

*Catalytic Construction of Carbon-  
Heteroatom Bonds by Shining Visible-Light  
on Transition-Metal Photocatalysts*

**Dissertation**

Zur Erlangung des Doktorgrades der Naturwissenschaften

(Dr. rer. nat.)

an der Fakultät für Chemie und Pharmazie

der **Universität Regensburg**



vorgelegt von

**Asik Hossain**

aus

West Bengal, Indien

**2019**



The experimental part of this work was carried out between April 2016 and July 2019 at the Institute of Organic Chemistry, University of Regensburg, Germany under the supervision of Prof. Dr. Oliver Reiser.

The thesis was submitted on 23.09.2019

Date of the colloquium: 28.10.2019

**Board of examiners**

PD Dr. Hans-Heiner Gorris chair

Prof. Dr. Oliver Reiser 1<sup>st</sup> referee

Prof. Dr. Burkhard König 2<sup>nd</sup> referee

Prof. Dr. Arno Pfitzner examiner

*.....dedicated to  
my Parents*



*“You have to dream before your dreams can come true.”*

**- Dr. A. P. J. Abdul Kalam**





## *Acknowledgements*

---

### **Acknowledgements**

Productive research and educational achievement always require the collaboration and support of many people. I would like to take the opportunity to express my appreciation for those people who have assisted and encouraged me in this long journey.

Foremost, I would like to express my sincere gratitude to my advisor, **Prof. Dr. Oliver Reiser**. I am very much thankful to him for accepting me into his research group. His kindness and generosity are deeply appreciated. His guidance and patience have led me to grow as a scientist, and motivated me to keep challenging myself. He did not give up on me during the difficult times, but instead he proactively provided me with sound advice and resources to get over the ‘nightmares’ that I was dealing with in my first year of graduate studies. Thanks to him for providing me the freedom and support for choosing the projects in my own way. In the past four years, his mentorship has been instrumental in my development, mentally, scientifically and professionally and I will always be grateful for each and every feedback from him. In general, now I think more deeply and critically about science, thanks to him, he is such an inspiring personality. In future, I will apply same type of scientific rigor to my future research endeavours.

I am also very much grateful to **Prof. Dr. Burkhard König** and **Prof. Dr. Arno Pfitzner** for being the doctoral committee members and reviewing this thesis. **Prof. König** is also thanked for providing the recommendation letter. I am also thankful to **PD Dr. Hans-Heiner Gorris** for being the chair person in my defense examination.

I would also like to express my gratitude to **Prof. Dr. Julia Rehbein** for the collaboration and her valuable feedback in one of my projects. I am very grateful to **Prof. Rehbein** for writing recommendation letter for me.

I would also like to thank **Prof. Indrapal Singh Aidhen**, my first research advisor during master studies at the Indian Institute of Technology Madras, India. It all began from his laboratory where I performed my first chromatographic separation. Many thanks to him for supporting me in every possible way during my master studies. I would also like extend my sincere gratitude to my teachers during bachelor studies at the University of Calcutta, Kolkata, India. **Dr. Amrit Mitra** (Private tutor, Singur Government College) and **Dr. Kaushik Basu** (St. Paul’s Cathedral Mission College) have guided me in the period of my college days with their outstanding knowledge in Organic Chemistry.

## *Acknowledgements*

---

I am very much grateful to **GRK 1626 (DFG)**, '*Chemical Photocatalysis*' for a scholarship throughout my graduate studies. I thank all the professors and other members of this programme for their feedback during progress of my research work.

I thank our international guests (visiting professors) who have provided their valuable comments for my research projects, especially Prof. Samir Z. Zard (LSO Polytechnique, France) and Prof. Huw M. L. Davies (Emory University, USA).

A big 'Thank You!' also goes to **Dr. Peter Kreitmeier** for his constant help and support in all the technical aspects. I am also thankful to **Antje Weigert** and **Michaela Schüle** for helping me in all the official works. Special thanks to **Michaela** for the cake recipe (I will definitely try this when I will visit my family and I am sure they will love it too). I am also thankful to Brigitte Eichenseher, Klaus Döring, Roxane Harteis, Helena Konkel for being kind to me whenever I needed their help.

I would like to thank the NMR department, the X-Ray crystallographic department and the mass department at the University of Regensburg for their excellent service. In this regard, I also thank Zulia Zach (König group) for her help during spectroscopic investigations in one of my research projects.

I sincerely thank all the past and present group members of **AK Reiser** who always kept a friendly environment in and outside of the laboratory. Special thanks to **Dr. Georgyi Kachkovskiy**, **Dr. Santosh K. Pagire** and **Dr. Thomas Rawner** for clearing all my scientific doubts in the first year of my graduate studies. You guys are amazing as a person as well as a scientist! I would also like to thank **Dr. Vidyasagar Adiyala** and **Dr. Aditya Bhattacharyya** for helping me with their great knowledge and experience in two of my important publications. Special thanks to **Dr. Aditya Bhattacharyya** for proofreading this thesis. **Dr. Christian Lankes**, **Dr. Eugen Lutsker**, **Christian Eichinger**, **Sebastian Engl**, **Jenny Phan** (AK Rehbein) are highly appreciated for their efforts in the collaborative projects. Thank you **Christian Eichinger** for your assistance in translating the summary of this thesis into German language. I am very much thankful to **Dr. Thomas Ertl**, **Dr. Verena Lehner**, **Dr. Sabine Kerres**, **Dr. Matthias Gnahn**, **Dr. Benjamin Kastl**, **Dr. Thomas Föll**, **Simon Budde**, **Peter Ehrnsberger** and other junior members of the 'AK Reiser' family for their fantastic company outside the laboratory during barbeque parties in summer and in Ph.D. parties. I know that I wouldn't have made it through without your friendship and support and I will miss all of you.

## *Acknowledgements*

---

I am very much glad to share room no. CH 33.1.23 with two awesome lab mates, **Dr. Julietta Yedoyan** and **Jinwei Shi**. Thank you so much for always keeping the lab environment calm and cool. Another special thanks to **Jinwei** for gifting me several packets of the *Chinese tea*, it tastes great as I love hot drinks.

I would also like to thank the members of the '**Welcome Center**' at the University of Regensburg for their help in finding (two times) apartment in Regensburg (very tough to find one!). This has saved lot of time for me.

I thank all the indian friends I have met during my stay at Regensburg – Dr. Indrajit Ghosh, Dr. Uttam Chakraborty, Dr. Somnath Das, Dr. Rizwan Shaikh, Dr. Anup Adhikary, Dr. Binoy Maity, Dr. Mukund Pramanik, Dr. Anamitra Chatterjee, Dr. Mitashree Maity, Dr. Amrita Das, Dr. Tamal Ghosh, Dr. Saikat Das, Dr. Jagadish Khamrai, Dr. Veera Reddy Yatham, Dr. Kathiravan Murugesan, Swarupa, Gunjan, Ria di, Rony di for their friendship and support.

Lastly, I would like to thank my family members for their constant encouragement, inspiration, affection and support.

## Publications

- 1) **A. Hossain**, O. Reiser\*  
Recent developments in visible-light-photocatalysis.  
**2019**. (manuscript in preparation).
- 2) **A. Hossain**,<sup>†</sup> A. Bhattacharyya,<sup>†</sup> O. Reiser\*  
Copper's rapid ascent in visible-light photoredox catalysis.  
*Science* **2019**, *364*, eaav9713. **DOI:** 10.1126/science.aav9713. (cited by 7).  
Altmetric score 39 (*top 5% of all research outputs ever tracked* by Altmetric).
- 3) **A. Hossain**,<sup>†</sup> S. Engl,<sup>†</sup> E. Lutsker,<sup>†</sup> O. Reiser\*  
Visible-Light-Mediated Regioselective Chlorosulfonylation of Alkenes and Alkynes:  
Introducing the Cu(II) Complex [Cu(dap)Cl<sub>2</sub>] to Photochemical ATRA Reactions.  
*ACS Catal.* **2019**, *9*, 1103-1109; **DOI:** 10.1021/acscatal.8b04188. (cited by 13).  
Among *the most read articles* (2nd) of the months January and February 2019.
- 4) **A. Hossain**, A. Vidyasagar, C. Eichinger, C. Lankes, J. Phan, J. Rehbein\*, O. Reiser\*  
Visible-Light-Accelerated Copper(II)-Catalyzed Regio- and Chemoselective Oxo-  
Azidation of Vinyl Arenes.  
*Angew. Chem. Int. Ed.* **2018**, *57*, 8288-8292; **DOI:** 10.1002/anie.201801678. (cited by 22).  
Regio- und chemoselektive Oxo-Azidierung von Vinylarenen, katalysiert durch Kupfer(II) und sichtbares Licht.  
*Angew. Chem.* **2018**, *130*, 8420-8424; **DOI:** 10.1002/ange.201801678.  
This article appears in *HOT Topic: Photocatalysis*.
- 5) S. K. Pagire, **A. Hossain**, O. Reiser\*  
Temperature Controlled Selective C-S or C-C Bond Formation: Photocatalytic  
Sulfonylation versus Arylation of Unactivated Heterocycles Utilizing Aryl Sulfonyl  
Chlorides.  
*Org. Lett.* **2018**, *20*, 648-651; **DOI:** 10.1021/acs.orglett.7b03790. (cited by 23).  
This article was highlighted in *Nature Index*.

- 6) **A. Hossain**, S. K. Pagire, O. Reiser\*  
Visible-Light-Mediated Synthesis of Pyrazines from Vinyl Azides Utilizing a Photocascade Process.  
*Synlett* **2017**, 28, 1707-1714; **DOI:** 10.1055/s-0036-1590888. (cited by 12).  
This article is a part of *Heterocycles: Special Issue*, ISHC Conference held in Regensburg, Germany (September 2017). Also nominated for *the best paper of the year* award.
- 7) S. K. Pagire, **A. Hossain**, L. Traub, S. Kerres, O. Reiser\*  
Photosensitised regioselective [2+2]-cycloaddition of cinnamates and related alkenes.  
*Chem. Commun.* **2017**, 53, 12072-12075; **DOI:** 10.1039/C7CC06710K. (cited by 25).  
Selected for inside front *cover picture* of the article; **DOI:** 10.1039/C7CC90428B.
- 8) T. Rawner, M. Knorn, E. Lutsker, **A. Hossain**, O. Reiser\*  
Synthesis of Trifluoromethylated Sultones from Alkenols Using a Copper Photoredox Catalyst.  
*J. Org. Chem.* **2016**, 81, 7139-7147; **DOI:** 10.1021/acs.joc.6b01001. (cited by 43).  
This article is a part of *Photocatalysis special issue*.

† denotes equal contribution.

\* denotes corresponding author.

## *Abbreviations*

---

### Abbreviations

AIBN	azobisisobutyronitrile	MHz	mega hertz
atm	atmosphere	min	minute
ATRA	atom transfer radical addition	mL	milliliter
Ar	Aryl	MLCT	metal-to-ligand charge transfer
bpy	2,2'-bipyridine	mmol	millimole
Bu	butyl	mol%	mole percent
CDCl <sub>3</sub>	deuterated chloroform	Mp	melting point
CFL	compact fluorescent lamp	MS	mass spectroscopy
CV	cyclic voltametry	$\nu$	frequency
$\delta$	chemical shift	<sup>n</sup> Bu	<i>n</i> -butyl
DCM	dichloromethane	nm	nanometer
dap	2,9-bis(para-anisyl)-1,10-phenanthroline	NMR	nuclear magnetic resonance
dF(CF) <sub>3</sub> ppy	2-(2,4-difluorophenyl)-5-(trifluoromethyl) pyridine	nr	no reaction
dtbbpy	4,4'-di-tert-butyl-2,2'-bipyridine	Nu	nucleophile
DMF	dimethyl formamide	<i>o</i> -	<i>ortho</i>
e.g.	exempli gratia ( <i>Latin</i> : for example)	<i>p</i> -	<i>para</i>
E <sub>1/2</sub>	standard reduction	PC	photocatalyst
ed.	Edition	PE	petroleum ether
EtOAc	ethylacetate	phen	phenanthroline
EtOH	ethanol	ppm	parts per million
EI	electron impact (MS)	Ph	phenyl
equiv	equivalents	Pr	propyl
ESI	electrospray ionization (MS)	ppy	2-phenylpyridine
Et	ethyl	$\Phi$	quantum yield
eV	electronvolt	redox	reduction-oxidation
<i>et al.</i>	et alia ( <i>Latin</i> : and others)	R <sub>f</sub>	retardation factor
FTIR	Fourier transform infrared spectroscopy	rt	room temperature

## *Abbreviations*

---

g	gram	SCE	saturated calomel electrode
h	hour(s)	SET	single electron transfer
HRMS	high resolution mass spectrometry	t	triplet
Hz	Hertz	$\tau$	excited-state lifetime
<i>i.e.</i>	it est ( <i>Latin</i> : that is)	TEMPO	(2,2,6,6-Tetramethylpiperidin-1-yl)oxyl
<sup>i</sup> Pr	<i>iso</i> -propyl	Tf	triflyl (= trifluoromethane sulfonyl)
IR	infrared spectroscopy	Ts	tosyl (= 4-toluenesulfonyl)
ISC	inter system crossing	<sup>t</sup> Bu	<i>tert</i> -butyl
<i>J</i>	coupling constant	TLC	thin layer chromatography
L	ligand	TMS	trimethylsilyl
LMCT	Ligand-to-metal charge transfer	UV	ultraviolet
$\lambda_{max}$	absorption maxima	V	Volt
LED	light emitting diode	vis	visible
M	metal; molar (molL <sup>-1</sup> )	vs	versus ( <i>Latin</i> : against)
m	milli (10 <sup>-3</sup> ); multiplet	VLIH	Visible-light-induced homolysis
<i>m</i> -	meta	W	watt
<i>m/z</i>	mass to charge ratio	X	counter anion
Me	methyl		
MeCN	acetonitrile		





## Table of contents

<b>Chapter 1: Visible-Light Photocatalysis: Background and Recent Developments</b>	<b>1</b>
1.1. Introduction.....	3
1.1.1. Single-electron transfer (SET).....	4
1.1.2. Energy transfer (ET).....	5
1.1.3. Commonly used photocatalysts.....	5
1.2. Early examples.....	7
1.3. Revolution of visible-light photoredox catalysis in organic synthesis.....	9
1.4. Recent advancements.....	11
1.5. Bifunctional photocatalysts.....	14
1.6. Formation of electron donor-acceptor (EDA) complex.....	15
1.7. Photocascade process.....	17
1.8. References.....	19
<b>Chapter 2: Synthesis of Substituted Pyrazines from Vinyl Azides via a Photocascade Process</b>	<b>25</b>
2.1. Introduction.....	27
2.2. Results and discussion.....	29
2.2.1. Reaction Optimization.....	29
2.2.2. Scope and limitation of the reaction.....	32
2.2.3. Synthesis of unsymmetrical pyrazine.....	33
2.3. Proposed reaction mechanism.....	33
2.4. Conclusion.....	35
2.5. References.....	35
2.6. Experimental section.....	38
2.6.1. General information.....	38
2.6.2. Procedure for the synthesis of vinyl-azides and their characterization.....	38
2.6.3. General procedure for the photochemical synthesis of pyrazines.....	46
2.6.4. Experimental set-up for photochemical reaction.....	46
2.6.5. Characterization of synthesized pyrazines.....	47
2.6.6. NMR spectra.....	56

## *Table of contents*

---

2.6.7. Crystal data.....	89
<b>Chapter 3: Copper and Visible-Light: Highlighting Special Features Beyond Photoinduced Electron Transfer</b>	<b>103</b>
3.1. Introduction.....	106
3.2. Copper(I)-complexes as stand-alone photocatalysts.....	107
3.2.1. Olefin bifunctionalization.....	109
3.2.2. C( <i>sp</i> <sup>3</sup> / <i>sp</i> <sup>2</sup> )-Heteroatom cross coupling.....	111
3.3. Photoexcitation of in situ generated Cu(I)-substrate complexes.....	113
3.4. Cooperative photoredox-copper dual catalysis.....	116
3.5. Miscellaneous examples.....	121
3.6. Cu(II)-complexes as stand-alone photocatalysts.....	123
3.7. Conclusion.....	125
3.8. References.....	125
<b>Chapter 4: Copper and Visible-Light: Oxo-azidation of Vinylarenes</b>	<b>131</b>
4.1. Introduction.....	133
4.2. Results and discussion.....	135
4.2.1. Reaction optimization.....	135
4.2.1. Scope and limitation of the reaction.....	138
4.2.3. Regio- and chemoselectivity of the developed method.....	139
4.2.4. Further transformations.....	140
4.3. Proposed reaction mechanism.....	141
4.4. Conclusion.....	143
4.5. References.....	144
4.6. Experimental section.....	147
4.6.1. General information.....	147
4.6.2. Safety Statements.....	147
4.6.3. Reaction set up.....	148
4.6.4. Colour change during the reaction.....	149
4.6.5. Mechanistic experiments.....	149
4.6.6. General procedure for the oxo-azidation of vinylarenes .....	153

## *Table of contents*

---

4.6.7. Characterization of the azido ketones.....	154
4.6.8. NMR Spectra.....	169
4.6.9. Crystal data.....	200
<b>Chapter 5: Sulfonyl chlorides in Photocatalytic Transformations</b>	<b>213</b>
5.1. Introduction.....	215
5.2. Selected examples.....	215
5.2.1. Trifluoromethylation using triflyl chloride.....	215
5.2.2. Aryl sulfonyl chlorides.....	218
5.2.3. Temperature-controlled selectivity.....	218
5.3. References.....	219
<b>Chapter 6: Copper and Visible-Light: Introducing a Cu(II)-catalyst, [Cu(dap)Cl<sub>2</sub>] to Photochemical ATRA Reaction</b>	<b>221</b>
6.1. Introduction.....	224
6.2. Results and discussion.....	225
6.2.1. Reaction Optimization.....	226
6.2.2. Scope and limitation of the developed method.....	228
6.2.3. Sequential functionalization of two different olefins.....	229
6.2.4. Further transformations of ATRA products.....	230
6.3. Mechanistic studies.....	231
6.4. Proposed reaction mechanism.....	232
6.5. Conclusion.....	234
6.6. References and notes.....	234
6.7. Experimental section.....	237
6.7.1. General information.....	237
6.7.2. Experimental set up.....	238
6.7.3. General Procedure for chlorosulfonation of unactivated olefins.....	238
6.7.4. Compound characterization.....	239
6.7.5. NMR Spectra.....	249
6.7.6. Crystal data.....	266

## *Table of contents*

---

<b>Summary</b> .....	279
<b>Zusammenfassung</b> .....	281
<b>Curriculum vitae</b> .....	283
<b>Declaration</b> .....	288

# *Chapter 1*



## Visible-Light Photocatalysis: Background and Recent Developments

### Abstract:

Aspects of sustainability are very crucial for the development of new synthetic methods. In this context, visible-light has been used as an abundant source of energy to induce or activate chemical reactions. Photoredox catalysis provides the opportunity to generate highly reactive radical ion intermediates often with unusual or unconventional reactivities under mild reaction conditions. In this chapter, different types of photocatalytic transformations have been discussed with the selection of a few noteworthy examples in the respective topics.

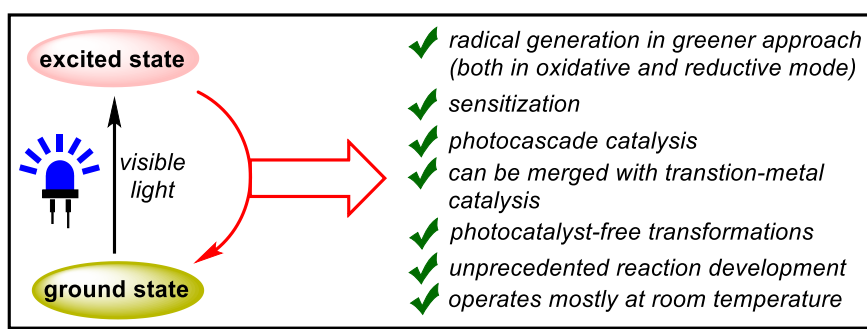


Figure 1: Photocatalysis in organic synthesis.

### Introduction:

In the field of catalysis, organic chemists primarily aim to find a simple method for the activation of small molecules. By sequential functionalization of small molecules, one can produce the desired valuable complex structures. In this context, visible-light photocatalysis<sup>[1]</sup> has received significant attention for the catalytic activation of such molecules. This method has allowed chemists to activate small molecules by efficiently converting photonic energy into chemical energy, to contrive unconventional modes of bond-formation. In principle, this approach relies on the ability of metal complexes and organic dyes to engage in single-electron transfer (SET), or energy transfer (ET) processes with organic substrates upon photoexcitation with visible light.<sup>[2]</sup> Thus, a photocatalyst can harness the energy of light (solar energy) and can convert this to chemical energy. Giacomo Ciamician, widely regarded as pioneering figure in the field of organic photochemistry, speculated that high-energy synthetic processes could be replaced with clean, cost-efficient photochemical transformations. He had this visionary idea in 1912, which has been documented in *Science* entitled 'The Photochemistry of the

*Future*'<sup>[3]</sup>. Almost after a century, chemists have made his visionary idea into a reality through the development of synthetic methods utilizing visible-light as one of the green and abundant reagents.<sup>[4]</sup>

A general schematic representation (mechanism) of majority of photocatalytic transformations is shown in Figure 2. In general, excited state of a photocatalyst can interact with an organic substance in two pathways: i) single electron transfer (SET) (Figure 2A) or energy transfer (ET) (Figure 2B).

### **Single electron transfer (SET)-mediated processes:**

A photocatalyst (PC) typically has higher oxidation and reduction potentials in excited state ( $PC^*$ ) compared to its ground state.<sup>[5]</sup> As a consequence, upon visible-light excitation,  $PC^*$  can either accept one electron from a donor (ED) generating corresponding radical-cation ( $ED^{\cdot+}$ ) of the quencher; this cycle is called '*reductive quenching cycle*'. On the other hand, in the presence of an electron acceptor (EA) substrate, corresponding radical anion ( $EA^{\cdot-}$ ) can be obtained which has been named as '*oxidative quenching cycle*' (Figure 2A). In photocatalysis, ED is often called '*reductive quencher*', likewise, EA is called '*oxidative quencher*'. Organic chemists typically design photocatalytic cycles by choosing different EA and ED for the

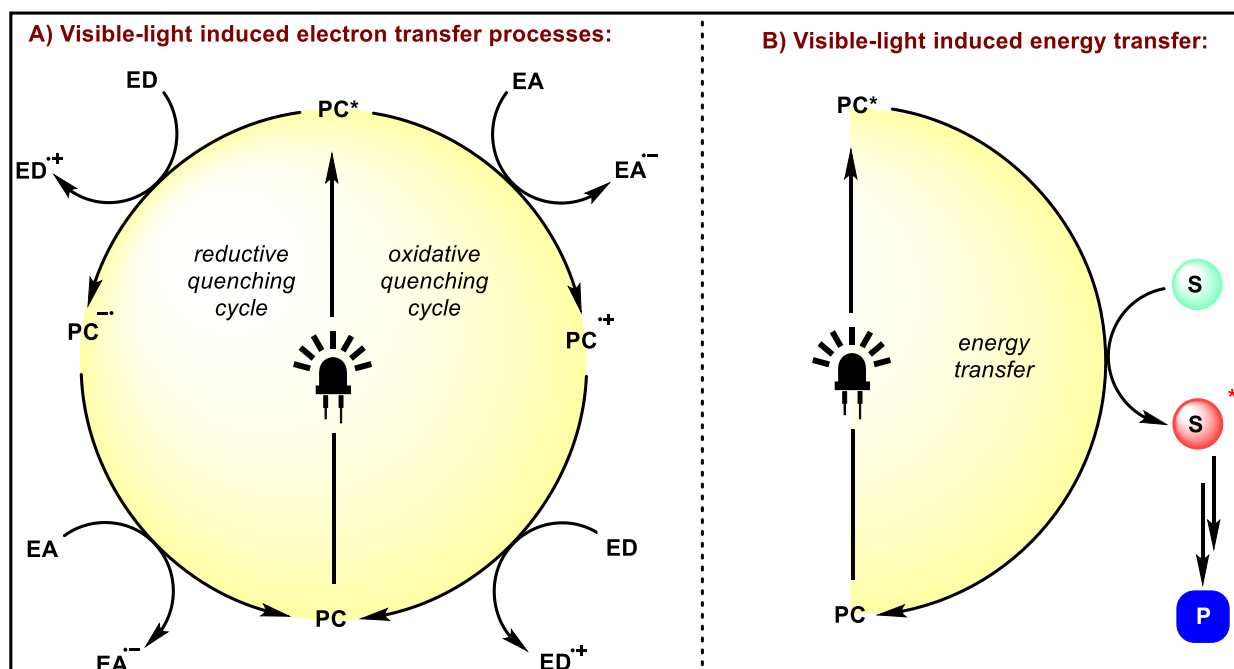


**Figure 2:** General representation of typical photoinduced processes. A) PC = Photocatalyst, EA = single electron acceptor, EA = single electron donor (EA and ED are mostly organic materials); B) S = Substrate, P = product.



development of new transformations. Very often simple amines (*e.g.* triethylamine) act as a ‘*reductive quencher*’ and molecular oxygen acts as ‘*oxidative quencher*’ which overall result very mild reaction conditions.<sup>[2]</sup>

### ***Energy transfer (ET) process:***

Another mode of action for an excited photocatalyst (PC\*) is energy transfer (ET)<sup>[6,7]</sup> pathway (Figure 2B) where a substrate (S) is sensitized through triplet energy transfer from PC\* forming S\*. S\*, reacts further either in an inter- or an intramolecular fashion to give desired products. Traditionally, this mode of activation is well-known with high energy UV-light without any external PC, but such activation has lower selectivity and often leads to undesired product formation in major amounts. To circumvent these issues, an alternative strategy employing milder conditions to access excited (triplet) states has been developed – visible-light-mediated energy transfer (ET). The combination of visible-light and a sensitizer (PC), can selectively activate a particular functionality present in organic molecules and hence, this is a more promising approach for the new reaction development. This activation principle typically provides a broader scope compared to the direct UV-light-mediated activation of organic molecules.

### **Commonly used photocatalysts:**

A series of different metal<sup>[2,5]</sup>-based and organic dye-based<sup>[8]</sup> photocatalysts are shown in Figure 3 and 4. An ideal photocatalyst should have strong absorption in the visible region and the lifetime of the excited state should be enough for bimolecular electron-transfer (with the *quencher*) in competition with other deactivation pathways. Another important aspect is photostability, which is often a major drawback for the organic photocatalysts although they have high excited state lifetimes. Most frequently used transition-metal photocatalysts are mainly composed of ruthenium(II) or iridium(III) and polypyridyl ligands. Specifically, [Ru(bpy)<sub>3</sub>]<sup>2+</sup> has been introduced as a photocatalyst by Kellogg and co-workers<sup>[9]</sup> in 1978. This complex has strong absorption maxima ( $\lambda_{max}$ ) at 452 nm (Figure 3). After absorption of a photon, the corresponding metal to ligand charge transfer (MLCT) state is long-lived enough (~1100 ns) to undergo single electron oxidation (*oxidative quenching*;  $E_{red} = -0.81$  V vs. SCE) or reduction (*reductive quenching*;  $E_{ox} = +0.77$  V vs. SCE).

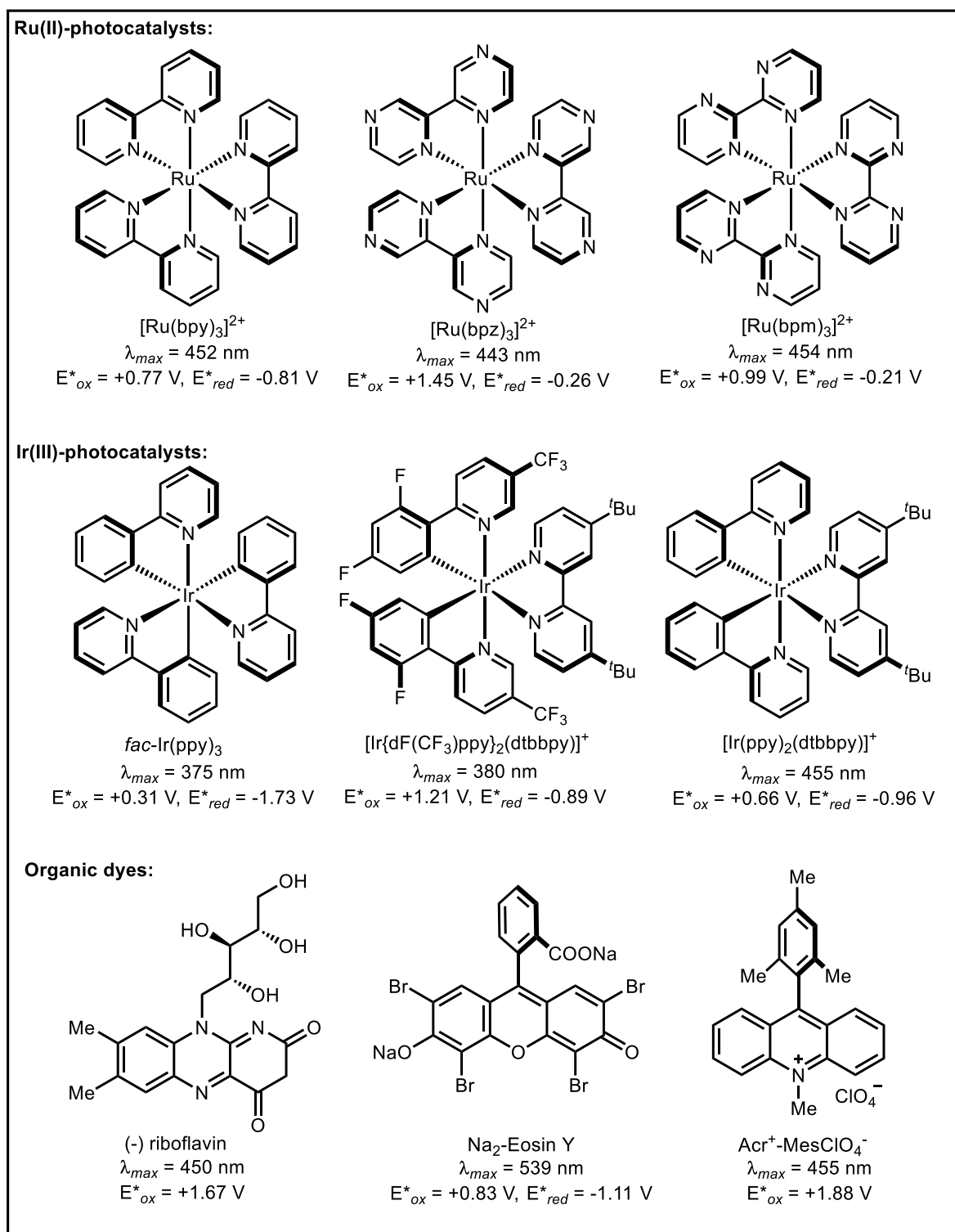


**Figure 3:** Structures of commonly used photocatalysts and their photochemical properties. All potential values are against saturated calomel electrode (SCE) in acetonitrile at room temperature.

Bifunctional photocatalysts are those which not only do photoinduced electron-transfer upon visible-light absorption, but can also interact with substrates or intermediate radicals within their coordination sphere. Copper-based photocatalysts are emerging in this area of research<sup>[10]</sup> including some engineered chiral iridium<sup>[11]</sup> or rhodium<sup>[12]</sup> octahedral complexes (Figure 4).

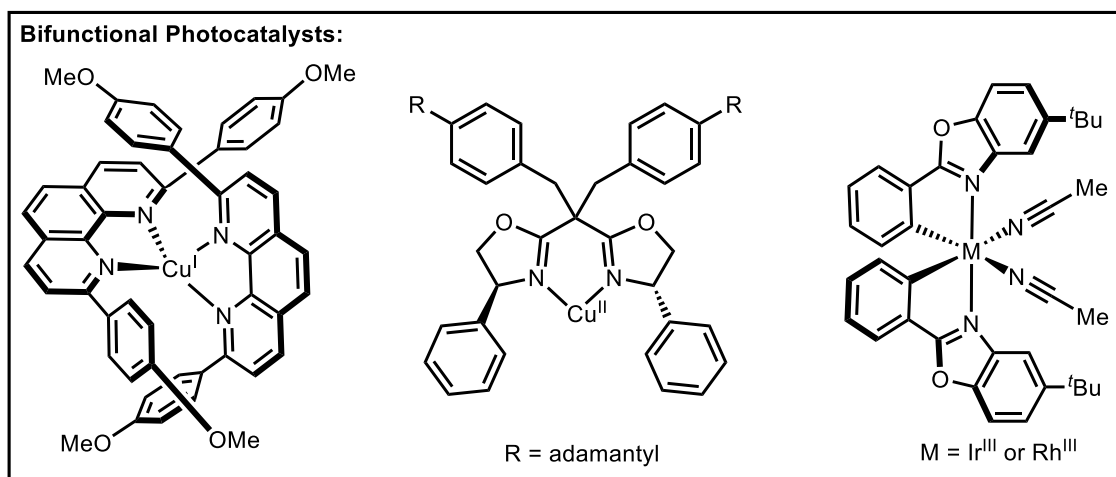
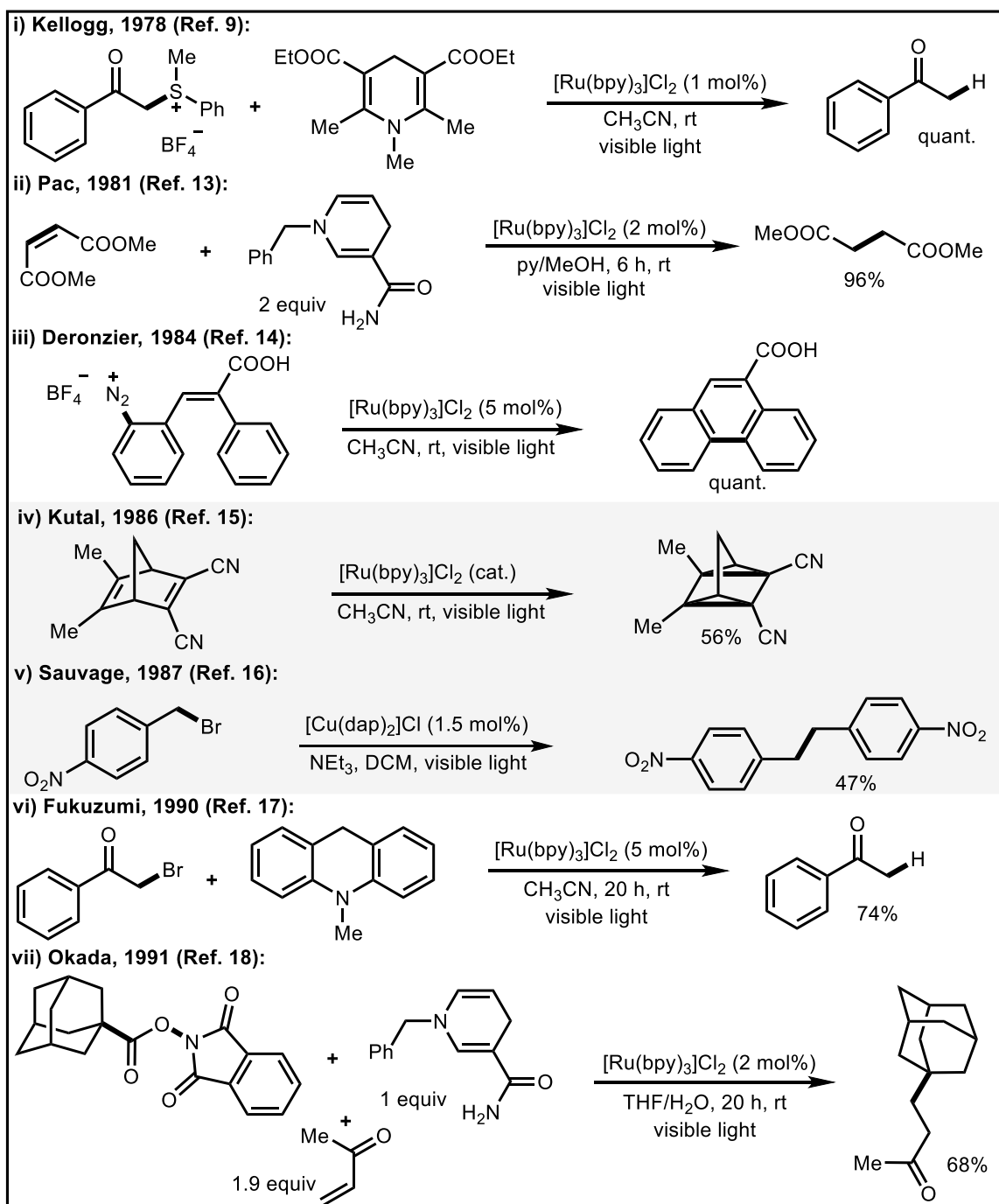


Figure 4: Bifunctional photocatalysts.

Copper photocatalysis is discussed in more detail in chapter 3. In this chapter, chiral iridium complex as bifunctional photocatalyst has been discussed.

### Early examples of visible-light photocatalyzed reactions:

The first set of reactions reported in this area of research were mostly reductive (not redox neutral), thus a stoichiometric ‘*reductive quencher*’ has always been used. In one of the earliest disclosure by Kellogg and co-workers<sup>[9]</sup> in 1978, [Ru(bpy)<sub>3</sub>]Cl<sub>2</sub> (1 mol%) was identified as an efficient photocatalyst to mediate the reduction of phenacyl sulfonium salt by Hantzsch ester (Figure 5, i). It was proposed that Hantzsch ester played the role of a ‘*reductive quencher*’. In 1981, Pac and co-workers<sup>[13]</sup> demonstrated that electron poor olefins can be reduced by using the same photocatalyst in presence of biological reductant 1,4-dihydronicotinamide adenine dinucleotide (NADH) as a stoichiometric ‘*reductive quencher*’ (Figure 5, ii). The first redox neutral photocatalyzed protocol was developed by Deronzier and co-workers<sup>[14]</sup> in 1984 (Figure 5, iii). Substituted phenanthrene has been synthesized in quantitative yield in presence of [Ru(bpy)<sub>3</sub>]Cl<sub>2</sub> (5 mol%) without using external oxidants or reductants. Two years later, Kutal and co-workers<sup>[15]</sup> found out for the first time that the same catalyst is also able to promote a [2+2]-cycloaddition reaction norboradiene system (Figure 5, iv). Then Sauvage *et al.* introduced [Cu(dap)<sub>2</sub>]Cl photocatalyst which could mediate reductive coupling of 4-



**Figure 5:** Pioneering examples of visible-light photocatalysis. quant. = quantitative; py = pyridine; THF = tetrahydrofuran.

nitrobenzyl bromide in presence of triethylamine<sup>[16]</sup> (Figure 5, v). In this case, triethylamine has been used to regenerate the Cu(I) catalyst. This is the first example for the utilization of an earth-abundant metal *i.e.* copper in visible-light photoredox catalysis. Fukuzumi *et al.* showed that phenacyl bromides can be converted to corresponding aldehydes under photocatalytic conditions using the ruthenium-based photocatalyst in presence of an aromatic

amine as ‘*reductive quencher*’<sup>[17]</sup> (Figure 5, vi). One year later, Okada *et al.* disclosed the first ever visible-light photocatalyzed decarboxylative coupling between activated acid derivatives (*N*-(acyloxy)phthalimides) and michael acceptors<sup>[18]</sup> (Figure 5, vii). In this reaction NADH has been used as the ‘*reductive quencher*’.

## Revolution of visible-light photoredox catalysis in organic synthesis:

### Pioneering studies by MacMillan, Yoon and Stephenson:

Although photoinduced electron-transfer reactions attracted considerable attention, but surprisingly, application of this method to organic synthesis has been limited to fewer examples (discussed in the above section). In 2008, two parallel studies by the research groups of MacMillan<sup>[19]</sup> and Yoon<sup>[20]</sup> have disclosed the use of [Ru(bpy)<sub>3</sub>]Cl<sub>2</sub> as a photocatalyst to perform enantioselective  $\alpha$ -alkylation of aldehydes and [2+2]-cycloaddition, respectively.

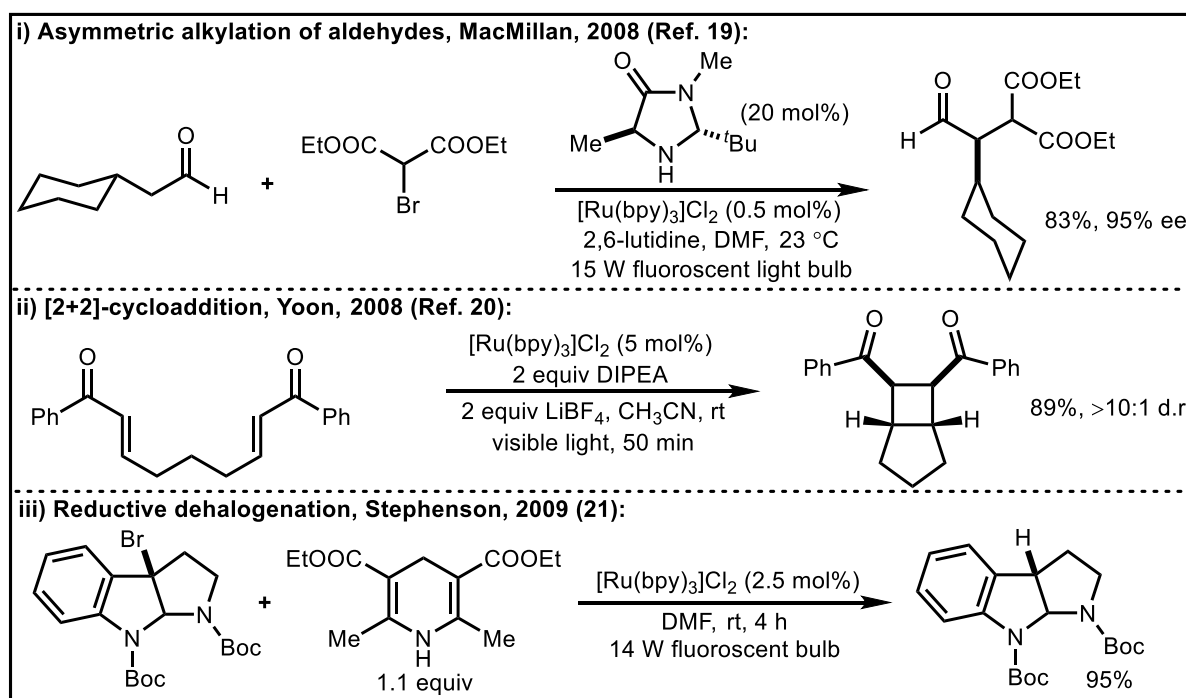


**Figure 6:** Revolution of photocatalysis in organic synthesis.

(Figure 6, i and ii) A year later, Stephenson and co-workers<sup>[21]</sup> reported a reductive dehalogenation protocol of alkyl halides using the same photocatalyst (Figure 6, iii). These three independent pioneering studies set the platform for further utilization of visible-light photocatalysis as a conceptually novel approach for the development of new organic reactions.

**Subsequent SET-mediated unique reaction developments:**

Immediately after these three pioneering studies, many scientific groups around the world have contributed to this field and developed a series of unprecedented reactions. In a noteworthy disclosure by Sanford and co-workers, palladium catalysis has been merged with

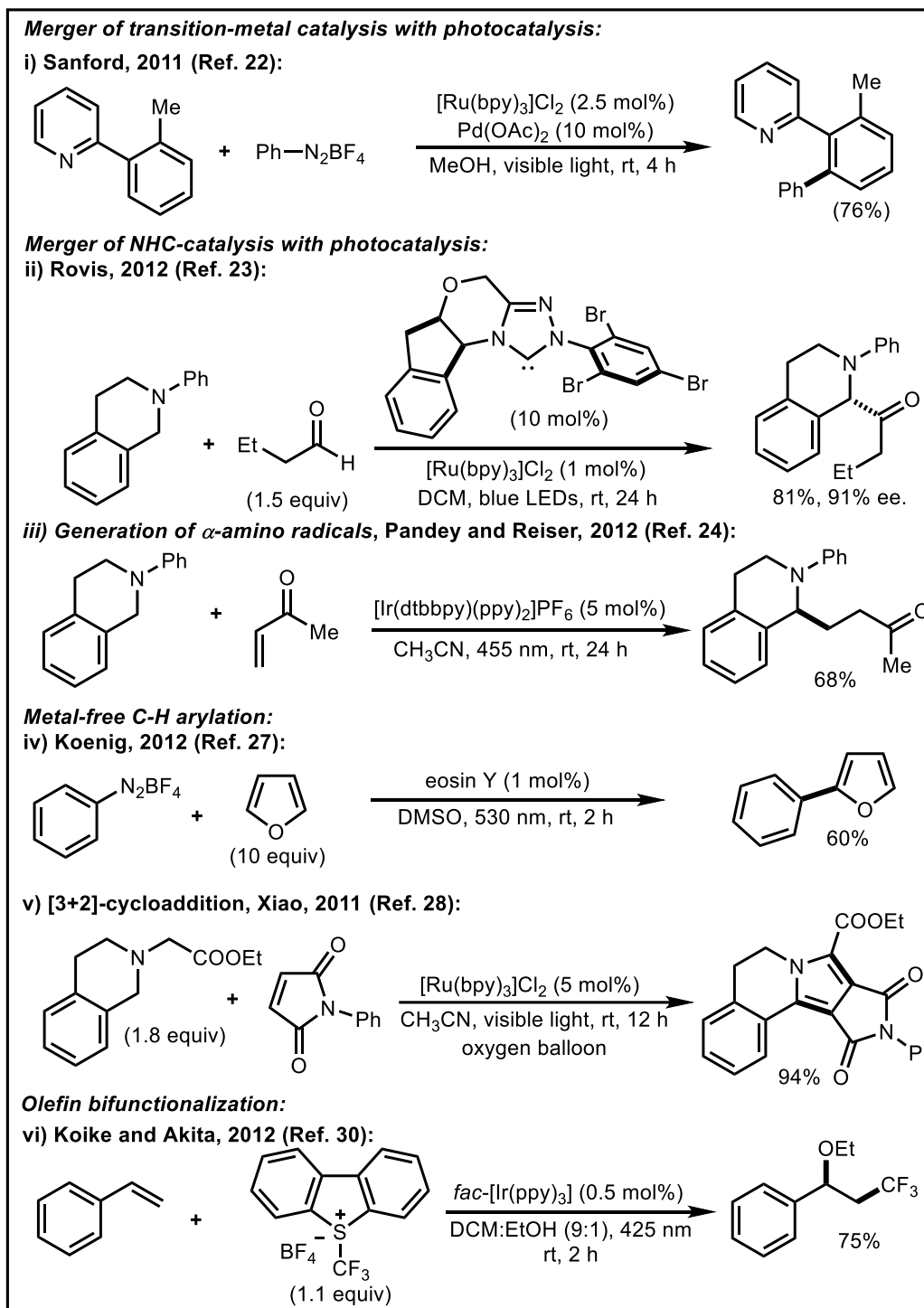
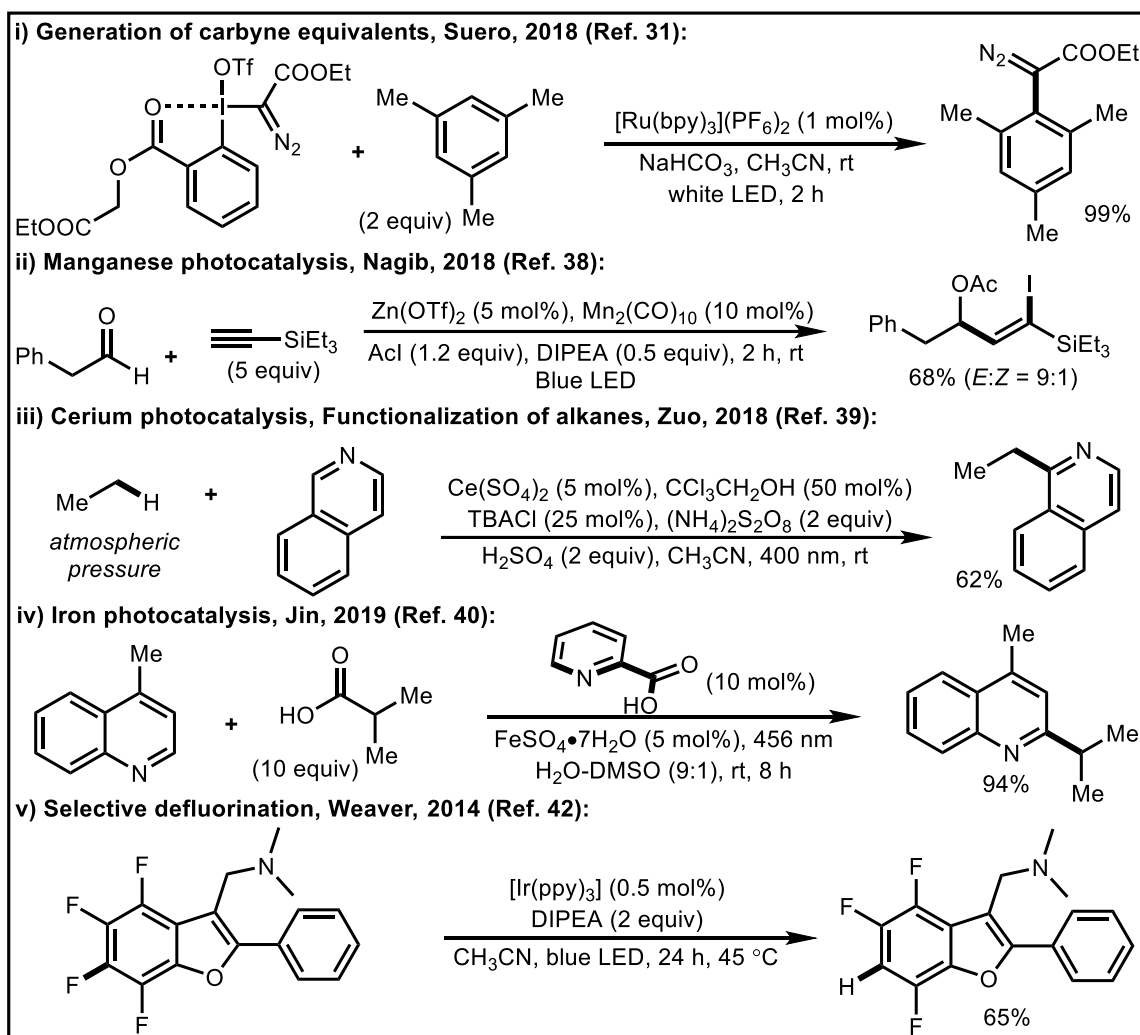


Figure 7: Further advancement of the field.

photocatalysis to achieve a room temperature C-H arylation reaction<sup>[22]</sup> (Figure 7, i). [Ru(bpy)<sub>3</sub>]Cl<sub>2</sub> photocatalyst after SET, generated aryl radicals from aryl diazonium salts via an ‘oxidative quenching cycle’, and while closing the photocatalytic cycle it also participated in the Pd-catalytic cycle for cross-coupling. A year later, Rovis and co-workers<sup>[23]</sup> have successfully merged photoredox catalysis with *N*-heterocyclic carbene (NHC) catalysis. By doing so, they could achieve  $\alpha$ -acylation of *tertiary*-amines in very good yield with high enantioselectivity (Figure 7, ii). At the same time, Pandey and Reiser<sup>[24]</sup> reported the generation of  $\alpha$ -amino radicals<sup>[25]</sup> from *tertiary*-amines which have been successfully trapped with Michael acceptors (Figure 7, iii) which ultimately produced *C*<sub>sp</sub><sup>3</sup>-*C*<sub>sp</sub><sup>3</sup> coupled products. The yield of the transformation can be increased in the presence of a Brønsted acid which has been nicely demonstrated by Yoon and co-workers<sup>[26]</sup>. Koenig and co-workers<sup>[27]</sup> utilized eosin Y for the development of a metal-free C-H arylation reaction in a short reaction time (Figure 7, iv). It was proposed that upon ‘oxidative quenching’ of eosin Y\* with aryl diazonium salt, corresponding aryl radicals were generated which subsequently reacted with heterocycles in a regioselective manner to give the arylated products. Xiao and co-workers<sup>[28]</sup> also found out the optimal reaction conditions for a [3+2]-cycloaddition between tertiary amines and activated olefins (Figure 7, v). In this case oxygen has been used as a terminal oxidant. Akita and co-workers have developed several methods for trifluoromethylation of olefinic compounds.<sup>[29]</sup> In one of their early studies in 2012, they could achieve oxy-trifluoromethylation<sup>[30]</sup> of vinylarenes using Umemoto’s reagent as a trifluoromethyl radical source (Figure 7, vi).

### Recent advancements in visible light photocatalysis:

In 2018, Suero and co-workers reported a photocatalytic strategy for the generation of diazomethyl radicals<sup>[31]</sup> from their corresponding hypervalent iodine precursors which have been successfully trapped by various functionalized arenes (Figure 8, i). Conceptually, this approach defines the smart generation of carbyne equivalents because the obtained diazo compounds can be subjected to a number of insertion reactions (C-H, N-H, C-S *etc.*). Quite recently, some scientific groups have disclosed interesting organic transformations<sup>[32]</sup> which do not utilize Ir or Ru-based photocatalysts, rather manganese<sup>[33]</sup>, cobalt<sup>[34]</sup>, nickel<sup>[35]</sup>, iron<sup>[36]</sup> or cerium<sup>[37]</sup> metal complexes have been used as photocatalysts. Nagib *et al.* found out that Mn<sub>2</sub>(CO)<sub>10</sub> can catalyze a carbo-iodination<sup>[38]</sup> reaction of alkynes under blue light irradiation (Figure 8, ii). Zuo and co-workers have published a number of synthetically useful transformations using cerium photocatalysis. Recently, they showed that gaseous ethane can



**Figure 8:** Selected recent examples in this field.

be used as an alkylating reagent<sup>[39]</sup> using catalytic cerium salt in the presence of an alcohol co-catalyst (Figure 8, iii). In the key step,  $\text{Ce}^{\text{IV}}\text{-O}$  bond undergoes a homolytic cleavage, generating an alkoxy radical which participates in a hydrogen atom transfer (HAT) from ethane to generate ethyl radical. Quite recently, in a noteworthy disclosure by Jin and co-workers<sup>[40]</sup> demonstrated that iron-complexes can also be used as a photocatalyst for selective alkylation of quinolines where free carboxylic acids have been employed as alkylating reagent (Figure 8, iv). C-F bond is considered to be a very strong bond and as a result, selective C-F defluorination/functionalization of a multi-fluorinated compound is a challenging task<sup>[41]</sup>. However, Weaver *et al.* showed that selective defluorination<sup>[42]</sup> (Scheme 8, v) or functionalization of C-F bonds are possible under photocatalytic conditions.



**ET-mediated reactions:**

As discussed in Figure 2A, visible-light-mediated sensitization of organic compounds in the presence of a sensitizer has offered a number of distinct reactions<sup>[43]</sup> and significant advancements have been made in this field.<sup>[6,7]</sup> In 2012, Xiao and co-workers<sup>[44]</sup> developed a visible-light-mediated intermolecular [2+2]-cycloaddition of 3-ylid-eneoxindoles via an

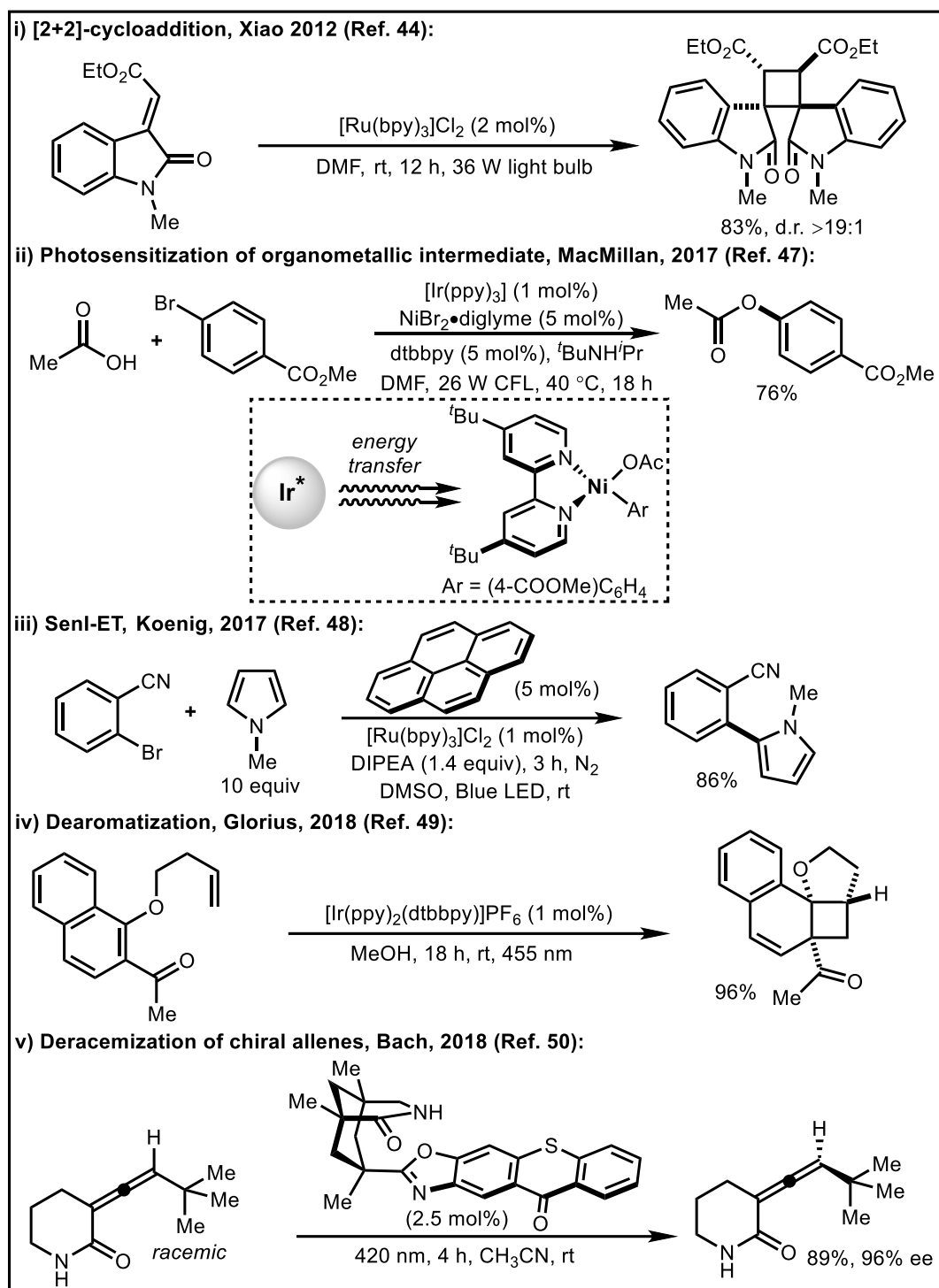


**Figure 9:** Selected examples for energy transfer mediated organic transformations.

energy transfer (ET) pathway (Figure 9, i). Almost at the same time, Yoon and co-workers<sup>[45]</sup> found out that styrenes can undergo [2+2]-cycloaddition in the presence of an Ir-based triplet sensitizer. Later, Reiser and Wu also contributed to this field through the independent development of [2+2]-cycloaddition protocol of cinnamates and related alkenes.<sup>[46]</sup> Another noteworthy disclosure by MacMillan and co-workers revealed that the reductive elimination step from an organo-nickel intermediate can be accelerated<sup>[47]</sup> in the presence of an Ir-sensitizer (Figure 9, ii). This study has huge impact in the field of transition-metal catalyzed cross-coupling reactions. In the same year, Koenig and co-workers<sup>[48]</sup> have developed a method mimicking the biological model, where energy has been transferred to a polyaromatic compound from  $^*[\text{Ru}(\text{bpy})_3]\text{Cl}_2$ . The resulting excited polyaromatic compound then participate in electron transfer process with DIPEA (Figure 9, iv). Glorius and co-workers<sup>[49]</sup> have advanced this field by the development of a novel approach for the dearomative [2+2]-cycloaddition through the action of an Ir-based sensitizer (Figure 9, iv). Very recently, Bach and co-workers<sup>[50]</sup> disclosed an unprecedented approach for the deracemization of chiral allenes (Figure 9, v). Both the enantiomers of the chiral allenes are obtainable in high enantiomeric excess depending upon the configuration of the chiral organo-sensitizer. This protocol operates at room temperature and showcases a conceptually new approach for making chiral compounds from their racemic mixtures.

### **Bifunctional photocatalyst in organic synthesis:**

Meggers *et. al.* has recently introduced a chiral iridium complex<sup>[11]</sup> can serve as a sensitizer for photocatalysis as well as can also control the stereochemistry of the product during the course of the reaction (Figure 10, i). This was a groundbreaking achievement in this field as because this study has opened up new avenues for asymmetric synthesis of organic molecules. When they changed the coupling partner *i.e.* instead of electron deficient benzyl bromide, electron rich *N,N*-dimethylaniline did not yield (<3%) significant amount of product formation using the chiral-iridium complex (Figure 10, ii). When they used corresponding rhodium complex, the desired coupled product was obtained in good yield with excellent enantioselectivity.<sup>[51]</sup> Although the major drawback for this study was to have engineered substrates which can coordinate with the metal center.

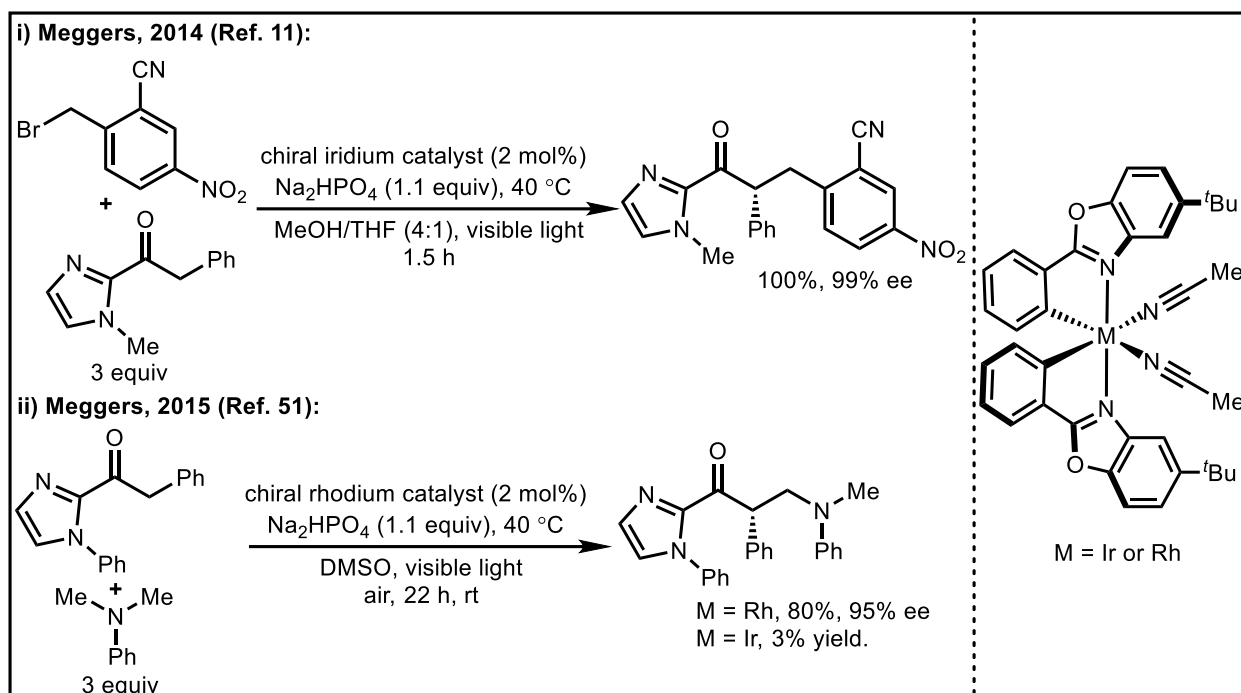


**Figure 10:** Chiral iridium complex as a bifunctional photocatalyst.

### Formation of electron donor-acceptor (EDA) complexes: Photocatalyst-free visible-light-induced reactions:

The methods which have been discussed so far always utilize a sensitizer in order to activate organic substrates via SET or ET. There are a few known visible-light-induced transformations which do not require any photocatalyst and the desired products still can be obtained in efficient manners. Such reactions are proposed to occur via the formation of electron donor-acceptor (EDA) complexes<sup>[52]</sup> (Figure 11A) between two colourless substrates, wherein one is electron-rich (donor) and another one is electron-deficient (acceptor). This coloured EDA complex can then undergo intermolecular electron transfer upon visible-light irradiation which results in the formation of the corresponding product without the need of an external photocatalyst.

In 2013, Melchiorre and co-workers<sup>[53]</sup> utilized this beautiful chemistry where an asymmetric  $\alpha$ -alkylation of aldehydes have been achieved (Figure 11B, i). The enantioselectivity in the product formation was controlled by a chiral *secondary*-amine catalyst which could form a chiral enamine intermediate after reacting with the aldehyde. In the next step, the enamine intermediate could form a coloured EDA complex with the electrophile (in this case, electron

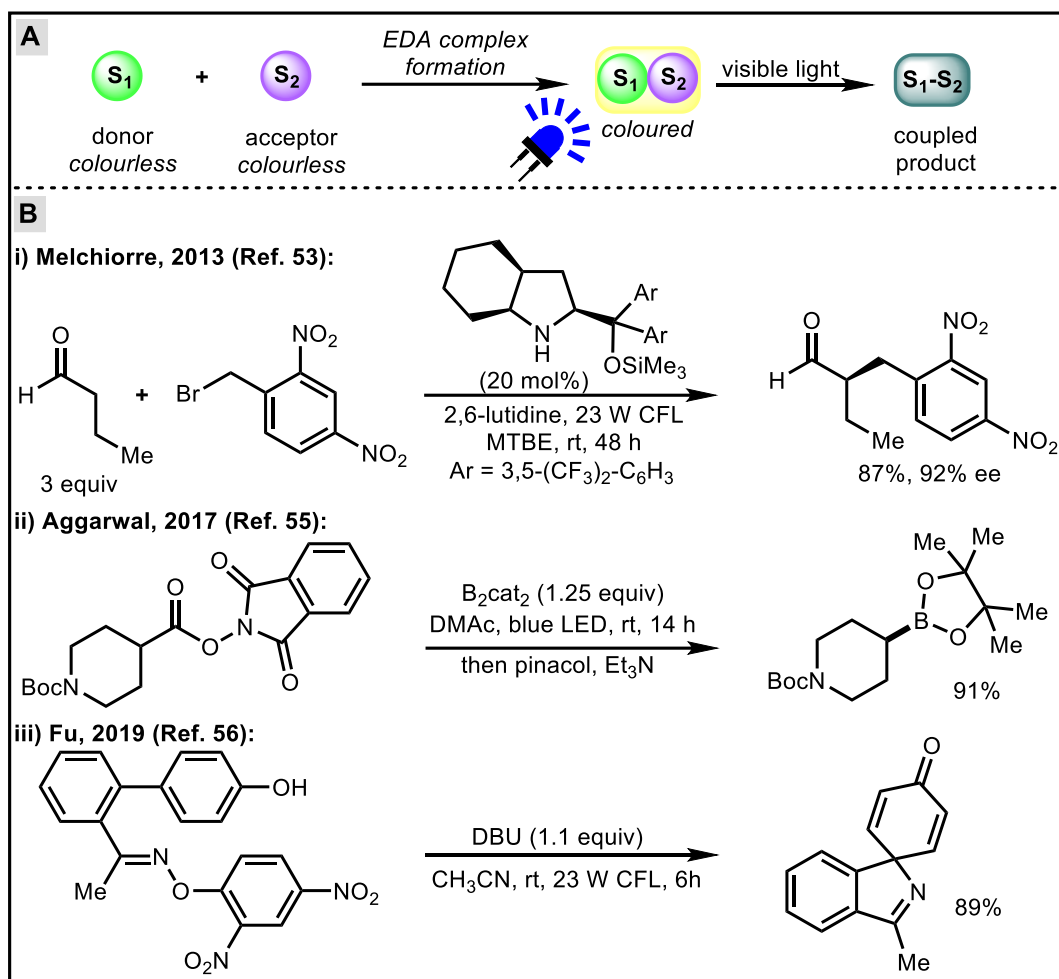


**Figure 11:** A) Photoreaction without external photocatalyst. S = substrate. EDA = electron donor-acceptor. B) Selected examples for photocatalyst free visible-light-induced reactions. MTBE = methyl *tert*-butyl ether; DMAc = *N,N*-Dimethylacetamide; DBU = 1,8-Diazabicyclo[5.4.0]undec-7-ene.

deficient benzyl bromide). This disclosure was the starting point for the development of several other photochemical methods which can be triggered without using a photocatalyst.<sup>[54]</sup> Quite recently, Aggarwal and co-workers<sup>[55]</sup> have established a decarboxylative borylation reaction which can be carried out only by using visible-light without a photocatalyst present (Figure 11B, ii). Intramolecular reaction is also feasible when both donor and acceptor moieties present in the same molecule (Figure 11B, iii). Very recently, Fu *et al.* were successful for the development of a method through visible-light excitation of an intramolecular charge-transfer complex, leading to spiropyrrolidines<sup>[56]</sup> in very good yields.

### Photocascade process: Two photons for one product formation:

Visible-light driven photocatalysis using a single catalyst to promote two or more catalytic cycles has also recently enjoyed impressive advances which is known as *photocascade catalysis*.<sup>[57]</sup> This idea is generalized in Figure 12. If the product **P<sup>1</sup>** is still active towards quenching with PC\*, it may get converted to another product **P<sup>2</sup>**, under the same reaction conditions. This unique sequential approach for the activation of small molecules often lead to complex structures through the action of a single photocatalyst and chemists have discovered many unprecedented reactions following the concept.<sup>[58]</sup>

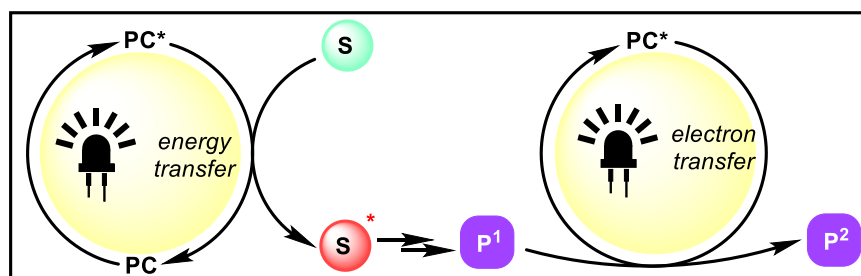


**Figure 12:** Photocascade Catalysis. The cycles define a visible-light induced sequential energy and electron transfer process.

An excellent example in this field was reported by Rueping *et al.* in 2013.<sup>[59]</sup> The authors reported the unexpected formation of synthetically useful indol-3-carbaldehydes starting from *N,N*-dibenzyl-2-iodoaniline-derived  $\alpha,\beta$ -unsaturated ketones (Figure 13, i). It was suggested that two sequential Ir-photocatalytic cycles (SET followed by another SET) were responsible for the unexpected product formation. Later, Pandey and co-workers<sup>[60]</sup> developed a double Michael addition protocol of benzylic compounds to obtain fused-ring system using [Ru(bpy)<sub>3</sub>]Cl<sub>2</sub> photocatalyst (Figure 13, ii). In the aforementioned two reactions, two photocatalytic cycles were involved and both of them were in SET mode. Xiao and co-workers could utilize ET followed by SET sequence<sup>[61]</sup> in a reaction between vinyl azides and alkynes which resulted in the formation of substituted pyrroles (Figure 13, iii). It was proposed that upon sensitization (ET), azirine-intermediates were formed which underwent a ring-opening step upon SET with the photoexcited Fukuzumi catalyst. A year later, Gilmour *et al.* could follow up this sequence of activation (ET followed by SET) for the synthesis of 2*H*-chromen-2-one derivatives from corresponding *trans* cinnamic acids (Figure 13, iv).<sup>[62]</sup> Recently, Reiser *et al.* further extended the concept by developing an excellent method for the synthesis of dihydroindeno[1,2-*c*]chromenes from easily accessible vinyl bromide precursors (Figure 13, v).<sup>[63]</sup> The authors could incorporate three oxygen atoms in the final compound which come

from molecular oxygen. Quite recently, Glorius *et al.* have developed a dual energy transfer sequence (ET followed by ET) to synthesize benzo-fused cyclobutanes through the action of a single Ir-photocatalyst (Figure 13, vi).<sup>[49]</sup>

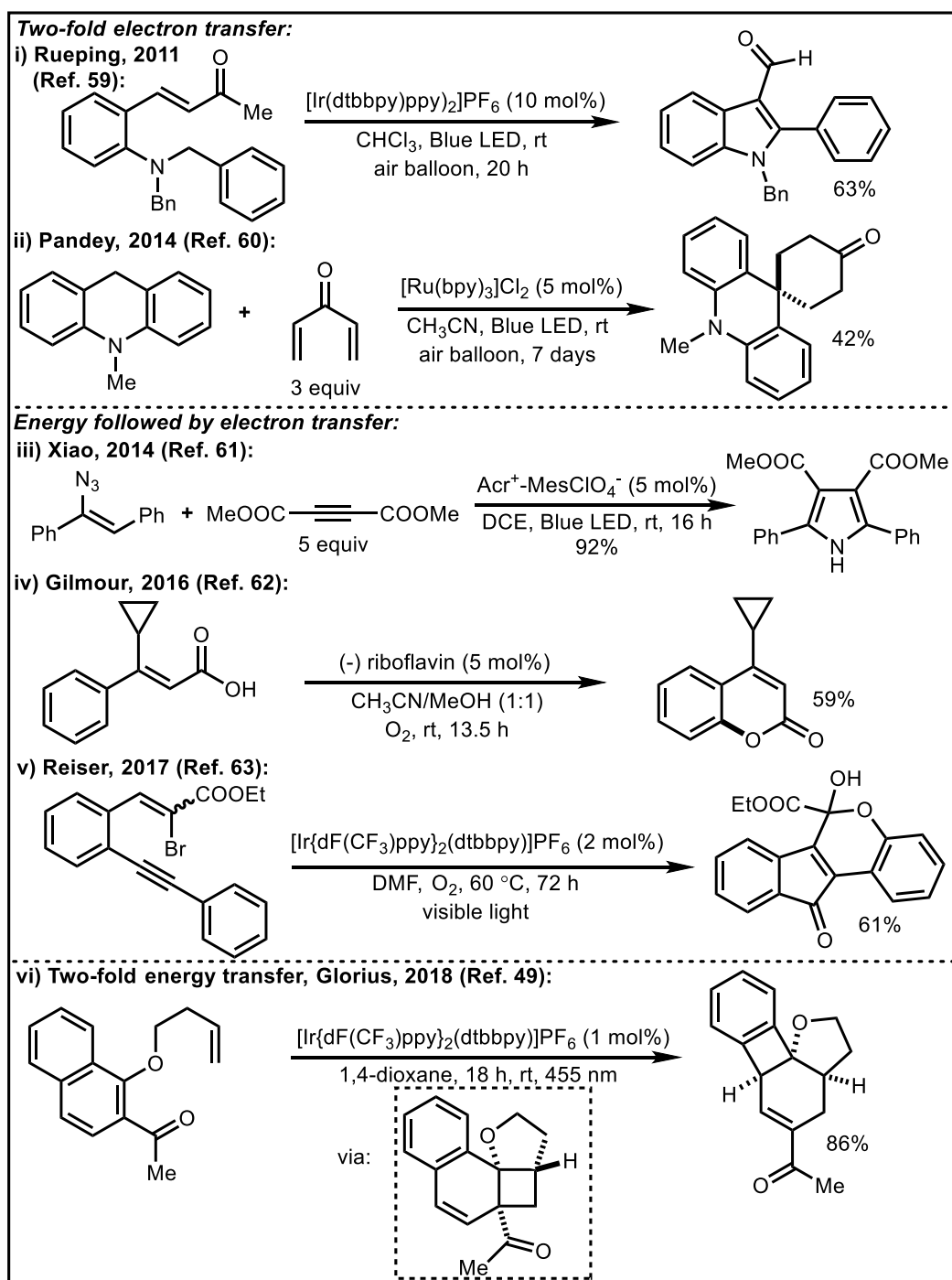


Figure 13: Selected examples of reactions.

### Conclusions and outlook:

Since 2008, photocatalysis has gained a mature growth and a wide array of new activation platforms and synthetic transformations have been developed through the conversion of visible light into chemical energy. In addition, the redox properties of the metal-based photocatalysts can be easily tuned (highly oxidizing or reducing) to suit almost any specific application. Recent advances in photocatalysis have shown that a broad array of radical intermediates can be accessed from readily available starting materials such as carboxylic acids and organohalides and, in some cases even alkanes through hydrogen atom transfer (HAT), thereby expanding the range of methods for native functionalization.

### References and notes:

- [1] M. H. Shaw, J. Twilton, D. W. C. MacMillan, *J. Org. Chem.* **2016**, *81*, 6898.
- [2] L. Marzo, S. K. Pagire, O. Reiser, B. König, *Angew. Chem. Int. Ed.* **2018**, *57*, 10034.
- [3] G. Ciamician, *Science* **1912**, *36*, 385.
- [4] a) T. Hering, A. U. Meyer, B. König, *J. Org. Chem.* **2016**, *81*, 6927; b) C. Stephenson, T. Yoon, D. W. C. MacMillan, *Visible Light Photocatalysis in Organic Chemistry*, Wiley-VCH Verlag GmbH & Co. KGaA, Weinheim, Germany, **2018**; c) M. N. Hopkinson, A. Tlahuext-Aca, F. Glorius, *Acc. Chem. Res.* **2016**, *49*, 2261; d) J. M. R. Narayanam, C. R. J. Stephenson, *Chem. Soc. Rev.* **2011**, *40*, 102; e) M. Majek, A. Jacobi von Wangelin, *Acc. Chem. Res.* **2016**, *49*, 2316; f) K. L. Skubi, T. R. Blum, T. P. Yoon, *Chem. Rev.* **2016**, *116*, 10035; g) O. Reiser, *Acc. Chem. Res.* **2016**, *49*, 1990; h) C. R. Jamison, L. E. Overman, *Acc. Chem. Res.* **2016**, *49*, 1578; i) N. A. Romero, D. A. Nicewicz, *Chem. Rev.* **2016**, *116*, 10075; j) I. Ghosh, L. Marzo, A. Das, R. Shaikh, B. König, *Acc. Chem. Res.* **2016**, *49*, 1566; k) E. C. Gentry, R. R. Knowles, *Acc. Chem. Res.* **2016**, *49*, 1546; l) A. C. Hernandez-Perez, S. K. Collins, *Acc. Chem. Res.* **2016**, *49*, 1557; m) J. C. Tellis, C. B. Kelly, D. N. Primer, M. Jouffroy, N. R. Patel, G. A. Molander, *Acc. Chem. Res.* **2016**, *49*, 1429; n) B. König, *Eur. J. Org. Chem.* **2017**, *2017*, 1979; o) J. Xuan, W.-J. Xiao, *Angew. Chem. Int. Ed.* **2012**, *51*, 6828; p) L. Buzzetti, G. E. M. Crisenza, P. Melchiorre, *Angew. Chem. Int. Ed.* **2019**, *58*, 3730; q) D. Ravelli, S. Protti, M. Fagnoni, *Chem. Rev.* **2016**, *116*, 9850.
- [5] C. K. Prier, D. A. Rankic, D. W. C. MacMillan, *Chem. Rev.* **2013**, *113*, 5322.
- [6] Tutorial review: F. Strieth-Kalthoff, M. J. James, M. Teders, L. Pitzer, F. Glorius, *Chem. Soc. Rev.* **2018**, *47*, 7190.

- [7] Excellent review for energy transfer reactions: Q.-Q. Zhou, Y.-Q. Zou, L.-Q. Lu, W.-J. Xiao, *Angew. Chem. Int. Ed.* **2019**, *58*, 1586.
- [8] Photocatalysis with organic dyes: a) D. P. Hari, B. König, *Chem. Commun.* **2014**, *50*, 6688; b) E. Silva, A. M. Edwards, *Flavins: Photochemistry and photobiology*, Royal Society of Chemistry, Cambridge, **2007**; c) E. Speckmeier, T. G. Fischer, K. Zeitler, *J. Am. Chem. Soc.* **2018**, *140*, 15353; d) B. Mühldorf, R. Wolf, *Angew. Chem. Int. Ed.* **2016**, *55*, 427.
- [9] D. M. Hedstrand, W. H. Kruizinga, R. M. Kellogg, *Tetrahedron Lett.* **1978**, *19*, 1255.
- [10] Use of copper in visible-light mediated transformations: A. Hossain, A. Bhattacharyya, O. Reiser, *Science* **2019**, *364*, eaav9713.
- [11] H. Huo, X. Shen, C. Wang, L. Zhang, P. Röse, L.-A. Chen, K. Harms, M. Marsch, G. Hilt, E. Meggers, *Nature* **2014**, *515*, 100.
- [12] X. Huang, E. Meggers, *Acc. Chem. Res.* **2019**, *52*, 833.
- [13] C. Pac, M. Ihama, M. Yasuda, Y. Miyauchi, H. Sakurai, *J. Am. Chem. Soc.* **1981**, *103*, 6495.
- [14] H. Cano-Yelo, A. Deronzier, *J. Chem. Soc., Perkin Trans. 2* **1984**, 1093.
- [15] H. Ikezawa, C. Kutal, K. Yasufuku, H. Yamazaki, *J. Am. Chem. Soc.* **1986**, *108*, 1589.
- [16] J.-M. Kern, J.-P. Sauvage, *J. Chem. Soc., Chem. Commun.* **1987**, 546.
- [17] S. Fukuzumi, S. Mochizuki, T. Tanaka, *J. Phys. Chem.* **1990**, *94*, 722.
- [18] K. Okada, K. Okamoto, N. Morita, K. Okubo, M. Oda, *J. Am. Chem. Soc.* **1991**, *113*, 9401.
- [19] D. A. Nicewicz, D. W. C. MacMillan, *Science* **2008**, *322*, 77.
- [20] M. A. Ischay, M. E. Anzovino, J. Du, T. P. Yoon, *J. Am. Chem. Soc.* **2008**, *130*, 12886.
- [21] J. M. R. Narayanam, J. W. Tucker, C. R. J. Stephenson, *J. Am. Chem. Soc.* **2009**, *131*, 8756.
- [22] D. Kalyani, K. B. McMurtrey, S. R. Neufeldt, M. S. Sanford, *J. Am. Chem. Soc.* **2011**, *133*, 18566.
- [23] D. A. DiRocco, T. Rovis, *J. Am. Chem. Soc.* **2012**, *134*, 8094.
- [24] P. Kohls, D. Jadhav, G. Pandey, O. Reiser, *Org. Lett.* **2012**, *14*, 672.
- [25] Y. Miyake, K. Nakajima, Y. Nishibayashi, *J. Am. Chem. Soc.* **2012**, *134*, 3338.
- [26] L. Ruiz Espelt, E. M. Wiensch, T. P. Yoon, *J. Org. Chem.* **2013**, *78*, 4107.
- [27] D. P. Hari, P. Schroll, B. König, *J. Am. Chem. Soc.* **2012**, *134*, 2958.
- [28] Y.-Q. Zou, L.-Q. Lu, L. Fu, N.-J. Chang, J. Rong, J.-R. Chen, W.-J. Xiao, *Angew. Chem. Int. Ed.* **2011**, *50*, 7171.
- [29] T. Koike, M. Akita, *Acc. Chem. Res.* **2016**, *49*, 1937.
- [30] Y. Yasu, T. Koike, M. Akita, *Angew. Chem. Int. Ed.* **2012**, *51*, 9567.



- [31] Z. Wang, A. G. Herraiz, A. M. Del Hoyo, M. G. Suero, *Nature* **2018**, 554, 86.
- [32] a) R. Kancherla, K. Muralirajan, A. Sagadevan, M. Rueping, *Trends in Chemistry* **2019**, 1, 510; b) C. B. Larsen, O. S. Wenger, *Chem. Eur. J.* **2018**, 24, 2039.
- [33] P. Nuhant, M. S. Oderinde, J. Genovino, A. Juneau, Y. Gagné, C. Allais, G. M. Chinigo, C. Choi, N. W. Sach, L. Bernier et al., *Angew. Chem. Int. Ed.* **2017**, 56, 15309.
- [34] L. M. Kreis, S. Krautwald, N. Pfeiffer, R. E. Martin, E. M. Carreira, *Org. Lett.* **2013**, 15, 1634.
- [35] Nickel photocatalysis: T. Mandal, S. Das, S. De Sarkar, *Adv. Synth. Catal.* **2019**, 361, 3200.
- [36] S. Parisien-Collette, A. C. Hernandez-Perez, S. K. Collins, *Org. Lett.* **2016**, 18, 4994.
- [37] J.-J. Guo, A. Hu, Y. Chen, J. Sun, H. Tang, Z. Zuo, *Angew. Chem. Int. Ed.* **2016**, 55, 15319.
- [38] Manganese photocatalysis: L. Wang, J. M. Lear, S. M. Rafferty, S. C. Fosu, D. A. Nagib, *Science* **2018**, 362, 225.
- [39] Cerium photocatalysis: A. Hu, J.-J. Guo, H. Pan, Z. Zuo, *Science* **2018**, 361, 668.
- [40] Iron photocatalysis: Z. Li, X. Wang, S. Xia, J. Jin, *Org. Lett.* **2019**, 21, 4259.
- [41] a) S. Senaweera, J. D. Weaver, *J. Am. Chem. Soc.* **2016**, 138, 2520; b) H. Wang, N. T. Jui, *J. Am. Chem. Soc.* **2018**, 140, 163; c) K. Chen, N. Berg, R. Gschwind, B. König, *J. Am. Chem. Soc.* **2017**, 139, 18444.
- [42] S. M. Senaweera, A. Singh, J. D. Weaver, *J. Am. Chem. Soc.* **2014**, 136, 3002.
- [43] a) E. P. Farney, T. P. Yoon, *Angew. Chem. Int. Ed.* **2014**, 53, 793; b) D. Ravelli, M. Fagnoni, *ChemCatChem* **2015**, 7, 735; c) E. Brachet, T. Ghosh, I. Ghosh, B. König, *Chem. Sci.* **2015**, 6, 987; d) S. Kerres, E. Plut, S. Malcherek, J. Rehbein, O. Reiser, *Adv. Synth. Catal.* **2018**, 361, 1400.
- [44] Y.-Q. Zou, S.-W. Duan, X.-G. Meng, X.-Q. Hu, S. Gao, J.-R. Chen, W.-J. Xiao, *Tetrahedron* **2012**, 68, 6914.
- [45] Z. Lu, T. P. Yoon, *Angew. Chem. Int. Ed.* **2012**, 51, 10329.
- [46] a) T. Lei, C. Zhou, M.-Y. Huang, L.-M. Zhao, B. Yang, C. Ye, H. Xiao, Q.-Y. Meng, V. Ramamurthy, C.-H. Tung et al., *Angew. Chem. Int. Ed.* **2017**, 56, 15407; b) S. K. Pagire, A. Hossain, L. Traub, S. Kerres, O. Reiser, *Chem. Commun.* **2017**, 53, 12072.
- [47] E. R. Welin, C. Le, D. M. Arias-Rotondo, J. K. McCusker, D. W. C. MacMillan, *Science* **2017**, 355, 380.

- [48] Sensitization-initiated electron transfer: a) I. Ghosh, R. S. Shaikh, B. König, *Angew. Chem. Int. Ed.* **2017**, *56*, 8544; b) I. Ghosh, J. I. Bardagi, B. König, *Angew. Chem. Int. Ed.* **2017**, *56*, 12822.
- [49] M. J. James, J. L. Schwarz, F. Strieth-Kalthoff, B. Wibbeling, F. Glorius, *J. Am. Chem. Soc.* **2018**, *140*, 8624.
- [50] A. Hölzl-Hobmeier, A. Bauer, A. V. Silva, S. M. Huber, C. Bannwarth, T. Bach, *Nature* **2018**, *564*, 240.
- [51] Y. Tan, W. Yuan, L. Gong, E. Meggers, *Angew. Chem. Int. Ed.* **2015**, *54*, 13045.
- [52] C. G. S. Lima, T. de M. Lima, M. Duarte, I. D. Jurberg, M. W. Paixão, *ACS Catal.* **2016**, *6*, 1389.
- [53] E. Arceo, I. D. Jurberg, A. Alvarez-Fernández, P. Melchiorre, *Nat. Chem.* **2013**, *5*, 750.
- [54] a) Z.-Y. Cao, T. Ghosh, P. Melchiorre, *Nat. Commun.* **2018**, *9*, 3274; b) Q.-Q. Ge, J.-S. Qian, J. Xuan, *J. Org. Chem.* **2019**, *84*, 8691; c) L. Marzo, S. Wang, B. König, *Org. Lett.* **2017**, *19*, 5976.
- [55] A. Fawcett, J. Pradeilles, Y. Wang, T. Mutsuga, E. L. Myers, V. K. Aggarwal, *Science* **2017**, *357*, 283.
- [56] Y. Han, Y. Jin, M. Jiang, H. Yang, H. Fu, *Org. Lett.* **2019**, *21*, 1799.
- [57] Leading review on photocascade catalysis: J.-R. Chen, D.-M. Yan, Q. Wei, W.-J. Xiao, *ChemPhotoChem* **2017**, *1*, 148.
- [58] a) D. Chandrasekhar, S. Borra, J. B. Nanubolu, R. A. Maurya, *Org. Lett.* **2016**, *18*, 2974; b) A. Hossain, S. Pagire, O. Reiser, *Synlett* **2017**, *28*, 1707; c) S. Borra, D. Chandrasekhar, S. Adhikary, S. Rasala, S. Gokulnath, R. A. Maurya, *J. Org. Chem.* **2017**, *82*, 2249.
- [59] S. Zhu, A. Das, L. Bui, H. Zhou, D. P. Curran, M. Rueping, *J. Am. Chem. Soc.* **2013**, *135*, 1823.
- [60] G. Pandey, D. Jadhav, S. K. Tiwari, B. Singh, *Adv. Synth. Catal.* **2014**, *356*, 2813.
- [61] J. Xuan, X.-D. Xia, T.-T. Zeng, Z.-J. Feng, J.-R. Chen, L.-Q. Lu, W.-J. Xiao, *Angew. Chem. Int. Ed.* **2014**, *53*, 5653.
- [62] J. B. Metternich, R. Gilmour, *J. Am. Chem. Soc.* **2016**, *138*, 1040.
- [63] S. K. Pagire, P. Kreitmeier, O. Reiser, *Angew. Chem. Int. Ed.* **2017**, *56*, 10928.





# *Chapter 2*



## Synthesis of Substituted Pyrazines from Vinyl Azides via a Photocascade Process

### Abstract:

A visible-light mediated photocatalyzed method for the synthesis of substituted pyrazines from vinyl azides has been developed. This method utilizes a dual energy and electron transfer strategy from the photoexcited catalyst. Initially, vinyl azides are activated by a triplet sensitization process from an excited ruthenium-photocatalyst in the presence of water to form dihydropyrazines, followed by a single electron transfer (SET) process under oxygen (air) atmosphere that ultimately leads to the tetrasubstituted pyrazines in good to excellent yields. This method has broad substrate scope and does not require any additives, moreover, it operates at room temperature which is also advantageous in terms of handling azides.

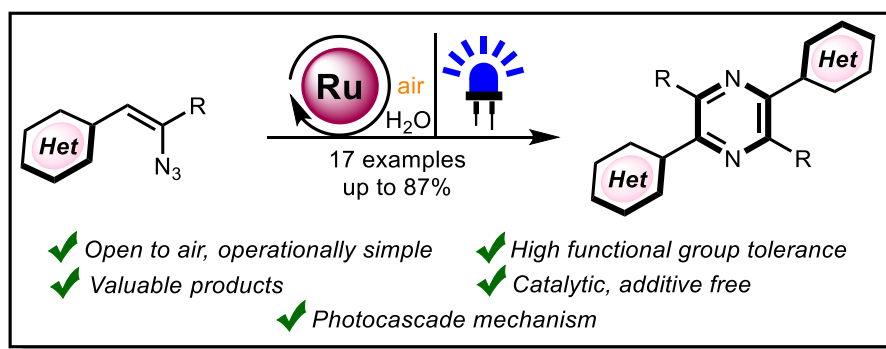


**Figure 1:** Synthesis of pyrazines from vinyl azides.

### Introduction:

Now-a-days, visible-light photocatalysis has gained significant attention for achieving challenging organic transformations.<sup>[1,2]</sup> It has also become an alternative tool to generate radicals in an environmentally benign way. Generally, the photoexcited catalysts activate the colourless organic substrate either by direct energy transfer (ET)<sup>[3,4]</sup> or by single-electron-transfer (SET)<sup>[5]</sup> processes and the respective reactive intermediates participate in non-

### This chapter has been published:

**A. Hossain**, S. K. Pagire, O. Reiser

*Synlett*, **2017**, 28, 1707-1714. (This article is a part of *Heterocycles: Special Issue*, IHSC Conference held in Regensburg, Germany (September 2017).

A.H. and S.K.P. wrote the manuscript.

traditional reaction pathways. By the independent use of these two activation modes, a number of synthetic transformations have been developed by various research groups.<sup>[6,7]</sup> However, the utilization of energy transfer followed by electron transfer modes or vice versa aiming at a photocascade processes is not well established.<sup>[8]</sup> The first example of such dual activation was reported by Xiao and co-workers<sup>[9]</sup> in the reaction between vinyl azides and alkynes to obtain poly-substituted pyrroles. Similarly, Reiser and co-workers<sup>[10]</sup> have also combined ET and SET-based pathways for the activation of vinyl bromides in the presence of oxygen. In the present study, we report the visible-light photocatalyzed transformation of vinyl-azides into 1,4-pyrazines by employing a single photocatalyst which works in different reaction modes in a cascade manner.<sup>[11]</sup> Pyrazines are an important nitrogen containing heterocycles which have interesting biological activities and great utility as precursors in organic synthesis.<sup>[12,13,14]</sup> For an example, the synthesis of Dragmacidin A<sup>[14]</sup> and 2,5-bis(6'-bromo-3'-indolyl)piperazine<sup>[13]</sup> (Figure 2) are achieved from the corresponding symmetrical pyrazines as key intermediates.<sup>[15]</sup> These are a class of compounds that occur almost ubiquitously in nature. The worldwide distribution of pyrazines in plants, insects, terrestrial vertebrates, marine organisms, fungi and bacteria and their specific properties including their using as drugs, fungicides and herbicides invite reasonable attention for their efficient synthesis.

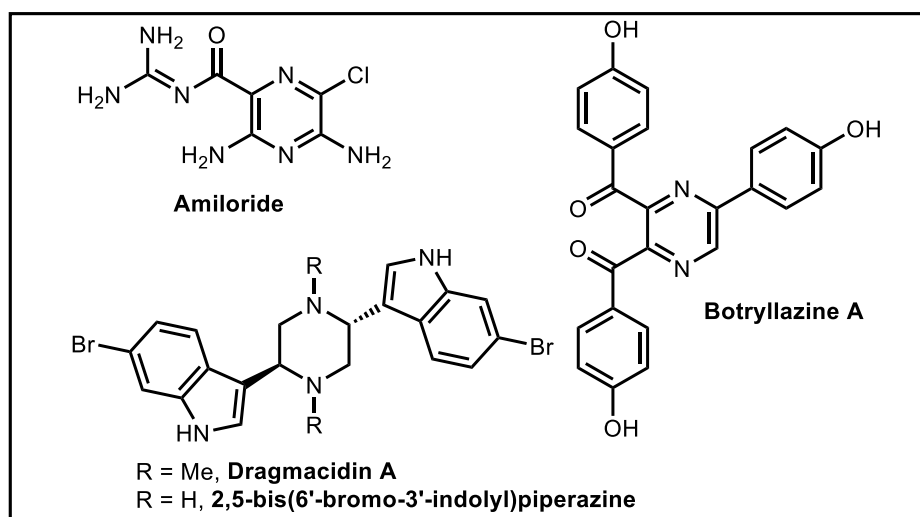


**Figure 2:** Selected biologically active pyrazine derivatives.

Various methods have been developed for the synthesis of pyrazines,<sup>[16]</sup> however, their synthesis from vinyl azides by thermal<sup>[17–20]</sup> or photochemical<sup>[21–24]</sup> approaches is not well-explored although these are well-known precursors for the synthesis of *N*-containing

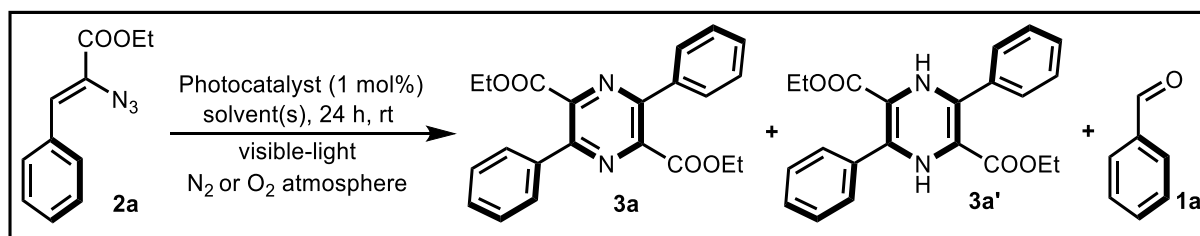


heterocycles such as phenanthridines,<sup>[25]</sup> indoles,<sup>[17–20]</sup> pyridines,<sup>[26]</sup> pyrroles,<sup>[21–24]</sup> and isoquinolines<sup>[27]</sup> for decades.<sup>[28]</sup> Recently, Yoon and co-workers<sup>[3]</sup> reported the photocatalytic, visible-light sensitization of dienylazides to azirines as key intermediates, which further rearrange to substituted pyrroles. We questioned if we could fill the gap, by developing a method for the synthesis of pyrazines and in this chapter the results have been discussed.

## Results and discussions:

We began our studies by exposing vinyl azide **2a**, being readily available from the corresponding ethyl cinnamate to blue light ( $\lambda_{max} = 455$  nm) employing 1 mol% of commonly used<sup>[1]</sup> iridium, ruthenium, copper<sup>[29]</sup> and organic dye-based<sup>[30]</sup> photocatalysts. Using  $[\text{Ir}(\text{dF}(\text{CF}_3)\text{ppy})_2(\text{dtbbpy})]\text{PF}_6$  ( $E_{\text{Ir(IV)/Ir(III)}^*} = -0.89$  V vs. SCE;  $T = 2300$  ns; dF = difluoro, ppy = 2-phenylpyridine, dtbbpy = 4,4'-di-*tert*-butyl-2,2'-dipyridyl) in a degassed acetonitrile-water (4:1) mixture at room temperature, we were pleased to observe the formation of a mixture of dihydro-pyrazine **3a'** and the desired pyrazine **3a** (**3a'**:**3a** = 6:1) in an overall isolated yield of 85% after 24 h (Table 1, entry 1). Similarly, other known photocatalysts such as *fac*- $[\text{Ir}(\text{ppy})_3]$  ( $E_{\text{Ir(IV)/Ir(III)}^*} = -1.73$  V vs. SCE;  $T = 1900$  ns; ppy = 2-phenylpyridine),  $[\text{Ir}(\text{dtbbpy})(\text{ppy})_2]\text{PF}_6$  ( $E_{\text{Ir(IV)/Ir(III)}^*} = -0.96$  V vs. SCE;  $T = 557$  ns; ppy = 2-phenylpyridine,

**Table 1: Reaction Optimization**



Entry	Photocatalyst	Solvent(s)	Under inert atmosphere		
			Yield <sup>a</sup> <b>3a</b>	Yield <sup>a</sup> <b>3a'</b>	Yield <sup>b</sup> <b>1a</b>
1	$[\text{Ir}(\text{dF}(\text{CF}_3)\text{ppy})_2(\text{dtbbpy})]\text{PF}_6$	$\text{CH}_3\text{CN}:\text{H}_2\text{O}$ (4:1)	12	73	-
2	<i>fac</i> - $[\text{Ir}(\text{ppy})_3]$	$\text{CH}_3\text{CN}:\text{H}_2\text{O}$ (4:1)	10	67	-
3	$[\text{Ir}(\text{dtbbpy})(\text{ppy})_2]\text{PF}_6$	$\text{CH}_3\text{CN}:\text{H}_2\text{O}$ (4:1)	11	69	-
4	$[\text{Ru}(\text{bpy})_3]\text{Cl}_2$	$\text{CH}_3\text{CN}:\text{H}_2\text{O}$ (4:1)	9	70	-
5 <sup>c</sup>	$[\text{Cu}(\text{dap})_2]\text{Cl}$	$\text{CH}_3\text{CN}:\text{H}_2\text{O}$ (4:1)	NR	-	-
6 <sup>c</sup>	$\text{Na}_2$ -Eosin Y	$\text{CH}_3\text{CN}:\text{H}_2\text{O}$ (4:1)			-

## Chapter 2: Synthesis of Pyrazines

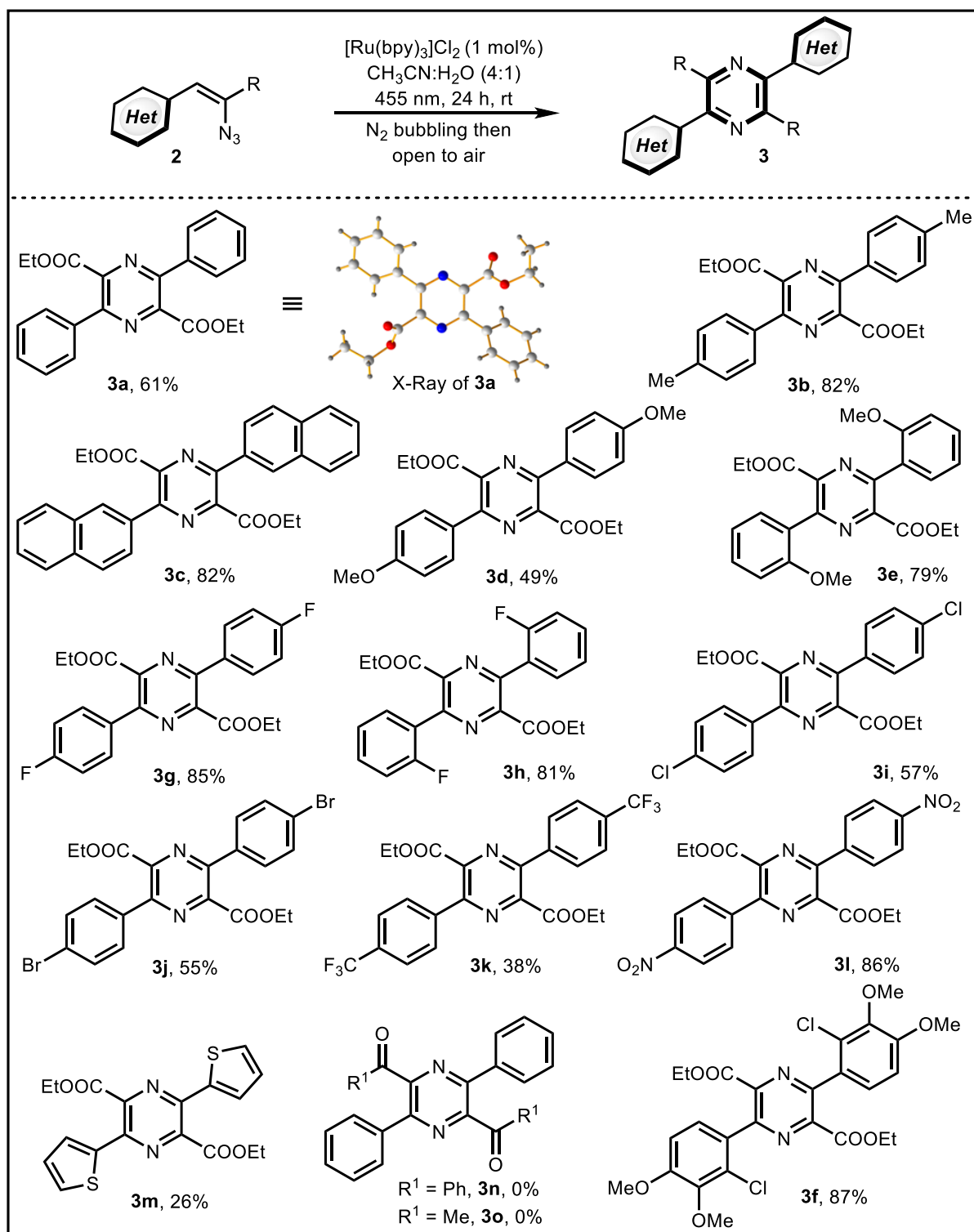
7	None	CH <sub>3</sub> CN:H <sub>2</sub> O (4:1)	trace	13	-
8 <sup>d</sup>	[Ru(bpy) <sub>3</sub> ]Cl <sub>2</sub>	CH <sub>3</sub> CN:H <sub>2</sub> O (4:1)	NR	-	-
9	[Ru(bpy) <sub>3</sub> ]Cl <sub>2</sub>	Dry CH <sub>3</sub> CN	ND	-	-
<i>Under aerobic atmosphere</i>					
10	[Ru(bpy) <sub>3</sub> ]Cl <sub>2</sub>	CH <sub>3</sub> CN:H <sub>2</sub> O (4:1)	61	-	15
11	<i>fac</i> -[Ir(ppy) <sub>3</sub> ]	CH <sub>3</sub> CN:H <sub>2</sub> O (4:1)	53	-	23
12	[Ir(dtbbpy)(ppy) <sub>2</sub> ]PF <sub>6</sub>	CH <sub>3</sub> CN:H <sub>2</sub> O (4:1)	40	-	35
13	[Ir(dF(CF <sub>3</sub> )ppy) <sub>2</sub> (dtbbpy)]PF <sub>6</sub>	CH <sub>3</sub> CN:H <sub>2</sub> O (4:1)	5	-	65
14 <sup>c</sup>	Na <sub>2</sub> -Eosin Y	CH <sub>3</sub> CN:H <sub>2</sub> O (4:1)	42	-	36
15	[Ru(bpy) <sub>3</sub> ]Cl <sub>2</sub>	CH <sub>3</sub> CN:CH <sub>3</sub> OH (4:1)	ND	-	-
16 <sup>e</sup>	[Ru(bpy) <sub>3</sub> ]Cl <sub>2</sub>	CH <sub>3</sub> CN:H <sub>2</sub> O (4:1)	34	-	45
17	[Ru(bpy) <sub>3</sub> ]Cl <sub>2</sub>	CH <sub>3</sub> CN:H <sub>2</sub> O (1:1)	57	-	30
18	[Ru(bpy) <sub>3</sub> ]Cl <sub>2</sub>	CH <sub>3</sub> CN:H <sub>2</sub> O (1:4)	trace	-	-
19	[Ru(bpy) <sub>3</sub> ]Cl <sub>2</sub>	CH <sub>3</sub> CN:H <sub>2</sub> O (6:1)	48	-	27
20	[Ru(bpy) <sub>3</sub> ]Cl <sub>2</sub>	DMF:H <sub>2</sub> O (4:1)	39	-	17
21	[Ru(bpy) <sub>3</sub> ]Cl <sub>2</sub>	DMSO:H <sub>2</sub> O (4:1)	trace	-	-
22	[Ru(bpy) <sub>3</sub> ]Cl <sub>2</sub>	CHCl <sub>3</sub> :H <sub>2</sub> O (4:1)	ND	-	-
23 <sup>f</sup>	[Ru(bpy) <sub>3</sub> ]Cl <sub>2</sub>	CH <sub>3</sub> CN:H <sub>2</sub> O (4:1)	51	-	18
24 <sup>g</sup>	[Ru(bpy) <sub>3</sub> ]Cl <sub>2</sub>	CH <sub>3</sub> CN:H <sub>2</sub> O (4:1)	60	-	18
25 <sup>h</sup>	[Ru(bpy) <sub>3</sub> ]Cl <sub>2</sub>	CH <sub>3</sub> CN:H <sub>2</sub> O (4:1)	ND	-	-

**Reaction conditions:** All reactions were performed in 0.5 mmol scale. **2a** (0.50 mmol, 1 equiv), photocatalyst (1 mol%) in 2 mL solvent mixture for 24 h under visible-light irradiation ( $\lambda_{max} = 455$  nm; unless otherwise noted) at room temperature. <sup>a</sup>Isolated yields. <sup>b</sup><sup>1</sup>H NMR yields of the crude reaction mixture using internal standard. <sup>c</sup>530 nm LED has been used for irradiation. <sup>d</sup>Dark reaction. <sup>e</sup>Oxygen balloon has been used. <sup>f</sup>In presence 0.5 mol% catalyst instead of 1 mol%. <sup>g</sup>In presence of 2 mol% catalyst. <sup>h</sup>In presence of additives (1 equiv) such as trifluoroacetic acid, K<sub>2</sub>S<sub>2</sub>O<sub>8</sub> and Na<sub>2</sub>CO<sub>3</sub> respectively.

dtbbpy = 4,4'-di-*tert*-butyl-2,2'-dipyridyl), [Ru(bpy)<sub>3</sub>]Cl<sub>2</sub> ( $E_{Ru(III)/Ru(II)^*} = -0.81$  V vs. SCE;  $T = 1100$  ns; bpy = 2,2'-bipyridine), Na<sub>2</sub>-Eosin Y ( $E_{EY^+/EY^*} = -1.11$  V vs. SCE,  $T = 24000$  ns), also provide comparable yields of **3a'** and **3a** (Table 1, entries 2-4, 6). Not surprisingly, [Cu(dap)<sub>2</sub>]Cl ( $E_{Cu(II)/Cu(I)^*} = -1.43$  V vs. SCE;  $T = 270$  ns; dap = 2,9-bis(*p*-anisyl)-1,10-phenanthroline, Table 1, entry 5) did not promote the transformation. This might be due to the

very low excited state lifetime ( $T = 270$  ns) of  $[\text{Cu}(\text{dap})_2]\text{Cl}$  which does not allow the efficient energy transfer from photoexcited state  $\text{Cu}(\text{I})^*$  to the substrate and makes at the same time the photocatalytic activation of the vinyl azides by electron transfer unlikely, given the high efficiency of SET triggered Atom Transfer Radical Addition (ATRA) reactions by  $[\text{Cu}(\text{dap})_2]\text{Cl}$ .<sup>[7,31]</sup> Finally, a series of control experiments (Table 1, entries 7-9), indicated the necessity of light, photocatalyst, and water in order to achieve complete conversion of **2a**. Aiming at an operationally simple procedure towards pyrazines **3**, we started looking for a suitable oxidant for the dehydrogenation of dihydropyrazines **3'**. At first, we thought oxygen would be sufficient to oxidize **3a'** to form **3a**. Indeed, carrying out the photoreaction of **2a** under oxygen atmosphere (open to air), thus utilizing oxygen as the terminal oxidant,<sup>[32]</sup> and employing 1 mol%  $[\text{Ru}(\text{bpy})_3]\text{Cl}_2$  gave rise to the desired product **3a** in 61% yield (Table 1, entry 10) along with 15% benzaldehyde **1a** as a byproduct. In contrast, Ir-photocatalysts (entries 11-13) or  $\text{Na}_2$ -Eosin Y (1 mol%, entry 14) provided **3a** in lower amounts. However, the undesired benzaldehyde was obtained in larger quantities. In line with our mechanistic proposal (Figure 3a), the addition of MeOH instead of water does not provide the desired product (Table 1, entry 15). Moreover, the use of an oxygen balloon (excess of oxygen) decreases the yield to 34% and the undesired benzaldehyde is obtained in a major amount (Table 1, entry 16). Reducing or increasing the amount of water resulted in inferior yields (Table 1, entries 17-19). Even varying the organic solvents such as DMF, DMSO or chloroform did not increase the yield of the desired product (Table 1, entries 20-22). Further optimization studies revealed that the addition of other oxidant such as  $\text{K}_2\text{S}_2\text{O}_8$  does not provide any product (entry 25), indicating the importance of oxygen. Other additives such as  $\text{Na}_2\text{CO}_3$  or trifluoroacetic acid, which were assumed to promote the opening of the azirine intermediate (Figure 3a), also have negative effect on the reaction (entry 25) and gave complex mixtures.

Employing the optimized reaction conditions (Table 1, entry 10) we started exploring the scope of this reaction. Before that, we slightly modified the protocol by simply degassing the reaction mixture via nitrogen bubbling, but then running the reaction open to air. In many cases *e.g.* **2e**, we have observed significant increase in the desired product yield of **3e** (from 52% to 79% (Scheme 1)). Many different functional groups on the aryl moiety of the vinyl azides **2** are tolerated well, including weak and strong electron donating and withdrawing groups, *ortho*- and extended  $\pi$ -substituents, providing good yields of the homodimerized products **3** (Scheme 1). Structure of **3a** was also confirmed by x-ray analysis. Most of the synthesized products are crystalline solids and no chromatographic separation were required. Only in a few cases the

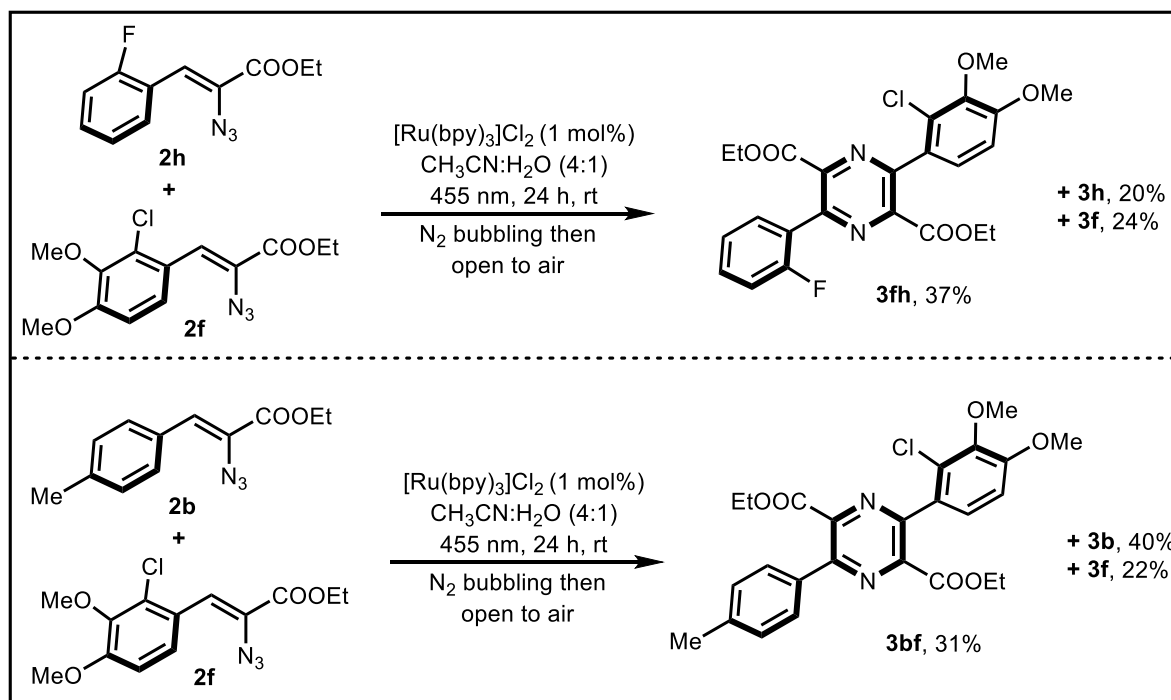


**Scheme 1: Scope of the reaction.** Reaction conditions: Vinyl azide **2** (0.50 mmol),  $[Ru(bpy)_3]Cl_2$  (1 mol%) in 2 mL  $CH_3CN:H_2O$  (4:1) at room temperature in presence of visible-light (455 nm LED) for 24 h. Isolated yields are given.

aldehyde byproducts (**1a** (15%) and **1d** (18%)) were obtained in significant amounts. It should be noted that all our attempts to separate the two reaction steps, *i.e.* running the transformation

of **2a/d** to **3a/d'** under nitrogen atmosphere, followed by irradiation of **3a/d'** under aerobic atmosphere did not suppress the formation of **1a** or **1d**. Switching the aryl group to heterocycle such as thiophene (**3m**) was met with only limited success, and surprisingly, the replacement of the ester moiety by  $-\text{COCH}_3$ ,  $-\text{COPh}$  groups did not result in any product formation (**3n** and **3o**).

### Crossover experiments: Access to unsymmetrical pyrazines:



**Scheme 2: Reaction conditions:** each substrate **2** 0.25 mmol. Isolated yields are provided.

Moreover, the union of two different vinyl azides in equimolar amounts (Scheme 2) is possible. Statistical distribution of product yields was expected. However, the self-coupled- and crossover products are all formed with a slight preference for the sterically less encumbered pyrazines. Hence, this method allows to accessing unsymmetrical pyrazines from vinyl azides only in moderate yields.

### Proposed reaction mechanism:

Following the mechanistic rationale put forward by Yoon and co-workers<sup>[3]</sup> for the photochemical activation of dienylazides to form substituted pyrroles, the reaction sequence to 1,4-pyrazines developed here starts with an energy transfer from the photoexcited  $\text{Ru}(\text{II})^*$  to substrate **2a** (Figure 3a). As a result, **2a** is converted to the triplet energy state **I**, which immediately loses nitrogen to form a highly reactive nitrene intermediate **II** that further

undergoes rearrangement to the reactive azirine **III**. This azirine **III** may undergo ring-opening by water, leading to the formation of  $\alpha$ -amino ketone **IV**. **IV** is very prone to undergo dimerization because this intermediate has an activated carbonyl functionality with an intramolecular nucleophile (amino) present. The condensation of **IV** to form dihydropyrazine<sup>[33]</sup> species **3a'** concludes the first transformation of the process.

The sensitization process *i.e.* the formation of **3'** from **2** is considerably faster (approximately, 3 h) under the reaction conditions employed then the subsequent oxidation of **3'** to **3** takes a bit longer (21 h). In line with control (light-on/off) experiments (Figure 3b), nevertheless, the

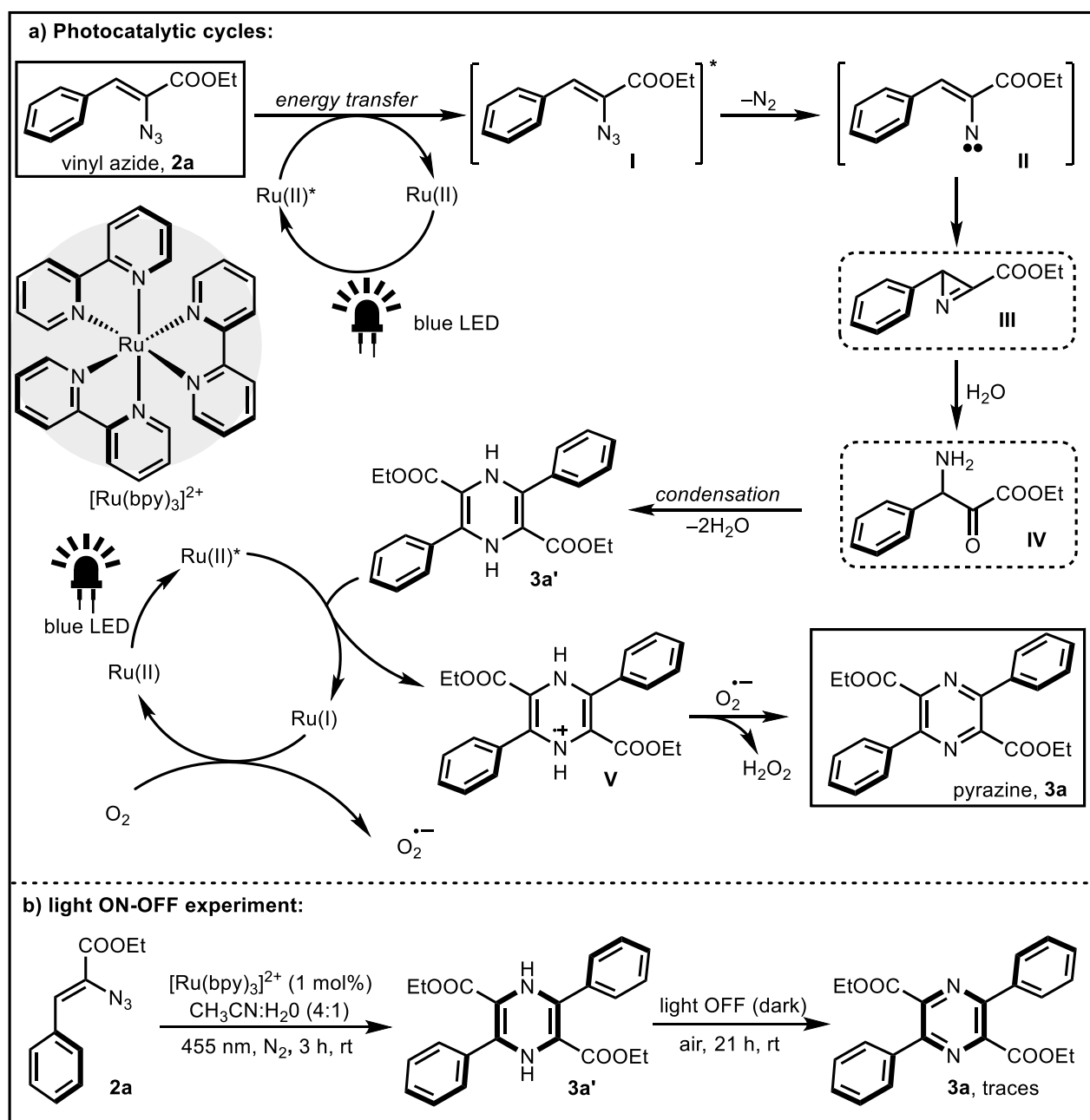


Figure 3: a) Proposed photocascade mechanism; b) mechanistic experiment

second step should also be a photocatalytic one, *i.e.* being initiated by excited state Ru(II)\* that may reductively quench **3a'** acting as an electron donor. This results in the generation of Ru(I) and the *N*-centered radical cation **V**, which can be oxidized by superoxide anion radical O<sub>2</sub><sup>•-</sup>, being in turn generated from Ru(I) and molecular oxygen.

### Conclusions:

To summarize, we have developed a visible-light photocatalyzed cascade to 1,4-pyrazines from the corresponding vinyl azides by combining energy and electron transfer initiated reaction steps operated by the same photocatalyst.

### References:

- [1] C. K. Prier, D. A. Rankic, D. W. C. MacMillan, *Chem. Rev.* **2013**, *113*, 5322.
- [2] a) K. Zeitler, *Angew. Chem. Int. Ed.* **2009**, *48*, 9785; b) M. H. Shaw, J. Twilton, D. W. C. MacMillan, *J. Org. Chem.* **2016**, *81*, 6898; c) J. C. Tellis, C. B. Kelly, D. N. Primer, M. Jouffroy, N. R. Patel, G. A. Molander, *Acc. Chem. Res.* **2016**, *49*, 1429; d) M. N. Hopkinson, A. Tlahuext-Aca, F. Glorius, *Acc. Chem. Res.* **2016**, *49*, 2261; e) K. L. Skubi, T. R. Blum, T. P. Yoon, *Chem. Rev.* **2016**, *116*, 10035; f) M. Majek, A. Jacobi von Wangelin, *Acc. Chem. Res.* **2016**, *49*, 2316; g) J. M. R. Narayanam, C. R. J. Stephenson, *Chem. Soc. Rev.* **2011**, *40*, 102.
- [3] E. P. Farney, T. P. Yoon, *Angew. Chem. Int. Ed.* **2014**, *53*, 793.
- [4] a) D. R. Heitz, J. C. Tellis, G. A. Molander, *J. Am. Chem. Soc.* **2016**, *138*, 12715; b) E. Brachet, T. Ghosh, I. Ghosh, B. König, *Chem. Sci.* **2015**, *6*, 987; c) E. R. Welin, C. Le, D. M. Arias-Rotondo, J. K. McCusker, D. W. C. MacMillan, *Science*. **2017**, *355*, 380; d) Z. Lu, T. P. Yoon, *Angew. Chem. Int. Ed.* **2012**, *51*, 10329.
- [5] a) P. Zhang, T. Xiao, S. Xiong, X. Dong, L. Zhou, *Org. Lett.* **2014**, *16*, 3264; b) D. Lenhart, A. Bauer, A. Pöthig, T. Bach, *Chem. Eur. J.* **2016**, *22*, 6519; c) G. Pandey, R. Laha, D. Singh, *J. Org. Chem.* **2016**, *81*, 7161; d) I. Ghosh, B. König, *Angew. Chem. Int. Ed.* **2016**, *55*, 7676; e) D. B. Bagal, G. Kachkovskiy, M. Knorn, T. Rawner, B. M. Bhanage, O. Reiser, *Angew. Chem. Int. Ed.* **2015**, *54*, 6999.
- [6] a) C. A. Huff, R. D. Cohen, K. D. Dykstra, E. Streckfuss, D. A. DiRocco, S. W. Krska, *J. Org. Chem.* **2016**, *81*, 6980; b) Z. Sun, N. Kumagai, M. Shibasaki, *Org. Lett.* **2017**, *19*, 3727; c) X.-z. Shu, M. Zhang, Y. He, H. Frei, F. D. Toste, *J. Am. Chem. Soc.* **2014**, *136*, 5844; d) A. J. Perkowski, C. L. Cruz, D. A. Nicewicz, *J. Am. Chem. Soc.* **2015**, *137*, 15684; e) J. J. Murphy, D. Bastida, S. Paria, M. Fagnoni, P. Melchiorre, *Nature* **2016**, *532*, 218; f)

- S. Paria, O. Reiser, *Adv. Synth. Catal.* **2014**, 356, 557; g) S. K. Pagire, O. Reiser, *Green. Chem.* **2017**, 19, 1721; h) S. K. Pagire, S. Paria, O. Reiser, *Org. Lett.* **2016**, 18, 2106; i) P. Kohls, D. Jadhav, G. Pandey, O. Reiser, *Org. Lett.* **2012**, 14, 672; j) G. Kachkovskiy, C. Faderl, O. Reiser, *Adv. Synth. Catal.* **2013**, 355, 2240.
- [7] S. Paria, O. Reiser, *ChemCatChem* **2014**, 6, 2477.
- [8] a) J. B. Metternich, R. Gilmour, *J. Am. Chem. Soc.* **2016**, 138, 1040; b) J.-R. Chen, D.-M. Yan, Q. Wei, W.-J. Xiao, *ChemPhotoChem* **2017**, 1, 148; c) D. Chandrasekhar, S. Borra, J. B. Nanubolu, R. A. Maurya, *Org. Lett.* **2016**, 18, 2974; d) S. Borra, D. Chandrasekhar, S. Adhikary, S. Rasala, S. Gokulnath, R. A. Maurya, *J. Org. Chem.* **2017**, 82, 2249.
- [9] J. Xuan, X.-D. Xia, T.-T. Zeng, Z.-J. Feng, J.-R. Chen, L.-Q. Lu, W.-J. Xiao, *Angew. Chem. Int. Ed.* **2014**, 53, 5653.
- [10] S. K. Pagire, P. Kreitmeier, O. Reiser, *Angew. Chem. Int. Ed.* **2017**, 56, 10928.
- [11] A. Hossain, S. Pagire, O. Reiser, *Synlett* **2017**, 28, 1707.
- [12] a) J. Loffing, B. Kaissling, *Am. J. Physiol. Renal physiology* **2003**, 284, F628-43; b) J.-F. Cavalier, M. Burton, F. Dussart, C. Marchand, J.-F. Rees, J. Marchand-Brynaert, *Bioorg. Med. Chem.* **2001**, 9, 1037; c) P. Miniyar, P. Murumkar, P. Patil, M. Barmade, K. Bothara, *Mini. Rev. Med. Chem.* **2013**, 13, 1607.
- [13] E. Fahy, B. C. M. Potts, D. J. Faulkner, K. Smith, *J. Nat. Prod.* **1991**, 54, 564.
- [14] S. A. Morris, R. J. Andersen, *Tetrahedron.* **1990**, 46, 715.
- [15] F. Y. Miyake, K. Yakushijin, D. A. Horne, *Org. Lett.* **2000**, 2, 3185.
- [16] a) K. Wu, Z. Huang, X. Qi, Y. L. G. Z. C. Liu, H. Yi, L. Meng, E. E. Bunel, J. T. Miller et al., *Sci. Adv.* **2015**, 1, e1500656; b) N. S. Y. Loy, S. Kim, C.-M. Park, *Org. Lett.* **2015**, 17, 395; c) T. Ryu, Y. Baek, P. H. Lee, *J. Org. Chem.* **2015**, 80, 2376; d) S. G. Modha, J. C. Trivedi, V. P. Mehta, D. S. Ermolat'ev, E. V. van der Eycken, *J. Org. Chem.* **2011**, 76, 846; e) R. P. Pandit, S. H. Kim, Y. R. Lee, *Adv. Synth. Catal.* **2016**, 358, 3586; f) K. K. D. R. Viswanadham, M. Prathap Reddy, P. Sathyanarayana, O. Ravi, R. Kant, S. R. Bathula, *Chem. Commun.* **2014**, 50, 13517; g) B. Gnanaprakasam, E. Balaraman, Y. Ben-David, D. Milstein, *Angew. Chem. Int. Ed.* **2011**, 50, 12240; h) D. Aparicio, O. A. Attanasi, P. Filippone, R. Ignacio, S. Lillini, F. Mantellini, F. Palacios, J. M. de Los Santos, *J. Org. Chem.* **2006**, 71, 5897; i) F. Palacios, Ochoa de Retana, Ana Maria, J. I. Gil, R. Lopez de Munain, *Org. Lett.* **2002**, 4, 2405.
- [17] B. J. Stokes, H. Dong, B. E. Leslie, A. L. Pumphrey, T. G. Driver, *J. Am. Chem. Soc.* **2007**, 129, 7500.
- [18] J. Bonnamour, C. Bolm, *Org. Lett.* **2011**, 13, 2012.



- [19] D. Hong, Z. Chen, X. Lin, Y. Wang, *Org. Lett.* **2010**, *12*, 4608.
- [20] Y. Zhang, S. Liu, W. Yu, M. Hu, G. Zhang, Y. Yu, *Tetrahedron*. **2013**, *69*, 2070.
- [21] F. Chen, T. Shen, Y. Cui, N. Jiao, *Org. Lett.* **2012**, *14*, 4926.
- [22] S. Chiba, Y.-F. Wang, G. Lapointe, K. Narasaka, *Org. Lett.* **2008**, *10*, 313.
- [23] Y.-F. Wang, K. K. Toh, S. Chiba, K. Narasaka, *Org. Lett.* **2008**, *10*, 5019.
- [24] R. Suresh, S. Muthusubramanian, M. Nagaraj, G. Manickam, *Tetrahedron Lett.* **2013**, *54*, 1779.
- [25] X. Sun, S. Yu, *Chem. Commun.* **2016**, *52*, 10898.
- [26] a) Y.-F. Wang, S. Chiba, *J. Am. Chem. Soc.* **2009**, *131*, 12570; b) Z.-B. Chen, D. Hong, Y.-G. Wang, *J. Org. Chem.* **2009**, *74*, 903.
- [27] a) Y.-F. Wang, K. K. Toh, J.-Y. Lee, S. Chiba, *Angew. Chem. Int. Ed.* **2011**, *50*, 5927; b) Y.-Y. Yang, W.-G. Shou, Z.-B. Chen, D. Hong, Y.-G. Wang, *J. Org. Chem.* **2008**, *73*, 3928.
- [28] a) T. G. Driver, *Org. Biomol. Chem.* **2010**, *8*, 3831; b) B. Hu, S. G. DiMagno, *Org. Biomol. Chem.* **2015**, *13*, 3844.
- [29] O. Reiser, *Acc. Chem. Res.* **2016**, *49*, 1990.
- [30] D. P. Hari, B. König, *Chem. Commun.* **2014**, *50*, 6688.
- [31] a) T. Rawner, M. Knorn, E. Lutsker, A. Hossain, O. Reiser, *J. Org. Chem.* **2016**, *81*, 7139; b) M. Pirtsch, S. Paria, T. Matsuno, H. Isobe, O. Reiser, *Chem. Eur. J.* **2012**, *18*, 7336.
- [32] Z. Lu, Y.-Q. Yang, H.-X. Li, *Synthesis* **2016**, *48*, 4221.
- [33] a) K. Banert, B. Meier, *Angew. Chem. Int. Ed.* **2006**, *45*, 4015; b) D. Knittel, *Synthesis* **1985**, 186; c) H. E. Smith, A. A. Hicks, *J. Org. Chem.* **1971**, *36*, 3659.

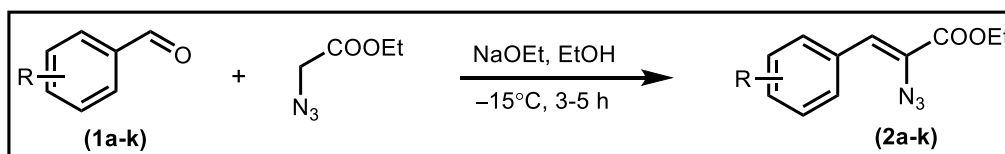
### General information:

The irradiation was done using blue light emitting diodes CREE XP or Oslon SSL (2.5 W electric power @700 mA,  $\lambda_{\max} = 455$  nm). All the reactions were monitored by TLC and visualized by a dual short/long wave UV lamp. Analytical thin layer chromatography was performed on Merck TLC aluminium sheets silica gel 60 F 254. Purifications by column chromatography were performed on silica gel (0.063 - 0.200 mm). All products were characterized by appropriate techniques such as  $^1\text{H-NMR}$ ,  $^{19}\text{F-NMR}$ ,  $^{13}\text{C-NMR}$ , FT-IR and HRMS analysis. NMR spectra were recorded on Bruker Avance 300 and 400 MHz spectrometers. Chemical shifts for  $^1\text{H-NMR}$  were reported as  $\delta$ , parts per million (ppm), relative to the signal of  $\text{CHCl}_3$  at 7.26 ppm. Chemical shifts for  $^{13}\text{C-NMR}$  were reported as  $\delta$ , parts per million, relative to the signal of  $\text{CHCl}_3$  at 77.2 ppm and TMS as an internal standard. Coupling constants ( $J$ ) are given in Hertz (Hz). The following notations indicate the multiplicity of the signals: s = singlet, d = doublet, t = triplet, q = quartet, dd = doublet of doublets, and m = multiplet. FT-IR (Cary 630) spectroscopy was carried out on a spectrometer, equipped with a Diamond Single Reflection ATR-System. Mass spectra were recorded at the Central Analytical Laboratory at the Department of Chemistry of the University of Regensburg on Agilent Technologies 6540 UHD Accurate-Mass Q-TOF LC/MS.

### General Procedure for the synthesis of Vinyl azides:

#### General Procedure 1 (GP-1):

The required vinyl azides (except **2a**, **2n** and **2o**) were synthesized in one step from the condensation of ethyl azidoacetate and aromatic or heteroaromatic aldehydes following a literature known procedure<sup>1</sup>. The obtained yields are not optimized.

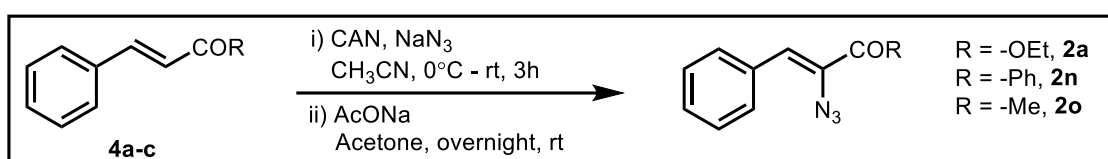


To a cooled ( $-15^\circ\text{C}$ ) solution of aldehyde **1** (1 equiv) and ethyl azidoacetate (2.5–4 equiv) in EtOH, freshly prepared NaOEt (2.5 equiv) was added dropwise via a cannula. The resulting reaction mixture was stirred at the same temperature. After 3-5 hours (judged by TLC analysis), the heterogeneous mixture was transferred to a separatory funnel containing saturated  $\text{NH}_4\text{Cl}$

(15 mL), 10 mL of water, and 20 mL of Et<sub>2</sub>O. The phases were separated and the resulting aqueous phase was extracted with an additional 2 × 20 mL of Et<sub>2</sub>O. The combined organic phases were washed with 2 × 20 mL of distilled water and 1 × 20 mL of brine solution. The resulting organic phase was dried over MgSO<sub>4</sub> and the heterogeneous mixture was filtered. The filtrate was concentrated *in vacuo*. Purification by column chromatography (EtOAc: hexanes) afforded the desired vinyl azide **2**.

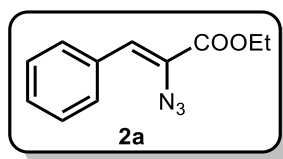
### General Procedure 2 (GP-2):

**2a**, **2n** and **2o** were synthesized following another known protocol.<sup>2</sup>



To a deoxygenated solution of cinnamic ester **4** (1 equiv) and NaN<sub>3</sub> (1.50 equiv.) in dry acetonitrile, a deoxygenated solution ceric ammonium nitrate (CAN) (2.50 equiv.) in the same solvent was added dropwise at 0°C and stirred well. On completion of the reaction, it was worked up using CH<sub>2</sub>Cl<sub>2</sub>-water, dried and concentrated. The crude residue, on treatment with anhydrous sodium acetate (1.50 equiv.) in dry acetone followed by usual work up and purification by silica gel column chromatography using hexane: ethyl acetate mixture as eluent, afforded **2**.

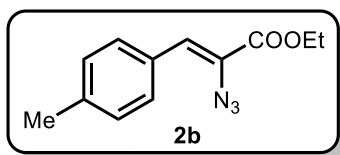
### Ethyl (Z)-2-azido-3-phenylacrylate (**2a**):



**GP-2** was followed using ethyl cinnamate **4a** (1.76 g, 10.00 mmol, 1.00 equiv.) and NaN<sub>3</sub> (975 mg, 15.00 mmol, 1.50 equiv) in 50 mL dry acetonitrile was added CAN (13.7 g, 25.00 mmol, 2.50 equiv.) in 100 mL dry Acetonitrile. After 3 h, the reaction mixture was quenched and the crude residue was treated with sodium acetate (1.23 g, 15.00 mmol, 1.50 equiv.) in 50 mL dry acetone for overnight at room temperature. After usual work up and purification by column chromatography (silica gel, hexanes:EtOAc-98:2, R<sub>f</sub> = 0.44) afforded **2a** as a pale yellow solid (1.34 g, 62%).

**<sup>1</sup>H-NMR (300 MHz, CDCl<sub>3</sub>):** δ 7.83 – 7.80 (m, 2H), 7.42 – 7.32 (m, 3H), 6.91 (s, 1H), 4.37 (q, *J* = 7.1 Hz, 2H), 1.40 (t, *J* = 7.1 Hz, 3H); **<sup>13</sup>C-NMR (75 MHz, CDCl<sub>3</sub>):** δ 163.7, 133.3, 130.7, 129.5, 128.6, 125.7, 125.4, 62.4, 14.3.

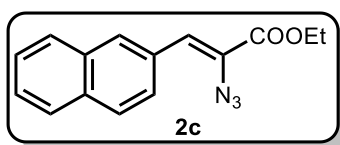
**Ethyl (Z)-2-azido-3-(p-tolyl)acrylate (2b):**



**GP-1** was followed using *p*-tolualdehyde (3.40 mmol, 1.00 equiv.), ethyl azidoacetate (1.40 g, 10.88 mmol, 3.20 equiv.) in 6 mL dry EtOH followed by addition of freshly prepared NaOEt (10.88 mmol, 3.20 equiv.) in 6 mL dry EtOH. After 3h, the reaction mixture was quenched and purification by column chromatography (silica gel, hexanes:EtOAc-9:1, *R<sub>f</sub>* = 0.53) afforded **2b** as a white solid (414 mg, 53%).

**<sup>1</sup>H-NMR (300 MHz, CDCl<sub>3</sub>):** δ 7.72 (d, *J* = 8.1 Hz, 2H), 7.19 (d, *J* = 8.0 Hz, 2H), 6.90 (s, 1H), 4.36 (q, *J* = 7.1 Hz, 2H), 2.37 (s, 3H), 1.39 (t, *J* = 7.1 Hz, 3H); **<sup>13</sup>C-NMR (75 MHz, CDCl<sub>3</sub>):**δ 163.8, 139.9, 130.7, 130.6, 129.4, 125.7, 124.8, 62.3, 21.6, 14.4.

**Ethyl (Z)-2-azido-3-(naphthalen-2-yl)acrylate (2c):**

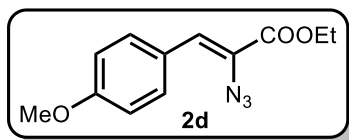


**GP-1** was followed using 2-naphthaldehyde (796.80 mg, 5.00 mmol, 1.00 equiv.), ethyl azidoacetate (1.93 g, 15.00 mmol, 3.00 equiv.) in 7 mL dry EtOH followed by addition of freshly prepared NaOEt (15.00 mmol, 3.00 equiv.) in 7 mL dry EtOH. After 4h, the reaction mixture was quenched and purification by column chromatography (silica gel, hexanes:EtOAc-9:1, *R<sub>f</sub>* = 0.44) afforded **2c** as a white solid (813 mg, 60%).

**<sup>1</sup>H-NMR (300 MHz, CDCl<sub>3</sub>):** δ 8.29 (s, 1H), 7.97 – 7.94 (m, 1H), 7.89 – 7.81 (m, 3H), 7.52 – 7.49 (m, 2H), 7.07 (s, 1H), 4.40 (q, *J* = 7.1 Hz, 2H), 1.43 (t, *J* = 7.1 Hz, 3H); **<sup>13</sup>C-NMR (75**

**MHz, CDCl<sub>3</sub>**):  $\delta$  163.7, 133.6, 133.2, 131.1, 130.9, 128.8, 128.1, 127.7, 127.5, 127.2, 126.5, 125.8, 125.4, 62.5, 14.4.

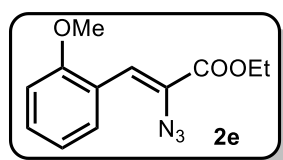
**Ethyl (Z)-2-azido-3-(4-methoxyphenyl)acrylate (2d):**



**GP-1** was followed using *p*-anisaldehyde (680.75 mg, 5.00 mmol, 1.00 equiv.), ethyl azidoacetate (1.61 g, 12.50 mmol, 2.50 equiv.) in 7 mL dry EtOH followed by addition of freshly prepared NaOEt (12.50 mmol, 2.50 equiv.) in 7 mL dry EtOH. After 4h, the reaction mixture was quenched and purification by column chromatography (silica gel, hexanes:EtOAc-9:1,  $R_f$  = 0.34) afforded **2d** as a pale yellow solid (692 mg, 56%).

**<sup>1</sup>H-NMR (300 MHz, CDCl<sub>3</sub>)**:  $\delta$  7.79 (d,  $J$  = 8.8 Hz, 2H), 6.90 (d,  $J$  = 8.9 Hz, 2H), 6.88 (s, 1H), 4.35 (q,  $J$  = 7.1 Hz, 2H), 3.84 (s, 3H), 1.39 (t,  $J$  = 7.1 Hz, 3H); **<sup>13</sup>C-NMR (75 MHz, CDCl<sub>3</sub>)**:  $\delta$  163.9, 160.6, 132.5, 126.2, 125.5, 123.4, 114.0, 62.2, 55.5, 14.4.

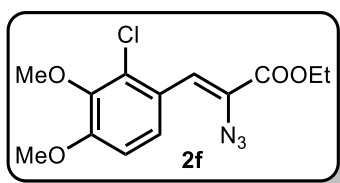
**Ethyl (Z)-2-azido-3-(2-methoxyphenyl)acrylate (2e):**



**GP-1** was followed using 2-methoxybenzaldehyde (680.75 mg, 5.00 mmol, 1.00 equiv.), ethyl azidoacetate (1.61 g, 12.50 mmol, 2.50 equiv.) in 7 mL dry EtOH followed by addition of freshly prepared NaOEt (12.50 mmol, 2.50 equiv.) in 7 mL dry EtOH. After 4h, the reaction mixture was quenched and purification by column chromatography (silica gel, hexanes:EtOAc-95:5,  $R_f$  = 0.25) afforded **2e** as a pale yellow solid (766 mg, 62%).

**<sup>1</sup>H-NMR (300 MHz, CDCl<sub>3</sub>)**:  $\delta$  8.18 (dd,  $J_1$  = 7.8 Hz,  $J_2$  = 1.5 Hz, 1H), 7.39 (s, 1H), 7.34 – 7.29 (m, 1H), 6.99 (t,  $J$  = 7.5 Hz, 1H), 6.88 (d,  $J$  = 8.2 Hz, 1H), 4.37 (q,  $J$  = 7.1 Hz, 2H), 3.86 (s, 3H), 1.40 (t,  $J$  = 7.1 Hz, 3H); **<sup>13</sup>C-NMR (75 MHz, CDCl<sub>3</sub>)**:  $\delta$  163.9, 157.6, 130.9, 130.6, 125.4, 122.2, 120.4, 119.5, 110.5, 62.2, 55.7, 14.3.

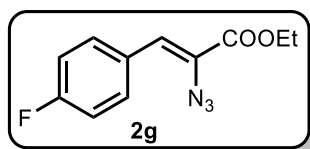
**Ethyl (Z)-2-azido-3-(2-chloro-3,4-dimethoxyphenyl)acrylate (2f):**



**GP-1** was followed using 2-chloro-3,4-dimethoxybenzaldehyde (1.00 g, 5.00 mmol, 1.00 equiv.), ethyl azidoacetate (1.61 g, 12.50 mmol, 2.50 equiv.) in 7 mL dry EtOH followed by addition of freshly prepared NaOEt (12.50 mmol, 2.50 equiv.) in 7 mL dry EtOH. After 4h, the reaction mixture was quenched and purification by column chromatography (silica gel, hexanes:EtOAc-95:5,  $R_f = 0.20$ ) afforded **2f** as a white solid (778 mg, 51%).

**$^1\text{H-NMR}$  (300 MHz,  $\text{CDCl}_3$ ):**  $\delta$  8.01 (d,  $J = 8.9$  Hz, 1H), 7.28 (s, 1H), 6.86 (d,  $J = 8.9$  Hz, 1H), 4.37 (q,  $J = 7.1$  Hz, 2H), 3.91 (s, 3H), 3.85 (s, 3H), 1.40 (t,  $J = 7.1$  Hz, 3H);  **$^{13}\text{C-NMR}$  (75 MHz,  $\text{CDCl}_3$ ):**  $\delta$  163.6, 154.3, 145.6, 129.7, 126.8, 125.8, 124.6, 120.8, 110.0, 62.5, 60.7, 56.2, 14.3.

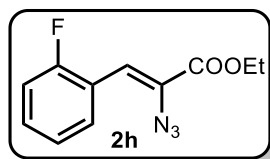
**Ethyl (Z)-2-azido-3-(4-fluorophenyl)acrylate (2g):**



**GP-1** was followed using 4-fluorobenzaldehyde (620.50 mg, 5.00 mmol, 1.00 equiv.), ethyl azidoacetate (1.61 g, 12.50 mmol, 2.50 equiv.) in 7 mL dry EtOH followed by addition of freshly prepared NaOEt (12.50 mmol, 2.50 equiv.) in 7 mL dry EtOH. After 4h, the reaction mixture was quenched and purification by column chromatography (silica gel, hexanes:EtOAc-95:5,  $R_f = 0.33$ ) afforded **2g** as yellow solid (771 mg, 64%).

**$^1\text{H-NMR}$  (300 MHz,  $\text{CDCl}_3$ ):**  $\delta$  7.84 – 7.80 (m, 2H), 7.09 – 7.40 (m, 2H), 6.88 (s, 1H), 4.37 (q,  $J = 7.1$  Hz, 2H), 1.39 (t,  $J = 7.1$  Hz);  **$^{13}\text{C-NMR}$  (75 MHz,  $\text{CDCl}_3$ ):**  $\delta$  163.6, 163.0 (d,  $^1J_{\text{C-F}} = 252.1$  Hz), 132.7 (d,  $^3J_{\text{C-F}} = 8.1$  Hz), 129.6 (d,  $^4J_{\text{C-F}} = 3.7$  Hz), 125.3, 124.1, 115.7 (d,  $^2J_{\text{C-F}} = 21.4$  Hz), 62.5, 14.3;  **$^{19}\text{F-NMR}$  (282 MHz,  $\text{CDCl}_3$ ):**  $\delta$  -110.4.

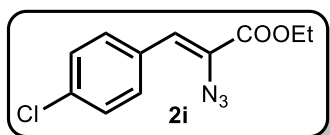
**Ethyl (Z)-2-azido-3-(2-fluorophenyl)acrylate (2h):**



**GP-1** was followed using 2-fluorobenzaldehyde (620.50 mg, 5.00 mmol, 1.00 equiv.), ethyl azidoacetate (1.61 g, 12.50 mmol, 2.50 equiv.) in 7 mL dry EtOH followed by addition of freshly prepared NaOEt (12.50 mmol, 2.50 equiv.) in 7 mL dry EtOH. After 4h, the reaction mixture was quenched and purification by column chromatography (silica gel, hexanes:EtOAc-9:1,  $R_f = 0.42$ ) afforded **2h** as yellow solid (733 mg, 62%).

**$^1\text{H-NMR}$  (300 MHz,  $\text{CDCl}_3$ ):**  $\delta$  8.27 (dt,  $J_1 = 7.7$  Hz,  $J_2 = 1.6$  Hz, 1H), 7.35 – 7.03 (m, 4H), 4.38 (q,  $J = 7.1$  Hz, 2H), 1.40 (t,  $J = 7.1$  Hz, 3H);  **$^{13}\text{C-NMR}$  (75 MHz,  $\text{CDCl}_3$ ):**  $\delta$  163.4, 160.8 (d,  $^1J_{\text{C-F}} = 252.7$  Hz), 131.0 (d,  $^3J_{\text{C-F}} = 8.8$  Hz), 130.8, 127.2, 124.1 (d,  $^4J_{\text{C-F}} = 3.6$  Hz), 121.4 (d,  $^2J_{\text{C-F}} = 11.0$  Hz), 116.0 (d,  $^3J_{\text{C-F}} = 8.0$  Hz), 115.4 (d,  $^2J_{\text{C-F}} = 22.1$  Hz), 62.6, 14.3;  **$^{19}\text{F-NMR}$  (282 MHz,  $\text{CDCl}_3$ ):**  $\delta$  -115.5.

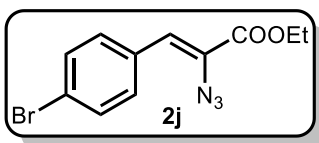
**Ethyl (Z)-2-azido-3-(4-chlorophenyl)acrylate (2i):**



**GP-1** was followed using 4-chlorobenzaldehyde (724.58 mg, 5.00 mmol, 1.00 equiv.), ethyl azidoacetate (1.90 g, 15.00 mmol, 3.00 equiv.) in 7 mL dry EtOH followed by addition of freshly prepared NaOEt (15.00 mmol, 3.00 equiv.) in 7 mL dry EtOH. After 4h, the reaction mixture was quenched and purification by column chromatography (silica gel, hexanes:EtOAc-95:5,  $R_f = 0.30$ ) afforded **2i** as white solid (895 mg, 69%).

**$^1\text{H-NMR}$  (300 MHz,  $\text{CDCl}_3$ ):**  $\delta$  7.78 – 7.73 (m, 2H), 7.36 – 7.32 (m, 2H), 6.84 (s, 1H), 4.37 (q,  $J = 7.1$  Hz, 2H), 1.39 (t,  $J = 7.1$  Hz, 3H);  **$^{13}\text{C-NMR}$  (75 MHz,  $\text{CDCl}_3$ ):**  $\delta$  163.5, 135.2, 131.9, 131.8, 128.8, 126.1, 123.8, 62.5, 14.3.

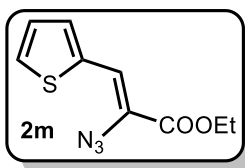
**Ethyl (Z)-2-azido-3-(4-bromophenyl)acrylate (2j):**



**GP-1** was followed using 4-bromobenzaldehyde (925.10 mg, 5.00 mmol, 1.00 equiv.), ethyl azidoacetate (1.90 g, 15.00 mmol, 3.00 equiv.) in 7 mL dry EtOH followed by addition of freshly prepared NaOEt (15.00 mmol, 3.00 equiv.) in 7 mL dry EtOH. After 4h, the reaction mixture was quenched and purification by column chromatography (silica gel, hexanes:EtOAc-95:5,  $R_f = 0.30$ ) afforded **2j** as white solid (596 mg, 40%).

**$^1\text{H-NMR}$  (300 MHz,  $\text{CDCl}_3$ ):**  $\delta$  7.70 – 7.66 (m, 2H), 7.52 – 7.47 (m, 2H), 6.82 (s, 1H), 4.36 (q,  $J = 7.1$  Hz, 2H), 1.39 (t,  $J = 7.1$  Hz, 3H);  **$^{13}\text{C-NMR}$  (75 MHz,  $\text{CDCl}_3$ ):**  $\delta$  163.5, 132.2, 132.1, 131.8, 126.3, 123.8, 123.6, 62.6, 14.3.

**Ethyl (Z)-2-azido-3-(thiophen-2-yl)acrylate (2m):**

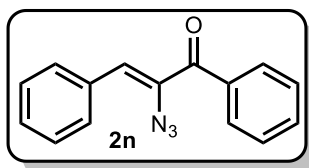


**GP-1** was followed using 2-thiophenecarboxaldehyde (560.75 mg, 5.00 mmol, 1.00 equiv.), ethyl azidoacetate (1.90 g, 15.00 mmol, 3.00 equiv.) in 7 mL dry EtOH followed by addition of freshly prepared NaOEt (15.00 mmol, 3.00 equiv.) in 7 mL dry EtOH. After 3h, the reaction mixture was quenched and purification by column chromatography (silica gel, hexanes:EtOAc-4:1,  $R_f = 0.52$ ) afforded **2m** as yellow solid (723 mg, 65%).

**$^1\text{H-NMR}$  (300 MHz,  $\text{CDCl}_3$ ):**  $\delta$  7.49 (d,  $J = 5.1$  Hz, 1H), 7.32 (d,  $J = 3.6$  Hz, 1H), 7.06 (dd,  $J_1 = 5.0$  Hz,  $J_2 = 3.7$  Hz, 2H), 4.35 (q,  $J = 7.1$  Hz, 2H), 1.39 (t,  $J = 7.1$  Hz, 3H);  **$^{13}\text{C-NMR}$  (75 MHz,  $\text{CDCl}_3$ ):**  $\delta$  163.3, 136.7, 132.1, 130.5, 127.1, 122.7, 119.3, 62.2, 14.3.



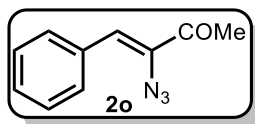
**(Z)-2-azido-1,3-diphenylprop-2-en-1-one (2n):**



**GP-2** was followed using (*E*)-chalcone **4b** (624.70 g, 3.00 mmol, 1.00 equiv.) and NaN<sub>3</sub> (293 mg, 4.50 mmol, 1.50 equiv) in 8 mL dry acetonitrile was added CAN (4.11 g, 7.50 mmol, 2.50 equiv.) in 30 mL dry Acetonitrile. After 3 h, the reaction mixture was quenched and the crude residue was treated with sodium acetate (369.13 mg, 4.5 mmol, 1.50 equiv.) in 20 mL dry acetone for overnight at room temperature. After usual work up and purification by column chromatography (silica gel, hexanes:EtOAc-9:1, R<sub>f</sub> = 0.42) afforded **2n** as a pale yellow solid (530 mg, 71%).

**<sup>1</sup>H-NMR (300 MHz, CDCl<sub>3</sub>):** δ 7.83 – 7.78 (m, 4H), 7.65 – 7.59 (m, 1H), 7.53 – 7.47 (m, 2H), 7.43 – 7.36 (m, 3H), 6.46 (s, 1H); **<sup>13</sup>C-NMR (75 MHz, CDCl<sub>3</sub>):** δ 192.4, 136.9, 133.8, 133.3, 132.8, 130.8, 129.98, 129.93, 129.8, 128.7, 128.6.

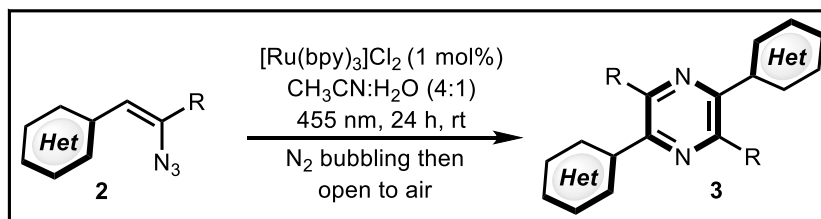
**(Z)-3-azido-4-phenylbut-3-en-2-one (2o):**



**GP-2** was followed using (*E*)-4-phenylbut-3-en-2-one **4c** (730.95 mg, 5.00 mmol, 1.00 equiv.) and NaN<sub>3</sub> (487.5 mg, 7.50 mmol, 1.50 equiv) in 15 mL dry acetonitrile was added CAN (6.85 g, 12.50 mmol, 2.50 equiv.) in 50 mL dry acetonitrile. After 3 h, the reaction mixture was quenched and the crude residue was treated with sodium acetate (615.22 mg, 7.5 mmol, 1.50 equiv.) in 25 mL dry acetone for overnight at room temperature. After usual work up and purification by column chromatography (silica gel, hexanes:EtOAc-9:1, R<sub>f</sub> = 0.34) afforded **2o** as a pale yellow solid (514 mg, 55%).

**<sup>1</sup>H-NMR (300 MHz, CDCl<sub>3</sub>):** δ 7.87 – 7.84 (m, 2H), 7.44 – 7.36 (m, 3H), 6.71 (s, 1H), 2.51 (s, 3H); **<sup>13</sup>C-NMR (75 MHz, CDCl<sub>3</sub>):** δ 194.5, 134.0, 133.2, 130.8, 129.9, 128.7, 126.8, 26.0.

General procedure 3 (GP-3) for the photochemical synthesis of pyrazines:



To an oven-dried Schlenk tube (10 mL size) equipped with a stirring bar was charged with  $[\text{Ru}(\text{bpy})_3]\text{Cl}_2 \cdot 6\text{H}_2\text{O}$  (3.74 mg, 0.01 equiv, 1mol%) followed by 1.60 mL Acetonitrile and 0.40 mL distilled water. The resulting solution was degassed via nitrogen bubbling for 5 minutes using a syringe niddle. Then vinyl azide **2** (0.50 mmol, 1 equiv) was added to the solution under nitrogen. Finally, irradiation with a Blue LED ( $\lambda_{\text{max}} = 455 \text{ nm}$ ) was started and the solution was kept open to air for 24 hours at room temperature. Then the reaction mixture was transferred to separatory funnel containing distilled water, extracted three times ethyl acetate. After drying the combined organic layers on  $\text{Na}_2\text{SO}_4$ , the resulting solution was concentrated *in vacuo*. The pure product **3** was obtained either by recrystallization from dichloromethane/pentane or by silica-gel column chromatography using hexanes and ethyl acetate as eluents.

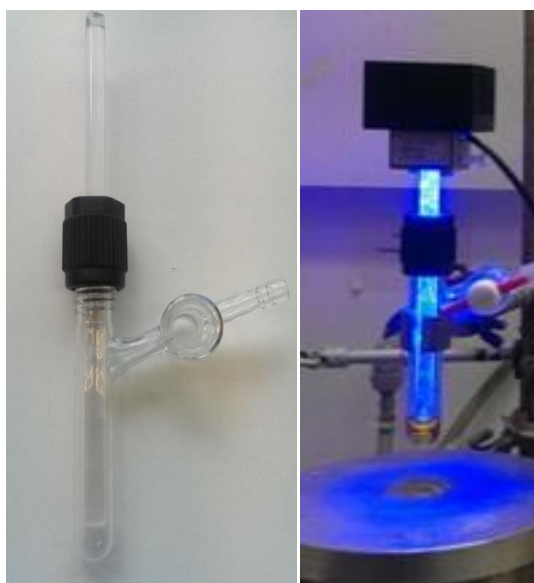
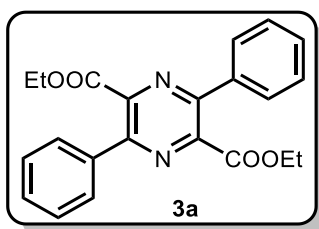


**Fig. S1:** Experimental set-up for photochemical reaction

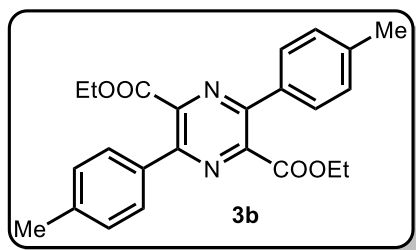
Diethyl 3,6-diphenylpyrazine-2,5-dicarboxylate (**3a**):



Following **GP-3**, **3a** was prepared from ethyl (Z)-2-azido-3-phenylacrylate **2a** (108.60 mg, 0.50 mmol, 1.00 equiv) and [Ru(bpy)<sub>3</sub>]Cl<sub>2</sub>·6H<sub>2</sub>O (3.74 mg, 0.01 equiv, 1mol%). The crude product was purified by column chromatography (silica gel, hexanes–EtOAc, 9:1, R<sub>f</sub> = 0.20) to afford **3a** as a white solid (57 mg, 61% yield).

<sup>1</sup>H-NMR (300 MHz, CDCl<sub>3</sub>): δ 7.74 – 7.71 (m, 4H), 7.49 – 7.47 (m, 6H), 4.31 (q, *J* = 7.14 Hz, 4H), 1.16 (t, *J* = 7.14 Hz, 6H); <sup>13</sup>C-NMR (75 MHz, CDCl<sub>3</sub>): δ 166.2, 149.9, 144.8, 136.2, 130.0, 128.9, 128.7, 62.5, 13.8; HRMS (ESI): exact m/z calculated for C<sub>22</sub>H<sub>20</sub>N<sub>2</sub>O<sub>4</sub> (M+H)<sup>+</sup>: 377.1423; Found: 377.1502; IR (neat, cm<sup>-1</sup>): 3059, 2986, 2925, 2854, 1731, 1449, 1405, 1380, 1293, 1173, 1137, 1094, 1057, 1021, 856, 766, 705.

Diethyl 3,6-di-p-tolylpyrazine-2,5-dicarboxylate (**3b**):

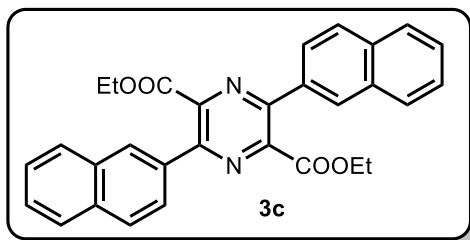


Following **GP-3**, **3b** was prepared from ethyl (Z)-2-azido-3-(p-tolyl)acrylate **2b** (115.50 mg, 0.50 mmol, 1.00 equiv) and [Ru(bpy)<sub>3</sub>]Cl<sub>2</sub>·6H<sub>2</sub>O (3.74 mg, 0.01 equiv, 1mol%). The crude product was dissolved in minimum amount of dichloromethane, then the solution was saturated with n-pentane. After 30 minutes, the solvent mixture was decanted, and the solid was again washed two times with n-pentane. The residual solvents were removed *in vacuo* which afforded **3b** as white solid (83 mg, 82%).

<sup>1</sup>H-NMR (300 MHz, CDCl<sub>3</sub>): δ 7.62 (d, *J* = 8.16 Hz, 4H), 7.27 (d, *J* = 7.98 Hz, 4H), 4.32 (q, *J* = 7.14 Hz, 4H), 2.41 (s, 6H), 1.19 (t, *J* = 7.11 Hz, 6H); <sup>13</sup>C-NMR (75 MHz, CDCl<sub>3</sub>): δ 166.4, 149.4, 144.6, 140.2, 133.3, 129.5, 128.7, 62.4, 21.5, 13.9; HRMS (ESI): exact m/z calculated

for  $C_{24}H_{24}N_2O_4$  ( $M+H$ )<sup>+</sup>: 405.1736; Found: 405.1814; **IR** (neat,  $cm^{-1}$ ): 2986, 2871, 1723, 1609, 1462, 1442, 1408, 1292, 1247, 1174, 1137, 1095, 1057, 1012, 853, 828, 775, 700.

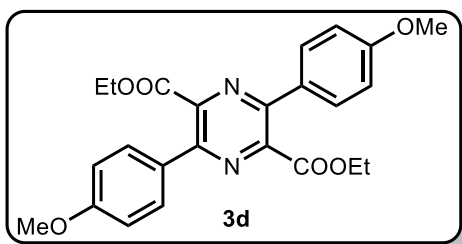
**Diethyl 3,6-di(naphthalen-2-yl)pyrazine-2,5-dicarboxylate (3c):**



Following **GP-3**, **3c** was prepared from ethyl (*Z*)-2-azido-3-(naphthalen-2-yl)acrylate **2c** (133.64 mg, 0.50 mmol, 1equiv) and  $[Ru(bpy)_3]Cl_2 \cdot 6H_2O$  (3.74 mg, 0.01 equiv, 1mol%). The crude product was purified by column chromatography (silica gel, hexanes–EtOAc, 4:1,  $R_f$  = 0.30) to afford **3c** as a white solid (81 mg, 70% yield).

**<sup>1</sup>H-NMR** (400 MHz,  $CDCl_3$ ):  $\delta$  8.28 (s, 2H), 7.97 – 7.85 (m, 8H), 7.59 – 7.53 (m, 4H), 4.33 (d,  $J$  = 7.12 Hz, 4H), 1.13 (t,  $J$  = 7.12 Hz, 6H); **<sup>13</sup>C-NMR** (100 MHz,  $CDCl_3$ ):  $\delta$  166.4, 149.6, 145.1, 134.0, 133.5, 133.2, 129.0, 128.8, 128.6, 127.9, 127.4, 126.8, 125.9, 62.6, 13.9; **HRMS** (ESI): exact  $m/z$  calculated for  $C_{30}H_{24}N_2O_4$  ( $M+H$ )<sup>+</sup>: 477.1736; Found : 477.1821; **IR** (neat,  $cm^{-1}$ ): 3056, 2974, 2927, 2854, 1729, 1686, 1462, 1405, 1381, 1304, 1236, 1169, 1140, 1004, 906, 871, 852, 830, 750.

**Diethyl 3,6-bis(4-methoxyphenyl)pyrazine-2,5-dicarboxylate (3d):**

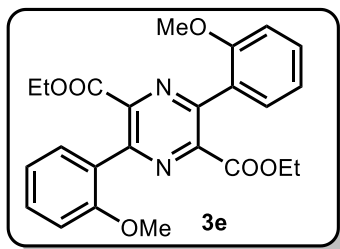


Following **GP-3**, **3d** was prepared from ethyl (*Z*)-2-azido-3-(4-methoxyphenyl)acrylate **2d** (123.60 mg, 0.50 mmol, 1equiv) and  $[Ru(bpy)_3]Cl_2 \cdot 6H_2O$  (3.74 mg, 0.01 equiv, 1mol%). The crude product was purified by column chromatography (silica gel, hexanes–EtOAc, 3:1,  $R_f$  = 0.28) to afford **3d** as a white solid (53 mg, 49% yield).

**<sup>1</sup>H-NMR** (300 MHz,  $CDCl_3$ ):  $\delta$  7.70 – 7.67 (m, 4H), 6.99 – 6.96 (m, 4H), 4.33 (q,  $J$  = 7.11 Hz, 4H), 3.85 (s, 6H), 1.21 (t,  $J$  = 7.11 Hz, 6H); **<sup>13</sup>C-NMR** (75 MHz,  $CDCl_3$ ):  $\delta$  166.5, 161.2, 148.5, 144.1, 130.3, 128.5, 114.2, 62.4, 55.5, 13.9; **HRMS** (ESI): exact  $m/z$  calculated for

$C_{24}H_{24}N_2O_6$  (M+H)<sup>+</sup>: 437.1634; Found: 437.1740; **IR** (neat,  $cm^{-1}$ ): 2980, 2955, 2926, 2851, 1732, 1607, 1580, 1518, 1414, 1295, 1253, 1177, 1148, 1060, 1017, 841, 811, 786, 752.

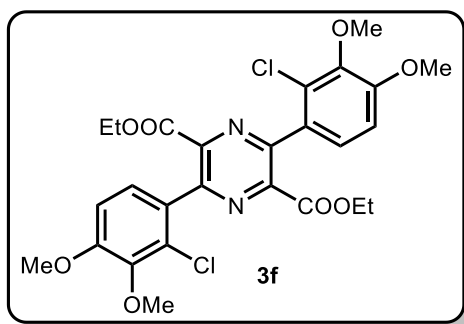
**Diethyl 3,6-bis(2-methoxyphenyl)pyrazine-2,5-dicarboxylate (3e):**



Following **GP-3**, **3e** was prepared from ethyl (*Z*)-2-azido-3-(2-methoxyphenyl)acrylate **2e** (123.60 mg, 0.50 mmol, 1.00 equiv) and [Ru(bpy)<sub>3</sub>]Cl<sub>2</sub>·6H<sub>2</sub>O (3.74 mg, 0.01 equiv, 1mol%). The crude product was dissolved in minimum amount of dichloromethane, then the solution was saturated with n-pentane. After 30 minutes, the solvent mixture was decanted, and the solid was again washed two times with n-pentane. The residual solvents were removed *in vacuo* which afforded **3e** as white solid (86 mg, 79%).

**<sup>1</sup>H-NMR (300 MHz, CDCl<sub>3</sub>):**  $\delta$  7.78 (dd,  $J_1 = 7.53$  Hz,  $J_2 = 1.65$  Hz, 2H), 7.44 – 7.38 (m, 2H), 7.14 – 7.09 (m, 2H), 6.89 (d,  $J = 8.22$  Hz, 2H), 4.25 (q,  $J = 7.14$  Hz, 4H), 3.73 (s, 6H), 1.14 (t,  $J = 7.14$  Hz, 6H); **<sup>13</sup>C-NMR (75 MHz, CDCl<sub>3</sub>):**  $\delta$  165.5, 156.5, 147.6, 145.9, 131.4, 131.2, 126.5, 121.4, 110.1, 61.8, 55.1, 13.9; **HRMS (ESI):** exact m/z calculated for  $C_{24}H_{24}N_2O_6$  (M+H)<sup>+</sup>: 437.1634; Found: 437.1739; **IR** (neat,  $cm^{-1}$ ): 2968, 2924, 2843, 1733, 1601, 1495, 1465, 1439, 1411, 1390, 1280, 1248, 1226, 1182, 1149, 1111, 1061, 1014, 854, 759, 697.

**Diethyl 3,6-bis(2-chloro-3,4-dimethoxyphenyl)pyrazine-2,5-dicarboxylate (3f):**

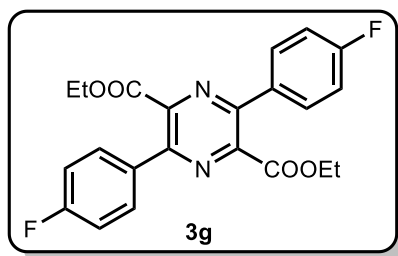


Following **GP-3**, **3f** was prepared from ethyl (*Z*)-2-azido-3-(2-chloro-3,4-dimethoxyphenyl)acrylate **2f** (155.86 mg, 0.50 mmol, 1.00 equiv) and [Ru(bpy)<sub>3</sub>]Cl<sub>2</sub>·6H<sub>2</sub>O (3.74 mg, 0.01 equiv, 1mol%). The crude product was dissolved in minimum amount of

dichloromethane, then the solution was saturated with n-pentane. After 30 minutes, the solvent mixture was decanted, and the solid was again washed two times with n-pentane. The residual solvents were removed *in vacuo* which afforded **3f** as white solid (122 mg, 87%).

**<sup>1</sup>H-NMR (400 MHz, CDCl<sub>3</sub>):** δ 7.36 (d, *J* = 8.56 Hz, 2H), 6.98 (d, *J* = 8.64 Hz, 2H), 4.28 (q, *J* = 7.12 Hz, 4H), 3.94 (s, 6H), 3.87 (s, 6H), 1.17 (t, *J* = 7.12 Hz, 6H); **<sup>13</sup>C-NMR (100 MHz, CDCl<sub>3</sub>):** δ 164.6, 154.8, 149.8, 145.5, 145.1, 129.5, 127.8, 126.4, 110.9, 62.5, 60.8, 56.3, 13.9; **HRMS (ESI):** exact *m/z* calculated for C<sub>26</sub>H<sub>26</sub>Cl<sub>2</sub>N<sub>2</sub>O<sub>8</sub> (M+H)<sup>+</sup>: 565.1066; Found: 565.1143; **IR (neat, cm<sup>-1</sup>):** 3090, 2980, 2938, 2841, 1735, 1590, 1490, 1447, 1412, 1392, 1293, 1269, 1220, 1202, 1099, 1038, 1003, 819, 790, 778.

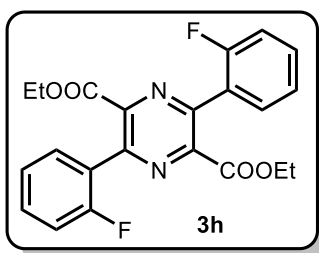
**Diethyl 3,6-bis(4-fluorophenyl)pyrazine-2,5-dicarboxylate (3g):**



Following **GP-3**, **3g** was prepared from ethyl (*Z*)-2-azido-3-(4-fluorophenyl)acrylate **2g** (117.60 mg, 0.50 mmol, 1.00 equiv) and [Ru(bpy)<sub>3</sub>]Cl<sub>2</sub>·6H<sub>2</sub>O (3.74 mg, 0.01 equiv, 1mol%). The crude product was dissolved in minimum amount of dichloromethane, then the solution was saturated with n-pentane. After 30 minutes, the solvent mixture was decanted, and the solid was again washed two times with n-pentane. The residual solvents were removed *in vacuo* which afforded **3g** as white solid (87 mg, 85%).

**<sup>1</sup>H-NMR (300 MHz, CDCl<sub>3</sub>):** δ 7.74 – 7.70 (m, 4H), 7.20 – 7.15 (m, 4H), 4.33 (q, *J* = 7.17 Hz, 4H), 1.20 (t, *J* = 7.15 Hz, 6H); **<sup>13</sup>C-NMR (75 MHz, CDCl<sub>3</sub>):** δ 165.9, 164.1 (d, <sup>1</sup>*J*<sub>C-F</sub> = 250.6 Hz), 148.8, 144.5, 132.1 (d, <sup>4</sup>*J*<sub>C-F</sub> = 3.1 Hz), 130.9 (d, <sup>3</sup>*J*<sub>C-F</sub> = 8.65 Hz), 116.0 (d, <sup>2</sup>*J*<sub>C-F</sub> = 21.8 Hz), 62.7, 13.9; **<sup>19</sup>F-NMR (282 MHz, CDCl<sub>3</sub>):** δ -110.9; **HRMS (ESI):** exact *m/z* calculated for C<sub>22</sub>H<sub>18</sub>F<sub>2</sub>N<sub>2</sub>O<sub>4</sub> (M+H)<sup>+</sup>: 413.1235; Found: 413.1320; **IR (neat, cm<sup>-1</sup>):** 3084, 2985, 2925, 2854, 1733, 1599, 1512, 1409, 1383, 1289, 1227, 1179, 1155, 1096, 1053, 1012, 845, 815, 766.

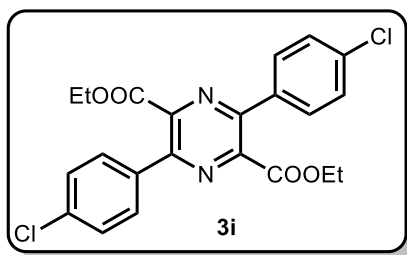
**Diethyl 3,6-bis(2-fluorophenyl)pyrazine-2,5-dicarboxylate (3h):**



Following **GP-3**, **3h** was prepared from ethyl (*Z*)-2-azido-3-(2-fluorophenyl)acrylate **2g** (117.60 mg, 0.50 mmol, 1.00 equiv) and [Ru(bpy)<sub>3</sub>]Cl<sub>2</sub>·6H<sub>2</sub>O (3.74 mg, 0.01 equiv, 1mol%). The crude product was dissolved in minimum amount of dichloromethane, then the solution was saturated with n-pentane. After 30 minutes, the solvent mixture was decanted, and the solid was again washed two times with n-pentane. The residual solvents were removed *in vacuo* which afforded **3g** as white solid (83 mg, 81%).

**<sup>1</sup>H-NMR (300 MHz, CDCl<sub>3</sub>):** δ 7.86 – 7.80 (m, 2H), 7.51 – 7.44 (m, 2H), 7.35 – 7.30 (m, 2H), 7.16 – 7.09 (m, 2H), 4.35 (q, *J* = 7.14 Hz, 4H), 1.21 (t, *J* = 7.13 Hz, 6H); **<sup>13</sup>C-NMR (75 MHz, CDCl<sub>3</sub>):** δ 164.7, 160.1 (d, <sup>1</sup>*J*<sub>C-F</sub> = 248.7 Hz), 146.5, 145.4 (d, *J* = 1.95 Hz), 132.0 (d, <sup>3</sup>*J*<sub>C-F</sub> = 8.5 Hz), 131.7 (d, <sup>4</sup>*J*<sub>C-F</sub> = 2.37 Hz), 124.9 (d, <sup>3</sup>*J*<sub>C-F</sub> = 3.3 Hz), 124.7, 115.4 (d, <sup>2</sup>*J*<sub>C-F</sub> = 21.7 Hz), 62.5, 13.9; **<sup>19</sup>F-NMR (282 MHz, CDCl<sub>3</sub>):** δ -116.6; **HRMS (ESI):** exact *m/z* calculated for C<sub>22</sub>H<sub>18</sub>F<sub>2</sub>N<sub>2</sub>O<sub>4</sub> (M+H)<sup>+</sup>: 413.1235; Found: 413.1320; **IR (neat, cm<sup>-1</sup>):** 3071, 2985, 2939, 2906, 1730, 1613, 1581, 1490, 1454, 1399, 1384, 1245, 1172, 1140, 1093, 1059, 1014, 859, 757.

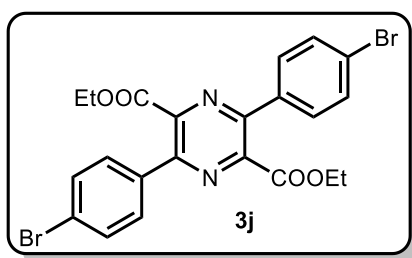
**Diethyl 3,6-bis(4-chlorophenyl)pyrazine-2,5-dicarboxylate (3i):**



Following **GP-3**, **3i** was prepared from ethyl (*Z*)-2-azido-3-(4-chlorophenyl)acrylate **2i** (125.83 mg, 0.50 mmol, 1.00 equiv) and [Ru(bpy)<sub>3</sub>]Cl<sub>2</sub>·6H<sub>2</sub>O (3.74 mg, 0.01 equiv, 1mol%). The crude product was dissolved in minimum amount of dichloromethane, then the solution was saturated with n-pentane. After 30 minutes, the solvent mixture was decanted, and the solid was again washed two times with n-pentane. The residual solvents were removed *in vacuo* which afforded **3i** as white solid (63 mg, 57%).

**<sup>1</sup>H-NMR (300 MHz, CDCl<sub>3</sub>):** δ 7.68 – 7.66 (m, 4H), 7.47 – 7.45 (m, 4H), 4.34 (q, *J* = 7.14 Hz, 4H), 1.22 (t, *J* = 7.14 Hz, 6H); **<sup>13</sup>C-NMR (75 MHz, CDCl<sub>3</sub>):** δ 165.8, 148.9, 144.5, 136.7, 134.4, 130.2, 129.1, 62.8, 13.9; **HRMS (ESI):** exact *m/z* calculated for C<sub>22</sub>H<sub>18</sub>Cl<sub>2</sub>N<sub>2</sub>O<sub>4</sub> (M+H)<sup>+</sup>: 445.0644; Found: 445.0713; **IR (neat, cm<sup>-1</sup>):** 2985, 2937, 1728, 1595, 1494, 1426, 1401, 1378, 1277, 1234, 1187, 1158, 1109, 1090, 1053, 1010, 854, 830, 778, 745.

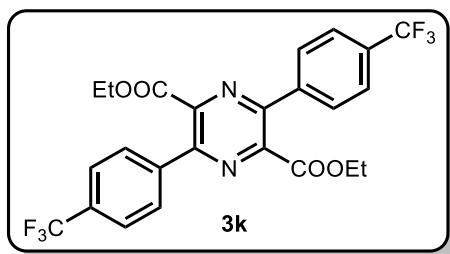
**Diethyl 3,6-bis(4-bromophenyl)pyrazine-2,5-dicarboxylate (3j):**



Following **GP-3**, **3j** was prepared from ethyl (*Z*)-2-azido-3-(4-bromophenyl)acrylate **2j** (148.06 mg, 0.50 mmol, 1equiv) and [Ru(bpy)<sub>3</sub>]Cl<sub>2</sub>·6H<sub>2</sub>O (3.74 mg, 0.01 equiv, 1mol%). The crude product was purified by column chromatography (silica gel, hexanes–EtOAc, 3:1, *R<sub>f</sub>* = 0.22) to afford **3j** as a white solid (73 mg, 55% yield).

**<sup>1</sup>H-NMR (300 MHz, CDCl<sub>3</sub>):** δ 7.64 – 7.58 (m, 8H), 4.34 (q, *J* = 7.20 Hz, 4H), 1.22 (t, *J* = 7.20 Hz, 6H); **<sup>13</sup>C-NMR (75 MHz, CDCl<sub>3</sub>):** δ 165.8, 149.0, 144.5, 134.9, 132.0, 130.4, 125.0, 62.8, 13.9; **HRMS (ESI):** exact *m/z* calculated for C<sub>22</sub>H<sub>18</sub>Br<sub>2</sub>N<sub>2</sub>O<sub>4</sub> (M+H)<sup>+</sup>: 532.9633; Found: 532.9708; **IR (neat, cm<sup>-1</sup>):** 2983, 2925, 2854, 1728, 1588, 1474, 1423, 1399, 1376, 1279, 1234, 1186, 1159, 1051, 1006, 854, 826, 776, 734.

**Diethyl 3,6-bis(4-(trifluoromethyl)phenyl)pyrazine-2,5-dicarboxylate (3k):**

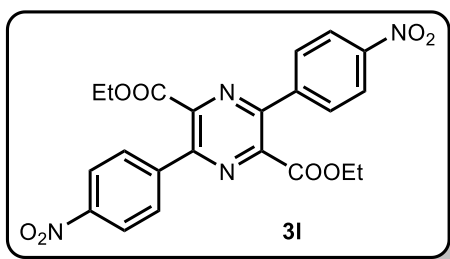


Following **GP-3**, **3k** was prepared from ethyl (*Z*)-2-azido-3-(4-(trifluoromethyl)phenyl)acrylate **2k** (142.61 mg, 0.50 mmol, 1equiv) and [Ru(bpy)<sub>3</sub>]Cl<sub>2</sub>·6H<sub>2</sub>O (3.74 mg, 0.01 equiv, 1mol%). The crude product was purified by column chromatography (silica gel, hexanes–EtOAc, 3:1, *R<sub>f</sub>* = 0.30) to afford **3j** as a white solid (48 mg, 38% yield).



**<sup>1</sup>H-NMR (300 MHz, CDCl<sub>3</sub>):** δ 7.86 (d, *J* = 8.19 Hz, 4H), 7.76 (d, *J* = 8.31 Hz, 4H), 4.34 (q, *J* = 7.14 Hz, 4H), 1.20 (t, *J* = 7.14 Hz, 6H); **<sup>13</sup>C-NMR (75 MHz, CDCl<sub>3</sub>):** δ 165.4, 149.4, 144.9, 139.4, 132.1 (q, *J* = 33.1 Hz), 129.4, 125.7 (q, *J* = 3.67 Hz), 122.1, 62.9, 13.8; **<sup>19</sup>F-NMR (282 MHz, CDCl<sub>3</sub>):** δ – 63.2; **HRMS (ESI):** exact *m/z* calculated for C<sub>24</sub>H<sub>18</sub>F<sub>6</sub>N<sub>2</sub>O<sub>4</sub> (M+H)<sup>+</sup>: 513.1171; Found: 513.1254; **IR (neat, cm<sup>-1</sup>):** 2982, 2965, 2927, 2856, 1721, 1414, 1324, 1254, 1138, 1105, 1072, 1053, 1016, 858, 832, 790, 717.

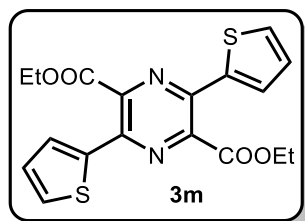
**Diethyl 3,6-bis(4-nitrophenyl)pyrazine-2,5-dicarboxylate (3l):**



Following **GP-3**, **3l** was prepared from Ethyl (Z)-2-azido-3-(4-nitrophenyl)acrylate **2l** (131.11 mg, 0.50 mmol, 1.00 equiv) and [Ru(bpy)<sub>3</sub>]Cl<sub>2</sub>·6H<sub>2</sub>O (3.74 mg, 0.01 equiv, 1mol%). The crude product was dissolved in minimum amount of dichloromethane, then the solution was saturated with n-pentane. After 30 minutes, the solvent mixture was decanted, and the solid was again washed two times with n-pentane. The residual solvents were removed *in vacuo* which afforded **3l** as yellow solid (99 mg, 86%).

**<sup>1</sup>H-NMR (300 MHz, CDCl<sub>3</sub>):** δ 8.38 – 8.35 (m, 4H), 7.93 – 7.90 (m, 4H), 4.37 (q, *J* = 7.14 Hz, 4H), 1.24 (t, *J* = 7.11 Hz, 6H); **<sup>13</sup>C-NMR (75 MHz, CDCl<sub>3</sub>):** δ 164.9, 149.08, 149.00, 144.8, 141.8, 130.1, 124.0, 63.2, 14.0; **HRMS (ESI):** exact *m/z* calculated for C<sub>22</sub>H<sub>18</sub>N<sub>4</sub>O<sub>8</sub> (M+H)<sup>+</sup>: 467.1125; Found: 467.1198; **IR (neat, cm<sup>-1</sup>):** 3110, 2985, 2958, 2919, 2851, 1721, 1601, 1516, 1466, 1408, 1344, 1296, 1259, 1144, 1100, 1009, 850, 800, 749, 689.

**Diethyl 3,6-di(thiophen-2-yl)pyrazine-2,5-dicarboxylate (3m):**

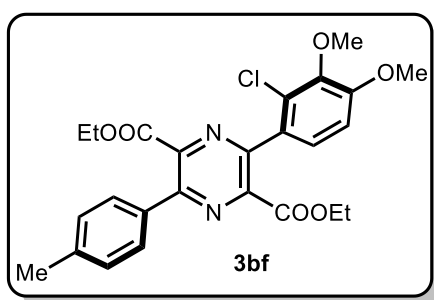


Following **GP-3**, **3m** was prepared from Ethyl (Z)-2-azido-3-(thiophen-2-yl)acrylate **2m** (111.60 mg, 0.50 mmol, 1equiv) and [Ru(bpy)<sub>3</sub>]Cl<sub>2</sub>·6H<sub>2</sub>O (3.74 mg, 0.01 equiv, 1mol%). The

crude product was purified by column chromatography (silica gel, hexanes–EtOAc, 5:1,  $R_f = 0.52$ ) to afford **3j** as a pale yellow solid (25 mg, 26%).

**$^1\text{H-NMR}$  (300 MHz,  $\text{CDCl}_3$ ):**  $\delta$  7.54 – 7.50 (m, 4H), 7.12 – 7.09 (m, 2H), 4.48 (q,  $J = 7.16$  Hz, 4H), 1.37 (t,  $J = 7.17$  Hz, 6H);  **$^{13}\text{C-NMR}$  (75 MHz,  $\text{CDCl}_3$ ):**  $\delta$  165.9, 142.5, 141.9, 139.1, 130.4, 128.6, 128.4, 62.8, 14.0; **HRMS (ESI):** exact  $m/z$  calculated for  $\text{C}_{18}\text{H}_{16}\text{N}_2\text{O}_4\text{S}_2$  ( $\text{M}+\text{H}$ ) $^+$ : 389.0551; Found: 389.0644; **IR (neat,  $\text{cm}^{-1}$ ):** 3097, 2991, 2963, 2924, 2853, 1719, 1531, 1435, 1418, 1381, 1330, 1270, 1145, 1109, 852, 830, 706.

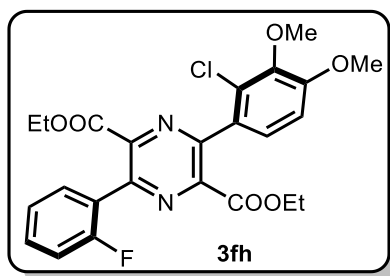
**Diethyl 3-(2-chloro-3,4-dimethoxyphenyl)-6-(*p*-tolyl)pyrazine-2,5-dicarboxylate (**3bf**):**



Following **GP-3**, **3bf** was prepared from ethyl (*Z*)-2-azido-3-(2-chloro-3,4-dimethoxyphenyl)acrylate **2f** (77.93 mg, 0.25 mmol, 1equiv), ethyl (*Z*)-2-azido-3-(*p*-tolyl)acrylate **2b** (57.77 mg, 0.25 mmol, 1.00 equiv) and  $[\text{Ru}(\text{bpy})_3]\text{Cl}_2 \cdot 6\text{H}_2\text{O}$  (3.74 mg, 0.01 equiv, 1mol%). The crude product was purified by column chromatography (silica gel, hexanes–EtOAc, 3:1,  $R_f = 0.25$ ) to afford **3bf** as a white solid (37 mg, 31% yield).

**$^1\text{H-NMR}$  (300 MHz,  $\text{CDCl}_3$ ):**  $\delta$  7.66 (d,  $J = 8.13$  Hz, 2H), 7.33 – 7.27 (m, 3H), 6.97 (d,  $J = 8.64$  Hz, 1H), 4.36 – 4.25 (m, 4H), 3.93 (s, 3H), 3.87 (s, 3H), 2.42 (s, 3H), 1.22 – 1.16 (m, 6H);  **$^{13}\text{C-NMR}$  (75 MHz,  $\text{CDCl}_3$ ):**  $\delta$  166.2, 164.7, 154.7, 150.5, 148.7, 145.5, 144.9, 144.8, 140.5, 133.2, 129.6, 129.5, 128.9, 127.8, 126.3, 110.8, 62.6, 62.4, 60.8, 56.3, 21.6, 13.97, 13.94; **HRMS (ESI):** exact  $m/z$  calculated for  $\text{C}_{25}\text{H}_{25}\text{ClN}_2\text{O}_6$  ( $\text{M}+\text{H}$ ) $^+$ : 485.1401; Found: 485.1494; **IR (neat,  $\text{cm}^{-1}$ ):** 2982, 2927, 2854, 1739, 1591, 1487, 1450, 1397, 1291, 1277, 1236, 1224, 1198, 1153, 1120, 1077, 1030, 1013, 964, 809, 755.

**Diethyl 3-(2-chloro-3,4-dimethoxyphenyl)-6-(2-fluorophenyl)pyrazine-2,5-dicarboxylate (3fh):**

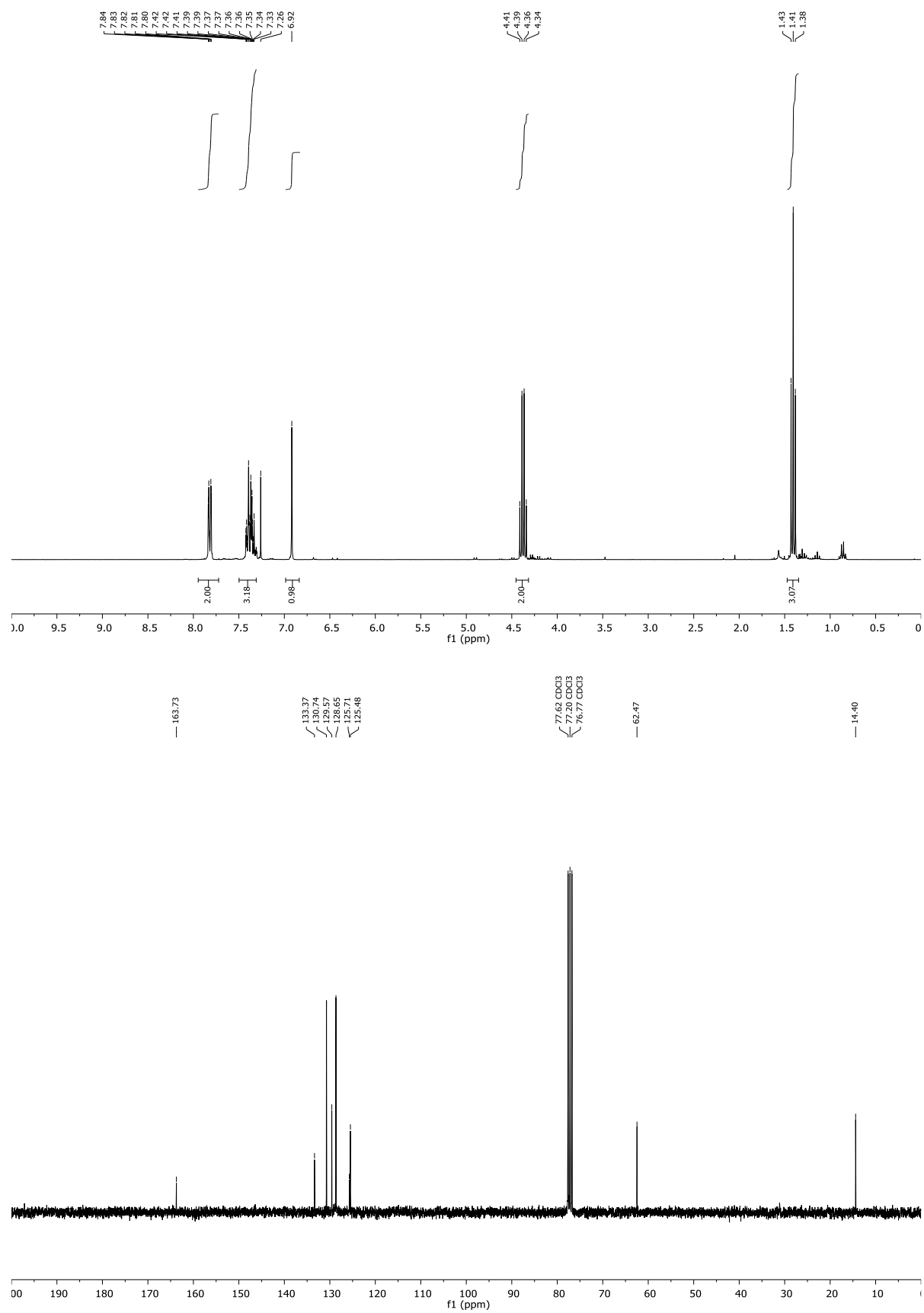


Following **GP-3**, **3fh** was prepared from ethyl (*Z*)-2-azido-3-(2-chloro-3,4-dimethoxyphenyl)acrylate **2f** (77.93 mg, 0.25 mmol, 1equiv), ethyl (*Z*)-2-azido-3-(2-fluorophenyl)acrylate **2h** (58.86 mg, 0.25 mmol, 1.00 equiv) and [Ru(bpy)<sub>3</sub>]Cl<sub>2</sub>·6H<sub>2</sub>O (3.74 mg, 0.01 equiv, 1mol%). The crude product was purified by column chromatography (silica gel, hexanes–EtOAc, 3:1, R<sub>f</sub> = 0.34) to afford **3fh** as a white solid (45 mg, 37% yield).

**<sup>1</sup>H-NMR (300 MHz, CDCl<sub>3</sub>):** δ 7.87 – 7.82 (m, 1H), 7.59 – 7.30 (m, 3H), 7.16 – 7.09 (m, 1H), 6.99 – 6.97 (m, 1H), 4.38 – 4.26 (m, 4H), 3.93 (s, 3H), 3.87 (s, 3H), 1.23 – 1.16 (m, 6H); **<sup>13</sup>C-NMR (75 MHz, CDCl<sub>3</sub>):** δ 164.8, 164.5, 160.1 (d, <sup>1</sup>J<sub>C-F</sub> = 248.3 Hz), 154.8, 149.7, 146.5, 145.5, 145.1, 132.0 (d, <sup>3</sup>J<sub>C-F</sub> = 8.5 Hz), 131.7 (d, <sup>4</sup>J<sub>C-F</sub> = 2.2 Hz), 129.4, 127.7, 126.4, 125.0, 124.9 (d, <sup>3</sup>J<sub>C-F</sub> = 3.3 Hz), 124.9, 115.4 (d, <sup>2</sup>J<sub>C-F</sub> = 21.6 Hz), 110.9, 62.5 (x2), 60.8, 56.3, 13.95, 13.92; **<sup>19</sup>F-NMR (282 MHz, CDCl<sub>3</sub>):** δ -116.6; **HRMS (ESI):** exact m/z calculated for C<sub>24</sub>H<sub>22</sub>ClFN<sub>2</sub>O<sub>6</sub> (M+H)<sup>+</sup>: 489.1150; Found: 489.1257; **IR (neat, cm<sup>-1</sup>):** 2981, 2934, 2843, 1723, 1616, 1558, 1490, 1450, 1408, 1296, 1269, 1248, 1224, 1173, 1142, 1099, 1075, 1040, 1016, 812, 758.

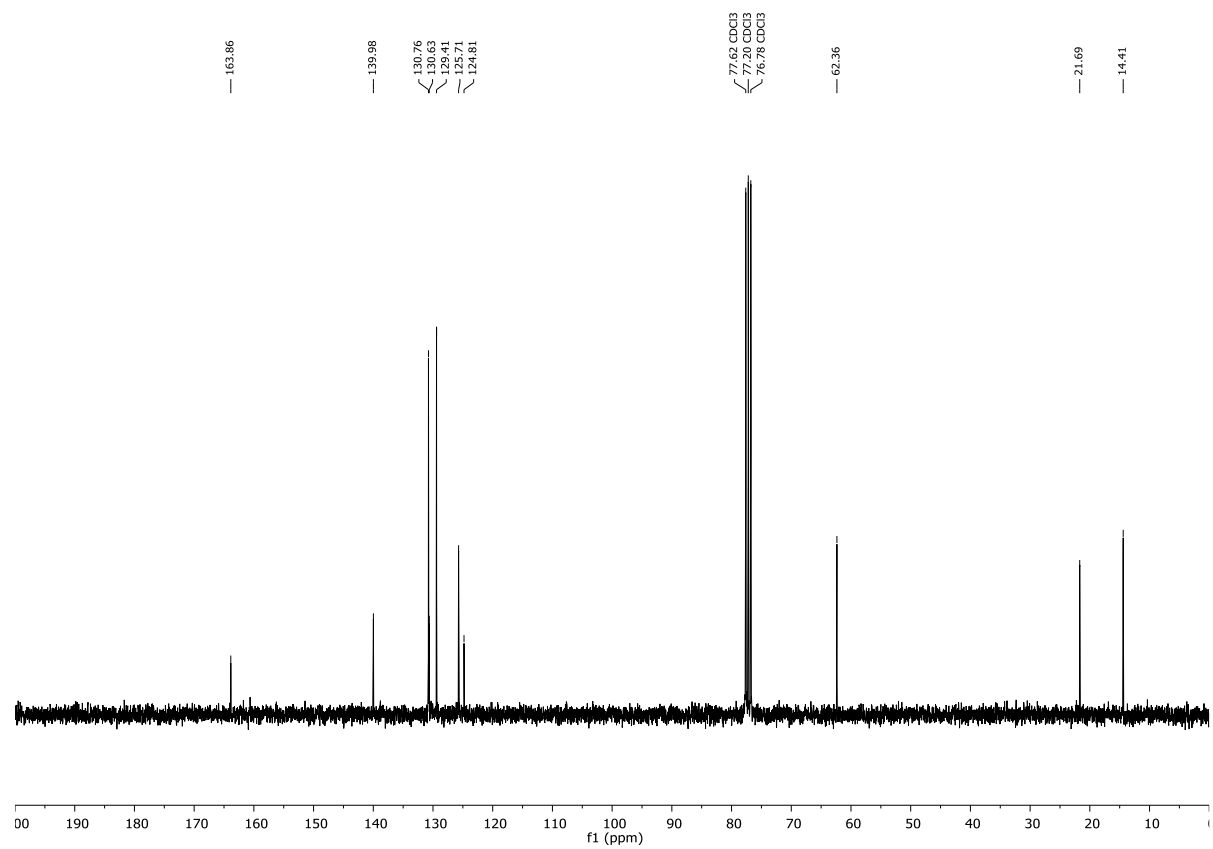
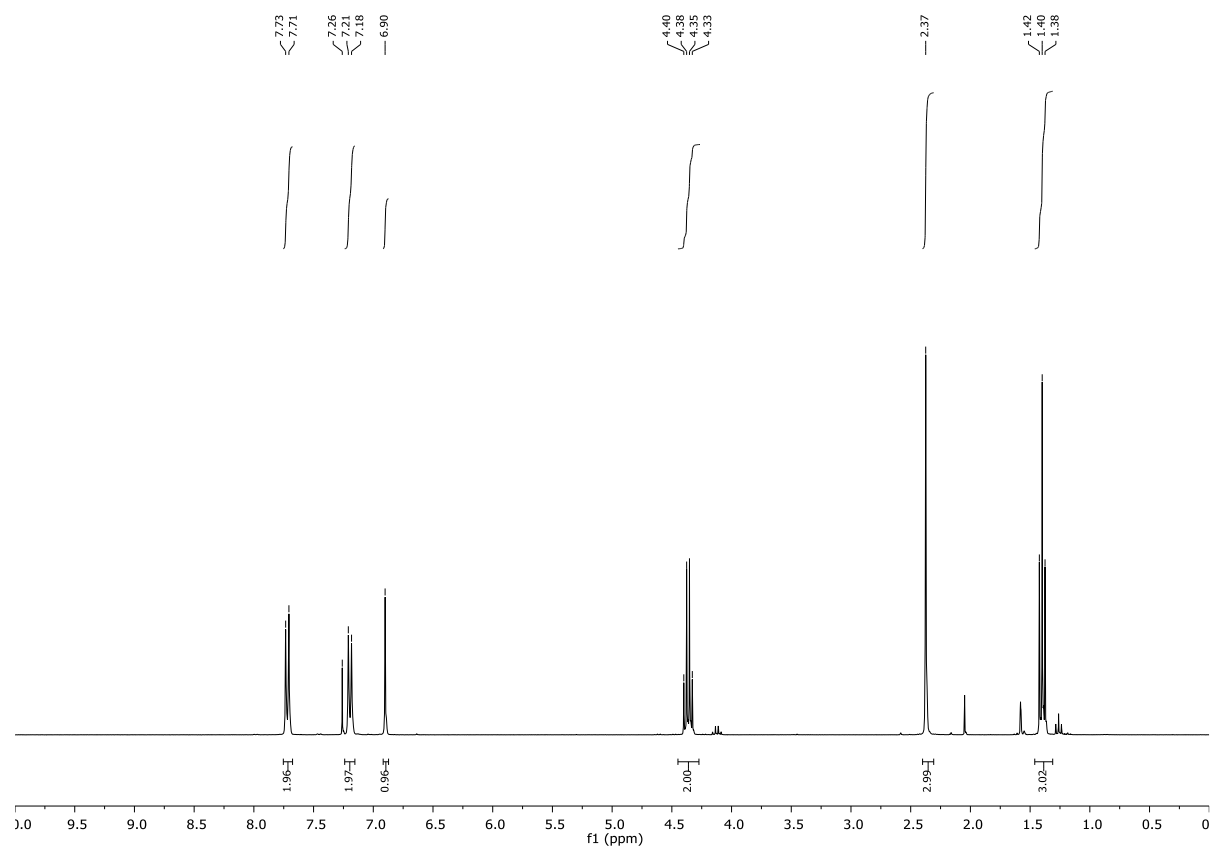
## Chapter 2: Synthesis of Pyrazines

### $^1\text{H}$ and $^{13}\text{C}$ NMR of **2a**



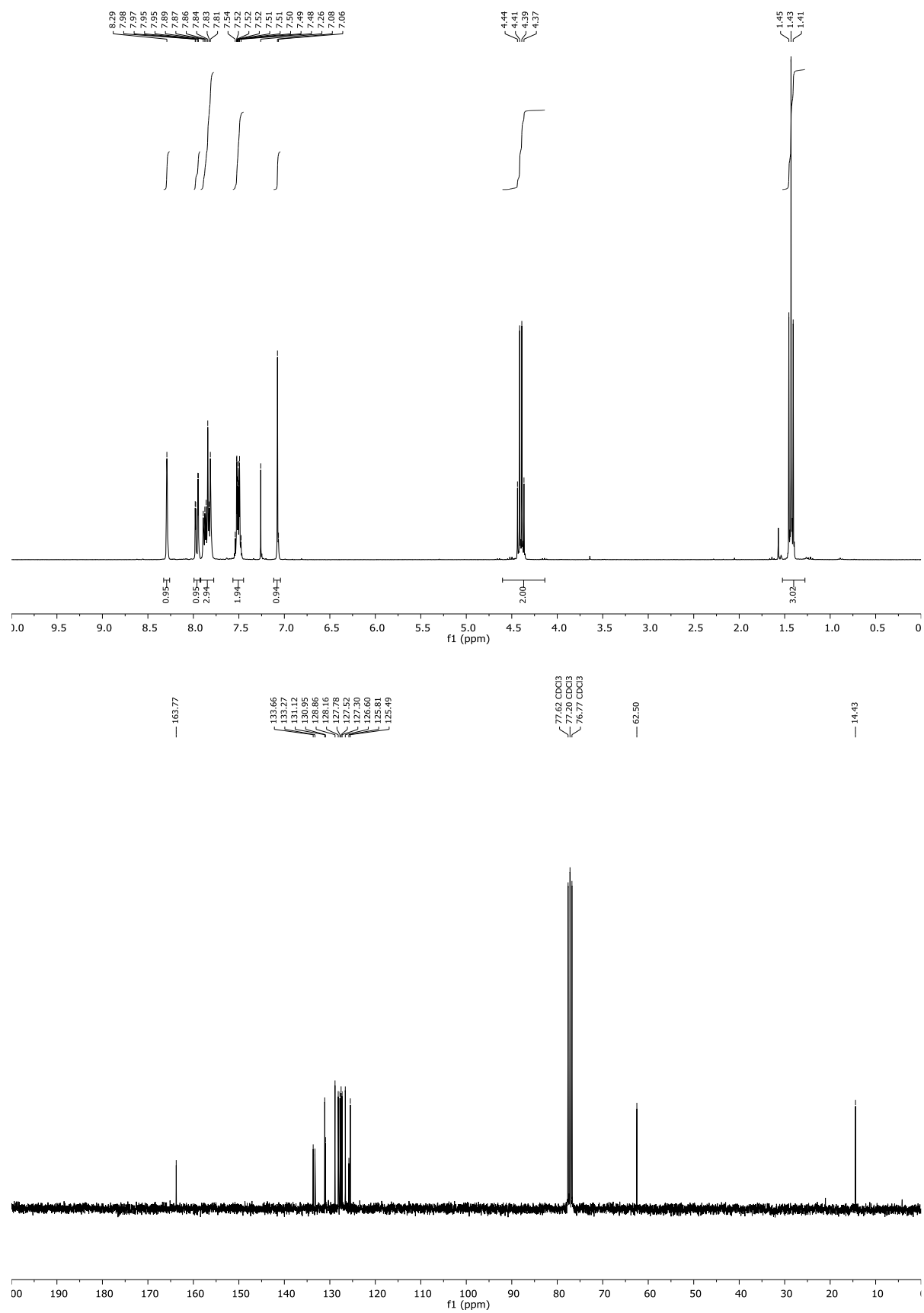
## Chapter 2: Synthesis of Pyrazines

### $^1\text{H}$ and $^{13}\text{C}$ NMR of **2b**



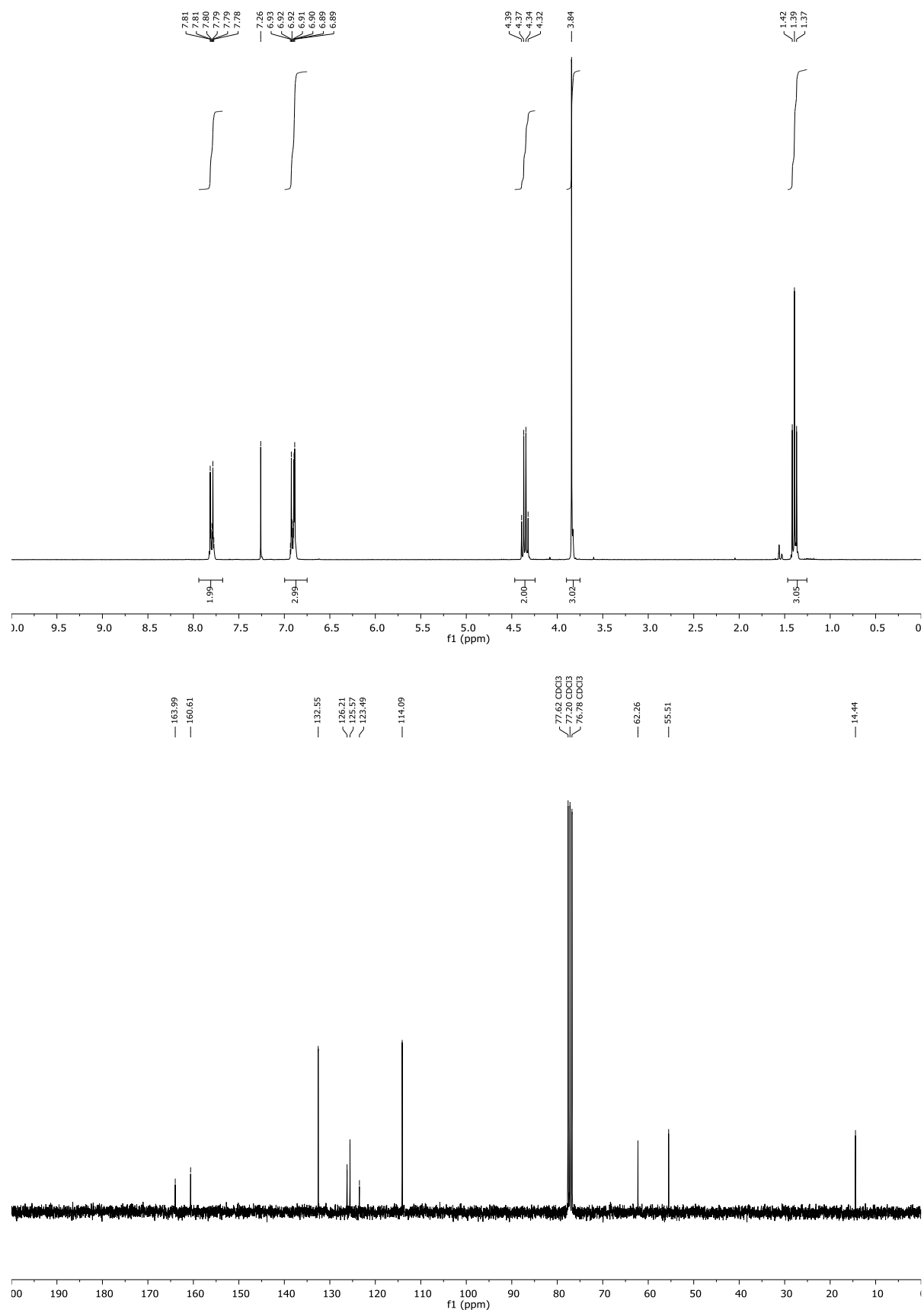
## Chapter 2: Synthesis of Pyrazines

### $^1\text{H}$ and $^{13}\text{C}$ NMR of **2c**



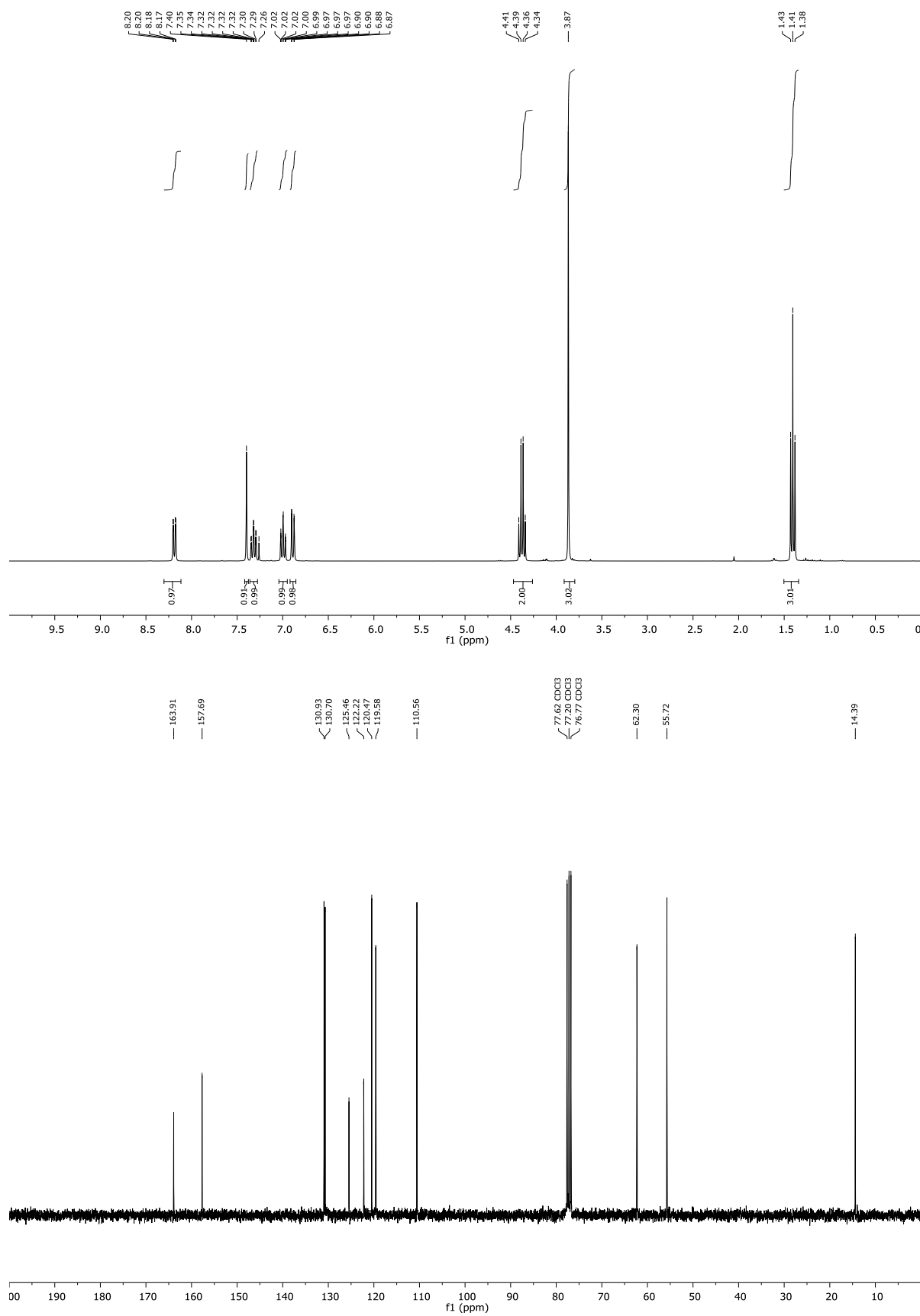
## Chapter 2: Synthesis of Pyrazines

### $^1\text{H}$ and $^{13}\text{C}$ NMR of **2d**



## Chapter 2: Synthesis of Pyrazines

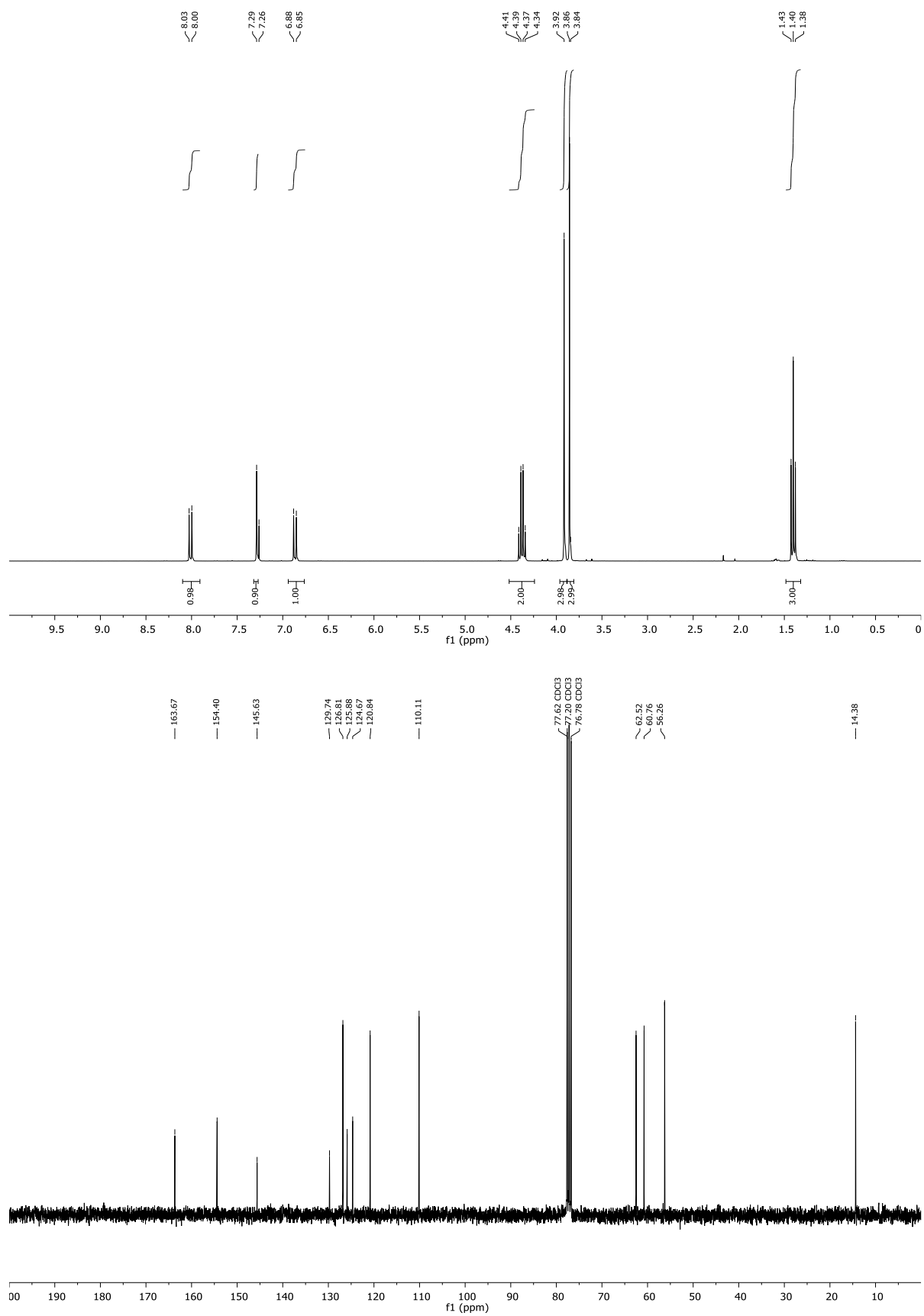
### $^1\text{H}$ and $^{13}\text{C}$ NMR of **2e**





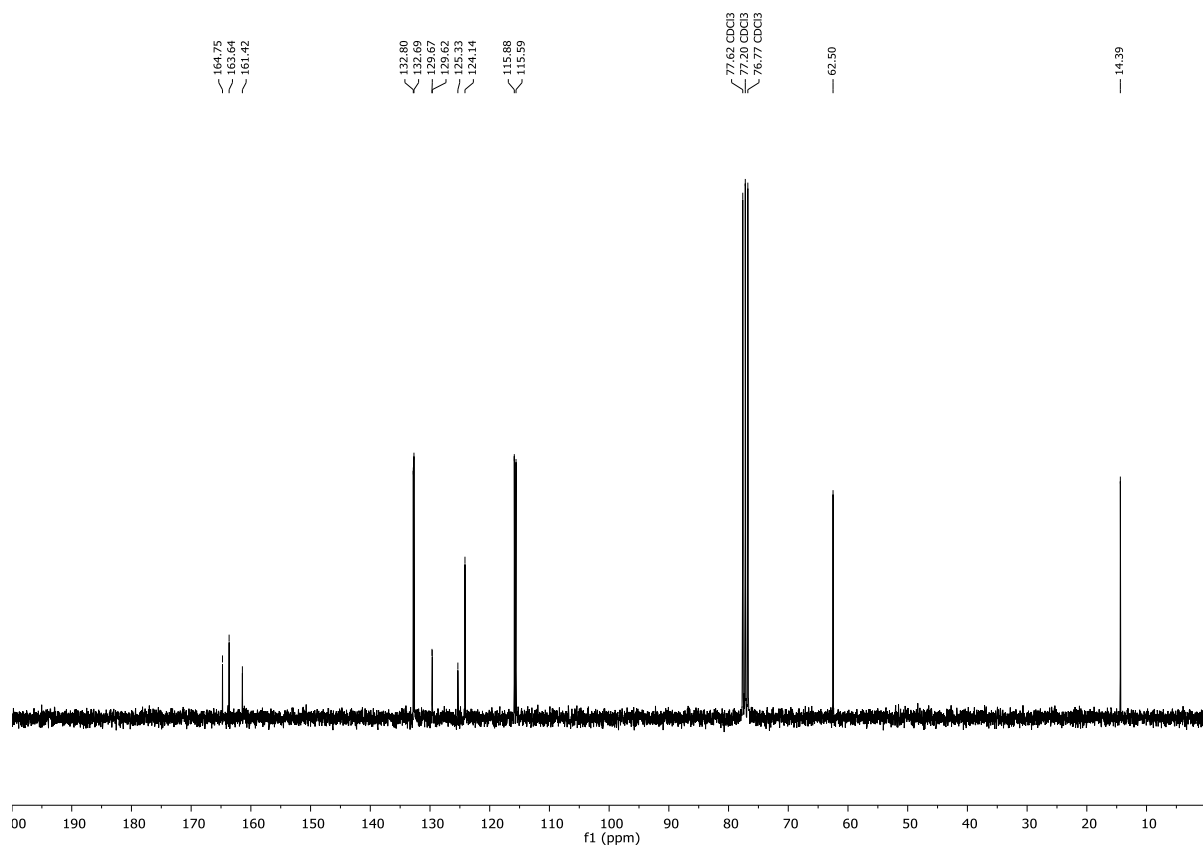
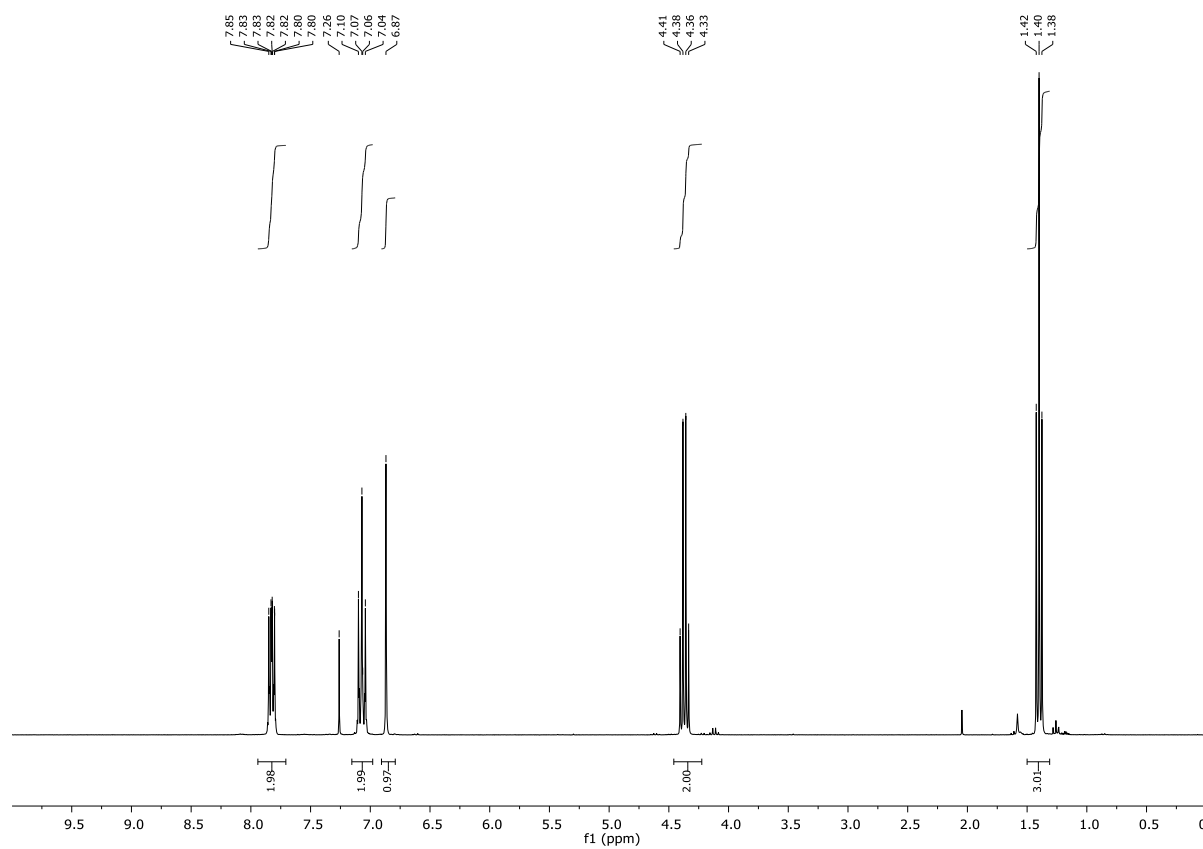
## Chapter 2: Synthesis of Pyrazines

### $^1\text{H}$ and $^{13}\text{C}$ NMR of **2f**



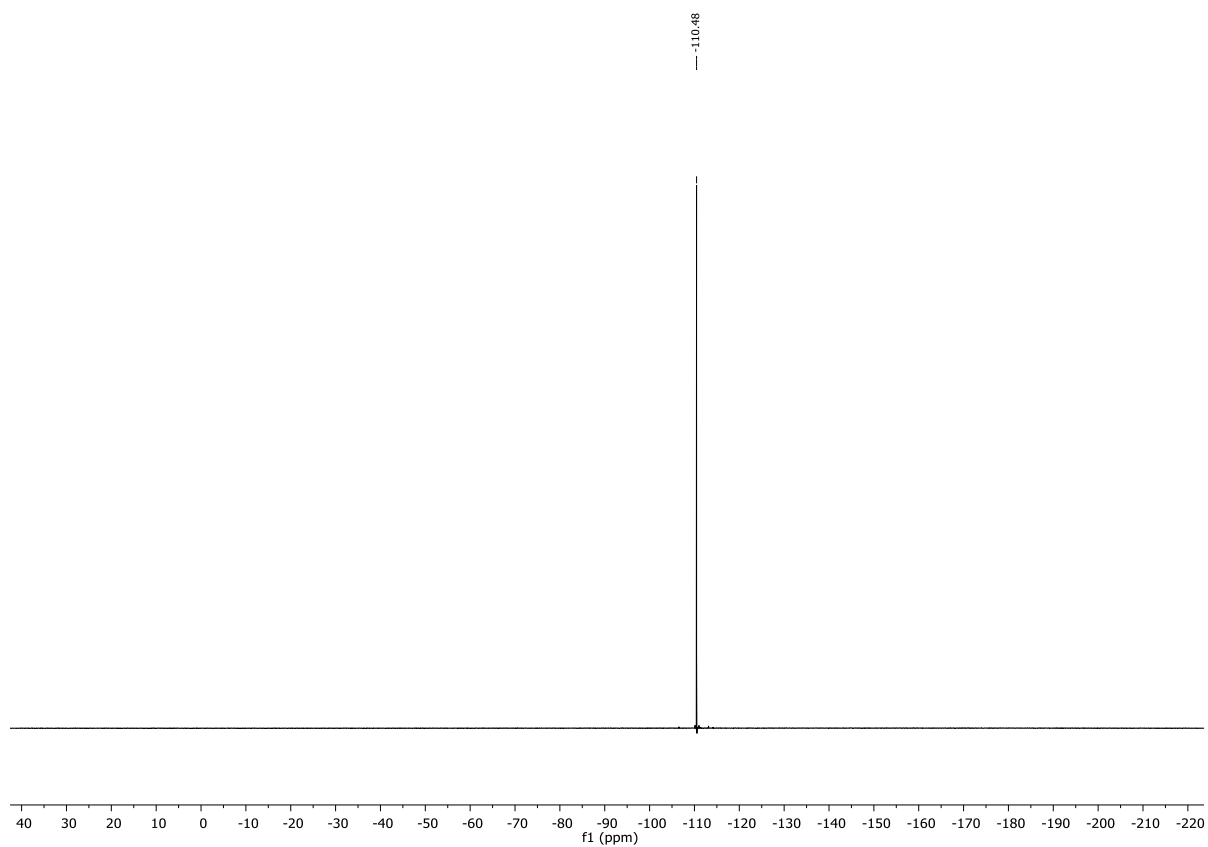
## Chapter 2: Synthesis of Pyrazines

$^1\text{H}$ ,  $^{13}\text{C}$  and  $^{19}\text{F}$  NMR of **2g**



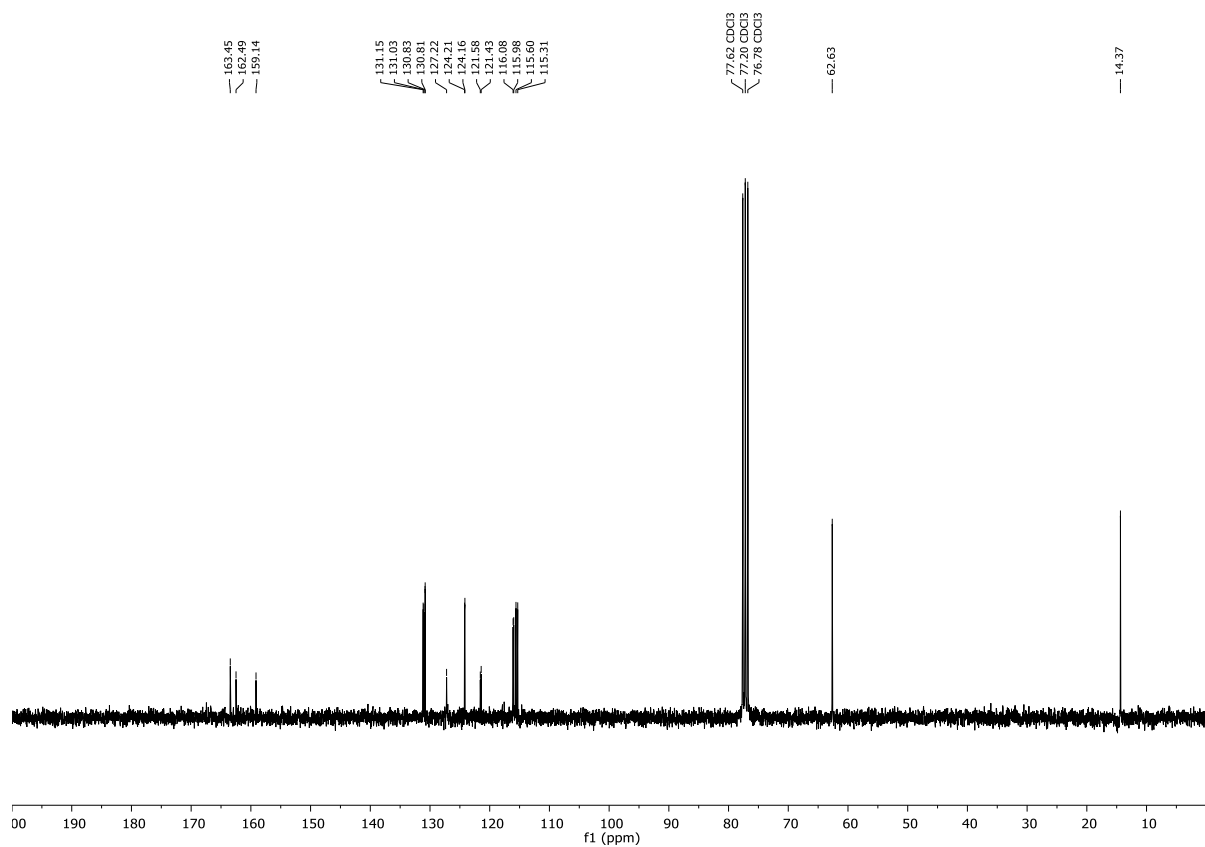
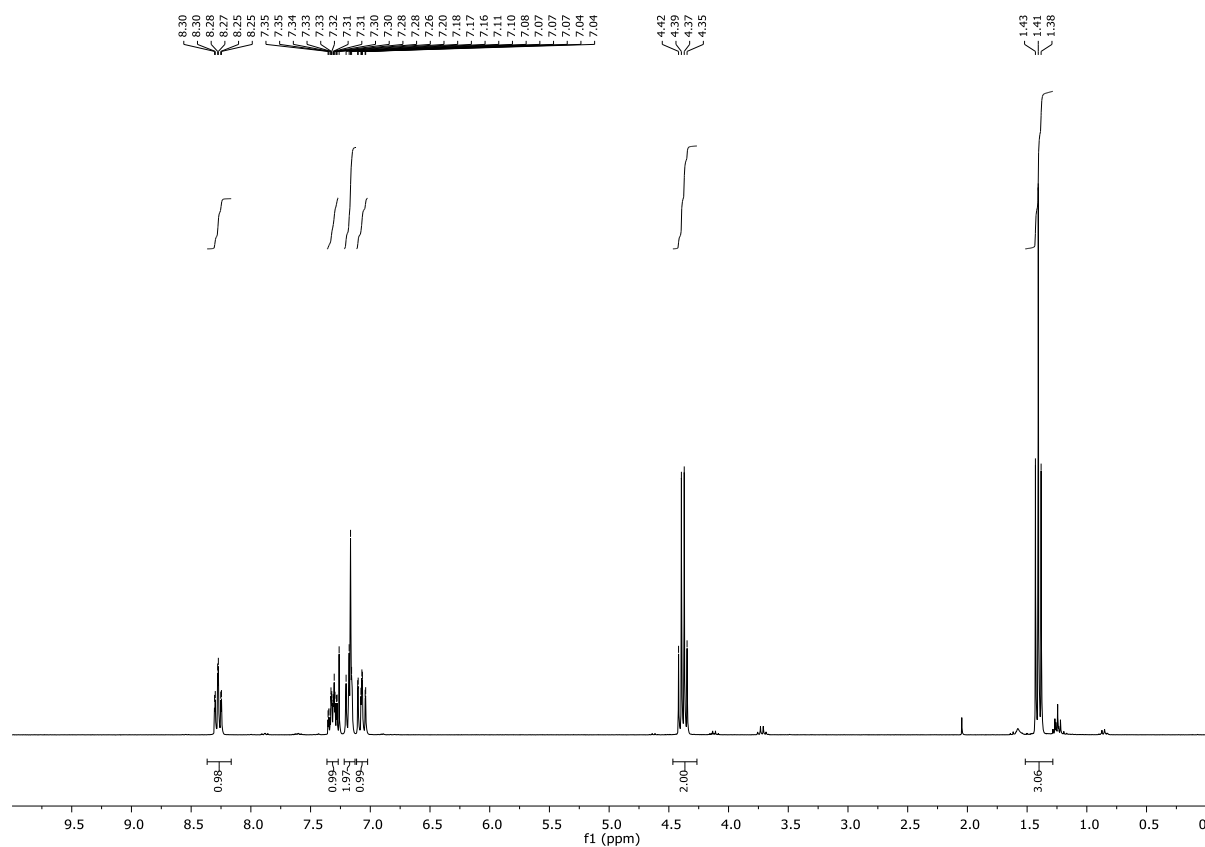
## Chapter 2: Synthesis of Pyrazines

---



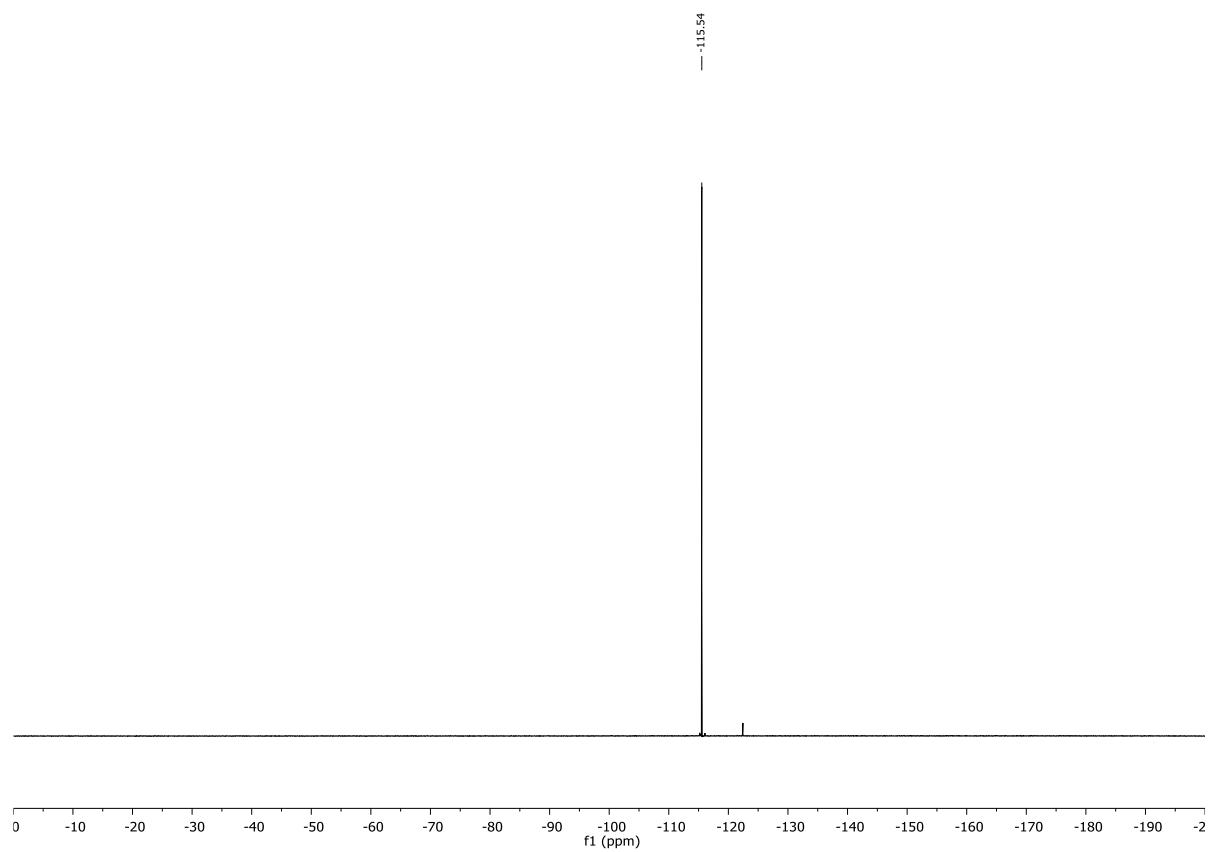
## Chapter 2: Synthesis of Pyrazines

### $^1\text{H}$ , $^{13}\text{C}$ and $^{19}\text{F}$ NMR of **2h**



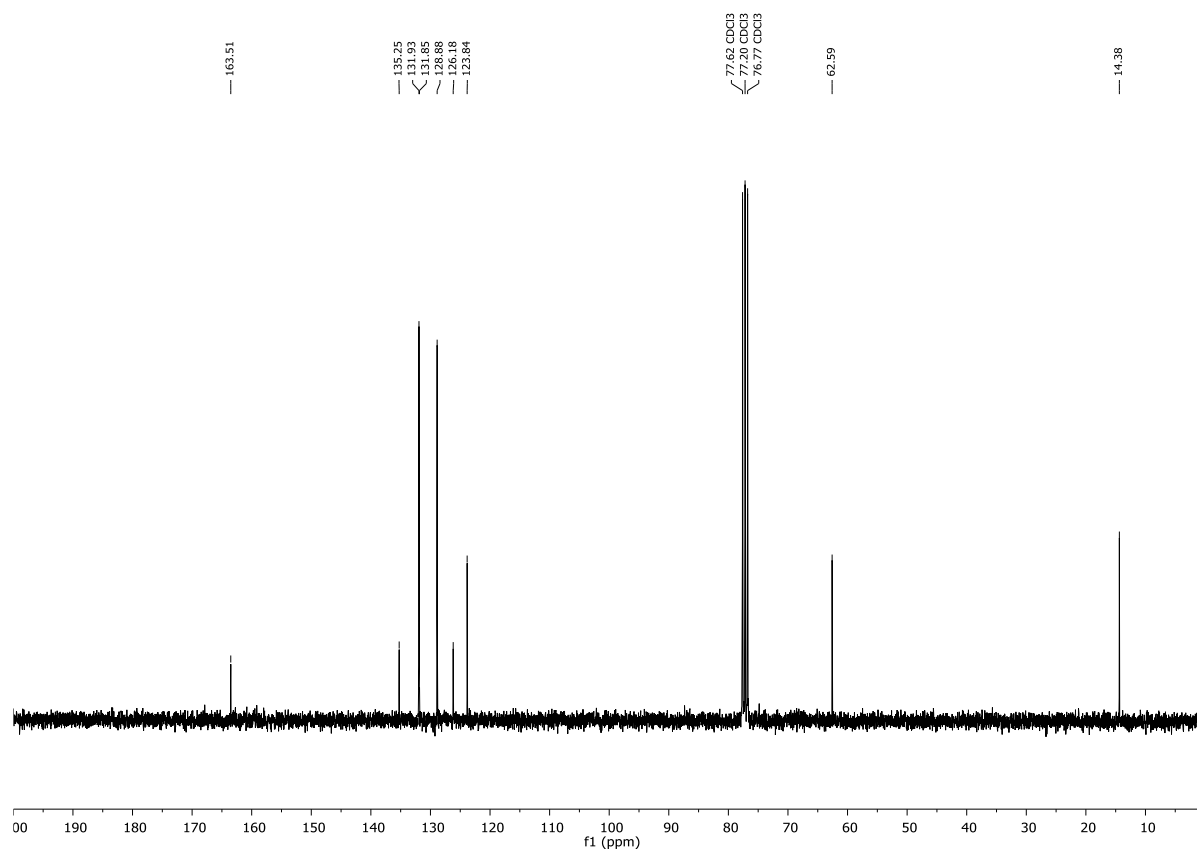
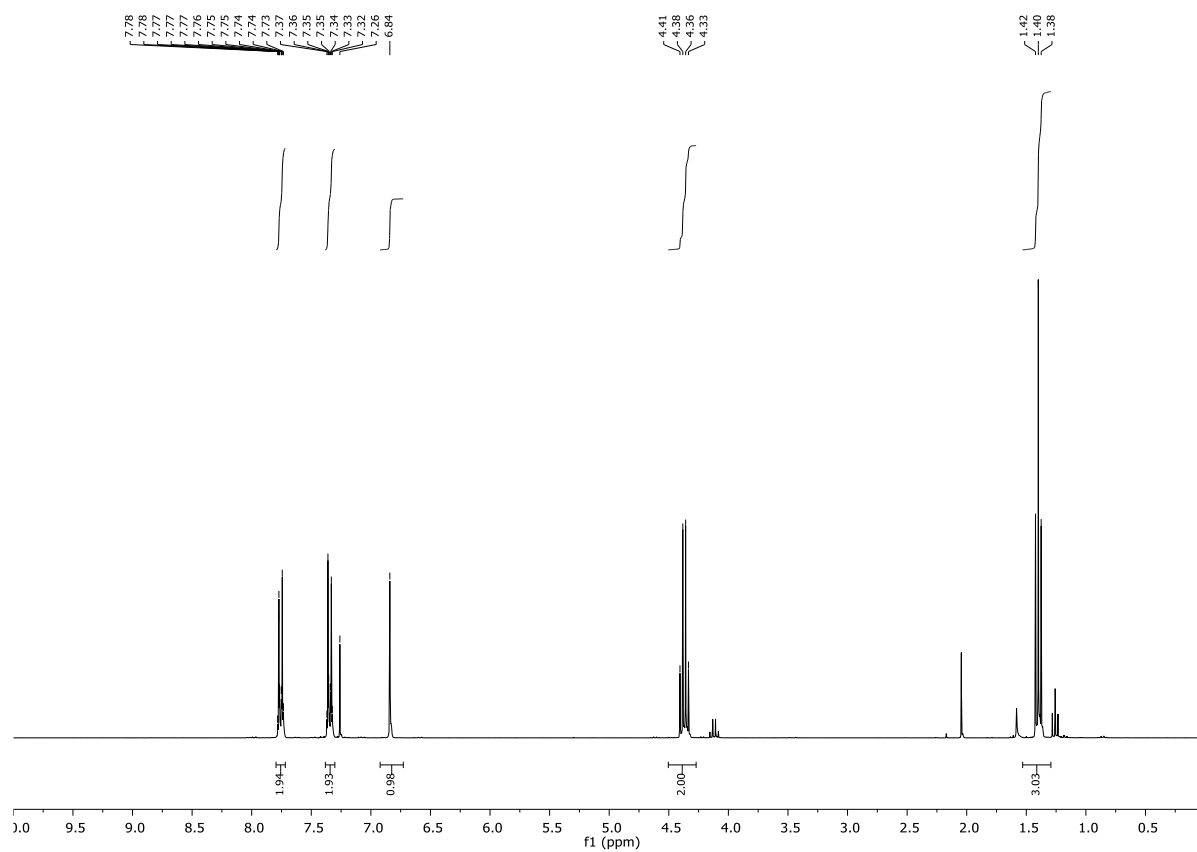
## Chapter 2: Synthesis of Pyrazines

---



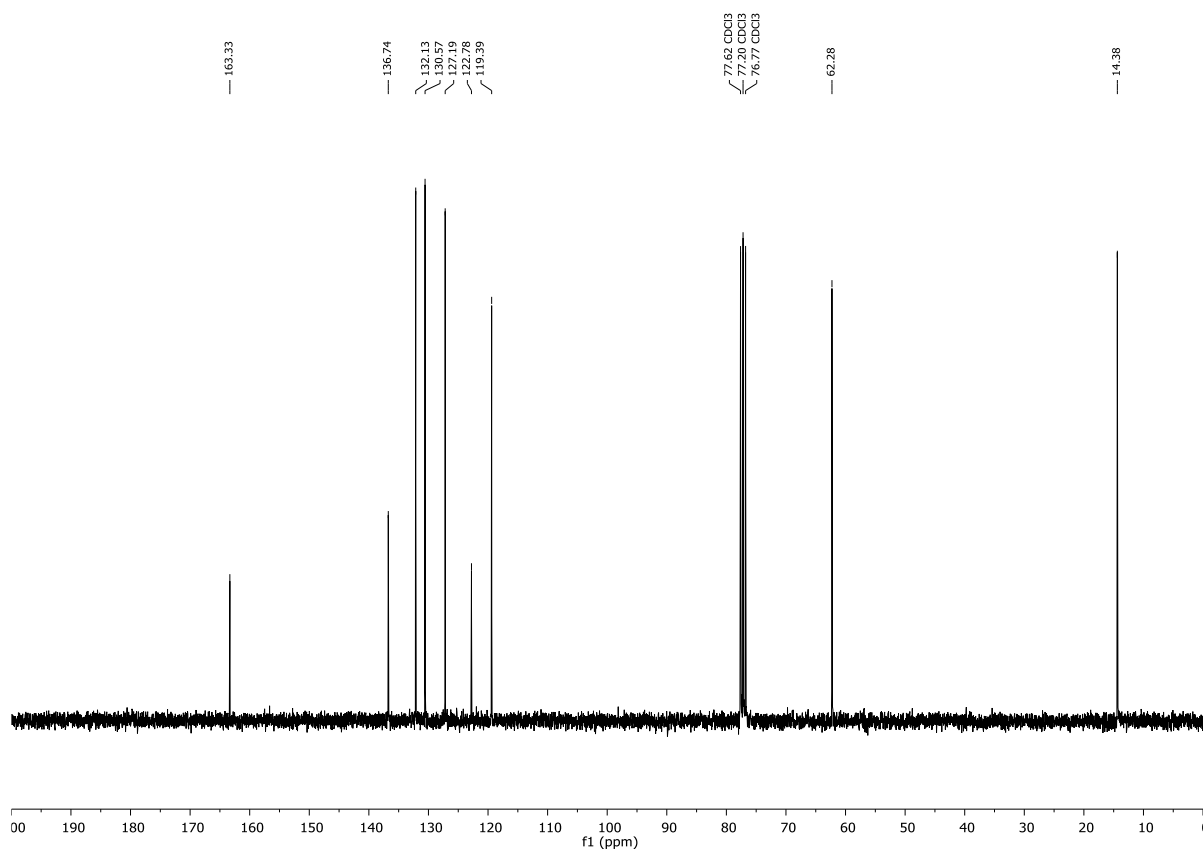
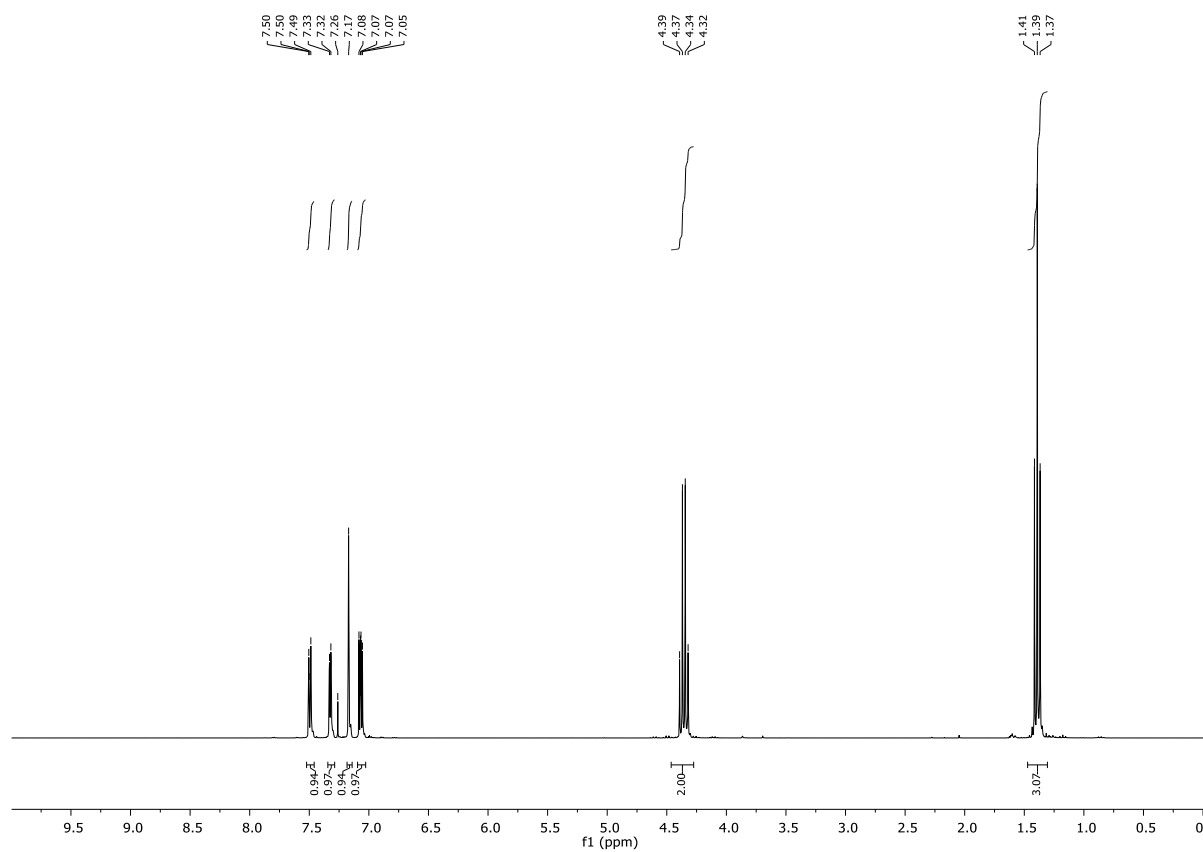
## Chapter 2: Synthesis of Pyrazines

### $^1\text{H}$ and $^{13}\text{C}$ NMR of **2i**



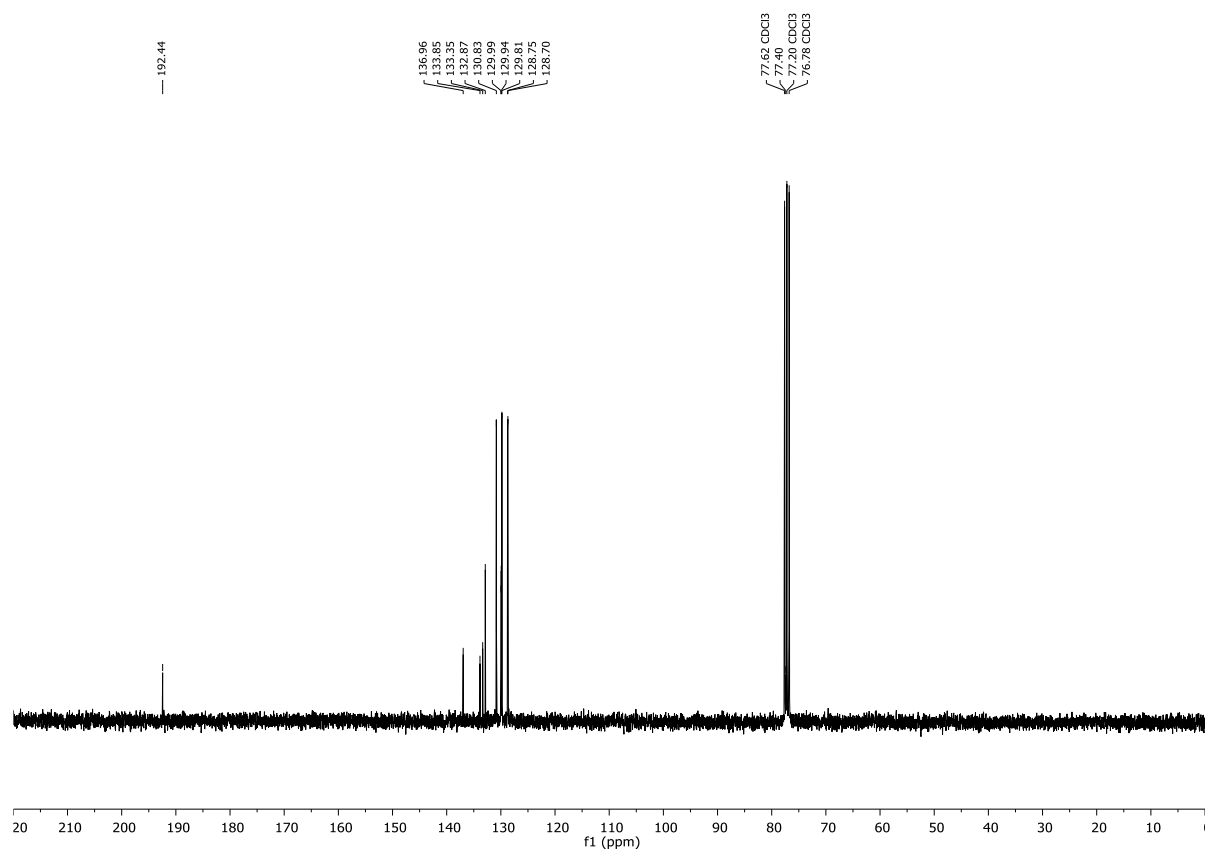
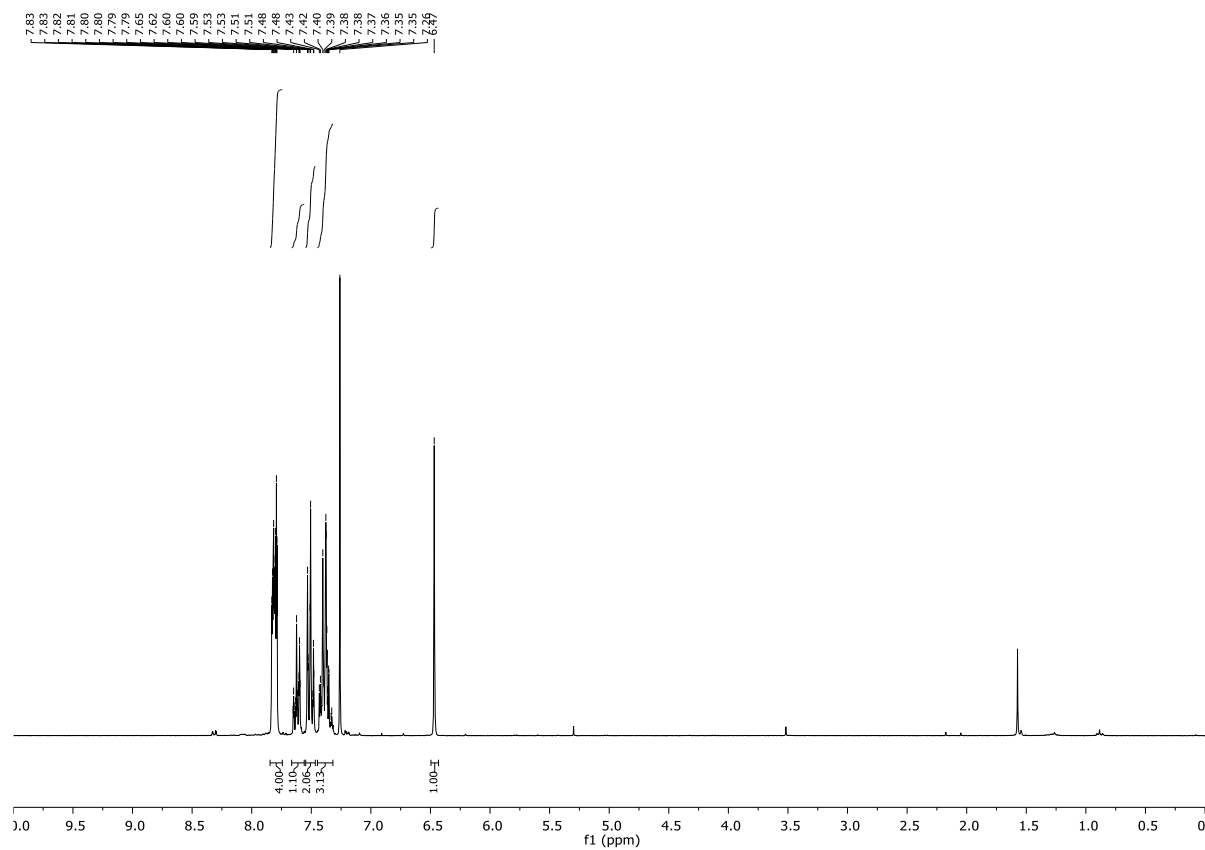
## Chapter 2: Synthesis of Pyrazines

### $^1\text{H}$ and $^{13}\text{C}$ NMR of **2m**



## Chapter 2: Synthesis of Pyrazines

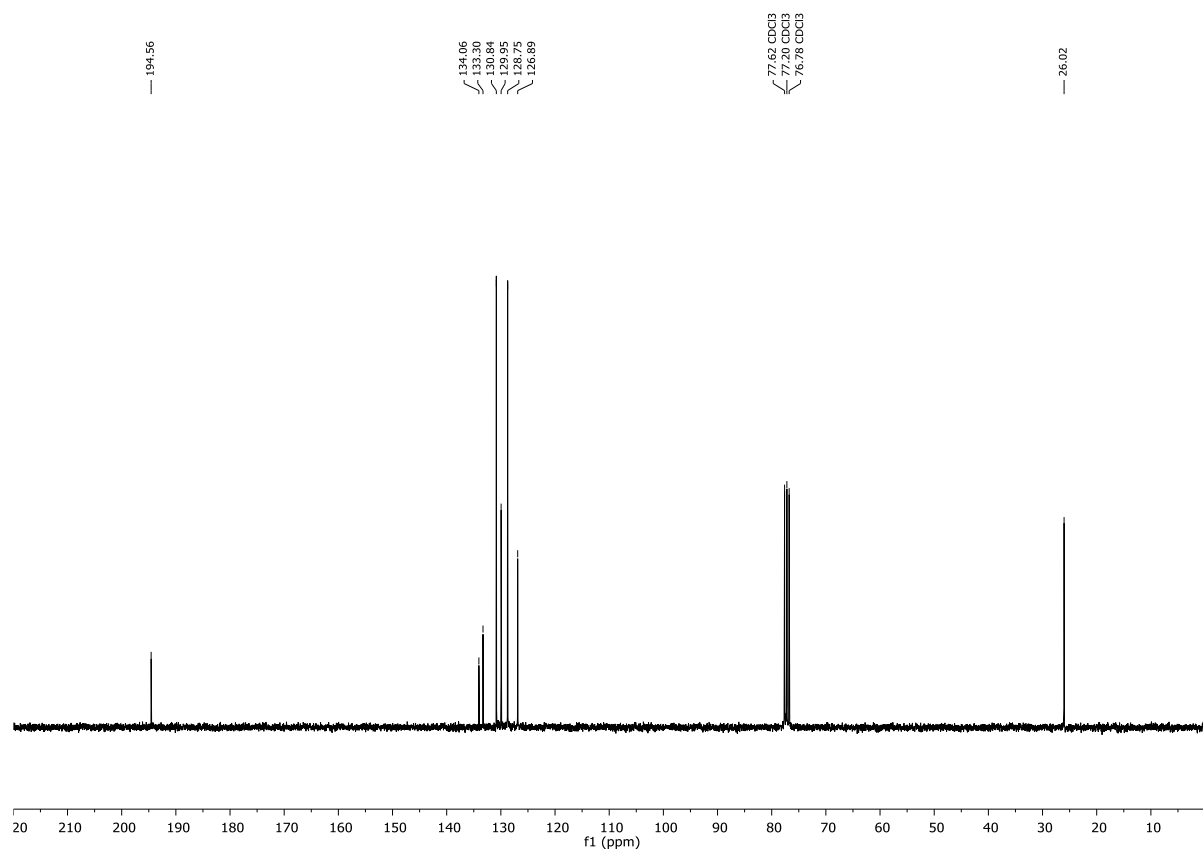
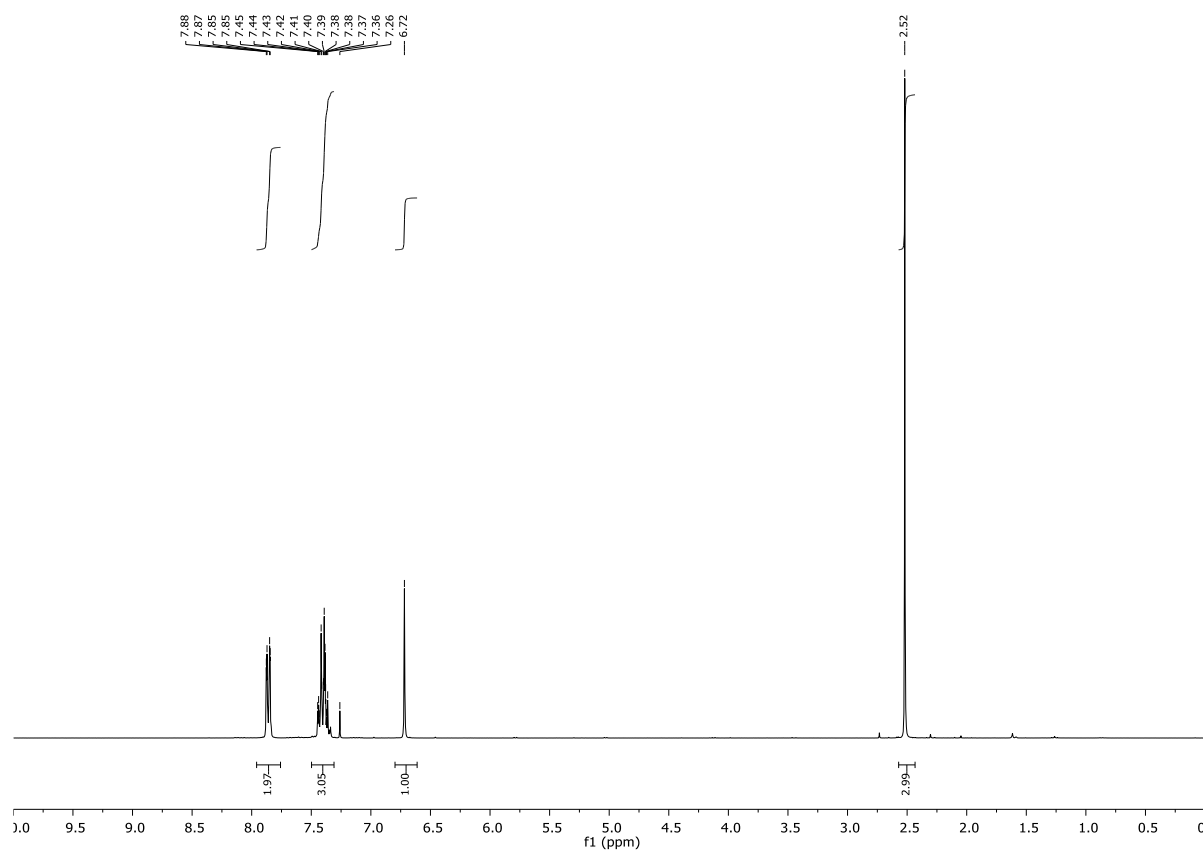
### $^1\text{H}$ and $^{13}\text{C}$ NMR of **2n**





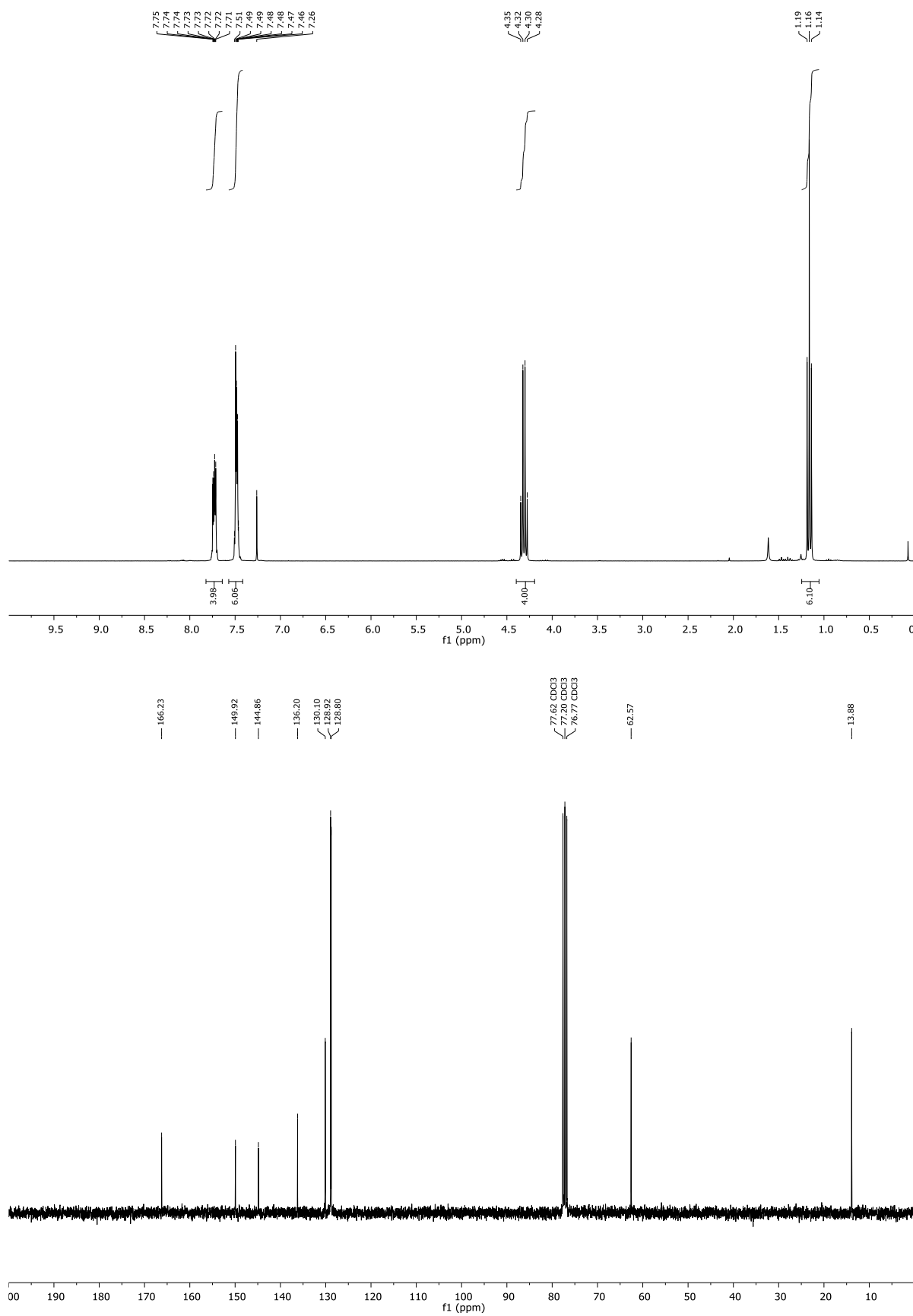
## Chapter 2: Synthesis of Pyrazines

### $^1\text{H}$ and $^{13}\text{C}$ NMR of **2o**



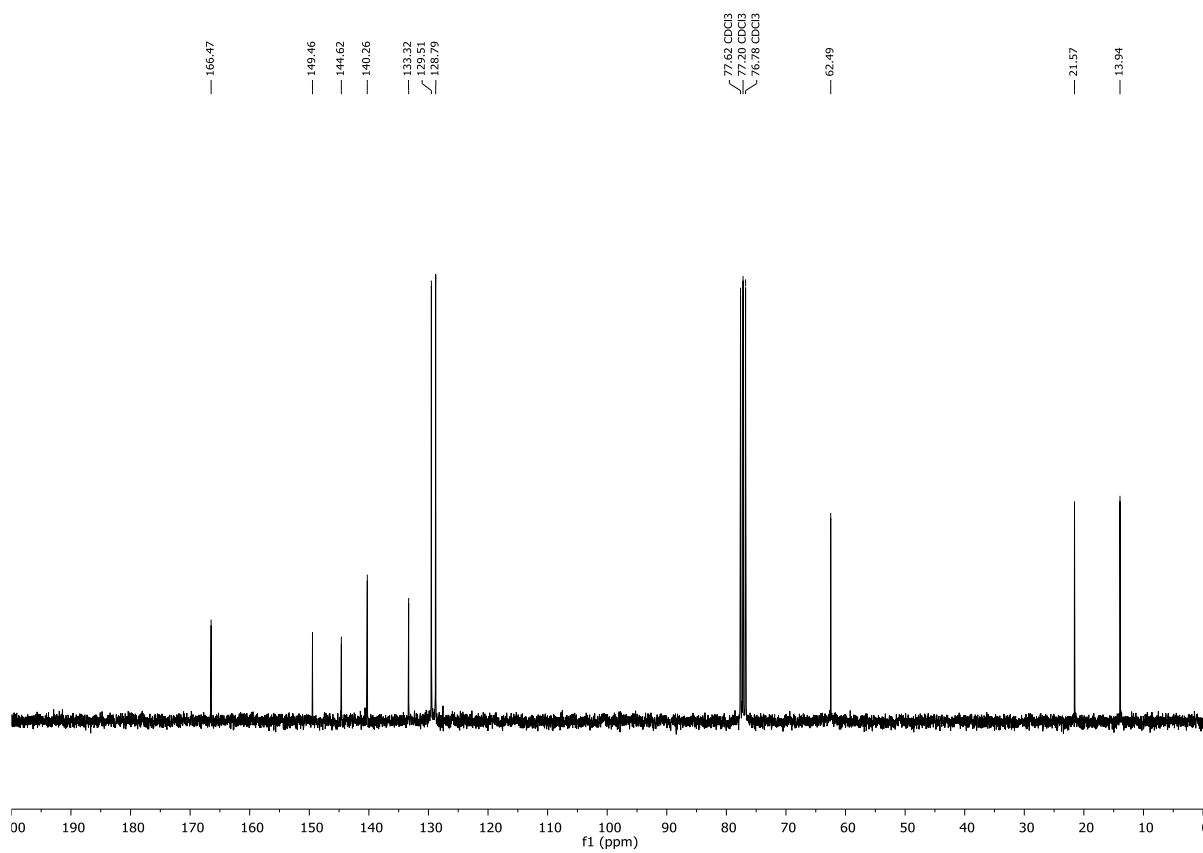
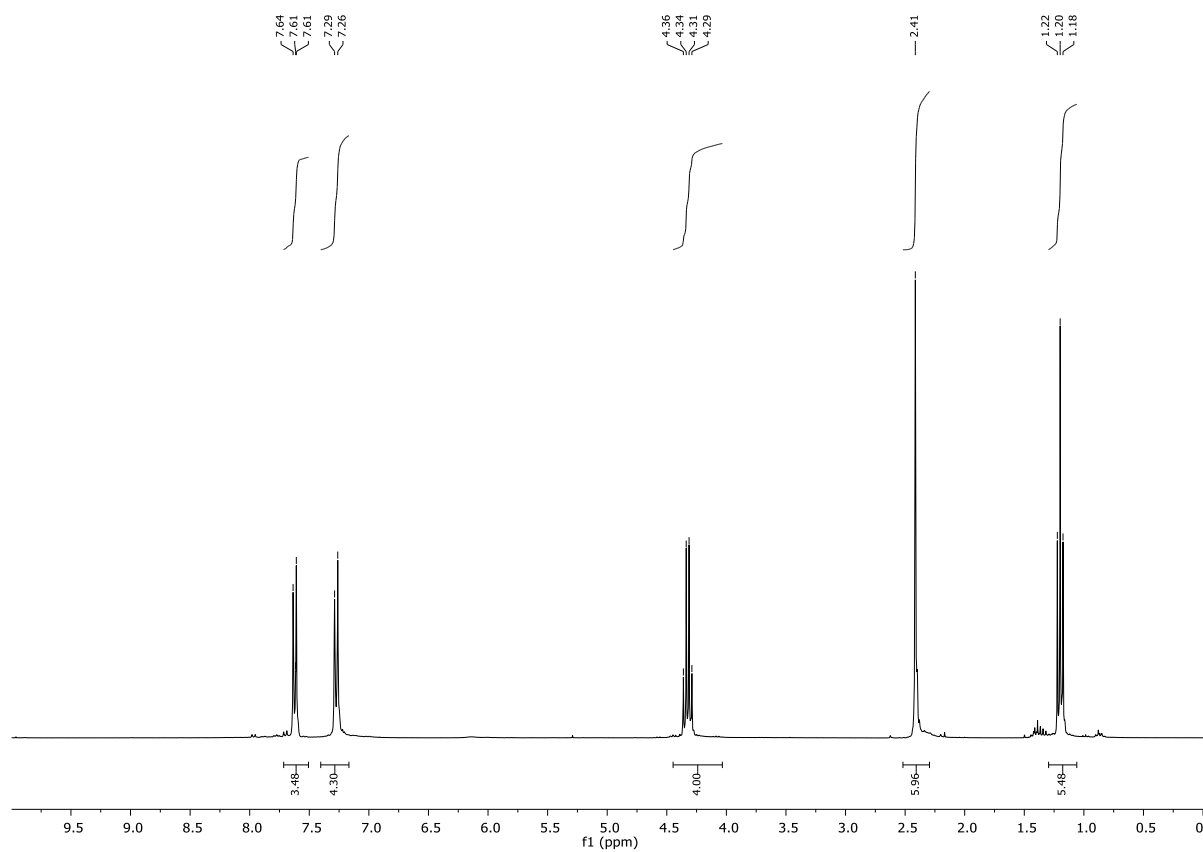
## Chapter 2: Synthesis of Pyrazines

### $^1\text{H}$ and $^{13}\text{C}$ NMR of **3a**



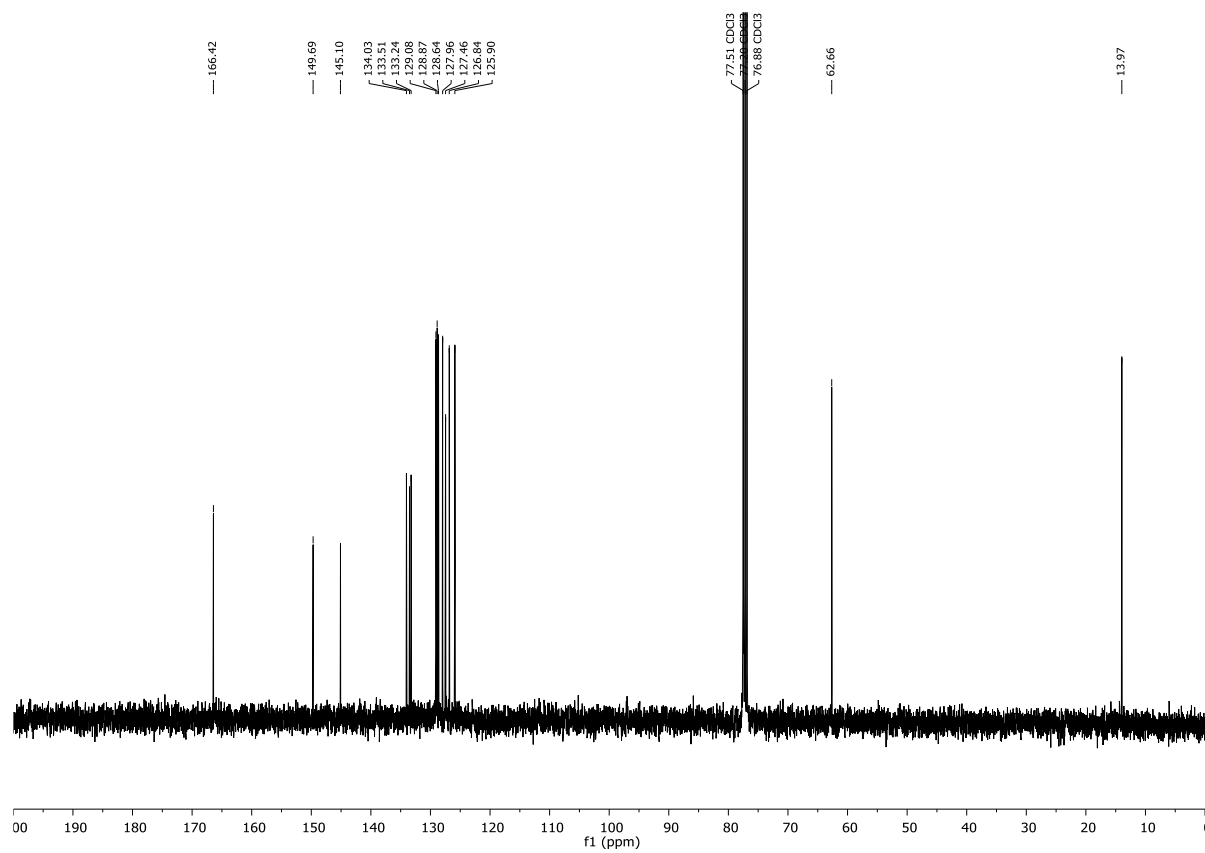
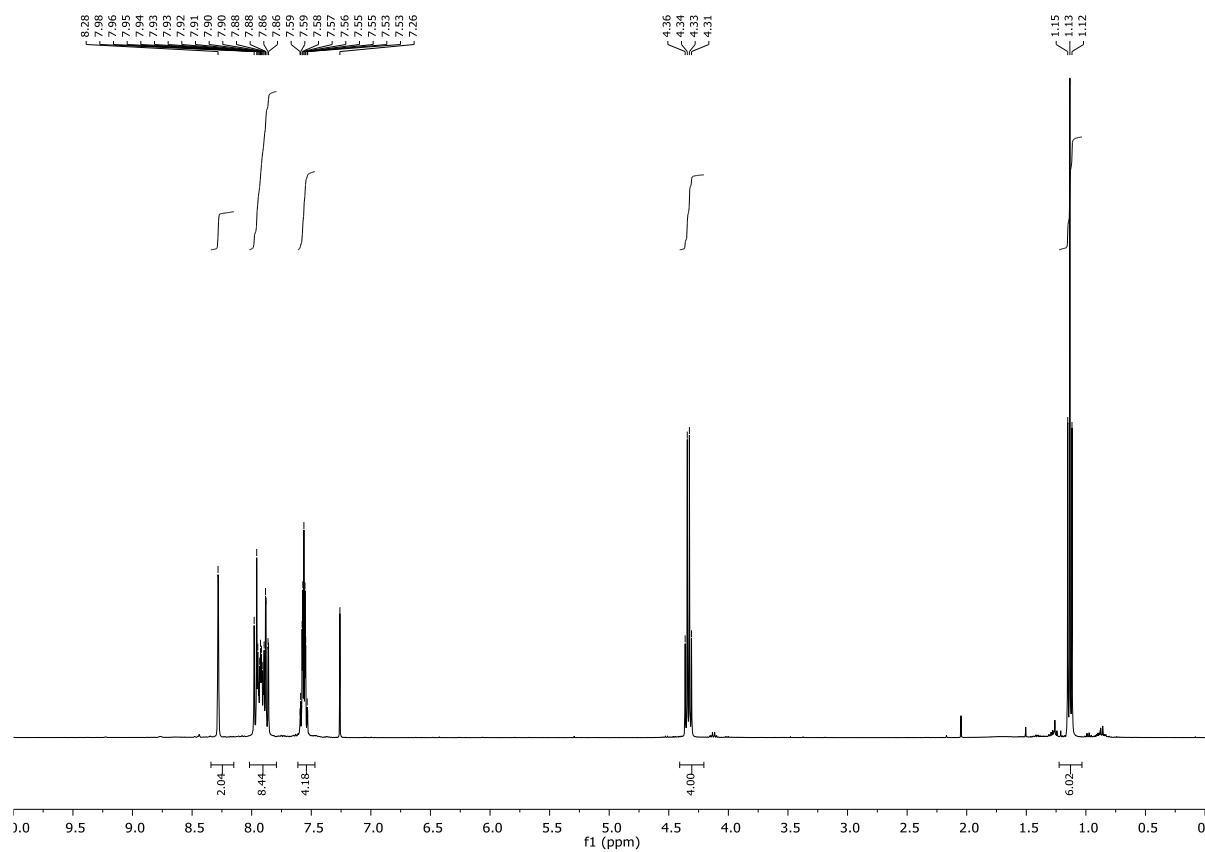
## Chapter 2: Synthesis of Pyrazines

### $^1\text{H}$ and $^{13}\text{C}$ NMR of **3b**



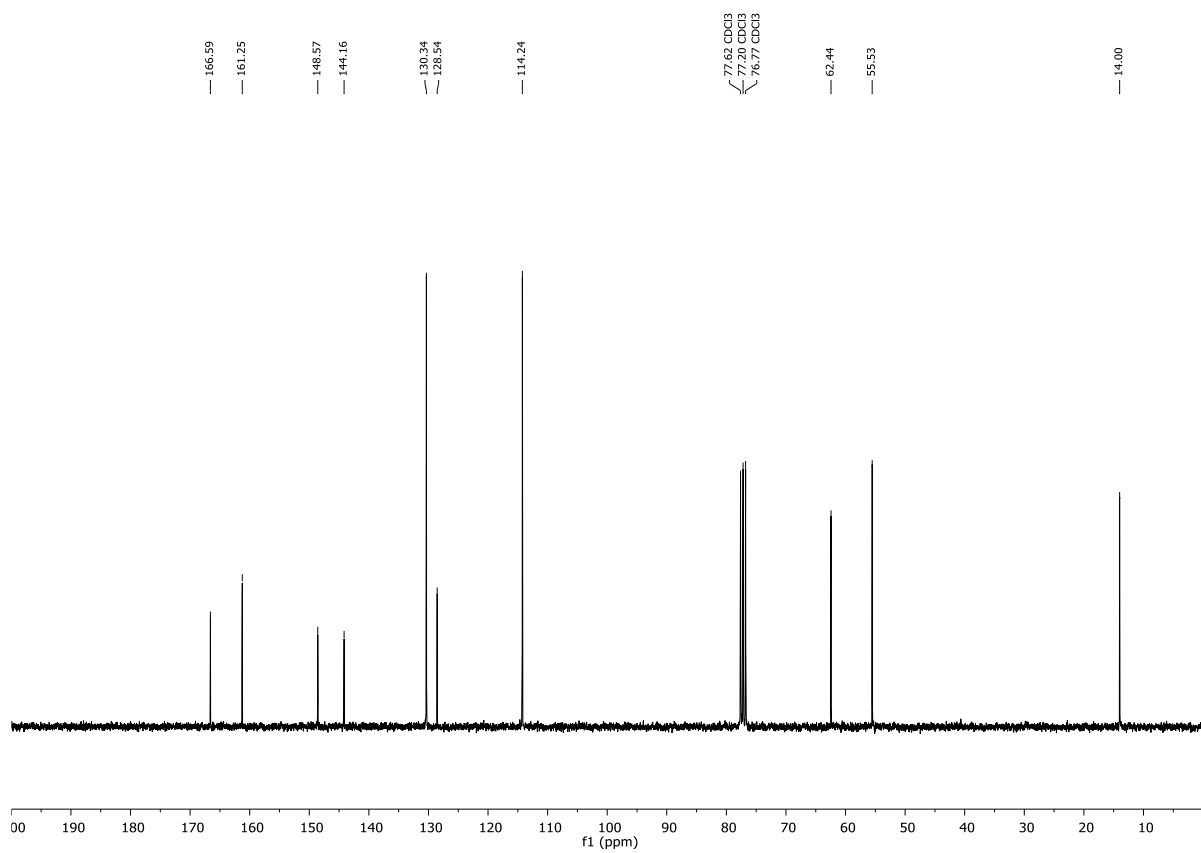
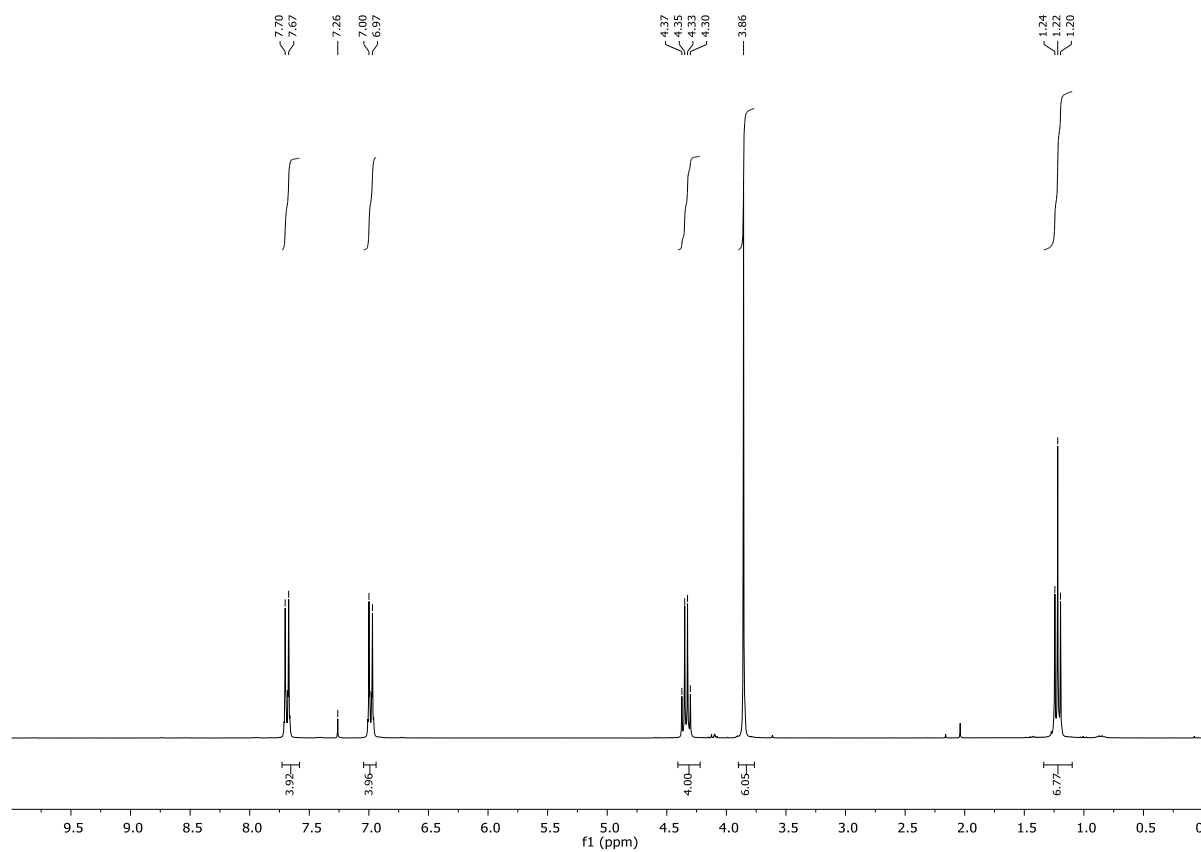
## Chapter 2: Synthesis of Pyrazines

### $^1\text{H}$ and $^{13}\text{C}$ NMR of **3c**



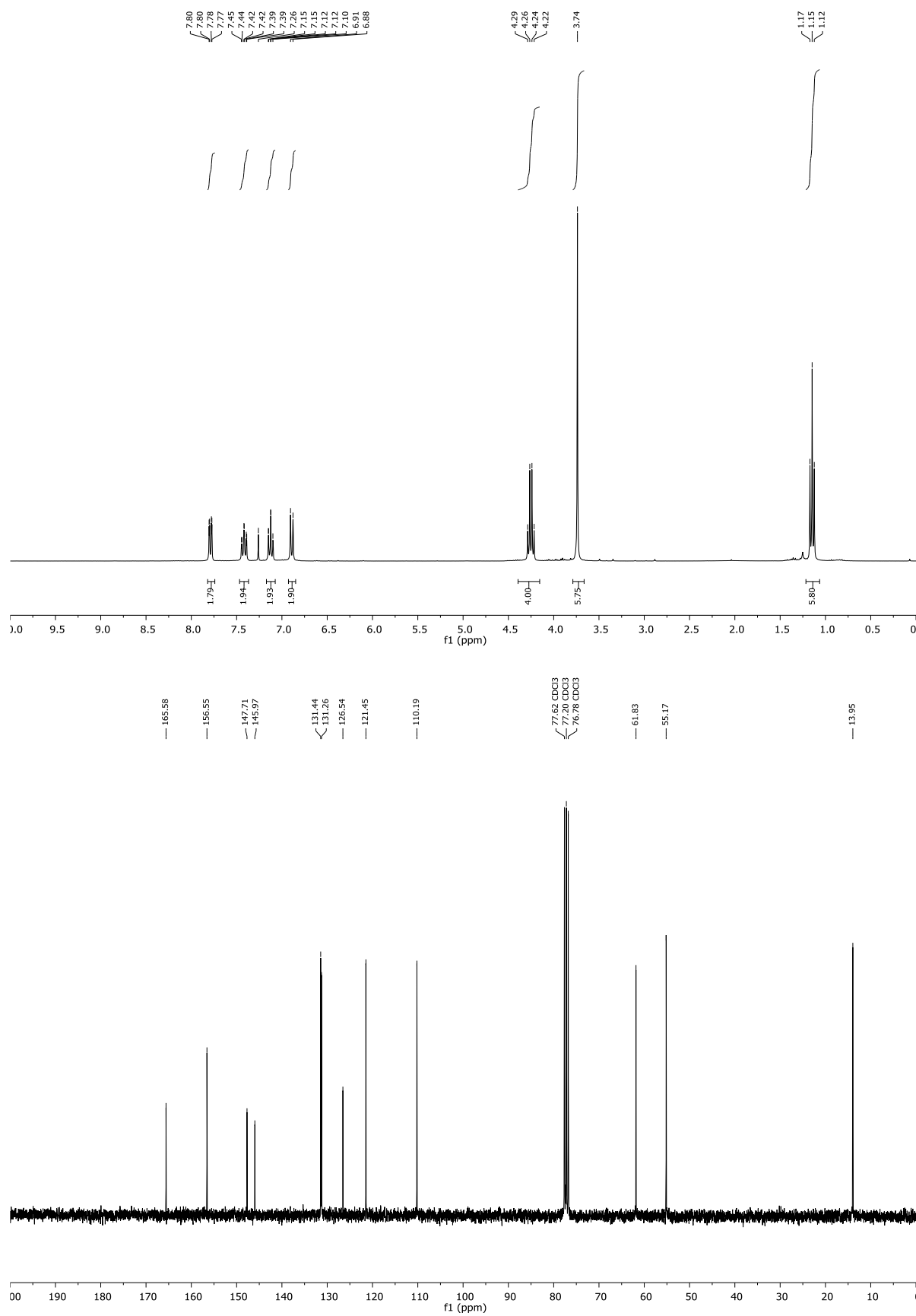
## Chapter 2: Synthesis of Pyrazines

### $^1\text{H}$ and $^{13}\text{C}$ NMR of **3d**



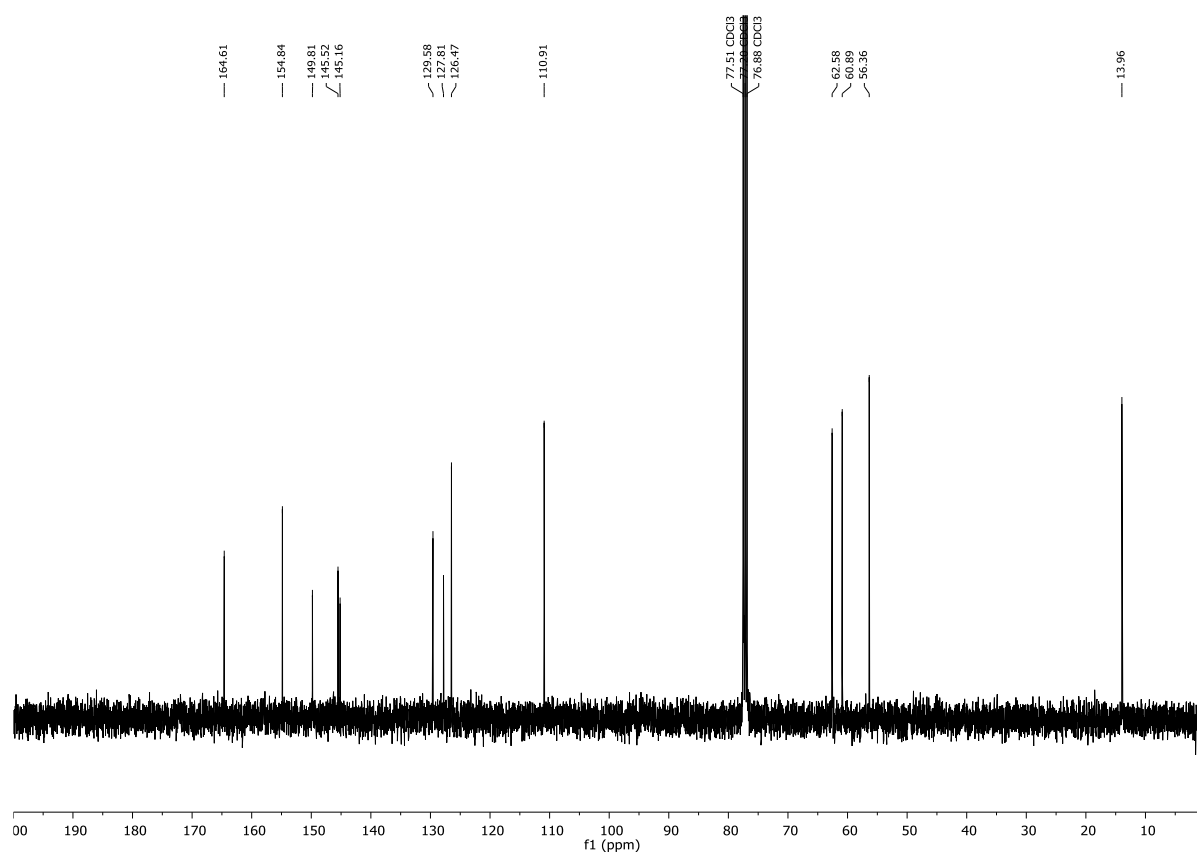
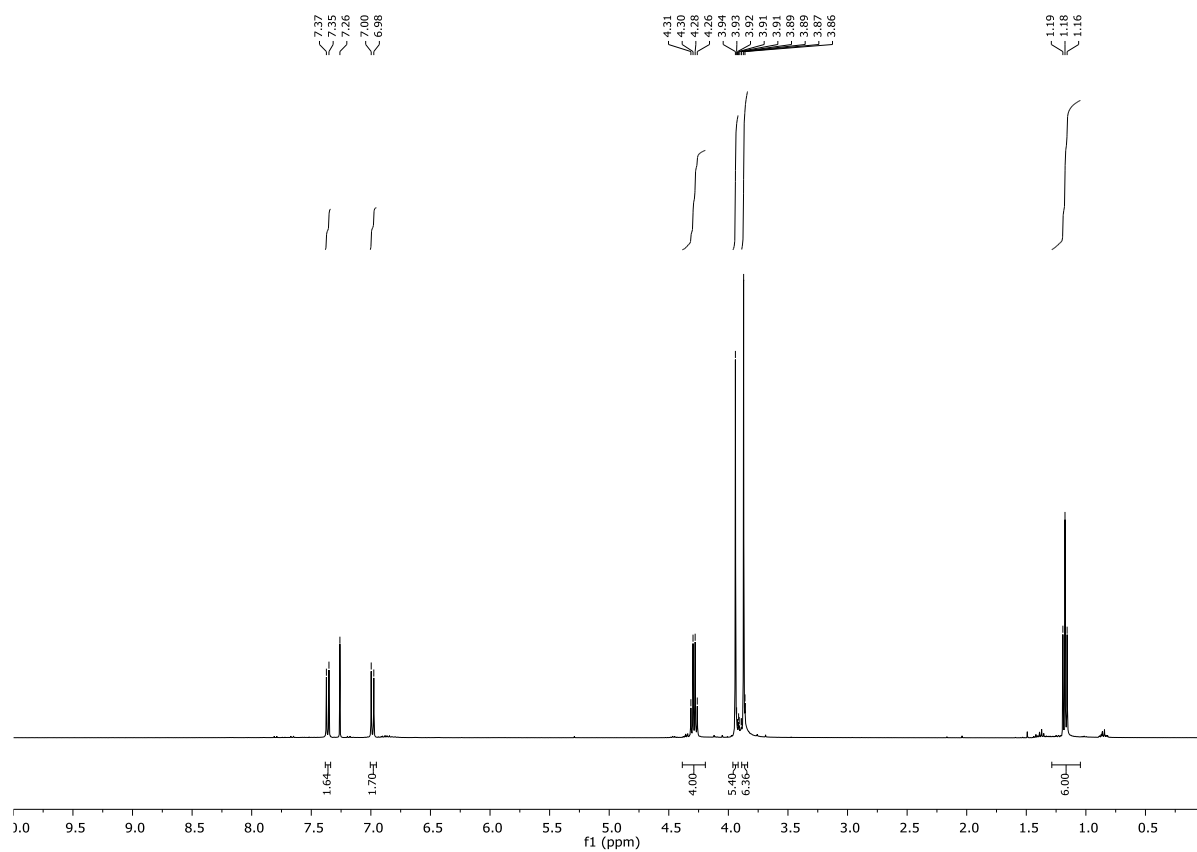
## Chapter 2: Synthesis of Pyrazines

### $^1\text{H}$ and $^{13}\text{C}$ NMR of **3e**



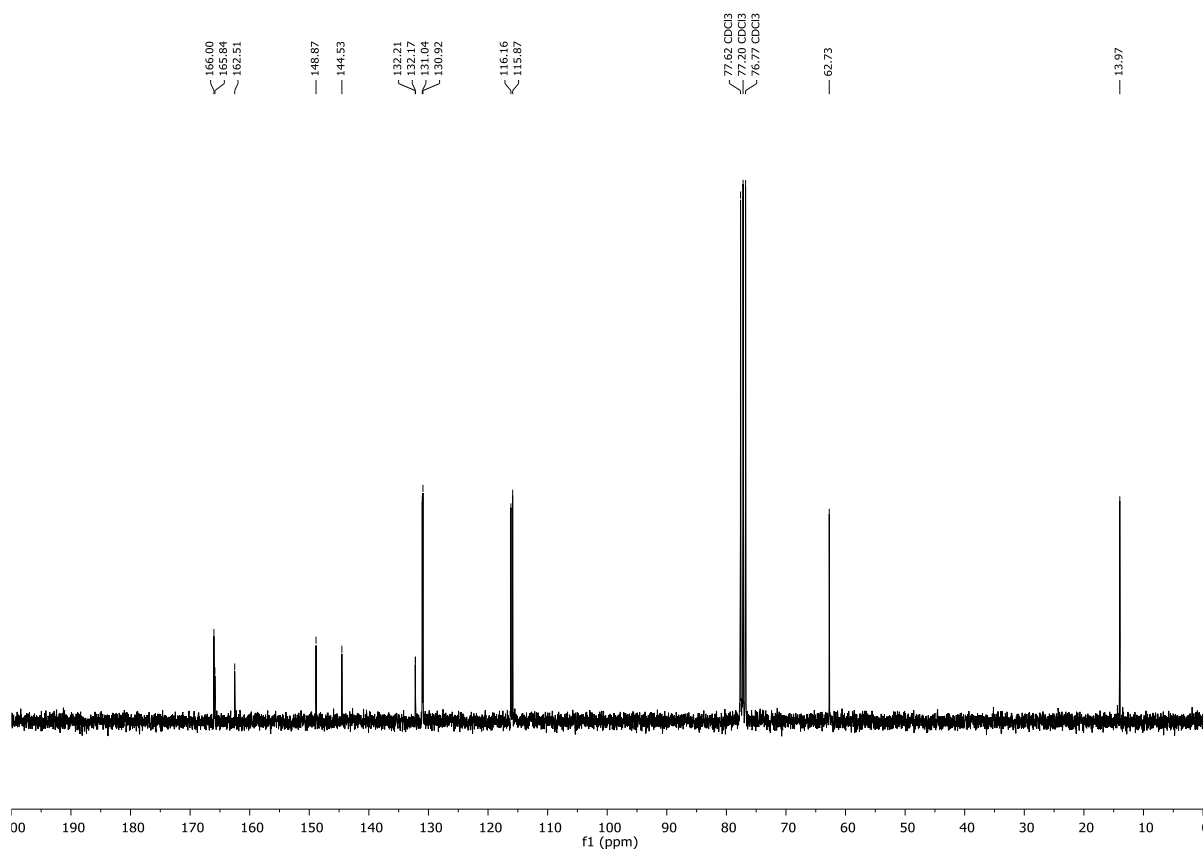
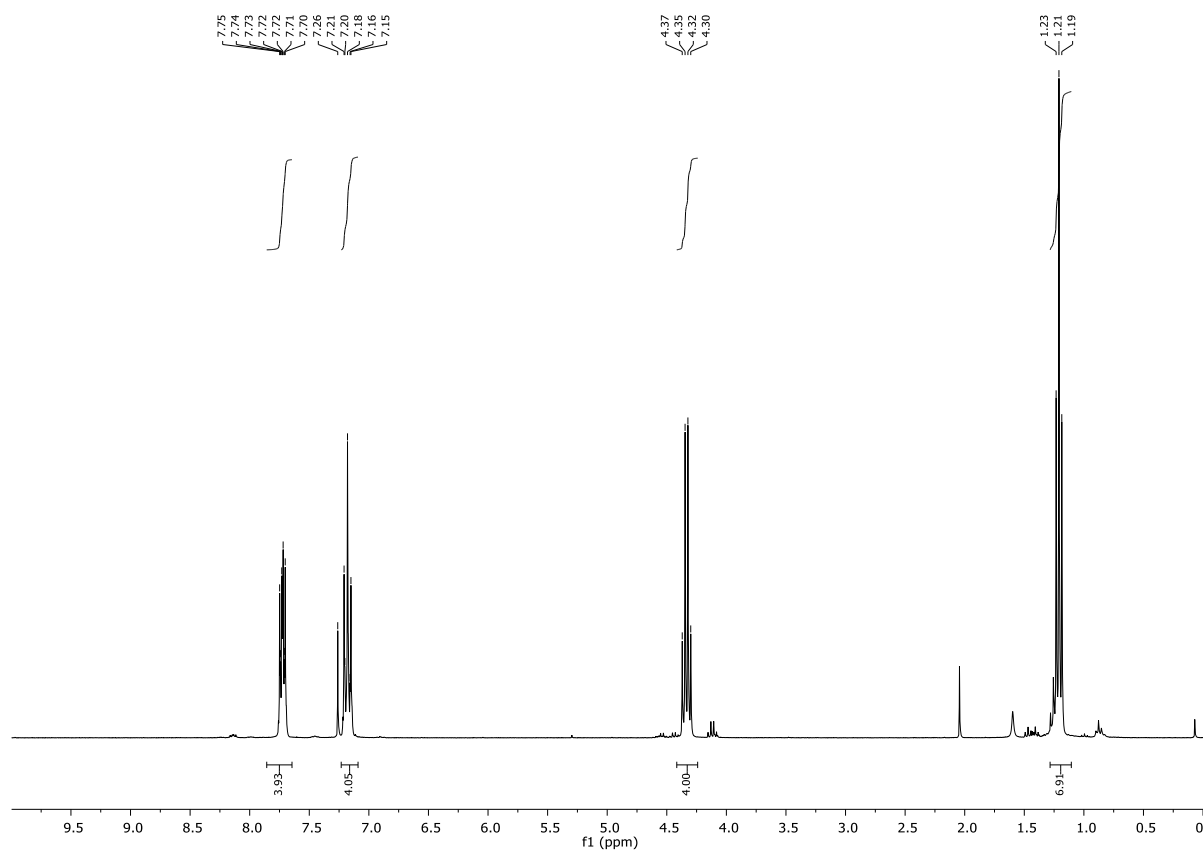
## Chapter 2: Synthesis of Pyrazines

### $^1\text{H}$ and $^{13}\text{C}$ NMR of **3f**



## Chapter 2: Synthesis of Pyrazines

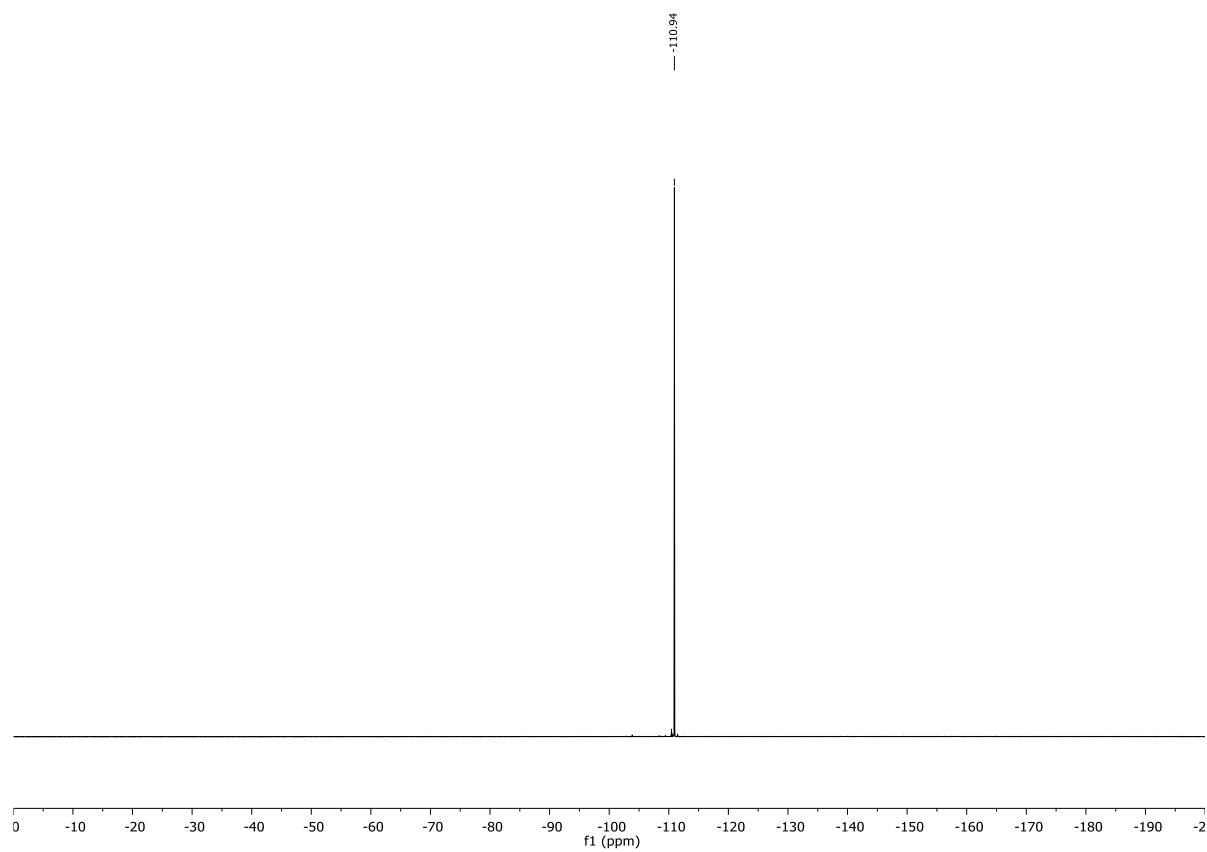
$^1\text{H}$ ,  $^{13}\text{C}$  and  $^{19}\text{F}$  NMR of **3g**





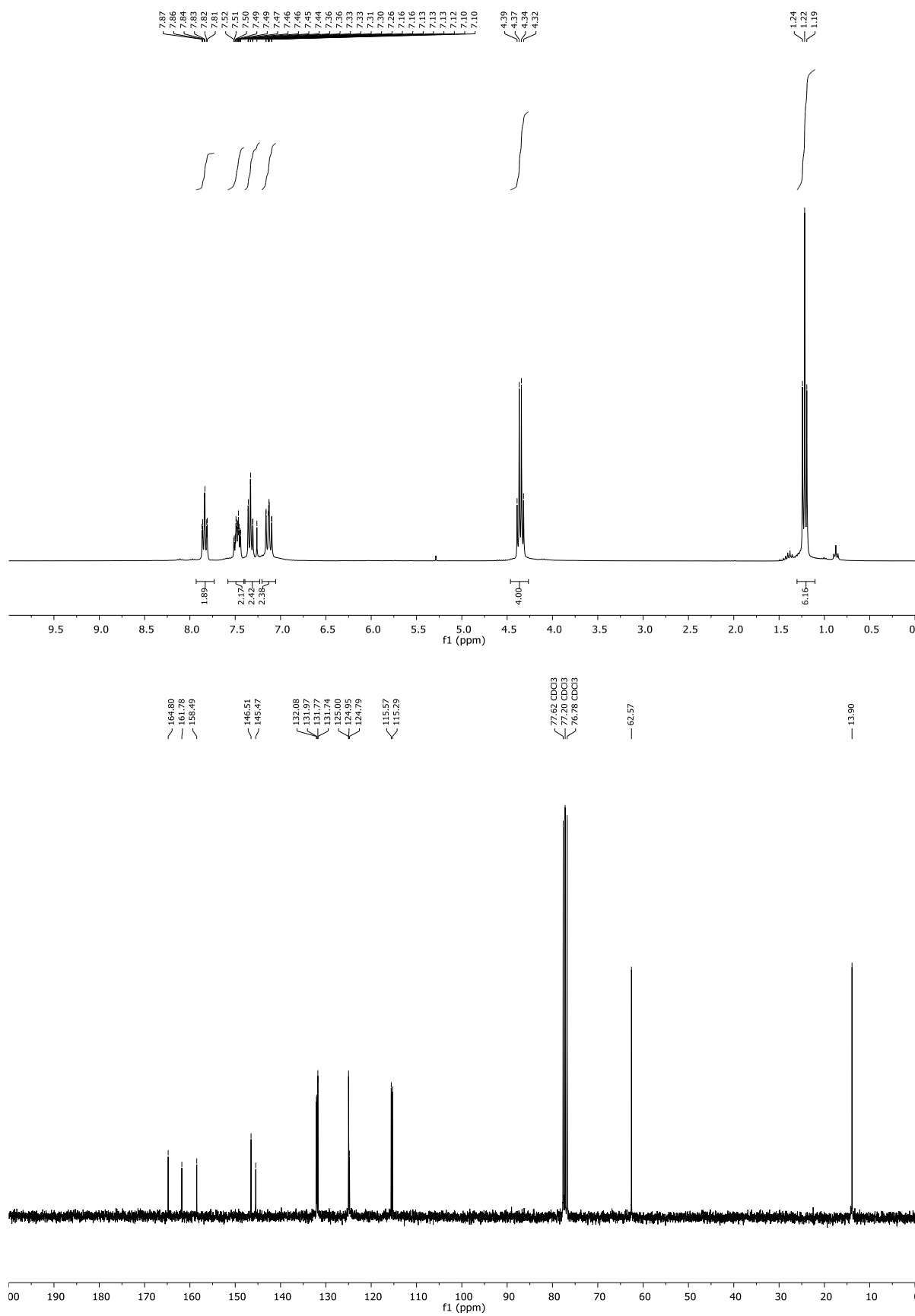
## Chapter 2: Synthesis of Pyrazines

---



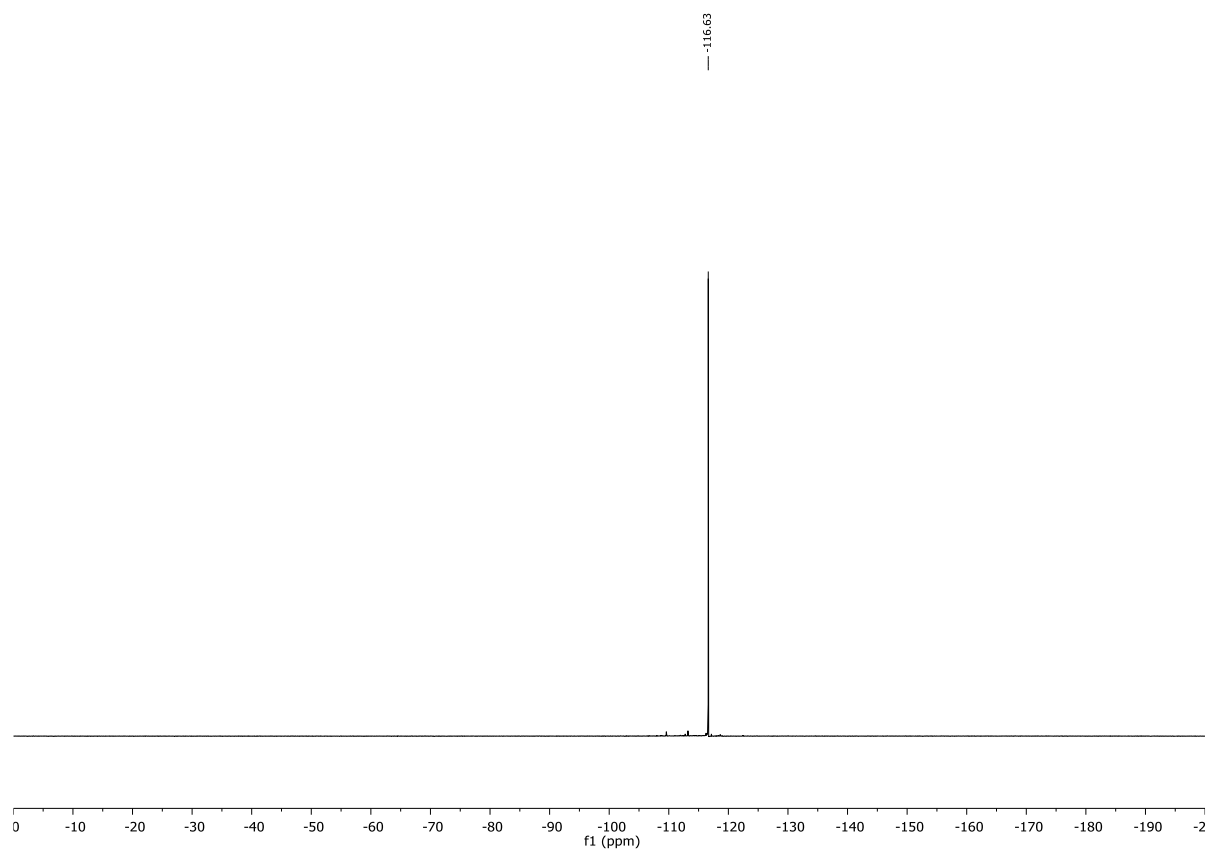
## Chapter 2: Synthesis of Pyrazines

### $^1\text{H}$ , $^{13}\text{C}$ and $^{19}\text{F}$ NMR of **3h**



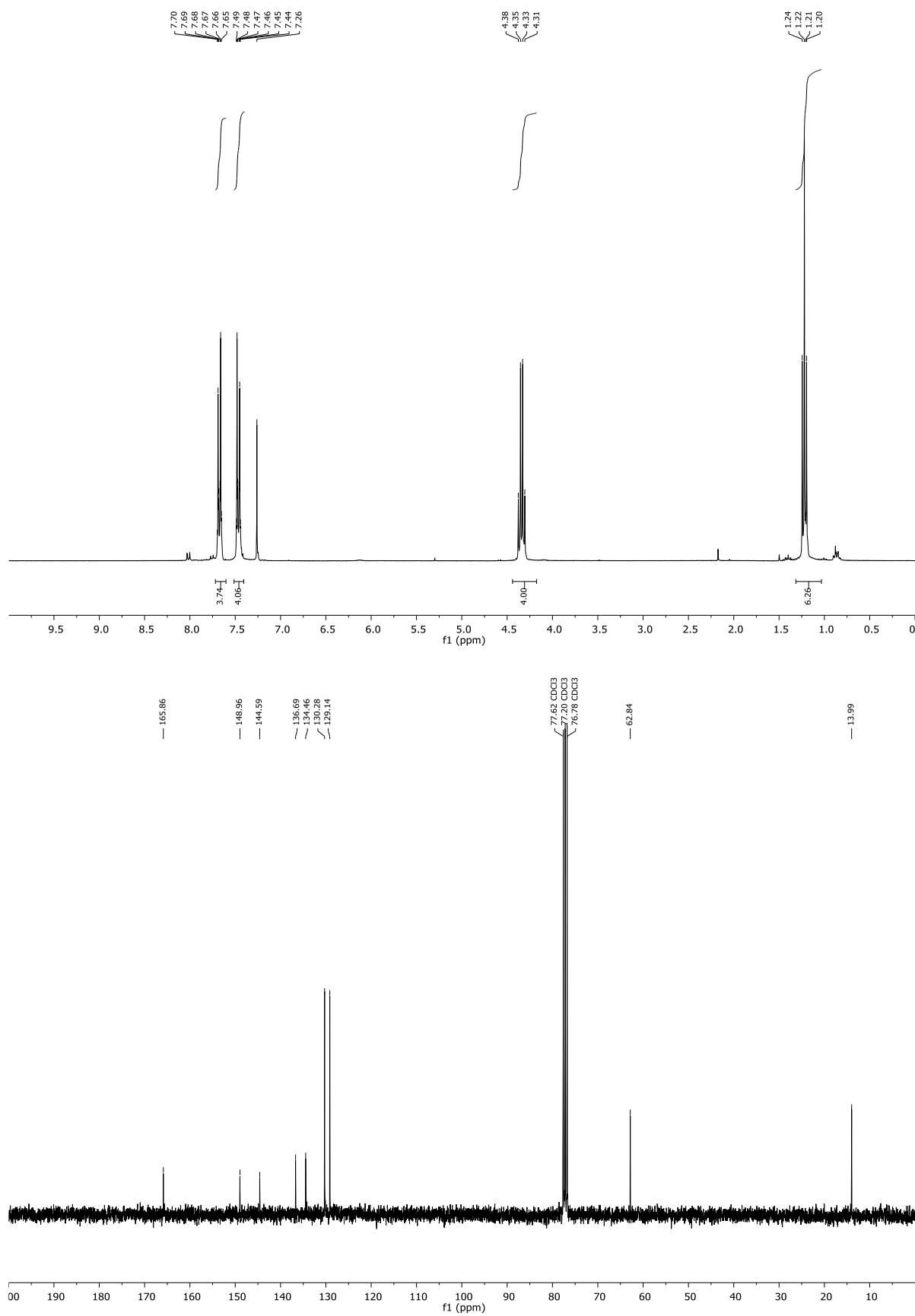
## Chapter 2: Synthesis of Pyrazines

---



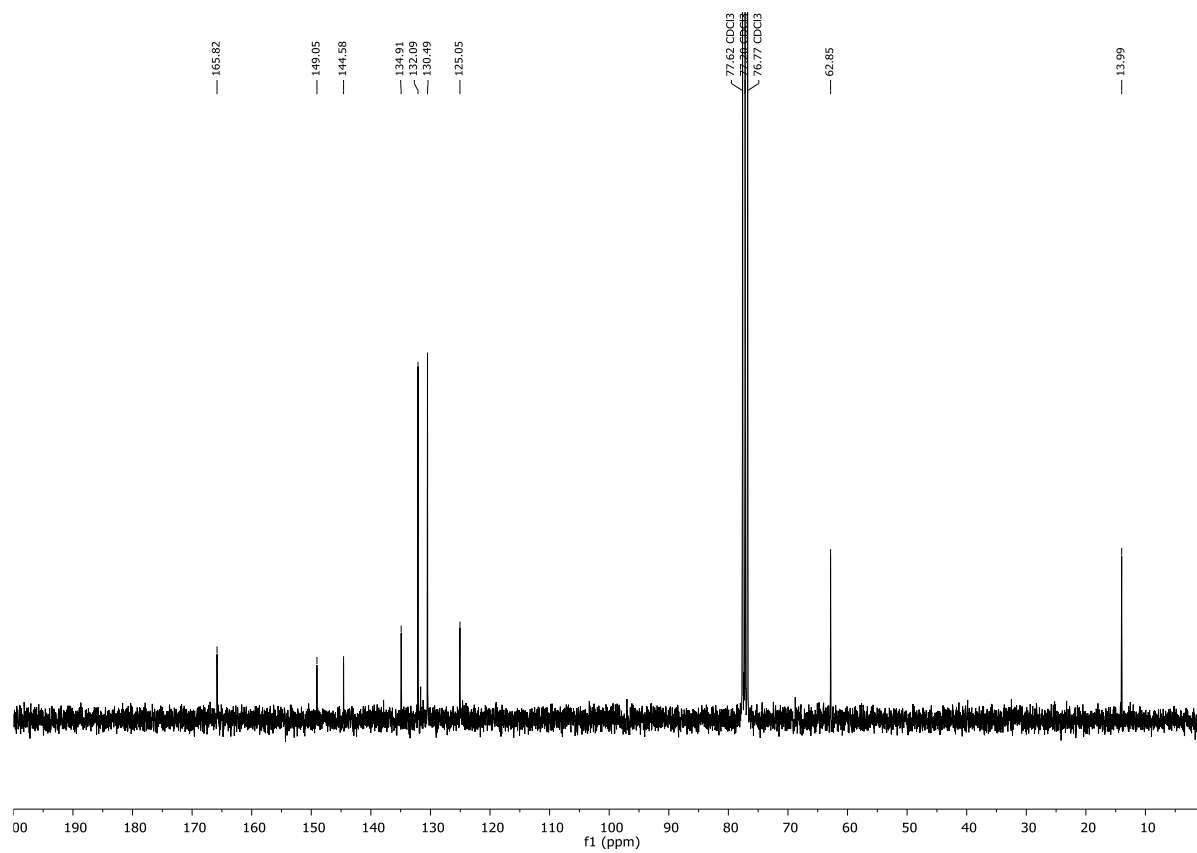
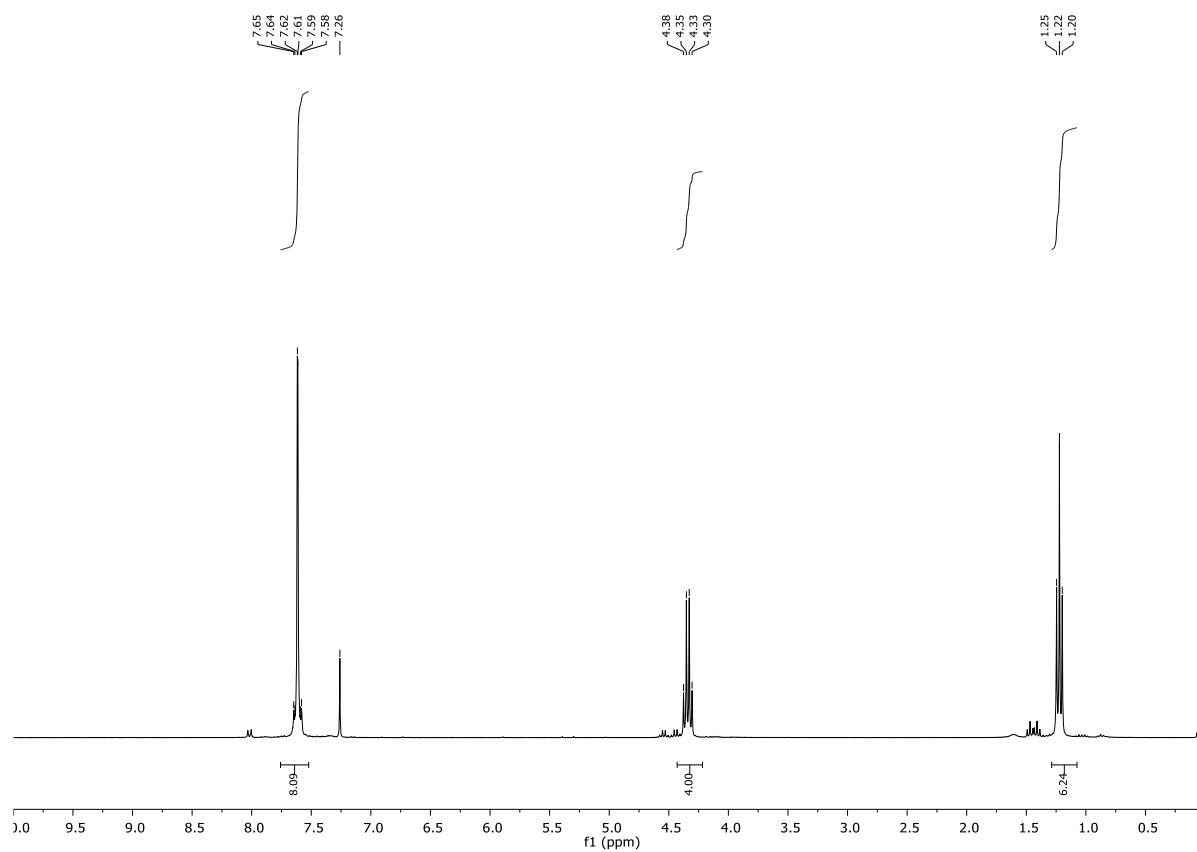
## Chapter 2: Synthesis of Pyrazines

### $^1\text{H}$ and $^{13}\text{C}$ NMR of **3i**



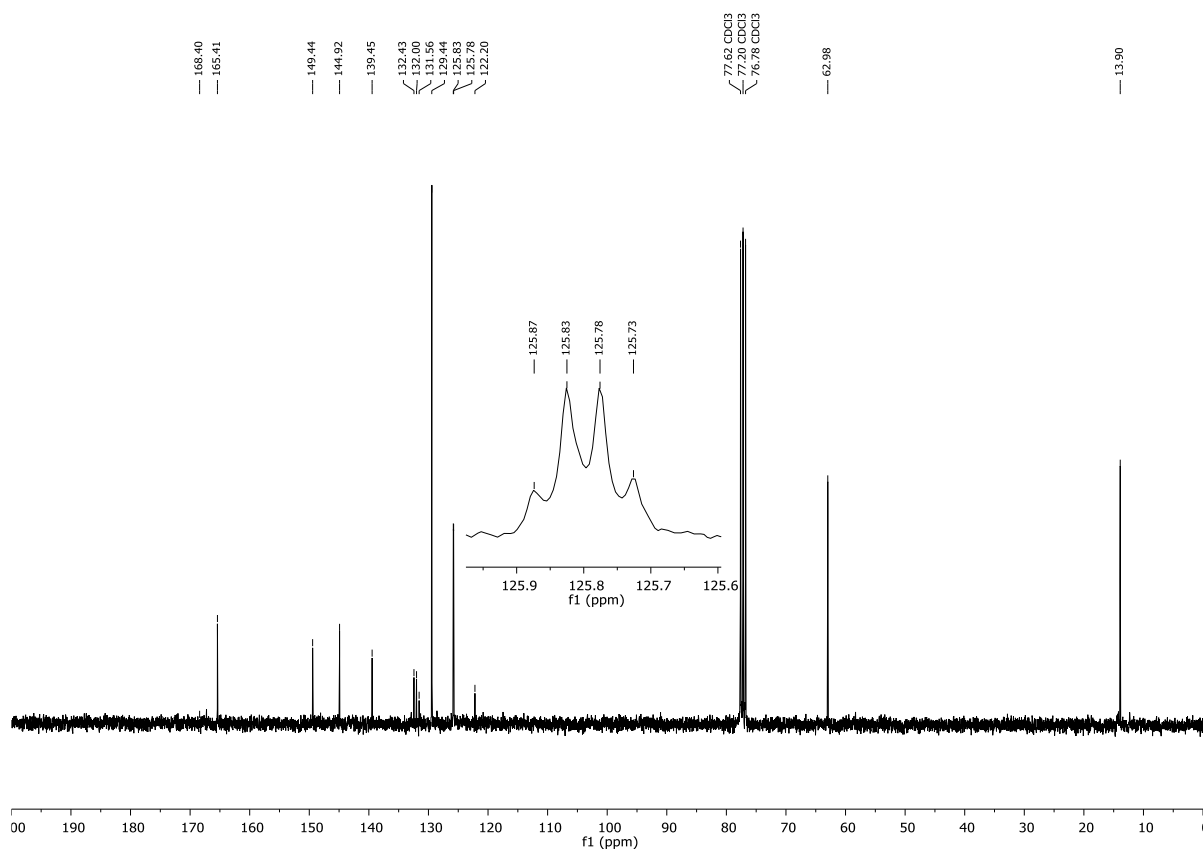
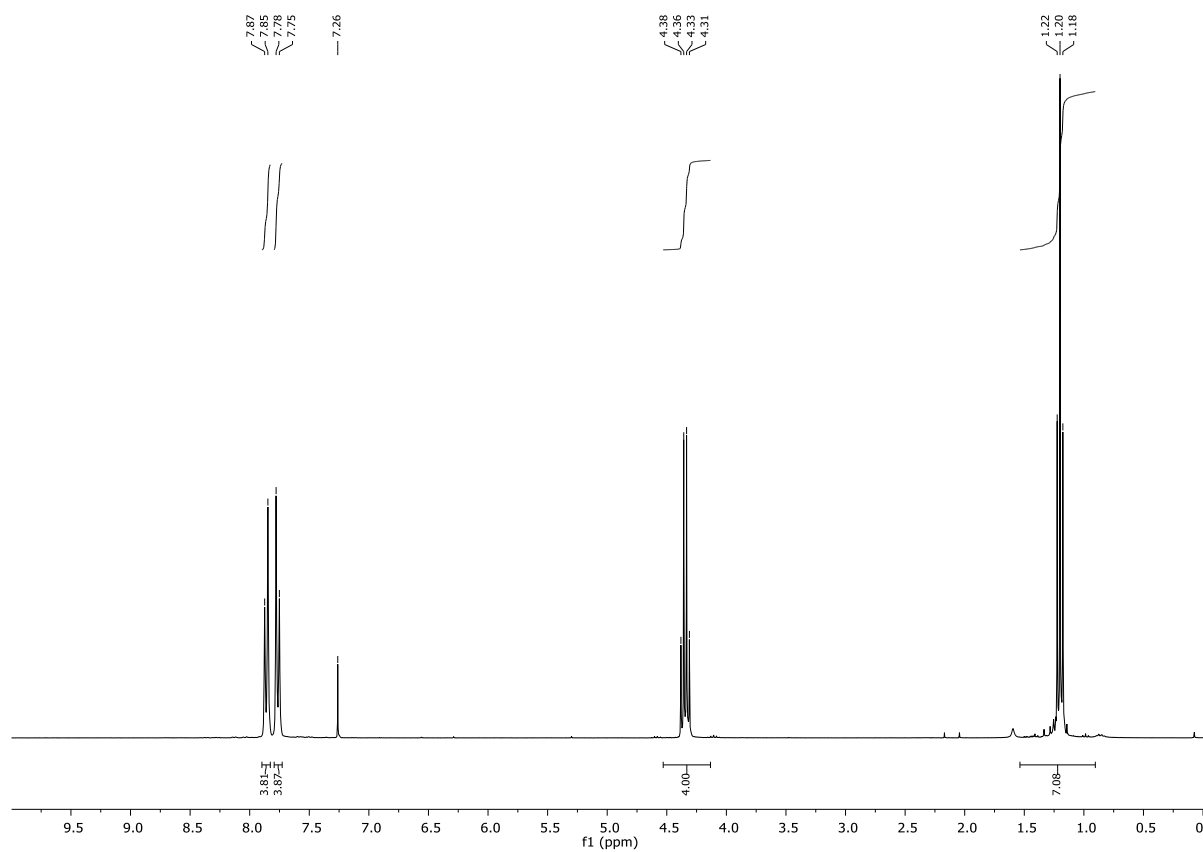
## Chapter 2: Synthesis of Pyrazines

### $^1\text{H}$ and $^{13}\text{C}$ NMR of **3j**



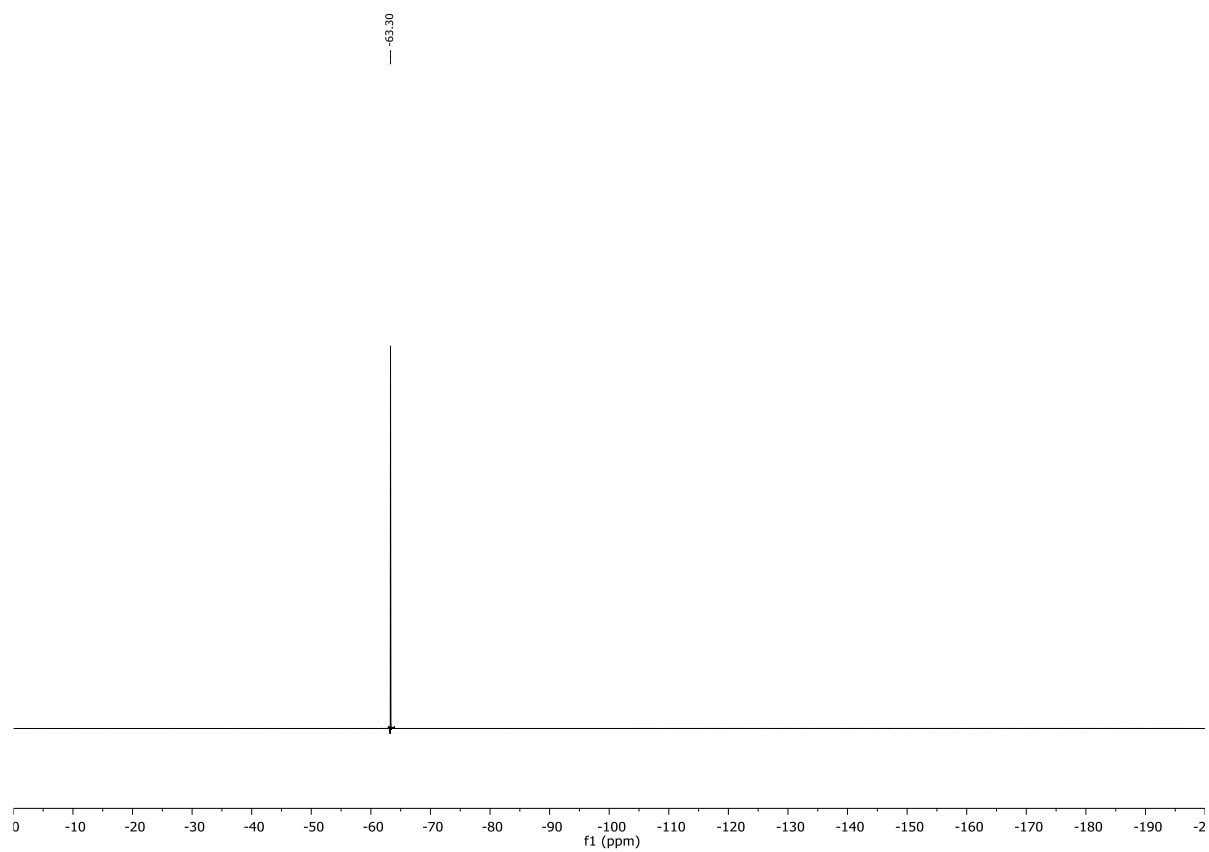
## Chapter 2: Synthesis of Pyrazines

$^1\text{H}$ ,  $^{13}\text{C}$  and  $^{19}\text{F}$  NMR of **3k**

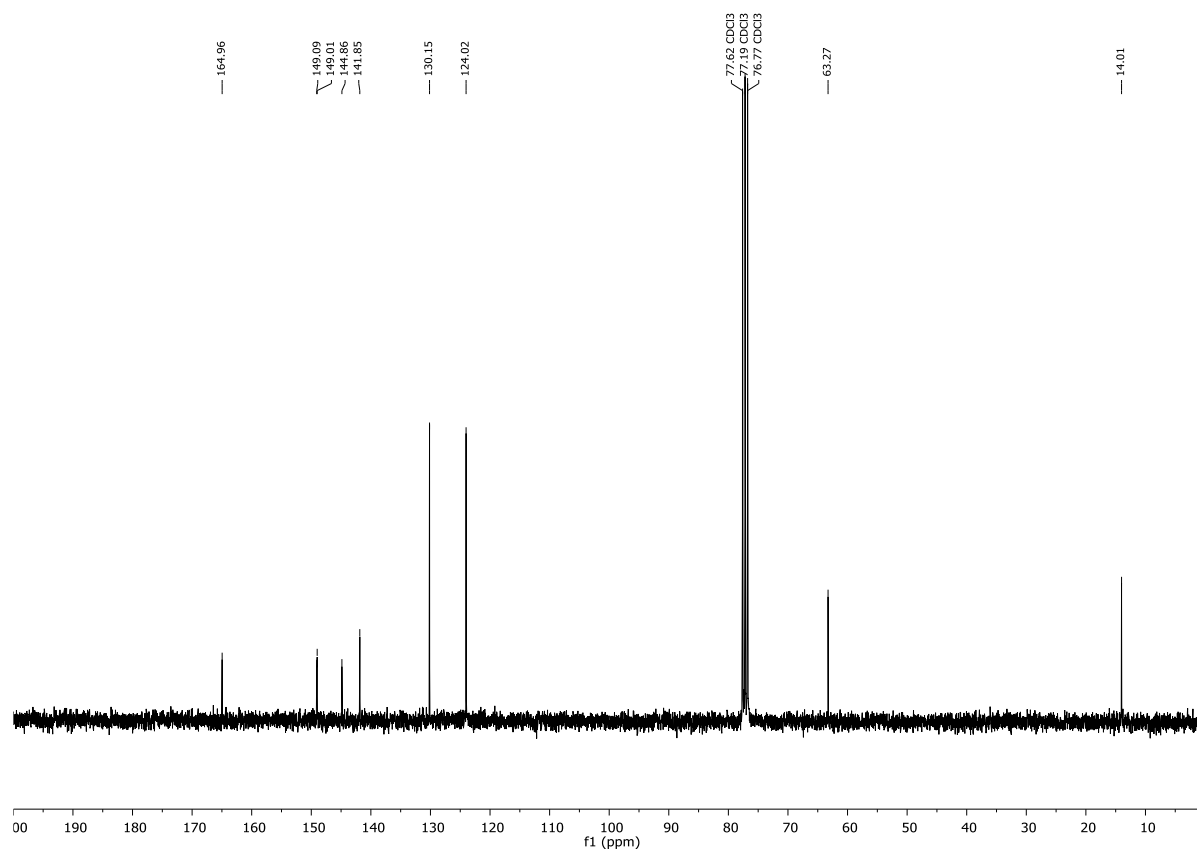
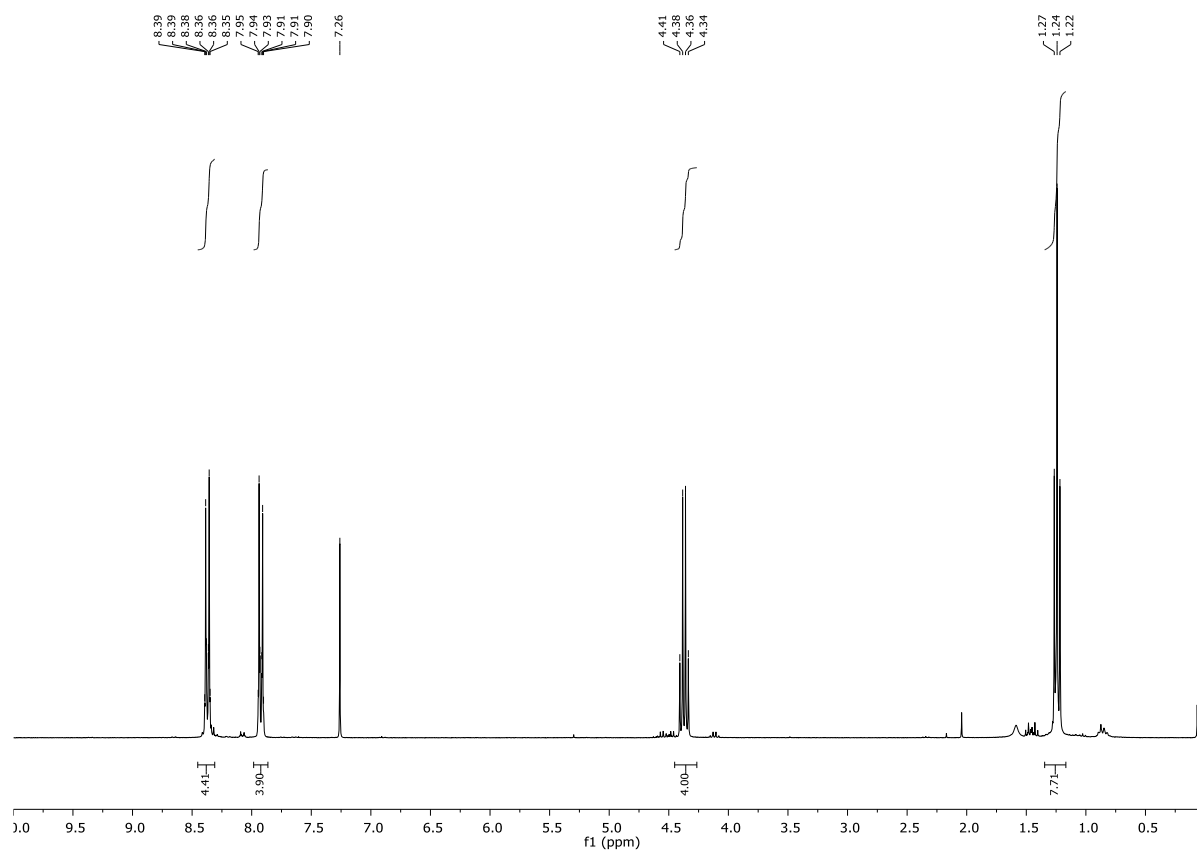


## Chapter 2: Synthesis of Pyrazines

---



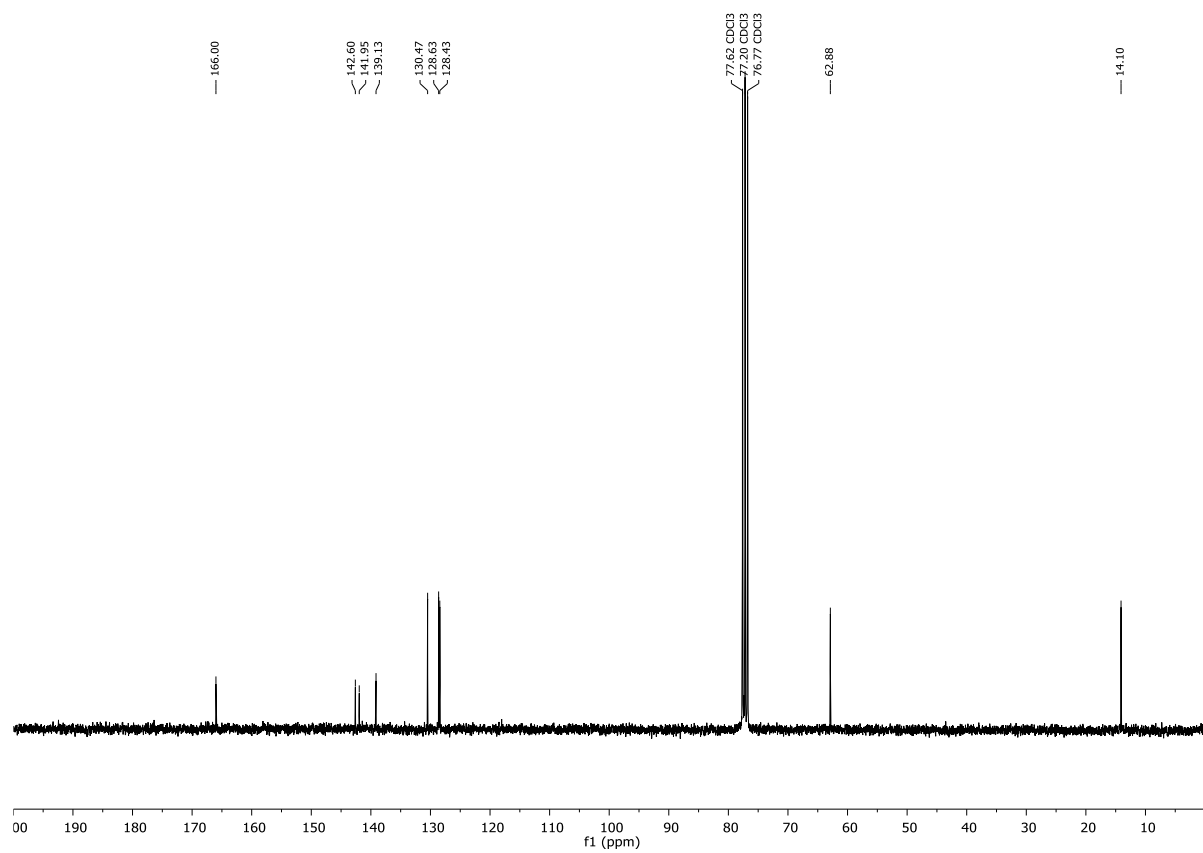
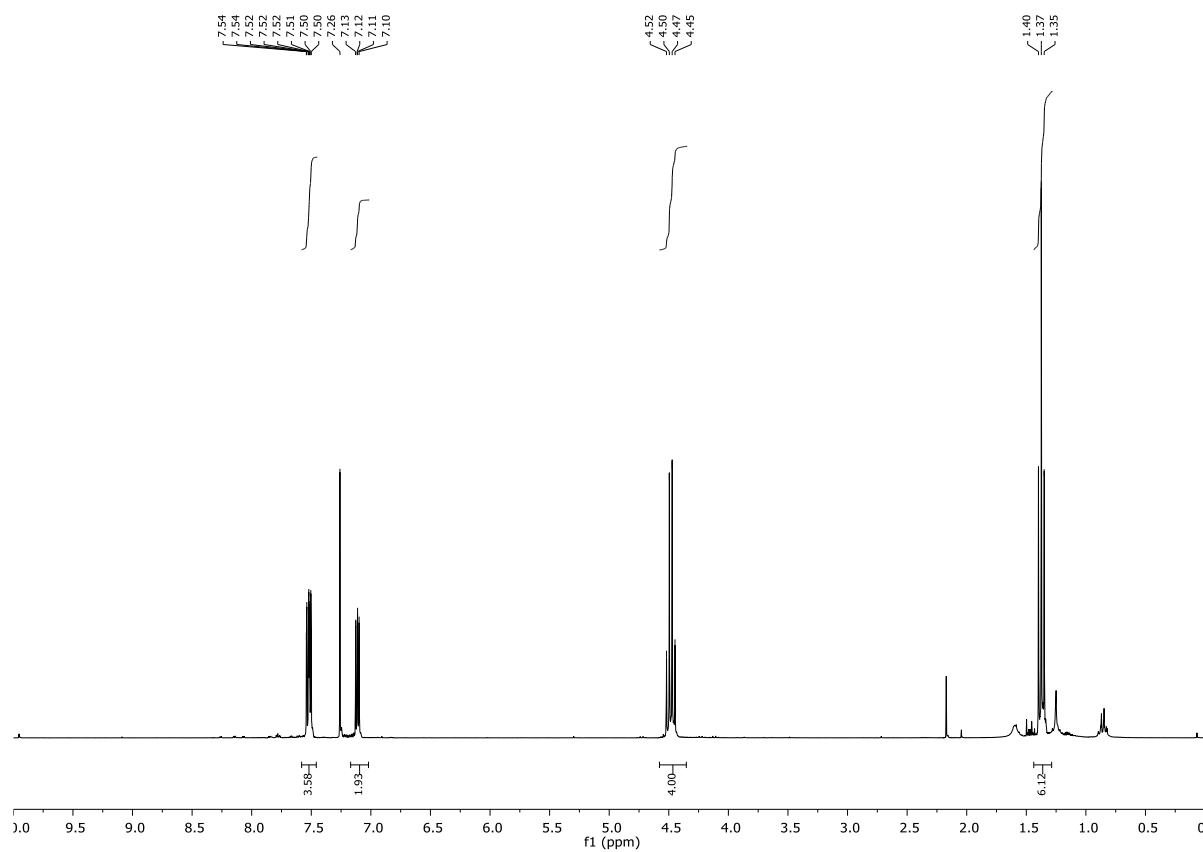
$^1\text{H}$  and  $^{13}\text{C}$  NMR of **31**





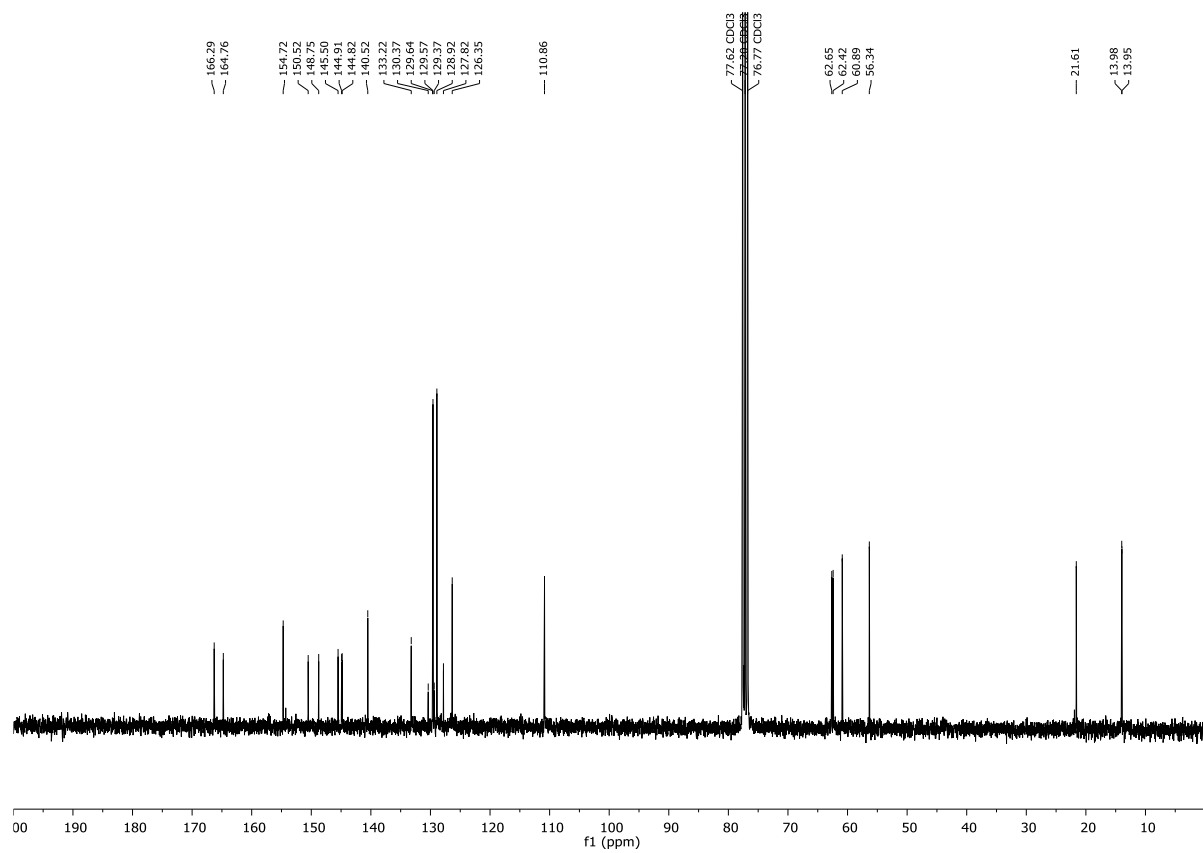
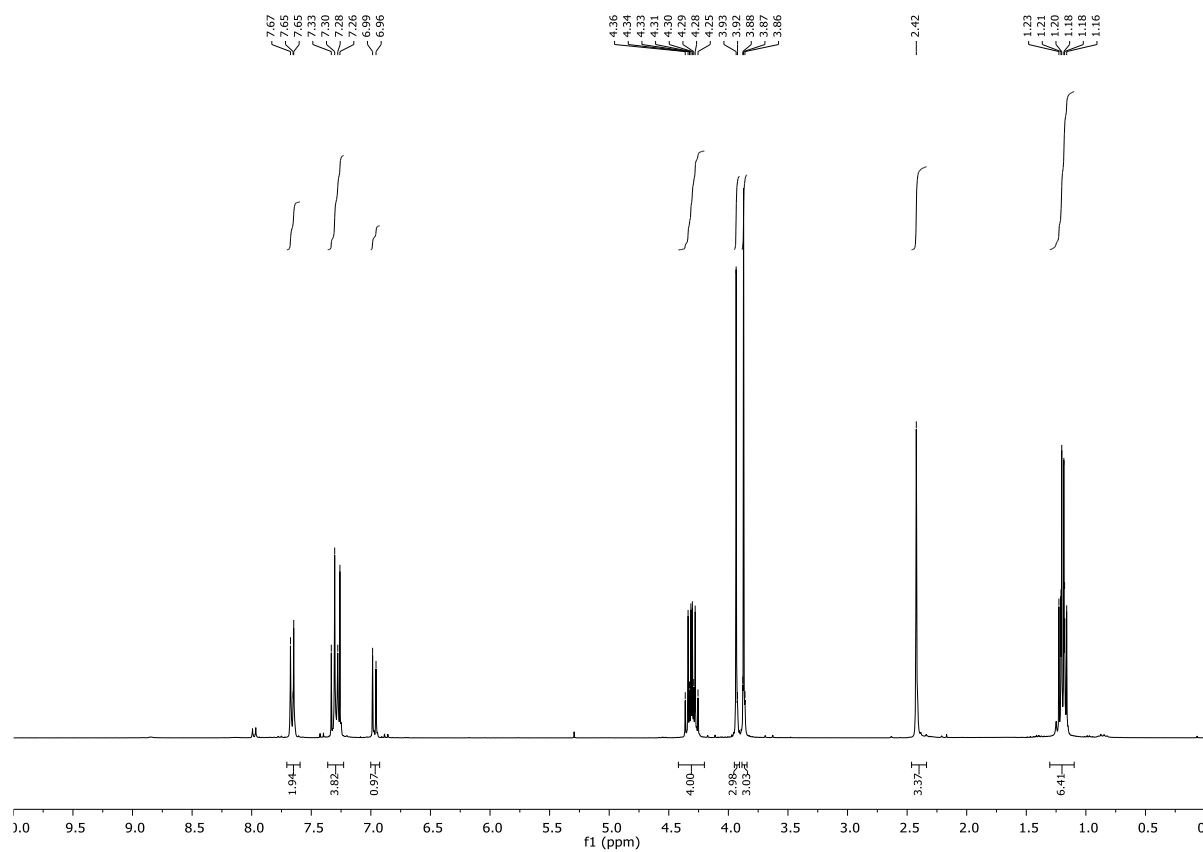
## Chapter 2: Synthesis of Pyrazines

### $^1\text{H}$ and $^{13}\text{C}$ NMR of **3m**



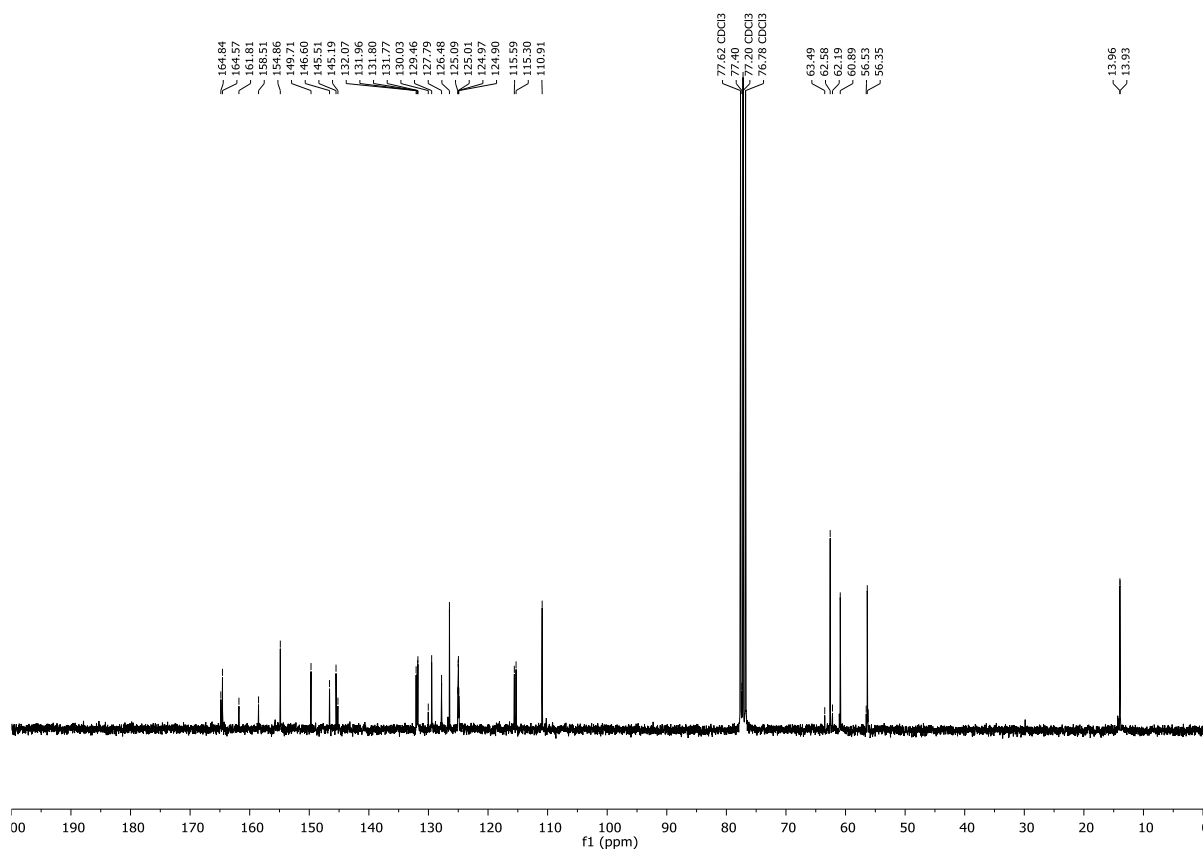
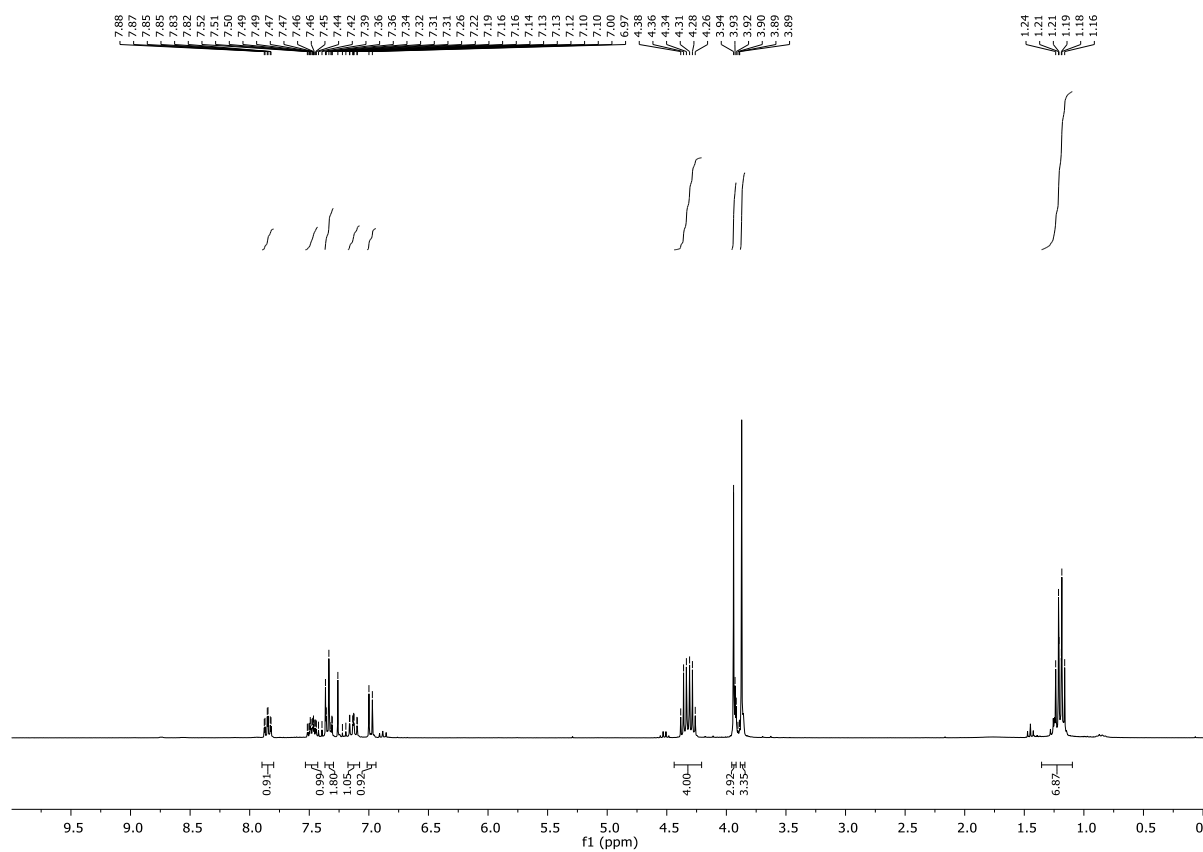
## Chapter 2: Synthesis of Pyrazines

### $^1\text{H}$ and $^{13}\text{C}$ NMR of **3bf**



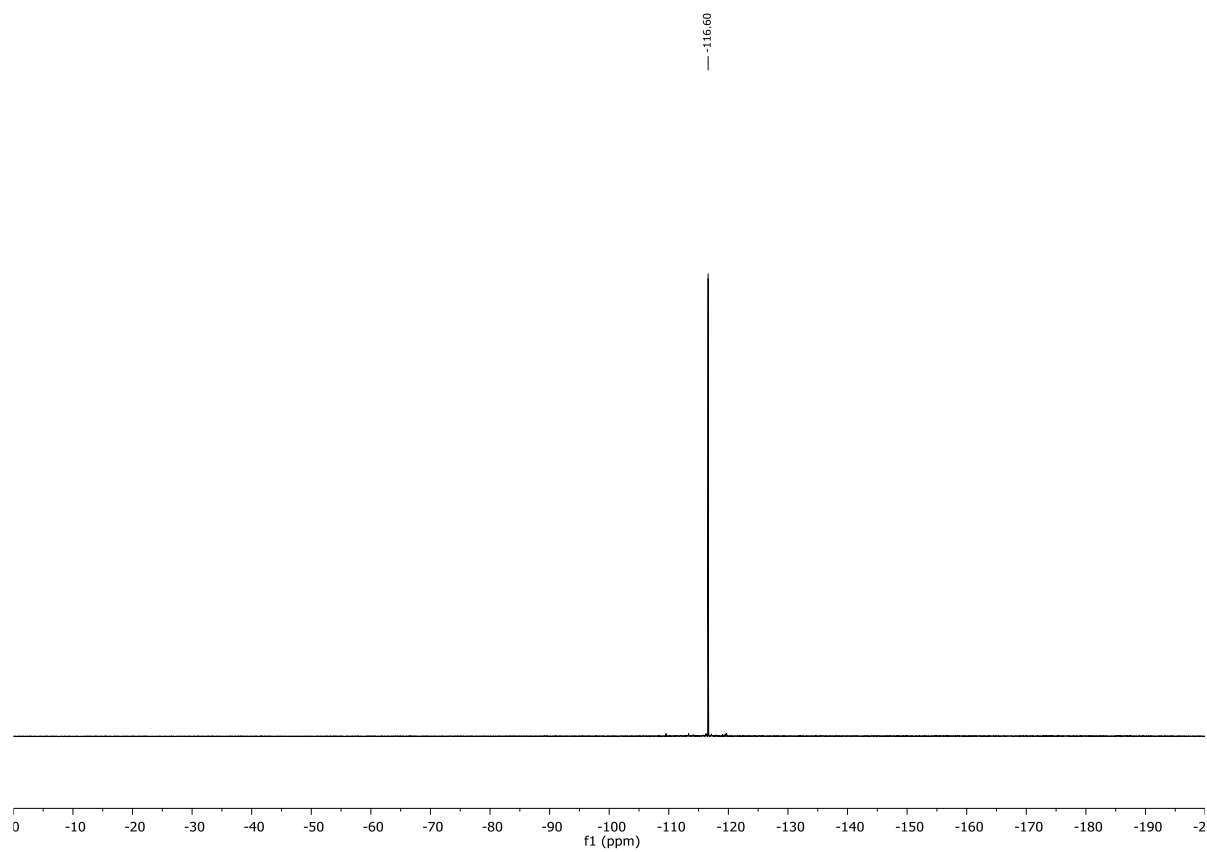
## Chapter 2: Synthesis of Pyrazines

### $^1\text{H}$ , $^{13}\text{C}$ and $^{19}\text{F}$ NMR of **3fh**

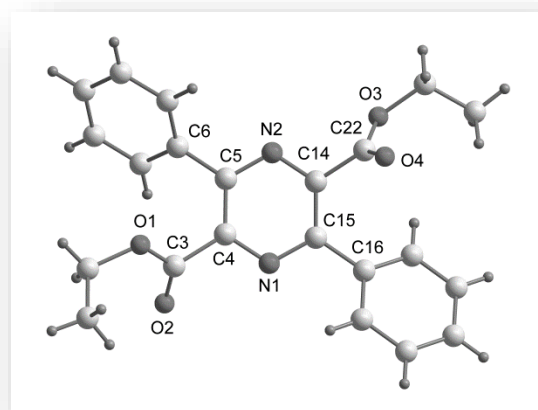


## Chapter 2: Synthesis of Pyrazines

---



### Crystal Data:



Crystal structure of **3a**

**Experimental.** Single clear colourless block-shaped crystals of (**3a**) were obtained by recrystallisation from DCM/pentane. A suitable crystal (0.52×0.20×0.11) mm<sup>3</sup> was selected and mounted on a MITIGEN holder with inert oil on a SuperNova, Single source at offset, Atlas diffractometer. The crystal was kept at  $T = 123.01(10)$  K during data collection. Using **Olex2** (Dolomanov et al., 2009), the structure was solved with the **ShelXT** (Sheldrick, 2015) structure solution program, using the Intrinsic Phasing solution method. The model was refined with version 2014/7 of **ShelXL** (Sheldrick, 2015) using Least Squares minimisation.

**Crystal Data.** C<sub>22</sub>H<sub>20</sub>N<sub>2</sub>O<sub>4</sub>,  $M_r = 376.40$ , monoclinic, P2<sub>1</sub>/c (No. 14),  $a = 5.9445(2)$  Å,  $b = 37.8883(11)$  Å,  $c = 9.1124(3)$  Å,  $\beta = 106.639(3)^\circ$ ,  $\alpha = \gamma = 90^\circ$ ,  $V = 1966.42(11)$  Å<sup>3</sup>,  $T = 123.01(10)$  K,  $Z = 4$ ,  $Z' = 1$ ,  $\mu(\text{CuK}\alpha) = 0.723$ , 8532 reflections measured, 3783 unique ( $R_{int} = 0.0216$ ) which were used in all calculations. The final  $wR_2$  was 0.1001 (all data) and  $R_1$  was 0.0380 ( $I > 2(I)$ ).

## Chapter 2: Synthesis of Pyrazines

---

Compound	3a
Formula	C <sub>22</sub> H <sub>20</sub> N <sub>2</sub> O <sub>4</sub>
$D_{calc.}/\text{g cm}^{-3}$	1.271
$\mu/\text{mm}^{-1}$	0.723
Formula Weight	376.40
Colour	clear colourless
Shape	block
Size/ $\text{mm}^3$	0.52×0.20×0.11
$T/\text{K}$	123.01(10)
Crystal System	monoclinic
Space Group	P2 <sub>1</sub> /c
$a/\text{Å}$	5.9445(2)
$b/\text{Å}$	37.8883(11)
$c/\text{Å}$	9.1124(3)
$\alpha/^\circ$	90
$\beta/^\circ$	106.639(3)
$\gamma/^\circ$	90
$V/\text{Å}^3$	1966.42(11)
$Z$	4
$Z'$	1
Wavelength/Å	1.54184
Radiation type	CuK $\alpha$
$\theta_{min}/^\circ$	4.668
$\theta_{max}/^\circ$	73.948
Measured Refl.	8532
Independent Refl.	3783
Reflections Used	3304
$R_{int}$	0.0216
Parameters	332
Restraints	180
Largest Peak	0.222

## Chapter 2: Synthesis of Pyrazines

---

Deepest Hole	-0.174
GooF	1.040
$wR_2$ (all data)	0.1001
$wR_2$	0.0951
$R_I$ (all data)	0.0460
$R_I$	0.0380

**Table 1:** Fractional Atomic Coordinates ( $\times 10^4$ ) and Equivalent Isotropic Displacement Parameters ( $\text{\AA}^2 \times 10^3$ ) for **3a**.  $U_{eq}$  is defined as 1/3 of the trace of the orthogonalised  $U_{ij}$ .

Atom	x	y	z	$U_{eq}$
O(3)	4207(10)	6921.7(18)	2631(7)	36.8(10)
O(2)	1943(10)	5358.9(11)	6358(5)	35.5(7)
O(1)	-1461(3)	5663.3(5)	5782(3)	28.5(4)
O(4)	3688(15)	7148(2)	4819(8)	34.7(10)
N(1)	3726.8(18)	6071.3(3)	6154.6(12)	26.6(2)
N(2)	1354.1(18)	6390.7(3)	3400.8(12)	24.8(2)
C(14)	3259(2)	6535.2(3)	4353.7(14)	23.7(3)
C(15)	4563(2)	6369.2(3)	5711.2(14)	24.4(3)
C(5)	597(2)	6082.6(3)	3811.5(15)	25.4(3)
C(22)	3766(2)	6906.9(3)	3962.7(14)	26.8(3)
C(6)	-1457(2)	5912.9(3)	2724.9(15)	27.9(3)
C(4)	1743(2)	5938.1(3)	5250.2(15)	26.2(3)
C(16)	6793(2)	6507.0(3)	6727.4(14)	25.8(3)
C(17)	8436(2)	6679.4(3)	6157.7(15)	27.6(3)
C(7)	-3420(2)	6111.9(3)	1985.9(16)	30.6(3)
C(18)	10513(2)	6803.1(4)	7138.1(16)	32.8(3)
C(3)	803(2)	5623.3(3)	5902.1(16)	31.4(3)
C(21)	7287(2)	6459.1(4)	8308.7(15)	32.1(3)
C(11)	-1476(3)	5549.9(4)	2470.9(18)	37.0(3)
C(19)	10976(3)	6755.1(4)	8704.6(17)	37.6(3)
C(20)	9368(3)	6583.3(4)	9285.2(16)	38.0(3)
C(8)	-5383(3)	5949.4(4)	1040.2(18)	39.1(3)

Atom	x	y	z	$U_{eq}$
C(10)	-3443(3)	5389.6(4)	1522(2)	44.8(4)
C(9)	-5397(3)	5588.3(4)	808(2)	45.8(4)
C(2)	-2624(4)	5362.9(6)	6239(3)	34.1(5)
C(13)	4684(8)	7277.6(13)	2161(5)	41.9(9)
C(1)	-2195(4)	5350.6(6)	7940(3)	48.7(6)
C(12)	7227(7)	7364.5(9)	2774(5)	76.5(13)
O(3A)	4770(20)	6938(4)	2821(16)	31.0(16)
C(13A)	5539(17)	7290(3)	2422(12)	40.8(17)
O(4A)	3260(30)	7169(6)	4520(20)	37(2)
C(12A)	7294(10)	7232.8(15)	1616(8)	51.5(17)
O(1A)	-1086(16)	5742(2)	6371(12)	29.3(17)
C(2A)	-2180(16)	5460(3)	7111(15)	32(2)
O(2A)	2050(50)	5421(6)	6720(20)	36(3)
C(0AA)	-3300(20)	5202(4)	5942(15)	48(3)

**Table 2:** Anisotropic Displacement Parameters ( $\times 10^4$ ) **3a**. The anisotropic displacement factor exponent takes the form:  $-2\pi^2[h^2a^{*2} \times U_{11} + \dots + 2hka^* \times b^* \times U_{12}]$

Atom	$U_{11}$	$U_{22}$	$U_{33}$	$U_{23}$	$U_{13}$	$U_{12}$
O(3)	63(3)	21.1(11)	25.2(15)	3.4(9)	10.3(15)	-13.7(15)
O(2)	24.4(10)	28.3(14)	55.1(19)	16.1(10)	13.5(13)	5.7(9)
O(1)	22.0(7)	24.3(8)	40.4(10)	6.9(7)	10.7(7)	1.0(5)
O(4)	53(3)	21.1(13)	29(3)	-5.5(16)	10.4(18)	-4.0(15)
N(1)	24.6(5)	28.3(5)	27.8(5)	6.8(4)	9.1(4)	2.7(4)
N(2)	27.9(5)	21.9(5)	24.0(5)	1.0(4)	6.3(4)	0.0(4)
C(14)	28.0(6)	22.7(6)	21.0(6)	0.4(4)	8.1(5)	0.2(5)
C(15)	26.3(6)	24.8(6)	23.3(6)	2.1(5)	9.0(5)	2.0(5)
C(5)	24.6(6)	22.0(6)	30.2(6)	2.6(5)	8.9(5)	2.2(4)
C(22)	31.1(7)	23.0(6)	22.7(6)	0.6(5)	2.0(5)	-0.9(5)
C(6)	26.1(6)	25.1(6)	31.9(7)	4.1(5)	7.4(5)	-0.7(5)
C(4)	22.2(6)	24.5(6)	33.1(7)	6.0(5)	10.1(5)	3.6(5)
C(16)	26.2(6)	25.6(6)	24.6(6)	1.1(5)	6.0(5)	3.8(5)



## Chapter 2: Synthesis of Pyrazines

Atom	$U_{11}$	$U_{22}$	$U_{33}$	$U_{23}$	$U_{13}$	$U_{12}$
C(17)	31.4(7)	27.0(6)	24.9(6)	-0.7(5)	8.8(5)	1.0(5)
C(7)	30.2(7)	25.4(6)	35.0(7)	4.7(5)	7.6(6)	1.8(5)
C(18)	29.1(7)	31.1(7)	38.9(8)	-4.6(5)	10.8(6)	-1.5(5)
C(3)	23.3(6)	30.5(7)	40.5(8)	11.9(6)	9.5(5)	3.0(5)
C(21)	30.3(7)	39.3(7)	26.0(7)	5.4(5)	6.9(5)	2.8(5)
C(11)	32.6(7)	25.1(7)	47.1(9)	2.4(6)	1.6(6)	2.9(5)
C(19)	29.6(7)	42.1(8)	35.5(8)	-6.6(6)	0.4(6)	-0.3(6)
C(20)	36.7(8)	49.6(8)	23.4(7)	1.7(6)	1.6(6)	4.6(6)
C(8)	28.2(7)	38.9(8)	44.6(8)	6.8(6)	1.3(6)	2.4(6)
C(10)	44.1(9)	25.6(7)	57(1)	-2.2(6)	2.3(7)	-4.9(6)
C(9)	35.0(8)	38.8(8)	53.5(10)	-0.1(7)	-3.5(7)	-11.0(6)
C(2)	23.6(10)	28.4(11)	52.0(14)	8.8(10)	13.7(9)	-1.8(8)
C(13)	64(2)	24.8(12)	32.5(15)	7.9(11)	7.0(16)	-18.4(17)
C(1)	41.2(11)	55.7(12)	53.8(14)	23.4(10)	20.8(9)	-1.4(9)
C(12)	74(2)	60.5(19)	89(3)	34.0(18)	13.3(19)	-29.5(16)
O(3A)	55(4)	17(2)	26(3)	-3(2)	20(3)	-4(3)
C(13A)	61(4)	23(3)	41(4)	5(2)	20(3)	-12(4)
O(4A)	51(5)	33(3)	27(5)	-1(3)	9(4)	-1(3)
C(12A)	50(3)	42(3)	57(3)	21(2)	5(3)	-8(2)
O(1A)	28(3)	23(3)	37(4)	8(3)	10(3)	-1(2)
C(2A)	24(3)	37(4)	37(4)	4(4)	14(3)	3(3)
O(2A)	25(4)	31(6)	52(7)	15(5)	11(5)	4(4)
C(0AA)	43(6)	50(6)	58(6)	8(5)	24(5)	4(5)

**Table 3:** Bond Lengths in Å for **3a**.

Atom	Atom	Length/Å
O(3)	C(22)	1.314(7)
O(3)	C(13)	1.467(8)
O(2)	C(3)	1.214(5)
O(1)	C(3)	1.327(2)
O(1)	C(2)	1.453(3)

## Chapter 2: Synthesis of Pyrazines

---

Atom	Atom	Length/Å
O(4)	C(22)	1.212(9)
N(1)	C(15)	1.3413(16)
N(1)	C(4)	1.3295(17)
N(2)	C(14)	1.3315(16)
N(2)	C(5)	1.3422(16)
C(14)	C(15)	1.4063(17)
C(14)	C(22)	1.5042(16)
C(15)	C(16)	1.4781(18)
C(5)	C(6)	1.4806(18)
C(5)	C(4)	1.4039(18)
C(22)	O(3A)	1.347(15)
C(22)	O(4A)	1.19(2)
C(6)	C(7)	1.3902(18)
C(6)	C(11)	1.3944(18)
C(4)	C(3)	1.5095(17)
C(16)	C(17)	1.3931(18)
C(16)	C(21)	1.3976(18)
C(17)	C(18)	1.3819(19)
C(7)	C(8)	1.382(2)
C(18)	C(19)	1.386(2)
C(3)	O(1A)	1.386(9)
C(3)	O(2A)	1.18(3)
C(21)	C(20)	1.383(2)
C(11)	C(10)	1.380(2)
C(19)	C(20)	1.381(2)
C(8)	C(9)	1.384(2)
C(10)	C(9)	1.380(2)
C(2)	C(1)	1.497(3)
C(13)	C(12)	1.491(5)
O(3A)	C(13A)	1.487(17)
C(13A)	C(12A)	1.454(12)
O(1A)	C(2A)	1.507(13)

Atom	Atom	Length/Å
C(2A)	C(0AA)	1.460(17)

**Table 4:** Bond Angles in ° for **3a**.

Atom	Atom	Atom	Angle/°
C(22)	O(3)	C(13)	114.5(5)
C(3)	O(1)	C(2)	116.19(14)
C(4)	N(1)	C(15)	118.16(10)
C(14)	N(2)	C(5)	117.79(10)
N(2)	C(14)	C(15)	122.77(11)
N(2)	C(14)	C(22)	114.92(10)
C(15)	C(14)	C(22)	121.99(11)
N(1)	C(15)	C(14)	118.87(11)
N(1)	C(15)	C(16)	116.86(11)
C(14)	C(15)	C(16)	124.24(11)
N(2)	C(5)	C(6)	117.99(11)
N(2)	C(5)	C(4)	119.18(11)
C(4)	C(5)	C(6)	122.83(11)
O(3)	C(22)	C(14)	111.4(3)
O(4)	C(22)	O(3)	128.1(5)
O(4)	C(22)	C(14)	120.4(4)
O(3A)	C(22)	C(14)	115.4(6)
O(4A)	C(22)	C(14)	126.0(11)
O(4A)	C(22)	O(3A)	118.5(12)
C(7)	C(6)	C(5)	120.36(11)
C(7)	C(6)	C(11)	119.27(12)
C(11)	C(6)	C(5)	120.33(11)
N(1)	C(4)	C(5)	122.56(11)
N(1)	C(4)	C(3)	114.74(11)
C(5)	C(4)	C(3)	122.69(11)
C(17)	C(16)	C(15)	122.08(11)
C(17)	C(16)	C(21)	118.84(12)

<b>Atom</b>	<b>Atom</b>	<b>Atom</b>	<b>Angle/°</b>
C(21)	C(16)	C(15)	119.07(12)
C(18)	C(17)	C(16)	120.65(12)
C(8)	C(7)	C(6)	120.16(12)
C(17)	C(18)	C(19)	119.90(13)
O(2)	C(3)	O(1)	125.2(3)
O(2)	C(3)	C(4)	123.6(3)
O(1)	C(3)	C(4)	111.00(12)
O(1A)	C(3)	C(4)	106.8(4)
O(2A)	C(3)	C(4)	122.0(14)
O(2A)	C(3)	O(1A)	115.8(14)
C(20)	C(21)	C(16)	120.28(13)
C(10)	C(11)	C(6)	120.19(13)
C(20)	C(19)	C(18)	120.09(13)
C(19)	C(20)	C(21)	120.23(13)
C(7)	C(8)	C(9)	120.18(13)
C(11)	C(10)	C(9)	120.20(13)
C(10)	C(9)	C(8)	119.98(13)
O(1)	C(2)	C(1)	111.5(3)
O(3)	C(13)	C(12)	110.7(3)
C(22)	O(3A)	C(13A)	120.2(9)
C(12A)	C(13A)	O(3A)	107.7(8)
C(3)	O(1A)	C(2A)	113.5(7)
C(0AA)	C(2A)	O(1A)	108.3(12)

**Table 5:** Torsion Angles in ° for **3a**.

<b>Atom</b>	<b>Atom</b>	<b>Atom</b>	<b>Atom</b>	<b>Angle/°</b>
N(1)	C(15)	C(16)	C(17)	146.00(12)
N(1)	C(15)	C(16)	C(21)	-33.11(17)
N(1)	C(4)	C(3)	O(2)	-54.5(3)
N(1)	C(4)	C(3)	O(1)	131.00(16)
N(1)	C(4)	C(3)	O(1A)	104.5(5)

## Chapter 2: Synthesis of Pyrazines

---

Atom	Atom	Atom	Atom	Angle/°
N(1)	C(4)	C(3)	O(2A)	-31.9(11)
N(2)	C(14)	C(15)	N(1)	-7.35(19)
N(2)	C(14)	C(15)	C(16)	174.58(11)
N(2)	C(14)	C(22)	O(3)	-63.2(3)
N(2)	C(14)	C(22)	O(4)	115.4(4)
N(2)	C(14)	C(22)	O(3A)	-78.4(6)
N(2)	C(14)	C(22)	O(4A)	97.8(9)
N(2)	C(5)	C(6)	C(7)	-44.67(18)
N(2)	C(5)	C(6)	C(11)	137.50(14)
N(2)	C(5)	C(4)	N(1)	-8.3(2)
N(2)	C(5)	C(4)	C(3)	170.72(12)
C(14)	N(2)	C(5)	C(6)	-177.34(11)
C(14)	N(2)	C(5)	C(4)	3.77(18)
C(14)	C(15)	C(16)	C(17)	-35.89(19)
C(14)	C(15)	C(16)	C(21)	144.99(13)
C(14)	C(22)	O(3A)	C(13A)	-174.9(7)
C(15)	N(1)	C(4)	C(5)	4.67(19)
C(15)	N(1)	C(4)	C(3)	-174.42(11)
C(15)	C(14)	C(22)	O(3)	123.2(3)
C(15)	C(14)	C(22)	O(4)	-58.3(4)
C(15)	C(14)	C(22)	O(3A)	108.0(6)
C(15)	C(14)	C(22)	O(4A)	-75.9(9)
C(15)	C(16)	C(17)	C(18)	-179.53(12)
C(15)	C(16)	C(21)	C(20)	179.56(12)
C(5)	N(2)	C(14)	C(15)	3.75(18)
C(5)	N(2)	C(14)	C(22)	-169.84(11)
C(5)	C(6)	C(7)	C(8)	-176.31(13)
C(5)	C(6)	C(11)	C(10)	176.44(15)
C(5)	C(4)	C(3)	O(2)	126.5(2)
C(5)	C(4)	C(3)	O(1)	-48.1(2)
C(5)	C(4)	C(3)	O(1A)	-74.6(5)
C(5)	C(4)	C(3)	O(2A)	149.0(11)

## Chapter 2: Synthesis of Pyrazines

---

Atom	Atom	Atom	Atom	Angle/°
C(22)	O(3)	C(13)	C(12)	87.7(5)
C(22)	C(14)	C(15)	N(1)	165.80(12)
C(22)	C(14)	C(15)	C(16)	-12.3(2)
C(22)	O(3A)	C(13A)	C(12A)	158.7(9)
C(6)	C(5)	C(4)	N(1)	172.87(12)
C(6)	C(5)	C(4)	C(3)	-8.1(2)
C(6)	C(7)	C(8)	C(9)	-0.8(2)
C(6)	C(11)	C(10)	C(9)	0.6(3)
C(4)	N(1)	C(15)	C(14)	2.86(18)
C(4)	N(1)	C(15)	C(16)	-178.93(11)
C(4)	C(5)	C(6)	C(7)	134.18(14)
C(4)	C(5)	C(6)	C(11)	-43.7(2)
C(4)	C(3)	O(1A)	C(2A)	-177.8(7)
C(16)	C(17)	C(18)	C(19)	0.1(2)
C(16)	C(21)	C(20)	C(19)	-0.1(2)
C(17)	C(16)	C(21)	C(20)	0.4(2)
C(17)	C(18)	C(19)	C(20)	0.2(2)
C(7)	C(6)	C(11)	C(10)	-1.4(2)
C(7)	C(8)	C(9)	C(10)	-0.1(3)
C(18)	C(19)	C(20)	C(21)	-0.2(2)
C(3)	O(1)	C(2)	C(1)	81.8(3)
C(3)	O(1A)	C(2A)	C(0AA)	-68.0(11)
C(21)	C(16)	C(17)	C(18)	-0.41(19)
C(11)	C(6)	C(7)	C(8)	1.5(2)
C(11)	C(10)	C(9)	C(8)	0.2(3)
C(2)	O(1)	C(3)	O(2)	0.0(4)
C(2)	O(1)	C(3)	C(4)	174.4(2)
C(13)	O(3)	C(22)	O(4)	0.8(7)
C(13)	O(3)	C(22)	C(14)	179.1(3)
O(4A)	C(22)	O(3A)	C(13A)	8.6(14)
O(2A)	C(3)	O(1A)	C(2A)	-38.3(16)

**Table 6:** Hydrogen Fractional Atomic Coordinates ( $\times 10^4$ ) and Equivalent Isotropic Displacement Parameters ( $\text{\AA}^2 \times 10^3$ ) for **3a**.  $U_{eq}$  is defined as 1/3 of the trace of the orthogonalised  $U_{ij}$ .

<b>Atom</b>	<b>x</b>	<b>y</b>	<b>z</b>	<b><math>U_{eq}</math></b>
H(17)	8133	6712	5107	33
H(7)	-3410	6355	2129	37
H(18)	11598	6918	6748	39
H(21)	6212	6343	8706	39
H(11)	-158	5415	2942	44
H(19)	12371	6839	9365	45
H(20)	9685	6551	10337	46
H(8)	-6700	6083	558	47
H(10)	-3453	5147	1363	54
H(9)	-6722	5479	172	55
H(2A)	-2051	5147	5902	41
H(2B)	-4299	5378	5744	41
H(13A)	3765	7448	2537	50
H(13B)	4219	7292	1052	50
H(1A)	-3092	5162	8196	73
H(1B)	-2663	5571	8286	73
H(1C)	-555	5311	8428	73
H(12A)	7526	7590	2387	115
H(12B)	8142	7187	2458	115
H(12C)	7651	7373	3873	115
H(13C)	4210	7418	1775	49
H(13D)	6201	7427	3344	49
H(12D)	6602	7106	684	77
H(12E)	8574	7098	2252	77
H(12F)	7866	7456	1379	77
H(2AA)	-985	5346	7926	38
H(2AB)	-3334	5564	7549	38
H(0AA)	-4538	5314	5167	72
H(0AB)	-3949	5014	6403	72

## Chapter 2: Synthesis of Pyrazines

Atom	x	y	z	$U_{eq}$
H(0AC)	-2163	5107	5486	72

**Table 7:** Atomic Occupancies for all atoms that are not fully occupied in **3a**.

Atom	Occupancy
O(3)	0.690(6)
O(2)	0.833(5)
O(1)	0.833(5)
O(4)	0.690(6)
C(2)	0.833(5)
H(2A)	0.833(5)
H(2B)	0.833(5)
C(13)	0.690(6)
H(13A)	0.690(6)
H(13B)	0.690(6)
C(1)	0.833(5)
H(1A)	0.833(5)
H(1B)	0.833(5)
H(1C)	0.833(5)
C(12)	0.690(6)
H(12A)	0.690(6)
H(12B)	0.690(6)
H(12C)	0.690(6)
O(3A)	0.310(6)
C(13A)	0.310(6)
H(13C)	0.310(6)
H(13D)	0.310(6)
O(4A)	0.310(6)
C(12A)	0.310(6)
H(12D)	0.310(6)
H(12E)	0.310(6)
H(12F)	0.310(6)



<b>Atom</b>	<b>Occupancy</b>
O(1A)	0.167(5)
C(2A)	0.167(5)
H(2AA)	0.167(5)
H(2AB)	0.167(5)
O(2A)	0.167(5)
C(0AA)	0.167(5)
H(0AA)	0.167(5)
H(0AB)	0.167(5)
H(0AC)	0.167(5)

**References:**

- 1) Stokes, B. J.; Dong, H.; Leslie, B. E.; Pumphrey, A. L.; Driver, T. G., *J. Am. Chem. Soc.* **2007**, *129*, 7500.
- 2) Nair, V.; George, T. G., *Tetrahedron Lett.* **2000**, *41*, 3199.



# *Chapter 3*



## Copper and Visible-Light: Highlighting the Special Features beyond Photoinduced Electron Transfer

### Abstract:

Visible-light photoredox catalysis has led to a paradigm shift in organic synthesis by offering elusive reaction pathways. Ru(II) or Ir(III)-polypyridyl complexes and organic dye sensitizers have been the widely used chromophores owing to strong absorption in the visible region, long excited-state lifetimes, and high redox potentials. However, the cost and adverse environmental impact of these heavy transition-metal complexes, as well as their restrictive conformational stability (both with respect to inner-sphere substrate interactions and as consequence asymmetric transformations), limit their applications. Given the crucial need to develop

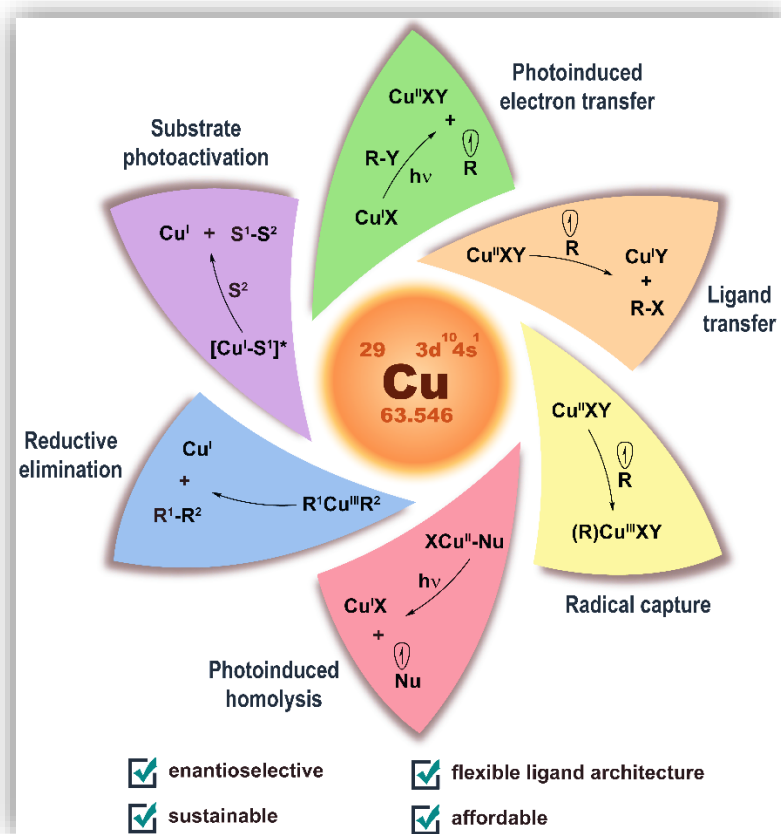


**Figure 1:** Various reactivities of copper in visible-light induced chemical transformations.

### This chapter has been published:

A. Hossain,<sup>†</sup> A. Bhattacharyya,<sup>†</sup> O. Reiser, *Science* **2019**, *364*, eaav9713. (<sup>†</sup>equal contribution).

A.H. and A.B. wrote the manuscript. O.R. directed throughout the manuscript preparation.

environmentally benign, cheap, multi-purpose, and flexible catalytic systems, copper has emerged as an appealing alternative. Copper-based photocatalysts display highly tunable redox properties in their excited states. Moreover, the combination of conventional photocatalysts with copper(I) or copper(II) salts has emerged as an efficient dual catalytic system for many cross-coupling reactions.

#### **Introduction:**

Visible-light photoredox catalysis<sup>[1,2]</sup> now a days has become a widely used method in organic synthesis. As because the small organic molecules do not absorb in the visible-light region of the electromagnetic spectrum, various photocatalysts have been employed to undergo single-electron transfer (SET) or energy transfer processes from their photoexcited states. This results in the formation of radical species which participate in various cross-coupling and cycloaddition reactions, respectively in non-traditional reaction pathways complementary to common, thermal two-electron processes.<sup>[3]</sup> Most commonly used photocatalysts are heavy transition metal catalysts such as Ru(II) or Ir(III)-polypyridyl complexes or metal-free organic dye sensitizers, owing to their favorable characteristics such as long excited-state lifetimes, strong absorption in the visible region, and high reduction or oxidation potentials of the corresponding excited states.<sup>[2]</sup> However, the major drawback with organic dyes is lower photostability. On the other hand, heavy transition metal-based complexes are expensive as well as environmentally unfriendly. Moreover, the high oxidation states of conventional Ir- or Ru-based photocatalysts make them very stable in terms of coordination which hinder their ability to undergo oxidative addition with organic electrophiles. In addition, although a few stereoselective reactions have been reported by employing Ir- or Ru-based photocatalysts (in presence of labile ligands) with prefunctionalized substrates<sup>[4]</sup>, but the synthesis of appropriate chiral octahedral complexes remains a substantial challenge. Catalysts that can undergo electron transfer processes in their inner coordination-sphere and thereby can also control reactions through their ligand environment are highly desirable. First row transition metal complexes are promising metal of choice in this context.<sup>[5]</sup> As a result, significant advancements have been made by various scientific groups by merging conventional Ir- or Ru-based photocatalysts with various nickel(II) salts or complexes that are capable of effecting oxidative addition to organic electrophiles leading to cross-coupled products.<sup>[6]</sup> However, with very recent discoveries copper has now come to the fore in the arena of photocatalysis<sup>[7]</sup>, owing to its versatile redox properties, capable both of initiating a reaction by SET as well as directly interacting with substrates in its coordination sphere. Moreover, copper complexes are highly

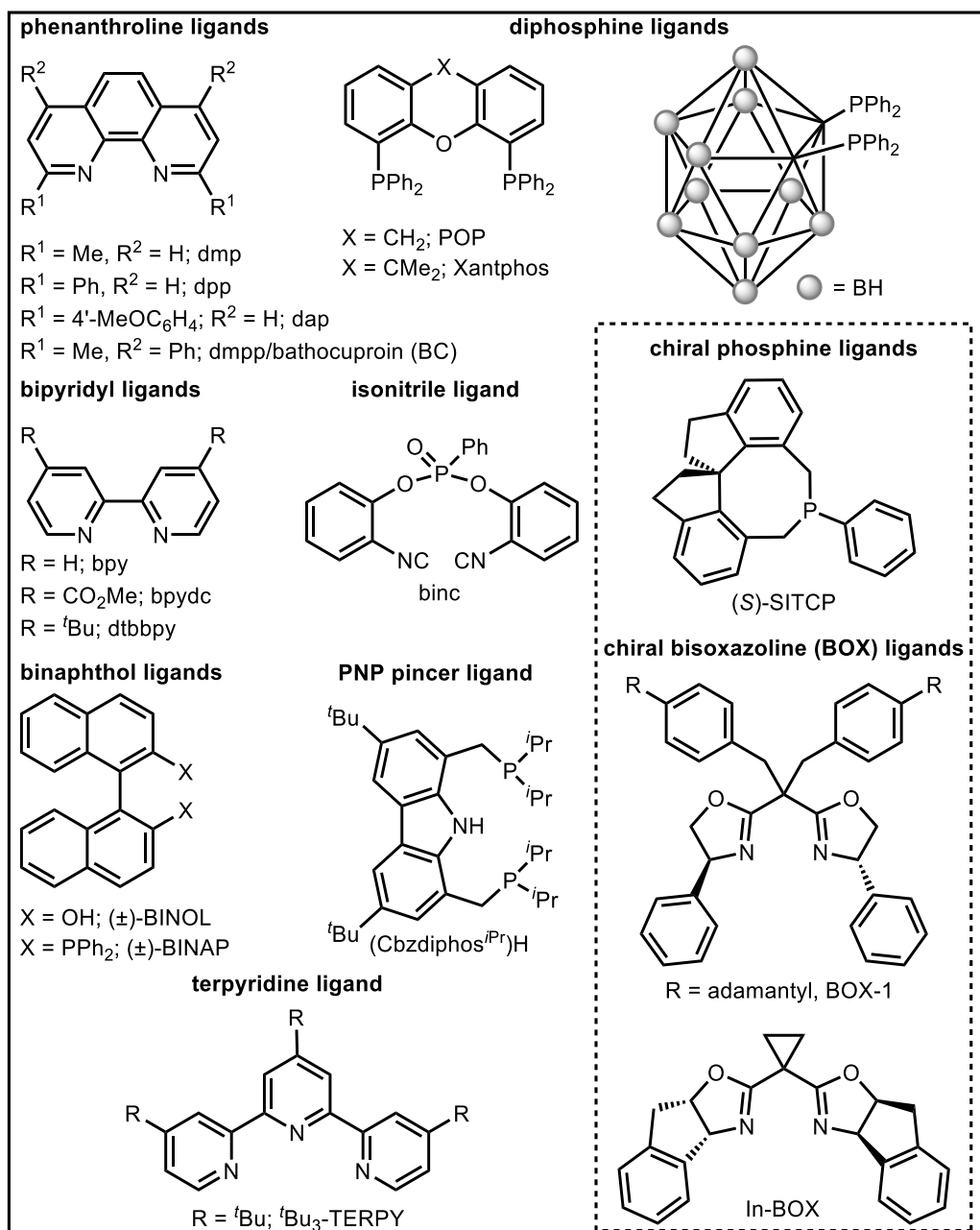


**Figure 2:** Representative ligands used in copper photocatalysis

dynamic which allows the synthesis of various heteroleptic complexes with N- and P-based multidentate ligands (Figure 2) to tune redox properties and enhance excited-state lifetime.<sup>[8]</sup>

### 1) Cu(I) complexes as stand-alone photocatalysts:

In 1977, McMillin *et al.* described the first ever visible-light-induced electron transfer process from a copper complex.<sup>[9]</sup> They synthesized [Cu(dmp)<sub>2</sub>]BF<sub>4</sub> (dmp = 2,9-dimethyl-1,10-phenanthroline) which could be photoexcited at 454 nm; the resulting metal-to-ligand charge transfer (MLCT) state could reduce Co(III) in K[*cis*-Co(IDA)<sub>2</sub>]·1.5H<sub>2</sub>O to the corresponding

Co(II) complex. A decade later, Sauvage *et al.* introduced<sup>[10]</sup> an engineered Cu(I) complex of two crescent-shaped phenanthroline ligands, which also resulted increase in the lifetime of its MLCT excited state ( $\leq 270$  ns). The complex, [Cu(dap)<sub>2</sub>]Cl (dap = 2,9-bis(*p*-anisyl)-1,10 phenanthroline;  $E_{red} = -1.43$  V vs. Saturated Calomel Electrode (SCE) in CH<sub>3</sub>CN), was employed to induce a reductive coupling of nitrobenzyl bromide to the corresponding bibenzylic compound in presence of triethylamine. Surprisingly, this catalyst went into hibernation until it was resuscitated in 2012 by Reiser and co-workers<sup>[11]</sup> for a C–C bond-forming atom transfer radical addition (ATRA) reaction. This particular study, along with

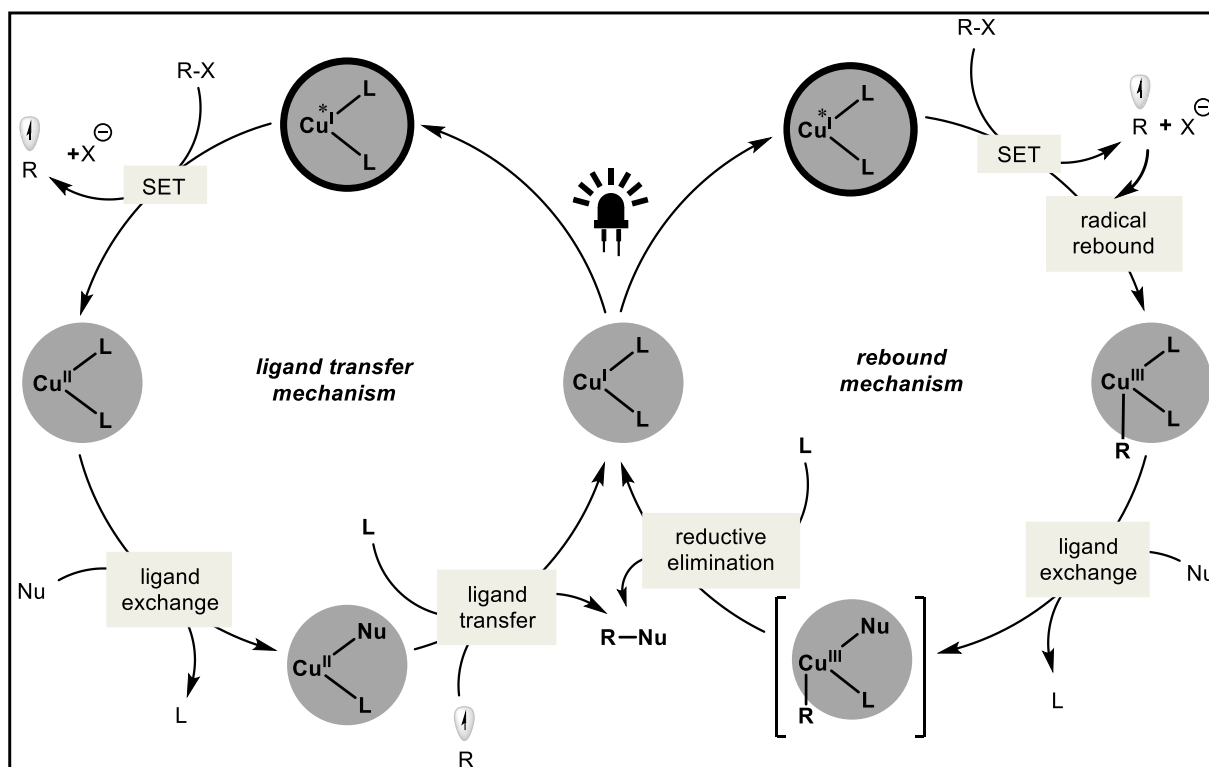


**Figure 3:** Mechanistic paradigms for Cu(I) photocatalysis. L = ligand; R-X = electron-accepting substrate (X = leaving group); Nu = nucleophile.

heteroleptic Cu(I)-phenanthroline- bisphosphine complex catalyzed  $6\pi$ -electrocyclization<sup>[12]</sup> by Collins *et al.* and palladium-free Sonogashira couplings via light-activated copper(I)-alkyne complexes<sup>[13]</sup> (Hwang and co-workers), set in motion the recent proliferation of studies involving Cu(I)- and Cu(II)-complexes as effective visible light photocatalysts.

The general mechanistic paradigm of Cu(I)L<sub>n</sub>-complexes as photocatalysts is shown in Figure 3. Upon photoexcitation with visible-light, Cu(I)L<sub>n</sub>\* transfers a single electron to an electrophile producing a radical species (R•) [which can further react with an alkene or alkyne resulting in a more nucleophilic radical species (R'•)] and a transient Cu(II)L<sub>n</sub> intermediate. At



this stage, two possibilities emerge: (i)  $\text{Cu(II)L}_n$  intermediate can exchange a ligand (L) with an incoming nucleophilic cross-coupling partner (Nu) to generate a  $\text{Nu-Cu(II)L}_{(n-1)}$  intermediate which transfers the nucleophilic moiety to  $\text{R}\cdot$  to furnish the cross-coupled product ( $\text{R-Nu}$ ) and reverts to the initial  $\text{Cu(I)L}_n$  complex upon coordinating with the previously departed ligand (L); (ii) the incipient radical ( $\text{R}\cdot$ ) can bind to the  $\text{Cu(II)L}_n$  intermediate which results in the formation of a high-valent  $\text{R-Cu(III)-L}_n$  intermediate.<sup>[14]</sup> This intermediate exchanges a ligand with Nu to form  $\text{R-Cu(III)L}_{(n-1)}\text{-Nu}$ , which undergoes facile reductive elimination to produce the desired cross-coupled product ( $\text{R-Nu}$ ) and regenerate the initial  $\text{Cu(I)L}_n$  complex with L.

### Olefin bifunctionalization

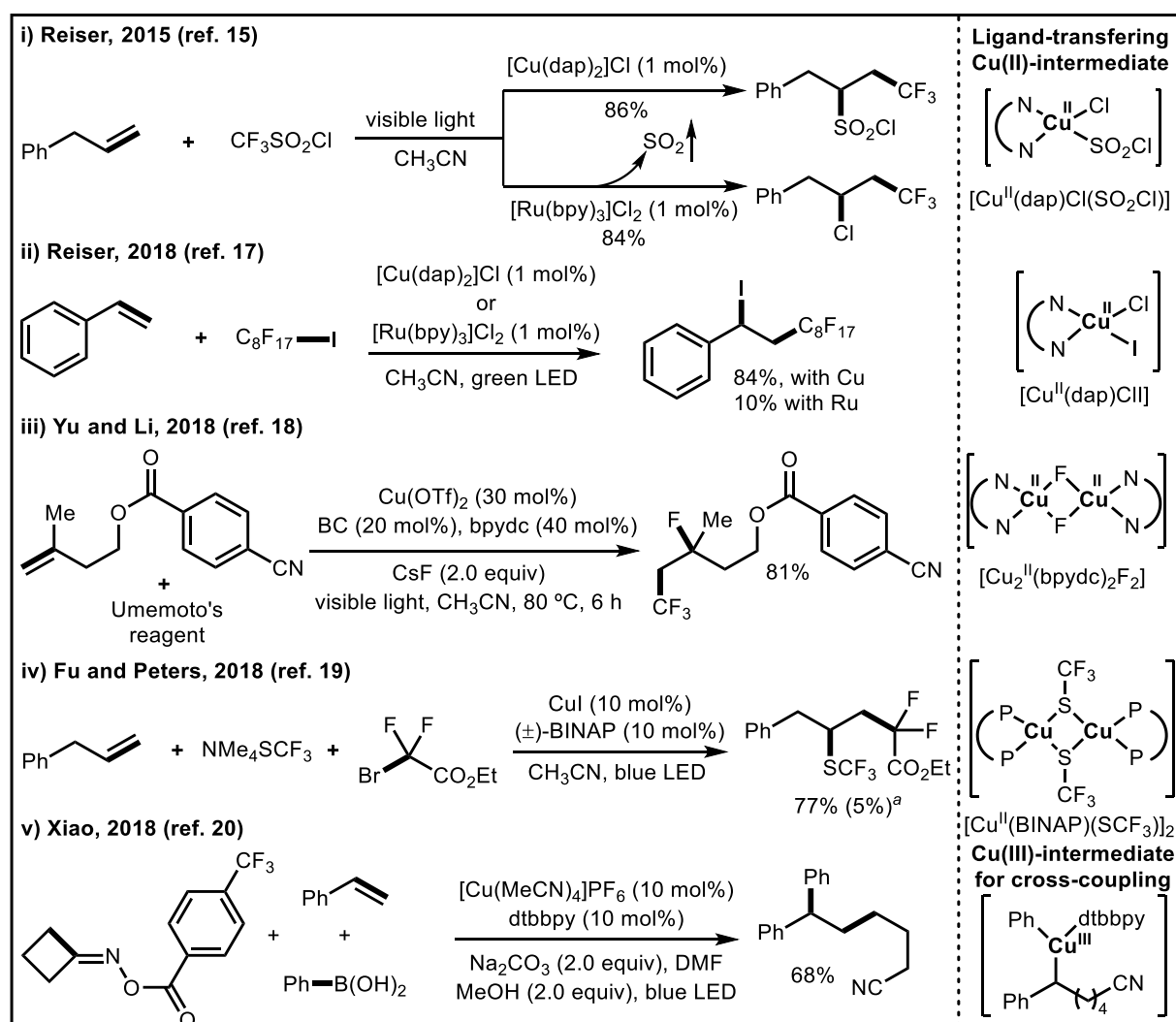


**Figure 4:** This represents mechanistically distinct copper-photocatalyzed olefin-bifunctionalization processes. OTf = Triflate.; LED = light-emitting diode.

A wide range of functionalities can bind to the Cu(II)-intermediate generated via SET from the photoexcited Cu(I)\*. As a result, the process of ligand-transfer to the intermediate radicals gets promoted in various atom-transfer radical addition (ATRA) reactions. The first such example was demonstrated in 2015 by Reiser and co-workers through the development of vicinal trifluoromethylation/chlorosulfonylation of unactivated olefins (Figure 4, i). When these olefins were exposed to triflyl chloride (CF<sub>3</sub>SO<sub>2</sub>Cl) in the presence of 1 mol% [Cu(dap)<sub>2</sub>]Cl, the corresponding trifluoromethyl-chlorosulfonylated products were obtained in high yields.<sup>[15]</sup> On the other hand, when [Ru(bpy)<sub>3</sub>]Cl<sub>2</sub> was employed as a photocatalyst, corresponding trifluoromethyl-chlorinated products were obtained.<sup>[16]</sup> The formation of the unexpected sulfonylchloride was explained in terms of coordination between the chlorosulfonyl anion, generated upon mesolysis of triflyl chloride after SET by excited-state [Cu(dap)<sub>2</sub>]Cl\*, and the concurrently formed Cu(II)-center. The same group also found out that the iodoperfluoroalkylation of styrenes fails with common ruthenium or iridium-based photocatalysts but proceeds efficiently with [Cu(dap)<sub>2</sub>]Cl, suggesting the intermediacy of an iodine-transferring [Cu<sup>II</sup>(dap)ClI] species (Figure 4, ii).<sup>[17]</sup> Yu, Li, and co-workers have recently shown a fluorine atom-transfer (FAT) capability of an innovative Cu(II)-F complex to efficiently promote carbofluorination of unactivated olefins (Figure 4, iii).<sup>[18]</sup> The reaction proceeds in the presence of Cu(OTf)<sub>2</sub>, as the catalyst with the assistance of two ligands *viz.* bathocuproine (BC) to reduce Cu(II) to Cu(I) and electron-deficient 4,4'-di(methoxycarbonyl)-2,2'-bipyridine (bpydc) to accelerate FAT from the LCu(II)-F complex. CsF and Umemoto's reagent have been used as the sources of F and CF<sub>3</sub> respectively. In the same year, a similar dicopper complex has been synthesized by Fu, Peters and co-workers to facilitate transfer of a thiotrifluoromethyl (SCF<sub>3</sub>) group (Figure 4, iv).<sup>[19]</sup> The ligand transferring process is initiated with the photoexcitation of a Cu<sup>I</sup>(BINAP)(SCF<sub>3</sub>) complex that reduces a electrophile to generate a radical, which is intercepted by an olefin to generate a more nucleophilic alkyl radical. At the same time, the newly-formed [Cu<sup>II</sup>(BINAP)(SCF<sub>3</sub>)<sub>2</sub>] complex effectively transfers the SCF<sub>3</sub> group to this radical species to furnish the targeted trifluoromethyl thioether with the concurrent regeneration of the initial CuI-complex with the SCF<sub>3</sub>-source.

All the discussed examples so far can be explained either by ligand transfer or rebound/reductive elimination of Cu(II)-species with a SET-generated radical. But the three-component cross-coupling protocol reported by Xiao and co-workers<sup>[20]</sup> involving redox-active cycloketone oxime esters, styrenes, and aryl boronic acids provides a strong case for the intermediacy of Cu(III)-species via a rebound pathway (Figure 4, v). The proposed mechanism

involves photoexcited Cu(I)(dtbbpy)\*-catalyzed SET-assisted formation of a cyanoalkyl radical that reacts with an olefin to generate another intermediate radical. Simultaneously, the newly-formed Cu(II) species undergoes transmetalation with aryl boronic acid to form an aryl-Cu(II) intermediate; which subsequently captures the intermediate radical to form a new aryl-Cu(III)(alkyl)-species. This intermediate undergoes reductive elimination to yield the cross-coupled product with the regeneration of the Cu(I) catalyst.

#### ***C(sp<sup>3</sup>/sp<sup>2</sup>)-Heteroatom cross coupling***

Shifting the classical pathway of nucleophilic substitution to a radical regime under visible-light irradiation conditions provides remarkable solutions to long-standing challenges for the (asymmetric) synthesis of amines as progressively addressed by the pioneering contributions from the groups of Peters and Fu. In 2016, they have disclosed an enantioconvergent cross-coupling reaction between racemic tertiary  $\alpha$ -chloroamides and carbazoles/indoles catalyzed by a novel Cu(I)/Nu/(*S*)-SITCP -complex (Nu = carbazole or indole) that acts both as a photocatalyst and as the source of enantioinduction (Figure 5, i).<sup>[21]</sup> The commercially available chiral phosphine ligand, (*S*)-SITCP, controls the absolute configuration of the products regardless of the initial stereochemistry of the electrophiles. It was proposed that *in situ* formed [Cu(I)-((*S*)-SITCP)<sub>2</sub>-carbazolide] complex acts as a photocatalyst. Later, the same groups have reported a generalized protocol for C-N cross-coupling by synthesizing a novel tridentate bisphosphine/carbazolide ligand-containing [Cu((Cbzdiphos<sup>i</sup>Pr)] photocatalyst. This photocatalyst was employed in combination with CuBr to accomplish C-N cross coupling between unactivated secondary alkyl halides and carbamates in an ‘out-of-cage’ process (Figure 5, ii).<sup>[22]</sup> They also found out that the use of Ru- or Ir-based photocatalysts instead of the aforementioned Cu(I)-photocatalyst led to <1% formation of the desired product. The scope of nitrogen-containing cross-coupling counterpart could be further extended to primary aliphatic amines by overcoming usual synthetic problems such as polyalkylation or steric hindrance. The same groups have employed a photoactive Cu(I)-binaphtholate complex to mediate the desired cross-coupling between the primary amines with unactivated secondary alkyl iodides under mild reaction conditions. The corresponding mono-alkylated amine products were obtained in very good yields (Figure 5, iii).<sup>[23]</sup> The *rac*-BINOL ligand was found to be essential in this reaction. According to the proposed reaction mechanism, the photoexcited Cu(I)/BINOL-complex undergoes SET to generate an alkyl radical and a Cu(II)/BINOL species. This Cu(II)/BINOL species upon ligand exchange with an amine forms the key Cu(II)-amine species which combines with the alkyl radical and subsequent cross-coupling furnishes

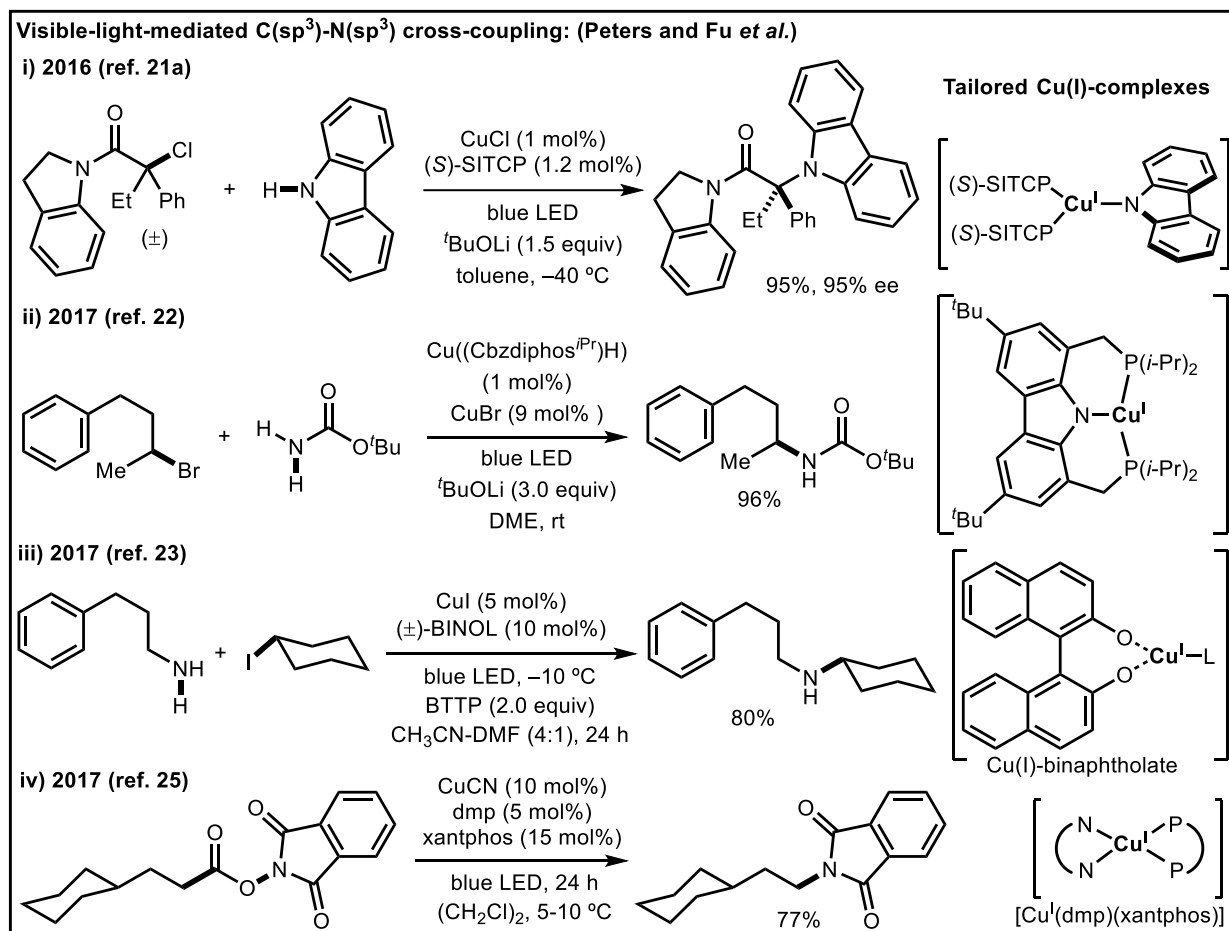


**Figure 5:** Cu(I)-complexes as stand-alone photocatalysts: Synthetic applications in carbon–nitrogen cross-coupling reactions. BTTP = Phosphazene base P<sub>1</sub>-*tert*-Bu-tris(tetramethylene).

the desired product.

Carboxylic acids are a more abundant, stable, and less toxic chemical feedstock in comparison to alkyl halides. *N*-(hydroxy)phthalimide (NHPI) esters are being widely exploited as superior sources of alkyl radicals through a SET-reduction-decarboxylation process, leading to the development of a wide variety of decarboxylative cross-coupling methodologies.<sup>[24]</sup> This principle was exploited by Peters, Fu and co-workers for the development of a decarboxylative C–N coupling protocol (Figure 5, iv). This is an azide-free alternative to the Curtius rearrangement.<sup>[25]</sup> As per their proposal, initial SET from a photoexcited \*Cu(I)/dmp/xantphos-complex resulted in the formation of a Cu(II)-species and the radical anion of the NHPI-ester. Fragmentation of this radical anion species produced an alkyl radical, CO<sub>2</sub> and the phthalimide anion, which binds to Cu(II). The recombination of the alkyl radical with this Cu(II)-phthalimide species and subsequent cross-coupling afforded the desired product with regeneration of the Cu(I) catalytic species.

## 2) Photoexcitation of in situ generated Cu(I)-substrate complexes

A mechanistically distinct class of reaction manifolds unique to copper has emerged wherein suitable substrates can form visible light-absorbing complexes by coordinating to copper salts (without using any external ligands). The excited  $^*Cu(I)$ -substrate complex reduces an electrophile by a SET process and the resulting  $Cu(II)$ -substrate species which then participates in a diverse range of synthetic transformations including cross-coupling reactions and functional group modifications (Figure 6). Based on this concept, Hwang and co-workers developed a visible-light-mediated, high-yielding palladium free Sonogashira cross-coupling reaction between aryl halides and alkyl- or aryl-substituted terminal alkynes in the presence of catalytic amounts of  $CuCl$ .<sup>[13]</sup>

This group has also applied this concept for the development of a three-component coupling reaction between anilines, terminal alkynes, and benzoquinones for making functionalized indoles (Figure 7, i).<sup>[26]</sup> The transformation operates via the formation of a photoactive  $Cu(I)$ -phenylacetylide species which, upon visible-light irradiation, reduces benzoquinone via SET ( $-2.048$  V vs. SCE in  $CH_3CN$ ) to enable further reactions with aniline. This principle has also

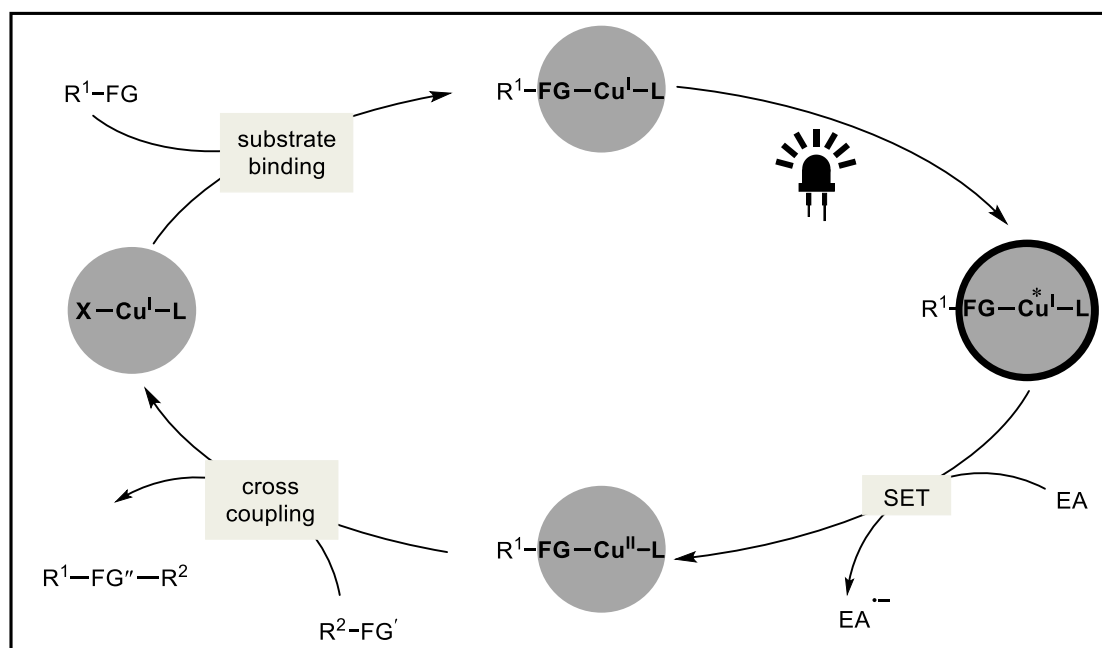


**Figure 6:** Cross-coupling reaction via photoexcitation of in situ generated  $Cu(I)$ -substrate complexes. In situ generated  $Cu(I)$ -substrate complexes reduce an electrophilic coupling partner upon irradiation with visible-light as a starting point for cross coupling. FG = Functional Group; X = counter anion; EA = electron acceptor.

been applied to denitrogenative oxidative  $C(sp^2)$ – $C(sp)$  cross-coupling between hydrazinylpyridines and terminal alkynes<sup>[27]</sup>, oxidative C–N coupling of anilines with terminal alkynes to synthesize  $\alpha$ -ketoamides<sup>[28]</sup>, oxidative C–N coupling of 2-aminopyridine with terminal alkynes via C–C triple bond cleavage<sup>[29]</sup>, and oxidative  $C(sp)$ – $C(sp)$  homo and cross-coupling of terminal alkynes.<sup>[30]</sup>

An interesting example of this strategy entailed the coupling of phenols and terminal alkynes in the presence of molecular oxygen to produce aryl and alkyl ketones. According to proposed mechanism, the excited state of the *in situ* generated Cu(I)-acetylide species reduces molecular oxygen by SET to generate a Cu(II)-acetylide species and a superoxide radical anion. Then, phenol is also converted to benzoquinone by the Cu(II)-superoxo intermediate. Sequential Paterno-Buchi-type [2+2] cycloaddition of Cu(II)-phenylacetylide and benzoquinone, oxetane ring-opening, fragmentation, formation of a peracid species, CO<sub>2</sub> extrusion, and keto-enol tautomerism furnish the desired aryl ketone product (Figure 7, ii).<sup>[31]</sup> On the other hand, the coupling between phenylacetylene and aliphatic alcohols in the presence of oxygen, stoichiometric 2-picolinic acid, and catalytic copper(I) iodide furnished  $\alpha$ -keto esters.<sup>[32]</sup> Quite recently, the same group has reported a CuCl catalyzed three-component reaction between N-alkylanilines, terminal alkynes and primary alcohols in the presence of stoichiometric benzoquinone as an oxidant to furnish propargylamines (Figure 7, iii).<sup>[33]</sup> The authors proposed that the photoexcited Cu(I)-phenylacetylide reduces benzoquinone and then the corresponding radical anion species triggers a hydrogen atom-transfer (HAT) process with a primary alcohol to generate a  $\alpha$ -oxy radical. This radical undergoes a radical-radical cross-coupling with aminyl radical cation previously generated upon LMCT excitation of a Cu(II)-amine species. Subsequent intramolecular proton-transfer followed by elimination of water molecule results in the formation of an iminium species which gets trapped by Cu(I)-phenylacetylide to produce the desired products. Recently, Lalic and co-workers established the right conditions for a  $C(sp)$ – $C(sp^3)$  cross-coupling reaction. They showed that catalytic amounts of CuCl in combination with a substituted terpyridine ligand can modulate the reactivity of the photoexcited Cu(I)-acetylide complex to achieve the coupling of unactivated alkyl iodides and terminal alkynes (Figure 7, iv).<sup>[34]</sup> Wu and co-workers have reported a C–H functionalization protocol wherein Cu(II) salts can bind 2-arylaminoacetates for the *in situ* formation of photoactive Cu(I) intermediates which can promote the alkylation of enolates (Figure 7, v).<sup>[35]</sup> Quite recently Liu and co-workers have discovered that *in situ* generated  $Cu(NCS)_2^-$  can play the dual roles, as a photocatalyst and as a Lewis acid (Figure 7, vi).<sup>[36]</sup> Energy transfer from

photoexcited  $\text{Cu}(\text{NCS})_2^-*$  to a vinyl azide causes a rearrangement to corresponding azirine intermediate which upon coordination by ground state  $\text{Cu}(\text{NCS})_2^-$  is activated and undergoes a ring-opening for the subsequent coupling with thiocyanide to give rise to 2-aminothiazole derivatives.

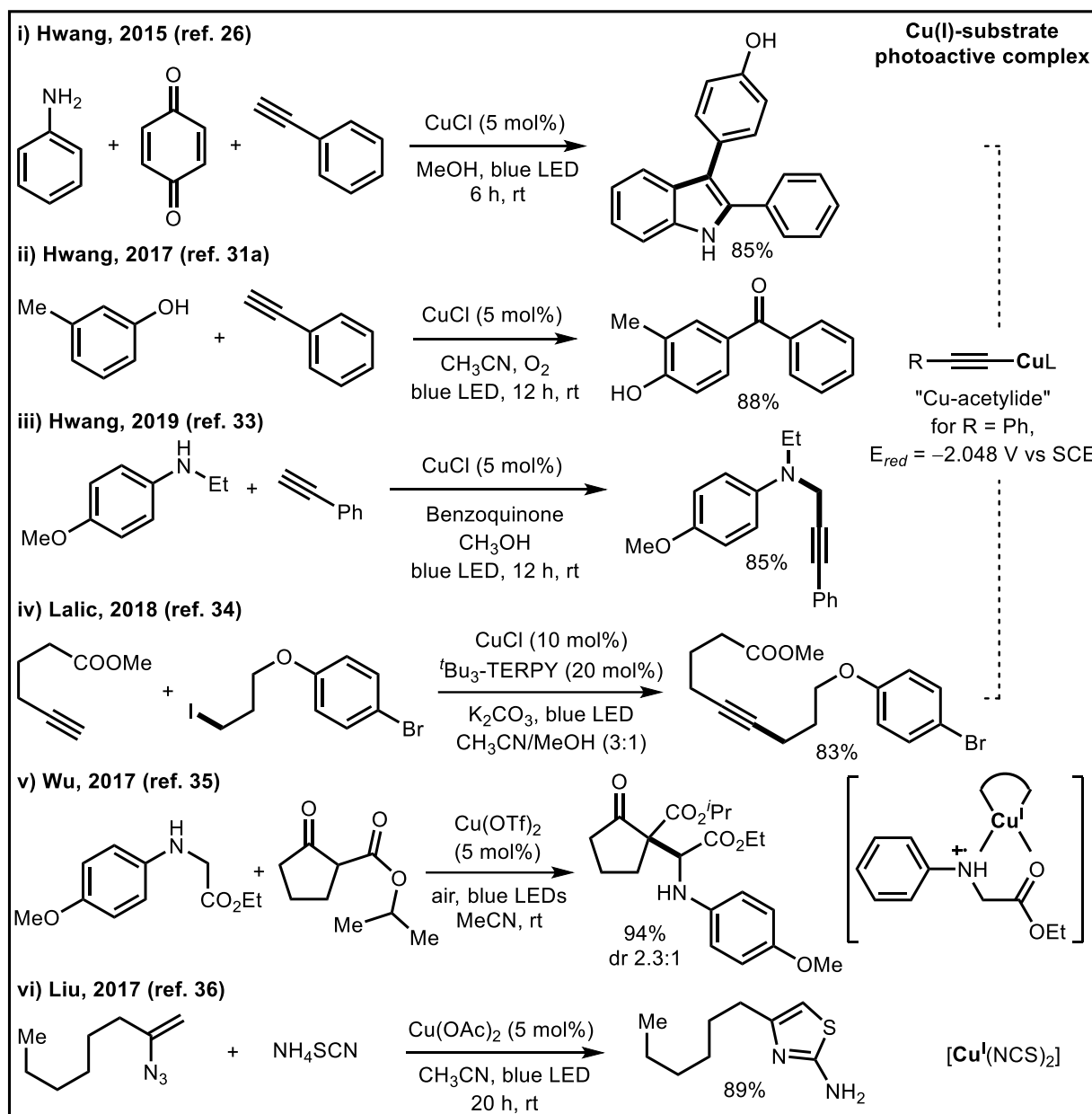


**Figure 7:** A few representative examples of the synthetic methodologies developed on the basis of this concept are shown, though (e) differs in that the *in situ* formed  $[\text{Cu}(\text{NCS})_2]^-$  complex acts as a sensitizer in the excited state and as a Lewis acid in the ground state. OAc = acetate.

### 3) Cooperative photoredox-copper dual catalysis

Cu(I) and Cu(II) salts have also recently been used as a co-catalyst in conjunction with traditional Ir- or Ru-based photocatalysts. Owing to the persistent radical effect (PRE) by copper, organic radical intermediates generated upon visible-light-induced photocatalytic cycles can be efficiently trapped by the metal center. The resulting organocopper intermediates display a variety of follow-up chemistry. The general representation of photo-copper dual catalytic cycle is shown in Figure 8 (irrespective of order): (i) the photocatalyst upon visible-light absorption, generates a radical species ( $R^1\bullet$ ) via single-electron reduction of the electrophile; (ii) simultaneous single-electron oxidation of the initial Cu(I) species to the ligated Cu(II) $L_n$  species by the oxidized-state of the photocatalyst; (iii) anionic ligand (Z) exchange from one of the reaction counterparts and formation of Cu(II) $L_{(n-1)}Z$  (or in some cases transmetallation); (iv) capture of the previously generated radical ( $R^1\bullet$ ) by Cu(II) $L_{(n-1)}Z$  and formation of the high-valent transient Cu(III) $R^1L_{(n-1)}Z$  species; and finally (v) collapse of Cu(III) $R^1L_{(n-1)}Z$  by reductive elimination to generate the desired cross-coupled product and to regenerate the initial Cu(I) species to close the copper-catalytic cycle (Figure 8). The carbophilic nature of copper allows access to various organo-copper species such as Cu-aryl

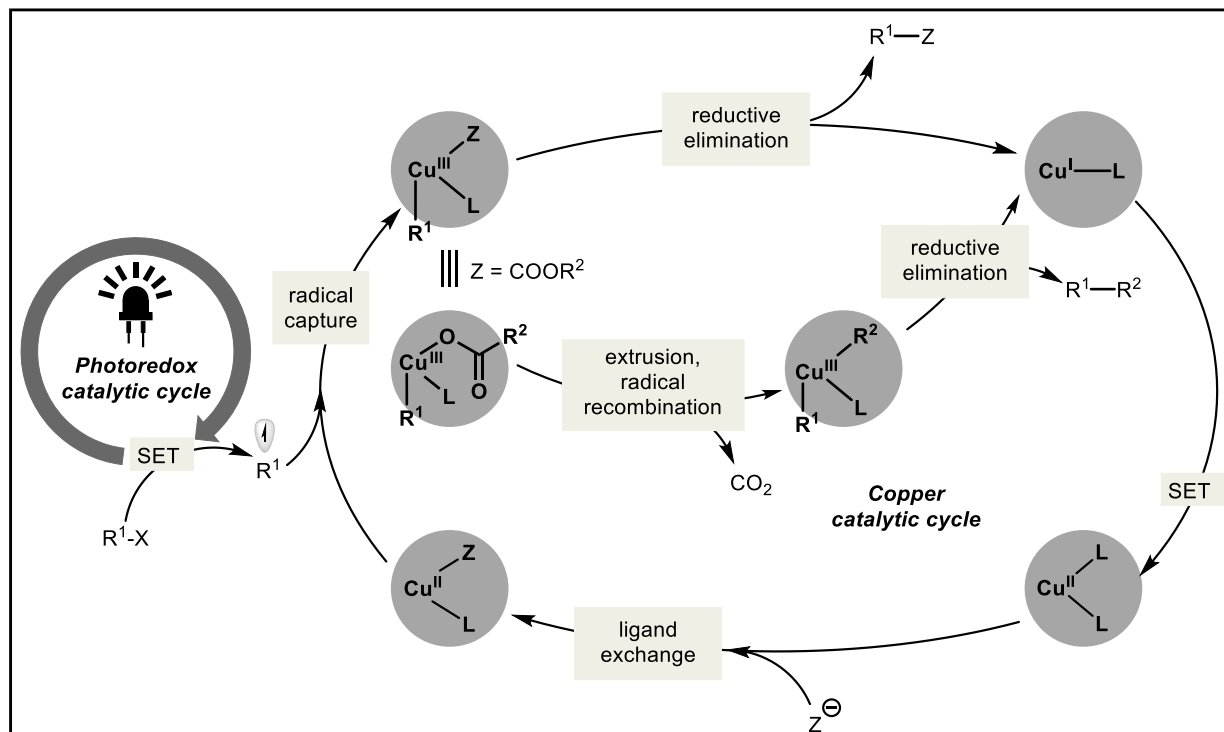


**Figure 8:** The general mechanistic pathways for cooperative photoredox/copper dual catalytic cycles.



and Cu-alkyl that in turn translate to several cross-coupling strategies with the formation of a wide variety of vital bonds such as  $C(sp^2)-C(sp^3)$ ,  $C(sp^2)-C(sp^2)$ ,  $C(sp^3)-N(sp^2)$ ,  $C(sp^3)-N(sp^3)$ ,  $C(sp^3)-O$ ,  $C(sp^3)-C(sp)$ , and  $C(sp^3)-C(sp^3)$ .

In an excellent study published in 2012, Sanford and co-workers have developed a mild synthetic method for the synthesis of perfluoroalkylated (hetero)aromatic compounds by the cross-coupling between (hetero)aryl boronic acids and perfluoroalkyl iodides in the presence of  $[Ru(bpy)_3]Cl_2 \cdot 6H_2O$  as the photocatalyst and CuOAc as the  $C(sp^2)-C(sp^3)$  bond-forming co-catalyst (Figure 9, i).<sup>[37]</sup>

Although high-valent Cu(III)-intermediate undergoes facile reductive elimination, oxidative addition of carbon-halogen bonds to low-valent Cu(I) species was a longstanding problem in the field of cross-coupling reactions that had barred the widespread use of copper as an efficient catalyst. In a noteworthy disclosure by MacMillan and co-workers have shown that an efficient cross-coupling reaction can be achieved between unactivated aryl bromides and a trifluoromethylating agent in the presence of an Ir-based photocatalyst and copper co-catalyst.<sup>[38]</sup> The transformation proceeds through the initial formation of a reactive silyl radical from tris(trimethylsilyl) silanol that abstracts bromine from the aryl bromide substrate to generate an aryl radical. At the same time, the Cu(I) complex combines with the trifluoromethyl radical generated during the closure of the Ir-photocatalytic cycle and forms a  $Cu(II)CF_3$  complex. This complex then captures the previously generated aryl radical forming a Cu(III)-intermediate which upon reductive elimination produces the trifluoromethylated arenes in excellent yields (Figure 9, ii).

Quite recently, Glorius and co-workers showed that a dual catalytic cycle involving a photocatalyst and a copper catalyst facilitates a decarboxylative olefination of redox-active esters.<sup>[39]</sup> Upon SET from excited state of the photocatalyst to the redox-active primary esters, alkyl radicals were obtained after  $CO_2$  extrusion, which were subsequently captured by the Cu(II) complex. The newly-formed Cu(III)alkyl species underwent  $\beta$ -hydride elimination to generate the desired terminal olefin in high yields concurrent with regeneration of the Cu(I) complex. Then the Cu(I)-complex was subsequently oxidized to the initial Cu(II) species to close the photocatalytic cycle (Figure 9, iii).

Hu and co-workers have recently established an efficient cross-coupling reaction between activated carboxylic acids and nitrogen nucleophiles for the synthesis of a wide range of alkyl amines.<sup>[40]</sup> In the initial step, benzophenone imine coordinates Cu(I), and subsequent

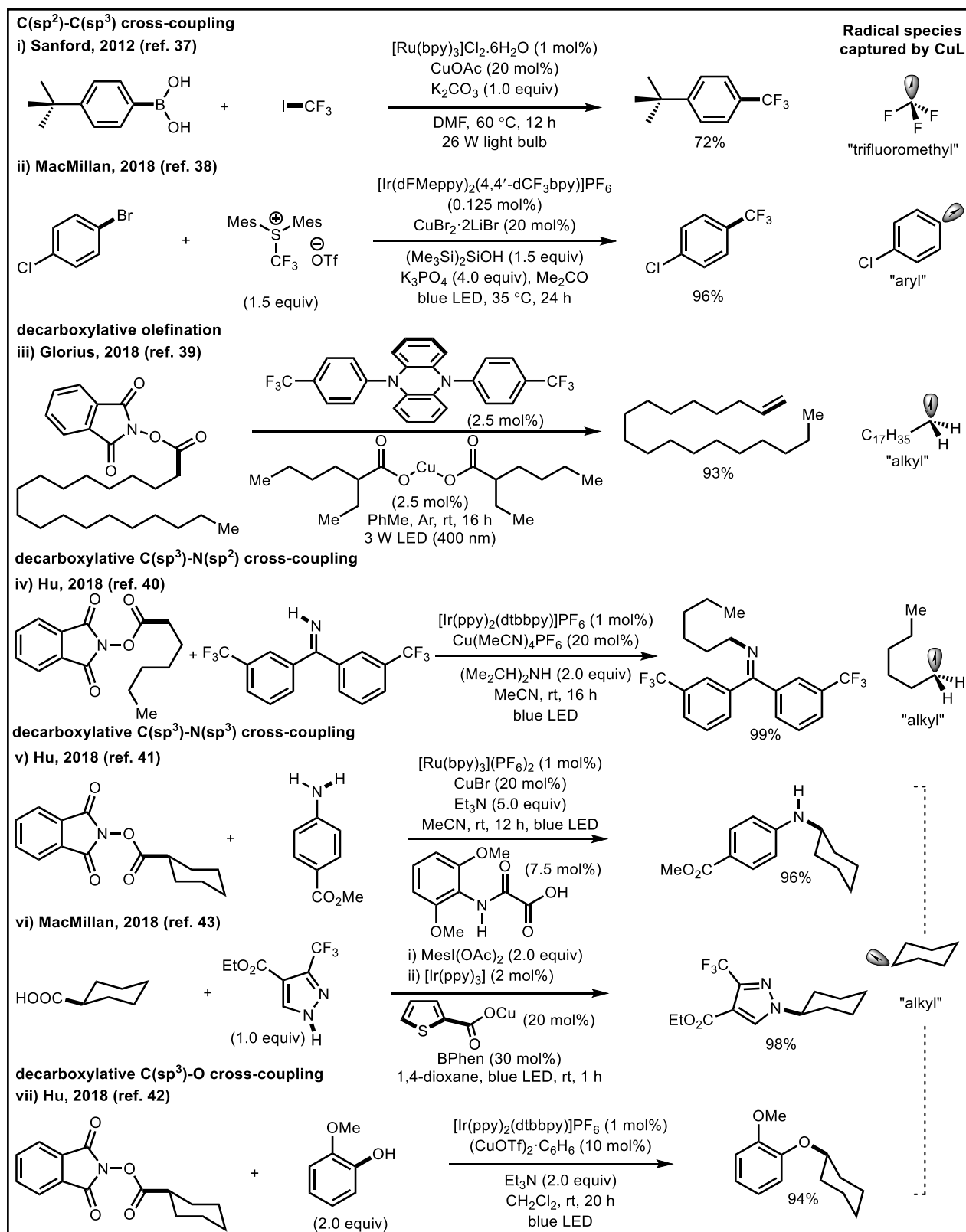


**Figure 9:** A series of non-stereoselective cross-coupling reactions.

deprotonation generates a Cu(I)-amido complex which then captures the alkyl radical generated from the alkyl NHPI ester and forms the alkyl-Cu(II) species. This species then gets converted to the corresponding Cu(III) complex by the oxidized photocatalyst, which then undergoes

reductive elimination to give the cross-coupled product with concurrent regeneration of the initial Cu(I) complex. The benzophenone imine group can be subsequently hydrolyzed or transaminated to give the corresponding primary amines (Figure 9, iv). Hu's group has further expanded the scope of the C-N bond-formation to anilines (Figure 9, v)<sup>[41]</sup> as well as to C-O bond forming reactions with phenols (Figure 9, vii)<sup>[42]</sup>.

Almost at the same time, MacMillan and co-workers<sup>[43]</sup> further extended the scope of this principle by employing a wide range of free (unactivated) primary, secondary, and tertiary alkyl carboxylic acids through *in situ* iodonium activation with a broad range of nitrogen nucleophiles such as heteroaromatics, amides, sulfonamides, and anilines (Figure 9, iv). The synthetic transformation proceeds via the initial formation of the Cu(I)-amido species which then gets oxidized by the photocatalyst to corresponding Cu(II)-amido species. Then the reduced photocatalyst generates alkyl radicals by SET to the iodomesitylene dicarboxylate, which then binds with previously generated Cu(II)-amido species to form the Cu(III)-intermediate which leads to the desired product formation.

Lin, Liu and co-workers<sup>[44]</sup> have developed a decarboxylative, enantioselective cyanation protocol of secondary benzylic NHPI esters using TMS-CN (as a cyanide source) in the presence of [Ir(ppy)<sub>3</sub>], CuBr and the chiral pyBOX ligand (Figure 10, i). The key step is the capture of the radical obtained by photoreduction of the NHPI ester by the chiral L\*Cu(II)CN complex to generate the corresponding Cu(III)-intermediate. Reductive elimination from this intermediate provided the nitrile products in good yields with excellent enantioselectivities. Later, Mei, Han and co-workers extended this concept to achieve an enantioselective bifunctionalization *i.e.* cyanoalkylation of olefins (Figure 10, ii).<sup>[45]</sup>

The aforementioned studies invariably required activation of the carboxylic acids either as their NHPI esters or through *in situ* iodonium formation. This potential drawback has recently been addressed in photocatalysis by using copper salts as the co-catalyst. Copper has the potential to enable the direct decarboxylation of the free carboxylic acids via formation of Cu(II)-carboxylate complexes, which can again capture the photochemically-generated radical to form Cu(III)(alkyl)-carboxylates. These Cu(III)-intermediate can then undergo decarboxylation, radical recombination, and reductive elimination to furnish the cross-coupled product (Figure 8). Liu and co-workers<sup>[46]</sup> showed that a decarboxylative cross-coupling reaction between  $\alpha,\beta$ -unsaturated carboxylic acids and ethyl iododifluoroacetate (Figure 10, iii) is possible following the idea. It was proposed that Cu(I) was first oxidized to Cu(II) by Ru(II)\*, which then forms

Cu(II)-carboxylate complex. Then while re-oxidation of Ru(I) to Ru(II), difluoroacetyl radical was obtained. This radical then adds to the  $\alpha$ -position of the olefinic double bonds of the Cu(II)-carboxylate complex, which subsequently undergoes CO<sub>2</sub> extrusion and elimination of Cu(I) to produce the desired products.

In line with this concept, MacMillan *et al.* have recently developed a decarboxylative trifluoromethylation of aliphatic carboxylic acids (Figure 10, iv).<sup>[47]</sup> The photoexcited Ir(III)\* initially oxidizes Cu(II)-carboxylate to corresponding Cu(III)-species. Then, subsequent extrusion of CO<sub>2</sub> and recombination of the newly generated alkyl radical produces the alkyl-Cu(III) intermediate which oxidizes Ir(II) to ground-state Ir(III) to close the photocatalytic cycle and generate an alkyl- Cu(II) intermediate. This intermediate further engages with

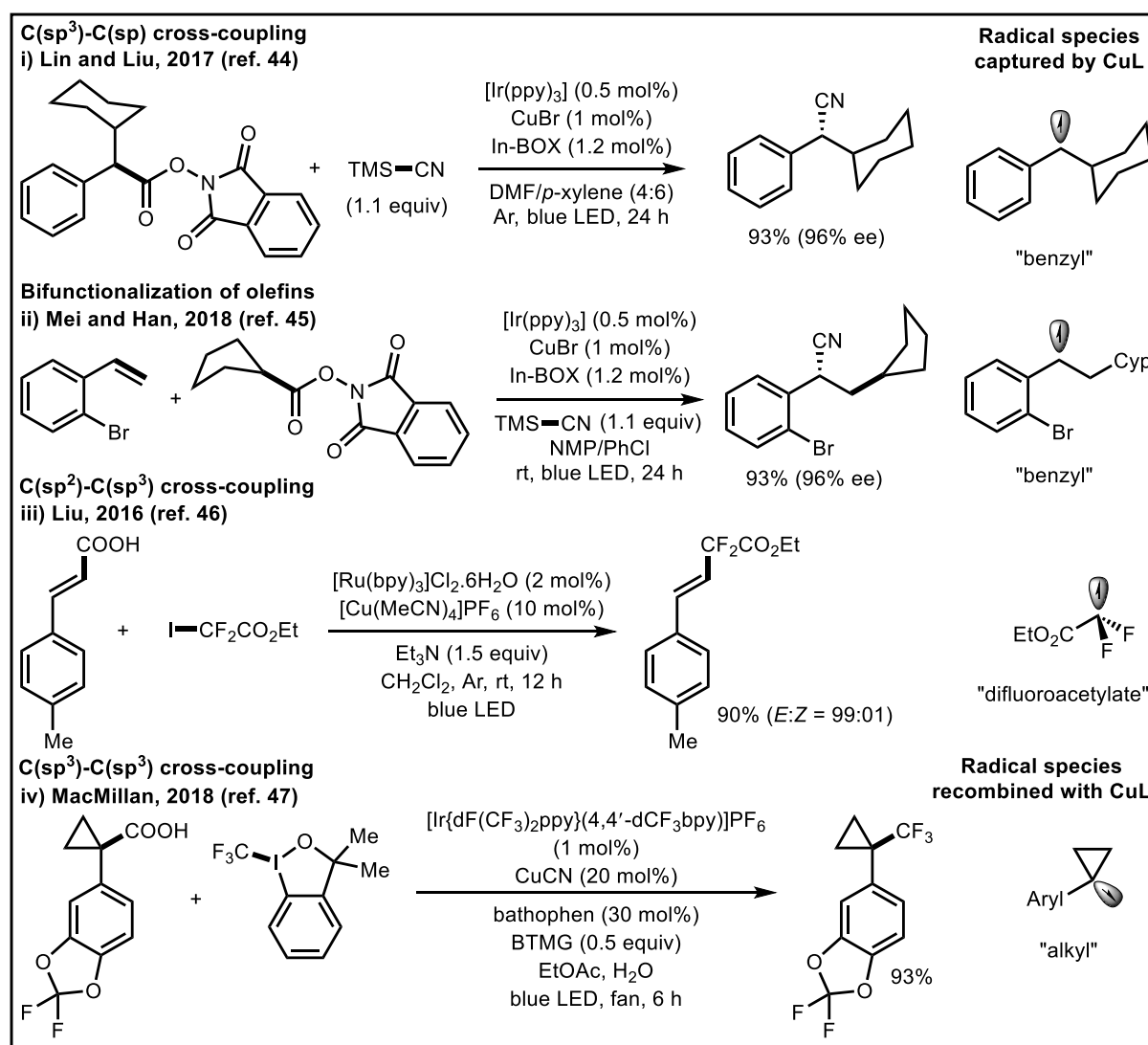
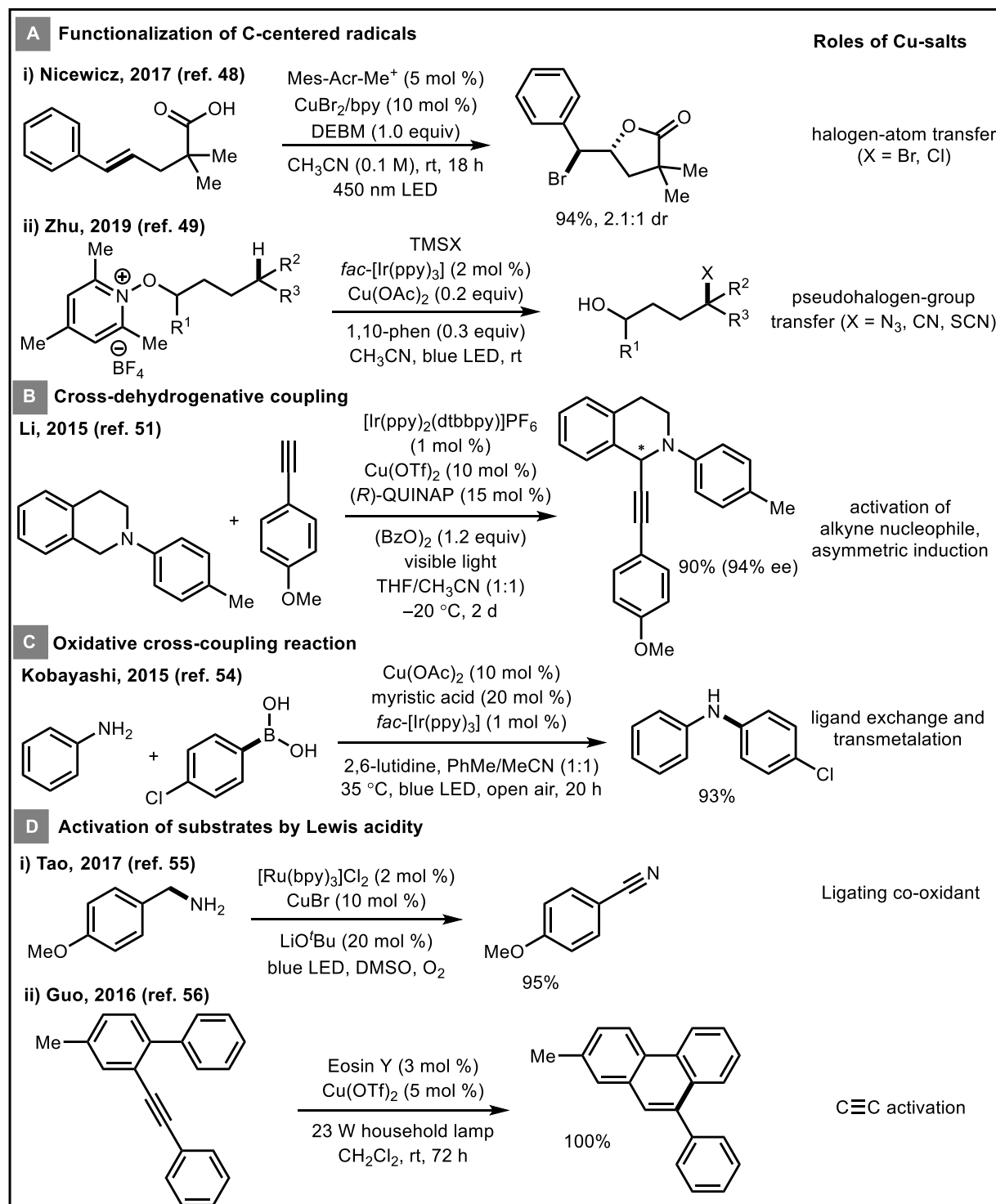


Figure 10: Few more selected examples including some enantioselective transformations.

BTMG = 2-tert-butyl-1,1,3,3-tetramethylguanidine

Togni's reagent to furnish the targeted alkyl-CF<sub>3</sub> products and regenerates the Cu(II) co-catalyst.

#### 4) Miscellaneous examples



**Figure 11:** Miscellaneous roles of copper in photoredox catalysis. DEBM = diethyl bromomalonate; QUINAP = 1-(2-Diphenylphosphino-1-naphthyl)isoquinoline.

Apart from the aforementioned studies, copper has played some special roles in photocatalytic transformations which will be discussed in this section. Nicewicz and co-workers<sup>[48]</sup> have combined photocatalysis with copper catalysis in order to achieve a regioselective halofunctionalization of unsaturated carboxylic acids (Figure 11A, i). The reaction proceeds via the initial oxidation of the alkene by the Fukuzumi's catalyst followed by the nucleophilic addition of the internal carboxylate to the radical cation intermediate. Then, Cu(II) co-catalyst assists in the halide transfer step from an external halide source to newly-generated C-centered radical which lead to the desired product formation. Zhu and co-workers have shown that a remote C(*sp*<sup>3</sup>)-H functionalization of N-alkoxy-pyridinium salts is possible in presence of copper salt under photocatalytic conditions (Figure 11A, ii). In this case also copper assisted pseudo-halogen transfer to the intermediate radical was responsible for the formation of various  $\delta$ -functionalized alcohols.<sup>[49]</sup>

In 2012, Rueping *et. al.* has shown that a photocatalytic oxidative alkylation reaction of tetrahydroisoquinolines can be achieved using [Cu(MeCN)<sub>4</sub>]PF<sub>6</sub> as a co-catalyst.<sup>[50]</sup> The role of copper salt was explained in terms of formation of copper acetylide as the active nucleophile from terminal alkynes. Later, Li and co-workers have extended concept through the development of its asymmetric variant by using a chiral Cu-QUINAP complex (Figure 11B).<sup>[51]</sup> The strategy has also been successfully used to functionalize isochromans with  $\beta$ -keto esters wherein catalytic amount of Cu(OTf)<sub>2</sub> has been used to activate the nucleophiles for their addition to the cationic intermediates.<sup>[52]</sup> Fu and co-workers<sup>[53]</sup> also contributed by the development of a photocatalyzed decarboxylative alkylation of NHPI esters of  $\alpha$ -amino acids. Presence of catalytic amounts of CuI was necessary to generate the active nucleophile in the form of copper acetylide.

Kobayashi and co-workers<sup>[54]</sup> established an improved Chan-Lam coupling reaction between electron-deficient aryl boronic acids and anilines (Figure 11C) by a combined copper/photocatalyst system. In the key step, a organo-Cu(III)-amide species was formed which underwent reductive elimination to give the desired cross-coupled product.

Aromatic nitriles can be obtained from primary amines through aerobic oxidation (Figure 11D, i) which was accomplished by Tao's group by employing [Ru(bpy)<sub>3</sub>]Cl<sub>2</sub>/CuBr dual catalytic system. The proposed mechanism involves the initial formation of a copper-amide intermediate which undergoes SET by photoexcited Ru(II)\* and subsequent hydrogen abstraction and neutralization by superoxide radical anion and hydrogen peroxide anion, respectively, to form

a copper-amido intermediate. Then, another similar catalytic cycle furnishes the desired nitrile derivative.<sup>[55]</sup>

Guo and co-workers have utilized copper's Lewis acidity for the activation of  $C(sp)\equiv C(sp)$  triple bonds through the formation of a  $\pi$ -complex (3c-2e) (Figure 11D, ii). This complex upon single-electron oxidation by a photocatalyst can form a new 3c-1e system which then undergoes an arene-yne cyclization reaction to produce phenanthrene derivatives.<sup>[56]</sup>

### 5) Cu(II)-complexes as stand-alone photocatalysts:

Very recently, the successful applications of Cu(II)-complexes as visible light photoredox catalysts have been reported by Rehbein, Reiser and co-workers. Following the seminal work of Kochi and co-workers, who demonstrated that  $CuCl_2$  undergoes homolysis to  $Cu(I)Cl$  and  $Cl\cdot$  upon UV-irradiation,<sup>[57]</sup> the activation of  $Cu(II)X_2$  complexes endowed with suitable ligands to redshift absorption into the visible region can produce radicals  $X\cdot$  that initiate

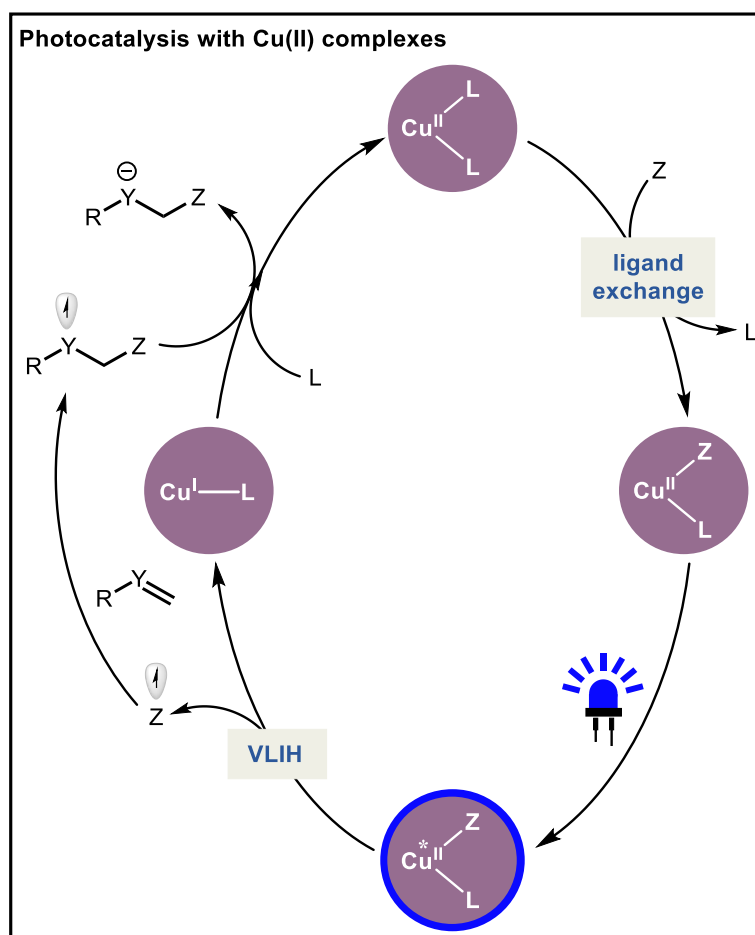


Figure 12: Z = Nucleophile; Y = Heteroatom; VLIH = visible-light induced homolysis.

productive organic transformations (Figure 12). Thus, rather than metal-to-ligand charge transfer (MLCT) states fundamental to photoexcitation of Cu(I) complexes, Cu(II) complexes react from ligand-to-metal charge transfer (LMCT) states<sup>[58]</sup>, which oxidize the nucleophile.

Following this concept, the synthesis of azido ketones from vinyl arenes, TMSN<sub>3</sub> and oxygen was developed using the copper(II) complex [Cu(dap)Cl<sub>2</sub>] as photoredox catalyst<sup>[59]</sup> (Chapter 4). The Cu(II) complex undergoes ligand exchange with azide to give rise to a new LCu(II)azide-bridged dimer. Upon visible light-induced homolysis (VLIH) LCu(I) and an azido radical are formed, and the latter can be intercepted by an alkene followed by molecular oxygen. Rebound of the *O*-centered radical with LCu(I) regenerates the LCu(II)-species, which upon elimination releases the product and closes the catalytic cycle.

A second, notable example was reported shortly after by Gong and coworkers<sup>[60]</sup> (Figure 13). In this case, a chiral Cu(II)-bisoxazoline complex is alkylated via transmetalation from trifluoroborate, and once again VLIH generates an alkyl radical and a Cu(I) intermediate. In a second catalytic cycle, this alkyl radical adds to the substrate, here an protected imine that is

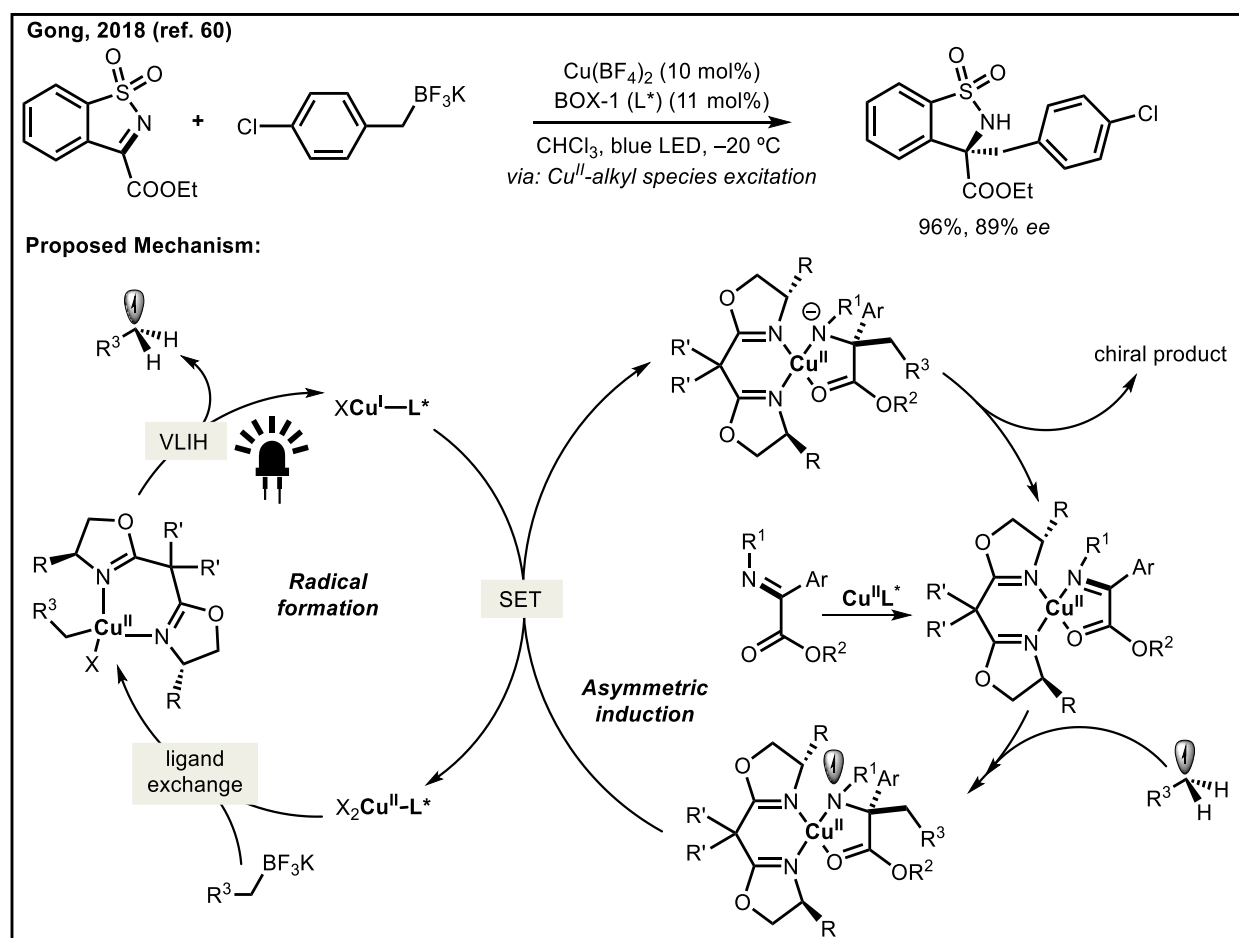


Figure 13: Example of a Cu(II)-photocatalyzed reaction.



activated by the same chiral Cu(II)-bisoxazoline complex. The newly generated *N*-centered radical is reduced by the previously-formed Cu(I) species in the first cycle to release the alkylated imine with high enantioselectivity.

Very recently, [Cu(dap)Cl<sub>2</sub>] has been successfully employed in a photochemical ATRA reaction between sulfonyl chloride and olefins<sup>[61]</sup> (Chapter 6).. In line with Kochi's proposal, VLIH of LCu(II)-Cl bond generates LCu(I)-species for reduction of sulfonyl chlorides. Interestingly, the presence of stoichiometric amount Na<sub>2</sub>CO<sub>3</sub> is necessary when unactivated olefins (*e.g.* allylbenzene) are subjected to the aforementioned reaction, in contrast to activated olefins (*e.g.* styrene) for which no additive is required. The role of Na<sub>2</sub>CO<sub>3</sub> is proven to prevent the catalyst poisoning during the reaction.

Another excellent report by Yuan and coworkers<sup>[62]</sup> disclosed the ability of CuCl<sub>2</sub> salt to form photoactive species with solvent (*viz.*, acetonitrile or acetone), which could efficiently convert benzyl alcohol to benzaldehyde in the presence of molecular oxygen. Detailed mechanistic studies suggested that molecular oxygen helped only in the regeneration of the catalyst but not acted as a source of oxygen in benzaldehyde.

#### Conclusion and outlook:

Although copper-based photocatalysts have mostly been used for SET from photoexcited states involving transition from Cu(I)\* to Cu(II), there have been a few reports which exploit the photo-oxidizing potential of transitions from Cu(I)\* to Cu(0)<sup>[63]</sup> or from Cu(II)\* to Cu(I).<sup>[64]</sup> More sophisticated catalytic systems can be designed because of the high degree of tunability in the coordination sphere and ligand-coordination mode which allows further optimization of redox properties and excited-state lifetimes (10). Likewise, a structurally pre-distorted bis(chelated) Cu(I)-complex with a guanidine-quinoline ligand system has been synthesized which retains its constrained geometry in both the +1 and +2 oxidation states to instigate photochemical reactions by facilitating faster MLCT transition.<sup>[65]</sup> In the coming years, copper complexes with such augmented potential will almost certainly have extensive impact in organic synthesis, materials science, and pharmaceutical chemistry.

#### References and notes:

- [1] a) C. K. Prier, D. A. Rankic, D. W. C. MacMillan, *Chem. Rev.* **2013**, *113*, 5322; b) D. M. Schultz, T. P. Yoon, *Science* **2014**, *343*, 1239176.
- [2] L. Marzo, S. K. Pagire, O. Reiser, B. König, *Angew. Chem. Int. Ed.* **2018**, *57*, 10034.

- [3] a) D. Ravelli, S. Protti, M. Fagnoni, *Chem. Rev.* **2016**, *116*, 9850; b) N. A. Romero, D. A. Nicewicz, *Chem. Rev.* **2016**, *116*, 10075.
- [4] H. Huo, X. Shen, C. Wang, L. Zhang, P. Röse, L.-A. Chen, K. Harms, M. Marsch, G. Hilt, E. Meggers, *Nature* **2014**, *515*, 100.
- [5] C. B. Larsen, O. S. Wenger, *Chem. Eur. J.* **2018**, *24*, 2039.
- [6] J. Twilton, C. Le, P. Zhang, M. H. Shaw, R. W. Evans, D. W. C. MacMillan, *Nat. Rev. Chem.* **2017**, *1*, 52.
- [7] O. Reiser, *Acc. Chem. Res.* **2016**, *49*, 1990.
- [8] a) C. Minozzi, A. Caron, J.-C. Grenier-Petel, J. Santandrea, S. K. Collins, *Angew. Chem. Int. Ed.* **2018**, *57*, 5477; b) M. Knorn, T. Rawner, R. Czerwieniec, O. Reiser, *ACS Catal.* **2015**, *5*, 5186; c) A. C. Hernandez-Perez, S. K. Collins, *Acc. Chem. Res.* **2016**, *49*, 1557.
- [9] D. R. McMillin, M. T. Buckner, B. T. Ahn, *Inorg. Chem.* **1977**, *16*, 943.
- [10] J.-M. Kern, J.-P. Sauvage, *J. Chem. Soc., Chem. Commun.* **1987**, 546.
- [11] M. Pirtsch, S. Paria, T. Matsuno, H. Isobe, O. Reiser, *Chem. Eur. J.* **2012**, *18*, 7336.
- [12] A. C. Hernandez-Perez, A. Vlassova, S. K. Collins, *Org. Lett.* **2012**, *14*, 2988.
- [13] A. Sagadevan, K. C. Hwang, *Adv. Synth. Catal.* **2012**, *354*, 3421.
- [14] M. Mitani, I. Kato, K. Koyama, *J. Am. Chem. Soc.* **1983**, *105*, 6719.
- [15] D. B. Bagal, G. Kachkovskyi, M. Knorn, T. Rawner, B. M. Bhanage, O. Reiser, *Angew. Chem. Int. Ed.* **2015**, *54*, 6999.
- [16] S. H. Oh, Y. R. Malpani, N. Ha, Y.-S. Jung, S. B. Han, *Org. Lett.* **2014**, *16*, 1310.
- [17] T. Rawner, E. Lutsker, C. A. Kaiser, O. Reiser, *ACS Catal.* **2018**, *8*, 3950.
- [18] Z. Liu, H. Chen, Y. Lv, X. Tan, H. Shen, H.-Z. Yu, C. Li, *J. Am. Chem. Soc.* **2018**, *140*, 6169.
- [19] J. He, C. Chen, G. C. Fu, J. C. Peters, *ACS Catal.* **2018**, 11741.
- [20] X.-Y. Yu, Q.-Q. Zhao, J. Chen, J.-R. Chen, W.-J. Xiao, *Angew. Chem. Int. Ed.* **2018**, *57*, 15505.
- [21] a) Q. M. Kainz, C. D. Matier, A. Bartoszewicz, S. L. Zultanski, J. C. Peters, G. C. Fu, *Science* **2016**, *351*, 681; b) M. F. Greaney, *Science* **2016**, *351*, 666.
- [22] J. M. Ahn, J. C. Peters, G. C. Fu, *J. Am. Chem. Soc.* **2017**, *139*, 18101.
- [23] C. D. Matier, J. Schwaben, J. C. Peters, G. C. Fu, *J. Am. Chem. Soc.* **2017**, *139*, 17707.
- [24] S. Murarka, *Adv. Synth. Catal.* **2018**, *360*, 1735.
- [25] W. Zhao, R. P. Wurz, J. C. Peters, G. C. Fu, *J. Am. Chem. Soc.* **2017**, *139*, 12153.
- [26] A. Sagadevan, A. Ragupathi, K. C. Hwang, *Angew. Chem. Int. Ed.* **2015**, *54*, 13896.
- [27] V. P. Charpe, A. A. Hande, A. Sagadevan, K. C. Hwang, *Green Chem.* **2018**, *20*, 4859.

- [28] A. Sagadevan, A. Ragupathi, C.-C. Lin, J. R. Hwu, K. C. Hwang, *Green Chem.* **2015**, *17*, 1113.
- [29] A. Ragupathi, A. Sagadevan, C.-C. Lin, J.-R. Hwu, K. C. Hwang, *Chem. Commun.* **2016**, *52*, 11756.
- [30] a) A. Sagadevan, P.-C. Lyu, K. C. Hwang, *Green Chem.* **2016**, *18*, 4526; b) A. Sagadevan, V. P. Charpe, K. C. Hwang, *Catal. Sci. Technol.* **2016**, *6*, 7688.
- [31] a) A. Sagadevan, V. P. Charpe, A. Ragupathi, K. C. Hwang, *J. Am. Chem. Soc.* **2017**, *139*, 2896; b) P. Xiao, C.-X. Li, W.-H. Fang, G. Cui, W. Thiel, *J. Am. Chem. Soc.* **2018**, *140*, 15099.
- [32] D. K. Das, V. K. Kumar Pampana, K. C. Hwang, *Chem. Sci.* **2018**, *9*, 7318.
- [33] A. Sagadevan, V. K. K. Pampana, K. C. Hwang, *Angew. Chem. Int. Ed.* **2019**, *58*, 3838.
- [34] A. Hazra, M. T. Lee, J. F. Chiu, G. Lalic, *Angew. Chem. Int. Ed.* **2018**, *57*, 5492.
- [35] Q.-Y. Meng, X.-W. Gao, T. Lei, Z. Liu, F. Zhan, Z.-J. Li, J.-J. Zhong, H. Xiao, K. Feng, B. Chen et al., *Sci. Adv.* **2017**, *3*, e1700666.
- [36] W.-L. Lei, T. Wang, K.-W. Feng, L.-Z. Wu, Q. Liu, *ACS Catal.* **2017**, *7*, 7941.
- [37] Y. Ye, M. S. Sanford, *J. Am. Chem. Soc.* **2012**, *134*, 9034.
- [38] C. Le, T. Q. Chen, T. Liang, P. Zhang, D. W. C. MacMillan, *Science* **2018**, *360*, 1010.
- [39] A. Tlahuext-Aca, L. Candish, R. A. Garza-Sanchez, F. Glorius, *ACS Catal.* **2018**, *8*, 1715.
- [40] R. Mao, J. Balon, X. Hu, *Angew. Chem. Int. Ed.* **2018**, *57*, 9501.
- [41] R. Mao, A. Frey, J. Balon, X. Hu, *Nat. Catal.* **2018**, *1*, 120.
- [42] R. Mao, J. Balon, X. Hu, *Angew. Chem. Int. Ed.* **2018**, *57*, 13624.
- [43] Y. Liang, X. Zhang, D. W. C. MacMillan, *Nature* **2018**, *559*, 83.
- [44] D. Wang, N. Zhu, P. Chen, Z. Lin, G. Liu, *J. Am. Chem. Soc.* **2017**, *139*, 15632.
- [45] W. Sha, L. Deng, S. Ni, H. Mei, J. Han, Y. Pan, *ACS Catal.* **2018**, *8*, 7489.
- [46] H.-R. Zhang, D.-Q. Chen, Y.-P. Han, Y.-F. Qiu, D.-P. Jin, X.-Y. Liu, *Chem. Commun.* **2016**, *52*, 11827.
- [47] J. A. Kautzky, T. Wang, R. W. Evans, D. W. C. MacMillan, *J. Am. Chem. Soc.* **2018**, *140*, 6522.
- [48] J. D. Griffin, C. L. Cavanaugh, D. A. Nicewicz, *Angew. Chem. Int. Ed.* **2017**, *56*, 2097.
- [49] X. Bao, Q. Wang, J. Zhu, *Angew. Chem. Int. Ed.* **2019**, *58*, 2139.
- [50] M. Rueping, R. M. Koenigs, K. Poscharny, D. C. Fabry, D. Leonori, C. Vila, *Chem. Eur. J.* **2012**, *18*, 5170.
- [51] I. Perepichka, S. Kundu, Z. Hearne, C.-J. Li, *Org. Biomol. Chem.* **2015**, *13*, 447.

- [52] M. Xiang, Q.-Y. Meng, J.-X. Li, Y.-W. Zheng, C. Ye, Z.-J. Li, B. Chen, C.-H. Tung, L.-Z. Wu, *Chem. Eur. J.* **2015**, *21*, 18080.
- [53] H. Zhang, P. Zhang, M. Jiang, H. Yang, H. Fu, *Org. Lett.* **2017**, *19*, 1016.
- [54] W.-J. Yoo, T. Tsukamoto, S. Kobayashi, *Angew. Chem. Int. Ed.* **2015**, *54*, 6587.
- [55] C. Tao, B. Wang, L. Sun, Z. Liu, Y. Zhai, X. Zhang, J. Wang, *Org. Biomol. Chem.* **2017**, *15*, 328.
- [56] R. Jin, Y. Chen, W. Liu, D. Xu, Y. Li, A. Ding, H. Guo, *Chem. Commun.* **2016**, *52*, 9909.
- [57] J. K. Kochi, *J. Am. Chem. Soc.* **1962**, *84*, 2121.
- [58] a) A. Hu, J.-J. Guo, H. Pan, Z. Zuo, *Science* **2018**, *361*, 668; b) J.-J. Guo, A. Hu, Y. Chen, J. Sun, H. Tang, Z. Zuo, *Angew. Chem. Int. Ed.* **2016**, *55*, 15319.
- [59] A. Hossain, A. Vidyasagar, C. Eichinger, C. Lankes, J. Phan, J. Rehbein, O. Reiser, *Angew. Chem. Int. Ed.* **2018**, *57*, 8288.
- [60] Y. Li, K. Zhou, Z. Wen, S. Cao, X. Shen, M. Lei, L. Gong, *J. Am. Chem. Soc.* **2018**, *140*, 15850.
- [61] a) S. Engl, O. Reiser, *Eur. J. Org. Chem.* **2019**, *116*, 9683; b) A. Hossain, S. Engl, E. Lutsker, O. Reiser, *ACS Catal.* **2019**, *9*, 1103.
- [62] C. Meng, K. Yang, X. Fu, R. Yuan, *ACS Catal.* **2015**, *5*, 3760.
- [63] a) B. Wang, D. P. Shelar, X.-Z. Han, T.-T. Li, X. Guan, W. Lu, K. Liu, Y. Chen, W.-F. Fu, C.-M. Che, *Chem. Eur. J.* **2015**, *21*, 1184; b) B. Michelet, C. Deldaele, S. Kajouj, C. Moucheron, G. Evano, *Org. Lett.* **2017**, *19*, 3576.
- [64] G. Fumagalli, P. T. G. Rabet, S. Boyd, M. F. Greaney, *Angew. Chem. Int. Ed.* **2015**, *54*, 11481.
- [65] B. Dicke, A. Hoffmann, J. Stanek, M. S. Rampp, B. Grimm-Lebsanft, F. Biebl, D. Rukser, B. Maerz, D. Göries, M. Naumova et al., *Nat. Chem.* **2018**, *10*, 355.





# *Chapter 4*





## Copper and Visible-Light: Oxo-azidation of Vinylarenes

### Abstract:

A visible-light-accelerated, copper(II)-catalyzed method for oxo-azidation of vinylarenes has been developed. This method operates at room temperature and utilizes molecular oxygen as the stoichiometric oxidant. In contrast to commonly used iridium, ruthenium or organic dye based photocatalysts, copper-based photocatalysts were found to be unique for this transformation, which is attributed to the inner-sphere mechanism. With spectroscopic evidences, Cu(II) has been proposed as the catalytically active species. In the key-step, a copper-azide species undergoes a light-accelerated homolysis to form Cu(I) and azido radicals. To the best of our knowledge, this represents the first visible-light photocatalyzed process triggered by copper in the oxidation state +2. This study also represents the first catalytic synthesis of azidoketones directly from olefins.

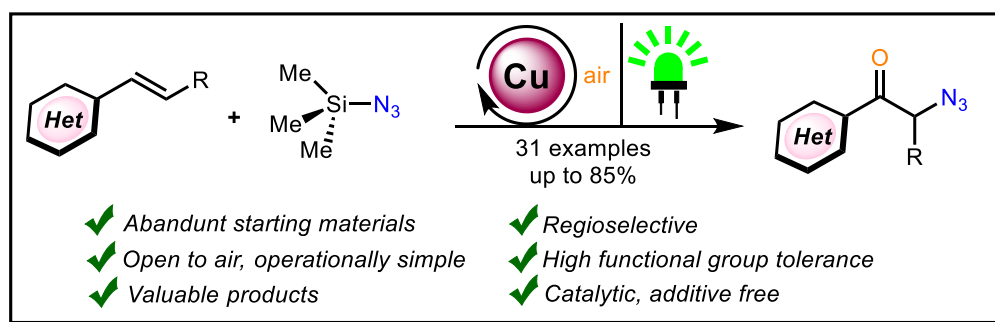


Figure 1: Copper-catalyzed oxo-azidation of vinylarenes.

### Introduction:

Visible-light photocatalysis has advanced organic synthesis during the last decade by offering unique opportunities to generate radical-intermediates in an environmentally benign and economic manner.<sup>[1]</sup> In this context, utilization of earth-abundant metals instead of heavy metals (ruthenium or iridium are always high on demand.<sup>[2]</sup> Particularly, photoactive Cu(I)-complexes has emerged as excellent catalysts<sup>[3]</sup> for the difunctionalization of carbon-carbon

### This chapter has been published:

**A. Hossain**, A. Vidyasagar, C. Eichinger, C. Lankes, J. Phan, J. Rehbein, O. Reiser  
*Angew. Chem. Int. Ed.* **2018**, *57*, 8288-8292; *Angew. Chem.* **2018**, *130*, 8420-8424.

A.H., J.R. and O.R. wrote the manuscript.

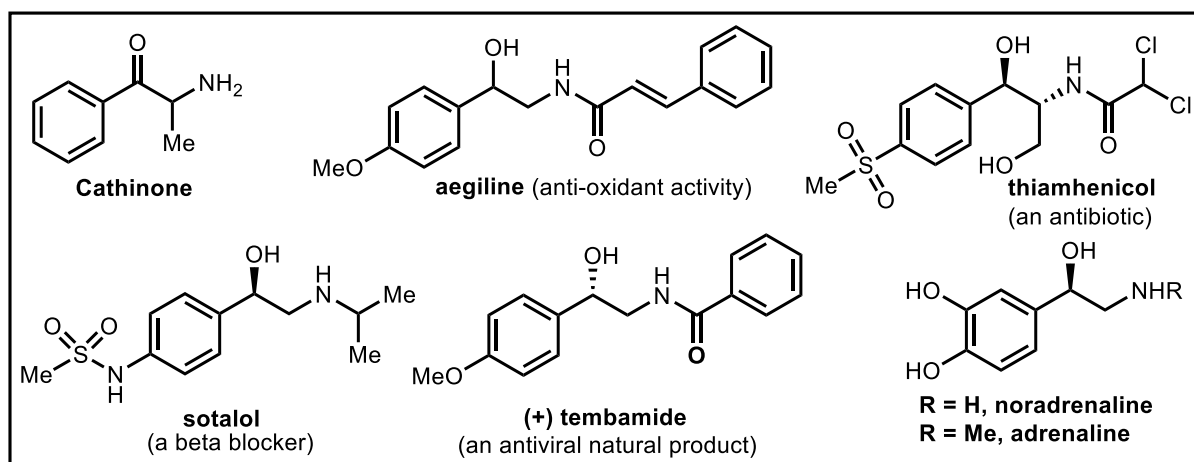
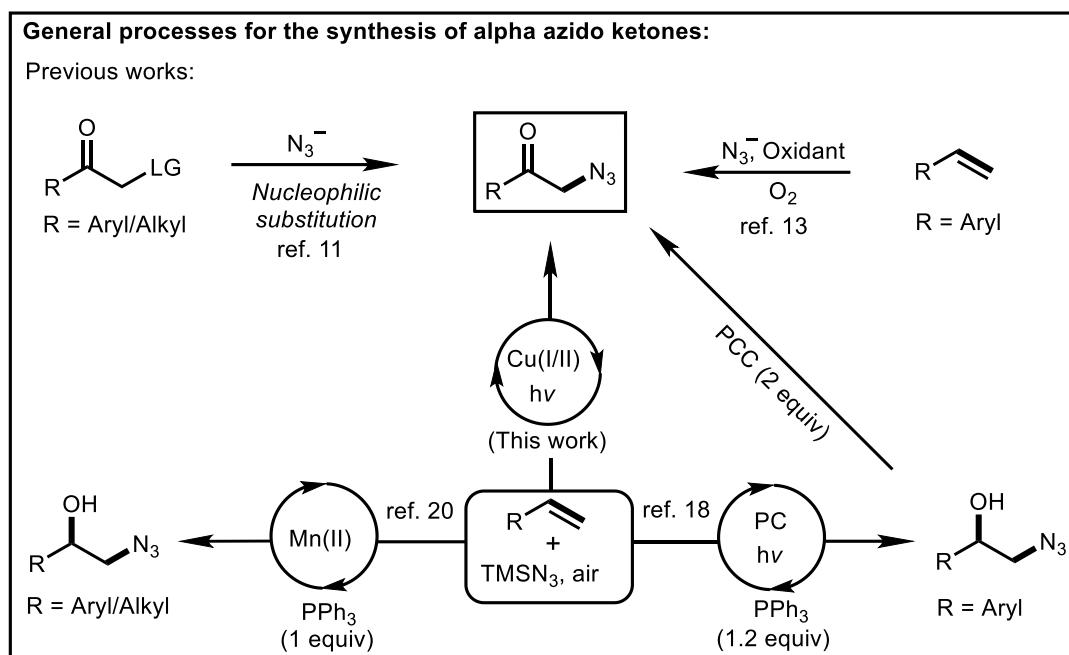


**Figure 2:** Selected bioactive compounds.

multiple bonds,<sup>[4,5]</sup> or in cross-coupling reactions<sup>[6]</sup> providing an attractive alternative to thermal activation by transition-metal or organic oxidants.<sup>[7]</sup>

Organic azides,<sup>[8]</sup> especially azidoketones,<sup>[9,10]</sup> are important class of compounds (Figure 2), and consequently, various methods have been developed for their synthesis. The most commonly used method is a nucleophilic substitution (Scheme 1)<sup>[11]</sup> reaction using sodium-azide as the azide source and pre-functionalized starting materials with a labile leaving group.<sup>[12]</sup> In 2000, Nair and co-workers<sup>[13]</sup> developed a method for their direct synthesis from olefins using molecular oxygen in the presence of stoichiometric amounts of a strong oxidant, ceric ammonium nitrate. However, there was no catalytic method available for the synthesis of azidoketones from olefins without using superstoichiometric amounts of strong oxidants.<sup>[13,14]</sup> Quite recently, Greaney and co-workers<sup>[15]</sup> disclosed the generation of azido radicals from an azidoiodinane (Zhdankin reagent) in the presence of a Cu(I)-complex which produced alkoxy- and diazido functionalized products under photochemical and thermal conditions, respectively. On the other hand, we have recently reported oxygen-mediated photocatalytic transformations of carbon-carbon multiple bond systems.<sup>[16]</sup> On the basis of these precedents, we envisioned that a three-component reaction between an azide radical source, an olefin, and molecular oxygen might lead to the formation of the desired  $\alpha$ -azidoketones.<sup>[17]</sup>

Our approach complements Lu's report in which peroxy-azidation of alkenes with 9-mesityl-10-methylacridiniumperchlorate (Fukuzumi's catalyst) has been achieved under photochemical conditions which actually utilizes the same precursors (Scheme 1)<sup>[18]</sup>. In fact, peroxy-azidation of olefins was also known under thermal conditions by catalysis with manganese(II), followed by reduction of the stoichiometrically generated hydroperoxides with



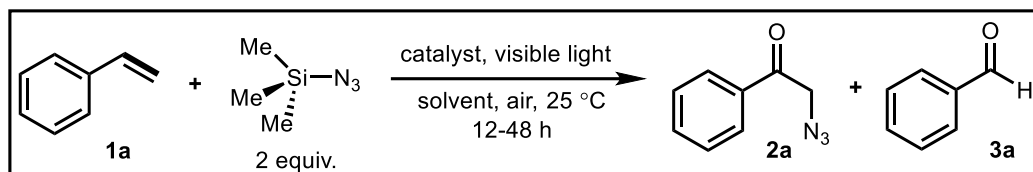
**Scheme 1:** LG = Leaving Group; PC = 9-mesityl-10-methylacridiniumperchlorate; PCC = pyridiumchlorochromate.

equimolar amounts of triphenylphosphine. It should be noted that, in the latter approach, copper catalysts failed to achieve this transformation. Alternatively, iodine or Sn(IV) catalysis using organic peroxides have been employed towards azido alcohols,<sup>[19,20]</sup> which, in turn, can then be oxidized to azidoketones with pyridiniumchlorochromate (PCC).

### Reaction optimization:

We began our investigation by testing different photocatalysts under visible-light irradiation, ( $\lambda_{max} = 455 \text{ nm}$ ) using trimethylsilyl azide as an inexpensive azido radical source and oxygen (reaction was run open to air) to achieve a coupling with styrene **1a**. Assuming that oxidation of the azide anion to its radical is required ( $E = +1.32 \text{ V vs. SCE}$ ), it was not unexpected that neither ruthenium ( $E_{\text{Ru(II)}/\text{Ru(I)}} = +0.77 \text{ V vs. SCE}$  for  $[\text{Ru}(\text{bpy})_3]\text{Cl}_2$ ; bpy = 2,2'-bipyridine), nor iridium ( $E_{\text{Ir(III)}/\text{Ir(II)}} = +0.31 \text{ V vs. SCE}$  for  $[\text{Ir}(\text{ppy})_3]$ ; ppy = 2-phenylpyridine) nor eosin Y ( $E_{\text{EY}^*/\text{EY}^-} = +0.83 \text{ V vs. SCE}$ )<sup>[21]</sup> would promote a reaction, given their low oxidation potential (Table 1, entries 1-3). However, azido radicals can be obtained from  $\text{TMSN}_3$  ( $E_{\text{N}_3^*/\text{N}_3^-} = +1.32 \text{ V}$ ) using highly oxidizing Fukuzumi's catalyst ( $E_{\text{dye}^*/\text{dye}^-} = +2.06 \text{ V vs. SCE}$ ; dye = 9-mesityl-10-methylacridiniumperchlorate). But in that case, azidoperoxides were obtained as major products in its presence. Nevertheless, when we performed the reaction in the presence of 1 mol%  $[\text{Cu}(\text{dap})_2]\text{Cl}$  ( $E_{\text{Cu(II)}/\text{Cu(I)}} = -1.43 \text{ V vs. SCE}$ ; dap = 2,9-bis(*p*-anisyl)-1,10-phenanthroline),<sup>[22]</sup> we were pleased to observe a full conversion of the starting material **1a**

Table 1: Optimization for reaction conditions:



Entry	catalyst (mol%)	$\lambda_{\text{vis}}$ (nm)	solvent (0.25 M)	time (h)	yield <sup>a</sup>	
					2a	3a
1	[Ir(ppy) <sub>3</sub> ] (1)	455	CH <sub>3</sub> CN	20	2	-
2	[Ru(bpy) <sub>3</sub> ]Cl <sub>2</sub> (1)	455	CH <sub>3</sub> CN	20	3	-
3	Na <sub>2</sub> -Eosin Y (1)	530	CH <sub>3</sub> CN	20	NR	-
4 <sup>b</sup>	[Cu(dap) <sub>2</sub> ]Cl (1)	530	CH <sub>3</sub> CN	12	79 (76)	18
5	[Cu(dap) <sub>2</sub> ]Cl (1)	No	CH <sub>3</sub> CN	12	11	3
6	[Cu(dap)Cl <sub>2</sub> ] (1)	530	CH <sub>3</sub> CN	12	72	21
7	CuCl <sub>2</sub> (1) + dap (2)	530	CH <sub>3</sub> CN	12	62	22
8	CuCl <sub>2</sub> (1) + dap (2)	No	CH <sub>3</sub> CN	12	12	4
9	CuCl <sub>2</sub> (1) + dap (2)	No	CH <sub>3</sub> CN	48	42	16
10	CuCl <sub>2</sub> (1) + dap (4)	No	CH <sub>3</sub> CN	48	45	19
11	No	530	CH <sub>3</sub> CN	12	NR	-
12	CuCl (5)	530	CH <sub>3</sub> CN	12	8	-
13	CuCl <sub>2</sub> (5)	No	CH <sub>3</sub> CN	48	18	4
14	CuBr <sub>2</sub> (5)	No	CH <sub>3</sub> CN	48	16	4
15	dap (5)	530	CH <sub>3</sub> CN	12	3	-
16	[Cu(dap) <sub>2</sub> ]Cl (0.5)	530	CH <sub>3</sub> CN	12	69	15
17 <sup>c</sup>	[Cu(dap) <sub>2</sub> ]Cl (1)	530	CH <sub>3</sub> CN	12	77	20
18 <sup>d</sup>	[Cu(dap) <sub>2</sub> ]Cl (1)	530	CH <sub>3</sub> CN	12	62	19
19 <sup>e</sup>	[Cu(dap) <sub>2</sub> ]Cl (1)	530	CH <sub>3</sub> CN	12	61	18
20	[Cu(dap) <sub>2</sub> ]Cl (1)	530	DMF	12	60	20
21	[Cu(dap) <sub>2</sub> ]Cl (1)	530	DCM	12	66	21
22	[Cu(dap) <sub>2</sub> ]Cl (1)	530	CH <sub>3</sub> OH	12	50	12
23	[Cu(dap) <sub>2</sub> ]Cl (1)	530	DMSO	12	39	16
24	[Cu(dap) <sub>2</sub> ]Cl (1)	530	DCE	12	26	6
25	[Cu(dap) <sub>2</sub> ]Cl (1)	530	CHCl <sub>3</sub>	12	13	4
26	[Cu(dap) <sub>2</sub> ]Cl (1)	455	CH <sub>3</sub> CN	12	65	12

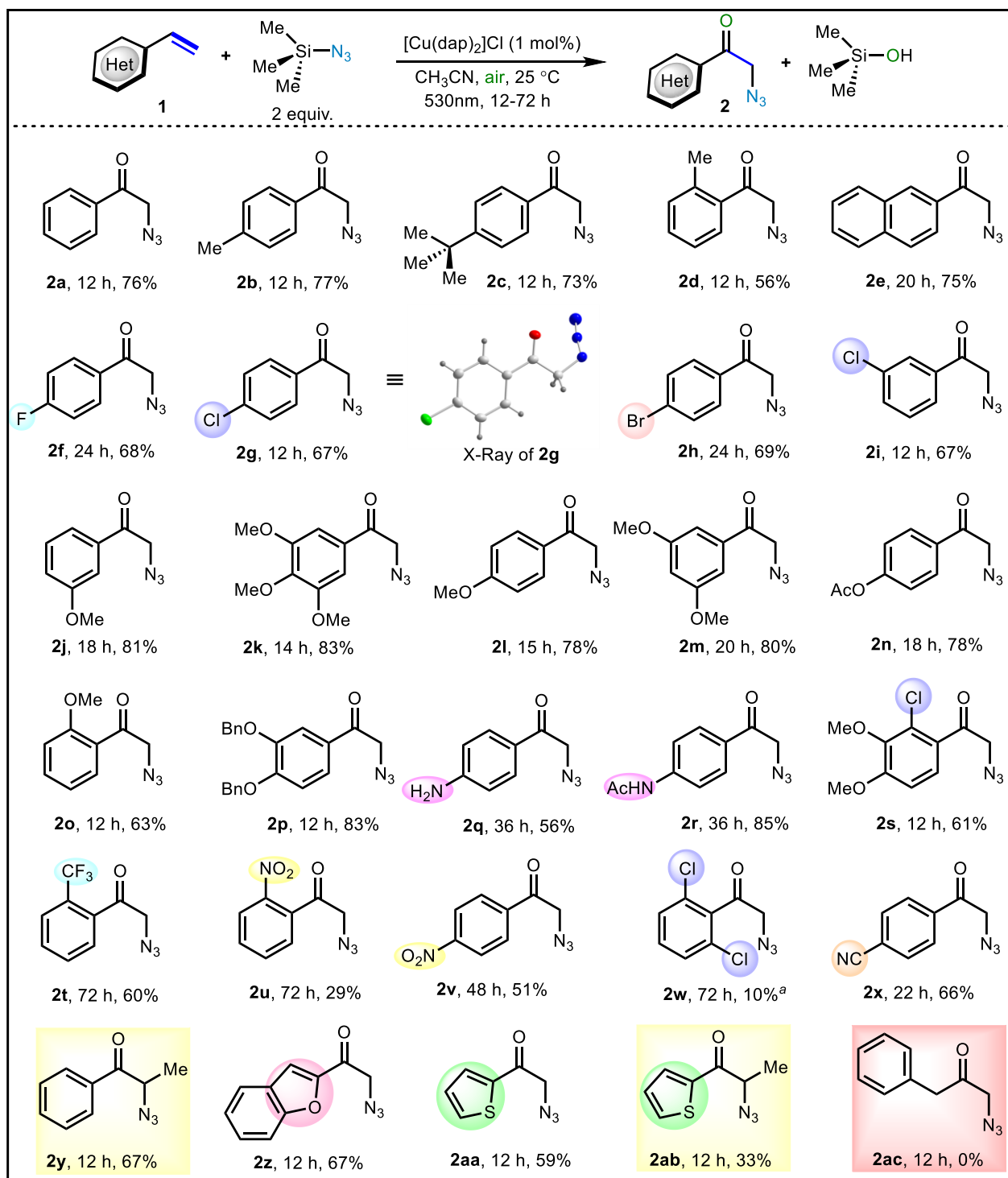
## Chapter 4: Copper(II)-catalyzed Oxo-azidation of Vinylarenes

27 <sup>f</sup>	[Cu(dap) <sub>2</sub> ]Cl (1)	530	CH <sub>3</sub> CN	12	NR	-
28 <sup>g</sup>	[Cu(dap) <sub>2</sub> ]Cl (1)	530	CH <sub>3</sub> CN	12	63	28
29 <sup>h</sup>	[Cu(dap) <sub>2</sub> ]Cl (1)	530	CH <sub>3</sub> CN	12	NR	-
30 <sup>i</sup>	[Cu(dap) <sub>2</sub> ]Cl (1)	530	CH <sub>3</sub> CN	12	58	32

**Reaction conditions:** Styrene **1a** (0.50 mmol, 1 equiv), TMSN<sub>3</sub> (1.00 mmol, 2 equiv), catalyst (1-5 mol%) in 0.25 M solvent under air at 25 °C (maintained by a temperature-controlled water bath). <sup>a</sup><sup>1</sup>H NMR yields using diphenylmethane as internal standard. <sup>b</sup>Isolated yield in parenthesis. <sup>c</sup>With oxygen balloon. <sup>d</sup>5 equiv TMSN<sub>3</sub> was used. <sup>e</sup>1 equiv TMSN<sub>3</sub> was used. <sup>f</sup>In the presence of 1 equiv Na<sub>2</sub>CO<sub>3</sub>. <sup>g</sup>In presence of 1 equiv acetic acid. <sup>h</sup>at 0 °C. <sup>i</sup>at 50 °C. NR = no reaction.

after 12 h visible-light-irradiation ( $\lambda_{max} = 530$  nm) and our desired product **2a** was isolated in 76% yield along with 18% (<sup>1</sup>H NMR yield) of benzaldehyde **3a** (Table 1, entry 4). Not surprisingly, when we employed the reaction in the presence of [Cu(dap)Cl<sub>2</sub>] or CuCl<sub>2</sub>/dap catalyst (Entries 6, 7), the reaction worked well upon visible-light irradiation. This indicates that an oxidation of azide anion takes place, which is triggered by Cu(II) (*vide infra*). Light proved to be very important for the transformation as because significantly lower yields of **2a** (entries 5 and 8 respectively) were obtained irrespective of Cu(I) or Cu(II) catalyst have been used in the dark. Increasing the reaction time to even 48 h under dark, did not resulted into full conversion of **1a** (entries 9 and 10). Without copper-catalysts, the reaction shut down completely (entry 11). When we lowered the catalyst loading to 0.5 mol%, the yield of the desired compounds **2a** dropped slightly to 69% (entry 16). Varying the amounts of oxygen (by using oxygen balloon) or TMSN<sub>3</sub>, did not increase the product yield (entries 17-19). Aiming to reduce the byproduct **3a**, several more parameters were screened (solvents, temperature, and effects of additives). We also found out that the under basic conditions (use of 1 equiv Na<sub>2</sub>CO<sub>3</sub>) the reaction did not work but under acidic conditions (use of 1 equiv acetic acid), **2a** was produced in 63% yield (entries 27 and 28). Interestingly, no conversion of **1a** was observed when the reaction was performed at 0 °C (entry 29). It should also be noted that when the reaction was performed with blue LED ( $\lambda_{max} = 455$  nm), the obtained yield of **2a** was lower compared to a green LED ( $\lambda_{max} = 530$  nm) (*vide infra*) (entry 26). Nevertheless, the conditions established in Table 1, entry 4, were found to be the best and were subsequently applied to explore the scope of the reaction. In the later experiments, the bench stable copper(I) complex [Cu(dap)<sub>2</sub>]Cl was used as the precatalyst since it can be prepared on gram scale and conveniently handled to set up the reactions.

Table 2: Scope of the reaction:



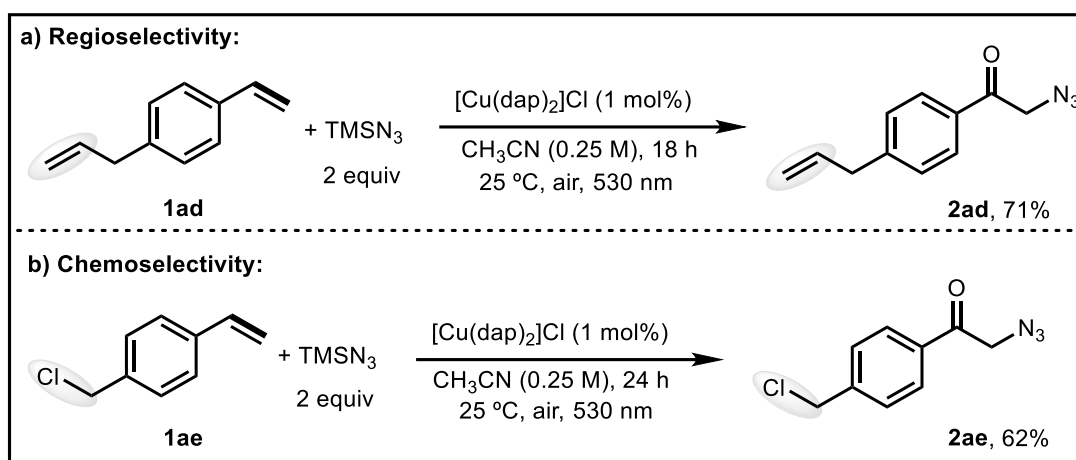
**Reaction conditions:** olefin **1** (0.50 mmol, 1 equiv), TMSN<sub>3</sub> (1.00 mmol, 2 equiv),  $[\text{Cu}(\text{dap})_2]\text{Cl}$  (1 mol%) in 2 mL  $\text{CH}_3\text{CN}$  under visible light irradiation (530 nm) in the presence of air at room temperature. <sup>1</sup>H NMR yield is provided. Ac = -COCH<sub>3</sub>, Bn = benzyl.

Different vinylarenes with a wide range of functionalities could be converted to the ketoazides (Table 2) following this protocol. Specifically, Alkyl-, halo-, amino-, alkoxy- and acetoxy,

nitro- and cyano- substituents in *meta* or *para* position of the arene ring were well tolerated under the reaction conditions. The structure of **2g** was confirmed by single crystal X-ray analysis. It was also observed that the presence of electron-donating groups (*e.g.* methoxy, **2j-2p**) minimizes the formation of the corresponding aldehyde as byproduct. On the other hand, considerable amount of aldehyde formation was observed when electron-withdrawing substituents (*e.g.* nitro, **2u** and **2v**) were present in the arene moiety. Protected amino functionality in the arene moiety produced higher yield of the desired product compared to the free amino substituted styrenes (**2q** and **2r**). A decrease in yield was observed for mono-*ortho*-substituted styrenes, which is attributed to the disordered conjugation between the arene and the alkene moiety, being further accentuated in case of the di-*ortho*-substituted styrene **1w**, which gave poor conversion even after 72 h of irradiation. Heterocycles such as thiophene and benzofuran substitution were also possible (**2z**, **2aa**, **2ab**). Internal aryl substituted alkenes can be also converted to the corresponding ketoazides, as demonstrated with **2y** and **2ab**.

### Regio- and chemoselectivity of the developed method:

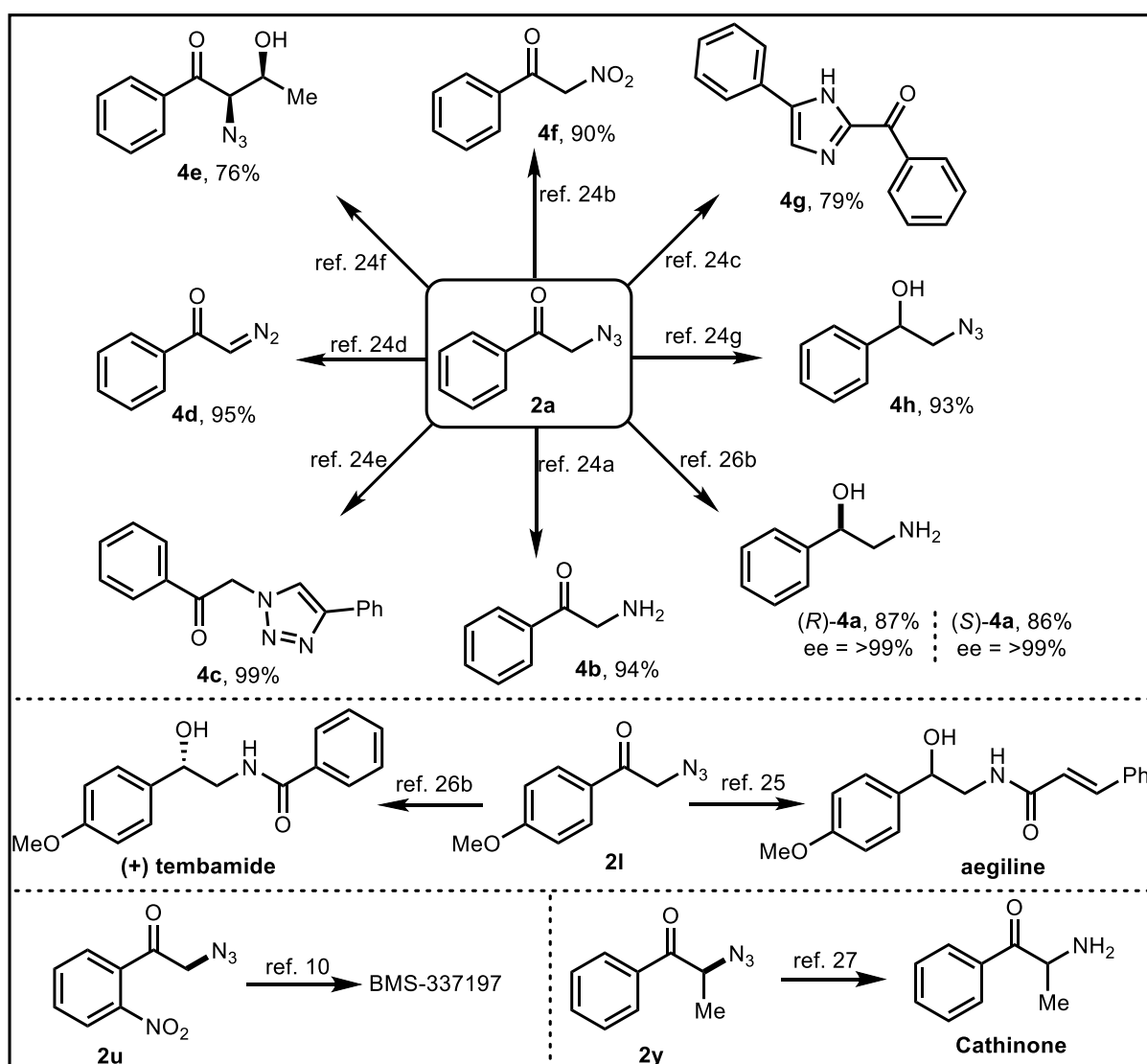
In the case of the unactivated olefin **1ac** (Table 1), no conversion was observed, which allows in turn the chemoselective oxo-azidation of **1ad** (Scheme 2a) and the desired product **2ad** was isolated in 71% yield. The unreacted olefinic part in **2ad** can be subjected to further important transformations. Moreover, trimethylsilylazide is known to readily react with organic halides such as benzyl chloride to the corresponding azides.<sup>[23]</sup> Nevertheless, under the photochemical protocol developed here, 1-(chloromethyl)-4-vinylbenzene (**1ae**) cleanly underwent oxo-azidation to give rise to **2ae** in 62% yield (Scheme 2b).



**Scheme 2:** Reactions were performed in 0.5 mmol scale following standard conditions.

**Further transformations of the obtained products:**

The great synthetic utility of  $\alpha$ -azido ketones is amply documented in the literature. Representative transformations of  $\alpha$ -azido ketones **2a**,<sup>[24]</sup> **2l**, **2u** and **2y** synthesized in this study are shown in Scheme 3. Especially, **2l** has been used as a key intermediate in the synthesis of the antihyperlipidemic and antihyperglycemic Aegiline<sup>[25]</sup> and the antiviral natural product (+)-Tembamide.<sup>[26]</sup> **2u** is an intermediate for the synthesis of BMS-337197, being a potent uncompetitive inhibitor of IMPDH II enzyme,<sup>[10]</sup> while **2y** has been used for the synthesis of Cathinone,<sup>[27]</sup> which has similar biological activity like amphetamines, especially on the cardiovascular system<sup>[28]</sup> and metabolism of dopamine.<sup>[29]</sup>

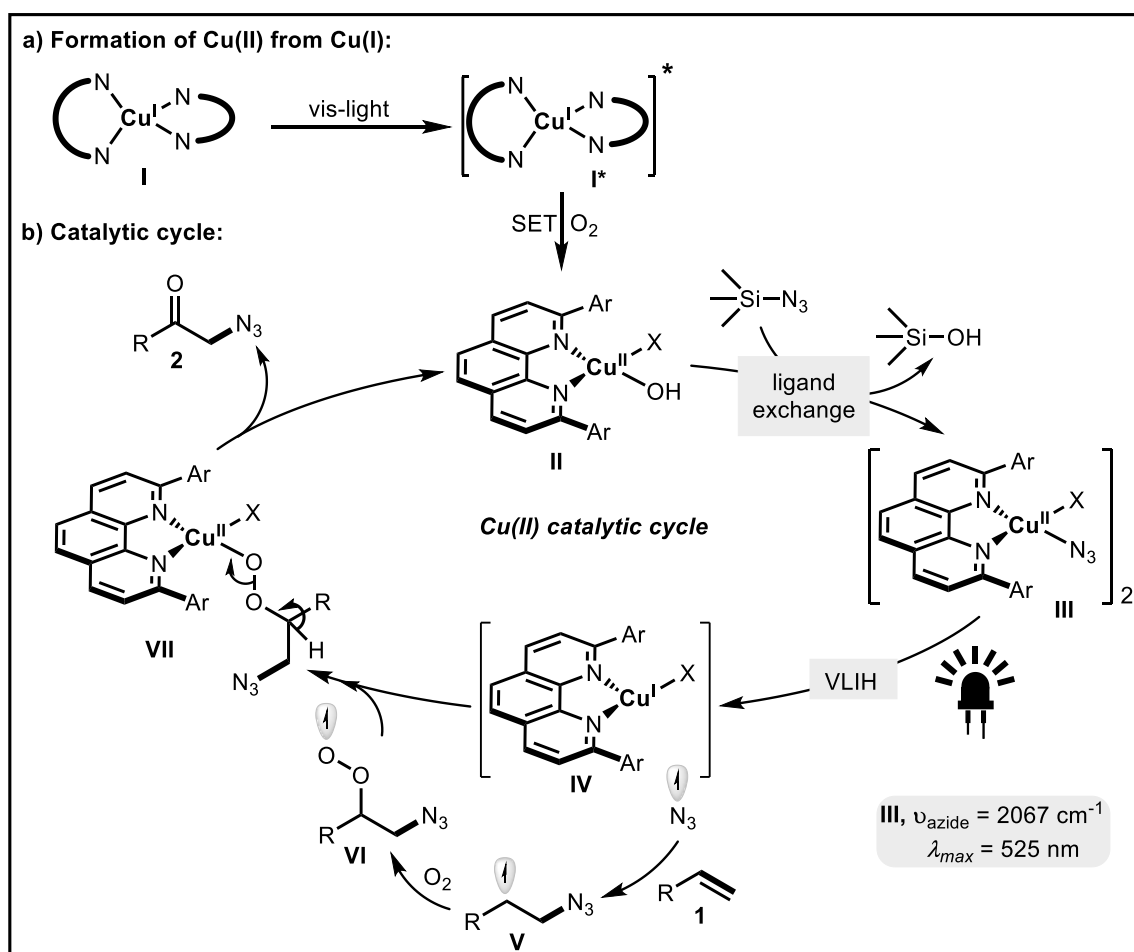


**Scheme 3:** Further transformations.



**Proposed reaction mechanism:**

A plausible mechanism (Scheme 4) for the aforementioned reaction features a Cu(II)-complex like **II** as the catalytically active species. **II** can be obtained easily from [Cu(dap)<sub>2</sub>]Cl **I** by oxidation with dioxygen ( $E_{\text{Cu(II)/Cu(I)}^*} = -1.43$  V vs. SCE;  $E_{\text{ox}} = +0.33$  V for molecular oxygen). When we investigated this step through EPR, indeed, the formation of an EPR-active copper species was observed during the reaction sequence starting with **I** (Figure 3b; yellow signal belongs to **I** under nitrogen atmosphere whereas under aerobic conditions blue signal indicates the formation of a Cu(II)-species). Interestingly, when we studied this step by NMR spectroscopy, we found out that one equivalent of dap ligand was released from the coordination-sphere upon change in the oxidation state at the metal center. The unbound ‘dap’ ligand was confirmed by NMR spectroscopy.<sup>[5]</sup> The stoichiometry of the Cu(II) dap complex was also confirmed by an independent synthesis of the [Cu(dap)Cl<sub>2</sub>] **5** and X-ray analysis.



**Scheme 4:** a) Formation of active Cu(II) catalyst and b) the proposed catalytic cycle for this transformation.

Interestingly, even with 2 equivalents of ‘dap’ ligand  $[\text{Cu}(\text{dap})\text{Cl}_2]$  is formed selectively (Figure 4c). The formation of an azide-bridged dimer<sup>[30]</sup> **III** was confirmed by ATR-IR spectroscopy and rapidly occurs upon mixing of  $[\text{Cu}(\text{dap})\text{Cl}_2]$  already without irradiation (experimental section). The formation and photophysical properties of **III** also explain the wavelength dependence of the overall reaction. **III** has a  $\lambda_{\text{max}}$  of 525 nm (Figure 3a) contrary to the  $[\text{Cu}(\text{dap}_2)]\text{Cl}$  or  $[\text{Cu}(\text{dap})\text{Cl}_2]$  complexes, and consequently, irradiation of **III** with green LEDs (530 nm) leads to a faster onward reaction than with blue LEDs (455 nm).

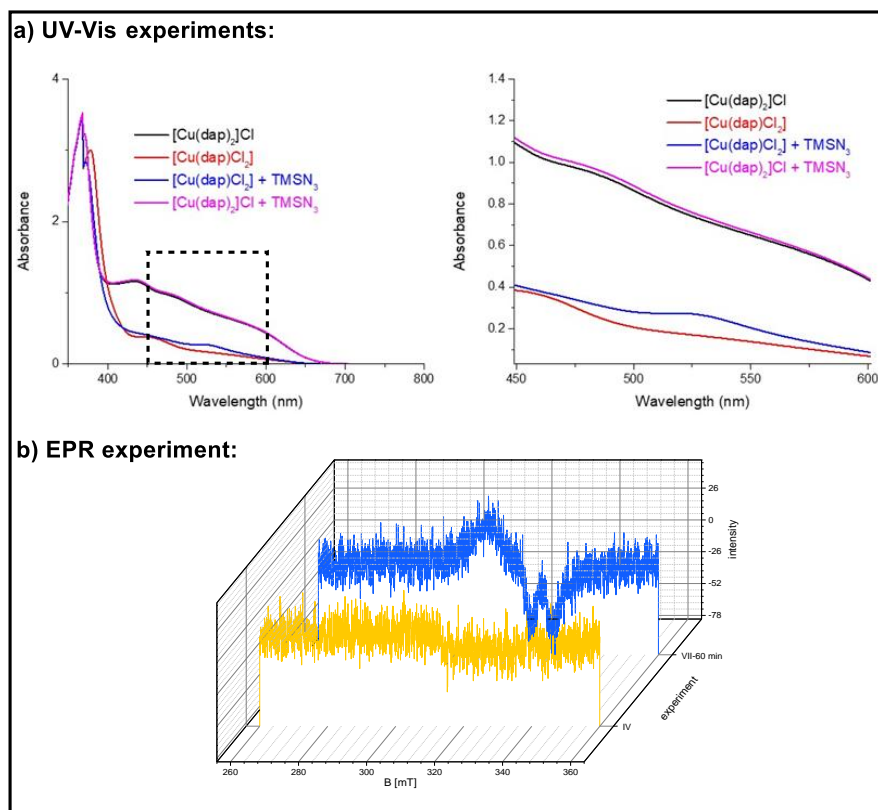


**Figure 3:** a) formation of Cu(II)-N<sub>3</sub> species. b) EPR-active Cu(II) formation from Cu(I) complex, this experiment was performed by J. Phan.

Elemental steps from **III** onwards are proposed to consist of a visible-light-induced homolysis (VLIH) of **III** to a Cu(I) species **IV** and azide radical. In this step the importance of visible-light was monitored with comparing the reaction times between light and dark reaction (Figure 4d). The change of the Cu(II) concentration during the reaction sequence was followed by quantitative EPR experiments and are in line with this mechanistic postulate. In the next step, the azido radical can add to the olefin **1** in a regioselective way to form a stabilized radical **V**. The formation of the benzylic radical **V** (confirmed by TEMPO trapping (Figure 4a)), further reacts with oxygen to form **VI**. Because of copper’s persistent radical effect, the newly formed

O-centered radical can now bind to **IV** forming a Cu(II) species **VII**. Formation of product **2** with concurrent elimination of **II** from **VII** closes the catalytic cycle. In agreement with this proposal, no conversion is observed if the reaction is carried out under a nitrogen atmosphere, neither starting with Cu(I) nor with Cu(II) (Figure 4b). Moreover, no azidoperoxides, being the products in related processes<sup>[18,20]</sup> (cf. Scheme 1) were detected. The overall mechanistic proposal is in line with recent reports<sup>[31]</sup> where Ni(II) intermediates were excited by using an external Ir-based photocatalyst to facilitate a reductive elimination.

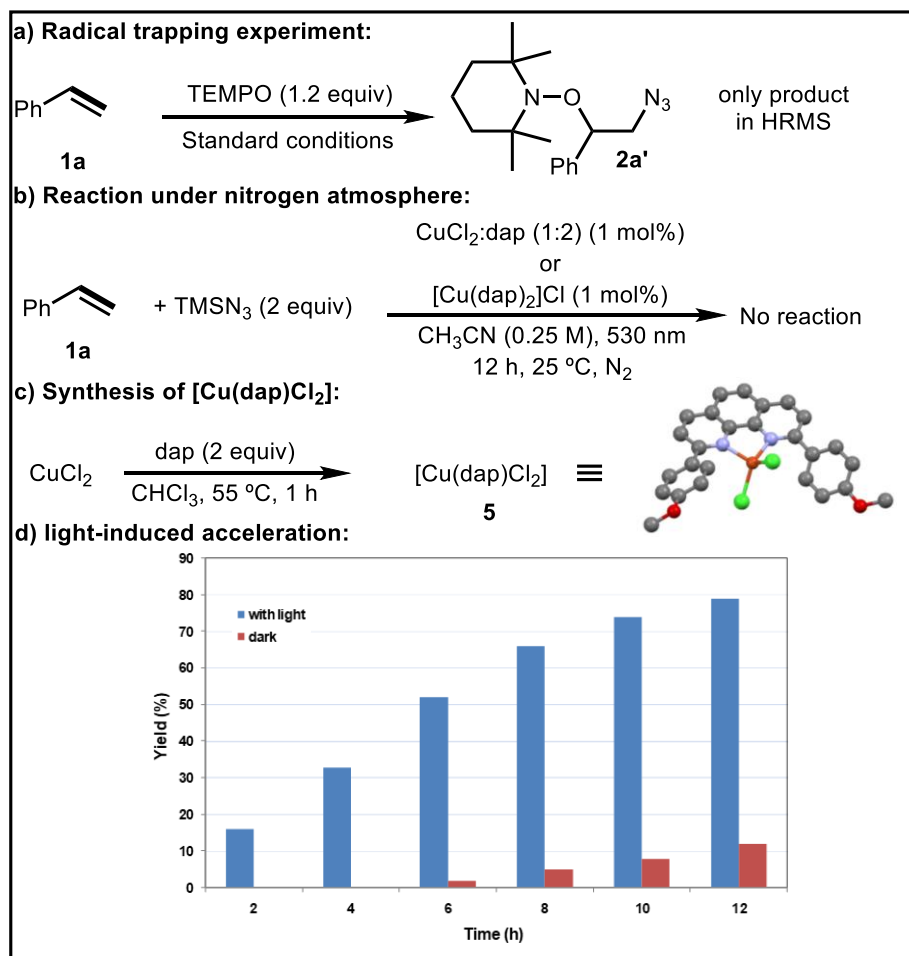


Figure 4: Mechanistic experiments. ‘c’ was performed by Dr. C. Lankes.

## Conclusion and outlook:

In conclusion, we have developed a highly versatile visible-light photocatalytic strategy for the step-economical synthesis of  $\alpha$ -azido ketones from vinylarenes and commercially available  $\text{TMSN}_3$  under aerobic condition without the need of an additional stoichiometric strong oxidant. To best of our knowledge, the developed method is the first example of a visible light accelerated Cu(II)-catalyzed process where the radical was generated oxidatively. This might

open up new opportunities to develop radical based redox transformations based on a light induced homolysis of Cu(II)-X species to give rise to Cu(I) and X•.

**References and notes:**

- [1] a) L. Marzo, S. K. Pagire, O. Reiser, B. König, *Angew. Chem. Int. Ed.* **2018**, *57*, 10034; b) C. K. Prier, D. A. Rankic, D. W. C. MacMillan, *Chem. Rev.* **2013**, *113*, 5322.
- [2] a) J. M. R. Narayanam, C. R. J. Stephenson, *Chem. Soc. Rev.* **2011**, *40*, 102; b) N. A. Romero, D. A. Nicewicz, *Chem. Rev.* **2016**, *116*, 10075; c) K. L. Skubi, T. R. Blum, T. P. Yoon, *Chem. Rev.* **2016**, *116*, 10035; d) K. Zeitler, *Angew. Chem. Int. Ed.* **2009**, *48*, 9785.
- [3] a) S. Paria, O. Reiser, *ChemCatChem* **2014**, *6*, 2477; b) O. Reiser, *Acc. Chem. Res.* **2016**, *49*, 1990; c) C. Minozzi, A. Caron, J.-C. Grenier-Petel, J. Santandrea, S. K. Collins, *Angew. Chem. Int. Ed.* **2018**, *57*, 5477.
- [4] a) M. Knorn, T. Rawner, R. Czerwieniec, O. Reiser, *ACS Catal.* **2015**, *5*, 5186; b) S. K. Pagire, S. Paria, O. Reiser, *Org. Lett.* **2016**, *18*, 2106; c) T. Rawner, M. Knorn, E. Lutsker, A. Hossain, O. Reiser, *J. Org. Chem.* **2016**, *81*, 7139; d) D. B. Bagal, G. Kachkovskiy, M. Knorn, T. Rawner, B. M. Bhanage, O. Reiser, *Angew. Chem. Int. Ed.* **2015**, *54*, 6999; e) S. Paria, M. Pirtsch, V. Kais, O. Reiser, *Synthesis* **2013**, *45*, 2689; f) M. Pirtsch, S. Paria, T. Matsuno, H. Isobe, O. Reiser, *Chem. Eur. J.* **2012**, *18*, 7336; g) X.-J. Tang, W. R. Dolbier, *Angew. Chem. Int. Ed.* **2015**, *54*, 4246; h) X.-W. Lan, N.-X. Wang, Y. Xing, *Eur. J. Org. Chem.* **2017**, *2017*, 5821; i) T. Courant, G. Masson, *J. Org. Chem.* **2016**, *81*, 6945; j) D. Menigaux, P. Belmont, E. Brachet, *Eur. J. Org. Chem.* **2017**, *2017*, 2008; k) G. Yin, X. Mu, G. Liu, *Acc. Chem. Res.* **2016**, *49*, 2413; l) R. Bag, D. Sar, T. Punniyamurthy, *Org. Lett.* **2015**, *17*, 2010; m) C.-J. Wallentin, J. D. Nguyen, P. Finkbeiner, C. R. J. Stephenson, *J. Am. Chem. Soc.* **2012**, *134*, 8875.
- [5] T. Rawner, E. Lutsker, C. A. Kaiser, O. Reiser, *ACS Catal.* **2018**, *8*, 3950.
- [6] a) J. M. Ahn, J. C. Peters, G. C. Fu, *J. Am. Chem. Soc.* **2017**, *139*, 18101; b) Q. M. Kainz, C. D. Matier, A. Bartoszewicz, S. L. Zultanski, J. C. Peters, G. C. Fu, *Science* **2016**, *351*, 681.
- [7] a) B. Zhang, A. Studer, *Org. Lett.* **2014**, *16*, 1790; b) A. A. Andia, M. R. Miner, K. A. Woerpel, *Org. Lett.* **2015**, *17*, 2704; c) L. Legnani, B. Morandi, *Angew. Chem. Int. Ed.* **2016**, *55*, 2248; d) K. Shen, Q. Wang, *J. Am. Chem. Soc.* **2017**, *139*, 13110; e) L. Xu, X.-Q. Mou, Z.-M. Chen, S.-H. Wang, *Chem. Commun.* **2014**, *50*, 10676; f) J. Xu, X. Li, Y.

- Gao, L. Zhang, W. Chen, H. Fang, G. Tang, Y. Zhao, *Chem. Commun.* **2015**, *51*, 11240; g) R. Zhu, S. L. Buchwald, *J. Am. Chem. Soc.* **2015**, *137*, 8069; h) L. Huang, J.-S. Lin, B. Tan, X.-Y. Liu, *ACS Catal.* **2015**, *5*, 2826; i) H. Zhou, W. Jian, B. Qian, C. Ye, D. Li, J. Zhou, H. Bao, *Org. Lett.* **2017**, *19*, 6120; j) M.-Z. Lu, C.-Q. Wang, T.-P. Loh, *Org. Lett.* **2015**, *17*, 6110; k) L. Zhu, H. Yu, Z. Xu, X. Jiang, L. Lin, R. Wang, *Org. Lett.* **2014**, *16*, 1562; l) F. Wang, X. Qi, Z. Liang, P. Chen, G. Liu, *Angew. Chem. Int. Ed.* **2014**, *53*, 1881.
- [8] a) S. Bräse, C. Gil, K. Knepper, V. Zimmermann, *Angew. Chem. Int. Ed.* **2005**, *44*, 5188; b) M. Minozzi, D. Nanni, P. Spagnolo, *Chem. Eur. J.* **2009**, *15*, 7830; c) J. H. Boyer, F. C. Canter, *Chem. Rev.* **1954**, *54*, 1; d) M. Goswami, B. de Bruin, *Eur. J. Org. Chem.* **2017**, *2017*, 1152; e) E. F. V. Scriven, K. Turnbull, *Chem. Rev.* **1988**, *88*, 297; f) Y.-F. Zeng, X. Hu, F.-C. Liu, X.-H. Bu, *Chem. Soc. Rev.* **2009**, *38*, 469.
- [9] T. Patonay, K. Kónya, É. Juhász-Tóth, *Chem. Soc. Rev.* **2011**, *40*, 2797.
- [10] S. Faiz, A. F. Zahoor, N. Rasool, M. Yousaf, A. Mansha, M. Zia-Ul-Haq, H. Z. E. Jaafar, *Molecules* **2015**, *20*, 14699.
- [11] T. Patonay, R. V. Hoffman, *J. Org. Chem.* **1994**, *59*, 2902.
- [12] a) D. Kumar, S. Sundaree, V. S. Rao, *Synth. Commun.* **2006**, *36*, 1893; b) O. Prakash, K. Pannu, R. Prakash, A. Batra, *Molecules* **2006**, *11*, 523; c) M. V. Vita, J. Waser, *Org. Lett.* **2013**, *15*, 3246.
- [13] V. Nair, L. G. Nair, T. G. George, A. Augustine, *Tetrahedron* **2000**, *56*, 7607.
- [14] R. Badri, M. Gorjizadeh, *Synth. Commun.* **2012**, *42*, 2058.
- [15] G. Fumagalli, P. T. G. Rabet, S. Boyd, M. F. Greaney, *Angew. Chem. Int. Ed.* **2015**, *54*, 11481.
- [16] a) S. K. Pagire, P. Kreitmeier, O. Reiser, *Angew. Chem. Int. Ed.* **2017**, *56*, 10928; b) A. Hossain, S. Pagire, O. Reiser, *Synlett* **2017**, *28*, 1707.
- [17] Immediately after our report, two more papers appeared within months. Photocatalyzed protocol see: a) W. Wei, H. Cui, H. Yue, D. Yang, *Green Chem.* **2018**, *20*, 3197; thermal activation see: b) M. I. Hussain, Y. Feng, L. Hu, Q. Deng, X. Zhang, Y. Xiong, *J. Org. Chem.* **2018**, *83*, 7852; Our report: c) A. Hossain, A. Vidyasagar, C. Eichinger, C. Lankes, J. Phan, J. Rehbein, O. Reiser, *Angew. Chem. Int. Ed.* **2018**, *57*, 8288.
- [18] B. Yang, Z. Lu, *ACS Catal.* **2017**, *7*, 8362.
- [19] a) I. Sakurada, S. Yamasaki, M. Kanai, M. Shibasaki, *Tetrahedron Lett.* **2000**, *41*, 2415; b) P. K. Prasad, R. N. Reddi, A. Sudalai, *Chem. Commun.* **2015**, *51*, 10276.
- [20] X. Sun, X. Li, S. Song, Y. Zhu, Y.-F. Liang, N. Jiao, *J. Am. Chem. Soc.* **2015**, *137*, 6059.

- [21] D. P. Hari, B. König, *Chem. Commun.* **2014**, 50, 6688.
- [22] a) J.-M. Kern, J.-P. Sauvage, *J. Chem. Soc. Chem. Commun.* **1987**, 546; b) C. Dietrich-Buchecker, J.-P. Sauvage, *Tetrahedron* **1990**, 46, 503.
- [23] K. Nishiyama, H. Karigomi, *Chem. Lett.* **1982**, 11, 1477.
- [24] a) J. H. Boyer, *J. Am. Chem. Soc.* **1951**, 73, 5865; b) M. Carmeli, S. Rozen, *J. Org. Chem.* **2006**, 71, 4585; c) J. Chen, W. Chen, Y. Yu, G. Zhang, *Tetrahedron Lett.* **2013**, 54, 1572; d) N. A. McGrath, R. T. Raines, *Chem. Sci.* **2012**, 3, 3237; e) S. B. Ötvös, I. M. Mándity, L. Kiss, F. Fülöp, *Chem. Asian J.* **2013**, 8, 800; f) T. Patonay, É. Juhász-Tóth, A. Bényei, *Eur. J. Org. Chem.* **2002**, 2002, 285; g) C. Rodríguez, W. Borzęcka, J. H. Sattler, W. Kroutil, I. Lavandera, V. Gotor, *Org. Biomol. Chem.* **2014**, 12, 673.
- [25] T. Narender, K. Rajendar, S. Sarkar, V. K. Singh, U. Chaturvedi, A. K. Khanna, G. Bhatia, *Bioorganic Med. Chem. Lett.* **2011**, 21, 6393.
- [26] a) M.-J. Cheng, K.-H. Lee, I.-L. Tsai, I.-S. Chen, *Bioorganic Med. Chem.* **2005**, 13, 5915; b) J. H. Schrittwieser, F. Coccia, S. Kara, B. Grischek, W. Kroutil, N. d'Alessandro, F. Hollmann, *Green Chem.* **2013**, 15, 3318.
- [27] P. Besse, H. Veschambre, M. Dickman, R. Chenevert, *J. Org. Chem.* **1994**, 59, 8288.
- [28] J. D. Kohli, L. I. Goldberg, *J. Pharm. Pharmacol.* **1982**, 34, 338.
- [29] P. Kalix, *Life Sci.* **1983**, 32, 801.
- [30] a) M. Liang, W.-Z. Wang, Z.-Q. Liu, D.-Z. Liao, Z.-H. Jiang, S.-P. Yan, P. Cheng, *J. Coord. Chem.* **2003**, 56, 1473; b) A. Jana, S. Konar, K. Das, S. Ray, J. A. Golen, A. L. Rheingold, L. M. Carrella, E. Rentschler, T. K. Mondal, S. K. Kar, *Polyhedron* **2012**, 38, 258; c) W.-B. Shi, A.-L. Cui, H.-Z. Kou, *ChemPlusChem* **2014**, 79, 310.
- [31] a) E. R. Welin, C. Le, D. M. Arias-Rotondo, J. K. McCusker, D. W. C. MacMillan, *Science* **2017**, 355, 380; b) T. Kim, S. J. McCarver, C. Lee, D. W. C. MacMillan, *Angew. Chem. Int. Ed.* **2018**, 57, 3488.

### **General information:**

All commercial chemical materials were used as received without further purification and weight was calculated based on purity mentioned in the container. All photochemical reactions were performed under aerobic atmosphere. All the reactions were monitored by TLC and visualized by a dual short (254 nm) / long (366 nm) wavelength UV lamp. Analytical thin layer chromatography was performed on Merck TLC aluminum sheets silica gel 60 F 254. Purifications by column chromatography were performed on silica gel (0.063-0.200 mm). All products were characterized by appropriate techniques such as <sup>1</sup>H-NMR, <sup>19</sup>F-NMR, <sup>13</sup>C-NMR, FT-IR and HRMS analysis. FT-IR (Cary 630) spectroscopy was carried out on a spectrometer, equipped with a Diamond Single Reflection ATR-System. NMR spectra were recorded on Bruker Advance 300 MHz, 400 MHz and 600 MHz spectrometers. Chemical shifts for <sup>1</sup>H-NMR were reported as δ, parts per million, relative to the signal of CHCl<sub>3</sub> at 7.26 ppm and for DMSO at 2.50 ppm. Chemical shifts for <sup>13</sup>C-NMR were reported as δ, parts per million, relative to the signal of CHCl<sub>3</sub> at 77.2 ppm and for DMSO at 39.52 ppm and TMS as an internal standard. Coupling constants (*J*) are given in Hertz (Hz). The following notations indicate the multiplicity of the signals: s = singlet, br-s = broad singlet, d = doublet, t = triplet, q = quartet, dd = doublet of doublets, dt = doublet of triplets, and m = multiplet. Mass spectra were recorded at the Central Analytical Laboratory at the Department of Chemistry of the University of Regensburg on Agilent Technologies 6540 UHD Accurate-Mass Q-TOF LC/MS. UV-Vis measurements were performed with Varian Cary 50 UV/Vis spectrophotometer. The photochemical reactions were performed with 530 nm LEDs (Cree XPEGRN G4 Q4 (green, λ<sub>max</sub> = 530 nm, I<sub>max</sub> = 1000 mA, 1.12 W)).

### **Safety Statements:**

Organic azides are considered as potentially explosive substances whenever the azido content is high. Although we have never observed any safety problem one has to be extra careful while dealing with organic azides. All the compounds synthesized in this study can be considered to be safe according to the equation below.

$$[\text{N}(\text{C}) + \text{N}(\text{O})] / \text{N}(\text{N}) \geq 3$$

Reference: H. C. Kolb, M. G. Finn, K. B. Sharpless, *Angew. Chem. Int. Ed.* **2001**, *40*, 2004.

Reaction set up:

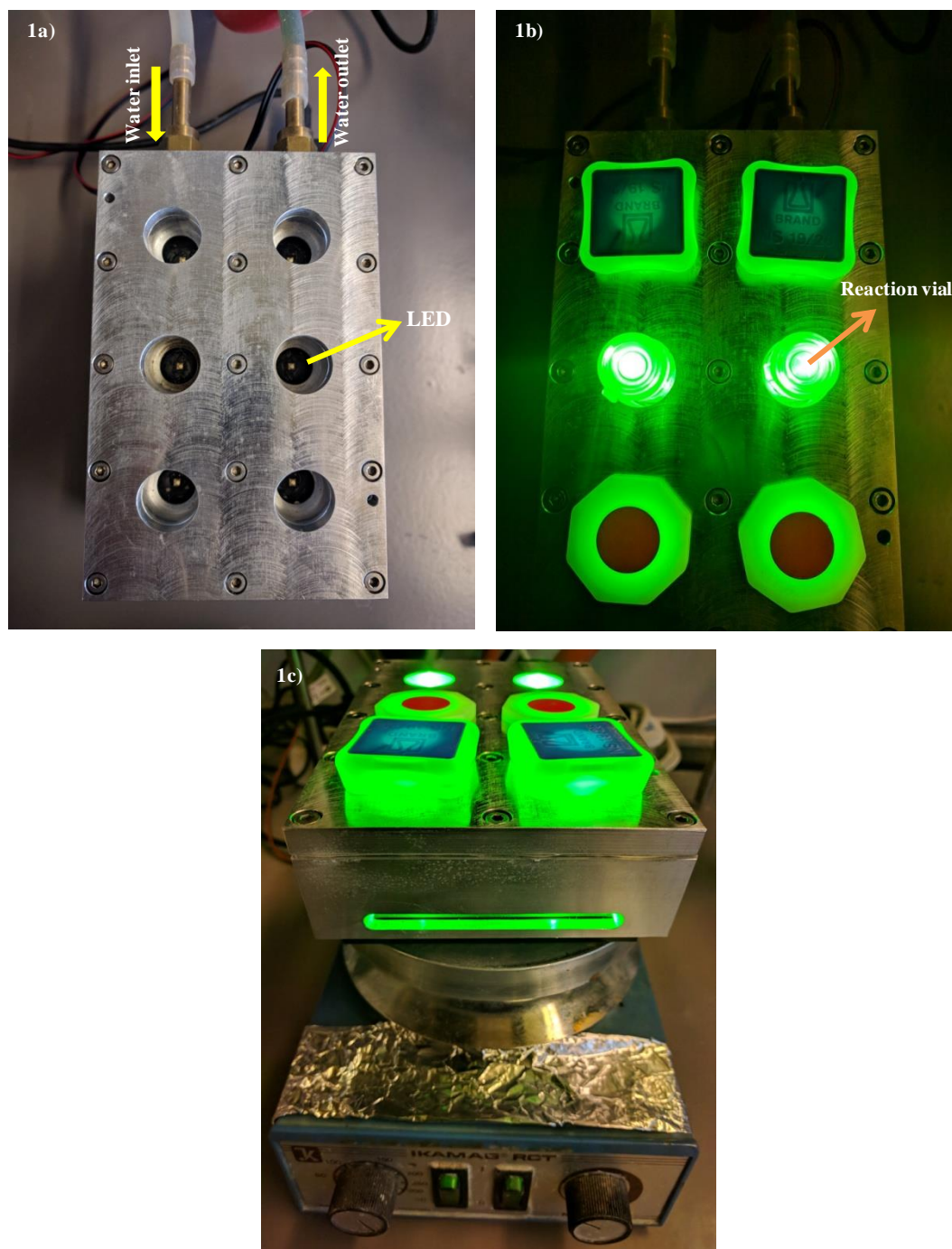


Figure S1: Photochemical set up for oxo-azidation of vinylarenes



### Reaction Optimization:

All the reactions for optimization were performed on 0.50 mmol scale and  $^1\text{H-NMR}$  yield is given. The light reactions were performed with the set up shown above. After mentioned time, the reaction mixture was diluted with Dichloromethane, transferred to a round bottom flask and concentrated in vacuo. The residue was dissolved in  $\text{CDCl}_3$  and  $83\mu\text{L}$  (0.50 mmol, 1 equiv) diphenylmethane (internal standard) was added. The yield was determined by integrating the characteristic peaks of the internal standard and the product.

### Colour change during the reaction:

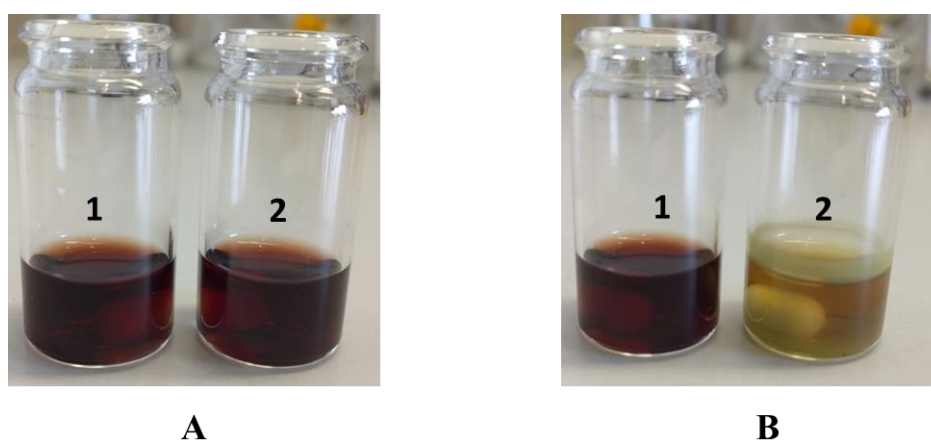
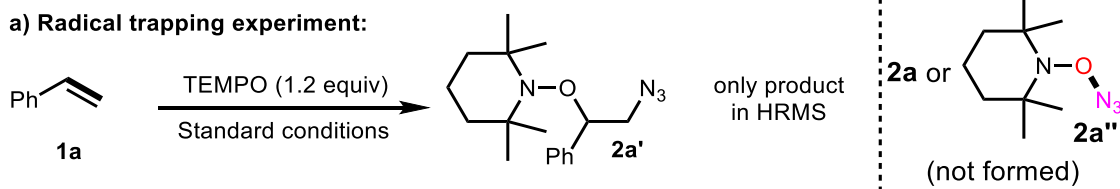


**Figure S2:** Photographs of reaction mixtures before (**A**) and after (**B1** (no irradiation); **B2** (with irradiation)) the reaction

Each of the vial (**A**) contains 0.5 mmol styrene **1a**, 1.0 mmol  $\text{TMSN}_3$ , 1 mol%  $[\text{Cu}(\text{dap})_2]\text{Cl}$  and 2mL  $\text{CH}_3\text{CN}$ . Note that after 12 h reaction time in presence of air, the solution looks same when left in the dark (left, **B1**) and different (right, **B2**) when it was irradiated with visible-light ( $\lambda_{\text{max}} = 530 \text{ nm}$ ).

### Radical trap experiment:

a) Radical trapping experiment:



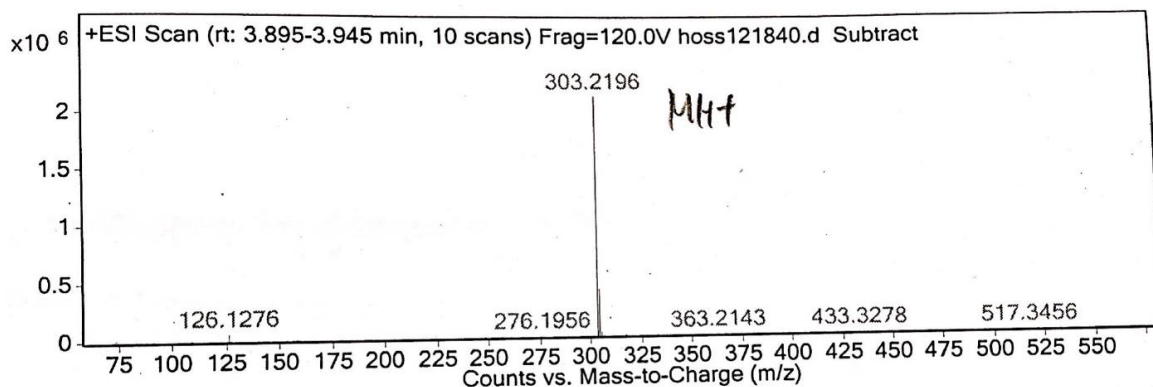


Figure S3: HRMS of TEMPO trap experiment (crude reaction mixture was submitted for analysis).

### Detection of TMSOH with GC-MS:

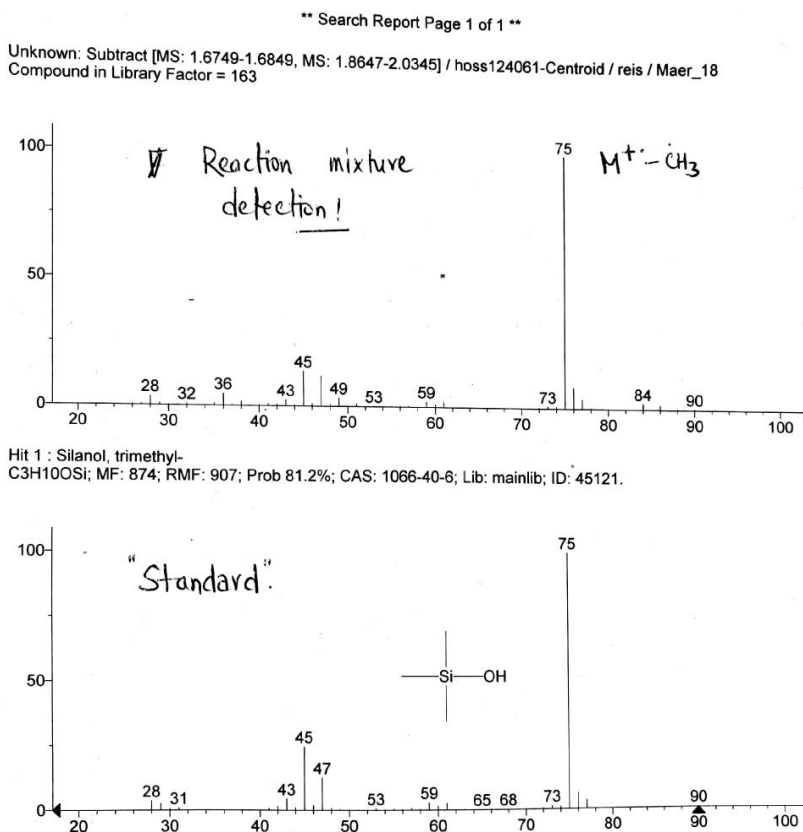


Figure S4: TMSOH detection from crude reaction mixture (top), TMS-OH is detected as  $M^+-CH_3$  (75) in comparison to TMSOH standard (bottom).

IR Experiment:

**Note:** IR experiments were performed in DCM instead of CH<sub>3</sub>CN in order to characterize the azide stretching frequency properly. The title reaction also works well in DCM (66% yield) instead of acetonitrile (79% yield).

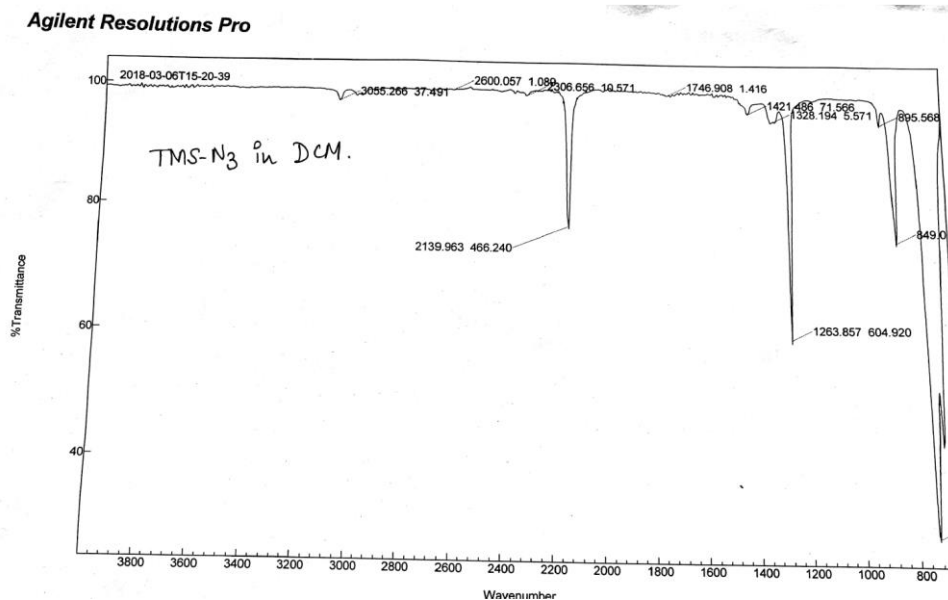


Figure S5: azide stretching frequency of TMSN<sub>3</sub> in DCM

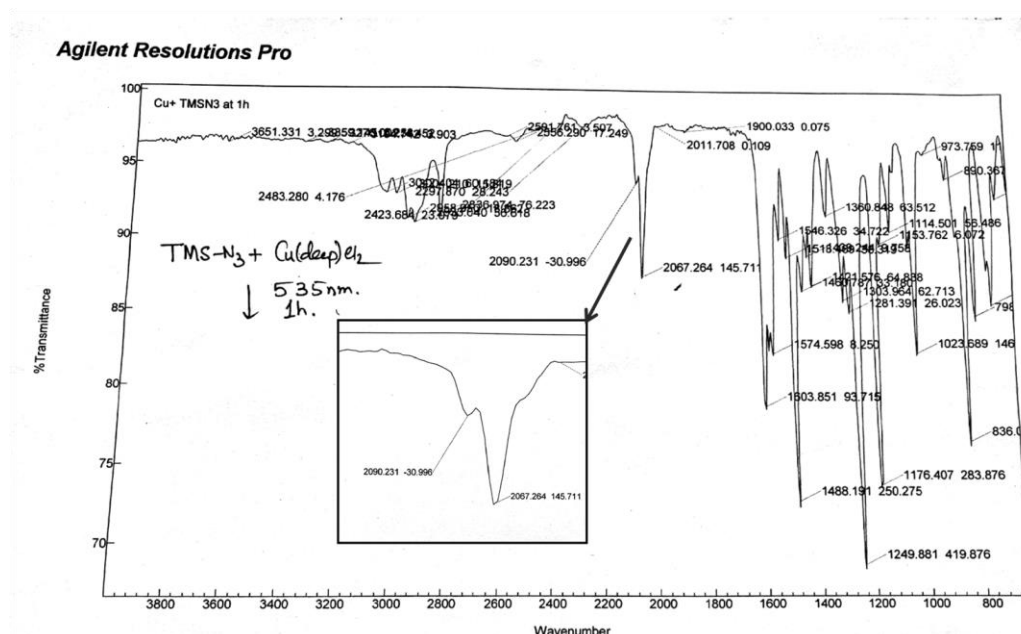
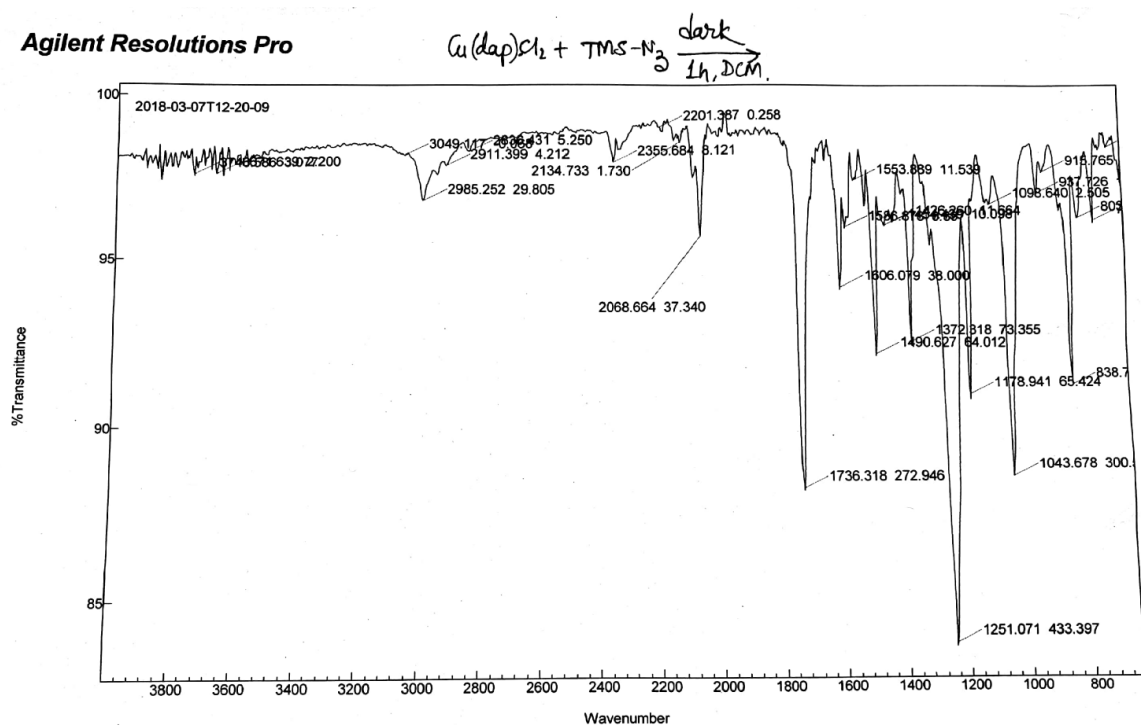


Figure S6(a): 1:1 mixture of [Cu(dap)Cl<sub>2</sub>] and TMSN<sub>3</sub> in DCM with irradiation



**Figure S6(b):** 1:1 mixture of  $[\text{Cu}(\text{dap})\text{Cl}_2]$  and  $\text{TMSN}_3$  in DCM without irradiation

Note that the strong band at  $2067\text{ cm}^{-1}$  in S7(a) ( $2068\text{ cm}^{-1}$  in S7(b)) corresponds to a  $\text{Cu}(\text{II})\text{-N}_3$  species (possibly the binuclear complex of  $\text{Cu}(\text{II})$ , where  $\text{N}_3$  acts as a bridged ligand). Literature<sup>[ref]</sup> value:  $2064\text{ cm}^{-1}$ .

References: a) Kar *et al.* *Polyhedron* **2012**, 38, 258; b) Kou *et al.* *ChemPlusChem* **2014**, 79, 310.

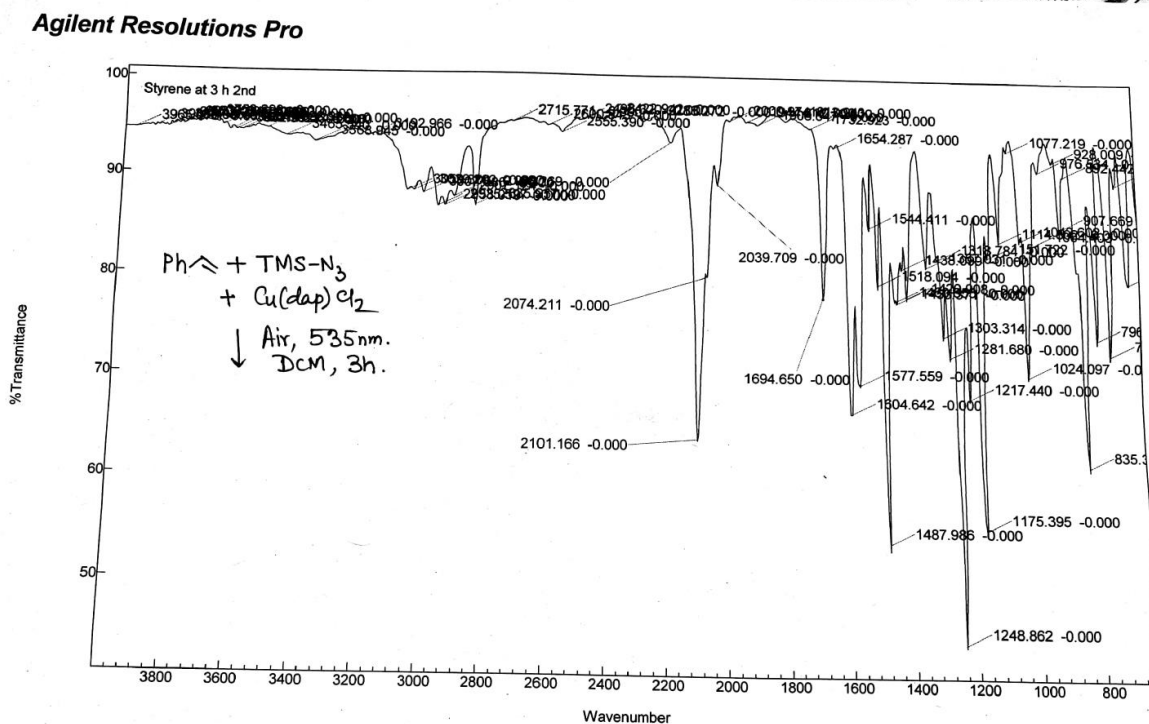
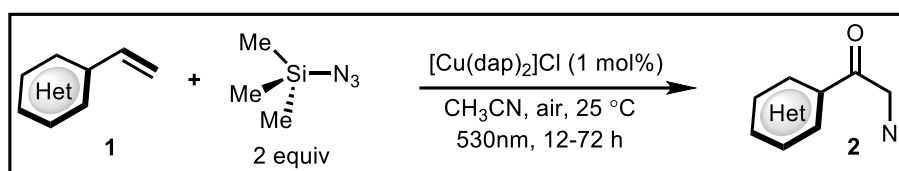


**Figure S7:** IR Spectra after irradiation of a mixture of all three components under air in DCM

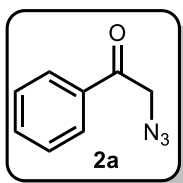
After 3 h irradiation, product formation was observed. Strong bands at  $2101\text{ cm}^{-1}$  and  $1694\text{ cm}^{-1}$  belong to N<sub>3</sub> and C=O respectively of the product **2a**.

### General Procedure for the oxo-azidation of vinyl arenes (GP):



To a glass vial (5 mL size) equipped with a stirring bar was charged with styrene derivative **1** (0.50 mmol, 1.00 equiv) and [Cu(dap)<sub>2</sub>]Cl (4.5 mg, 0.01 equiv, 1.00 mol%). Then 2 mL CH<sub>3</sub>CN was added followed by TMSN<sub>3</sub> (0.140 mL, 1.00 mmol, 2.00 equiv). Then the vial was irradiated with Green LED ( $\lambda_{max} = 530\text{ nm}$ ) under air and the solution was stirred at room temperature ( $25\text{ }^\circ\text{C} \pm 3$ ) (maintained by continuous cold-water flow through the LED “Box”). Upon completion (judged by TLC analysis) the reaction mixture was diluted with Dichloromethane (20 mL), transferred to a round bottom flask and then concentrated *in vacuo*. The pure product **2** was obtained by silica-gel column chromatography using hexanes and ethyl acetate as eluent.

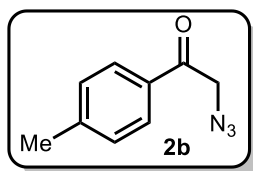
2-azido-1-phenylethan-1-one (**2a**)<sup>[1]</sup>:



Following the general procedure, **2a** was prepared from styrene **1a** (52 mg, 0.50 mmol). Reaction time was 12 hours. The crude product was purified by column chromatography (silica-gel, hexanes-EtOAc = 9:1,  $R_f = 0.30$ ) to afford **2a** as a colourless liquid (60mg, 76% yield).

**<sup>1</sup>H-NMR (300 MHz, CDCl<sub>3</sub>):**  $\delta$  7.92 – 7.88 (m, 2H), 7.65 – 7.59 (m, 1H), 7.51 – 7.46 (m, 2H), 4.56 (s, 2H); **<sup>13</sup>C-NMR (75 MHz, CDCl<sub>3</sub>):**  $\delta$  193.3, 134.4, 134.2, 129.1, 128.0, 55.0; **IR (neat, cm<sup>-1</sup>):** 3064, 2896, 2099, 1692, 1595, 1450, 1282, 1215, 1182, 910, 753, 686; **HRMS (ESI):** exact m/z calculated for C<sub>8</sub>H<sub>7</sub>N<sub>3</sub>O (M+H)<sup>+</sup>: 162.0667; Found: 162.0663 (M+H)<sup>+</sup>.

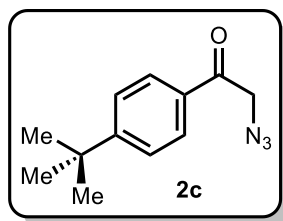
2-azido-1-(*p*-tolyl)ethan-1-one (**2b**)<sup>[2]</sup>:



Following the general procedure, **2b** was prepared from 1-methyl-4-vinylbenzene **1b** (61.5 mg, 0.50 mmol). Reaction time was 12 hours. The crude product was purified by column chromatography (silica-gel, hexanes-EtOAc = 9:1,  $R_f = 0.25$ ) to afford **2b** as a white solid (67 mg, 77% yield).

**<sup>1</sup>H-NMR (300 MHz, CDCl<sub>3</sub>):**  $\delta$  7.80 (d,  $J = 8.1$  Hz, 2H), 7.28 (d,  $J = 8.1$  Hz, 2H), 4.53 (s, 2H), 2.42 (s, 3H); **<sup>13</sup>C-NMR (75 MHz, CDCl<sub>3</sub>):**  $\delta$  192.9, 145.3, 132.0, 129.8, 128.1, 54.9, 21.9; **IR (neat, cm<sup>-1</sup>):** 2963, 2907, 2095, 1685, 1603, 1446, 1409, 1342, 1290, 1223, 1185, 1122, 1006, 910, 805; **HRMS (ESI):** exact m/z calculated for C<sub>9</sub>H<sub>9</sub>N<sub>3</sub>O (M+H)<sup>+</sup>: 176.0824; Found: 176.0814 (M+H)<sup>+</sup>.

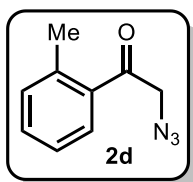
**2-azido-1-(4-(*tert*-butyl)phenyl)ethan-1-one (2c):**



Following the general procedure, **2c** was prepared from 1-(*tert*-butyl)-4-vinylbenzene **1c** (86.1 mg, 0.50 mmol). Reaction time was 12 hours. The crude product was purified by column chromatography (silica-gel, hexanes-EtOAc = 9:1,  $R_f$  = 0.35) to afford **2c** as a colourless liquid (77 mg, 73% yield).

**$^1\text{H-NMR}$  (300 MHz,  $\text{CDCl}_3$ ):**  $\delta$  7.84 (d,  $J$  = 8.6 Hz, 2H), 7.50 (d,  $J$  = 8.7 Hz, 2H), 4.54 (s, 2H), 1.34 (s, 9H);  **$^{13}\text{C-NMR}$  (75 MHz,  $\text{CDCl}_3$ ):**  $\delta$  192.9, 158.2, 131.9, 128.0, 126.1, 54.9, 35.4, 31.1; **IR (neat,  $\text{cm}^{-1}$ ):** 3340, 2963, 2870, 2102, 1692, 1602, 1461, 1408, 1364, 1267, 1226, 1193, 1107; **HRMS (ESI):** exact  $m/z$  calculated for  $\text{C}_{12}\text{H}_{15}\text{N}_3\text{O}$  ( $\text{M}+\text{H}$ ) $^+$ : 218.1293; Found: 218.1284 ( $\text{M}+\text{H}$ ) $^+$ .

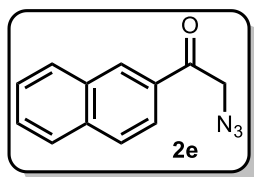
**2-azido-1-(*o*-tolyl)ethan-1-one (2d):**



Following the general procedure, **2d** was prepared from 1-methyl-2-vinylbenzene **1d** (60.2 mg, 0.50 mmol). Reaction time was 12 hours. The crude product was purified by column chromatography (silica-gel, hexanes-EtOAc = 9:1,  $R_f$  = 0.30) to afford **2d** as a colourless liquid (49 mg, 56% yield).

**$^1\text{H-NMR}$  (300 MHz,  $\text{CDCl}_3$ ):**  $\delta$  7.57 (d,  $J$  = 7.9 Hz, 1H), 7.47 – 7.41 (m, 1H), 7.31 – 7.29 (m, 2H), 4.45 (s, 2H), 2.55 (s, 3H);  **$^{13}\text{C-NMR}$  (75 MHz,  $\text{CDCl}_3$ ):**  $\delta$  196.4, 139.6, 134.4, 132.7, 132.6, 128.5, 126.1, 56.5, 21.6; **IR (neat,  $\text{cm}^{-1}$ ):** 3064, 2971, 2930, 2099, 1692, 1603, 1569, 1487, 1457, 1338, 1279, 1211, 1133, 992, 910, 753; **HRMS (ESI):** exact  $m/z$  calculated for  $\text{C}_9\text{H}_9\text{N}_3\text{O}$  ( $\text{M}+\text{H}$ ) $^+$ : 176.0824; Found: 176.0815 ( $\text{M}+\text{H}$ ) $^+$ .

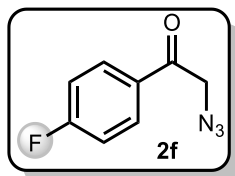
2-azido-1-(naphthalen-2-yl)ethan-1-one (**2e**)<sup>[5]</sup>:



Following the general procedure, **2e** was prepared from 2-vinylnaphthalene **1e** (81.0 mg, 0.50 mmol). Reaction time was 20 hours. The crude product was purified by column chromatography (silica-gel, hexanes-EtOAc = 9:1,  $R_f = 0.20$ ) to afford **2e** as a white solid (79 mg, 75% yield).

**<sup>1</sup>H-NMR (300 MHz, CDCl<sub>3</sub>):**  $\delta$  8.38 (s, 1H), 7.98 – 7.87 (m, 4H), 7.66 – 7.55 (m, 2H), 4.69 (s, 2H); **<sup>13</sup>C-NMR (75 MHz, CDCl<sub>3</sub>):**  $\delta$  193.2, 136.0, 132.4, 131.7, 129.9, 129.7, 129.2, 129.1, 128.0, 127.3, 123.4, 55.1; **IR (neat, cm<sup>-1</sup>):** 3310, 3063, 2982, 2907, 2099, 1677, 1625, 1468, 1357, 1275, 1215, 1003, 898, 850, 816, 772; **HRMS (ESI):** exact  $m/z$  calculated for C<sub>12</sub>H<sub>9</sub>N<sub>3</sub>O (M+H)<sup>+</sup>: 212.0824; Found: 212.0817 (M+H)<sup>+</sup>.

2-azido-1-(4-fluorophenyl)ethan-1-one (**2f**)<sup>[3]</sup>:

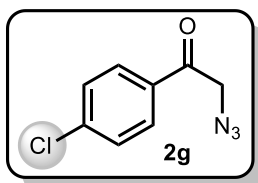


Following the general procedure, **2f** was prepared from 1-fluoro-4-vinylbenzene **1f** (62.0 mg, 0.50 mmol). Reaction time was 24 hours. The crude product was purified by column chromatography (silica-gel, hexanes-EtOAc = 9:1,  $R_f = 0.20$ ) to afford **2f** as a colourless oil (61 mg, 68% yield).

**<sup>1</sup>H-NMR (300 MHz, CDCl<sub>3</sub>):**  $\delta$  7.96 – 7.91 (m, 2H), 7.20 – 7.14 (s, 2H), 4.53 (s, 2H); **<sup>13</sup>C-NMR (75 MHz, CDCl<sub>3</sub>):**  $\delta$  191.8, 166.3 (d,  $^1J_{C-F} = 256.8$  Hz), 130.9 (d,  $^4J_{C-F} = 4.6$  Hz), 130.8 (d,  $^3J_{C-F} = 9.5$  Hz), 116.3 (d,  $^2J_{C-F} = 22.2$  Hz), 54.9; **<sup>19</sup>F-NMR (282 MHz, CDCl<sub>3</sub>):**  $\delta$  -103.3; **IR (neat, cm<sup>-1</sup>):** 3362, 3109, 3079, 2989, 2903, 2184, 2095, 1689, 1592, 1505, 1416, 1349, 1279, 1211, 1155, 1100, 999, 906, 831, 805; **HRMS (ESI):** exact  $m/z$  calculated for C<sub>8</sub>H<sub>6</sub>FN<sub>3</sub>O (M+H)<sup>+</sup>: 180.0573; Found: 180.0570 (M+H)<sup>+</sup>.



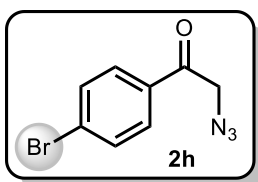
**2-azido-1-(4-chlorophenyl)ethan-1-one (2g)**<sup>[3]</sup>:



Following the general procedure, **2g** was prepared from 1-chloro-4-vinylbenzene **1g** (71.4 mg, 0.50 mmol). Reaction time was 12 hours. The crude product was purified by column chromatography (silica-gel, hexanes-EtOAc = 9:1,  $R_f$  = 0.22) to afford **2g** as a pale yellow solid (61 mg, 61% yield).

**<sup>1</sup>H-NMR (300 MHz, CDCl<sub>3</sub>):**  $\delta$  7.84 (d,  $J$  = 8.6 Hz, 2H), 7.47 (d,  $J$  = 8.6 Hz, 2H), 4.53 (s, 2H); **<sup>13</sup>C-NMR (75 MHz, CDCl<sub>3</sub>):**  $\delta$  192.2, 140.8, 132.7, 129.5, 129.4, 54.9; **IR (neat, cm<sup>-1</sup>):** 3360, 3094, 2960, 2926, 2087, 1916, 1681, 1588, 1487, 1402, 1334, 1257, 1211, 1174, 1088, 976, 910, 808, 734; **HRMS (ESI):** exact  $m/z$  calculated for C<sub>8</sub>H<sub>6</sub>ClN<sub>3</sub>O (M+H)<sup>+</sup>: 196.0277; Found: 196.0268 (M+H)<sup>+</sup>.

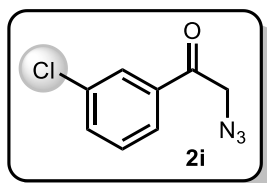
**2-azido-1-(4-bromophenyl)ethan-1-one (2h):**



Following the general procedure, **2h** was prepared from 1-bromo-4-vinylbenzene **1h** (95.0 mg, 0.50 mmol). Reaction time was 24 hours. The crude product was purified by column chromatography (silica-gel, hexanes-EtOAc = 9:1,  $R_f$  = 0.20) to afford **2h** as a white solid (83 mg, 69% yield).

**<sup>1</sup>H-NMR (300 MHz, CDCl<sub>3</sub>):**  $\delta$  7.76 (d,  $J$  = 8.1 Hz, 2H), 7.64 (d,  $J$  = 8.3 Hz, 2H), 4.52 (s, 2H); **<sup>13</sup>C-NMR (75 MHz, CDCl<sub>3</sub>):**  $\delta$  192.4, 133.1, 132.5, 129.6, 129.5, 54.9; **IR (neat, cm<sup>-1</sup>):** 3370, 3094, 2968, 2907, 2095, 1916, 1685, 1584, 1484, 1398, 1338, 1282, 1211, 1170, 1070, 995, 910, 805; **HRMS (ESI):** exact  $m/z$  calculated for C<sub>8</sub>H<sub>6</sub>BrN<sub>3</sub>O (M+H)<sup>+</sup>: 239.9722; Found: 239.9761 (M+H)<sup>+</sup>.

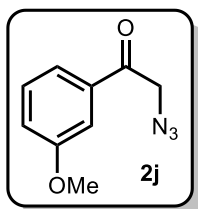
2-azido-1-(3-chlorophenyl)ethan-1-one (**2i**):



Following the general procedure, **2i** was prepared from 1-chloro-3-vinylbenzene **1i** (70.7 mg, 0.50 mmol). Reaction time was 12 hours. The crude product was purified by column chromatography (silica-gel, hexanes-EtOAc = 9:1,  $R_f$  = 0.25) to afford **2i** as a white solid (65 mg, 67% yield).

**$^1\text{H-NMR}$  (300 MHz,  $\text{CDCl}_3$ ):**  $\delta$  7.88 (t,  $J$  = 1.8 Hz, 1H), 7.77 (dt,  $J_1$  = 7.7 Hz,  $J_2$  = 1.2 Hz, 1H), 7.61 – 7.57 (m, 1H), 7.47 – 7.42 (m, 1H), 4.54 (s, 2H);  **$^{13}\text{C-NMR}$  (75 MHz,  $\text{CDCl}_3$ ):**  $\delta$  192.1, 135.8, 135.4, 134.1, 130.3, 128.0, 125.9, 54.9; **IR (neat,  $\text{cm}^{-1}$ ):** 3071, 2919, 2855, 2106, 1685, 1569, 1472, 1416, 1289, 1211, 905, 1029, 980, 906, 787; **HRMS (ESI):** exact  $m/z$  calculated for  $\text{C}_8\text{H}_6\text{ClN}_3\text{O}$  ( $\text{M}+\text{H}$ ) $^+$ : 196.0277; Found: 196.0264 ( $\text{M}+\text{H}$ ) $^+$ .

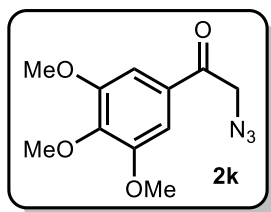
2-azido-1-(3-methoxyphenyl)ethan-1-one (**2j**):



Following the general procedure, **2j** was prepared from 1-methoxy-3-vinylbenzene **1j** (69.1 mg, 0.50 mmol). Reaction time was 18 hours. The crude product was purified by column chromatography (silica-gel, hexanes-EtOAc = 4:1,  $R_f$  = 0.22) to afford **2j** as a colourless oil (77 mg, 81% yield).

**$^1\text{H-NMR}$  (300 MHz,  $\text{CDCl}_3$ ):**  $\delta$  7.45 – 7.36 (m, 3H), 7.18 – 7.14 (m, 1H), 4.54 (s, 2H), 3.86 (s, 3H);  **$^{13}\text{C-NMR}$  (75 MHz,  $\text{CDCl}_3$ ):**  $\delta$  193.2, 160.2, 135.8, 130.1, 120.7, 120.4, 112.3, 55.6, 55.1; **IR (neat,  $\text{cm}^{-1}$ ):** 3078, 3008, 2945, 2840, 2102, 1692, 1584, 1487, 1454, 1420, 1252, 1197, 1150, 1040, 872, 775, 686; **HRMS (ESI):** exact  $m/z$  calculated for  $\text{C}_9\text{H}_9\text{N}_3\text{O}_2$  ( $\text{M}+\text{H}$ ) $^+$ : 192.0773; Found: 192.0765 ( $\text{M}+\text{H}$ ) $^+$ .

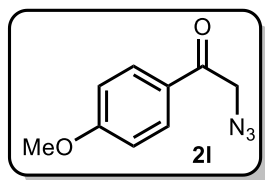
**2-azido-1-(3,4,5-trimethoxyphenyl)ethan-1-one (2k):**



Following the general procedure, **2k** was prepared from 1,2,3-trimethoxy-5-vinylbenzene **1k** (97.1 mg, 0.50 mmol). Reaction time was 14 hours. The crude product was purified by column chromatography (silica-gel, hexanes-EtOAc = 7:3,  $R_f$  = 0.22) to afford **2k** as a white solid (102 mg, 83% yield).

**$^1\text{H-NMR}$  (300 MHz,  $\text{CDCl}_3$ ):**  $\delta$  7.11 (s, 2H), 4.51 (s, 2H), 3.90 (s, 3H), 3.89 (s, 6H);  **$^{13}\text{C-NMR}$  (75 MHz,  $\text{CDCl}_3$ ):**  $\delta$  192.2, 153.3, 143.5, 129.5, 105.5, 61.1, 56.4, 54.8; **IR (neat,  $\text{cm}^{-1}$ ):** 3000, 2944, 2833, 2106, 1692, 1584, 1502, 1413, 1346, 1332, 1252, 1159, 1126, 995, 861; **HRMS (ESI):** exact  $m/z$  calculated for  $\text{C}_{11}\text{H}_{13}\text{N}_3\text{O}_4$  ( $\text{M}+\text{H}$ ) $^+$ : 252.0984; Found: 252.0977 ( $\text{M}+\text{H}$ ) $^+$ .

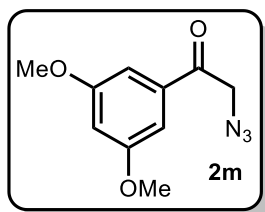
**2-azido-1-(4-methoxyphenyl)ethan-1-one (2l)<sup>[3]</sup>:**



Following the general procedure, **2l** was prepared from 1-methoxy-4-vinylbenzene **1l** (68.4 mg, 0.50 mmol). Reaction time was 15 hours. The crude product was purified by column chromatography (silica-gel, hexanes-EtOAc = 4:1,  $R_f$  = 0.20) to afford **2l** as a white solid (74 mg, 78% yield).

**$^1\text{H-NMR}$  (300 MHz,  $\text{CDCl}_3$ ):**  $\delta$  7.88 (d,  $J$  = 8.9 Hz, 2H), 6.95 (d,  $J$  = 8.9 Hz, 2H), 4.50 (s, 2H), 3.88 (s, 3H);  **$^{13}\text{C-NMR}$  (75 MHz,  $\text{CDCl}_3$ ):**  $\delta$  191.8, 164.3, 130.4, 127.5, 114.3, 55.7, 54.6; **IR (neat,  $\text{cm}^{-1}$ ):** 3330, 2933, 2844, 2106, 1681, 1599, 1513, 1454, 1423, 1356, 1305, 1260, 1238, 1174, 1021, 943, 824, 772; **HRMS (ESI):** exact  $m/z$  calculated for  $\text{C}_9\text{H}_9\text{N}_3\text{O}_2$  ( $\text{M}+\text{H}$ ) $^+$ : 192.0773; Found: 192.0762 ( $\text{M}+\text{H}$ ) $^+$ .

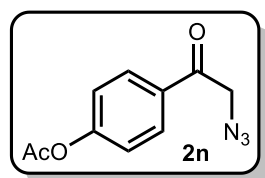
2-azido-1-(3,5-dimethoxyphenyl)ethan-1-one (**2m**):



Following the general procedure, **2m** was prepared from 1,3-dimethoxy-5-vinylbenzene **1m** (82.1 mg, 0.50 mmol). Reaction time was 20 hours. The crude product was purified by column chromatography (silica-gel, hexanes-EtOAc = 4:1,  $R_f$  = 0.25) to afford **2m** as a colourless oil (88 mg, 80% yield).

**$^1\text{H-NMR}$  (300 MHz,  $\text{CDCl}_3$ ):**  $\delta$  7.01 (d,  $J$  = 2.2 Hz, 2H), 6.68 (t,  $J$  = 2.2 Hz, 1H), 4.51 (s, 2H), 3.83 (s, 6H);  **$^{13}\text{C-NMR}$  (75 MHz,  $\text{CDCl}_3$ ):**  $\delta$  193.1, 161.2, 136.2, 106.2, 105.8, 55.8, 55.1; **IR (neat,  $\text{cm}^{-1}$ ):** 3093, 3011, 2952, 2896, 2844, 2214, 2102, 1699, 1591, 1454, 1428, 1349, 1297, 1267, 1208, 1156, 1059, 1021, 842; **HRMS (ESI):** exact  $m/z$  calculated for  $\text{C}_{10}\text{H}_{11}\text{N}_3\text{O}_3$  ( $\text{M}+\text{H}$ )<sup>+</sup>: 222.0878; Found: 222.0874 ( $\text{M}+\text{H}$ )<sup>+</sup>.

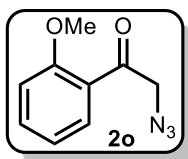
4-(2-azidoacetyl)phenyl acetate (**2n**)<sup>[4]</sup>:



Following the general procedure, **2n** was prepared from 4-vinylphenyl acetate **1n** (85.3 mg, 0.50 mmol). Reaction time was 18 hours. The crude product was purified by column chromatography (silica-gel, hexanes-EtOAc = 5:1,  $R_f$  = 0.20) to afford **2n** as a colourless oil (85 mg, 78% yield).

**$^1\text{H-NMR}$  (300 MHz,  $\text{CDCl}_3$ ):**  $\delta$  7.93 (d,  $J$  = 8.7 Hz, 2H), 7.22 (d,  $J$  = 8.6 Hz, 2H), 4.53 (s, 2H), 2.32 (s, 3H);  **$^{13}\text{C-NMR}$  (75 MHz,  $\text{CDCl}_3$ ):**  $\delta$  192.2, 168.8, 155.2, 131.9, 129.7, 122.3, 54.9, 21.2; **IR (neat,  $\text{cm}^{-1}$ ):** 3310, 3071, 2911, 2363, 2102, 1744, 1692, 1599, 1505, 1416, 1372, 1286, 1193, 1160, 1003, 910, 846; **HRMS (ESI):** exact  $m/z$  calculated for  $\text{C}_{10}\text{H}_9\text{N}_3\text{O}_3$  ( $\text{M}+\text{H}$ )<sup>+</sup>: 220.0722; Found: 220.0712 ( $\text{M}+\text{H}$ )<sup>+</sup>.

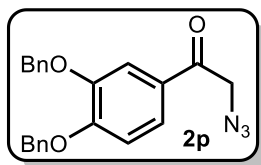
**2-azido-1-(2-methoxyphenyl)ethan-1-one (2o):**



Following the general procedure, **2o** was prepared from 1-methoxy-2-vinylbenzene **1o** (68.4 mg, 0.50 mmol). Reaction time was 12 hours. The crude product was purified by column chromatography (silica-gel, hexanes-EtOAc = 4:1,  $R_f$  = 0.22) to afford **2o** as a colourless oil (60 mg, 63% yield).

**$^1\text{H-NMR}$  (300 MHz,  $\text{CDCl}_3$ ):**  $\delta$  7.91 (dd,  $J_1 = 7.8$  Hz,  $J_2 = 1.8$  Hz, 1H), 7.56 – 7.50 (m, 1H), 7.07 – 6.97 (m, 2H), 4.51 (s, 2H), 3.93 (s, 3H);  **$^{13}\text{C-NMR}$  (75 MHz,  $\text{CDCl}_3$ ):**  $\delta$  194.5, 159.4, 135.2, 131.2, 124.6, 121.2, 111.7, 59.5, 55.7; **IR (neat,  $\text{cm}^{-1}$ ):** 3291, 2948, 2844, 2099, 1730, 1677, 1595, 1484, 1345, 1282, 1241, 1200, 1160, 1114, 1018, 910, 820, 753; **HRMS (ESI):** exact  $m/z$  calculated for  $\text{C}_9\text{H}_9\text{N}_3\text{O}_2$  ( $\text{M}+\text{H}$ ) $^+$ : 192.0773; Found: 192.0762 ( $\text{M}+\text{H}$ ) $^+$ .

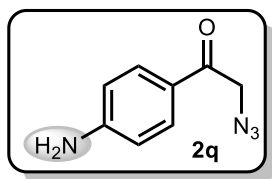
**2-azido-1-(3,4-bis(benzyloxy)phenyl)ethan-1-one (2p):**



Following the general procedure, **2p** was prepared from (((4-vinyl-1,2-phenylene)bis(oxy))bis(methylene))dibenzene **1p** (158.2 mg, 0.50 mmol). Reaction time was 12 hours. The crude product was purified by column chromatography (silica-gel, hexanes-EtOAc = 4:1,  $R_f$  = 0.30) to afford **2p** as a white solid (154 mg, 83% yield).

**$^1\text{H-NMR}$  (600 MHz,  $\text{CDCl}_3$ ):**  $\delta$  7.56 (d,  $J = 1.9$  Hz, 1H), 7.46 – 7.41 (m, 5H), 7.39 – 7.36 (m, 4H), 7.34 – 7.30 (m, 2H), 6.93 (d,  $J = 8.4$  Hz, 1H), 5.24 (s, 2H), 5.21 (s, 2H), 4.44 (s, 2H);  **$^{13}\text{C-NMR}$  (150 MHz,  $\text{CDCl}_3$ ):**  $\delta$  191.8, 154.1, 149.0, 136.7, 136.3, 128.8, 128.7, 128.3, 128.2, 127.9, 127.5, 127.2, 122.9, 113.7, 113.1, 71.3, 71.0, 54.6; **IR (neat,  $\text{cm}^{-1}$ ):** 3064, 3034, 2907, 2855, 2102, 1674, 1580, 1513, 1435, 1379, 1338, 1271, 1182, 1148, 1021, 809, 731, 693; **HRMS (ESI):** exact  $m/z$  calculated for  $\text{C}_{22}\text{H}_{19}\text{N}_3\text{O}_3$  ( $\text{M}+\text{H}$ ) $^+$ : 374.1504; Found: 374.1499 ( $\text{M}+\text{H}$ ) $^+$ .

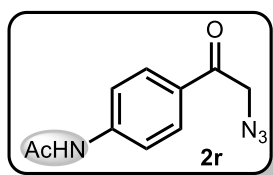
1-(4-aminophenyl)-2-azidoethan-1-one (**2q**):



Following the general procedure, **2q** was prepared from 4-vinylaniline **1q** (61.4 mg, 0.50 mmol). Reaction time was 36 hours. The crude product was purified by column chromatography (silica-gel, hexanes-EtOAc = 2:1,  $R_f$  = 0.20) to afford **2q** as a yellow solid (49 mg, 56% yield).

**$^1\text{H-NMR}$  (300 MHz,  $\text{CDCl}_3$ ):**  $\delta$  7.74 (d,  $J$  = 8.6 Hz, 2H), 6.65 (d,  $J$  = 8.7 Hz, 2H), 4.45 (s, 2H), 4.23 (br-s, 2H);  **$^{13}\text{C-NMR}$  (75 MHz,  $\text{CDCl}_3$ ):**  $\delta$  191.2, 152.0, 130.6, 124.8, 114.0, 54.4; **IR (neat,  $\text{cm}^{-1}$ ):** 3377, 3332, 3228, 2918, 2098, 1670, 1588, 1517, 1442, 1346, 1234, 1182, 910, 828, 675; **HRMS (ESI):** exact  $m/z$  calculated for  $\text{C}_8\text{H}_8\text{N}_4\text{O}$  ( $\text{M}+\text{H}$ ) $^+$ : 177.0776; Found: 177.0770 ( $\text{M}+\text{H}$ ) $^+$ .

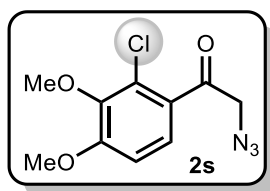
*N*-(4-(2-azidoacetyl)phenyl)acetamide (**2r**):



Following the general procedure, **2r** was prepared from *N*-(4-vinylphenyl)acetamide **1r** (80.6 mg, 0.50 mmol). Reaction time was 36 hours. The crude product was purified by column chromatography (silica-gel, hexanes-EtOAc = 2:3,  $R_f$  = 0.22) to afford **2r** as a pale yellow solid (93 mg, 85% yield).

**$^1\text{H-NMR}$  (400 MHz,  $\text{DMSO-d}^6$ ):**  $\delta$  10.32 (s, 1H), 7.90 (d,  $J$  = 8.7 Hz, 2H), 7.72 (d,  $J$  = 8.7 Hz, 2H), 4.81 (s, 2H), 2.09 (s, 3H);  **$^{13}\text{C-NMR}$  (100 MHz,  $\text{DMSO-d}^6$ ):**  $\delta$  192.8, 169.0, 144.2, 129.2, 128.8, 118.2, 54.3, 24.1; **IR (neat,  $\text{cm}^{-1}$ ):** 3325, 3284, 3194, 2915, 2110, 1677, 1599, 1536, 1409, 1372, 1327, 1260, 1180, 945, 831, 716; **HRMS (ESI):** exact  $m/z$  calculated for  $\text{C}_{10}\text{H}_{10}\text{N}_4\text{O}_2$  ( $\text{M}+\text{H}$ ) $^+$ : 219.0882; Found: 219.0873 ( $\text{M}+\text{H}$ ) $^+$ .

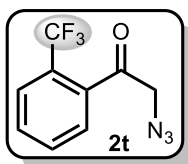
**2-azido-1-(2-chloro-3,4-dimethoxyphenyl)ethan-1-one (2s):**



Following the general procedure, **2s** was prepared from 2-chloro-3,4-dimethoxy-1-vinylbenzene **1s** (99.3 mg, 0.50 mmol). Reaction time was 12 hours. The crude product was purified by column chromatography (silica-gel, hexanes-EtOAc = 5:2,  $R_f$  = 0.30) to afford **2s** as a white solid (77 mg, 61% yield).

**$^1\text{H-NMR}$  (300 MHz,  $\text{CDCl}_3$ ):**  $\delta$  7.48 (d,  $J$  = 8.7 Hz, 1H), 6.90 (d,  $J$  = 8.7 Hz, 1H), 4.52 (s, 2H), 3.93 (s, 3H), 3.86 (s, 3H);  **$^{13}\text{C-NMR}$  (75 MHz,  $\text{CDCl}_3$ ):**  $\delta$  194.4, 157.2, 145.9, 128.8, 127.5, 126.6, 110.5, 60.8, 58.0, 56.4; **IR (neat,  $\text{cm}^{-1}$ ):** 3090, 2978, 2940, 2848, 2113, 1670, 1580, 1490, 1442, 1401, 1338, 1282, 1241, 1062, 1029, 992, 820, 779; **HRMS (ESI):** exact  $m/z$  calculated for  $\text{C}_{10}\text{H}_{10}\text{ClN}_3\text{O}_3$  ( $\text{M}+\text{H}$ ) $^+$ : 256.0489; Found: 256.0484 ( $\text{M}+\text{H}$ ) $^+$ .

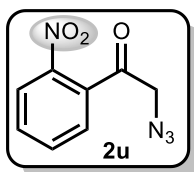
**2-azido-1-(2-(trifluoromethyl)phenyl)ethan-1-one (2t):**



Following the general procedure, **2t** was prepared from 1-(trifluoromethyl)-2-vinylbenzene **1t** (87.0 mg, 0.50 mmol). Reaction time was 72 hours. The crude product was purified by column chromatography (silica-gel, hexanes-EtOAc = 9:1,  $R_f$  = 0.20) to afford **2t** as a colourless oil (69 mg, 60% yield).

**$^1\text{H-NMR}$  (300 MHz,  $\text{CDCl}_3$ ):**  $\delta$  7.77 – 7.74 (m, 1H), 7.66 – 7.63 (m, 2H), 7.45 – 7.42 (m, 1H), 4.33 (s, 2H);  **$^{13}\text{C-NMR}$  (75 MHz,  $\text{CDCl}_3$ ):**  $\delta$  197.9, 136.9, 132.2, 131.2, 127.29, 127.18 (q,  $J_1$  = 5.0 Hz,  $J_2$  = 9.5 Hz), 127.18 (q,  $J$  = 14.1 Hz,  $J$  = 18.6 Hz), 126.5 (q,  $J_1$  = 273.8,  $J_2$  = 460.8 Hz), 57.8 (d,  $J$  = 1.9 Hz);  **$^{19}\text{F-NMR}$  (282 MHz,  $\text{CDCl}_3$ ):**  $\delta$  -58.5; **IR (neat,  $\text{cm}^{-1}$ ):** 3083, 2654, 2162, 2110, 1703, 1584, 1312, 1274, 1167, 1111, 1036, 767; **HRMS (ESI):** exact  $m/z$  calculated for  $\text{C}_9\text{H}_6\text{F}_3\text{N}_3\text{O}$  ( $\text{M}+\text{Na}$ ) $^+$ : 252.0361; Found: 252.0354 ( $\text{M}+\text{Na}$ ) $^+$ .

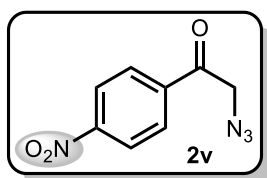
**2-azido-1-(2-nitrophenyl)ethan-1-one (2u)**<sup>[6]</sup>:



Following the general procedure, **2u** was prepared from 1-nitro-2-vinylbenzene **1u** (74.6 mg, 0.50 mmol). Reaction time was 72 hours. The crude product was purified by column chromatography (silica-gel, hexanes-EtOAc = 4:1,  $R_f$  = 0.20) to afford **2u** as a pale-yellow oil (30 mg, 29% (42% based on conversion) yield).

**<sup>1</sup>H-NMR (300 MHz, CDCl<sub>3</sub>):**  $\delta$  8.21 (dd,  $J_1$  = 8.2 Hz,  $J_2$  = 1.0 Hz, 1H), 7.82 – 7.77 (m, 1H), 7.71 – 7.66 (m, 1H), 7.42 (dd,  $J_1$  = 7.4 Hz,  $J_2$  = 1.4 Hz, 1H), 4.31 (s, 2H); **<sup>13</sup>C-NMR (75 MHz, CDCl<sub>3</sub>):**  $\delta$  197.2, 145.8, 135.1, 135.0, 131.5, 127.8, 124.6, 57.8; **IR (neat, cm<sup>-1</sup>):** 3034, 2922, 2855, 2106, 1689, 1584, 1521, 1342, 1282, 1219, 992, 854, 746, 701; **HRMS (ESI):** exact m/z calculated for C<sub>8</sub>H<sub>6</sub>N<sub>4</sub>O<sub>3</sub> (M+Na)<sup>+</sup>: 229.0338; Found: 229.0329 (M+Na)<sup>+</sup>.

**2-azido-1-(4-nitrophenyl)ethan-1-one (2v)**<sup>[3]</sup>:

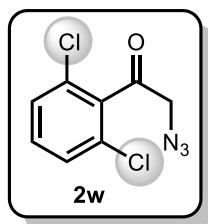


Following the general procedure, **2v** was prepared from 1-nitro-4-vinylbenzene **1v** (78.5 mg, 0.50 mmol). Reaction time was 48 hours (Note: *more than 48 hours leads to decomposition of the product!*). The crude product was purified by column chromatography (silica-gel, hexanes-EtOAc = 9:1,  $R_f$  = 0.15) to afford **2v** as a yellow solid (52 mg, 51% yield).

**<sup>1</sup>H-NMR (400 MHz, CDCl<sub>3</sub>):**  $\delta$  8.36 (d,  $J$  = 8.9 Hz, 2H), 8.09 (d,  $J$  = 8.6 Hz, 2H), 4.60 (s, 2H); **<sup>13</sup>C-NMR (125 MHz, CDCl<sub>3</sub>):**  $\delta$  192.1, 151.1, 138.9, 129.3, 124.4, 55.5; **IR (neat, cm<sup>-1</sup>):** 3111, 2906, 2107, 1704, 1604, 1525, 1345, 1212, 854; **HRMS (ESI):** exact m/z calculated for C<sub>8</sub>H<sub>6</sub>N<sub>4</sub>O<sub>3</sub> (M+H)<sup>+</sup>: 207.0517; Found: 207.0511 (M+H)<sup>+</sup>.

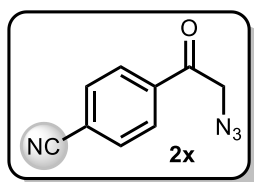


2-azido-1-(2,6-dichlorophenyl)ethan-1-one (**2w**):



Following the general procedure, **2w** was prepared from 1,3-dichloro-2-vinylbenzene **1w** (86.5 mg, 0.50 mmol). After 72 h, very little conversion of the starting material was observed. The yield of the product was determined by  $^1\text{H}$  NMR using diphenylmethane as internal standard.  $^1\text{H}$ -NMR yield (10 %).

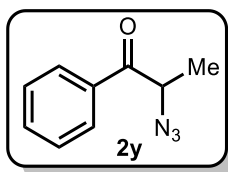
4-(2-azidoacetyl)benzonitrile (**2x**):



Following the general procedure, **2x** was prepared from 4-vinylbenzonitrile **1x** (66.5 mg, 0.50 mmol). Reaction time was 22 hours. The crude product was purified by column chromatography (silica-gel, hexanes-EtOAc = 5:1,  $R_f$  = 0.20) to afford **2x** as a yellow solid (61 mg, 66% yield).

$^1\text{H}$ -NMR (300 MHz,  $\text{CDCl}_3$ ):  $\delta$  8.01 (d,  $J$  = 8.5 Hz, 2H), 7.81 (d,  $J$  = 8.5 Hz, 2H), 4.57 (s, 2H);  $^{13}\text{C}$ -NMR (75 MHz,  $\text{CDCl}_3$ ):  $\delta$  192.3, 137.3, 132.9, 128.5, 117.7, 117.5, 55.2; IR (neat,  $\text{cm}^{-1}$ ): 3101, 2956, 2915, 2233, 2184, 2102, 1692, 1607, 1402, 1342, 1271, 1211, 1003, 913, 831, 764; HRMS (ESI): exact  $m/z$  calculated for  $\text{C}_9\text{H}_6\text{N}_4\text{O}$  ( $\text{M}+\text{H}$ ) $^+$ : 187.0619; Found: 187.0612 ( $\text{M}+\text{H}$ ) $^+$ .

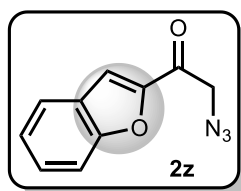
**2-azido-1-phenylpropan-1-one (2y)**<sup>[7]</sup>:



Following the general procedure, **2y** was prepared from (*E*)-prop-1-en-1-ylbenzene **1y** (60.0 mg, 0.50 mmol). Reaction time was 12 hours. The crude product was purified by column chromatography (silica-gel, hexanes-EtOAc = 95:5,  $R_f$  = 0.20) to afford **2y** as a colourless oil (58 mg, 67% yield).

**<sup>1</sup>H-NMR (300 MHz, CDCl<sub>3</sub>):**  $\delta$  7.96 – 7.93 (m, 2H), 7.64 – 7.59 (m, 1H), 7.53 – 7.48 (m, 2H), 4.71 (q,  $J$  = 7.1 Hz, 1H), 1.57 (d,  $J$  = 7.0 Hz, 3H); **<sup>13</sup>C-NMR (75 MHz, CDCl<sub>3</sub>):**  $\delta$  196.8, 134.4, 134.1, 129.1, 128.8, 58.5, 16.6; **IR (neat, cm<sup>-1</sup>):** 3064, 2989, 2937, 2091, 1689, 1595, 1450, 1256, 1215, 1066, 962, 697; **HRMS (ESI):** exact  $m/z$  calculated for C<sub>9</sub>H<sub>9</sub>N<sub>3</sub>O (M+H)<sup>+</sup>: 176.0824; Found: 176.0819 (M+H)<sup>+</sup>.

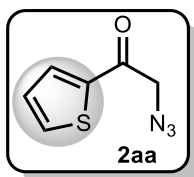
**2-azido-1-(benzofuran-2-yl)ethan-1-one (2z):**



Following the general procedure, **2z** was prepared from 2-vinylbenzofuran **1z** (72.1 mg, 0.50 mmol). Reaction time was 12 hours. The crude product was purified by column chromatography (silica-gel, hexanes-EtOAc = 9:1,  $R_f$  = 0.20) to afford **2z** as a white solid (67 mg, 67% yield).

**<sup>1</sup>H-NMR (400 MHz, CDCl<sub>3</sub>):**  $\delta$  7.74 (d,  $J$  = 7.9 Hz, 1H), 7.62 (d,  $J$  = 0.7 Hz, 1H), 7.59 – 7.50 (m, 2H), 4.56 (s, 2H); **<sup>13</sup>C-NMR (100 MHz, CDCl<sub>3</sub>):**  $\delta$  184.8, 155.9, 150.6, 129.1, 126.9, 124.5, 123.7, 113.9, 112.6, 55.0; **IR (neat, cm<sup>-1</sup>):** 3116, 2967, 2929, 2102, 1666, 1547, 1439, 1364, 1271, 1163, 1029, 932, 734; **HRMS (ESI):** exact  $m/z$  calculated for C<sub>10</sub>H<sub>7</sub>N<sub>3</sub>O<sub>2</sub> (M+H)<sup>+</sup>: 202.0616; Found: 202.0616 (M+H)<sup>+</sup>.

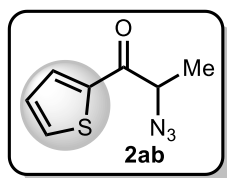
**2-azido-1-(thiophen-2-yl)ethan-1-one (2aa)**<sup>[5]</sup>:



Following the general procedure, **2aa** was prepared from 2-vinylthiophene **1aa** (55.0 mg, 0.50 mmol). Reaction time was 12 hours. The crude product was purified by column chromatography (silica-gel, hexanes-EtOAc = 9:1,  $R_f$  = 0.20) to afford **2y** as a pale-yellow oil (49 mg, 59% yield).

**<sup>1</sup>H-NMR (400 MHz, CDCl<sub>3</sub>):**  $\delta$  7.73 – 7.72 (m, 2H), 7.16 (m, 1H), 4.45 (s, 2H); **<sup>13</sup>C-NMR (100 MHz, CDCl<sub>3</sub>):**  $\delta$  186.4, 140.8, 135.0, 132.6, 128.5, 55.0; **IR (neat, cm<sup>-1</sup>):** 3094, 2900, 2099, 1666, 1513, 1409, 1357, 1282, 1223, 1059, 891, 854, 723; **HRMS (ESI):** exact m/z calculated for C<sub>6</sub>H<sub>5</sub>N<sub>3</sub>OS (M+H)<sup>+</sup>: 168.0231; Found: 168.0225 (M+H)<sup>+</sup>.

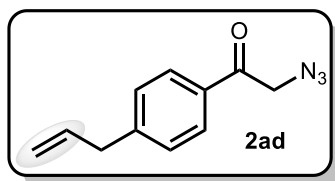
**2-azido-1-(thiophen-2-yl)propan-1-one (2ab)**:



Following the general procedure, **2ab** was prepared from (*E*)-2-(prop-1-en-1-yl)thiophene **1ab** (62.1 mg, 0.50 mmol). Reaction time was 12 hours. The crude product was purified by column chromatography (silica-gel, hexanes-EtOAc = 9:1,  $R_f$  = 0.22) to afford **2ab** as a yellow solid (30 mg, 33% yield).

**<sup>1</sup>H-NMR (400 MHz, CDCl<sub>3</sub>):**  $\delta$  7.79 (d,  $J$  = 3.6 Hz, 1H), 7.73 (d,  $J$  = 4.7 Hz, 1H), 7.18 – 7.16 (m, 1H), 4.52 (q,  $J$  = 6.8 Hz, 1H), 1.60 (d,  $J$  = 7.0 Hz, 3H); **<sup>13</sup>C-NMR (100 MHz, CDCl<sub>3</sub>):**  $\delta$  189.9, 141.0, 135.4, 133.3, 128.6, 59.9, 17.1; **IR (neat, cm<sup>-1</sup>):** 3094, 2985, 2937, 2095, 1659, 1517, 1450, 1409, 1357, 1215, 1054, 999, 913, 828, 723; **HRMS (ESI):** exact m/z calculated for C<sub>7</sub>H<sub>7</sub>N<sub>3</sub>OS (M+H)<sup>+</sup>: 182.0388; Found: 182.0382 (M+H)<sup>+</sup>.

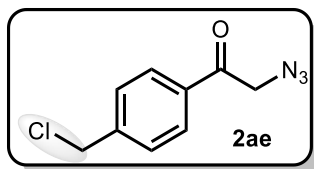
1-(4-allylphenyl)-2-azidoethan-1-one (**2ad**):



Following the general procedure, **2ad** was prepared from 1-allyl-4-vinylbenzene **1ad** (72.2 mg, 0.50 mmol). Reaction time was 18 hours. The crude product was purified by column chromatography (silica-gel, hexanes-EtOAc = 9:1,  $R_f$  = 0.30) to afford **2ad** as a colourless oil (71 mg, 71% yield).

**$^1\text{H-NMR}$  (400 MHz,  $\text{CDCl}_3$ ):**  $\delta$  7.83 (d,  $J$  = 8.2 Hz, 2H), 7.31 (d,  $J$  = 8.2 Hz, 2H), 5.99 – 5.89 (m, 1H), 5.14 – 5.07 (m, 2H), 4.53 (s, 2H), 3.44 (d,  $J$  = 6.6 Hz, 2H);  **$^{13}\text{C-NMR}$  (100 MHz,  $\text{CDCl}_3$ ):**  $\delta$  192.9, 147.1, 136.0, 132.6, 129.3, 128.3, 117.1, 54.9, 40.2; **IR (neat,  $\text{cm}^{-1}$ ):** 3310, 3079, 2982, 2900, 2102, 1689, 1607, 1416, 1346, 1275, 1223, 1178, 1111, 995, 910, 757; **HRMS (ESI):** exact  $m/z$  calculated for  $\text{C}_{11}\text{H}_{11}\text{N}_3\text{O}$  ( $\text{M}+\text{H}$ ) $^+$ : 202.0980; Found: 202.0975 ( $\text{M}+\text{H}$ ) $^+$ .

2-azido-1-(4-(chloromethyl)phenyl)ethan-1-one (**2ae**):

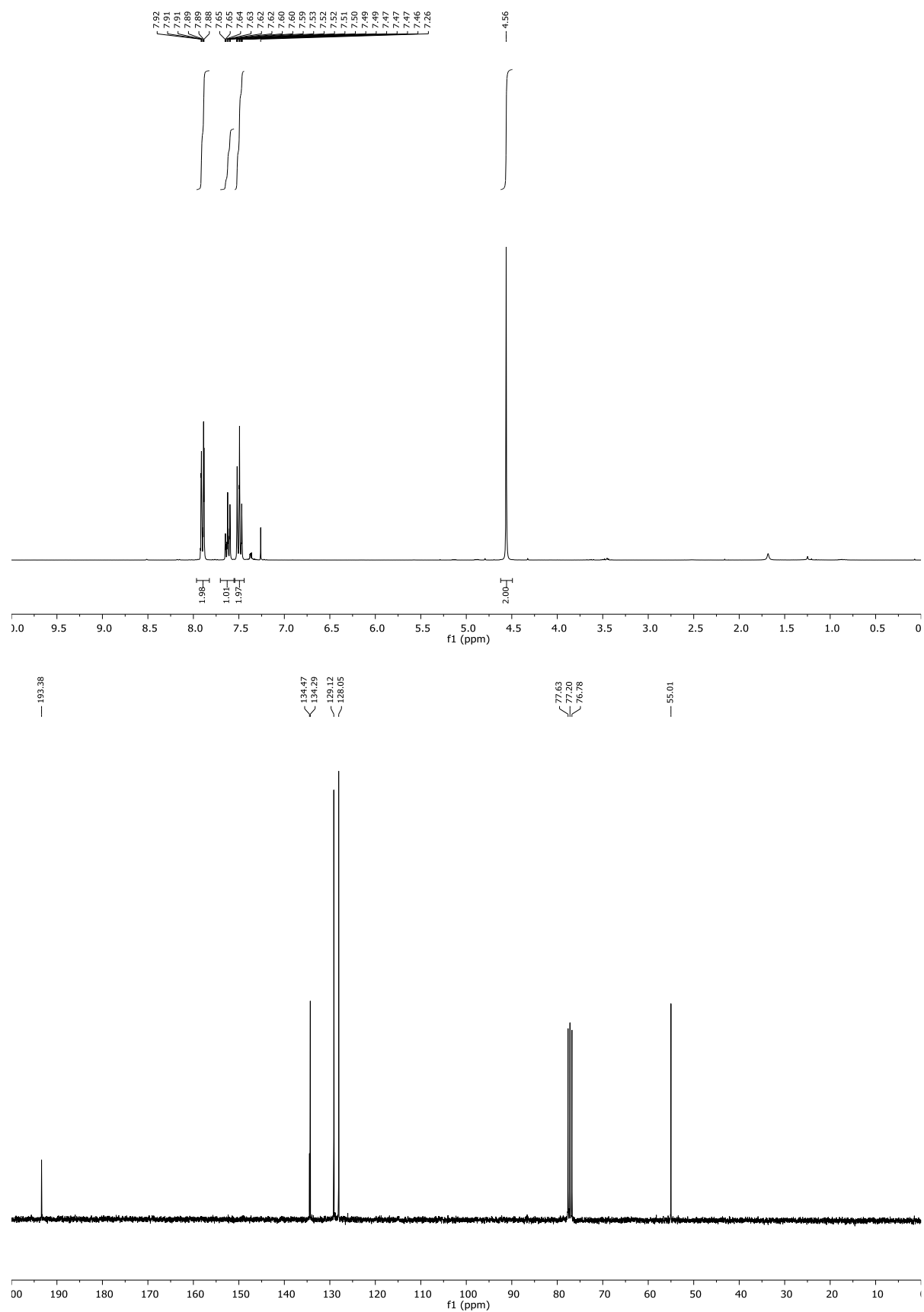


Following the general procedure, **2ae** was prepared from 1-(chloromethyl)-4-vinylbenzene **1ae** (76.3 mg, 0.50 mmol). Reaction time was 24 hours. The crude product was purified by column chromatography (silica-gel, hexanes-EtOAc = 4:1,  $R_f$  = 0.25) to afford **2ae** as a white solid (65 mg, 62% yield).

**$^1\text{H-NMR}$  (300 MHz,  $\text{CDCl}_3$ ):**  $\delta$  7.90 (d,  $J$  = 8.3 Hz, 2H), 7.52 (d,  $J$  = 8.3 Hz, 2H), 4.61 (s, 2H), 4.55 (s, 2H);  **$^{13}\text{C-NMR}$  (75 MHz,  $\text{CDCl}_3$ ):**  $\delta$  192.8, 143.6, 134.2, 129.1, 128.5, 55.0, 45.2; **IR (neat,  $\text{cm}^{-1}$ ):** 2907, 2191, 2099, 1692, 1606, 1416, 1346, 1267, 1219, 1182, 999, 906, 835, 790, 746, 682; **HRMS (ESI):** exact  $m/z$  calculated for  $\text{C}_9\text{H}_8\text{ClN}_3\text{O}$  ( $\text{M}+\text{H}$ ) $^+$ : 210.0434; Found: 210.0430 ( $\text{M}+\text{H}$ ) $^+$ .

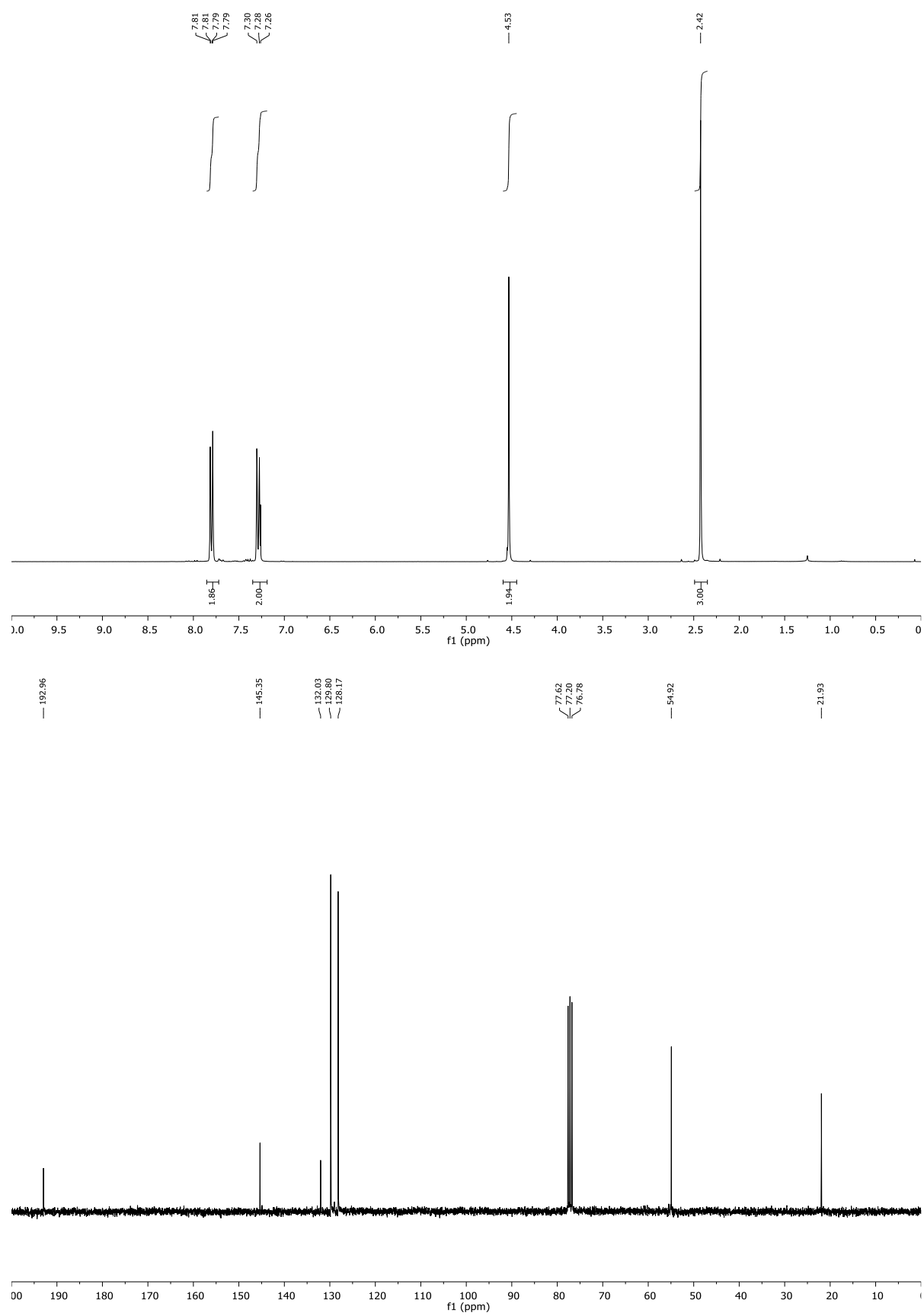
## Chapter 4: Copper(II)-catalyzed Oxo-azidation of Vinylarenes

$^1\text{H}$  and  $^{13}\text{C}$  NMR of **2a**:



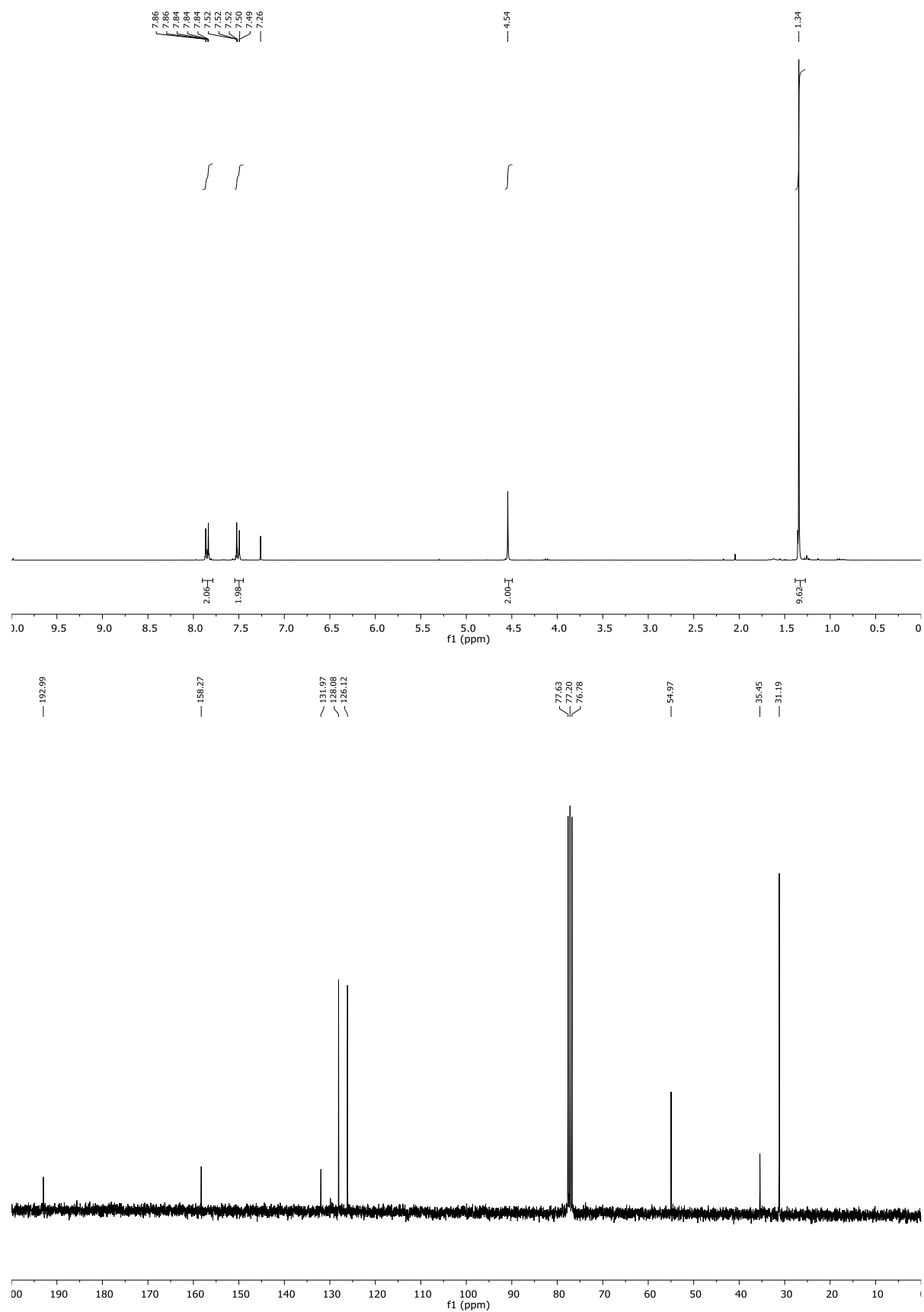
## Chapter 4: Copper(II)-catalyzed Oxo-azidation of Vinylarenes

$^1\text{H}$  and  $^{13}\text{C}$  NMR of **2b**:



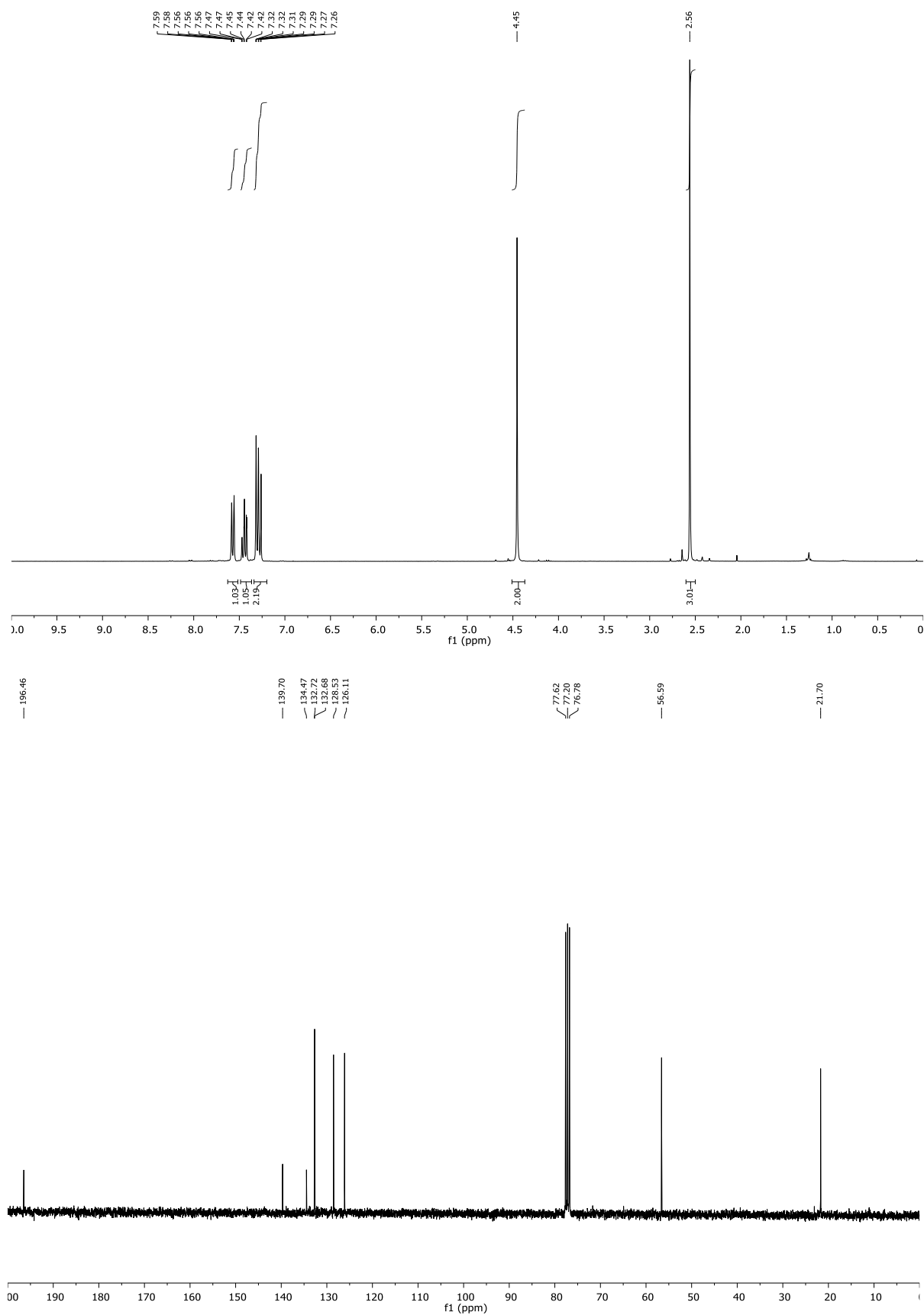
## Chapter 4: Copper(II)-catalyzed Oxo-azidation of Vinylarenes

$^1\text{H}$  and  $^{13}\text{C}$  NMR of **2c**:



## Chapter 4: Copper(II)-catalyzed Oxo-azidation of Vinylarenes

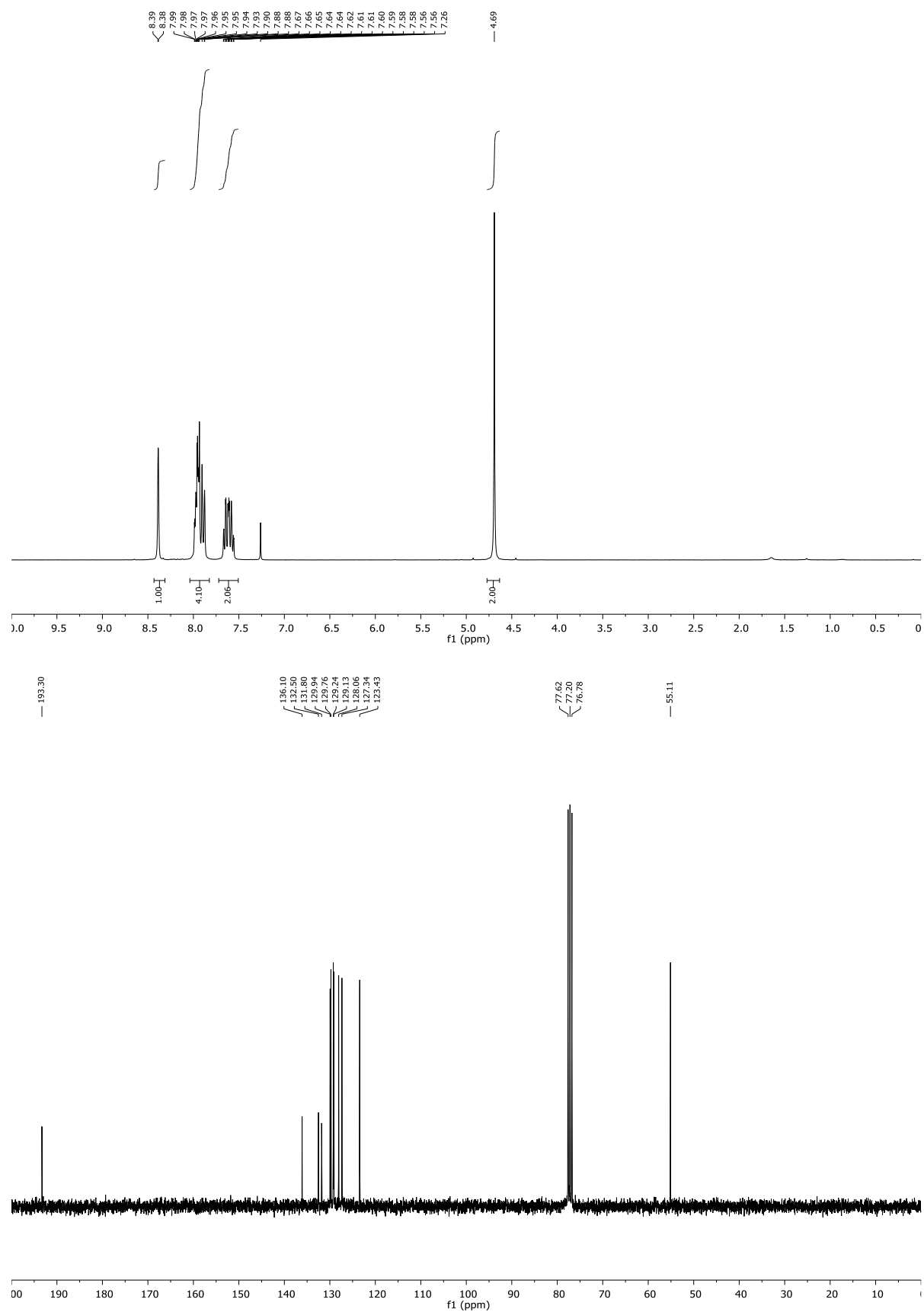
$^1\text{H}$  and  $^{13}\text{C}$  NMR of **2d**:





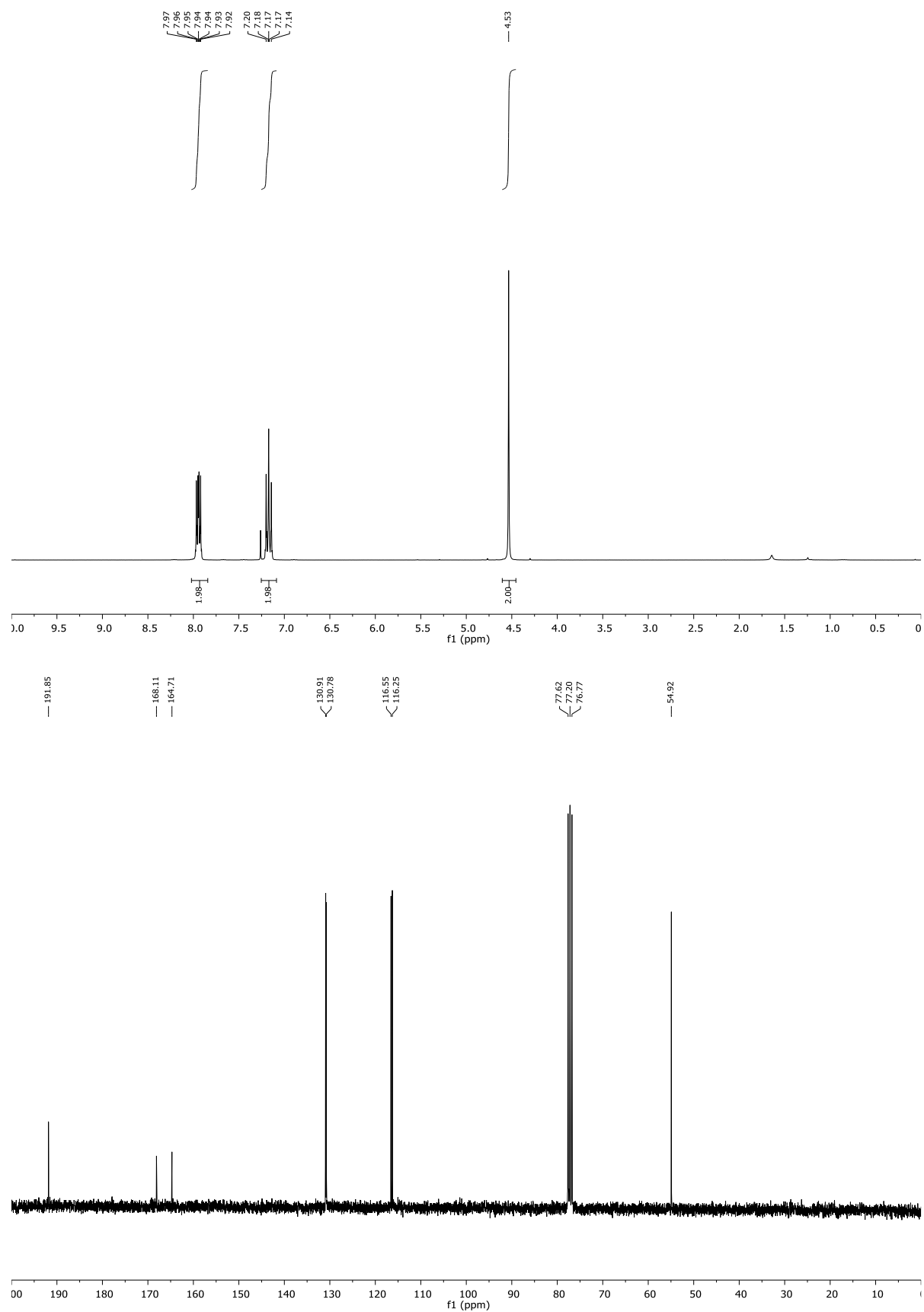
## Chapter 4: Copper(II)-catalyzed Oxo-azidation of Vinylarenes

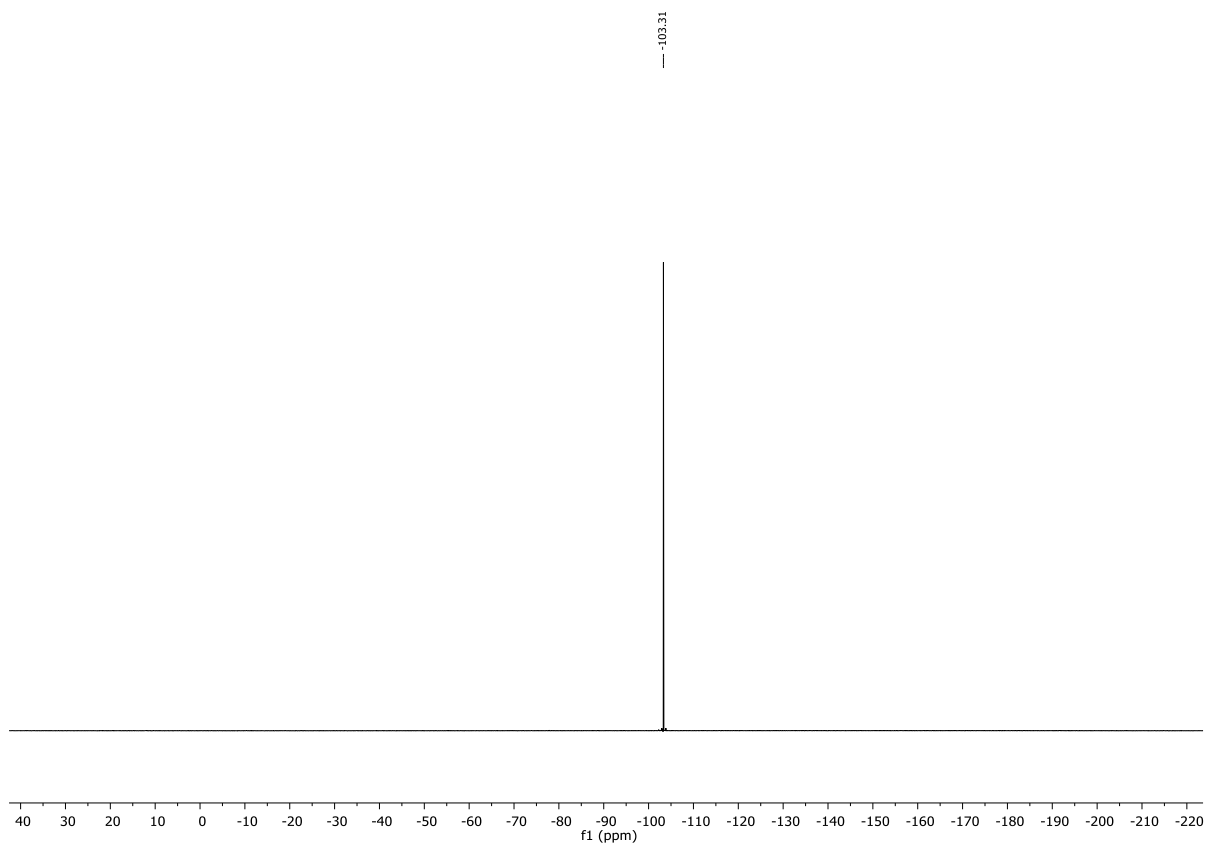
$^1\text{H}$  and  $^{13}\text{C}$  NMR of **2e**:



## Chapter 4: Copper(II)-catalyzed Oxo-azidation of Vinylarenes

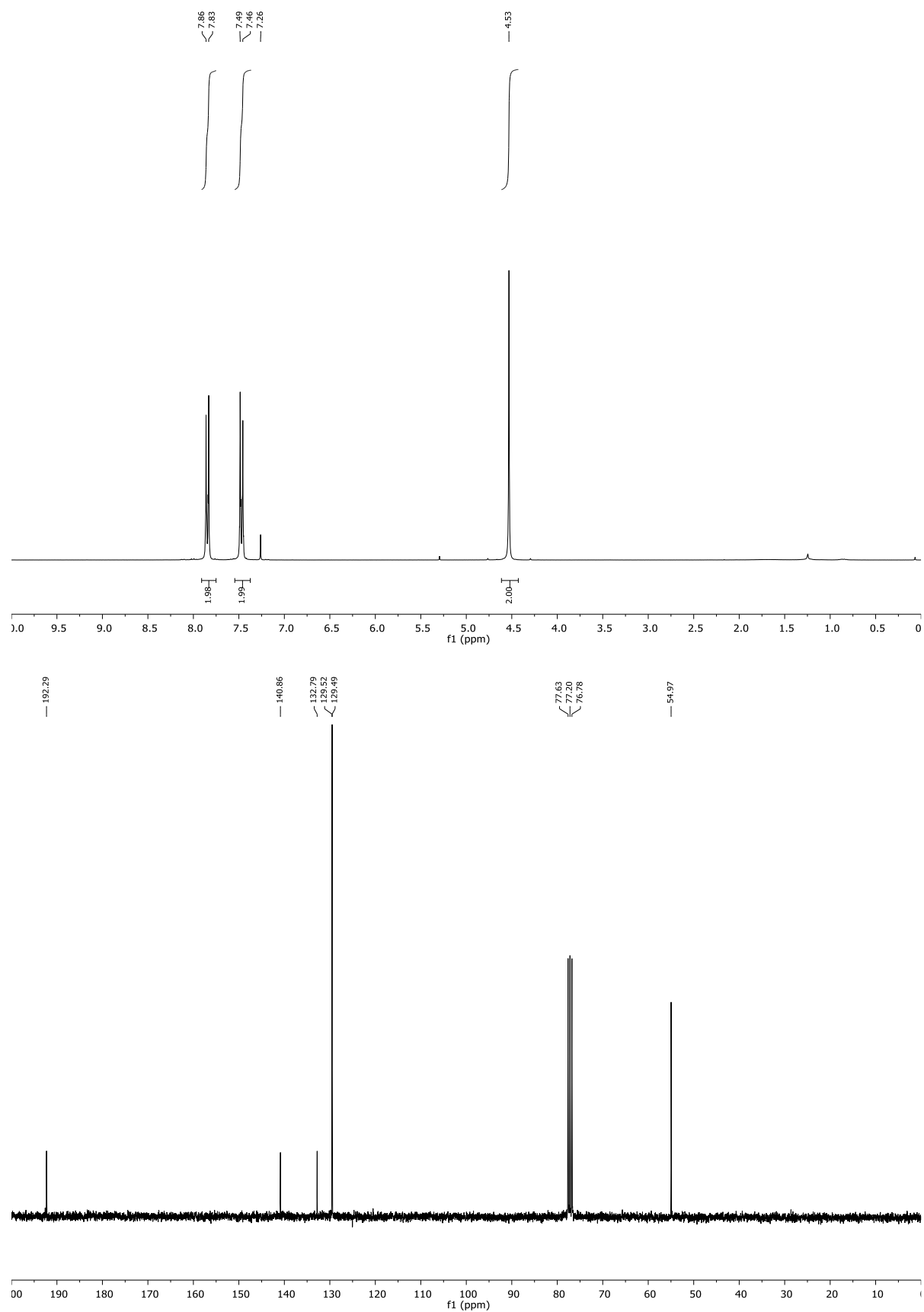
$^1\text{H}$ ,  $^{13}\text{C}$  and  $^{19}\text{F}$  NMR of **2f**:





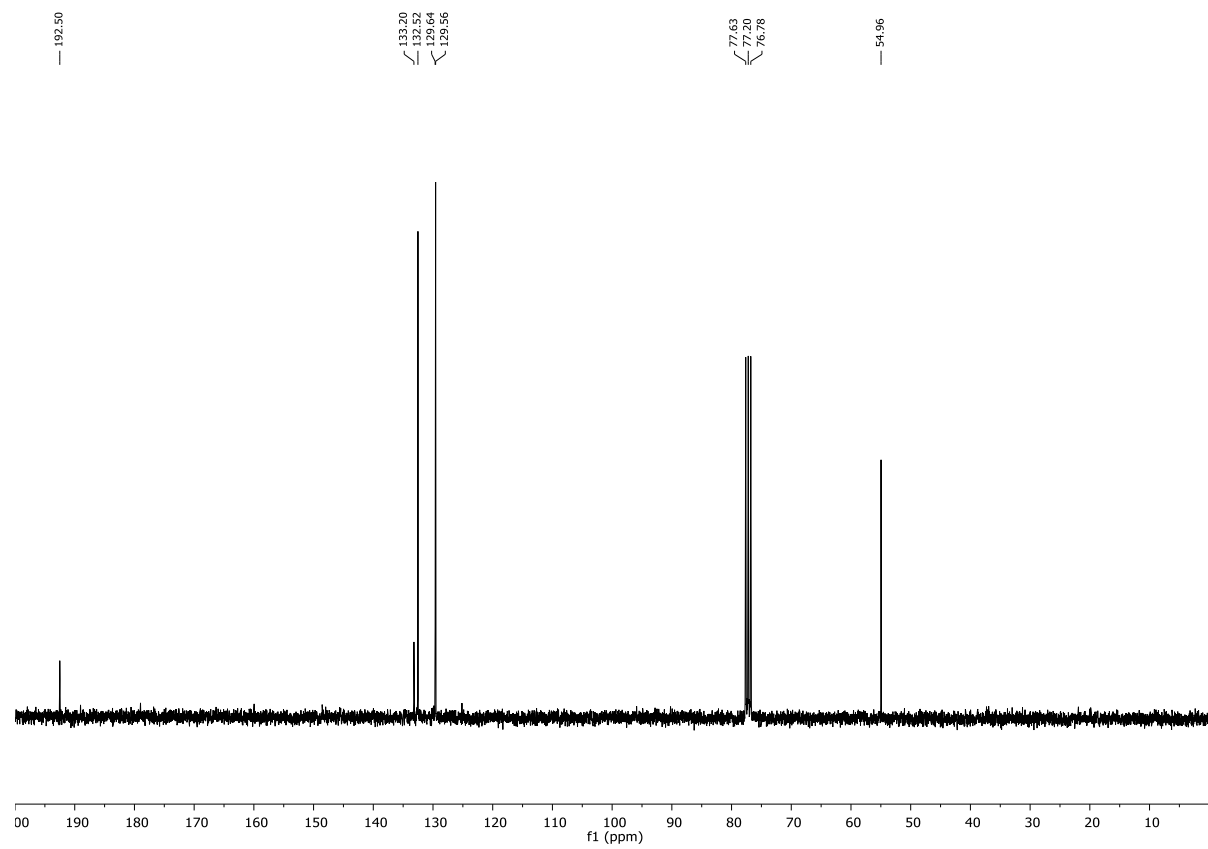
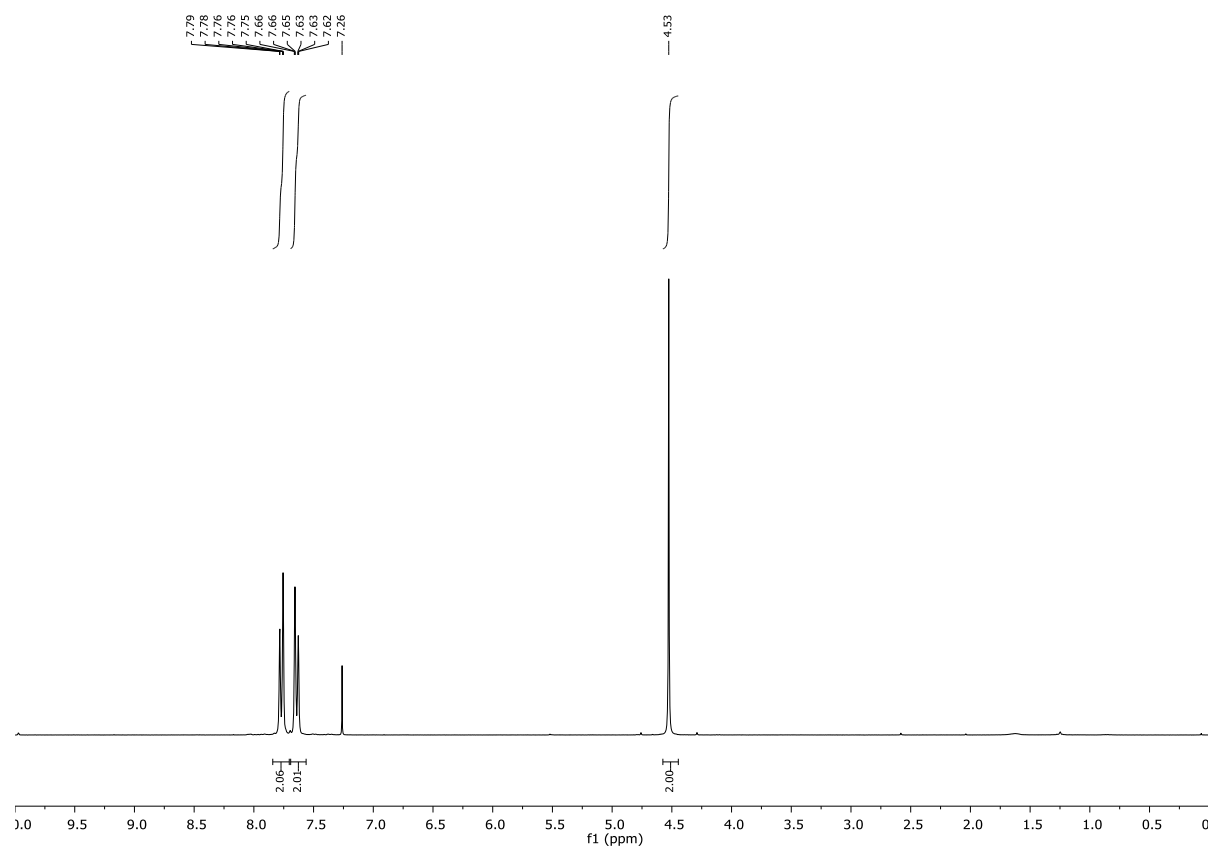
## Chapter 4: Copper(II)-catalyzed Oxo-azidation of Vinylarenes

$^1\text{H}$  and  $^{13}\text{C}$  NMR of **2g**:



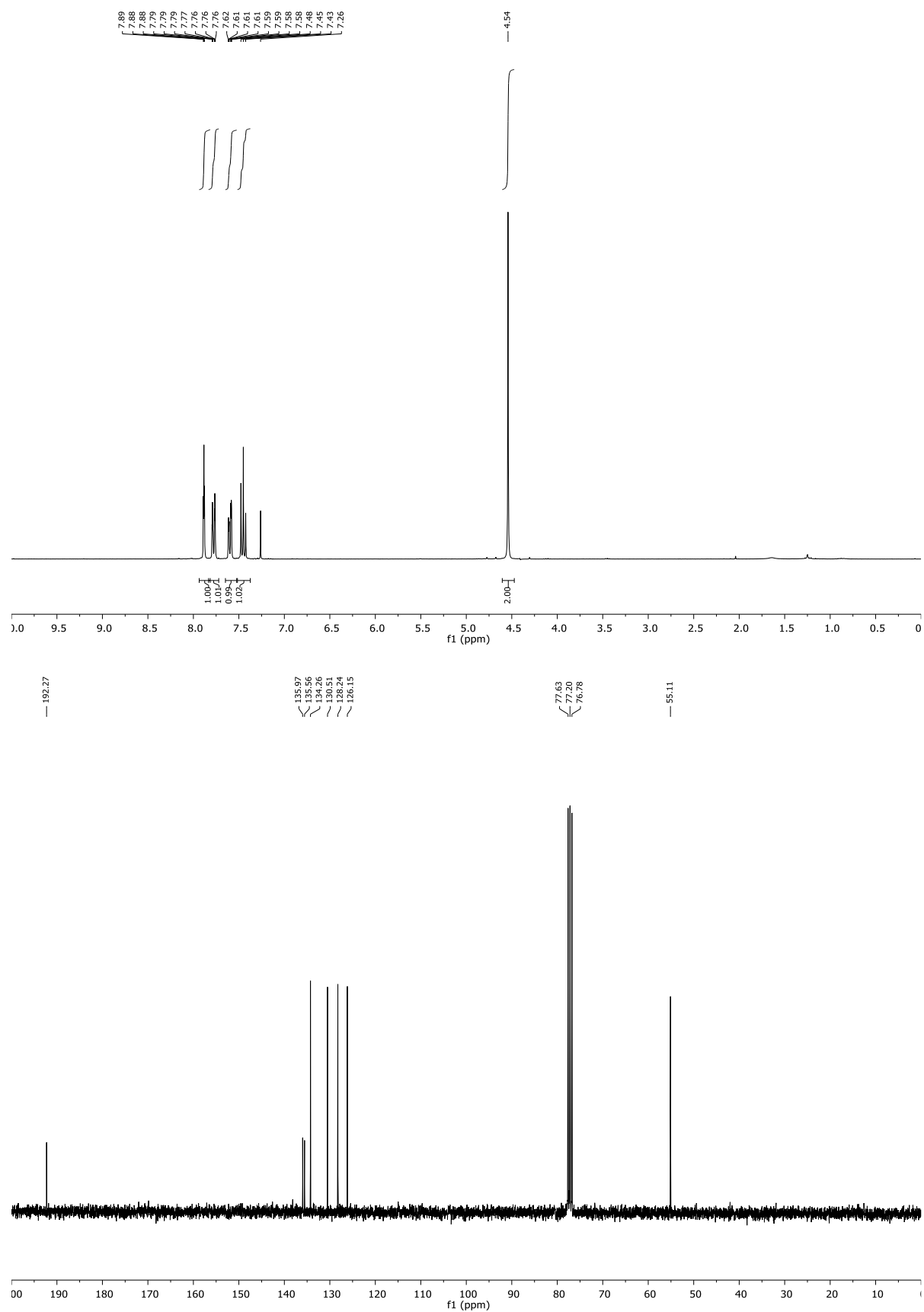
## Chapter 4: Copper(II)-catalyzed Oxo-azidation of Vinylarenes

$^1\text{H}$  and  $^{13}\text{C}$  NMR of **2h**:



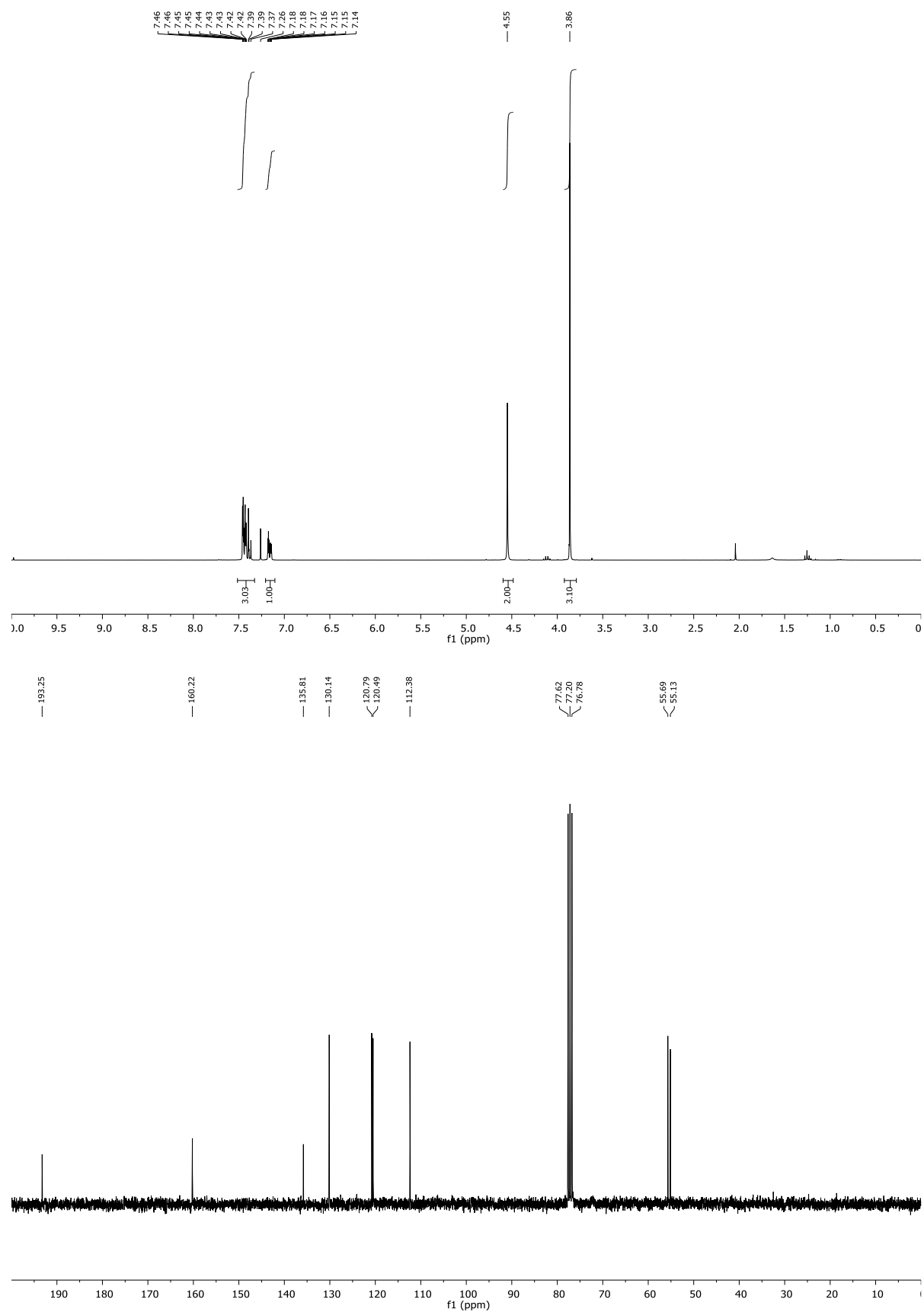
## Chapter 4: Copper(II)-catalyzed Oxo-azidation of Vinylarenes

$^1\text{H}$  and  $^{13}\text{C}$  NMR of **2i**:



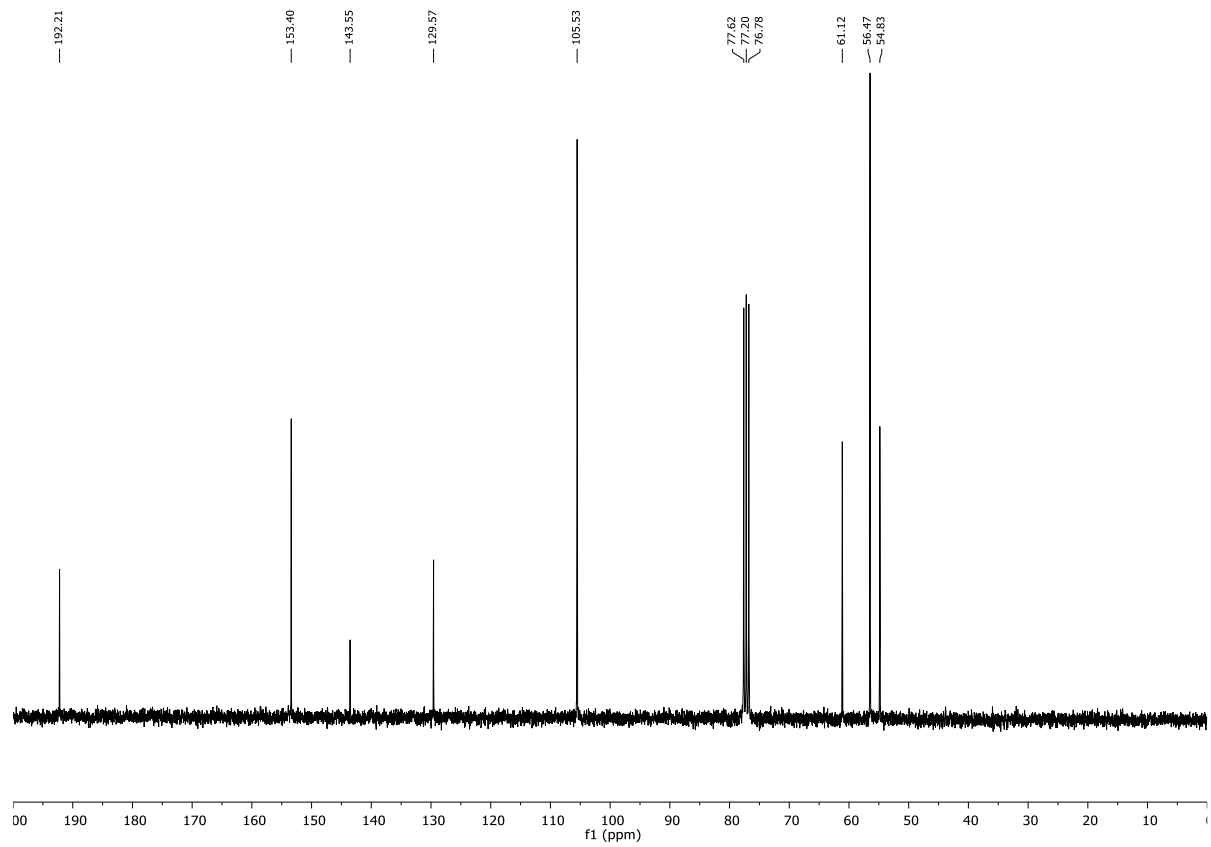
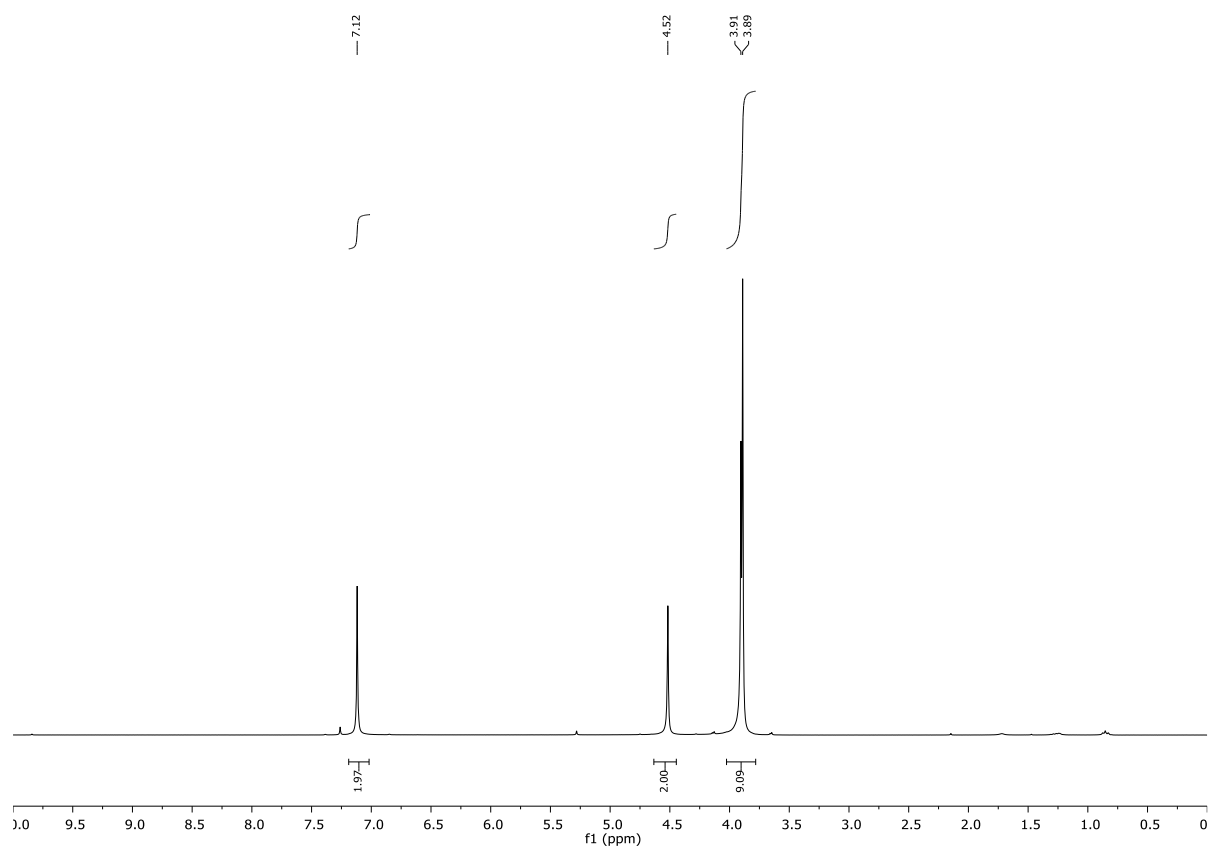
## Chapter 4: Copper(II)-catalyzed Oxo-azidation of Vinylarenes

$^1\text{H}$  and  $^{13}\text{C}$  NMR of **2j**:



## Chapter 4: Copper(II)-catalyzed Oxo-azidation of Vinylarenes

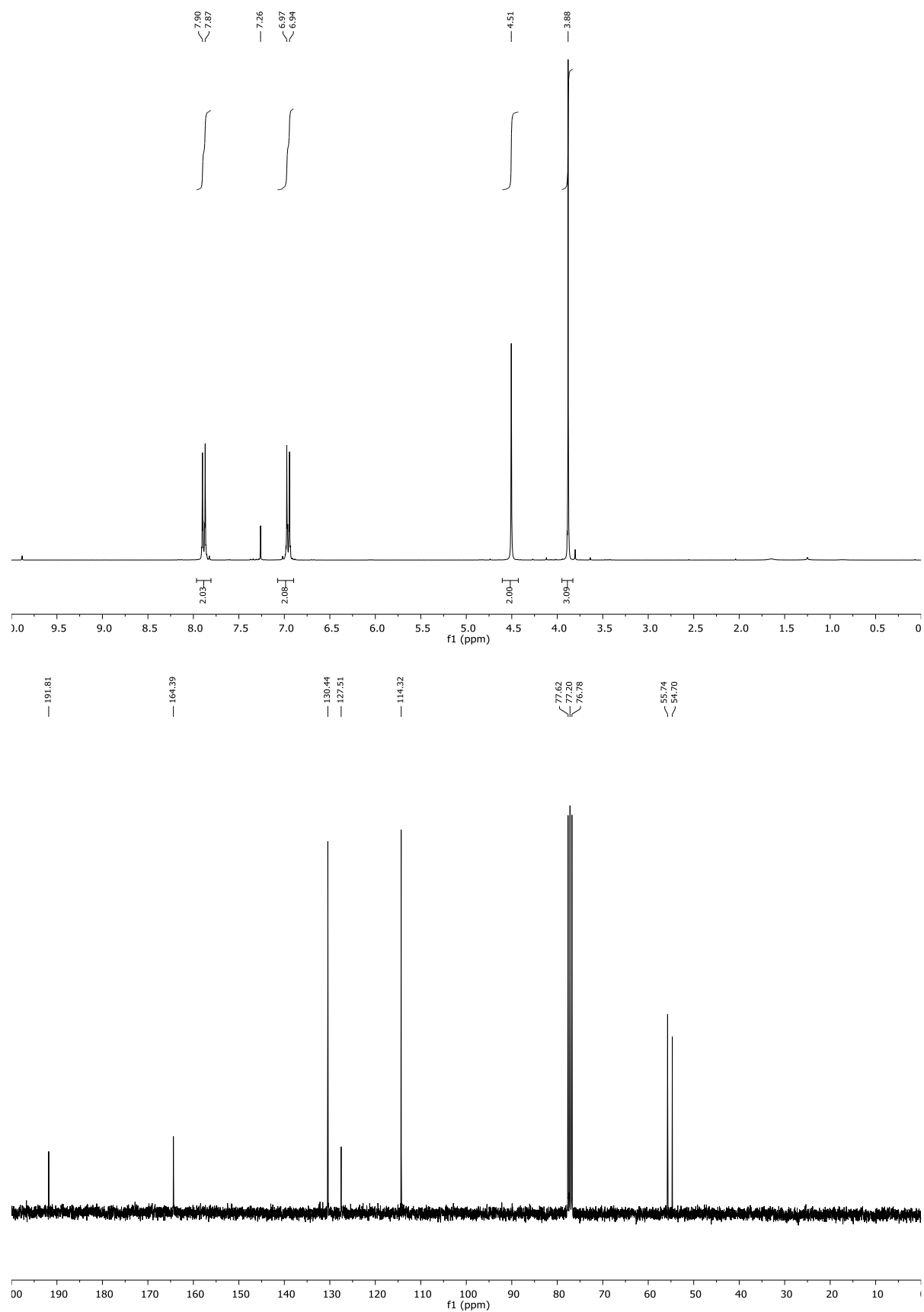
$^1\text{H}$  and  $^{13}\text{C}$  NMR of **2k**:





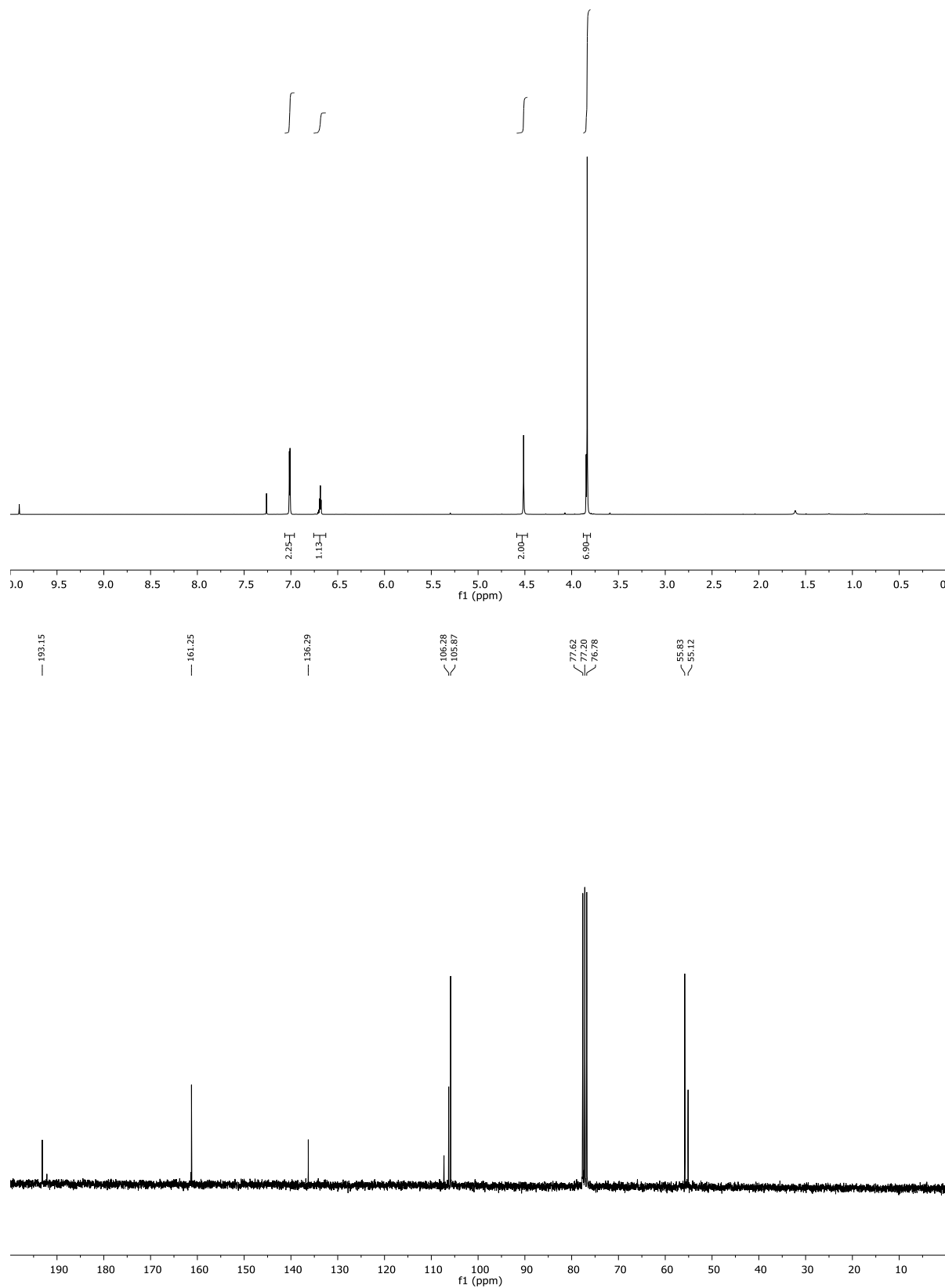
## Chapter 4: Copper(II)-catalyzed Oxo-azidation of Vinylarenes

$^1\text{H}$  and  $^{13}\text{C}$  NMR of **2l**:



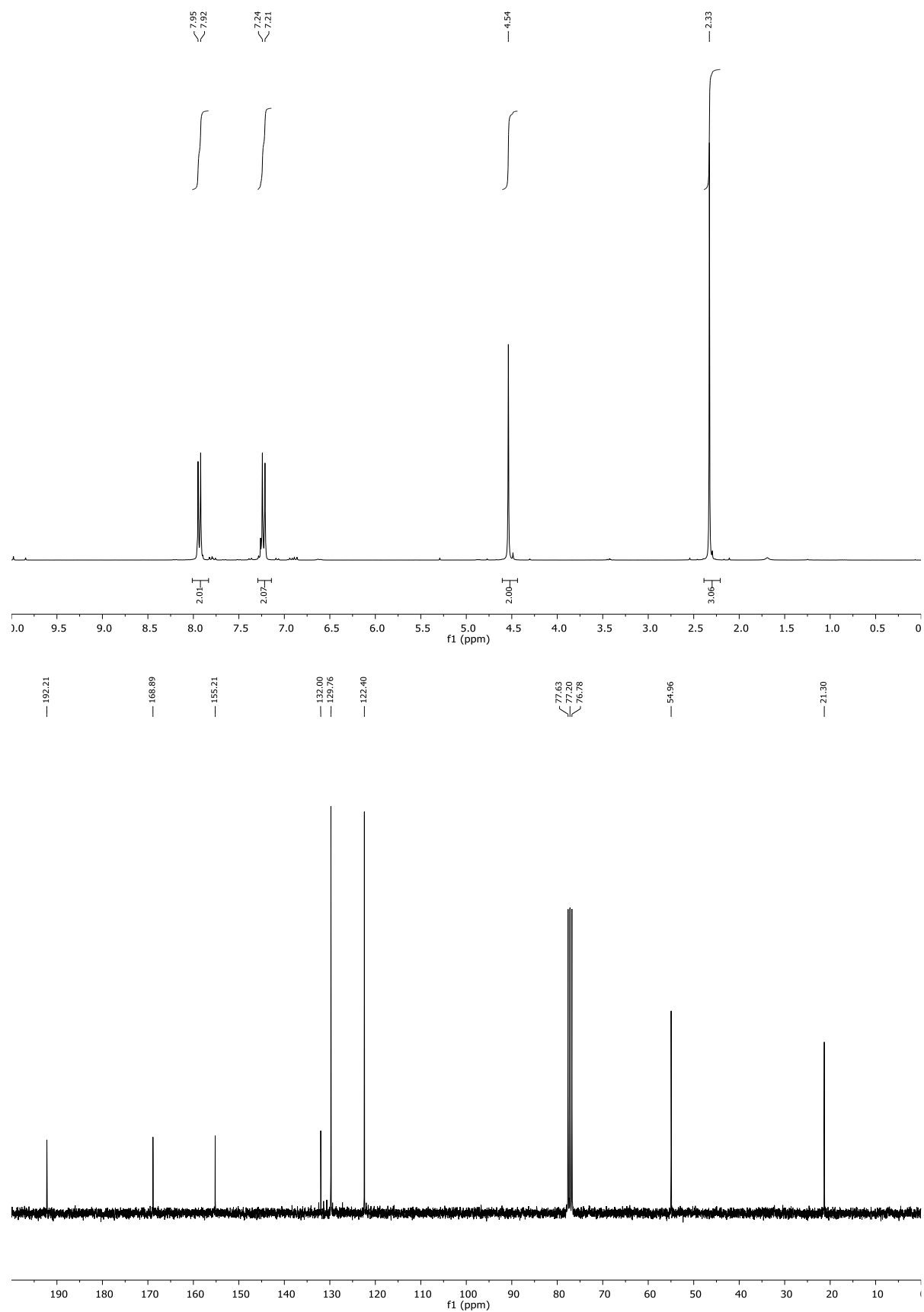
## Chapter 4: Copper(II)-catalyzed Oxo-azidation of Vinylarenes

$^1\text{H}$  and  $^{13}\text{C}$  NMR of **2m**:



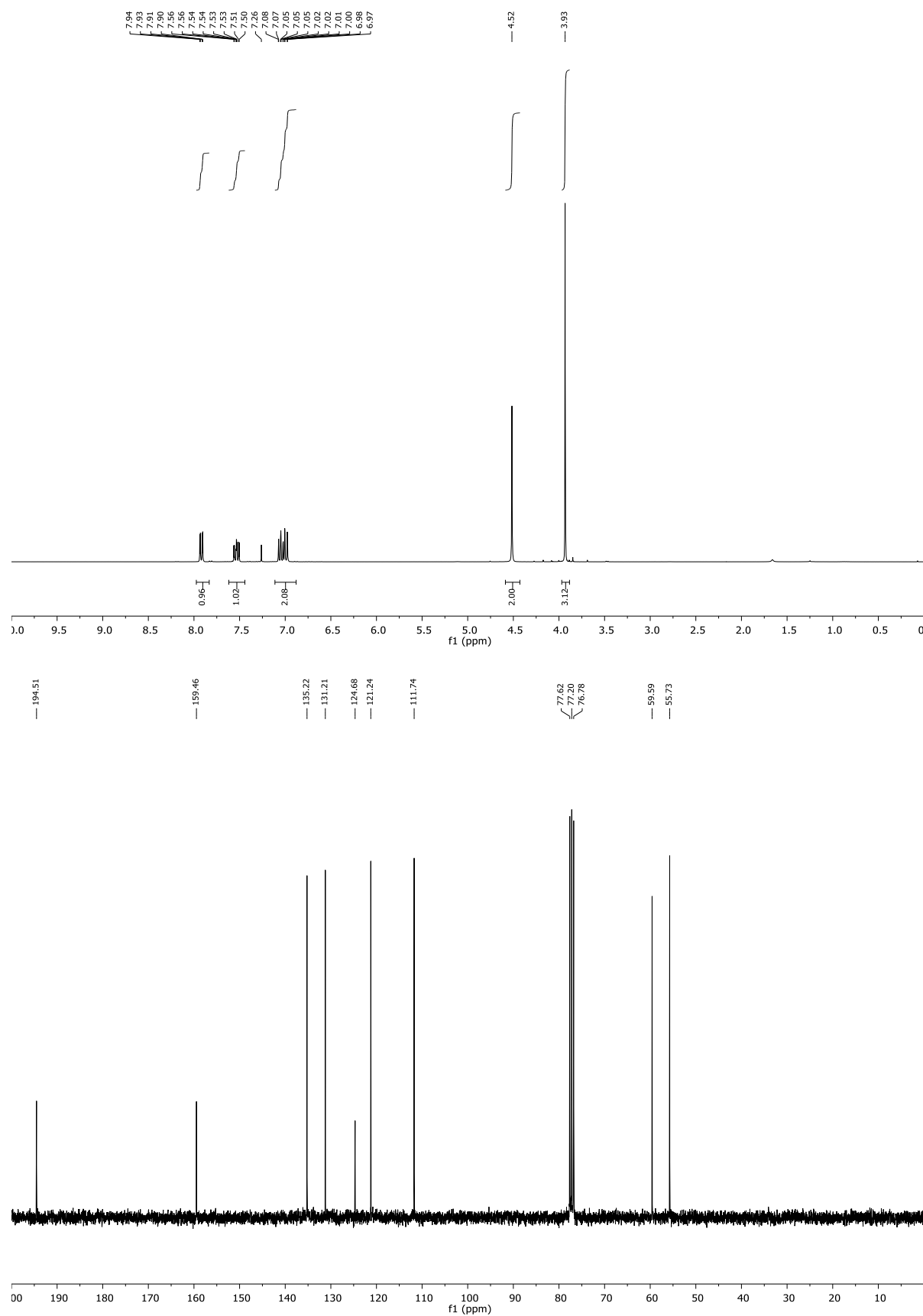
## Chapter 4: Copper(II)-catalyzed Oxo-azidation of Vinylarenes

$^1\text{H}$  and  $^{13}\text{C}$  NMR of **2n**:



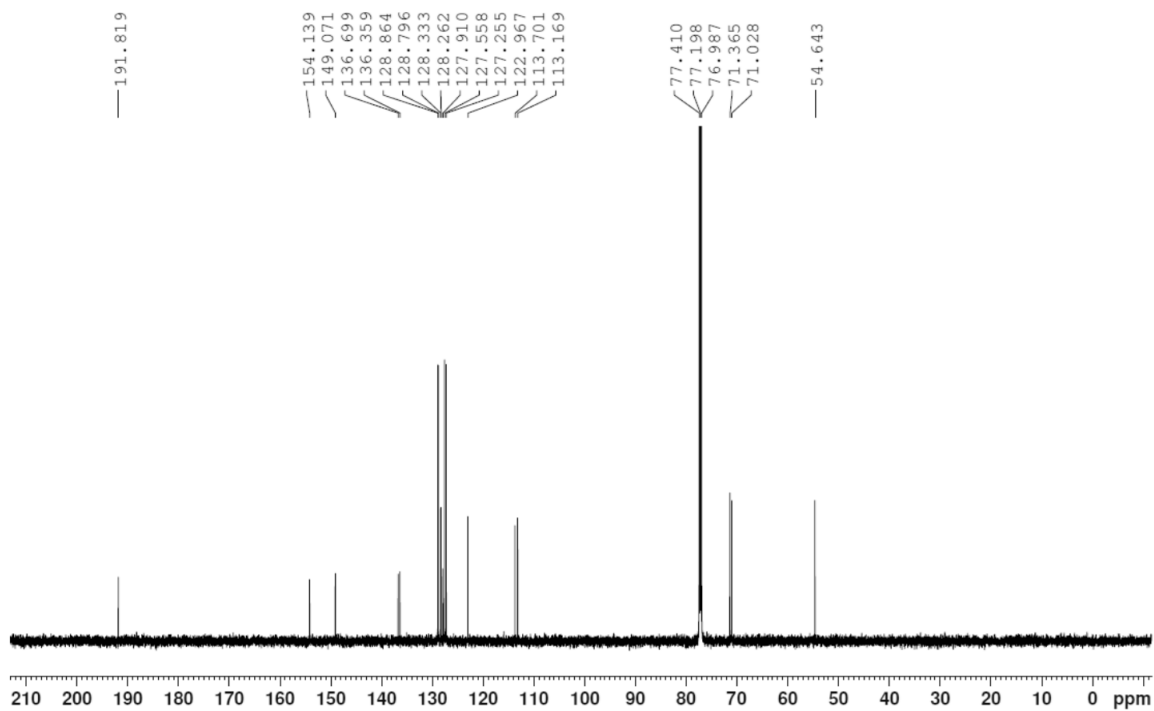
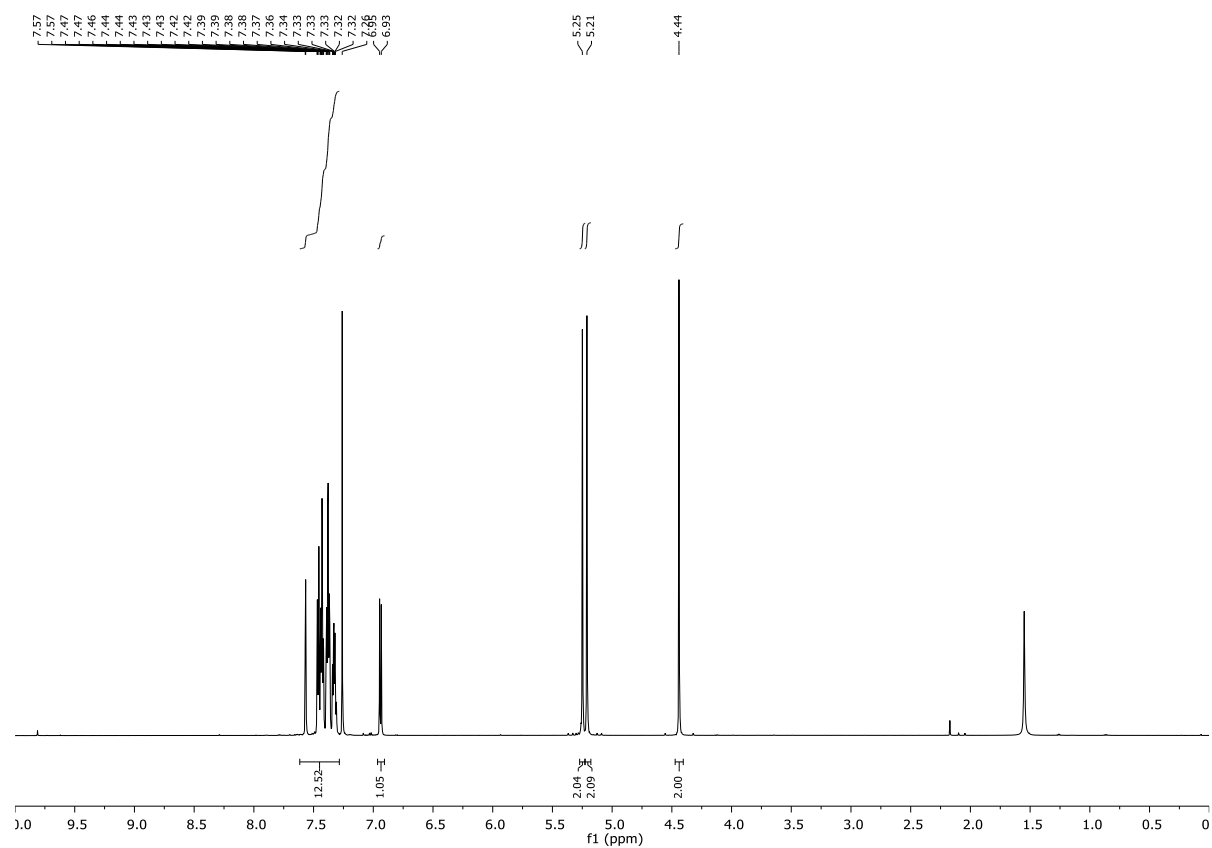
## Chapter 4: Copper(II)-catalyzed Oxo-azidation of Vinylarenes

$^1\text{H}$  and  $^{13}\text{C}$  NMR of **2o**:



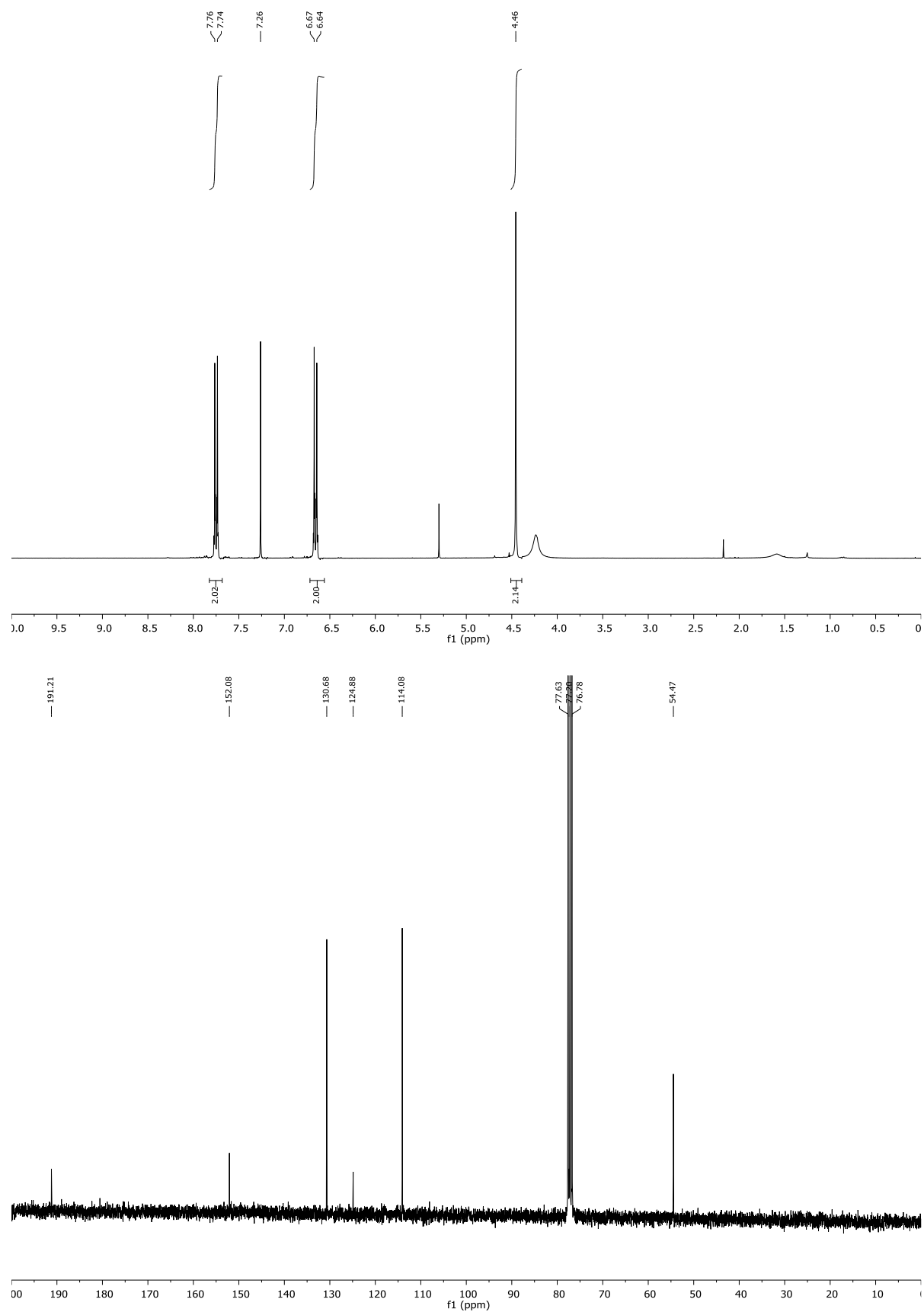
## Chapter 4: Copper(II)-catalyzed Oxo-azidation of Vinylarenes

$^1\text{H}$  and  $^{13}\text{C}$  NMR of **2p**:



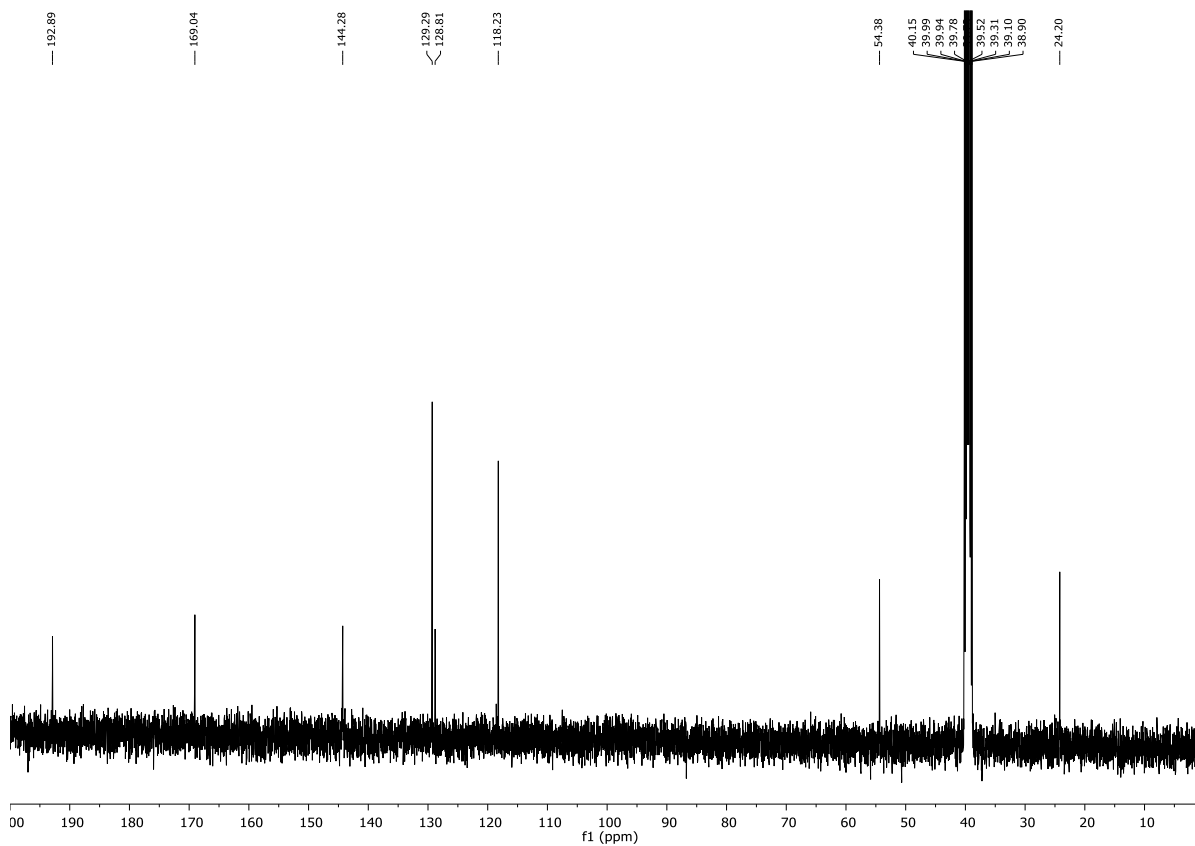
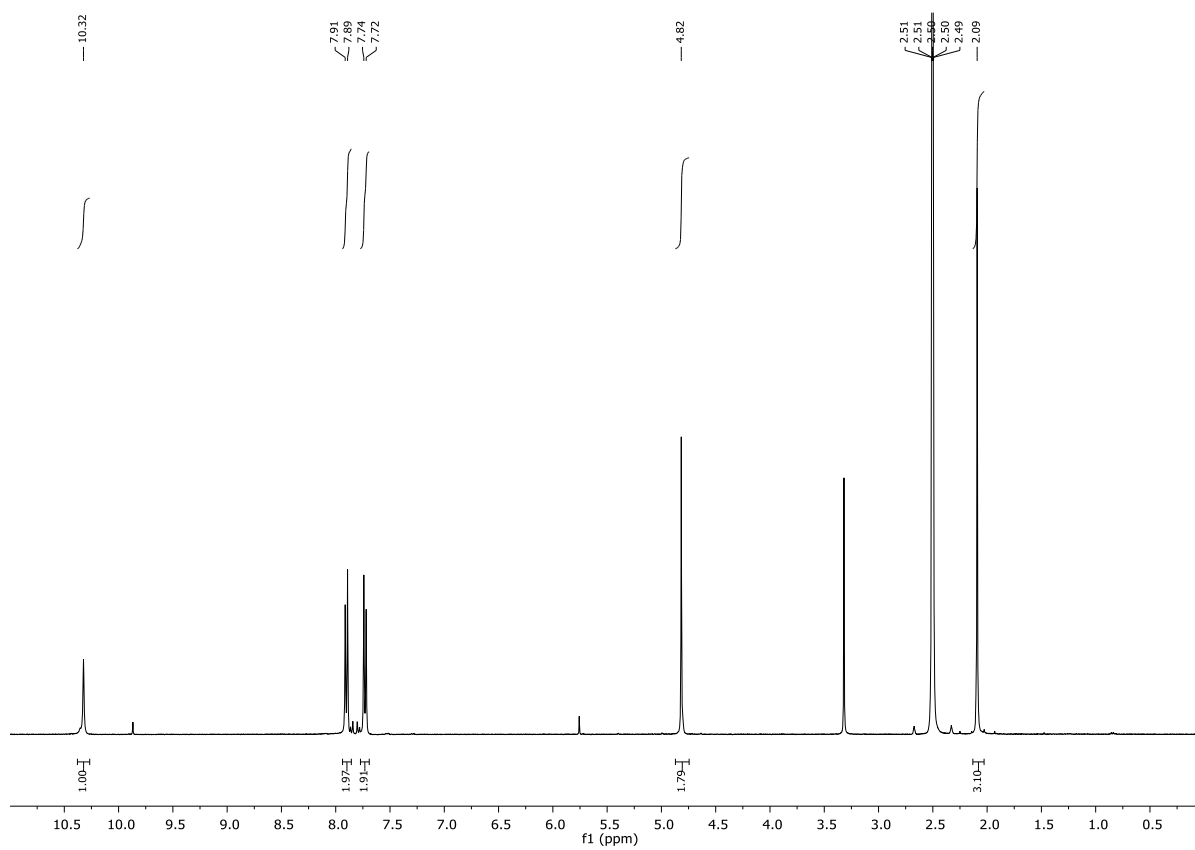
## Chapter 4: Copper(II)-catalyzed Oxo-azidation of Vinylarenes

$^1\text{H}$  and  $^{13}\text{C}$  NMR of **2q**:



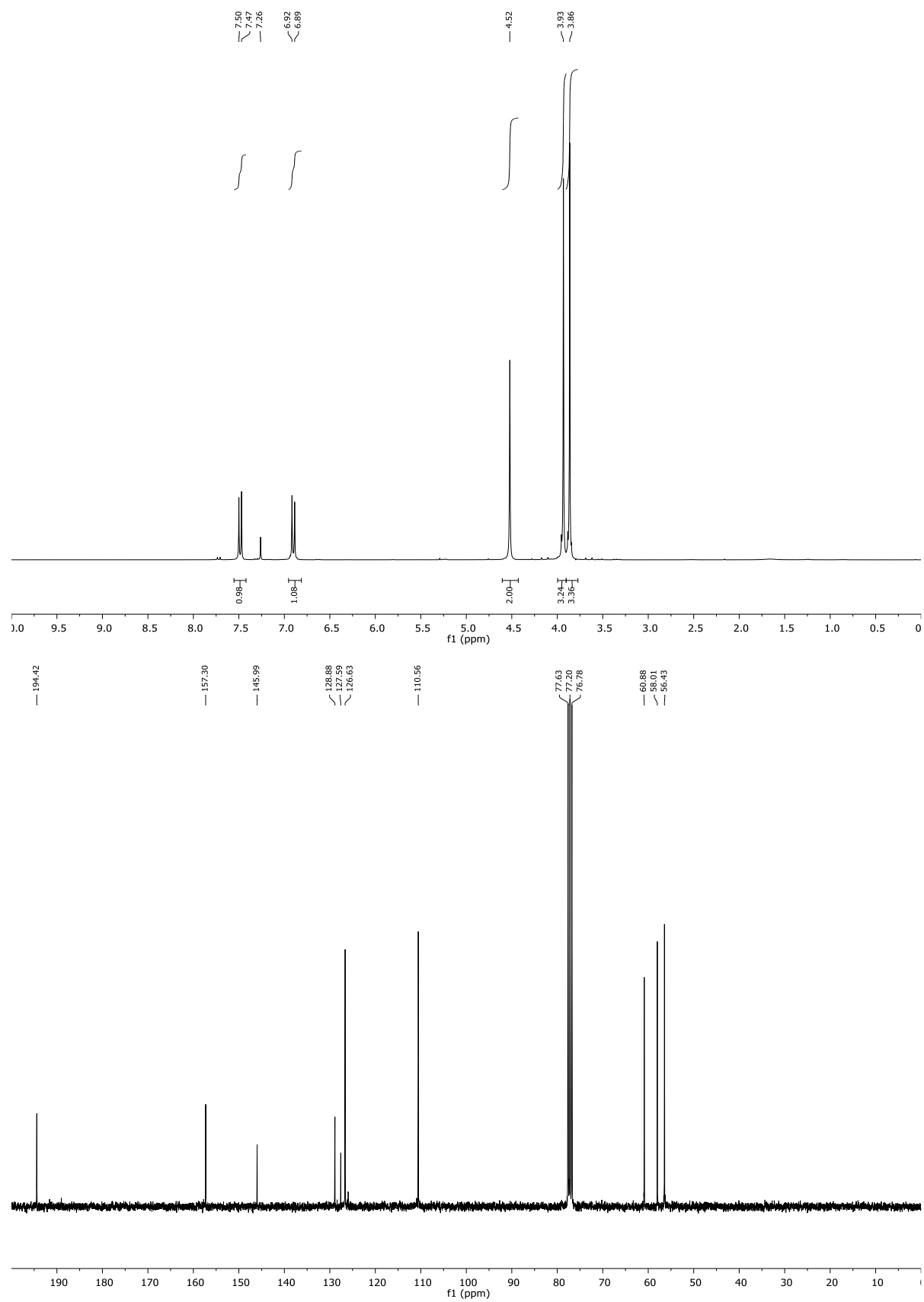
## Chapter 4: Copper(II)-catalyzed Oxo-azidation of Vinylarenes

$^1\text{H}$  and  $^{13}\text{C}$  NMR of **2r**:



## Chapter 4: Copper(II)-catalyzed Oxo-azidation of Vinylarenes

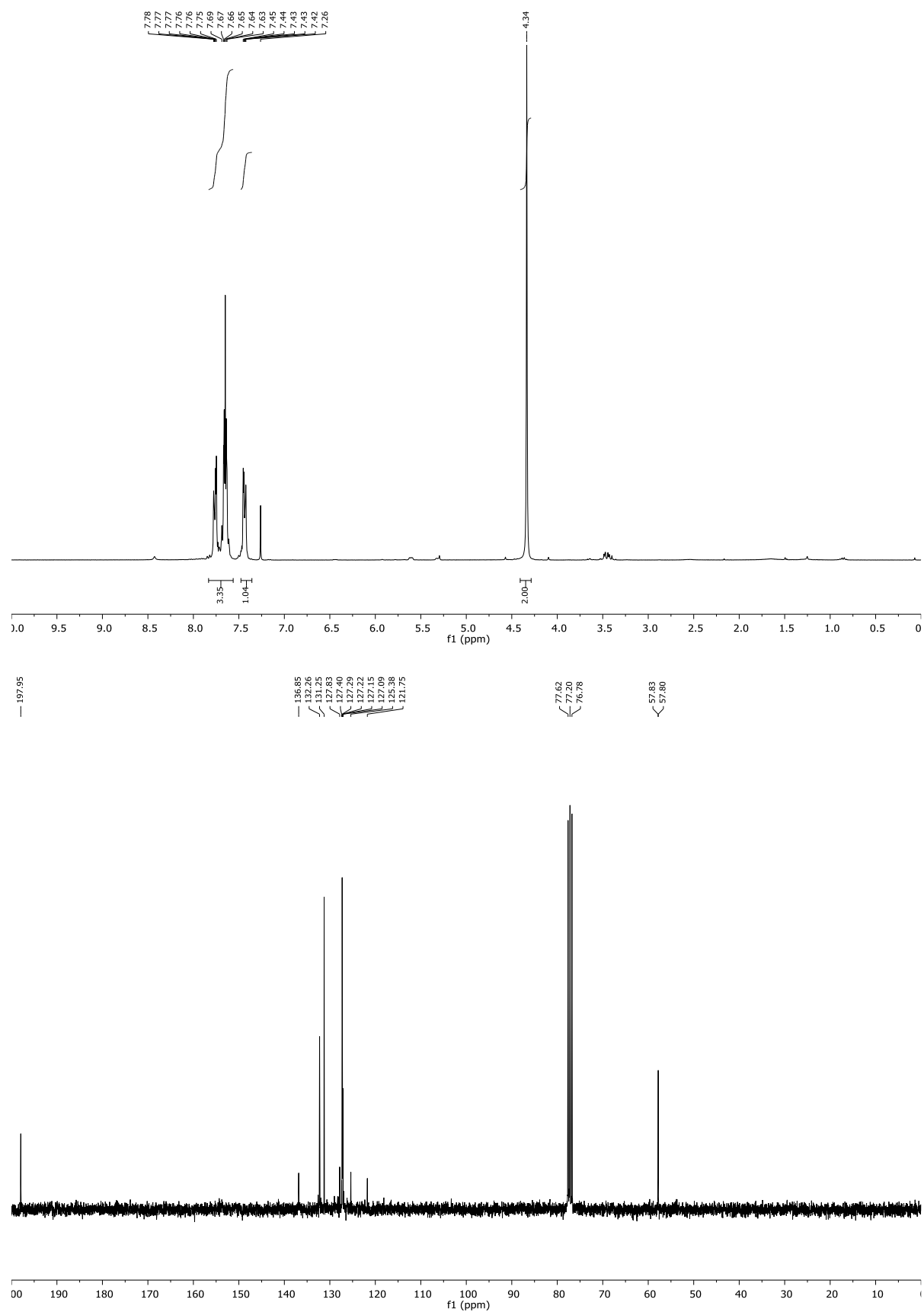
$^1\text{H}$   $^{13}\text{C}$  and  $^{19}\text{F}$  NMR of **2s**:

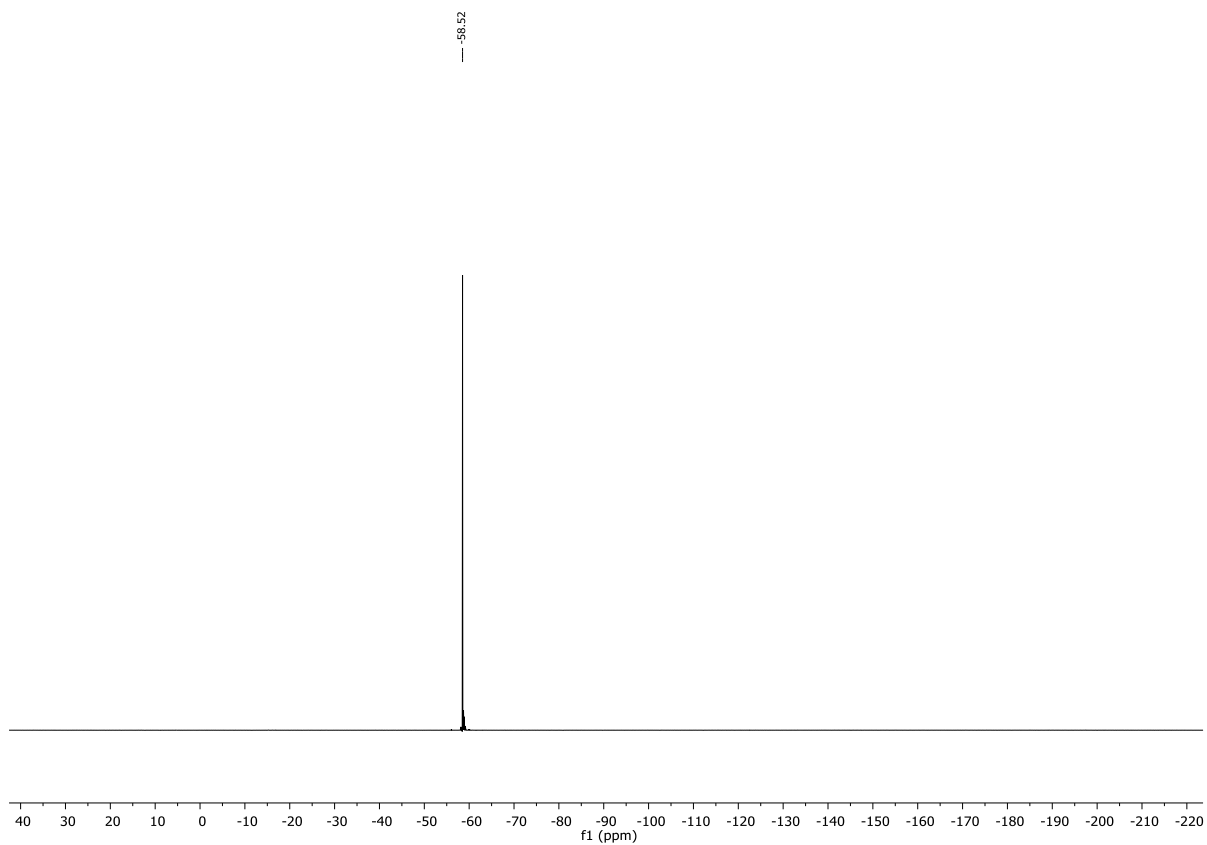




## Chapter 4: Copper(II)-catalyzed Oxo-azidation of Vinylarenes

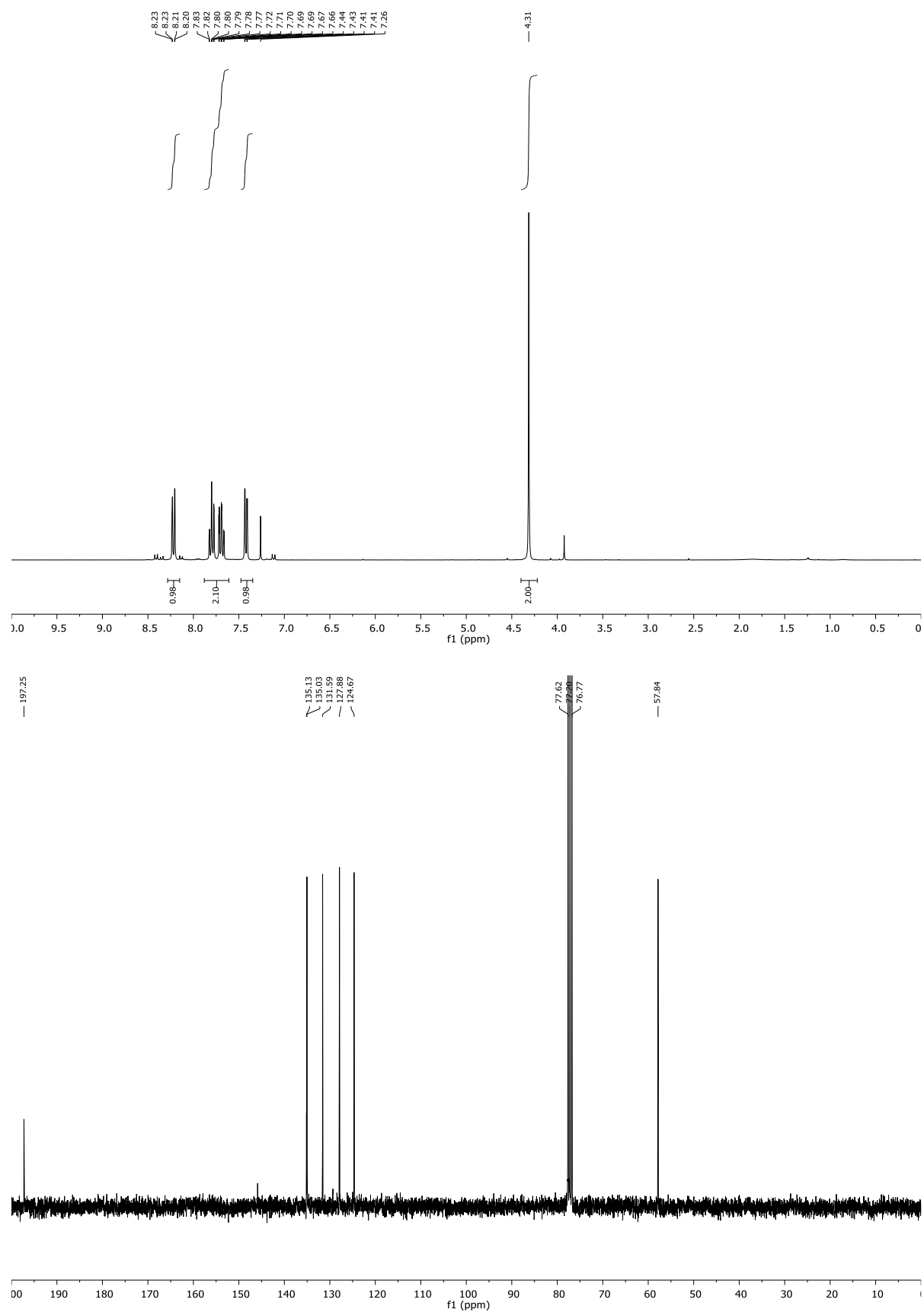
$^1\text{H}$  and  $^{13}\text{C}$  NMR of **2t**:





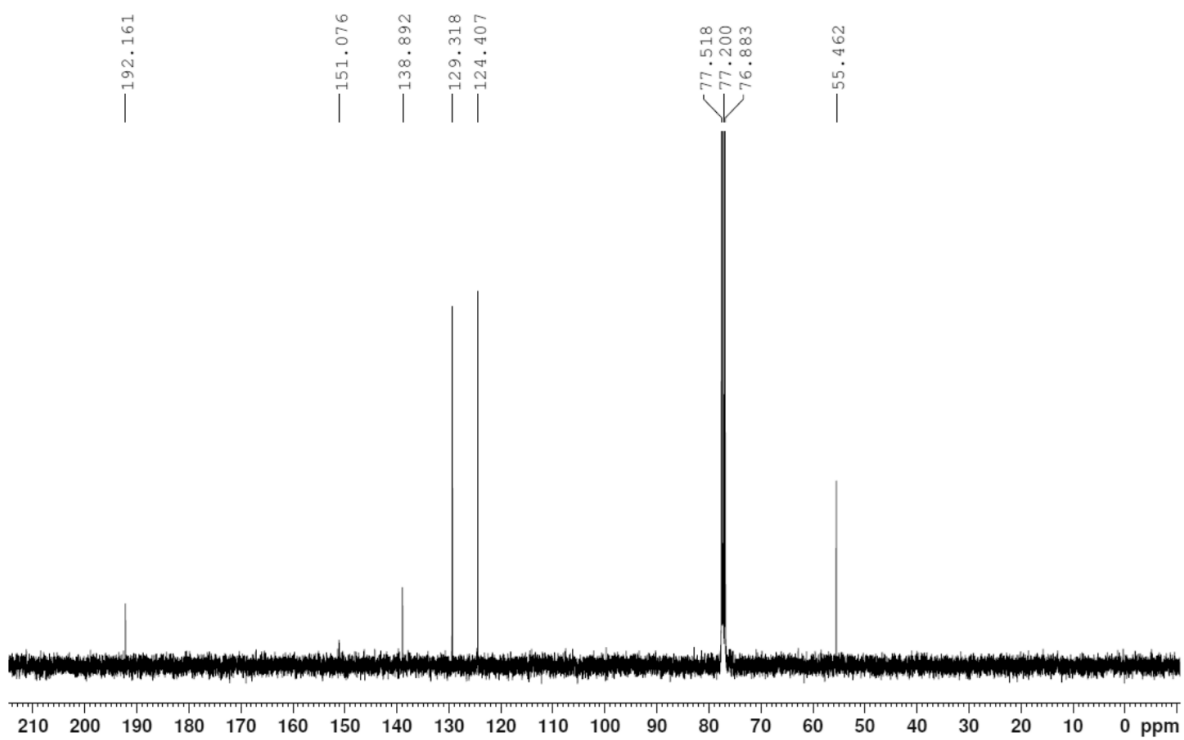
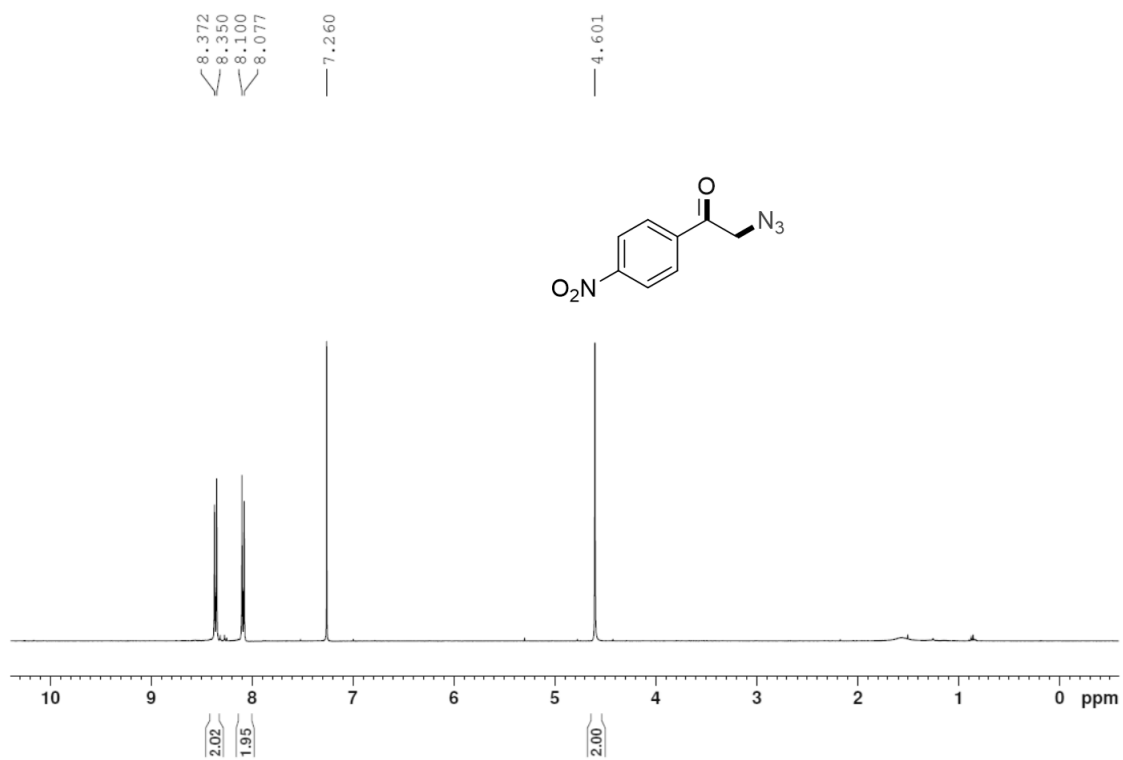
## Chapter 4: Copper(II)-catalyzed Oxo-azidation of Vinylarenes

$^1\text{H}$  and  $^{13}\text{C}$  NMR of **2u**:



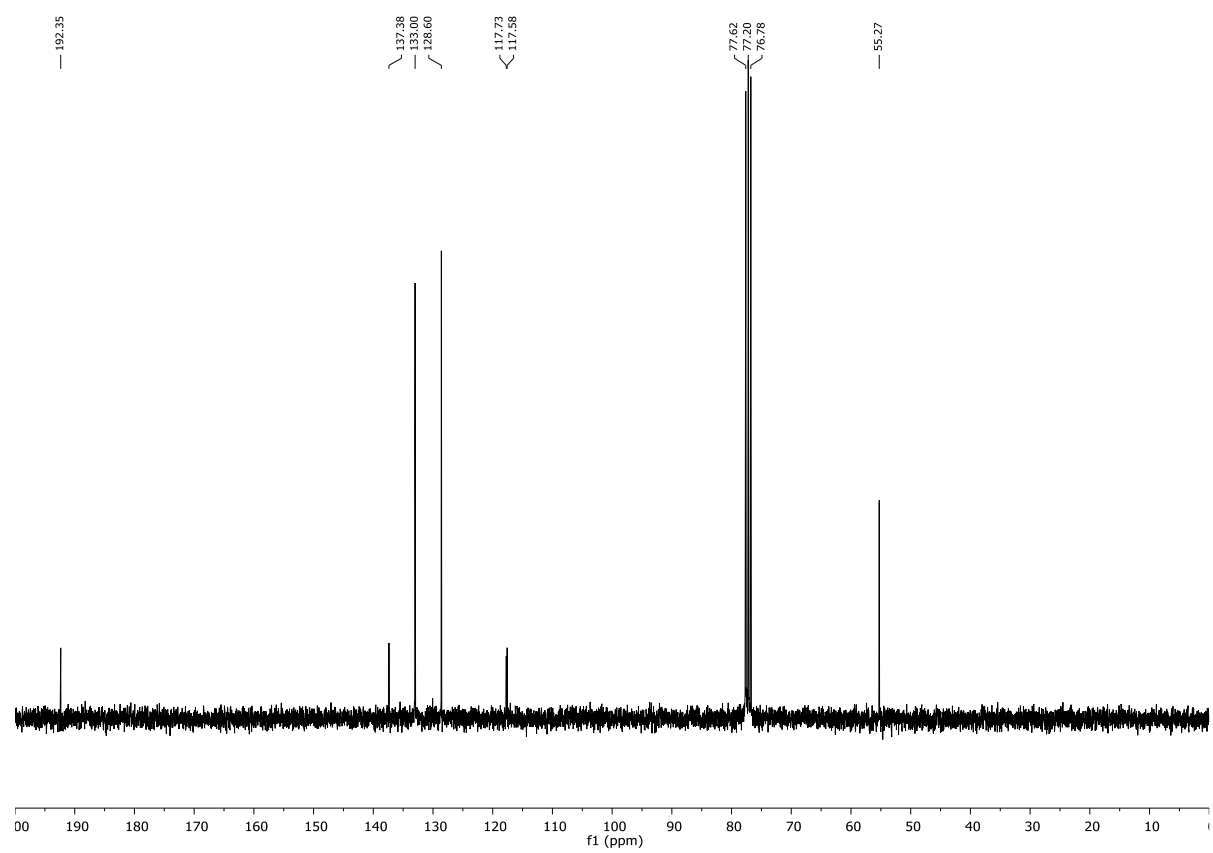
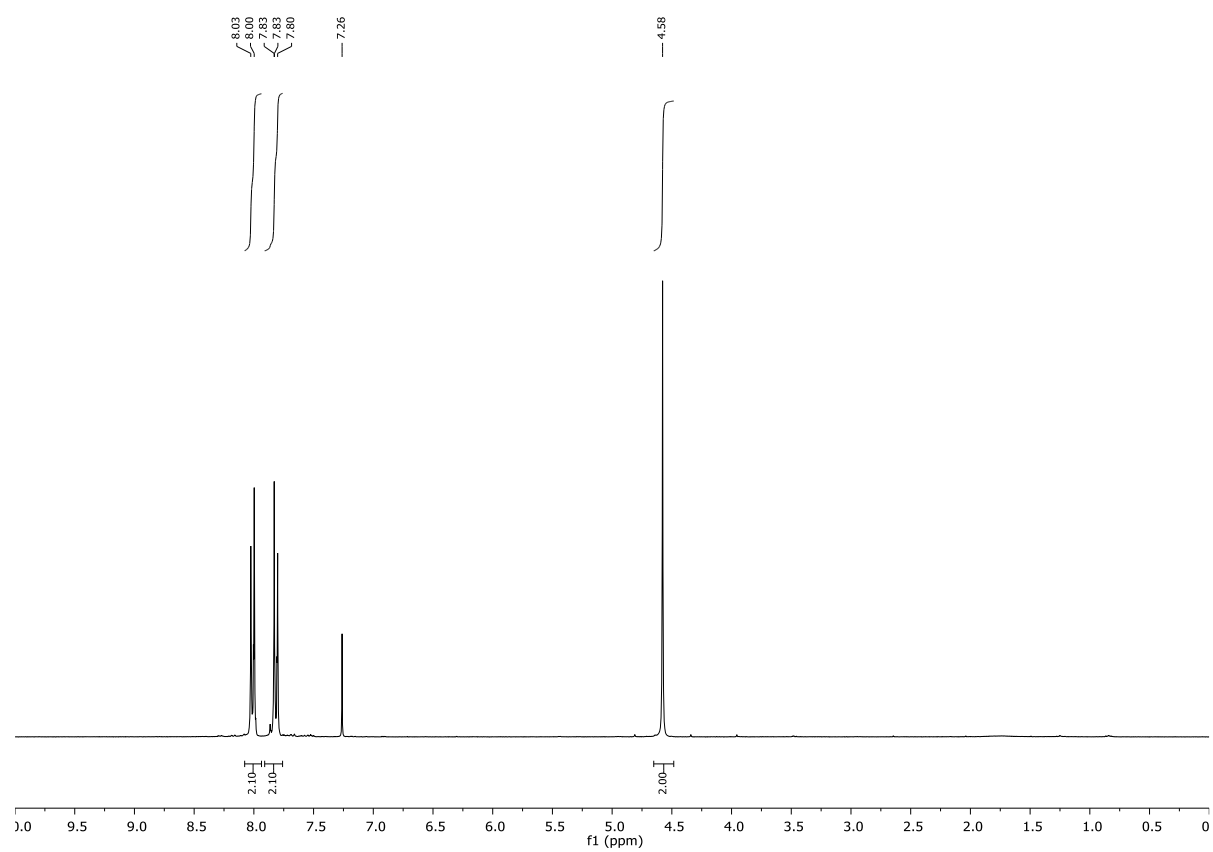
## Chapter 4: Copper(II)-catalyzed Oxo-azidation of Vinylarenes

$^1\text{H}$  and  $^{13}\text{C}$  NMR of **2v**:



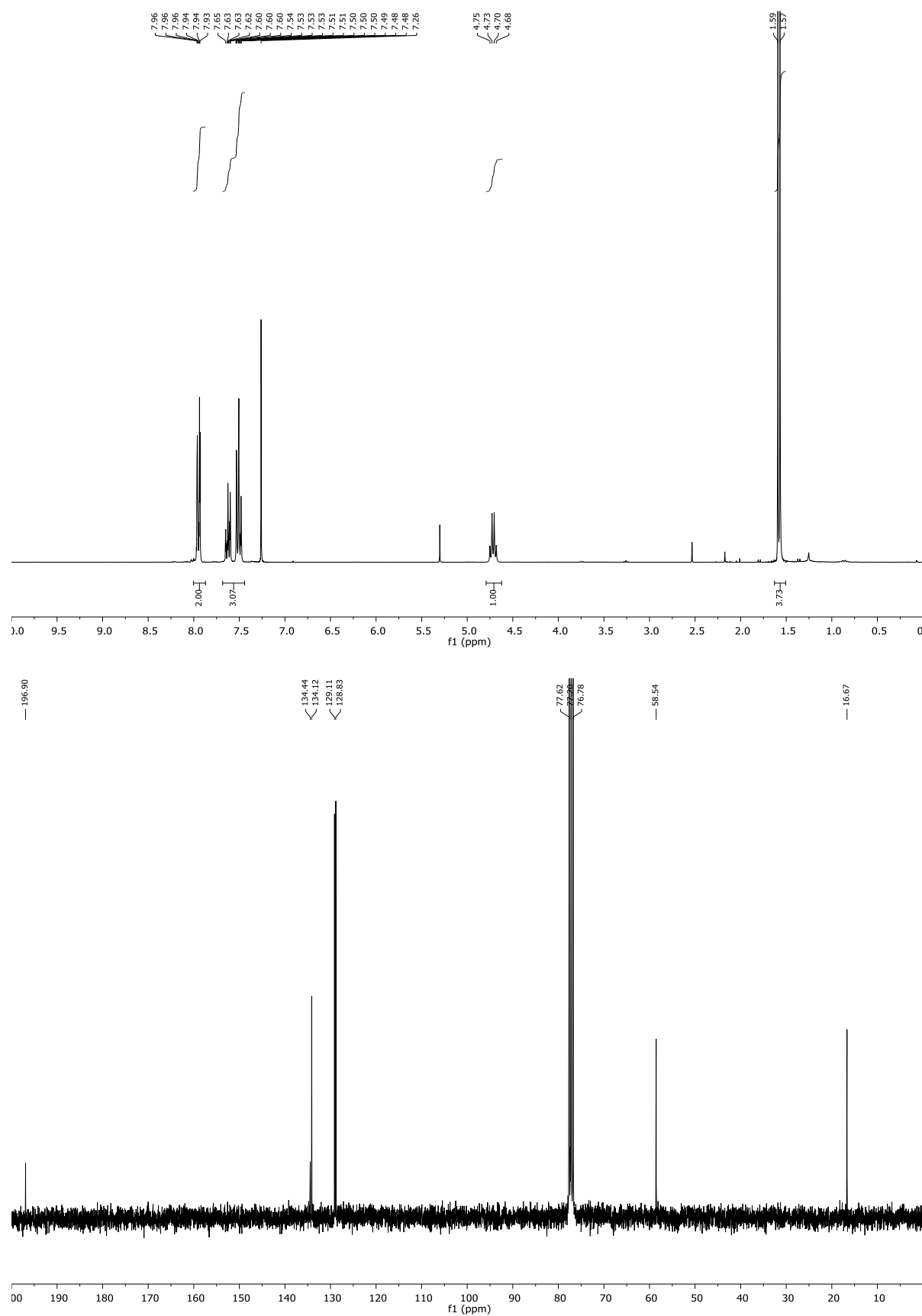
## Chapter 4: Copper(II)-catalyzed Oxo-azidation of Vinylarenes

$^1\text{H}$  and  $^{13}\text{C}$  NMR of **2x**:



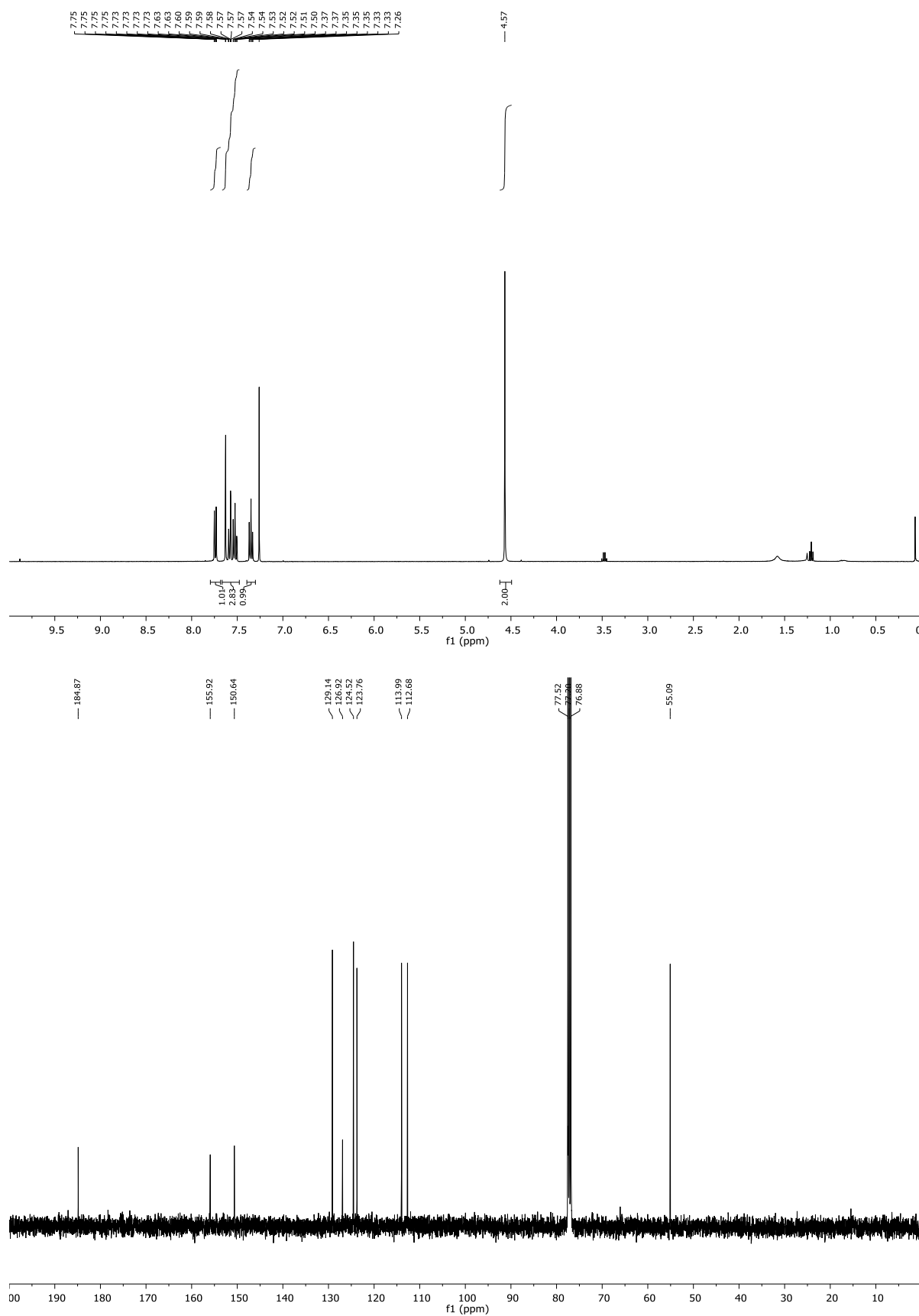
## Chapter 4: Copper(II)-catalyzed Oxo-azidation of Vinylarenes

$^1\text{H}$  and  $^{13}\text{C}$  NMR of **2y**:



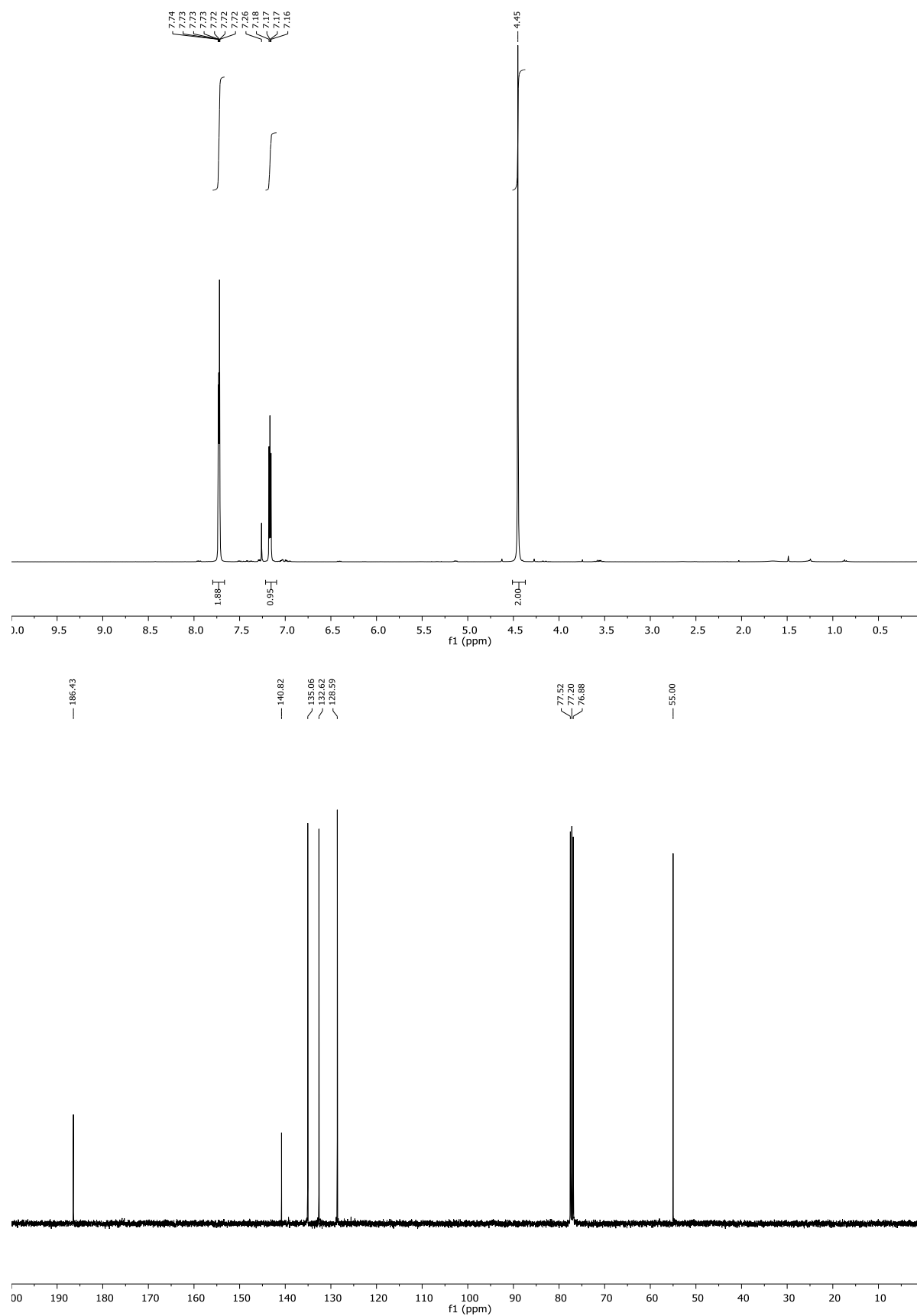
## Chapter 4: Copper(II)-catalyzed Oxo-azidation of Vinylarenes

$^1\text{H}$  and  $^{13}\text{C}$  NMR of **2z**:



## Chapter 4: Copper(II)-catalyzed Oxo-azidation of Vinylarenes

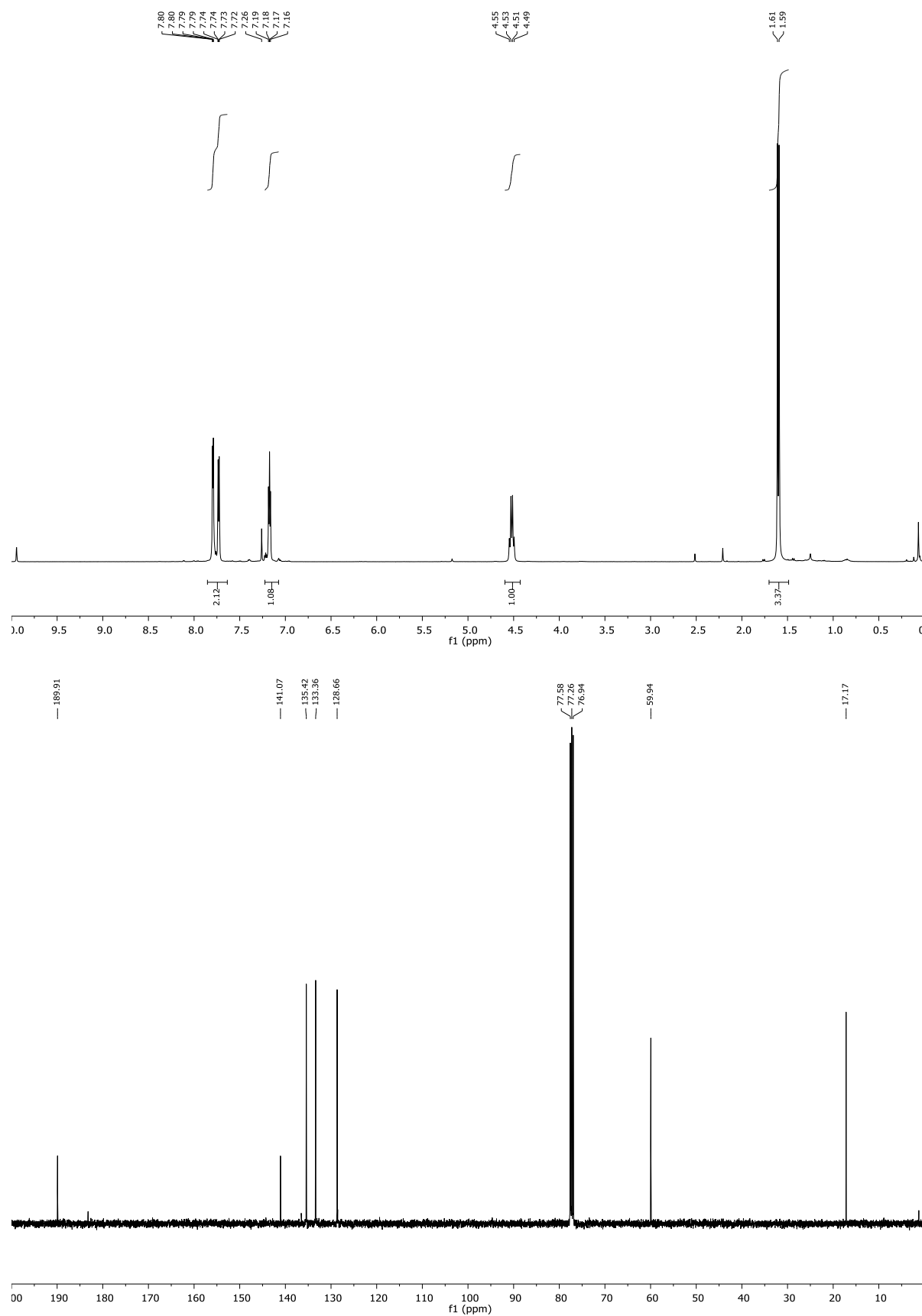
$^1\text{H}$  and  $^{13}\text{C}$  NMR of **2aa**:





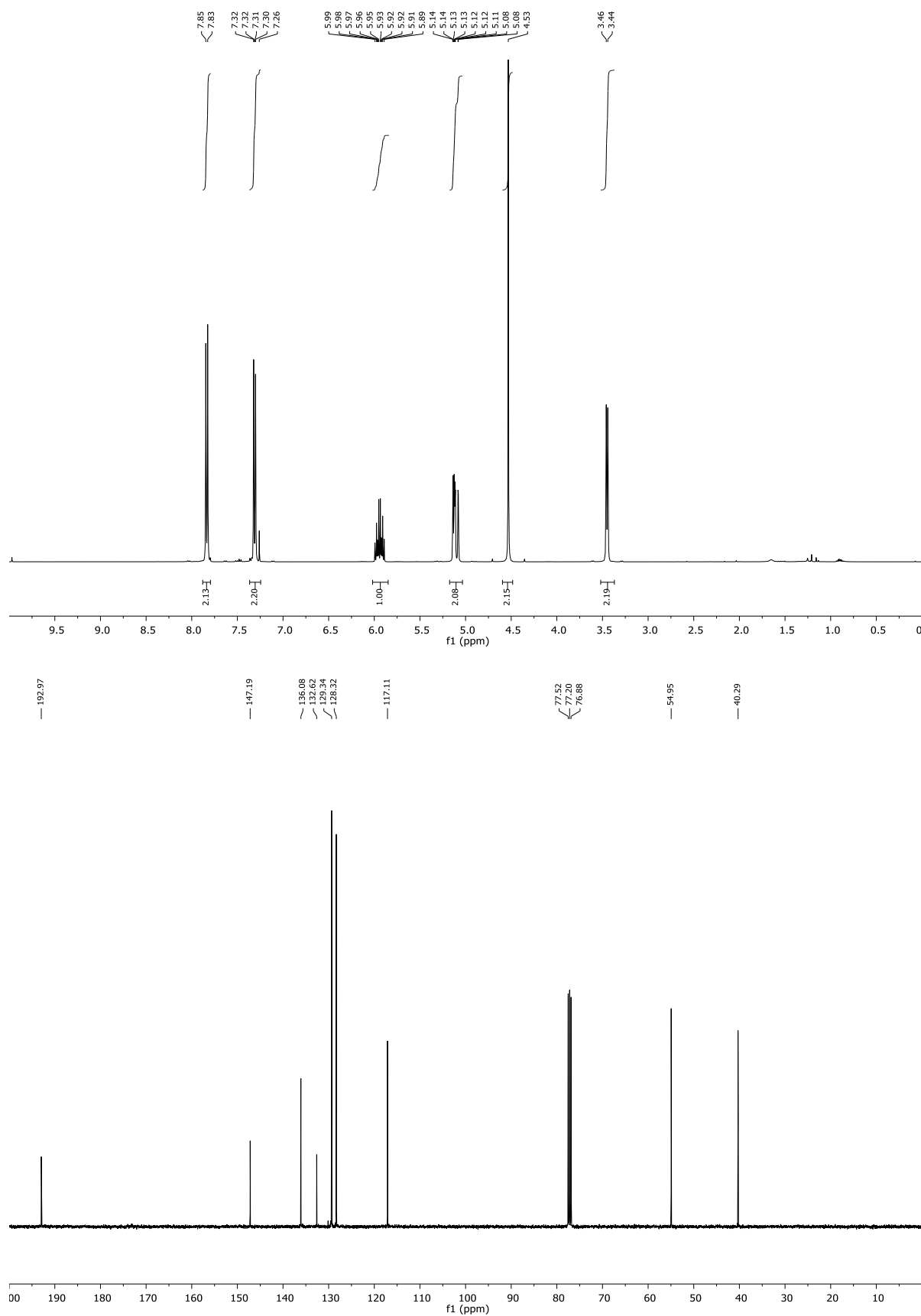
## Chapter 4: Copper(II)-catalyzed Oxo-azidation of Vinylarenes

$^1\text{H}$  and  $^{13}\text{C}$  NMR of **2ab**:



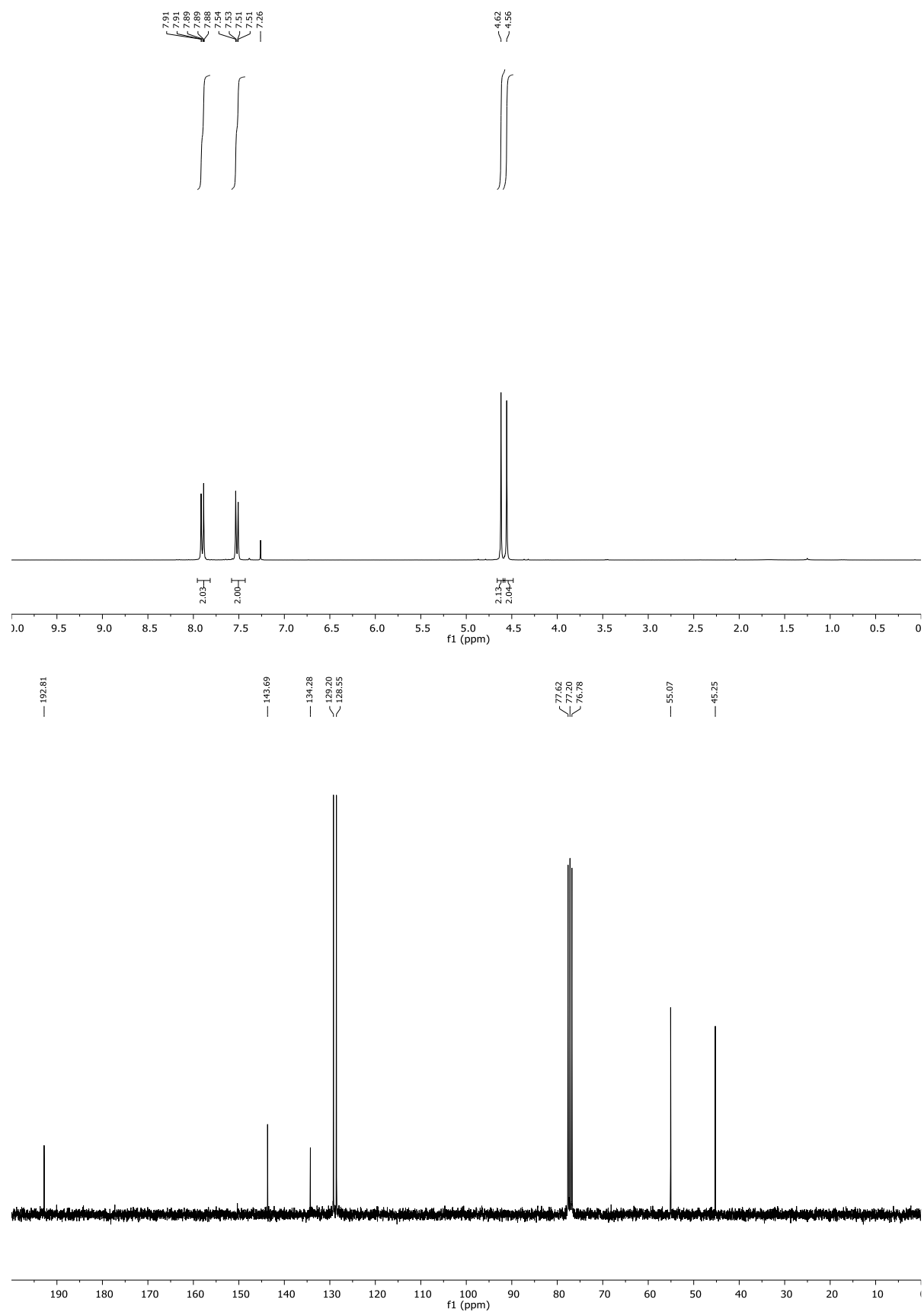
## Chapter 4: Copper(II)-catalyzed Oxo-azidation of Vinylarenes

$^1\text{H}$  and  $^{13}\text{C}$  NMR of **2ad**:

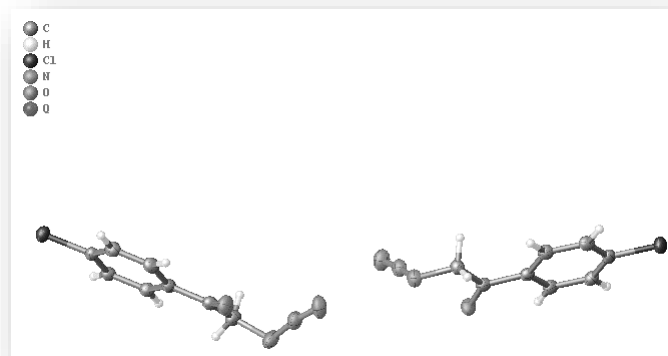


## Chapter 4: Copper(II)-catalyzed Oxo-azidation of Vinylarenes

$^1\text{H}$  and  $^{13}\text{C}$  NMR of **2ae**:



Crystal data:



**Experimental.** Single clear colorless plate-shaped crystals of compound **2q** were obtained by recrystallization from dichloromethane. A suitable crystal (0.16×0.10×0.02) was selected and mounted on a MITIGEN holder oil on a SuperNova, Single source at offset, Atlas diffractometer. The crystal was kept at  $T = 122.98(10)$  K during data collection. Using **Olex2** (Dolomanov et al., 2009), the structure was solved with the **ShelXT** (Sheldrick, 2015) structure solution program, using the Intrinsic Phasing solution method. The model was refined with ShelXL (Sheldrick, 2015) using Least Squares minimisation.

**Crystal Data.**  $C_8H_6ClN_3O$ ,  $M_r = 195.61$ , triclinic, P-1 (No. 2),  $a = 3.8012(3)$  Å,  $b = 13.0808(5)$  Å,  $c = 17.3898(9)$  Å,  $\alpha = 80.022(4)^\circ$ ,  $\beta = 84.470(5)^\circ$ ,  $\gamma = 86.690(5)^\circ$ ,  $V = 846.89(9)$  Å<sup>3</sup>,  $T = 122.98(10)$  K,  $Z = 4$ ,  $Z' = 2$ ,  $\mu(\text{CuK}\alpha) = 3.678$ , 17639 reflections measured, 3528 unique ( $R_{int} = 0.0838$ ) which were used in all calculations. The final  $wR_2$  was 0.1120 (all data) and  $R_1$  was 0.0433 ( $I > 2(I)$ ).

<b>Compound</b>	<b>2g</b>
Formula	C <sub>8</sub> H <sub>6</sub> ClN <sub>3</sub> O
$D_{calc.}/\text{g cm}^{-3}$	1.534
$\mu/\text{mm}^{-1}$	3.678
Formula Weight	195.61
Colour	clear colourless
Shape	plate
Max Size/mm	0.16
Mid Size/mm	0.10
Min Size/mm	0.02
$T/\text{K}$	122.98(10)
Crystal System	triclinic
Space Group	P-1
$a/\text{\AA}$	3.8012(3)
$b/\text{\AA}$	13.0808(5)
$c/\text{\AA}$	17.3898(9)
$\alpha^\circ$	80.022(4)
$\beta^\circ$	84.470(5)
$\gamma^\circ$	86.690(5)

$V/\text{\AA}^3$	846.89(9)
$Z$	4
$Z'$	2
$\theta_{min}/^\circ$	3.434
$\theta_{max}/^\circ$	76.748
Measured Refl.	17639
Independent Refl.	3528
Reflections Used	2811
$R_{int}$	0.0838
Parameters	235
Restraints	0
Largest Peak	0.366
Deepest Hole	-0.359
GooF	1.075
$wR_2$ (all data)	0.1120
$wR_2$	0.0998
$R_1$ (all data)	0.0594
$R_1$	0.0433

### Structure Quality Indicators

<b>Reflections:</b>	d min (Cu) 0.79	$I/\sigma$ 9.4	Rint 8.38%	complete at $2\theta=144^\circ$ 99%
<b>Refinement:</b>	Shift -0.001	Max Peak 0.4	Min Peak -0.4	GooF 1.075

A clear colourless plate-shaped crystal with dimensions 0.16×0.10×0.02 was mounted on a MITIGEN holder oil. Data were collected using a SuperNova, Single source at offset, Atlas diffractometer equipped with an Oxford Cryosystems CryoStream 700 low-temperature apparatus operating at  $T = 122.98(10)$  K.

Data were measured using scans scans of  $1.0^\circ$  per frame for 2.5 s using  $\text{CuK}\alpha$  radiation (micro-focus sealed X-ray tube). The total number of runs and images was based on the strategy calculation from the program CrysAlisPro (Agilent). The actually achieved resolution was  $\theta = 76.748$ .

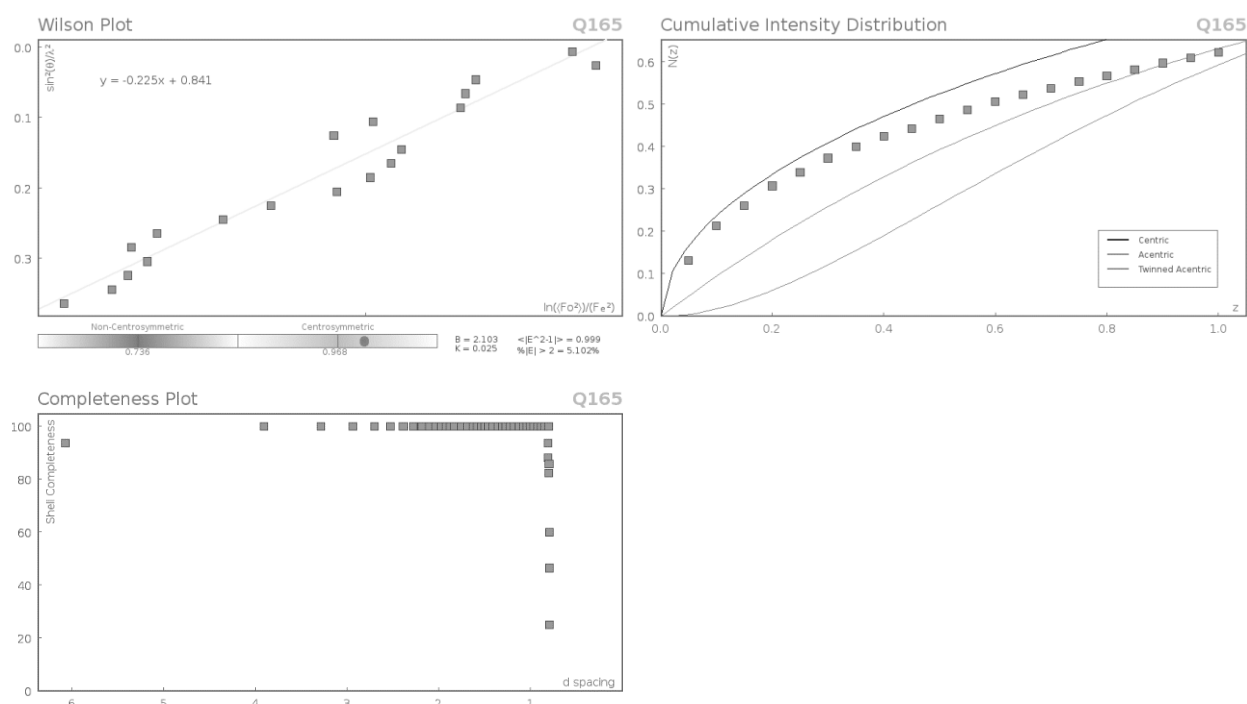
## Chapter 4: Copper(II)-catalyzed Oxo-azidation of Vinylarenes

Cell parameters were retrieved using the CrysAlisPro (Agilent) software and refined using CrysAlisPro (Agilent) on 4438 reflections, 25 of the observed reflections. Data reduction was performed using the CrysAlisPro (Agilent) software which corrects for Lorentz polarisation. The final completeness is 100.00 out to 76.748 in  $\theta$ . The absorption coefficient ( $\mu$ ) of this material is 3.678 and the minimum and maximum transmissions are 0.837 and 1.000.

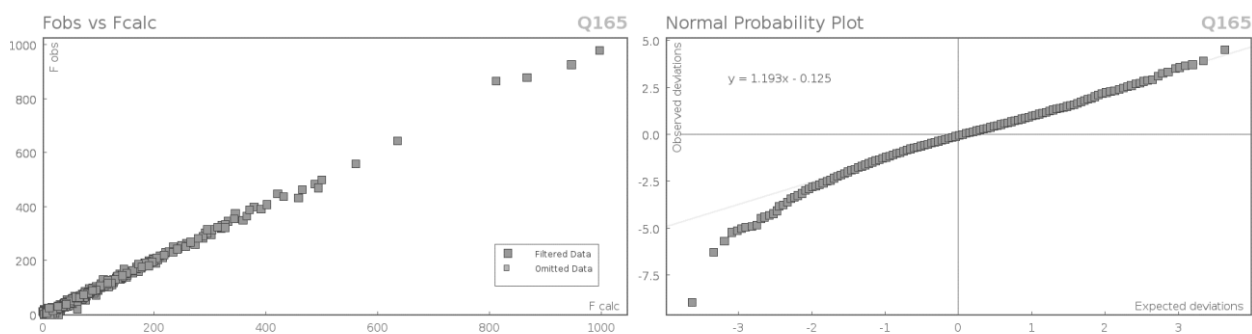
The structure was solved in the space group P-1 (# 2) by Intrinsic Phasing using the **ShelXT** (Sheldrick, 2015) structure solution program and refined by Least Squares using ShelXL (Sheldrick, 2015). All non-hydrogen atoms were refined anisotropically. Hydrogen atom positions were calculated geometrically and refined using the riding model.

The value of Z' is 2. This means that there are two independent molecules in the asymmetric unit.

### Data Plots: Diffraction Data



**Data Plots: Refinement and Data**



**Reflection Statistics**

Total reflections (after filtering)	17639	Unique reflections	3528
Completeness	0.988	Mean I/ $\sigma$	9.39
hkls <sub>sub</sub> >max</sub> collected	(4, 16, 21)	hkls <sub>sub</sub> >min</sub> collected	(-4, -16, -21)
hkl <sub>max</sub> used	(4, 16, 21)	hkl <sub>min</sub> used	(-4, -16, 0)
Lim d <sub>max</sub> collected	100.0	Lim d <sub>min</sub> collected	0.77
d <sub>max</sub> used	12.87	d <sub>min</sub> used	0.79
Friedel pairs	2954	Friedel pairs merged	1
Inconsistent equivalents	39	R <sub>int</sub>	0.0838
R <sub>sigma</sub>	0.0612	Intensity transformed	0
Omitted reflections	0	Omitted by user (OMIT hkl)	0
Multiplicity	(1284, 2142, 1407, 872, 454, 209, 79, 30, 5)	Maximum multiplicity	16
Removed systematic absences	0	Filtered off (Shel/OMIT)	0



Images of the Crystal on the Diffractometer

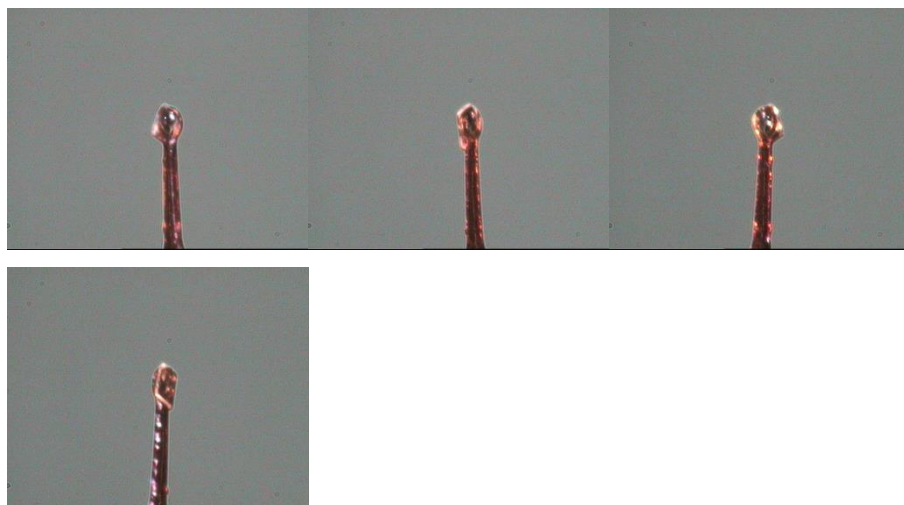


**Table 1:** Fractional Atomic Coordinates ( $\times 10^4$ ) and Equivalent Isotropic Displacement Parameters ( $\text{\AA}^2 \times 10^3$ ) for **2g**.  $U_{eq}$  is defined as 1/3 of the trace of the orthogonalised  $U_{ij}$ .

Atom	x	y	z	$U_{eq}$
C12	8121.9(16)	3140.8(4)	502.2(3)	28.25(15)
C11	4007.8(17)	11598.7(4)	9388.6(3)	32.83(16)
O1	-197(5)	8469.8(13)	6988.7(10)	31.1(4)
O2	585(6)	6567.9(13)	2654.2(11)	36.6(4)
N2	3329(6)	8076.1(16)	5629.1(12)	30.2(4)
N1	2069(6)	8974.2(15)	5451.6(12)	29.4(4)
N5	-742(7)	6669.0(17)	4164.5(13)	35.5(5)
N4	-2066(7)	5829.4(18)	4146.0(14)	39.5(5)
N3	4351(8)	7236.0(17)	5717.7(14)	40.9(6)
C7	1420(6)	9264.8(16)	6838.3(13)	23.7(4)
C4	2114(6)	9864.6(16)	7454.0(13)	22.9(4)
C10	6109(7)	4930.5(18)	1028.3(14)	27.6(5)
C15	1142(6)	5640.4(17)	2852.7(14)	26.9(5)
C13	3009(6)	3899.9(17)	2451.5(13)	25.1(5)
C12	2930(6)	4985.5(16)	2292.4(14)	24.5(5)
N6	123(8)	7460.6(19)	4237.1(15)	46.7(6)
C9	6130(6)	3852.6(17)	1199.2(13)	24.1(4)
C1	3259(6)	10932.8(17)	8641.6(14)	25.5(5)

Atom	x	y	z	$U_{eq}$
C14	4611(6)	3328.8(16)	1902.5(13)	24.1(4)
C2	1755(6)	9969.1(17)	8834.2(13)	26.4(5)
C5	3655(6)	10832.6(16)	7277.7(14)	25.6(5)
C6	4211(7)	11375.3(17)	7868.7(14)	27.1(5)
C8	2773(7)	9667.8(17)	5994.6(13)	25.5(5)
C3	1180(6)	9444.0(16)	8236.4(14)	24.8(5)
C11	4485(7)	5492.3(17)	1579.4(15)	27.9(5)
C16	62(7)	5132.7(18)	3686.9(15)	30.5(5)

**Table 2:** Anisotropic Displacement Parameters ( $\times 10^4$ ) **2g**. The anisotropic displacement factor exponent takes the form:  $-2\pi^2[h^2a^{*2} \times U_{11} + \dots + 2hka^* \times b^* \times U_{12}]$

Atom	$U_{11}$	$U_{22}$	$U_{33}$	$U_{23}$	$U_{13}$	$U_{12}$
Cl2	30.6(3)	25.2(2)	28.8(3)	-6.64(19)	0.5(2)	0.8(2)
Cl1	35.5(3)	31.9(3)	34.5(3)	-15.2(2)	-2.9(2)	-1.7(2)
O1	37.4(10)	24.4(8)	31.9(8)	-6.6(6)	2.3(7)	-8.7(7)
O2	47.6(12)	21.8(8)	40.4(10)	-7.4(7)	-2.4(8)	3.4(7)
N2	36.6(12)	28.1(10)	25.7(9)	-3.6(8)	-3.4(8)	-1.8(9)
N1	37.9(12)	24.3(9)	25.6(9)	-2.6(7)	-4.4(8)	-0.8(8)
N5	38.9(13)	33.0(11)	36.2(11)	-12.6(9)	-2.8(9)	5.3(9)
N4	39.2(13)	33.9(11)	45.2(13)	-14.1(9)	10.7(10)	-1.8(10)
N3	54.4(16)	29.2(11)	39.1(12)	-7.9(9)	-5.1(11)	6(1)
C7	22.5(11)	19.1(9)	28.0(11)	-1.6(8)	-0.1(8)	0.3(8)
C4	21.3(11)	20.5(9)	26.2(10)	-2.9(8)	-1.3(8)	1.1(8)
C10	29.8(12)	25.1(10)	26.7(11)	0.0(8)	-2.1(9)	-4.2(9)
C15	23.0(12)	24.1(11)	34.1(12)	-5.9(9)	-4.3(9)	-0.3(9)
C13	24.2(11)	21.8(10)	28.3(11)	-1.9(8)	-1.5(9)	-1.4(8)
C12	23.8(11)	20.5(10)	30.3(11)	-6.0(8)	-4.6(9)	-0.6(8)
N6	64.4(18)	35.7(12)	45.2(14)	-19.5(10)	-11.2(12)	2.4(12)
C9	21.7(11)	24.5(10)	27.1(11)	-6.8(8)	-3.8(9)	0.5(8)
C1	24.3(12)	24.6(10)	29.5(11)	-11.0(8)	-3.1(9)	3.3(9)
C14	23.9(11)	18.4(9)	30.0(11)	-3.7(8)	-2.8(9)	-1.1(8)

**Chapter 4: Copper(II)-catalyzed Oxo-azidation of Vinylarenes**

Atom	$U_{11}$	$U_{22}$	$U_{33}$	$U_{23}$	$U_{13}$	$U_{12}$
C2	27.0(12)	25(1)	25.5(11)	-2.6(8)	1.7(9)	2.3(9)
C5	27.4(12)	20.1(10)	27.4(11)	0.7(8)	-1.4(9)	0.2(9)
C6	26.5(12)	18.9(10)	35.6(12)	-3.6(8)	-3.4(9)	-1.2(8)
C8	27.4(12)	23.6(10)	25.6(10)	-2.9(8)	-4.0(9)	-2.6(9)
C3	26.6(12)	18.1(9)	29.3(11)	-4.0(8)	-0.1(9)	-0.3(8)
C11	30.7(13)	17.5(9)	35.6(12)	-2.8(8)	-5.2(10)	-2.3(9)
C16	30.8(13)	23.7(10)	36.5(12)	-7.3(9)	2.9(10)	-0.3(9)

**Table 3:** Bond Lengths in Å for **2g**.

Atom	Atom	Length/Å
Cl2	C9	1.744(2)
Cl1	C1	1.738(2)
O1	C7	1.215(3)
O2	C15	1.215(3)
N2	N1	1.242(3)
N2	N3	1.134(3)
N1	C8	1.470(3)
N5	N4	1.241(3)
N5	N6	1.135(3)
N4	C16	1.471(3)
C7	C4	1.484(3)
C7	C8	1.521(3)
C4	C5	1.399(3)
C4	C3	1.396(3)
C10	C9	1.389(3)
C10	C11	1.384(3)
C15	C12	1.496(3)
C15	C16	1.516(3)
C13	C12	1.398(3)
C13	C14	1.387(3)
C12	C11	1.395(3)

Atom	Atom	Length/Å
C9	C14	1.385(3)
C1	C2	1.389(3)
C1	C6	1.390(4)
C2	C3	1.382(3)
C5	C6	1.384(3)

**Table 4:** Bond Angles in ° for **2g**.

Atom	Atom	Atom	Angle/°
N3	N2	N1	172.5(3)
N2	N1	C8	113.6(2)
N6	N5	N4	171.9(3)
N5	N4	C16	115.6(2)
O1	C7	C4	122.0(2)
O1	C7	C8	119.5(2)
C4	C7	C8	118.49(19)
C5	C4	C7	122.4(2)
C3	C4	C7	118.5(2)
C3	C4	C5	119.1(2)
C11	C10	C9	118.5(2)
O2	C15	C12	121.3(2)
O2	C15	C16	119.7(2)
C12	C15	C16	118.99(19)
C14	C13	C12	120.2(2)
C13	C12	C15	122.5(2)
C11	C12	C15	117.8(2)
C11	C12	C13	119.7(2)
C10	C9	C12	118.75(18)
C14	C9	C12	119.17(17)
C14	C9	C10	122.1(2)
C2	C1	C11	119.03(19)
C2	C1	C6	121.9(2)

Atom	Atom	Atom	Angle/°
C6	C1	C11	119.11(18)
C9	C14	C13	118.9(2)
C3	C2	C1	118.6(2)
C6	C5	C4	120.6(2)
C5	C6	C1	118.8(2)
N1	C8	C7	112.90(19)
C2	C3	C4	121.0(2)
C10	C11	C12	120.6(2)
N4	C16	C15	113.4(2)

(d, TorsionAngles) **Table 5:** Hydrogen Fractional Atomic Coordinates ( $\times 10^4$ ) and Equivalent Isotropic Displacement Parameters ( $\text{\AA}^2 \times 10^3$ ) for **2g**.  $U_{eq}$  is defined as 1/3 of the trace of the orthogonalised  $U_{ij}$ .

Atom	x	y	z	$U_{eq}$
H10	7162.18	5267.27	554.27	33
H13	1982.38	3559.52	2927.15	30
H14	4665.47	2606.57	2004.92	29
H2	1146.57	9683.1	9354.71	32
H5	4312.77	11114.23	6758.6	31
H6	5201.6	12023.6	7750.97	32
H8A	1659.65	10345.95	5828.72	31
H8B	5302.99	9751.73	5968.93	31
H3	155.9	8800.51	8356.93	30
H11	4430.49	6214.41	1473.09	34
H16A	-1287.55	4529.37	3674.78	37
H16B	2174.94	4893.15	3947.5	37

### References:

- [1] T. Patonay, R. V. Hoffman, *J. Org. Chem.* **1994**, *59*, 2909.
- [2] T. Narender, K. Rajendar, S. Sarkar, V. K. Singh, U. Chaturvedi, A. K. Khanna, G. Bhatia, *Bioorganic Med. Chem. Lett.* **2011**, *21*, 6393.

- [3] T. Patonay, É. Juhász-Tóth, A. Bényei, *Eur. J. Org. Chem.* **2002**, 2002, 285.
- [4] V. Nair, L. G. Nair, T. G. George, A. Augustine, *Tetrahedron* **2000**, 56, 7607.
- [5] R. Moumné, V. Larue, B. Seijo, T. Lecourt, L. Micouin, C. Tinsé, *Org. Biomol. Chem.* **2010**, 8, 1154.
- [6] R. Zhao, B. -C. Chen, M. S. Bednarz, B. Wang, A. P. Skoumbourdis, J. E. Sundeen, T. G. M. Dhar, E. J. Ewanowicz, B. Balasubramanian, J. C. Barrish, *Arcivoc*, **2007**, 36.
- [7] H.-M. Wang, R.-S. Hou, J.-L. Wu, L.-C. Chen, *J. Chin. Chem. Soc.* **2007**, 54, 1333.







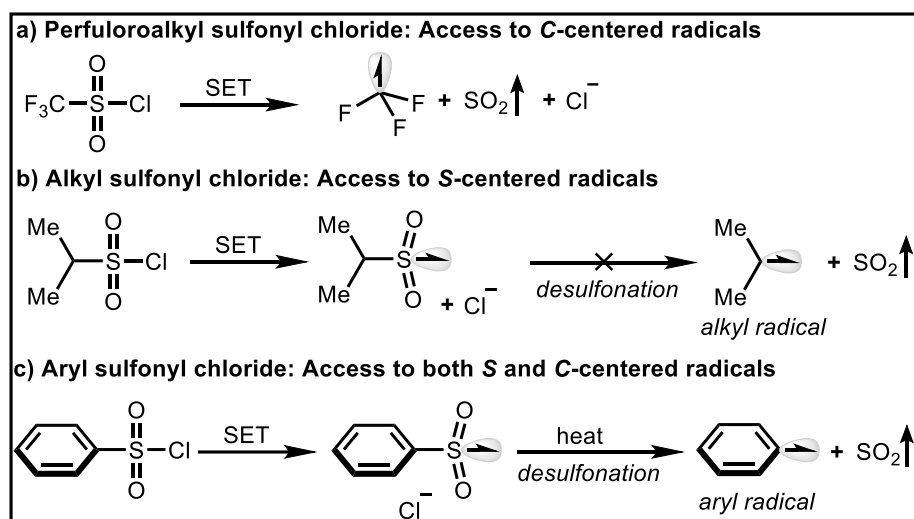
# *Chapter 5*



## Sulfonyl chlorides in Photocatalytic Transformations

## Introduction:

Alkyl/aryl-sulfonyl chlorides are biocompatible, relatively cheap and readily available radical precursors which can be employed in various organic transformations. Upon single-electron transfer (SET), one can easily get access to S- or C-centered radicals depending upon temperature or substituents present (Scheme 1). Perfluoroalkyl sulfonyl chlorides, *e.g.*  $\text{CF}_3\text{SO}_2\text{Cl}$ , upon SET, can easily undergo desulfonation at room temperature generating trifluoromethyl radical (Scheme 1a), whereas other alkyl sulfonyl chlorides cannot be desulfonated (Scheme 1b). On the other hand, in case the of aryl sulfonyl chlorides, the desulfonation step is temperature dependent (Scheme 1c). Many scientific groups have employed these versatile precursors in photocatalytic C-S and C-C bond-forming reactions, which are recently summarized by Natarajan *et. al.* in their outstanding review<sup>[1]</sup>.



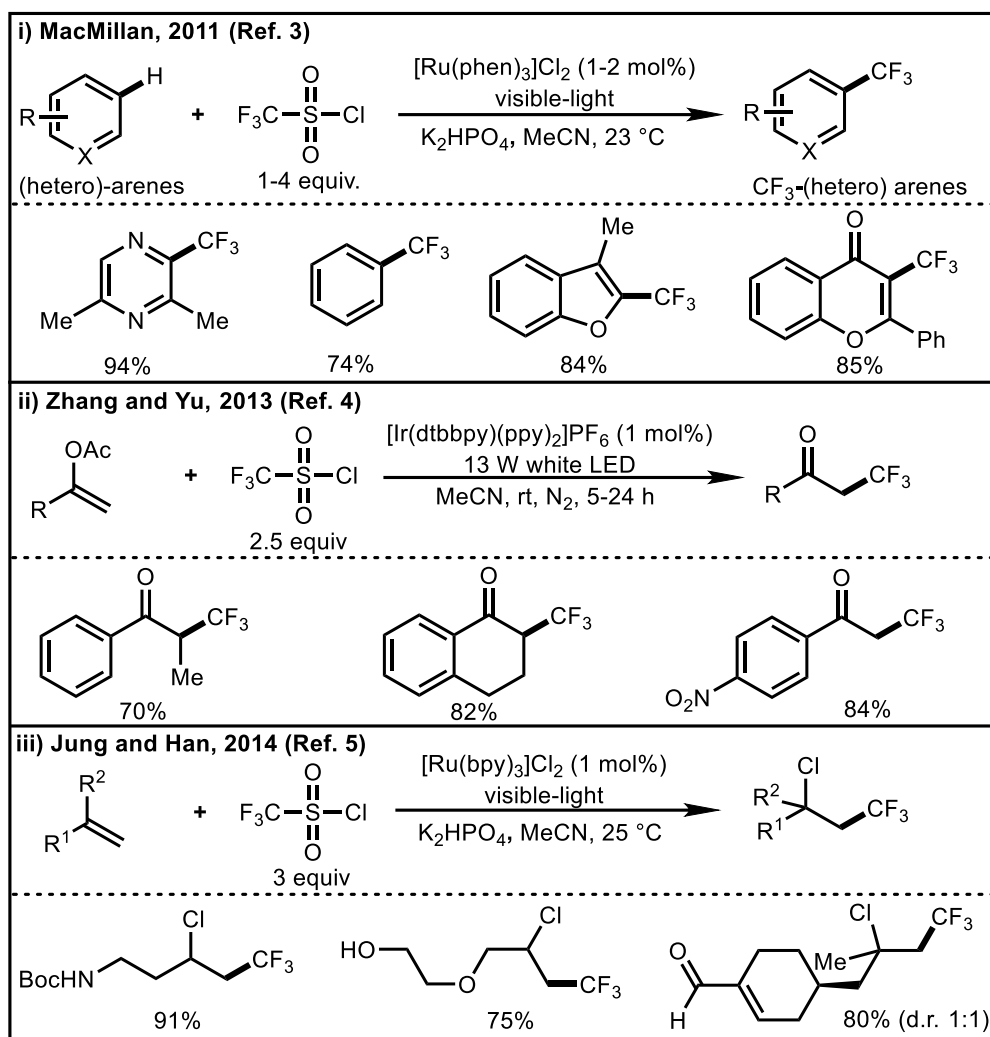
**Scheme 1:** Generation of S or C-centered radicals from sulfonyl chlorides.

## Selected examples:

*Triflyl chloride as a source of trifluoromethyl radical source:*

Introduction of trifluoromethyl ( $\text{CF}_3$ ) functionality into organic molecules can dramatically increase their biological activities and chemical stabilities<sup>[2]</sup>. As a consequence, the development of efficient methods for the direct incorporation of  $\text{CF}_3$ -functionality into organic molecules are highly desirable. MacMillan *et al.* showed for the first time that  $\text{CF}_3\text{SO}_2\text{Cl}$  can be used as a trifluoromethyl radical source under photoredox conditions<sup>[3]</sup>. A wide variety of

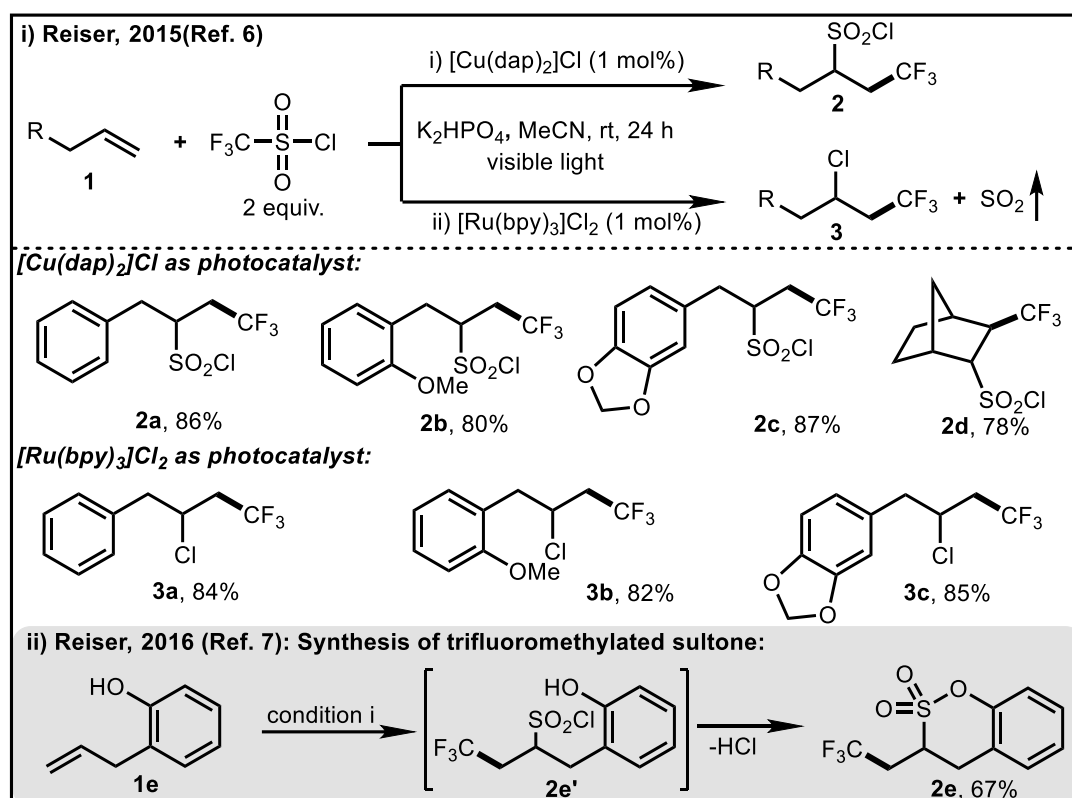
arenes and heteroarenes can be trifluoromethylated following the protocol (Scheme 2, i). Later on, Zhang and Yu *et al.* have reported a general protocol for the synthesis of  $\alpha$ -trifluoromethylated ketones<sup>[4]</sup> through the action of an iridium-based photocatalyst (Scheme 2, ii). A year later, Jun, Han and co-workers showed that  $\text{CF}_3\text{SO}_2\text{Cl}$  can be used as a source of both  $\text{CF}_3$  and Cl groups in the presence of a ruthenium-based photocatalyst<sup>[5]</sup> (Scheme 2, iii).



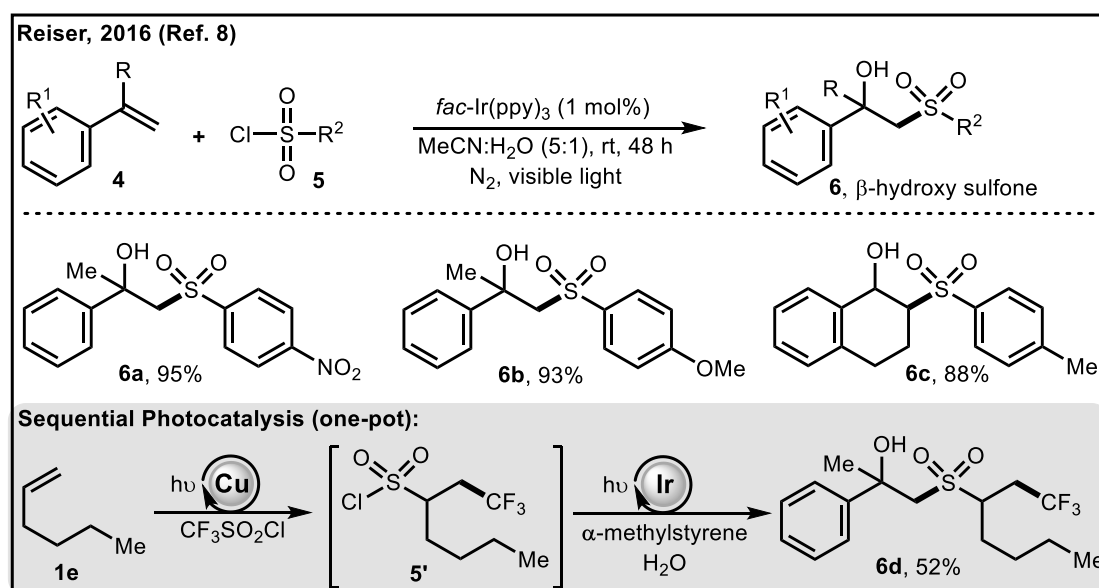
**Scheme 2:** Photocatalytic synthesis of  $\text{CF}_3$ -containing organic compounds.

In a noteworthy disclosure, Reiser and co-workers<sup>[6]</sup> have shown that the reactivity of  $\text{CF}_3\text{SO}_2\text{Cl}$  towards an unactivated olefin **1** can give rise to two different products **2** and **3**, by switching from ruthenium-based photocatalyst to a copper-based photocatalyst, respectively (Scheme 3).

Specifically, trifluoromethyl-chlorosulfonation **2a-d** of an unactivated olefin was facilitated by  $[\text{Cu}(\text{dap})_2]\text{Cl}$ . On the other hand,  $[\text{Ru}(\text{bpy})_3]\text{Cl}_2$  produced trifluoromethylchlorinated products **3a-c**. It was suggested that upon SET, the generated counter anion  $^-\text{SO}_2\text{Cl}$  was bound to the



Scheme 3: Inner-sphere reactivity of copper-based photocatalyst.


 Scheme 4: Photocatalytic synthesis of  $\beta$ -hydroxy sulfones.

copper catalyst, stabilizing and delivering this molecule to the intermediate radical. In absence of a copper catalyst, this anion immediately decomposed to generate  $\text{SO}_2$  and chloride. This unique discovery by Reiser and co-workers was further extended to the synthesis of

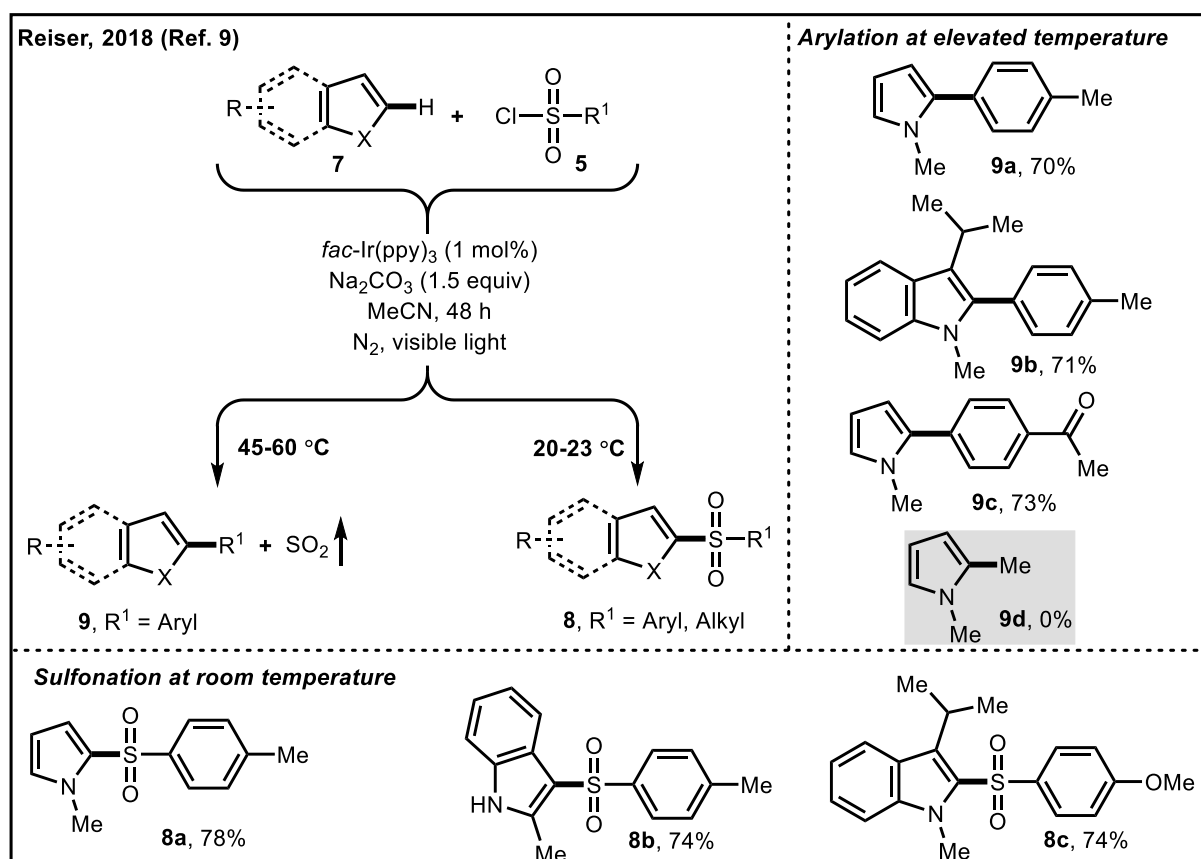
trifluoromethylated sultone **2e** (Scheme 3, ii)<sup>[7]</sup>. The intermediate alkyl sulfonyl chloride **2e'** could react with an internal *O*-nucleophile to form sultone **2e** in 67% isolated yield.

### Aryl-sulfonyl chlorides in photocatalysis:

The synthesis of  $\beta$ -hydroxysulfones **6** from sulfonyl chlorides **5** and activated olefin **4** in presence of water through the action of [Ir(ppy)<sub>3</sub>] photocatalyst was developed by the same group (Scheme 4)<sup>[8]</sup>. This method was further utilized in a photocatalytic sequence process shown in Scheme 4 which allowed the synthesis of highly substituted trifluoromethylated sulfone **6d** in one pot.

### Temperature-controlled selectivity:

Later, Reiser and co-workers have also found out that SO<sub>2</sub> extrusion, in case of aryl sulfonyl chlorides can be controlled thermally (Scheme 5)<sup>[9]</sup>. Through this method, one can achieve C-H sulfonation (**8a-c**) /arylation (**9a-c**) of heteroarenes at room temperature (20-23 °C), and at



**Scheme 5:** Influence of temperature in photocatalytic reaction between aryl sulfonyl chlorides and various heterocycles.

elevated temperature (45-60 °C) respectively. In case of alkyl sulfonyl chloride, instead of C-C (**9d**), C-S bond formation was observed even at elevated temperature.

**References:**

- [1] R. Chaudhary, P. Natarajan, *ChemistrySelect* **2017**, 2, 6458.
- [2] a) X.-F. Wu, H. Neumann, M. Beller, *Chem. Asian. J.* **2012**, 7, 1744; b) T. Furuya, A. S. Kamlet, T. Ritter, *Nature* **2011**, 473, 470; c) Y. Ye, M. S. Sanford, *Synlett* **2012**, 23, 2005; d) J. Wang, M. Sánchez-Roselló, J. L. Aceña, C. del Pozo, A. E. Sorochinsky, S. Fustero, V. A. Soloshonok, H. Liu, *Chem. Rev.* **2014**, 114, 2432.
- [3] D. A. Nagib, D. W. C. MacMillan, *Nature* **2011**, 480, 224.
- [4] H. Jiang, Y. Cheng, Y. Zhang, S. Yu, *Eur. J. Org. Chem.* **2013**, 2013, 5485.
- [5] S. H. Oh, Y. R. Malpani, N. Ha, Y.-S. Jung, S. B. Han, *Org. Lett.* **2014**, 16, 1310.
- [6] D. B. Bagal, G. Kachkovskiy, M. Knorn, T. Rawner, B. M. Bhanage, O. Reiser, *Angew. Chem. Int. Ed.* **2015**, 54, 6999.
- [7] T. Rawner, M. Knorn, E. Lutsker, A. Hossain, O. Reiser, *J. Org. Chem.* **2016**, 81, 7139.
- [8] S. K. Pagire, S. Paria, O. Reiser, *Org. Lett.* **2016**, 18, 2106.
- [9] S. K. Pagire, A. Hossain, O. Reiser, *Org. Lett.* **2018**, 20, 648.





# *Chapter 6*



## Copper and Visible-Light: Introducing a Cu(II)-Catalyst [Cu(dap)Cl<sub>2</sub>] to Photochemical ATRA Reaction

### Abstract:

A visible-light-mediated chloro-sulfonation of unactivated olefins has been developed utilizing commercially available sulfonyl chlorides and copper-phenanthroline-based catalysts. Besides the Cu(I) complex [Cu(dap)<sub>2</sub>]Cl, the corresponding Cu(II) complex [Cu(dap)Cl<sub>2</sub>] proved to be an efficient catalyst in this reaction, being advantageous from an economic point of view but also opening up new avenues for photoredox catalysis. Moreover, these copper complexes outperformed commonly used ruthenium, iridium, or organic dye based photocatalysts, owing to their ability to stabilize or interact with transient radicals by inner-sphere mechanisms due to the persistent radical effect. The use of stoichiometric Na<sub>2</sub>CO<sub>3</sub> in combination with the copper photocatalysts was found to be essential for this reaction. As suggested by appropriate control experiments, the role of Na<sub>2</sub>CO<sub>3</sub> is attributed to prevention of poisoning of the catalyst. The obtained products could be subjected to elimination (mono or double) which produced vinyl-sulfones or alkynes in very good yields.

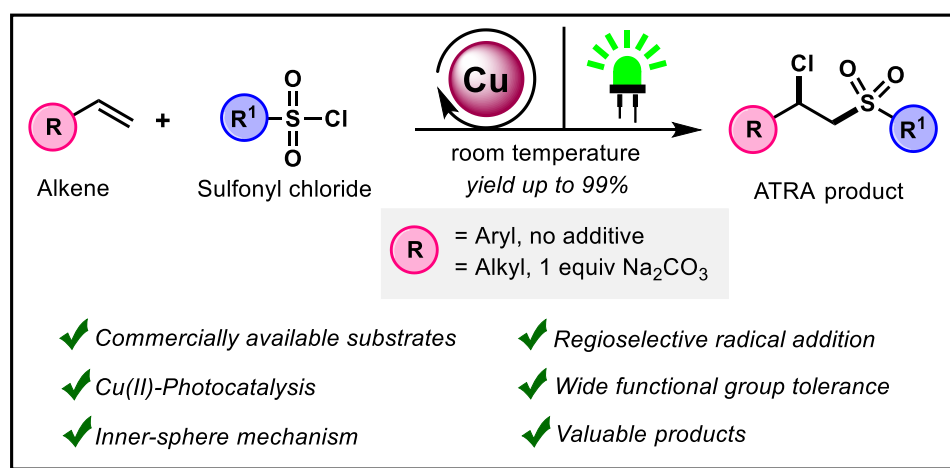


Figure 1: Visible-light mediated copper catalyzed chloro-sulfonation of olefins.

This chapter has been published:

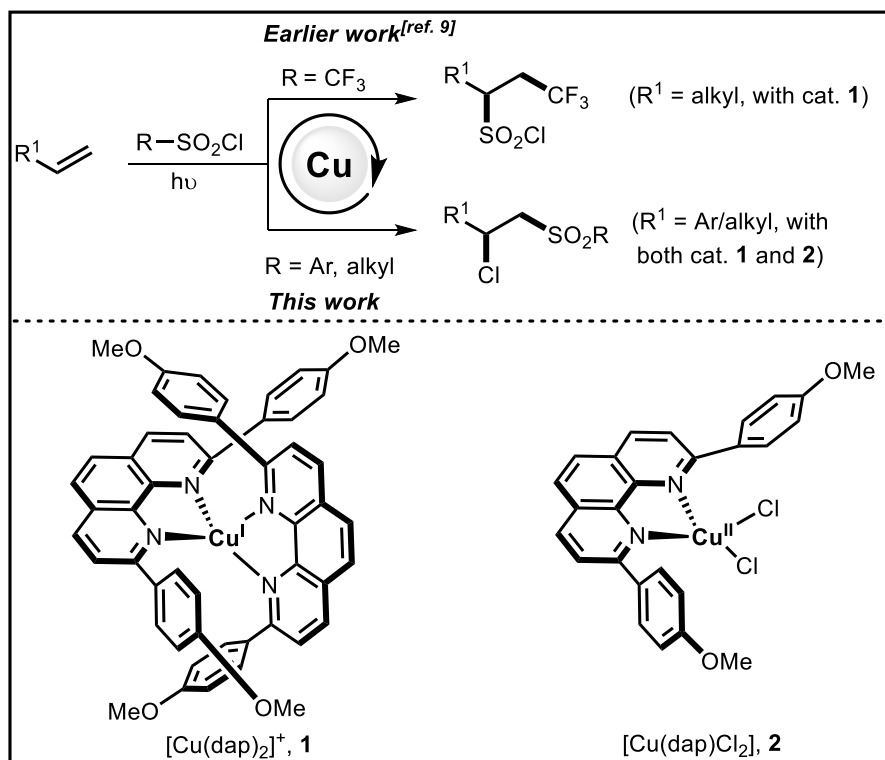
A. Hossain,<sup>†</sup> S. Engl,<sup>†</sup> E. Lutsker,<sup>†</sup> O. Reiser, *ACS Catal.* **2019**, 9, 1103-1109. (<sup>†</sup>equal contribution).

A.H. wrote the manuscript. S.E. and E.L. also assisted to finalize the manuscript.

## Chapter 6: Introducing Copper(II)-Catalyst to Photochemical ATRA Reactions

### Introduction:

The development of efficient methods for the construction of carbon-carbon and carbon-heteroatom bonds is highly desirable in synthetic organic chemistry, and organic chemists are on a perpetual path of discovery to identify new protocols for making such bonds. As a consequence, new catalytic strategies by employing inexpensive catalysts at low loadings are high on demand in terms of sustainable chemistry. Recently, difunctionalization<sup>[1]</sup>, a reaction which introduces two new chemical bonds across a functional group in a substrate has attracted considerable attention from organic chemists as it can increase the molecular complexity in a single step. In this context, visible-light photocatalysis<sup>[2]</sup> has become very useful for the difunctionalization of carbon-carbon multiple bonds<sup>[3,4]</sup>.



**Scheme 1:** Different sulfonyl chlorides under Copper Photocatalysis.

Sulfones are important motifs which can be found in many drugs and natural products<sup>[5,6]</sup>. Considerable efforts have been given by various scientific groups for the direct incorporation of sulfone moiety into organic molecules<sup>[7]</sup>. Reiser and co-workers<sup>[8,9]</sup> have recently revealed that  $\text{CF}_3\text{SO}_2\text{Cl}$  can be used as an ATRA reagent without extrusion of  $\text{SO}_2$ , under photochemical conditions using an earth-abundant metal-based (copper) photocatalyst<sup>[10,11]</sup> (Scheme 1). Therefore, the olefin was difunctionalized by forming two new chemical bonds, namely, C- $\text{CF}_3$  and C- $\text{SO}_2\text{Cl}$  in a single-step. On the other hand, ruthenium, iridium or organic-dye-based

## Chapter 6: Introducing Copper(II)-Catalyst to Photochemical ATRA Reactions

photocatalysts failed to achieve this transformation, and produced chlorinated products<sup>[9,12]</sup>. In this chapter, the reactivity of other (aryl/alkyl)-sulfonyl chlorides<sup>[13]</sup> with an unactivated olefin<sup>[14]</sup> in the presence of a copper photocatalyst<sup>[15]</sup> has been documented (Scheme 1).

In 2012, Stephenson and co-workers<sup>[16]</sup> have disclosed visible-light-mediated ATRA reactions of a series of organo-halogen compounds including two examples where *p*-toluenesulfonyl chloride **3a** has been used as ATRA reagent. Very recently, Niu *et al.*<sup>[17]</sup> have broadened the scope of Stephenson's protocol using [Ru(bpy)<sub>3</sub>]Cl<sub>2</sub> photocatalyst but they found out that certain number of olefins including unactivated olefins **5** were unsuccessful towards chloro-sulfonation reaction. We questioned if we can develop a more efficient protocol using a copper photocatalyst for the chloro-sulfonation reaction.

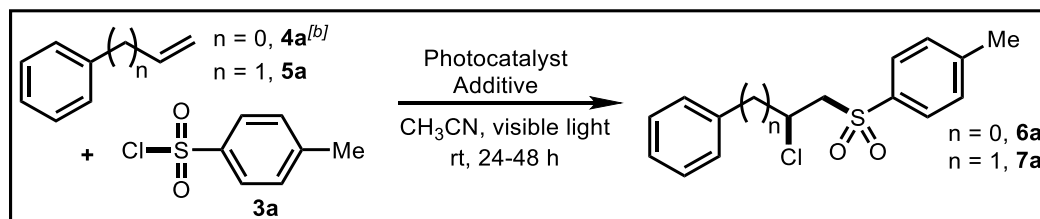
### Results and discussion:

Indeed, when we started our investigation with **3a** ( $E_{red} = -0.94$  V vs. SCE) and styrene **4a** (1 equiv), in the presence of 1 mol% of [Cu(dap)<sub>2</sub>]Cl **1** ( $E_{Cu(II)/Cu(I)^*} = -1.43$  V vs. SCE; dap = 2,9-bis(*p*-anisyl)-1,10-phenanthroline) as a photocatalyst under visible-light irradiation ( $\lambda_{max} = 530$  nm), we were pleased to observe the desired product **6a** formation in 96% yield (Table 1, entry 1) after 24 h. Instead, with [Ru(bpy)<sub>3</sub>]Cl<sub>2</sub> ( $E_{Ru(III)/Ru(II)^*} = -0.81$  V vs. SCE; bpy = 2,2'-bipyridine), highly reducing *fac*-[Ir(ppy)<sub>3</sub>] ( $E_{Ir(IV)/Ir(III)^*} = -1.73$  V vs. SCE; ppy = 2-phenylpyridine) or [Ir(dF(CF<sub>3</sub>)ppy)<sub>2</sub>(dtbbpy)]PF<sub>6</sub> ( $E_{Ir(IV)/Ir(III)^*} = -0.89$  V vs. SCE; dF(CF<sub>3</sub>)ppy = 2-(2,4-difluorophenyl)-5-trifluoromethylpyridine, dtbbpy = 4,4'-di-*tert*-butyl-2,2'-dipyridyl) or Na<sub>2</sub>-Eosin Y ( $E_{EY^+/EY^*} = -1.11$  V vs. SCE) under irradiation the yield of the desired product **6a** was found to be significantly lower (Table 1, entries 3-6) which is consistent with the report by Stephenson and co-workers<sup>[16]</sup> but surprisingly not consistent with Niu's report<sup>[17]</sup>, according to which **3a** does not result in any product formation in this reaction. It should be noted that the reduction potentials of all catalysts are sufficient to generate the toluylsulfonyl radical upon SET to TsCl (**3a**). Surprisingly, the analogous copper(II) complex [Cu(dap)Cl<sub>2</sub>] **2** also produced the desired product **6a** in 95% yield (Table 1, entry 2). Control experiments revealed that both light and catalyst were necessary to achieve this transformation (Table 1, entries 7-8).

Under the best conditions established for styrene (**4a**, Table 1, entry 1), employing the unactivated olefin **5a** gave poor yield of the desired ATRA product **7a**, even after doubling the amount of olefin (Table 1, entry 9). Then, we started investigating effects of an additive on this

**Chapter 6: Introducing Copper(II)-Catalyst to Photochemical ATRA  
Reactions**

**Catalyst screening and reaction optimization<sup>a</sup>**



Entry	photocatalyst (1 mol%)	additive (equiv)	olefin (equiv)	yield (%) <sup>c</sup>
1 <sup>d</sup>	[Cu(dap) <sub>2</sub> ]Cl	no	<b>4a</b> (1)	96 (96)
2	[Cu(dap)Cl <sub>2</sub> ]	no	<b>4a</b> (1)	95
3	[Ru(bpy) <sub>3</sub> ]Cl <sub>2</sub>	no	<b>4a</b> (1)	80
4	<i>fac</i> -[Ir(ppy) <sub>3</sub> ]	no	<b>4a</b> (1)	45
5	[Ir(dF(CF <sub>3</sub> )ppy) <sub>2</sub> (dtbbpy)]PF <sub>6</sub>	no	<b>4a</b> (1)	7
6	Na <sub>2</sub> -Eosin Y	no	<b>4a</b> (1)	NR
7	no	no	<b>4a</b> (1)	NR
8	[Cu(dap) <sub>2</sub> ]Cl (dark)	no	<b>4a</b> (1)	NR
9	[Cu(dap) <sub>2</sub> ]Cl	no	<b>5a</b> (1 or 2)	5 or 9
10	[Cu(dap) <sub>2</sub> ]Cl	K <sub>2</sub> HPO <sub>4</sub> (1)	<b>5a</b> (2)	60
11	[Cu(dap) <sub>2</sub> ]Cl	K <sub>2</sub> CO <sub>3</sub> (1)	<b>5a</b> (2)	18
12 <sup>d</sup>	[Cu(dap) <sub>2</sub> ]Cl	Na <sub>2</sub> CO <sub>3</sub> (1)	<b>5a</b> (2)	97 (92)
13	[Cu(dap) <sub>2</sub> ]Cl	NaCl (1)	<b>5a</b> (2)	8
14	[Cu(dap) <sub>2</sub> ]Cl	Cs <sub>2</sub> CO <sub>3</sub> (1)	<b>5a</b> (2)	NR
15	[Cu(dap) <sub>2</sub> ]Cl	NaOAc (1)	<b>5a</b> (2)	41
16	[Cu(dap) <sub>2</sub> ]Cl	Na <sub>2</sub> CO <sub>3</sub> (0.3)	<b>5a</b> (2)	55
17 <sup>d,e</sup>	[Cu(dap)Cl <sub>2</sub> ]	Na <sub>2</sub> CO <sub>3</sub> (1)	<b>5a</b> (2)	77 (72)
18	[Cu(dap) <sub>2</sub> ]Cl	Na <sub>2</sub> CO <sub>3</sub> (1)	<b>5a</b> (1.5)	76
19	[Ru(bpy) <sub>3</sub> ]Cl <sub>2</sub>	Na <sub>2</sub> CO <sub>3</sub> (1)	<b>5a</b> (2)	26
20	[Ru(bpy) <sub>3</sub> ]Cl <sub>2</sub>	no	<b>5a</b> (2)	55
21	<i>fac</i> -[Ir(ppy) <sub>3</sub> ]	Na <sub>2</sub> CO <sub>3</sub> (1)	<b>5a</b> (2)	26
22	<i>fac</i> -[Ir(ppy) <sub>3</sub> ]	no	<b>5a</b> (2)	30
23	[Ir(dtbbpy)(ppy) <sub>2</sub> ]PF <sub>6</sub>	Na <sub>2</sub> CO <sub>3</sub> (1)	<b>5a</b> (2)	18
24	[Ir(dtbbpy)(ppy) <sub>2</sub> ]PF <sub>6</sub>	no	<b>5a</b> (2)	17

**Chapter 6: Introducing Copper(II)-Catalyst to Photochemical ATRA  
Reactions**

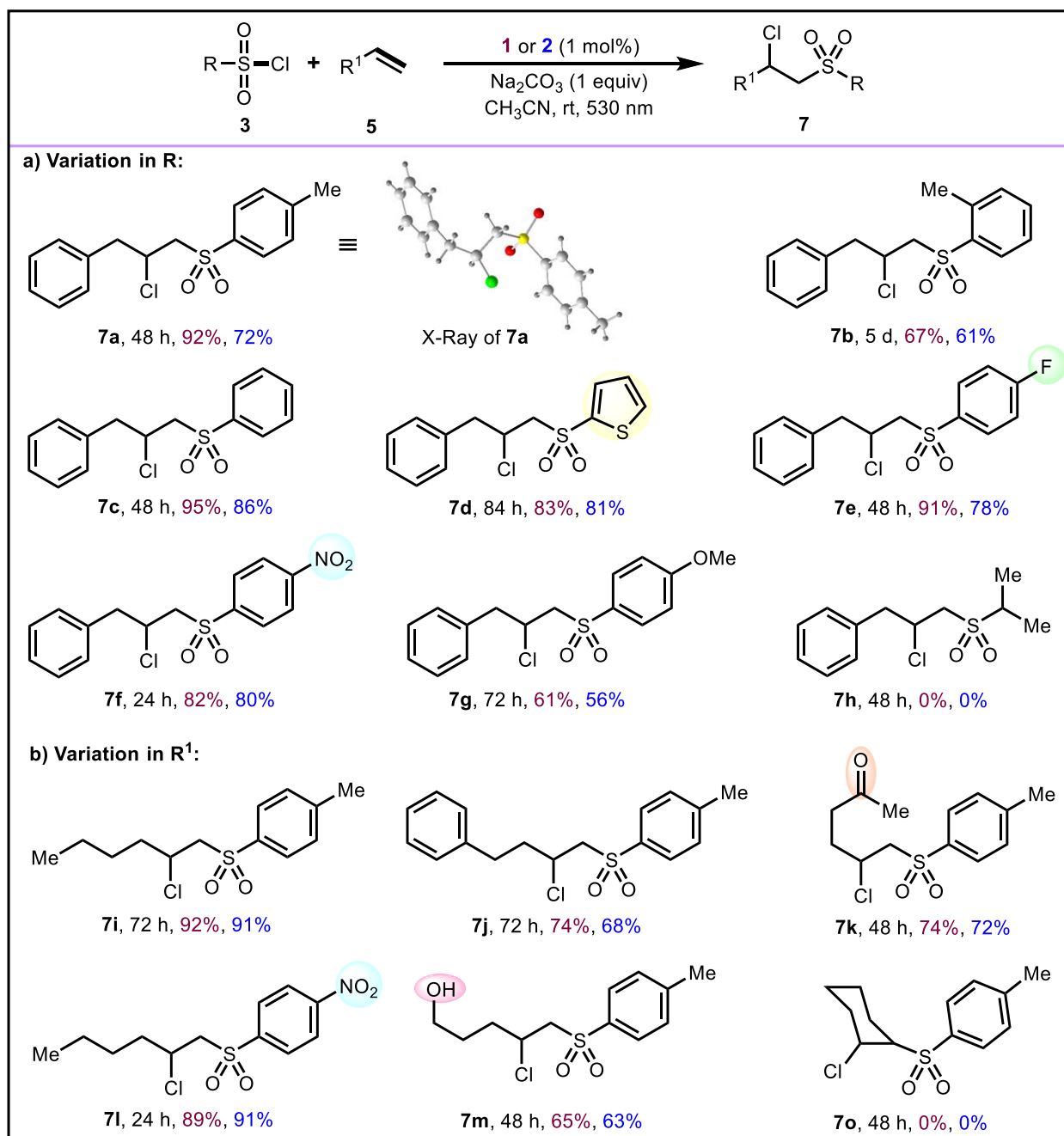
25	[Ir(dF(CF <sub>3</sub> )ppy) <sub>2</sub> (dtbbpy)]PF <sub>6</sub>	Na <sub>2</sub> CO <sub>3</sub> (1)	<b>5a</b> (2)	31
26	[Ir(dF(CF <sub>3</sub> )ppy) <sub>2</sub> (dtbbpy)]PF <sub>6</sub>	no	<b>5a</b> (2)	33
27	Na <sub>2</sub> -Eosin Y	Na <sub>2</sub> CO <sub>3</sub> (1)	<b>5a</b> (2)	3
28	Na <sub>2</sub> -Eosin Y	no	<b>5a</b> (2)	NR
29	no	Na <sub>2</sub> CO <sub>3</sub> (1)	<b>5a</b> (2)	NR
30	[Cu(dap) <sub>2</sub> ]Cl (dark)	Na <sub>2</sub> CO <sub>3</sub> (1)	<b>5a</b> (2)	NR
31 <sup>f</sup>	CuCl	Na <sub>2</sub> CO <sub>3</sub> (1)	<b>5a</b> (2)	NR
32 <sup>f</sup>	CuCl <sub>2</sub>	Na <sub>2</sub> CO <sub>3</sub> (1)	<b>5a</b> (2)	NR
33 <sup>f</sup>	dap	Na <sub>2</sub> CO <sub>3</sub> (1)	<b>5a</b> (2)	6
34 <sup>g</sup>	CuCl + phen	Na <sub>2</sub> CO <sub>3</sub> (1)	<b>5a</b> (2)	4
36 <sup>g</sup>	CuCl <sub>2</sub> + phen	Na <sub>2</sub> CO <sub>3</sub> (1)	<b>5a</b> (2)	4
37 <sup>h</sup>	[Cu(dap) <sub>2</sub> ]Cl	Na <sub>2</sub> CO <sub>3</sub> (1)	<b>5a</b> (2)	26
38 <sup>i</sup>	[Cu(dap) <sub>2</sub> ]Cl	Na <sub>2</sub> CO <sub>3</sub> (1)	<b>5a</b> (2)	NR

**Table 1: Reaction Conditions:** **3a** (0.50 mmol, 1 equiv), photocatalyst (1 mol%), in CH<sub>3</sub>CN (0.25 M) under N<sub>2</sub> at room temperature (25–30 °C). Reaction times were 24 h for **4a** and 48 h for **5a**. LEDs have been used for irradiation (see experimental section). For [Cu] and Na<sub>2</sub>-Eosin Y, Green LED ( $\lambda_{max}$  = 530 nm) and for other photocatalysts Blue LED ( $\lambda_{max}$  = 455 nm). <sup>b</sup>Reactions with styrene **4a** were performed by S. Engl. <sup>c</sup><sup>1</sup>H NMR yields. <sup>d</sup>Isolated yields are in parenthesis. <sup>e</sup>72 h reaction time, performed by Dr. E. Lutsker. <sup>f</sup>5 mol% catalyst was employed. <sup>g</sup>5 mol% copper salt with 10 mol% phen was used. <sup>h</sup>DCM instead of CH<sub>3</sub>CN. <sup>i</sup>DMF or DMSO instead of CH<sub>3</sub>CN. NR = No Reaction. phen = 1,10-phenanthroline.

reaction. Indeed, when this reaction was performed in the presence of 1 equivalent of K<sub>2</sub>HPO<sub>4</sub>, a drastic increase in product yield (60%) was observed (Table 1, entry 10). The use of stoichiometric amounts of K<sub>2</sub>CO<sub>3</sub> lowers the product yield to 18% (Table 1, entry 11), while the use of 1 equivalent Na<sub>2</sub>CO<sub>3</sub> instead of K<sub>2</sub>CO<sub>3</sub> increases the isolated product yield to 92% (Table 1, entry 12). Having these two entries (11 and 12) we speculate there might be a special effect of Na<sup>+</sup> cation itself. However, using 1 equivalent NaCl as an additive instead again drastically decreases the yield of **7a** to 8% (Table 1, entry 13), making it unlikely that the process is dependent on Na<sup>+</sup>-cocatalysis. Given that the overall reaction is a net addition, substoichiometric amounts of base should be sufficient, *i.e.* to scavenge traces of HCl that could form in the process. Nevertheless, catalytic amount of Na<sub>2</sub>CO<sub>3</sub> is also accompanied by a decrease in product formation (55%, Table 1, entry 16). The use of Cs<sub>2</sub>CO<sub>3</sub> as a base, completely shut down the reaction (Table 1, Entry 14) whereas use of NaOAc produced only

## Chapter 6: Introducing Copper(II)-Catalyst to Photochemical ATRA Reactions

### Scope of the reaction:



**Scheme 2: Reaction conditions:** Sulfonyl chloride **3** (0.50 mmol, 1 equiv), olefin **5** (1.00 mmol, 2 equiv), Na<sub>2</sub>CO<sub>3</sub> (0.50 mmol, 1 equiv), [Cu(dap)<sub>2</sub>]Cl **1** (1 mol %) or [Cu(dap)Cl<sub>2</sub>] **2** (1 mol %) in CH<sub>3</sub>CN. All reactions were performed under N<sub>2</sub> atmosphere at room temperature (25–30 °C) with green LED ( $\lambda_{max}$  = 530 nm). Isolated yields are given.

41% of the desired product **7a** (Table 1, entry 15). Again, the use of the copper(II)-catalyst **2** was also possible, producing **5a** in 72% isolated yield (Table 1, entry 17) after 72 h irradiation. Moreover, when other photocatalysts were employed such as [Ru(bpy)<sub>3</sub>]Cl<sub>2</sub>, *fac*-[Ir(ppy)<sub>3</sub>],



## Chapter 6: Introducing Copper(II)-Catalyst to Photochemical ATRA Reactions

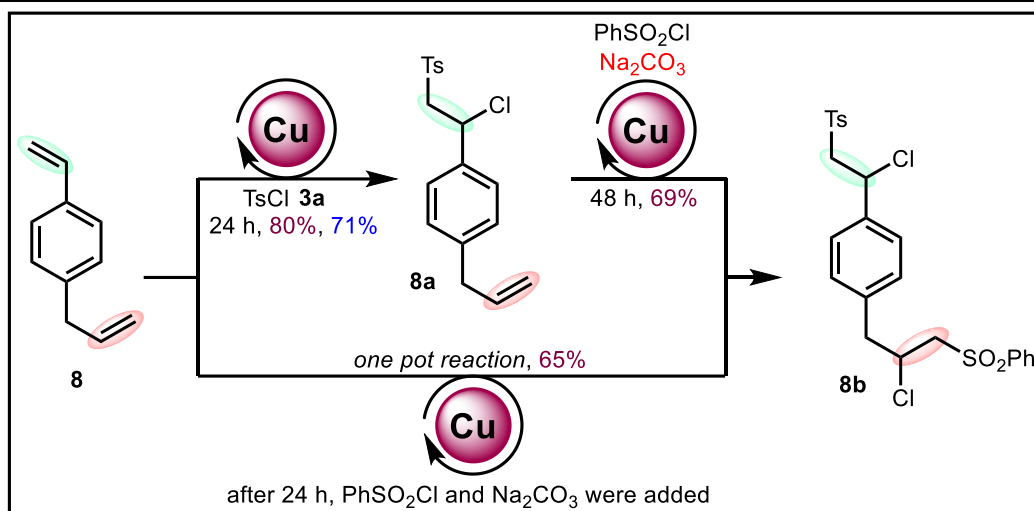
$[\text{Ir}(\text{dtbbpy})(\text{ppy})_2]\text{PF}_6$ ,  $[\text{Ir}(\text{dF}(\text{CF}_3)\text{ppy})_2(\text{dtbbpy})]\text{PF}_6$  or  $\text{Na}_2$ -Eosin Y, poor yields were observed and notably, irrespective of the use of  $\text{Na}_2\text{CO}_3$  as an additive (Table 1, entries 19–28). Control experiments proved the necessity of both catalyst and light since no reaction was observed in the absence of each of these components (Table 1, entries 29-30). Further optimization studies were performed (entries 31-36) which indicated the importance of the ‘dap’ ligand in combination with copper salts for this transformation. Changing the solvent from  $\text{CH}_3\text{CN}$  to DCM, DMF or DMSO either provided poor yields or no reaction was observed (Table 1, entries 37-38). Thus, the conditions established in entry 12 and 17 (for unactivated olefins **5**) were found to be best and were subsequently applied to explore the scope of this reaction. It should be noted that the possibility of using  $[\text{Cu}(\text{dap})\text{Cl}_2]$  **2** offers a considerable cost advantage, given that only half the amount of ‘dap’ ligand has to be employed.

For a wide variety of substrates **3**, both Cu(I)- and Cu(II)-dap catalysts (**1** and **2**) could be successfully employed in the title reaction (Schemes 2a and 2b). We were pleased to observe that both electron rich and electron poor sulfonyl chlorides underwent the addition reaction with allylbenzene **5a** in high yields. Structure of **7a** was confirmed by single crystal X-Ray analysis. In case of *ortho*-substituted sulfonyl chloride, (*e.g.* **7b**) the reaction time was 5 days and the yield was moderate. Considering thiophene derived substrates a potential poison for the copper-photocatalyst, they nevertheless also provided the ATRA products **7d** in good yield (>80%). Fluoro, nitro, methoxy-containing sulfonyl chlorides provided the desired products **7e-7g** in good yields (up to 91%). Surprisingly, alkyl sulfonyl chlorides did not give yield for **7h**. On the other hand, when we examined the limitation for olefinic partner, we found out that disubstituted olefin, for example, cyclohexene did not give any yield for **7o** after 48 h of irradiation. However, **7i-7m** were isolated in very good yields.

### Sequential functionalization of two different olefins:

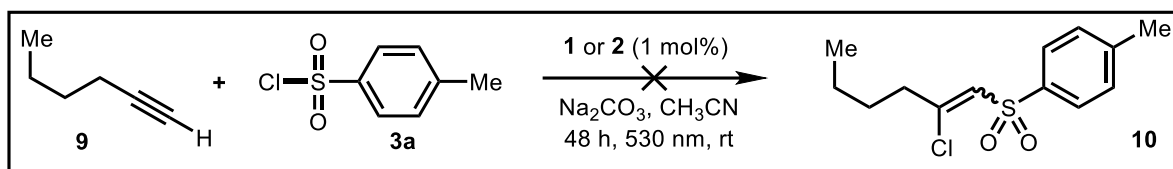
Given the necessity of employing  $\text{Na}_2\text{CO}_3$  as an additive for alkenes **5** for the chlorosulfonation, we seized the opportunity to perform the sequential functionalization of **8** (Scheme 3). Indeed, **8a** could be obtained in the first step in 80% yield using  $\text{TsCl}$ , followed by a second ATRA reaction with  $\text{PhSO}_2\text{Cl}$  in the presence of  $\text{Na}_2\text{CO}_3$  to give rise to **8b** in 69% isolated yield. An even better overall yield (65%) was obtained when a single flask reaction was performed in which 1 mol%  $[\text{Cu}(\text{dap})_2]\text{Cl}$  **1** was found to be sufficient for the sequential functionalization of the two different double bonds.

## Chapter 6: Introducing Copper(II)-Catalyst to Photochemical ATRA Reactions



**Scheme 3: Reaction conditions:** see experimental section.

### Alkyne difunctionalization:



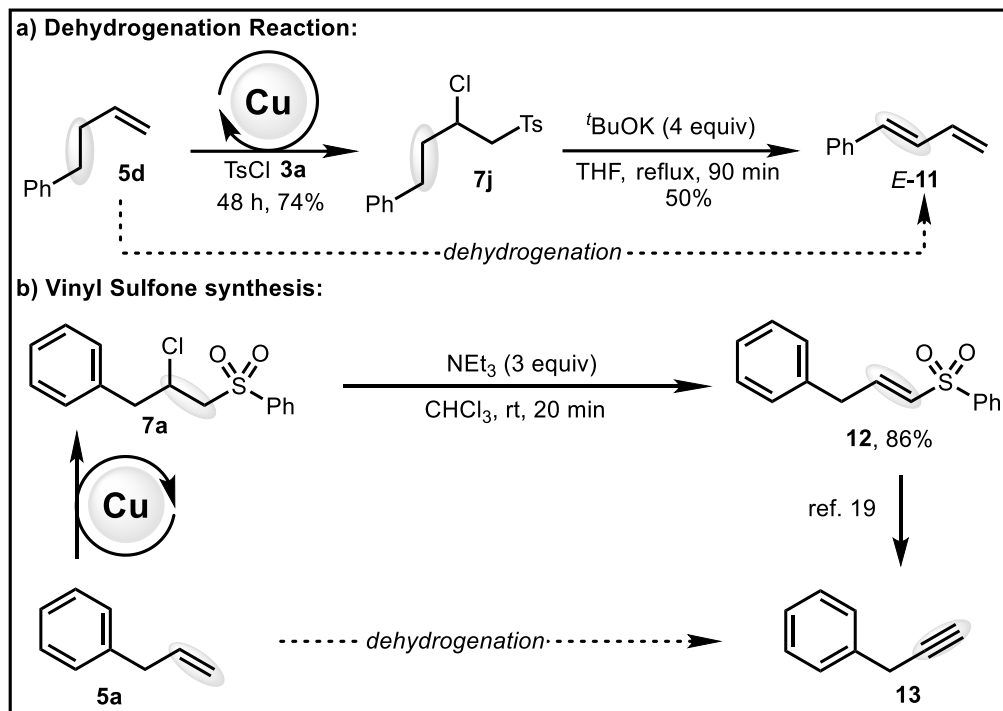
**Scheme 4: Reaction conditions:** **3a** (0.50 mmol, 1 equiv), alkyne **9** (1.00 mmol, 2 equiv), **Na<sub>2</sub>CO<sub>3</sub>** (0.50 mmol, 1 equiv), **[Cu(dap)<sub>2</sub>]Cl 1** (1 mol %) or **[Cu(dap)Cl<sub>2</sub>] 2** (1 mol %) in **CH<sub>3</sub>CN**.

Next, we aimed for chlorosulfonation of unactivated alkynes. Phenylacetylene derived substrates gave excellent yields of the desired products with our developed method (cite). However, when we subjected **9** into our reaction conditions, none of the catalysts **1** and **2** could produce the desired product **10** (Scheme 4). This result is in fact consistent with a very recent report<sup>[18]</sup> where an iridium-based photocatalyst was also shown to be ineffective towards unactivated alkynes.

### Further transformations of ATRA products:

Next, we explored the scope of the further transformations of the synthesized products. First, we tested some of the ATRA products in their reactivity with bases. Upon treatment of **7j** with potassium *tert*-butoxide<sup>[19]</sup> a two-fold elimination occurred giving rise to *E*-**11** (Scheme 5a), while weak bases (**NEt<sub>3</sub>**) resulted in the formation of vinylsulfones<sup>[6]</sup> **12** in high yield (Scheme 5b). Vinyl sulfones have been proven to be valuable synthons in asymmetric reactions<sup>[20]</sup>, cycloadditions<sup>[21]</sup>, and metalations<sup>[22]</sup>, but can also be transformed to alkynes<sup>[19]</sup> **13**, thus

## Chapter 6: Introducing Copper(II)-Catalyst to Photochemical ATRA Reactions



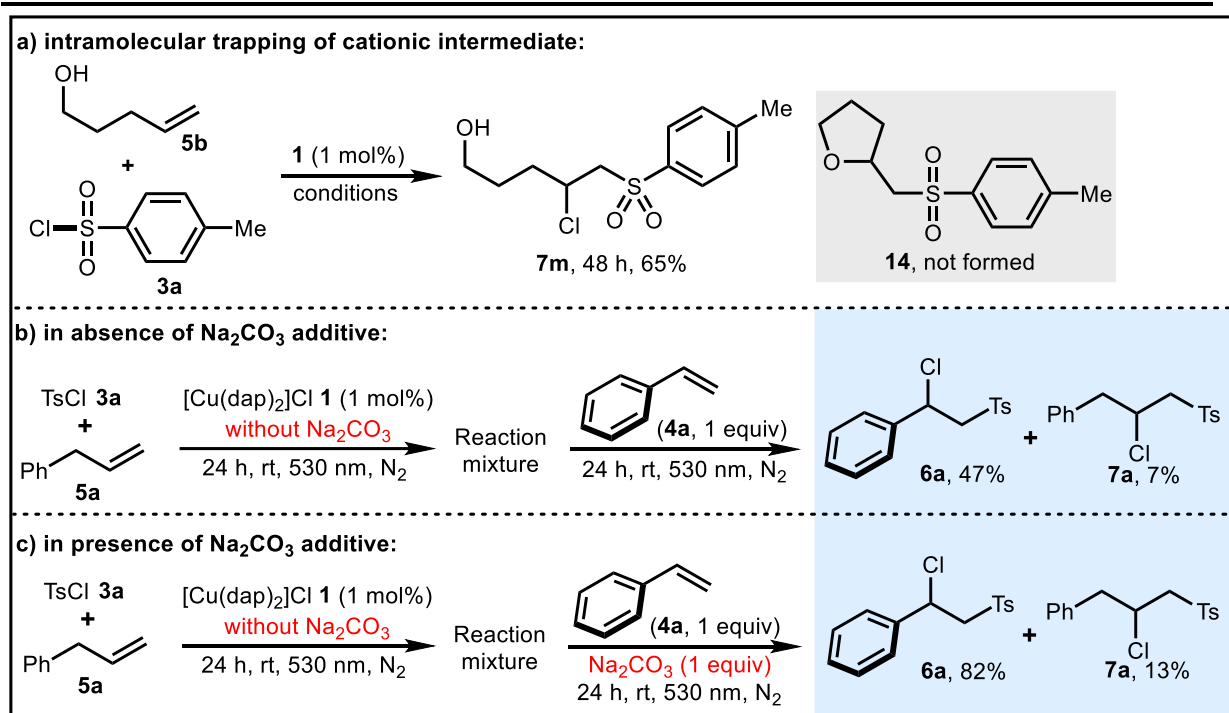
**Scheme 5: Reaction conditions:** a) **3a** (0.50 mmol, 1 equiv), **5d** (1.00 mmol, 2 equiv), Na<sub>2</sub>CO<sub>3</sub> (0.50 mmol, 1 equiv), [Cu(dap)<sub>2</sub>]Cl **1** (1 mol%) in CH<sub>3</sub>CN under N<sub>2</sub> atmosphere at room temperature (25–30 °C) with green LED ( $\lambda_{max} = 530$  nm). b) **7a** (0.30 mmol, 1 equiv), triethylamine (0.90 mmol, 3 equiv) in 2 mL chloroform. Isolated yields are given.

offering overall a route for the dehydrogenation of alkenes.

### Mechanistic studies:

In order to gain insight into the mechanism for this reaction, we first ruled out the possibility of formation of cationic intermediate through the reaction shown in Scheme 6a. Olefin **5b**, when treated with tosyl chloride **3a** under standard reaction condition (Table 1, Entry 12) the obtained product was **7m**, exclusively, no cyclized product **14** formation was observed. Next, we investigated the role of the additive, specifically, Na<sub>2</sub>CO<sub>3</sub> through a series of control experiments. We surmised that the distinct requirement for employing heterogeneous inorganic bases, in particular Na<sub>2</sub>CO<sub>3</sub>, which has also been shown to be beneficial in other photoredox reactions<sup>[9,12,23]</sup>, might also prevent the poisoning of the copper catalysts. Indeed, when a mixture of **3a** and **5a** was irradiated in the absence of Na<sub>2</sub>CO<sub>3</sub> for 24 h (Scheme 6b) followed by addition of styrene (**4a**) with continuing irradiation for another 24 h, the formation of only 47% (<sup>1</sup>H NMR yield) of **6a** was observed along with 7% **7a**. When the experiment was repeated but Na<sub>2</sub>CO<sub>3</sub> was added together with styrene, the respective yields were 82% and 13%,

## Chapter 6: Introducing Copper(II)-Catalyst to Photochemical ATRA Reactions

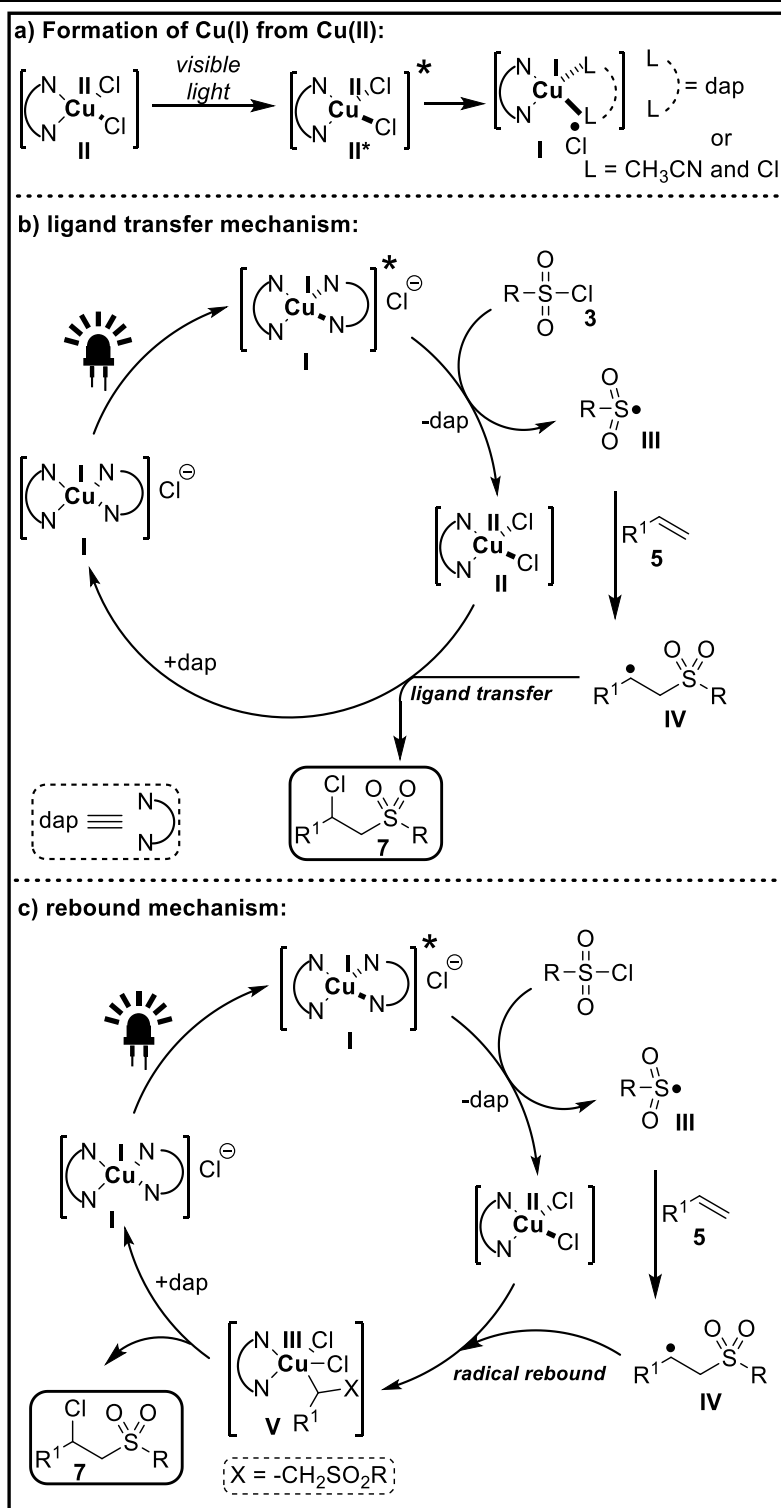


**Scheme 6: Reaction conditions:** a) **3a** (0.50 mmol, 1 equiv), **5b** (1.00 mmol, 2 equiv), Na<sub>2</sub>CO<sub>3</sub> (0.50 mmol, 1 equiv), [Cu(dap)<sub>2</sub>]Cl **1** (1 mol%) in CH<sub>3</sub>CN under N<sub>2</sub> atmosphere at room temperature (25–30 °C) with green LED ( $\lambda_{max}$  = 530 nm), 48 h. b, c) reactions were performed on 0.50 mmol scale.

clearly suggesting the protective nature of the heterogeneous base for the copper catalyst. The more reactive vinylarenes, being more efficient acceptors for radicals formed in the process, apparently prevent catalyst deactivation as well, since these alkenes do not require any base.

### Proposed Mechanism:

A plausible mechanism considering the unique role of the copper catalysts in the title transformation is outlined in Scheme 7. When the reaction was performed with [Cu(dap)Cl<sub>2</sub>] **2** as a catalyst, we assume that nevertheless a reduction to Cu(I) occurs being the catalytically active species, for example via a visible-light-induced homolytic cleavage of the Cu(II)-Cl bond<sup>[4,10,24]</sup> (Scheme 7a) forming a Cu(I) intermediate **I**. **I** might get coordinated either by another dap ligand with chloride as a counter anion (which results in the formation of [Cu(dap)<sub>2</sub>]Cl **1**) or by the solvent<sup>[25]</sup>. **I** in its excited state **I\*** can form sulfonyl radicals **III** upon one electron reduction of sulfonyl chloride **3** (Scheme 7b, c). In turn, a Cu(II) species of type **II** such as [Cu(dap)Cl<sub>2</sub>] is formed, which has been independently synthesized from CuCl<sub>2</sub> and dap<sup>[4]</sup> being found to be a capable photocatalyst for the title reaction in this study as well. The radical **III** can add to the olefin forming a C-centered radical **IV** which takes back chlorine



**Scheme 7:** Proposed catalytic cycles. a) Visible-light induced homolysis (VLH) of Cu(II)-Cl bond; b and c represent two possible ways for the product formation.

from **II** concurrent with the regeneration of catalyst **I** (Scheme 7b). Intermediate **IV** could also bind to the Cu(II) species **II** (Scheme 7c), being a persistent radical, to give rise to a Cu(III) intermediate<sup>[26]</sup> **V**. Reductive elimination from **V** leads to the formation of the desired product

## Chapter 6: Introducing Copper(II)-Catalyst to Photochemical ATRA Reactions

---

and the active catalyst **I** is regenerated by trapping the free ligand. We assume that for unactivated alkenes this pathway (Scheme 7c) is more feasible when Na<sub>2</sub>CO<sub>3</sub> assists the reductive elimination from Cu(III) intermediate **V**. This would explain that for other photocatalysts either a negative or no effect of this additive was observed since in those cases a normal oxidative quenching pathway is followed.

### Conclusion:

In conclusion, we have developed a highly efficient, first row transition-metal based photocatalytic protocol to convert a large variety of olefins to their corresponding vicinal chlorosulfonated adducts. Moreover, the obtained adducts can be subjected to mono elimination reaction which produced vinyl sulfones in high yields. On the other hand, double elimination can produce alkynes. In other words, sulfonyl chloride mimics traditionally used Br<sub>2</sub> for the conversion of alkenes to corresponding alkynes. During this study it was also realized that a very specific additive can play a crucial role to achieve a particular transformation.

### References and notes:

- [1] T. Courant, G. Masson, *J. Org. Chem.* **2016**, *81*, 6945.
- [2] a) L. Marzo, S. K. Pagire, O. Reiser, B. König, *Angew. Chem. Int. Ed.* **2018**, *57*, 10034–10072; b) B. König, *Eur. J. Org. Chem.* **2017**, *2017*, 1979; c) J.-R. Chen, X.-Q. Hu, L.-Q. Lu, W.-J. Xiao, *Acc. Chem. Res.* **2016**, *49*, 1911; d) J. M. R. Narayanam, C. R. J. Stephenson, *Chem. Soc. Rev.* **2011**, *40*, 102; e) M. H. Shaw, J. Twilton, D. W. C. MacMillan, *J. Org. Chem.* **2016**, *81*, 6898; f) G. Ciamician, *Science* **1912**, *36*, 385.
- [3] a) S. Paria, M. Pirtsch, V. Kais, O. Reiser, *Synthesis* **2013**, *45*, 2689; b) M. Pirtsch, S. Paria, T. Matsuno, H. Isobe, O. Reiser, *Chem. Eur. J.* **2012**, *18*, 7336; c) T. Rawner, E. Lutsker, C. A. Kaiser, O. Reiser, *ACS Catal.* **2018**, *8*, 3950; d) H. Jiang, A. Studer, *Angew. Chem. Int. Ed.* **2017**, *56*, 12273; e) J. Davies, S. G. Booth, S. Essafi, R. A. W. Dryfe, D. Leonori, *Angew. Chem. Int. Ed.* **2015**, *54*, 14017; f) D. H. Barton, M. A. Csiba, J. C. Jaszberenyi, *Tetrahedron Lett.* **1994**, *35*, 2869; g) A. J. Musacchio, B. C. Lainhart, X. Zhang, S. G. Naguib, T. C. Sherwood, R. R. Knowles, *Science* **2017**, *355*, 727; h) Y. Shen, J. Cornella, F. Juliá-Hernández, R. Martin, *ACS Catal.* **2016**, *7*, 409; i) T. Koike, M. Akita, *Acc. Chem. Res.* **2016**, *49*, 1937; j) K. A. Margrey, D. A. Nicewicz, *Acc. Chem. Res.* **2016**, *49*, 1997.
- [4] A. Hossain, A. Vidyasagar, C. Eichinger, C. Lankes, J. Phan, J. Rehbein, O. Reiser, *Angew. Chem. Int. Ed.* **2018**, *57*, 8288-8292.

## Chapter 6: Introducing Copper(II)-Catalyst to Photochemical ATRA Reactions

---

- [5] a) E. N. Prilezhaeva, *Russ. Chem. Rev.* **2000**, *69*, 367; b) A.-N. R. Alba, X. Companyó, R. Rios, *Chem. Soc. Rev.* **2010**, *39*, 2018; c) S. Y. Woo, J. H. Kim, M. K. Moon, S.-H. Han, S. K. Yeon, J. W. Choi, B. K. Jang, H. J. Song, Y. G. Kang, J. W. Kim et al., *J. Med. Chem.* **2014**, *57*, 1473.
- [6] D. C. Meadows, J. Gervay-Hague, *Med. Res. Rev.* **2006**, *26*, 793.
- [7] a) L. Kadari, R. K. Palakodety, L. P. Yallapragada, *Org. Lett.* **2017**, *19*, 2580; b) Z. Yuan, H.-Y. Wang, X. Mu, P. Chen, Y.-L. Guo, G. Liu, *J. Am. Chem. Soc.* **2015**, *137*, 2468; c) C. S. Gloor, F. Dénès, P. Renaud, *Angew. Chem. Int. Ed.* **2017**, *56*, 13329; d) J. Sun, P. Li, L. Guo, F. Yu, Y.-P. He, L. Chu, *Chem. Commun.* **2018**, *54*, 3162; e) J. Zhu, W.-C. Yang, X.-d. Wang, L. Wu, *Adv. Synth. Catal.* **2018**, *360*, 386; f) N.-W. Liu, S. Liang, G. Manolikakes, *Synthesis* **2016**, *48*, 1939; g) R. Chaudhary, P. Natarajan, *ChemistrySelect* **2017**, *2*, 6458; h) A. Wimmer, B. König, *Beilstein J. Org. Chem.* **2018**, *14*, 54.
- [8] T. Rawner, M. Knorn, E. Lutsker, A. Hossain, O. Reiser, *J. Org. Chem.* **2016**, *81*, 7139.
- [9] D. B. Bagal, G. Kachkovskyi, M. Knorn, T. Rawner, B. M. Bhanage, O. Reiser, *Angew. Chem. Int. Ed.* **2015**, *54*, 6999.
- [10] Use of copper in visible-light-mediated transformations see: A. Hossain, A. Bhattacharya, O. Reiser, *Science* **2019**, *364*, eaav9713.
- [11] a) S. Paria, O. Reiser, *ChemCatChem* **2014**, *6*, 2477; b) O. Reiser, *Acc. Chem. Res.* **2016**, *49*, 1990.
- [12] S. H. Oh, Y. R. Malpani, N. Ha, Y.-S. Jung, S. B. Han, *Org. Lett.* **2014**, *16*, 1310.
- [13] a) S. K. Pagire, S. Paria, O. Reiser, *Org. Lett.* **2016**, *18*, 2106; b) S. K. Pagire, A. Hossain, O. Reiser, *Org. Lett.* **2018**, *20*, 648.
- [14] a) M. Asscher, D. Vofsi, *J. Chem. Soc.* **1964**, 4962; b) W. Truce, C. Goralski, *J. Org. Chem.* **1970**, *35*, 4220.
- [15] a) A. Hossain, S. Engl, E. Lutsker, O. Reiser, *ACS Catal.* **2019**, *9*, 1103; b) This paper appeared immediately after acceptance of our manuscript. The authors have reported the same transformation using a copper-photocatalyst, but they could only use activated olefins as substrates, no successful example for an unactivated olefin. M. Alkan-Zambada, X. Hu, *J. Org. Chem.* **2019**, *84*, 4525.
- [16] C.-J. Wallentin, J. D. Nguyen, P. Finkbeiner, C. R. J. Stephenson, *J. Am. Chem. Soc.* **2012**, *134*, 8875.
- [17] T.-f. Niu, D. Lin, L.-s. Xue, D.-y. Jiang, B.-q. Ni, *Synlett* **2018**, *29*, 364.
- [18] This paper appeared when our manuscript was under revision. The authors have reported a [Ir(ppy)<sub>3</sub>]-catalyzed difunctionalization strategy of activated alkynes using aromatic

## Chapter 6: Introducing Copper(II)-Catalyst to Photochemical ATRA Reactions

---

- sulfonyl chlorides; no examples for alkenes as substrates. P. Chakrasali, K. Kim, Y.-S. Jung, H. Kim, S. B. Han, *Org. Lett.* **2018**, *20*, 7509.
- [19] S. Mao, Y.-R. Gao, X.-Q. Zhu, D.-D. Guo, Y.-Q. Wang, *Org. Lett.* **2015**, *17*, 1692.
- [20] a) P. Evans, M. Leffray, *Tetrahedron* **2003**, *59*, 7973; b) J.-N. Desrosiers, A. B. Charette, *Angew. Chem. Int. Ed.* **2007**, *46*, 5955.
- [21] a) B. M. Trost, D. M. T. Chan, *J. Am. Chem. Soc.* **1982**, *104*, 3733; b) D. Sahu, S. Dey, T. Pathak, B. Ganguly, *Org. Lett.* **2014**, *16*, 2100.
- [22] S. Farhat, I. Marek, *Angew. Chem. Int. Ed.* **2002**, *41*, 1410.
- [23] X.-J. Tang, W. R. Dolbier, *Angew. Chem. Int. Ed.* **2015**, *54*, 4246.
- [24] J. K. Kochi, *J. Am. Chem. Soc.* **1962**, *84*, 2121.
- [25] H.-C. Liang, E. Kim, C. D. Incarvito, A. L. Rheingold, K. D. Karlin, *Inorg. Chem.* **2002**, *41*, 2209.
- [26] a) C. Le, T. Q. Chen, T. Liang, P. Zhang, D. W. C. MacMillan, *Science* **2018**, *360*, 1010; b) M. Mitani, I. Kato, K. Koyama, *J. Am. Chem. Soc.* **1983**, *105*, 6719.



## Chapter 6: Introducing Copper(II)-Catalyst to Photochemical ATRA Reactions

---

### Experimental section:

#### General information:

All commercial chemical materials were used as received without further purification and weight was calculated based on purity mentioned in the container. All photochemical reactions were performed under nitrogen atmosphere. All the reactions were monitored by TLC and visualized by a dual short (254 nm) / long (366 nm) wavelength UV lamp. Analytical thin layer chromatography was performed on Merck TLC aluminum sheets silica gel 60 F 254. Purifications by column chromatography were performed on silica gel (0.063-0.200 mm). Melting points were recorded on Stanford Research Systems OptiMelt MPA 100 Automated melting point system. All products were characterized by appropriate techniques such as <sup>1</sup>H-NMR, <sup>19</sup>F-NMR, <sup>13</sup>C-NMR, FT-IR and HRMS analysis. FT-IR (Cary 630) spectroscopy was carried out on a spectrometer, equipped with a Diamond Single Reflection ATR-System. NMR spectra were recorded on Bruker Advance 300 MHz and 400 MHz spectrometers. Chemical shifts for <sup>1</sup>H-NMR were reported as  $\delta$ , parts per million, relative to the signal of CHCl<sub>3</sub> at 7.26 ppm. Chemical shifts for <sup>13</sup>C-NMR were reported as  $\delta$ , parts per million, relative to the signal of CHCl<sub>3</sub> at 77.2 ppm and TMS as an internal standard. Coupling constants (*J*) are given in Hertz (Hz). The following notations indicate the multiplicity of the signals: s = singlet, br-s = broad singlet, d = doublet, t = triplet, q = quartet, p = pentet, hept = heptet, dd = doublet of doublets, dt = doublet of triplets, td = triplet of doublets, tt = triplet of triplets, qd = quartet of doublets, ddd = doublet of doublet of doublets, dtd = doublet of triplet of doublets, dqd = doublet of quartet of doublets, tdd = triplet of doublet of doublets, dddd = doublet of doublet of doublet of doublets and m = multiplet. Mass spectra were recorded at the Central Analytical Laboratory at the Department of Chemistry of the University of Regensburg on Agilent Technologies 6540 UHD Accurate-Mass Q-TOF LC/MS. The irradiation was done using blue light emitting diodes CREE XP or Oslon SSL (2.5 W electric power @700 mA,  $\lambda_{\max}$  = 530 nm). In the case of no full conversion, the yields are also given based on recovered starting material (brsm).

Experimental set up:

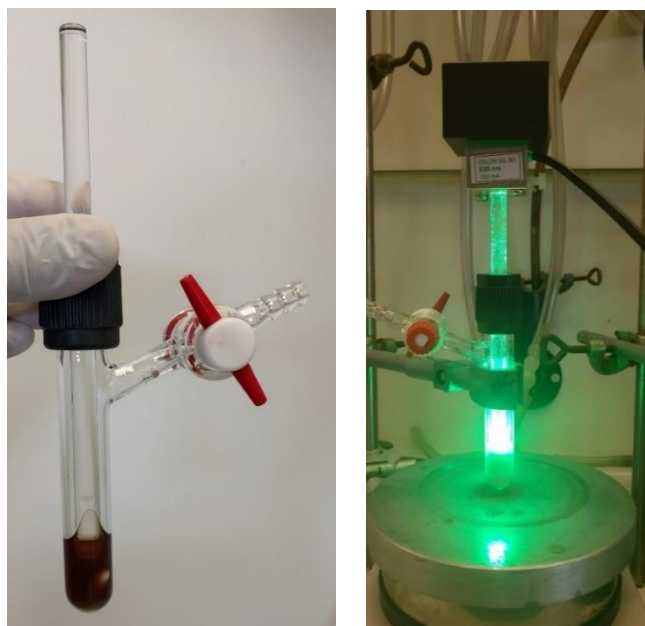
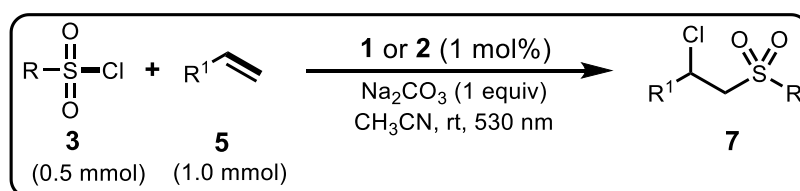


Figure 1: Experimental set up for chlorosulfonation of olefins

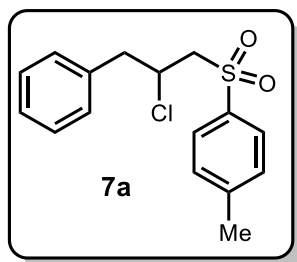
General Procedure for chlorosulfonylation of unactivated olefins (GP-A):



To an oven dried nitrogen tube (10 mL size) equipped with a stirring bar was charged with sulfonyl chloride derivative **3** (0.50 mmol, 1.00 equiv), Na<sub>2</sub>CO<sub>3</sub> (53 mg, 0.50 mmol, 1.00 equiv) and [Cu(dap)<sub>2</sub>]Cl (4.4 mg, 1.00 mol%, 0.01 equiv). Then 2 mL dry CH<sub>3</sub>CN was added under positive nitrogen atmosphere. The solution was degassed by three freeze-pump-thaw cycles. Then desired olefin **5** was added (1.00 mmol, 2.00 equiv) under nitrogen. The reaction mixture was exposed to the Green light emitting diode (LED, λ<sub>max</sub> = 530 nm) at room temperature for mentioned time. After complete conversion of sulfonyl chloride (judged by TLC), the reaction mixture was saturated by addition of brine solution (20 mL). The aqueous phase was washed with ethyl acetate (3 x 20 mL). The combined organic fractions were dried over Na<sub>2</sub>SO<sub>4</sub>, concentrated *in vacuo*, and the crude residue was purified by flash column chromatography on silica gel by using hexanes and ethyl acetate as eluents to afford the pure product **7**.

## Chapter 6: Introducing Copper(II)-Catalyst to Photochemical ATRA Reactions

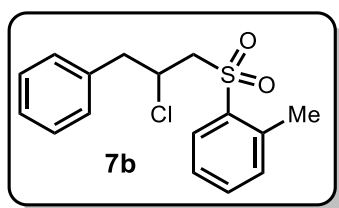
### 1-((2-chloro-3-phenylpropyl)sulfonyl)-4-methylbenzene (**7a**):



Following GP-A, **7a** was prepared from 4-methylbenzenesulfonyl chloride **3a** (95.3 mg, 0.50 mmol, 1.00 equiv) and allyl benzene **4a** (133  $\mu$ L, 1.00 mmol, 2.00 equiv). The crude product was purified by flash column chromatography (hexanes-EtOAc = 4:1,  $R_f$  = 0.22) to afford **7a** as a white solid (142 mg, 92% yield).

**$^1\text{H}$  NMR (400 MHz,  $\text{CDCl}_3$ ):**  $\delta$  7.68 (d,  $J$  = 8.3 Hz, 2H), 7.24 (d,  $J$  = 8.1 Hz, 2H), 7.20 – 7.14 (m, 3H), 7.11 – 7.09 (m, 2H), 4.41 – 4.35 (m, 1H), 3.40 (d,  $J$  = 6.2 Hz, 2H), 3.20 – 2.96 (m, 2H), 2.34 (s, 3H);  **$^{13}\text{C}$  NMR (100 MHz,  $\text{CDCl}_3$ ):**  $\delta$  145.3, 136.5, 136.0, 130.1, 129.7, 128.7, 128.3, 127.4, 62.5, 54.6, 44.0, 21.8; **IR (neat,  $\text{cm}^{-1}$ ):** 3061, 3030, 2924, 1596, 1495, 1453, 1400, 1316, 1300, 1147, 1085, 815, 746; **HRMS (ESI):** exact  $m/z$  calculated for  $\text{C}_{16}\text{H}_{17}\text{ClO}_2\text{S}$  ( $\text{M}+\text{H}$ ) $^+$ : 309.0718; Found: 309.0719 ( $\text{M}+\text{H}$ ) $^+$ .

### 1-((2-chloro-3-phenylpropyl)sulfonyl)-2-methylbenzene (**7b**):



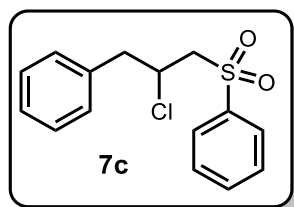
Following GP-A, **7b** was prepared from 2-methylbenzenesulfonyl chloride **3b** (98 mg, 0.50 mmol, 1.00 equiv) and allyl benzene **5a** (133  $\mu$ L, 1.00 mmol, 2.00 equiv). The crude product was purified by flash column chromatography (hexanes-EtOAc = 4:1,  $R_f$  = 0.20) to afford **7b** as a white solid (100 mg, 67% yield).

**$^1\text{H}$  NMR (300 MHz,  $\text{CDCl}_3$ ):**  $\delta$  8.03 (dd,  $J_1$  = 7.9 Hz,  $J_2$  = 1.3 Hz, 1H), 7.53 (dt,  $J_1$  = 7.5 Hz,  $J_2$  = 1.3 Hz, 1H), 7.41 – 7.27 (m, 5H), 7.20 – 7.17 (m, 2H), 4.54 – 4.56 (m, 1H), 3.55 (dd,  $J_1$  = 6.2 Hz,  $J_2$  = 1.3 Hz, 2H), 3.28 – 3.09 (m, 2H), 2.57 (s, 3H);  **$^{13}\text{C}$  NMR (75 MHz,  $\text{CDCl}_3$ ):**  $\delta$  138.1, 137.4, 136.0, 134.2, 133.0, 130.4, 129.7, 128.8, 127.5, 126.9, 61.3, 54.4, 44.1, 20.3; **IR**

## Chapter 6: Introducing Copper(II)-Catalyst to Photochemical ATRA Reactions

(neat,  $\text{cm}^{-1}$ ): 3062, 3029, 2928, 1596, 1495, 1471, 1453, 1390, 1306, 1150, 1125, 1059, 895; HRMS (ESI): exact  $m/z$  calculated for  $\text{C}_{16}\text{H}_{17}\text{ClO}_2\text{S}$  ( $\text{M}+\text{H}$ )<sup>+</sup>: 309.0718; Found: 309.0719 ( $\text{M}+\text{H}$ )<sup>+</sup>.

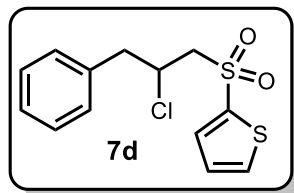
### (2-chloro-3-(phenylsulfonyl)propyl)benzene (7c):



Following GP-A, **7c** was prepared from benzenesulfonyl chloride **3c** (88 mg, 0.50 mmol, 1.00 equiv) and allyl benzene **5a** (133  $\mu\text{L}$ , 1.00 mmol, 2.00 equiv). The crude product was purified by flash column chromatography (hexanes-EtOAc = 4:1,  $R_f$  = 0.20) to afford **7c** as a colorless oil (140 mg, 95% yield).

<sup>1</sup>H NMR (300 MHz,  $\text{CDCl}_3$ ):  $\delta$  7.93 – 7.90 (m, 2H), 7.69 – 7.64 (m, 1H), 7.59 – 7.53 (m, 2H), 7.34 – 7.27 (m, 3H), 7.22 – 7.19 (m, 2H), 4.56 – 4.48 (m, 1H), 3.54 (d,  $J$  = 6.2 Hz, 2H), 3.33 – 3.07 (m, 2H); <sup>13</sup>C NMR (75 MHz,  $\text{CDCl}_3$ ):  $\delta$  139.3, 135.9, 134.2, 129.6, 129.5, 128.7, 128.2, 127.4, 62.2, 54.4, 43.9; IR (neat,  $\text{cm}^{-1}$ ): 3062, 3029, 2923, 1602, 1495, 1446, 1394, 1304, 1136, 1083, 1025; HRMS (ESI): exact  $m/z$  calculated for  $\text{C}_{15}\text{H}_{15}\text{ClO}_2\text{S}$  ( $\text{M}+\text{H}$ )<sup>+</sup>: 295.0561; Found: 295.0557 ( $\text{M}+\text{H}$ )<sup>+</sup>.

### 2-((2-chloro-3-phenylpropyl)sulfonyl)thiophene (7d):

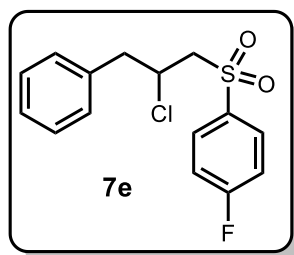


Following GP-A, **7d** was prepared from 2-thiophenesulfonyl chloride **3d** (95.3 mg, 0.50 mmol, 1.00 equiv) and allyl benzene **5a** (133  $\mu\text{L}$ , 1.00 mmol, 2.00 equiv). The crude product was purified by flash column chromatography (hexanes-EtOAc = 4:1,  $R_f$  = 0.20) to afford **7d** as a colorless oil (125 mg, 83% yield).

## Chapter 6: Introducing Copper(II)-Catalyst to Photochemical ATRA Reactions

$^1\text{H NMR}$  (300 MHz,  $\text{CDCl}_3$ ):  $\delta$  7.75 – 7.71 (m, 2H), 7.33 – 7.14 (m, 7H), 4.57 – 4.48 (m, 1H), 3.64 (d,  $J = 6.2$  Hz, 2H), 3.32 – 3.09 (m, 2H);  $^{13}\text{C NMR}$  (75 MHz,  $\text{CDCl}_3$ ):  $\delta$  140.1, 135.8, 134.97, 134.90, 129.7, 128.7, 128.2, 127.5, 63.6, 54.5, 43.9. **IR** (neat,  $\text{cm}^{-1}$ ): 3062, 3031, 1642, 1603, 1520, 1492, 1344, 1298, 1145, 1097, 988, 856; **HRMS** (ESI): exact  $m/z$  calculated for  $\text{C}_{13}\text{H}_{13}\text{ClO}_2\text{S}_2$  ( $\text{M}+\text{H}$ ) $^+$ : 301.0125; Found: 301.0123 ( $\text{M}+\text{H}$ ) $^+$ .

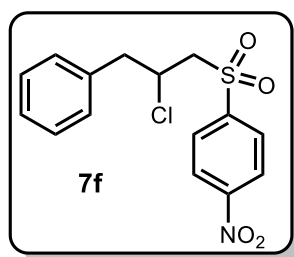
### 1-((2-chloro-3-phenylpropyl)sulfonyl)-4-fluorobenzene (7e):



Following GP-A, **7e** was prepared from 4-fluorobenzenesulfonyl chloride **3e** (99.3 mg, 0.50 mmol, 1.00 equiv) and allyl benzene **5a** (133  $\mu\text{L}$ , 1.00 mmol, 2.00 equiv). The crude product was purified by flash column chromatography (hexanes-EtOAc = 4:1,  $R_f = 0.38$ ) to afford **7e** as a yellow oil (159 mg, 91% yield).

$^1\text{H NMR}$  (300 MHz,  $\text{CDCl}_3$ ):  $\delta$  7.95 – 7.90 (m, 2H), 7.34 – 7.27 (m, 3H), 7.25 – 7.19 (m, 4H), 4.56 – 4.47 (m, 1H), 3.53 – 3.51 (m, 2H), 3.27 – 3.09 (m, 2H);  $^{13}\text{C NMR}$  (75 MHz,  $\text{CDCl}_3$ ):  $\delta$  166.0 (d,  $^1J_{\text{C-F}} = 257.0$  Hz), 135.7, 135.4 (d,  $^4J_{\text{C-F}} = 3.0$  Hz), 131.3 (d,  $^3J_{\text{C-F}} = 9.6$  Hz), 129.6, 128.8, 127.5, 116.8 (d,  $^2J_{\text{C-F}} = 22.7$  Hz), 62.4, 54.4, 44.1;  $^{19}\text{F NMR}$  (282 MHz,  $\text{CDCl}_3$ ):  $\delta$  -103.0; **IR** (neat,  $\text{cm}^{-1}$ ): 3066, 3030, 2925, 1589, 1492, 1453, 1404, 1318, 1289, 1232, 1137, 1083, 1010, 817; **HRMS** (ESI): exact  $m/z$  calculated for  $\text{C}_{15}\text{H}_{14}\text{ClFO}_2\text{S}$  ( $\text{M}+\text{H}$ ) $^+$ : 313.0467; Found: 313.0464 ( $\text{M}+\text{H}$ ) $^+$ .

### 1-((2-chloro-3-phenylpropyl)sulfonyl)-4-nitrobenzene (7f):

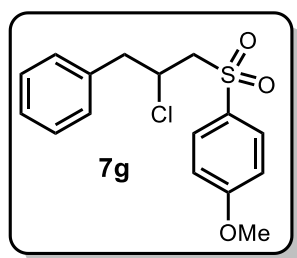


## Chapter 6: Introducing Copper(II)-Catalyst to Photochemical ATRA Reactions

Following GP-A, **7f** was prepared from 4-nitrobenzenesulfonyl chloride **3f** (114 mg, 0.50 mmol, 1.00 equiv) and allyl benzene **5a** (133  $\mu$ L, 1.00 mmol, 2.00 equiv). The crude product was purified by flash column chromatography (hexanes-EtOAc = 4:1,  $R_f$  = 0.25) to afford **7f** as a yellow solid (170 mg, 86% yield).

**$^1\text{H}$  NMR (300 MHz,  $\text{CDCl}_3$ ):**  $\delta$  8.38 (d,  $J$  = 8.8 Hz, 2H), 8.10 (d,  $J$  = 8.9 Hz, 2H), 7.33 – 7.29 (m, 3H), 7.20 – 7.17 (m, 2H), 4.58 – 4.49 (m, 1H), 3.58 – 3.56 (m, 2H), 3.16 (d,  $J$  = 6.8 Hz, 2H);  **$^{13}\text{C}$  NMR (75 MHz,  $\text{CDCl}_3$ ):**  $\delta$  151.1, 145.1, 135.4, 130.0, 129.6, 129.0, 127.8, 124.6, 62.3, 54.2, 44.3; **IR (neat,  $\text{cm}^{-1}$ ):** 3103, 2927, 1673, 1605, 1525, 1496, 1452, 1345, 1301, 1130, 1081, 1009, 898; **HRMS (ESI):** exact  $m/z$  calculated for  $\text{C}_{15}\text{H}_{14}\text{ClNO}_4\text{S}$  ( $\text{M}+\text{H}$ ) $^+$ : 340.0412; Found: 340.0411 ( $\text{M}+\text{H}$ ) $^+$ .

### 1-((2-chloro-3-phenylpropyl)sulfonyl)-4-methoxybenzene (**7g**):

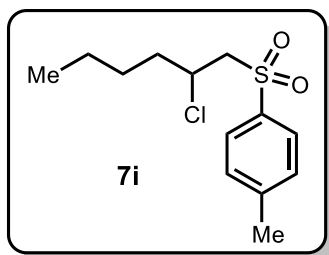


Following GP-A, **7g** was prepared from 4-methoxybenzenesulfonyl chloride **3g** (103 mg, 0.50 mmol, 1.00 equiv) and allyl benzene **5a** (133  $\mu$ L, 1.00 mmol, 2.00 equiv). The crude product was purified by flash column chromatography (hexanes-EtOAc = 4:1,  $R_f$  = 0.20) to afford **7g** as a colorless oil (100 mg, 61% yield/70% brsm).

**$^1\text{H}$  NMR (300 MHz,  $\text{CDCl}_3$ ):**  $\delta$  7.84 – 7.81 (m, 2H), 7.31 – 7.19 (m, 5H), 7.02 – 6.99 (m, 2H), 4.53 – 4.45 (m, 1H), 3.87 (s, 3H), 3.51 (d,  $J$  = 6.2 Hz, 2H), 3.31 - 3.06 (m, 2H);  **$^{13}\text{C}$  NMR (75 MHz,  $\text{CDCl}_3$ ):**  $\delta$  164.1, 136.0, 130.7, 130.4, 129.6, 128.6, 127.4, 114.6, 62.5, 55.8, 54.6, 43.9; **IR (neat,  $\text{cm}^{-1}$ ):** 3063, 3029, 2929, 2841, 1593, 1495, 1456, 1296, 1258, 1132, 1086, 1021, 942; **HRMS (ESI):** exact  $m/z$  calculated for  $\text{C}_{16}\text{H}_{17}\text{ClO}_3\text{S}$  ( $\text{M}+\text{H}$ ) $^+$ : 325.0667; Found: 325.0666 ( $\text{M}+\text{H}$ ) $^+$ .

## Chapter 6: Introducing Copper(II)-Catalyst to Photochemical ATRA Reactions

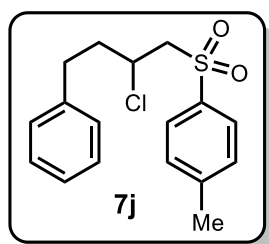
### 1-((2-chlorohexyl)sulfonyl)-4-methylbenzene (**7i**):



Following GP-A, **7i** was prepared from 4-methylbenzenesulfonyl chloride **3a** (95.3 mg, 0.50 mmol, 1.00 equiv) and 1-hexene **5c** (127  $\mu$ L, 1.00 mmol, 2.00 equiv). The crude product was purified by flash column chromatography (hexanes-EtOAc = 4:1,  $R_f$  = 0.35) to afford **7i** as a colorless oil (129 mg, 92% yield).

$^1\text{H NMR}$  (300 MHz,  $\text{CDCl}_3$ ):  $\delta$  7.79 (d,  $J$  = 8.2 Hz, 2H), 7.36 (d,  $J$  = 8.3 Hz, 2H), 4.33 – 4.25 (m, 1H), 3.59 – 3.41 (m, 2H), 2.45 (s, 3H), 2.03 – 1.92 (m, 1H), 1.81 – 1.68 (m, 1H), 1.49 – 1.26 (m, 4H), 0.89 (t,  $J$  = 7.1 Hz, 3H);  $^{13}\text{C NMR}$  (75 MHz,  $\text{CDCl}_3$ ):  $\delta$  145.3, 136.6, 130.1, 128.3, 63.6, 54.7, 37.7, 28.0, 22.0, 21.8, 14.0; IR (neat,  $\text{cm}^{-1}$ ): 2957, 2930, 2864, 1596, 1493, 1458, 1401, 1316, 1301, 1140, 1017, 938, 815; HRMS (ESI): exact  $m/z$  calculated for  $\text{C}_{13}\text{H}_{19}\text{ClO}_2\text{S}$  ( $\text{M}+\text{H}$ ) $^+$ : 275.0874; Found: 275.0874 ( $\text{M}+\text{H}$ ) $^+$ .

### 1-((2-chloro-4-phenylbutyl)sulfonyl)-4-methylbenzene (**7j**):



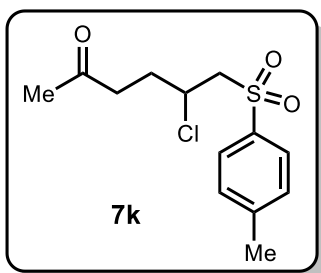
Following GP-A, **7j** was prepared from 4-methylbenzenesulfonyl chloride **3a** (95.3 mg, 0.50 mmol, 1.00 equiv) and homo allyl benzene **5d** (132 mg, 1.00 mmol, 2.00 equiv). The crude product was purified by flash column chromatography (hexanes-EtOAc = 4:1,  $R_f$  = 0.25) to afford **7j** as a colorless oil (119 mg, 74% yield).

$^1\text{H NMR}$  (300 MHz,  $\text{CDCl}_3$ ):  $\delta$  7.67 (d,  $J$  = 8.3 Hz, 2H), 7.33 – 7.17 (m, 7H), 4.21 – 4.13 (m, 1H), 3.61 – 3.44 (m, 2H), 2.93 – 2.69 (m, 2H), 2.44 (s, 3H), 2.41 – 1.99 (m, 2H);  $^{13}\text{C NMR}$  (75 MHz,  $\text{CDCl}_3$ ):  $\delta$  145.2, 140.1, 136.1, 130.1, 128.7, 128.6, 128.2, 126.4, 63.4, 53.8, 39.3,

## Chapter 6: Introducing Copper(II)-Catalyst to Photochemical ATRA Reactions

32.0, 21.7; **IR** (neat,  $\text{cm}^{-1}$ ): 3061, 3027, 2924, 1596, 1494, 1453, 1401, 1315, 1301, 1136, 1085, 1031, 814; **HRMS (ESI)**: exact  $m/z$  calculated for  $\text{C}_{17}\text{H}_{19}\text{ClO}_2\text{S}$  ( $\text{M}+\text{H}$ )<sup>+</sup>: 323.0874; Found: 323.0874 ( $\text{M}+\text{H}$ )<sup>+</sup>.

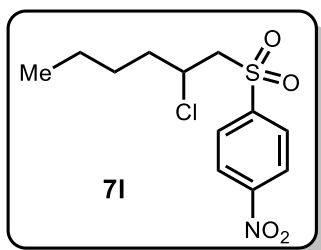
### 5-chloro-6-tosylhexan-2-one (**7k**):



Following GP-A, **7k** was prepared from 4-methylbenzenesulfonyl chloride **3a** (95.3 mg, 0.50 mmol, 1.00 equiv) and hex-5-en-2-one **5e** (116  $\mu\text{L}$ , 1.00 mmol, 2.00 equiv). The crude product was purified by flash column chromatography (hexanes-EtOAc = 4:1,  $R_f$  = 0.30) to afford **7k** as a colorless oil (108 mg, 74% yield).

**$^1\text{H}$  NMR (300 MHz,  $\text{CDCl}_3$ )**:  $\delta$  7.80 (d,  $J$  = 8.2 Hz, 2H), 7.36 (d,  $J$  = 8.3 Hz, 2H), 4.35 – 4.27 (m, 1H), 3.59 – 3.41 (m, 2H), 2.68 – 2.62 (m, 2H), 2.44 (s, 3H), 2.41 – 2.49 (m, 1H), 2.14 (s, 3H), 1.98 – 1.88 (m, 1H);  **$^{13}\text{C}$  NMR (75 MHz,  $\text{CDCl}_3$ )**:  $\delta$  206.9, 145.4, 136.3, 130.1, 128.3, 63.6, 53.9, 39.6, 31.7, 30.1, 21.8; **IR** (neat,  $\text{cm}^{-1}$ ): 2959, 2924, 1712, 1596, 1493, 1404, 1359, 1301, 1289, 1137, 1085, 815; **HRMS (ESI)**: exact  $m/z$  calculated for  $\text{C}_{13}\text{H}_{17}\text{ClO}_3\text{S}$  ( $\text{M}+\text{H}$ )<sup>+</sup>: 289.0667; Found: 289.0663 ( $\text{M}+\text{H}$ )<sup>+</sup>.

### 1-((2-chlorohexyl)sulfonyl)-4-nitrobenzene (**7l**):



Following GP-A, **7l** was prepared from 4-nitrobenzenesulfonyl chloride **3f** (114 mg, 0.50 mmol, 1.00 equiv) and 1-hexene **5c** (127  $\mu\text{L}$ , 1.00 mmol, 2.00 equiv). The crude product was

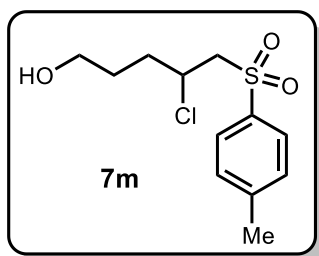


## Chapter 6: Introducing Copper(II)-Catalyst to Photochemical ATRA Reactions

purified by flash column chromatography (hexanes-EtOAc = 4:1,  $R_f = 0.30$ ) to afford **7l** as a yellow solid (140 mg, 89% yield).

**$^1\text{H}$  NMR (300 MHz,  $\text{CDCl}_3$ ):**  $\delta$  8.42 (d,  $J = 8.7$  Hz, 2H), 8.14 (d,  $J = 8.8$  Hz, 2H), 4.39 – 4.30 (m, 1H), 3.67 – 3.49 (m, 2H), 1.96 – 1.71 (m, 2H), 1.52 – 1.26 (m, 4H), 0.90 (t,  $J = 7.0$  Hz, 3H);  **$^{13}\text{C}$  NMR (75 MHz,  $\text{CDCl}_3$ ):**  $\delta$  151.1, 145.3, 130.0, 124.6, 63.7, 54.4, 37.9, 27.9, 22.0, 13.9; **IR (neat,  $\text{cm}^{-1}$ ):** 3105, 2958, 2931, 2867, 1606, 1528, 1463, 1400, 1347, 1302, 1143, 1084, 853; **HRMS (ESI):** exact  $m/z$  calculated for  $\text{C}_{12}\text{H}_{16}\text{ClNO}_4\text{S}$  ( $\text{M}+\text{H}$ ) $^+$ : 306.0569; Found: 306.0567 ( $\text{M}+\text{H}$ ) $^+$ .

### 4-chloro-5-tosylpentan-1-ol (**7m**):

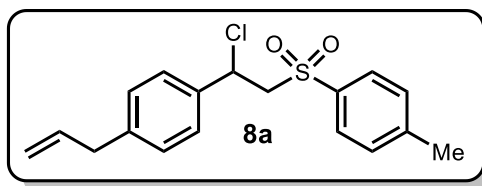


Following GP-A, **7m** was prepared from 4-methylbenzenesulfonyl chloride **3a** (95.3 mg, 0.50 mmol, 1.00 equiv) and 4-penten-1-ol **5b** (103  $\mu\text{L}$ , 1.00 mmol, 2.00 equiv). The crude product was purified by flash column chromatography (hexanes-EtOAc = 4:1,  $R_f = 0.20$ ) to afford **7m** as a yellow oil (91 mg, 65% yield).

**$^1\text{H}$  NMR (300 MHz,  $\text{CDCl}_3$ ):**  $\delta$  7.79 (d,  $J = 8.2$  Hz, 2H), 7.36 (d,  $J = 8.0$  Hz, 2H), 4.39 – 4.30 (m, 1H), 3.66 (t,  $J = 6.0$  Hz, 2H), 3.60 – 3.43 (m, 2H), 2.45 (s, 3H), 2.19 – 2.08 (m, 1H), 1.91 – 1.66 (m, 4H);  **$^{13}\text{C}$  NMR (75 MHz,  $\text{CDCl}_3$ ):**  $\delta$  145.4, 136.4, 130.2, 128.3, 63.5, 61.8, 54.4, 34.5, 28.9, 21.8. **IR (neat,  $\text{cm}^{-1}$ ):** 3529, 2926, 2875, 1596, 1445, 1400, 1289, 1136, 1084, 1056, 917; **HRMS (ESI):** exact  $m/z$  calculated for  $\text{C}_{12}\text{H}_{17}\text{ClO}_3\text{S}$  ( $\text{M}+\text{H}$ ) $^+$ : 277.0667; Found: 277.0666 ( $\text{M}+\text{H}$ ) $^+$ .

## Chapter 6: Introducing Copper(II)-Catalyst to Photochemical ATRA Reactions

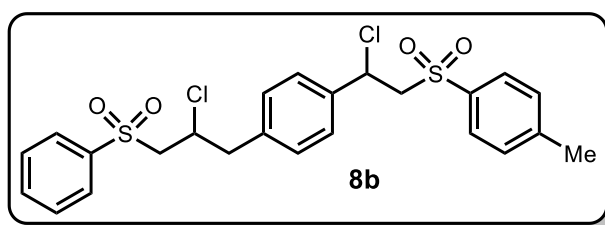
### 1-allyl-4-(1-chloro-2-tosylethyl)benzene (**8a**):



To an oven dried nitrogen tube (10 mL size) equipped with a stirring bar was charged with 4-methylbenzenesulfonyl chloride **3a** (72.4 mg, 0.38 mmol, 1.00 equiv) and [Cu(dap)<sub>2</sub>]Cl (4.4 mg, 1.00 mol%, 0.01 equiv) or [Cu(dap)Cl<sub>2</sub>] (2.6 mg, 1.00 mol%, 0.01 equiv). Then 2 mL dry CH<sub>3</sub>CN was added under positive nitrogen atmosphere. The solution was degassed by three freeze-pump-thaw cycles. Then olefin **8** was added (55 mg, 0.38 mmol, 1.00 equiv) under nitrogen. The reaction mixture was exposed to the green light emitting diode (LED,  $\lambda_{max}$  = 530 nm) at room temperature for 24 h. After complete conversion of sulfonyl chloride (judged by TLC), the reaction mixture was transferred to a round bottom flask, concentrated *in vacuo*, and the crude product was purified by flash column chromatography (hexanes-EtOAc = 4:1,  $R_f$  = 0.25) to afford **8a** as a white solid (99 mg, 80% yield).

**<sup>1</sup>H NMR (300 MHz, CDCl<sub>3</sub>):**  $\delta$  7.59 (d,  $J$  = 8.3 Hz, 2H), 7.23 – 7.16 (m, 4H), 7.07 (d,  $J$  = 8.2 Hz, 2H), 5.97 – 5.83 (m, 1H), 5.31 (t,  $J$  = 6.8 Hz, 1H), 5.11 – 5.04 (m, 2H), 3.97 – 3.81 (m, 2H), 3.33 (d,  $J$  = 6.7 Hz, 2H), 2.40 (s, 3H); **<sup>13</sup>C NMR (75 MHz, CDCl<sub>3</sub>):**  $\delta$  144.9, 141.4, 136.9, 136.4, 136.3, 129.8, 129.1, 128.3, 127.3, 116.4, 64.2, 55.2, 40.0, 21.8; **IR (neat, cm<sup>-1</sup>):** 2978, 2924, 1638, 1596, 1424, 1402, 1318, 1301, 1264, 1153, 1136, 1085, 912, 812; **HRMS (ESI):** exact  $m/z$  calculated for C<sub>18</sub>H<sub>19</sub>ClO<sub>2</sub>S (M+Na)<sup>+</sup>: 357.0647; Found: 357.0693 (M+Na)<sup>+</sup>.

### 1-((2-chloro-2-(4-(2-chloro-3-(phenylsulfonyl)propyl)phenyl)ethyl)sulfonyl)-4-methylbenzene (**8b**):



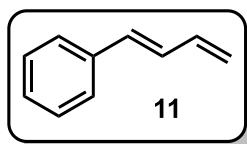
Following GP-A, **8b** was prepared from benzenesulfonyl chloride **3c** (17.6 mg, 0.10 mmol, 1.00 equiv) and 1-allyl-4-(1-chloro-2-tosylethyl)benzene **8a** (67 mg, 1.00 mmol, 2.00 equiv).

## Chapter 6: Introducing Copper(II)-Catalyst to Photochemical ATRA Reactions

The crude product was purified by flash column chromatography (hexanes-EtOAc = 3:1,  $R_f$  = 0.22) to afford **8b** as a colorless oil (51 mg, 69% yield).

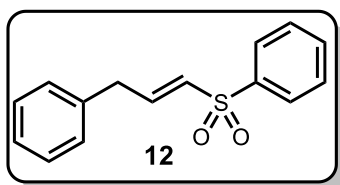
$^1\text{H NMR}$  (300 MHz,  $\text{CDCl}_3$ ):  $\delta$  7.91 (d,  $J$  = 7.3 Hz, 2H), 7.68 – 7.55 (m, 5H), 7.27 – 7.13 (m, 6H), 5.32 (t,  $J$  = 6.8 Hz, 1H), 4.51 – 4.44 (m, 1H), 3.96 – 3.78 (m, 2H), 3.53 – 3.49 (m, 2H), 3.34 – 3.28 (m, 1H), 3.10 – 3.01 (m, 1H), 2.40 (s, 3H);  $^{13}\text{C NMR}$  (75 MHz,  $\text{CDCl}_3$ ):  $\delta$  145.1, 139.3, 137.9, 137.1, 136.3, 134.4, 130.3, 129.9, 129.6, 128.3, 128.2, 127.5, (64.2, 64.1), 62.3, 54.9, (54.24, 54.21), (43.43, 43.40), 21.8; **IR** (neat,  $\text{cm}^{-1}$ ): 3062, 2983, 2926, 1597, 1513, 1492, 1446, 1426, 1401, 1318, 1303, 1267, 1153, 1138, 1085, 91; **HRMS** (ESI): exact  $m/z$  calculated for  $\text{C}_{24}\text{H}_{24}\text{Cl}_2\text{O}_4\text{S}_2$  ( $\text{M}+\text{H}$ ) $^+$ : 511.0573; Found: 511.0573 ( $\text{M}+\text{H}$ ) $^+$ .

### (*E*)-buta-1,3-dien-1-ylbenzene (**11**):



This double elimination protocol was inspired from previously reported work.<sup>[1]</sup> A schlenk tube (10 mL size) with stirring bar was charged with 1-((2-chloro-4-phenylbutyl)sulfonyl)-4-methylbenzene (**7j**) (65 mg, 0.2 mmol, 1.00 equiv) and dry THF (2 mL) was added. Then  $t\text{BuOK}$  (89.7 mg, 0.8 mmol, 4.00 equiv) was added to the solution under positive nitrogen atmosphere. The solution was then refluxed for 90 min. After work up, chromatographic purification afforded **11** (15 mg, 50% yield). The obtained NMR matched with previous report.<sup>[2]</sup>

### (*E*)-((3-phenylprop-1-en-1-yl)sulfonyl)benzene (**12**):



A mixture of (2-chloro-3-(phenylsulfonyl)propyl)benzene **7c** (85.0 mg, 0.30 mmol, 1.00 equiv.) and triethylamine (125  $\mu\text{L}$ , 0.90 mmol, 3.00 equiv.) in 2 mL  $\text{CHCl}_3$  was stirred at room temperature for 30 min and monitored by TLC. Afterwards, the reaction mixture was filtered

## ***Chapter 6: Introducing Copper(II)-Catalyst to Photochemical ATRA Reactions***

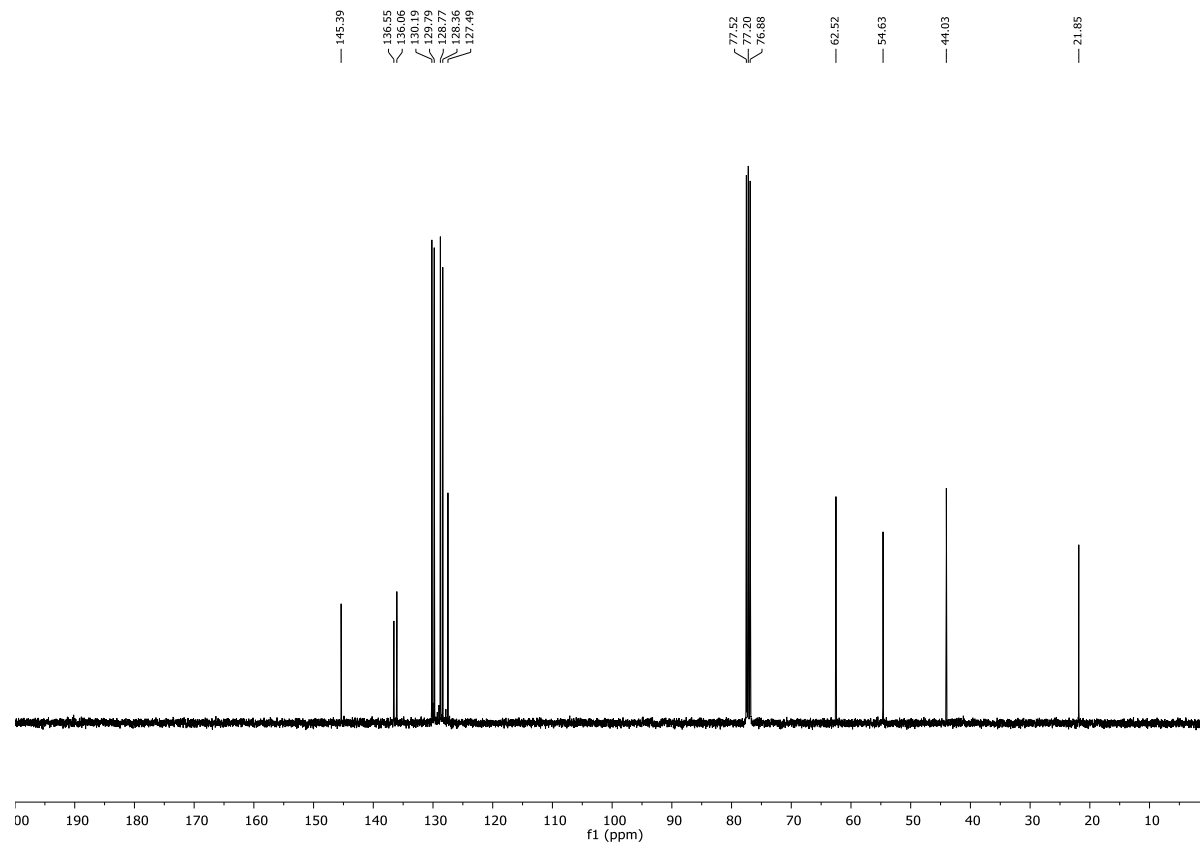
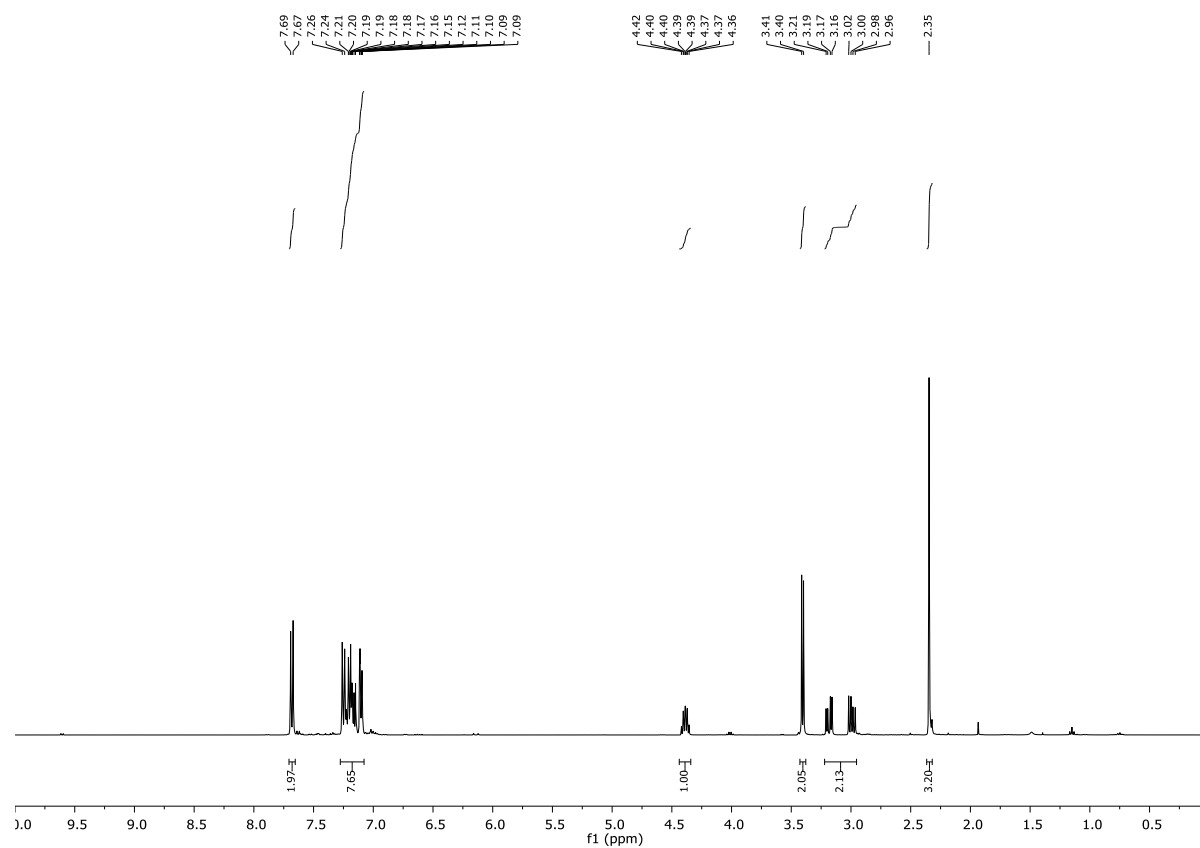
---

and the solvents as well as residues of triethylamine were removed under reduced pressure. Then the crude reaction mixture was purified by column chromatography (hexanes-EtOAc = 5:1,  $R_f = 0.35$ ) to afford **12** (63 mg, 86%) as white solid.

**$^1\text{H}$  NMR (300 MHz,  $\text{CDCl}_3$ ):**  $\delta$  7.89 – 7.86 (m, 2H), 7.66 – 7.60 (m, 1H), 7.55 – 7.50 (m, 2H), 7.31 – 7.27 (m, 5H), 6.39 – 6.34 (m, 1H), 6.15 – 6.04 (m, 1H), 3.95 (dd,  $J_1 = 7.5$  Hz,  $J_2 = 0.9$  Hz, 2H);  **$^{13}\text{C}$  NMR (75 MHz,  $\text{CDCl}_3$ ):**  $\delta$  139.3, 138.4, 135.8, 133.9, 129.2, 128.7, 128.64, 128.62, 126.7, 115.1, 60.5; **IR (neat,  $\text{cm}^{-1}$ ):** 3059, 3028, 2919, 1582, 1494, 1478, 1446, 1295, 1235, 1133, 1083, 966, 901, 728; **HRMS (ESI):** exact  $m/z$  calculated for  $\text{C}_{15}\text{H}_{14}\text{O}_2\text{S}$  ( $\text{M}+\text{NH}_4^+$ ): 276.1058; Found: 276.1064 ( $\text{M}+\text{NH}_4^+$ ).

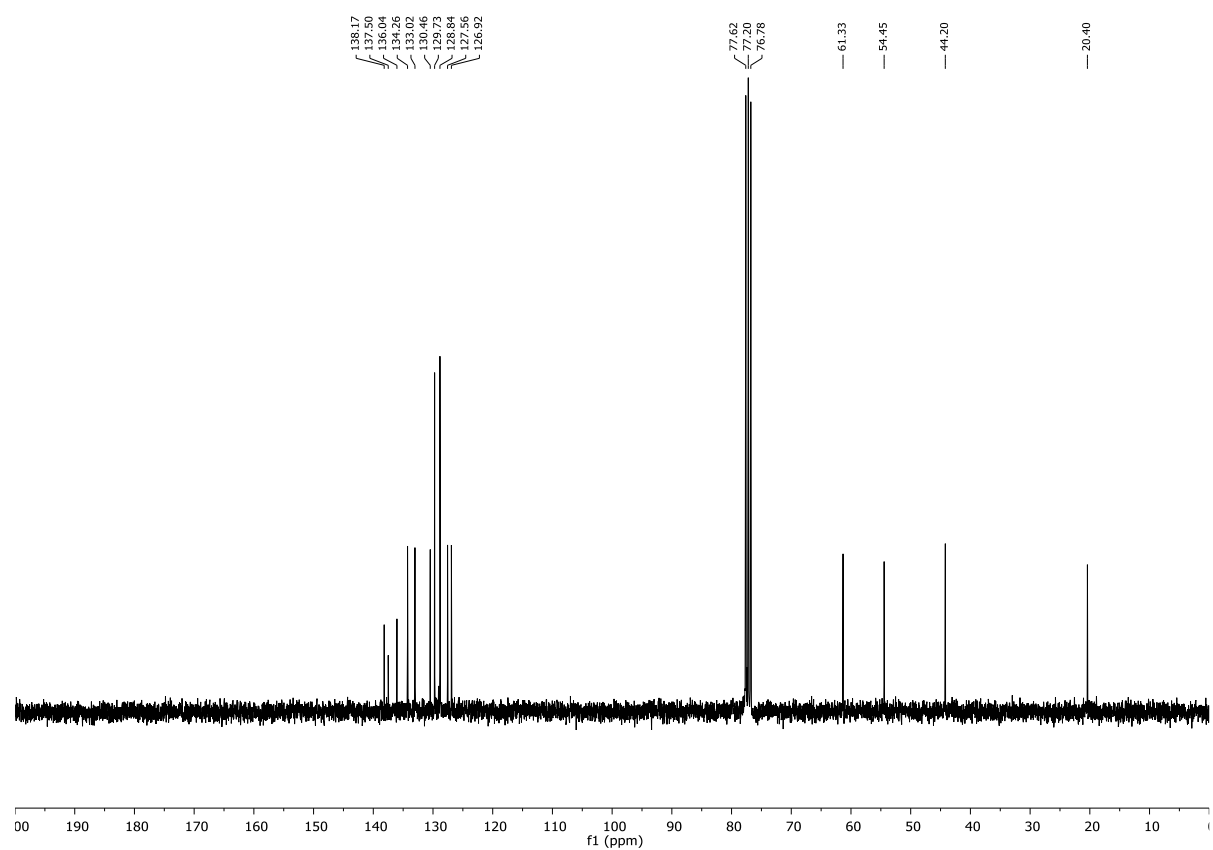
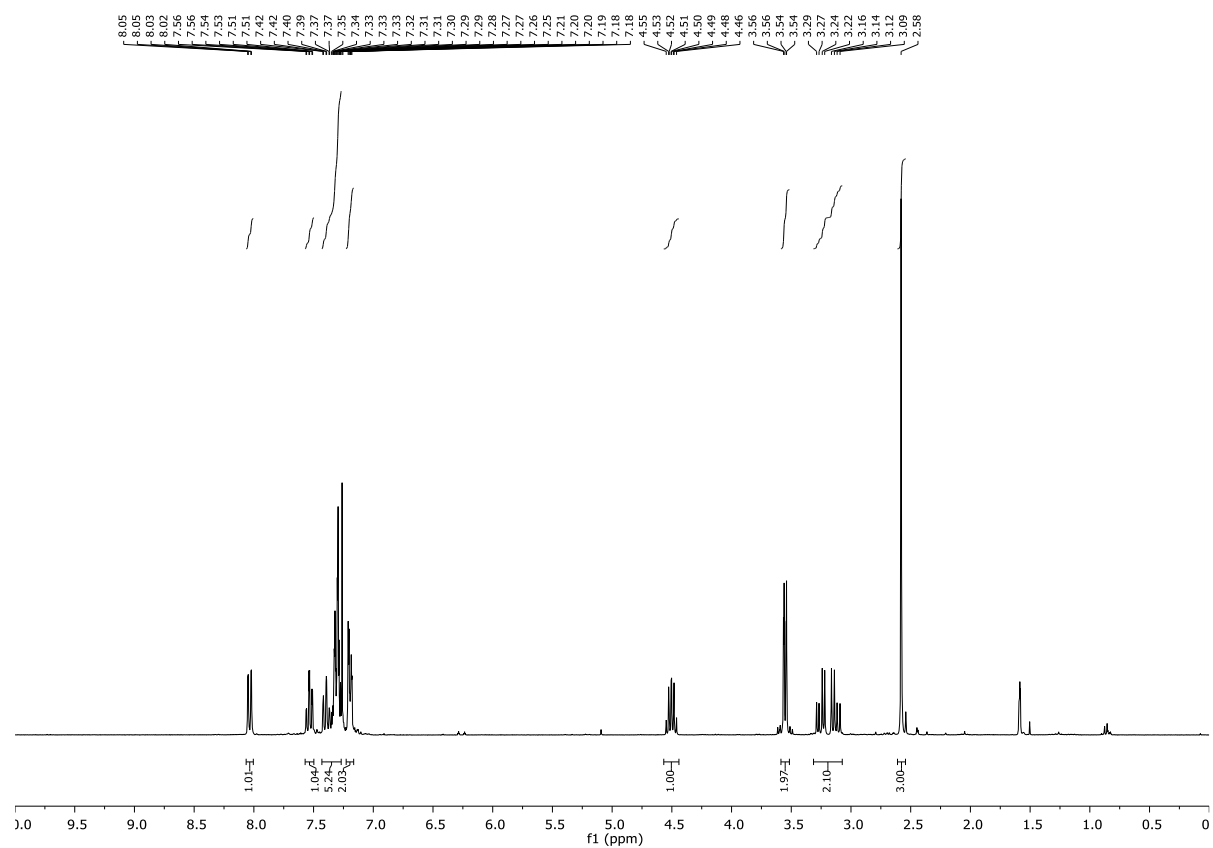
## Chapter 6: Introducing Copper(II)-Catalyst to Photochemical ATRA Reactions

$^1\text{H}$  and  $^{13}\text{C}$  NMR of **7a**:



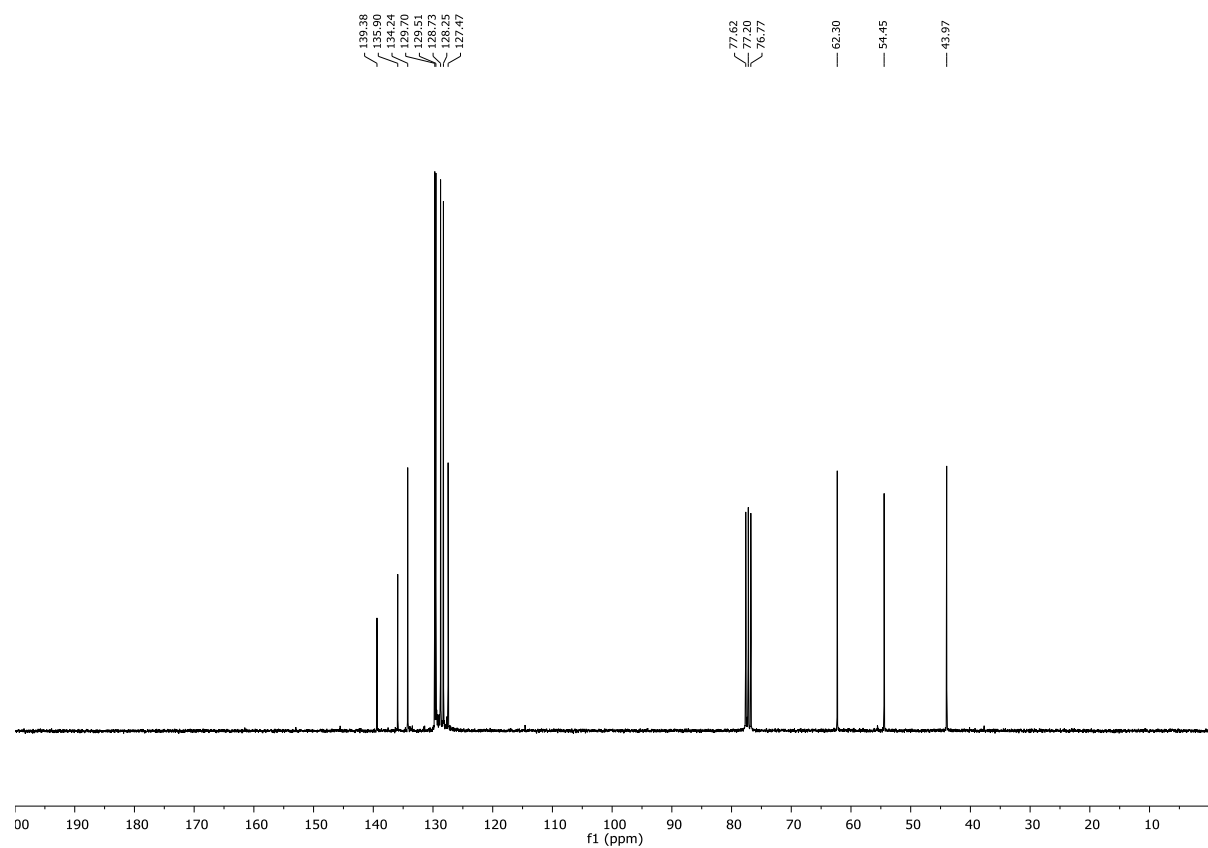
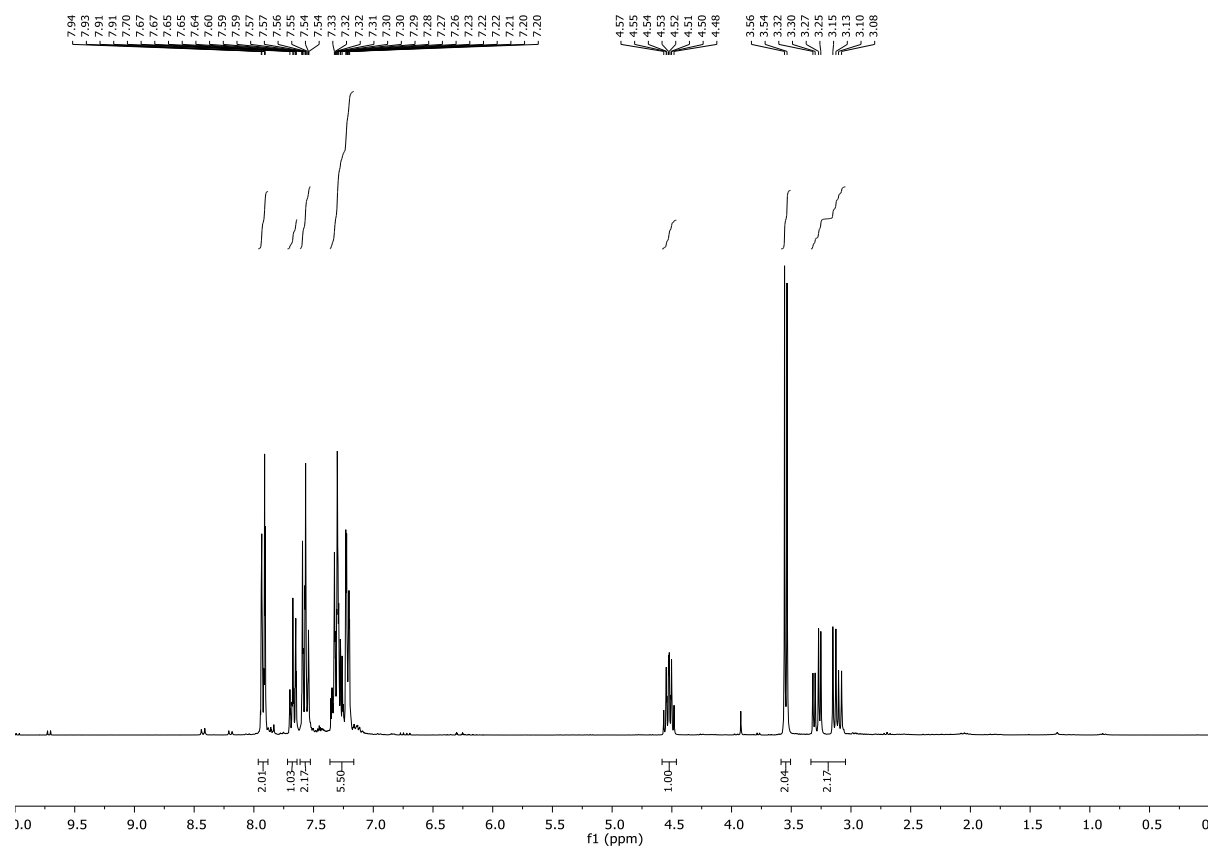
## Chapter 6: Introducing Copper(II)-Catalyst to Photochemical ATRA Reactions

$^1\text{H}$  and  $^{13}\text{C}$  NMR of **7b**:



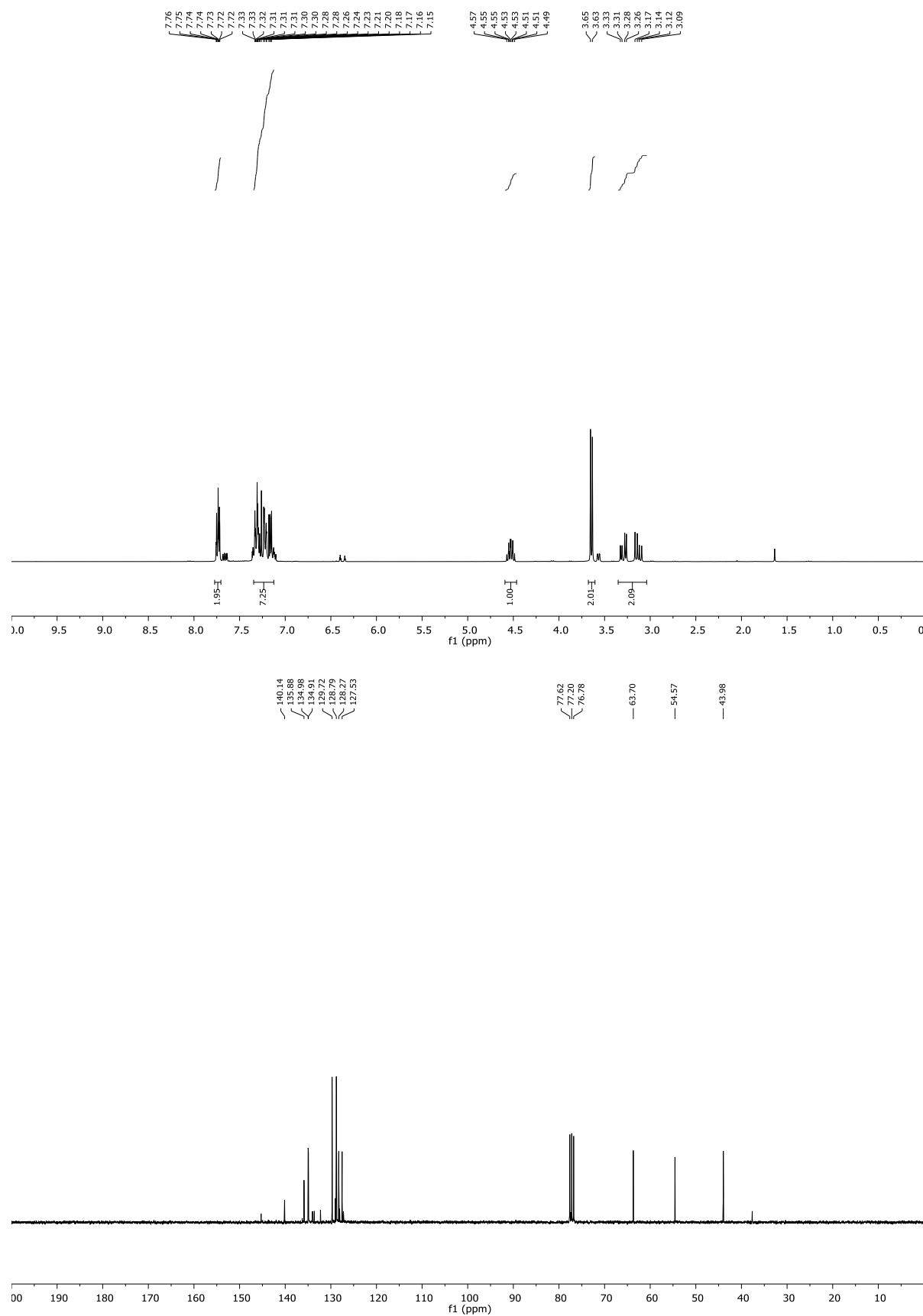
## Chapter 6: Introducing Copper(II)-Catalyst to Photochemical ATRA Reactions

$^1\text{H}$  and  $^{13}\text{C}$  NMR of **7c**:



## Chapter 6: Introducing Copper(II)-Catalyst to Photochemical ATRA Reactions

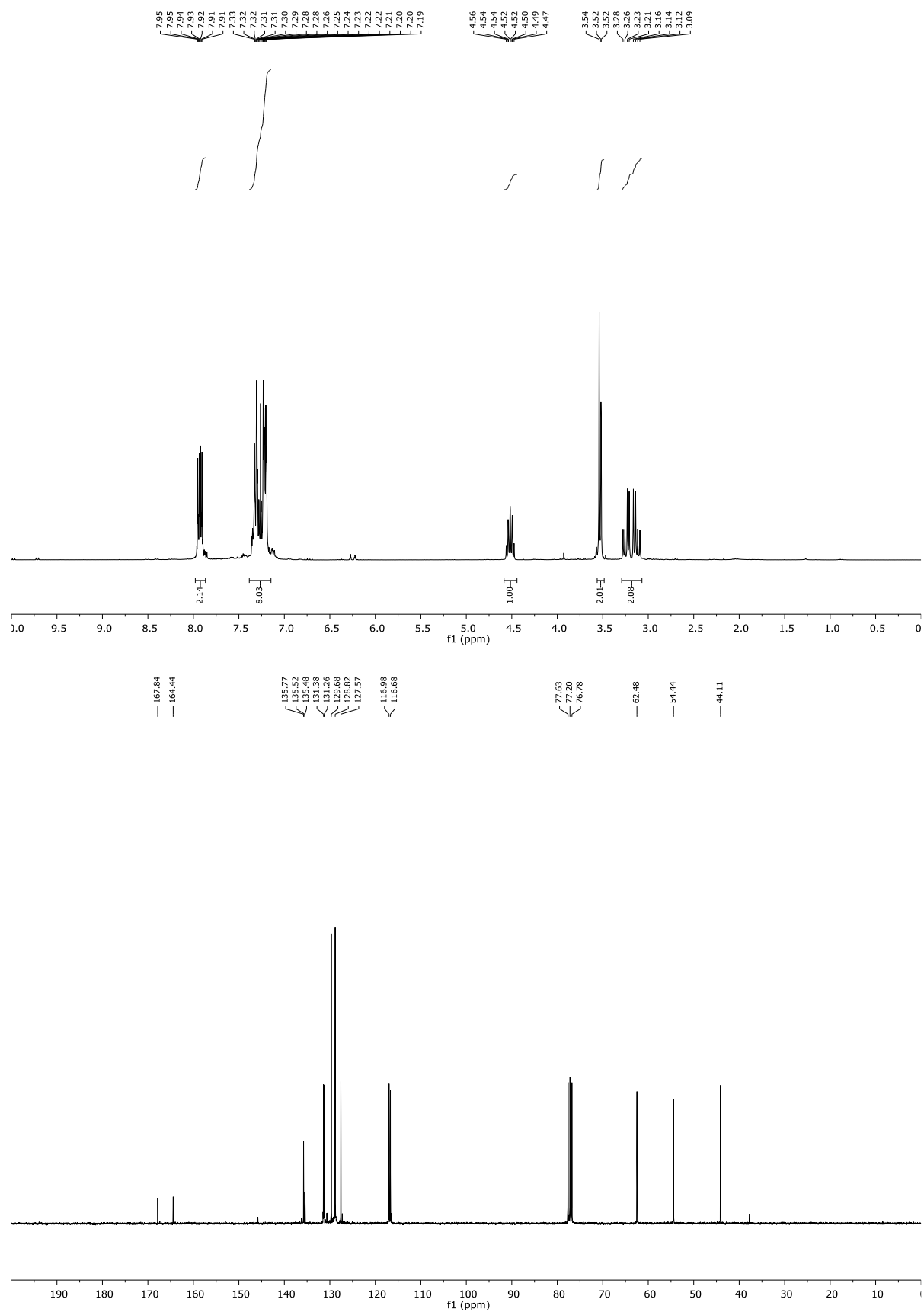
$^1\text{H}$  and  $^{13}\text{C}$  NMR of **7d**:





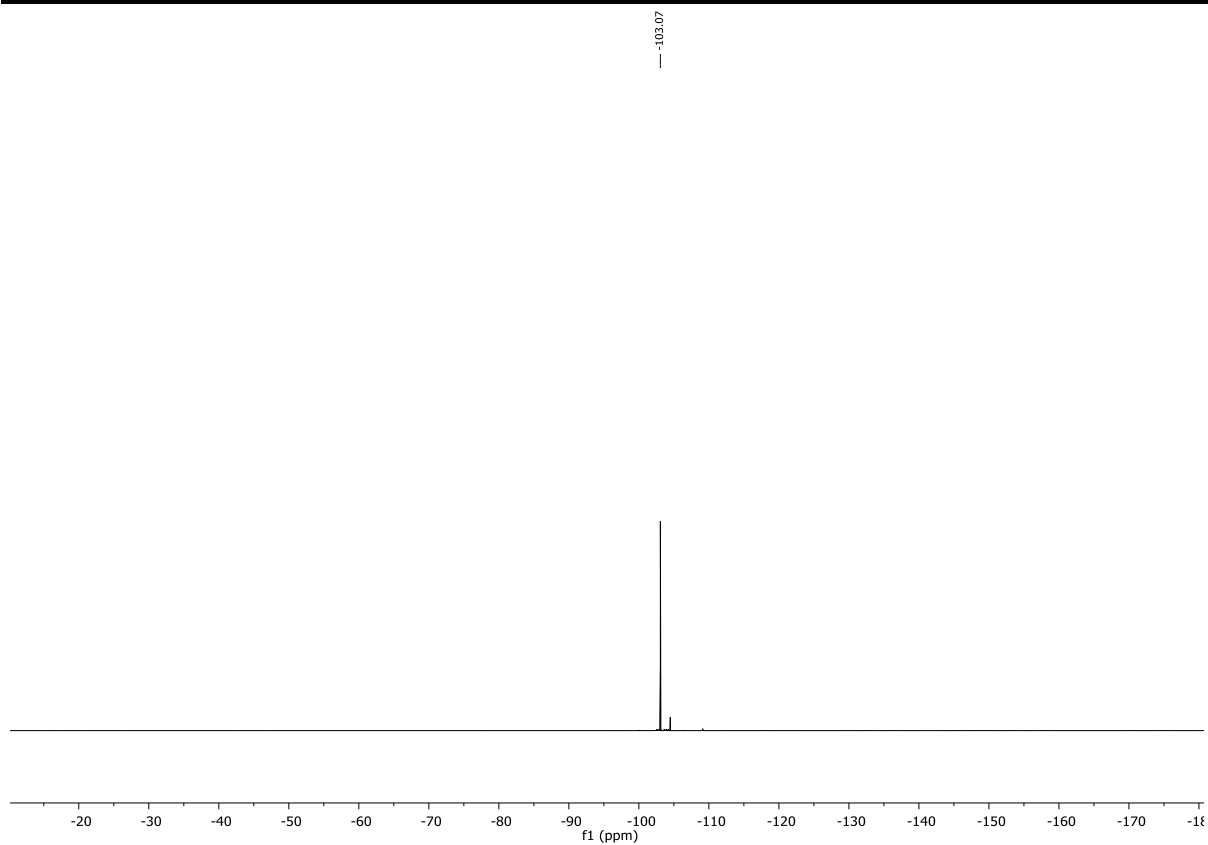
## Chapter 6: Introducing Copper(II)-Catalyst to Photochemical ATRA Reactions

$^1\text{H}$ ,  $^{13}\text{C}$  and  $^{19}\text{F}$  NMR of **7e**:



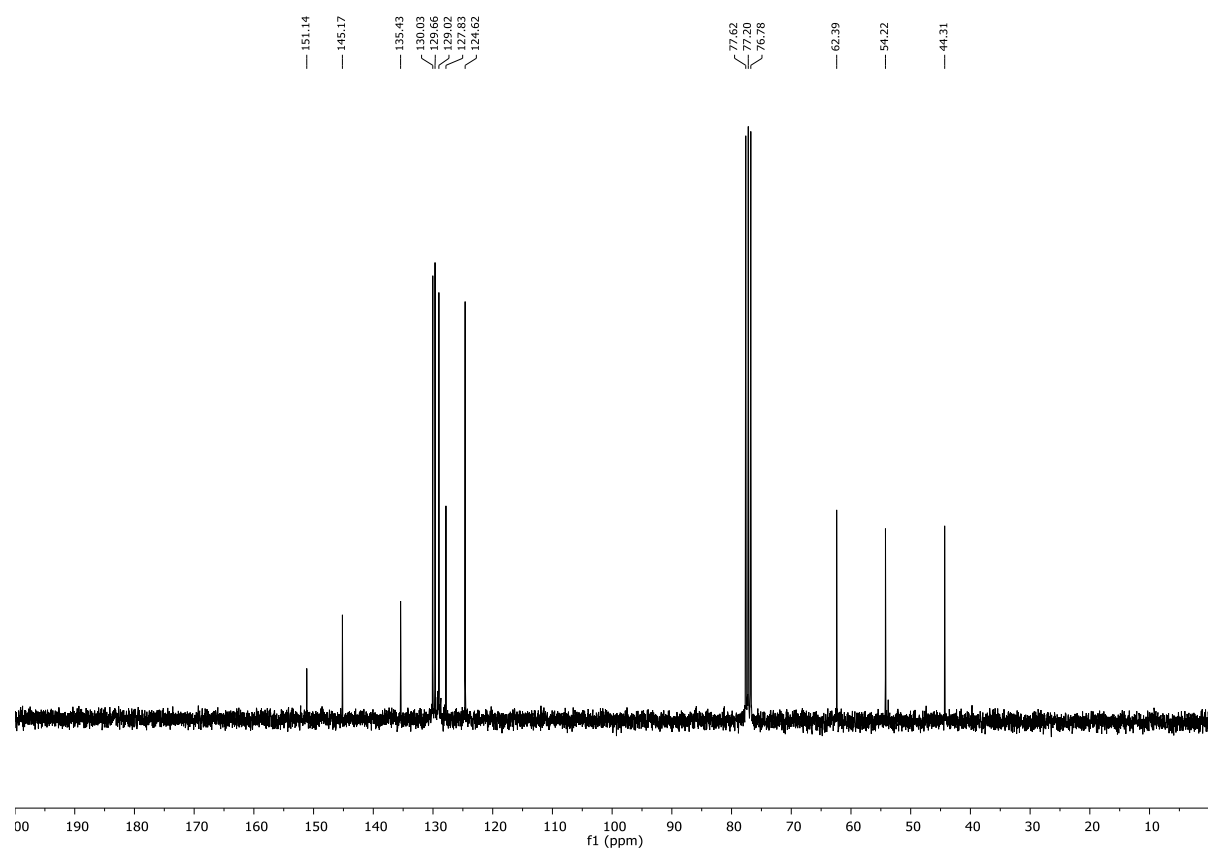
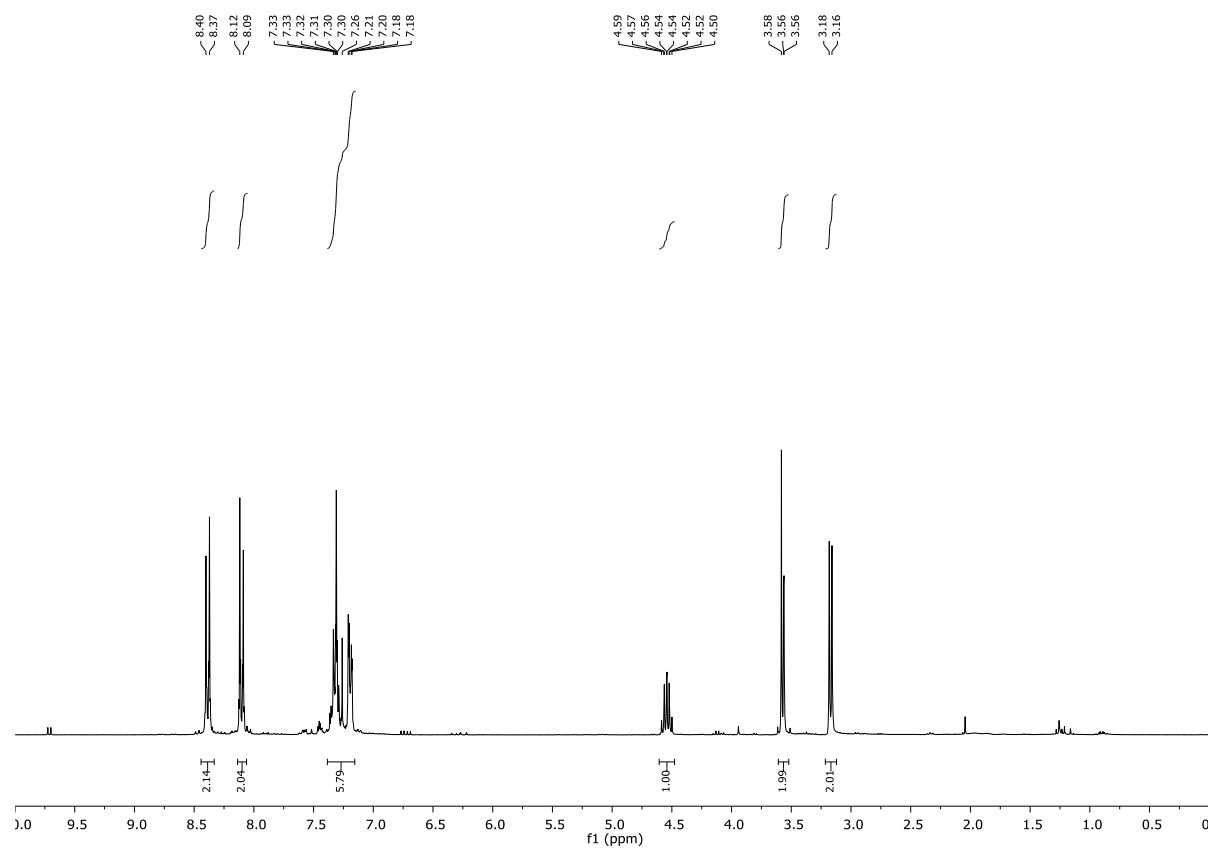
## Chapter 6: Introducing Copper(II)-Catalyst to Photochemical ATRA Reactions

---



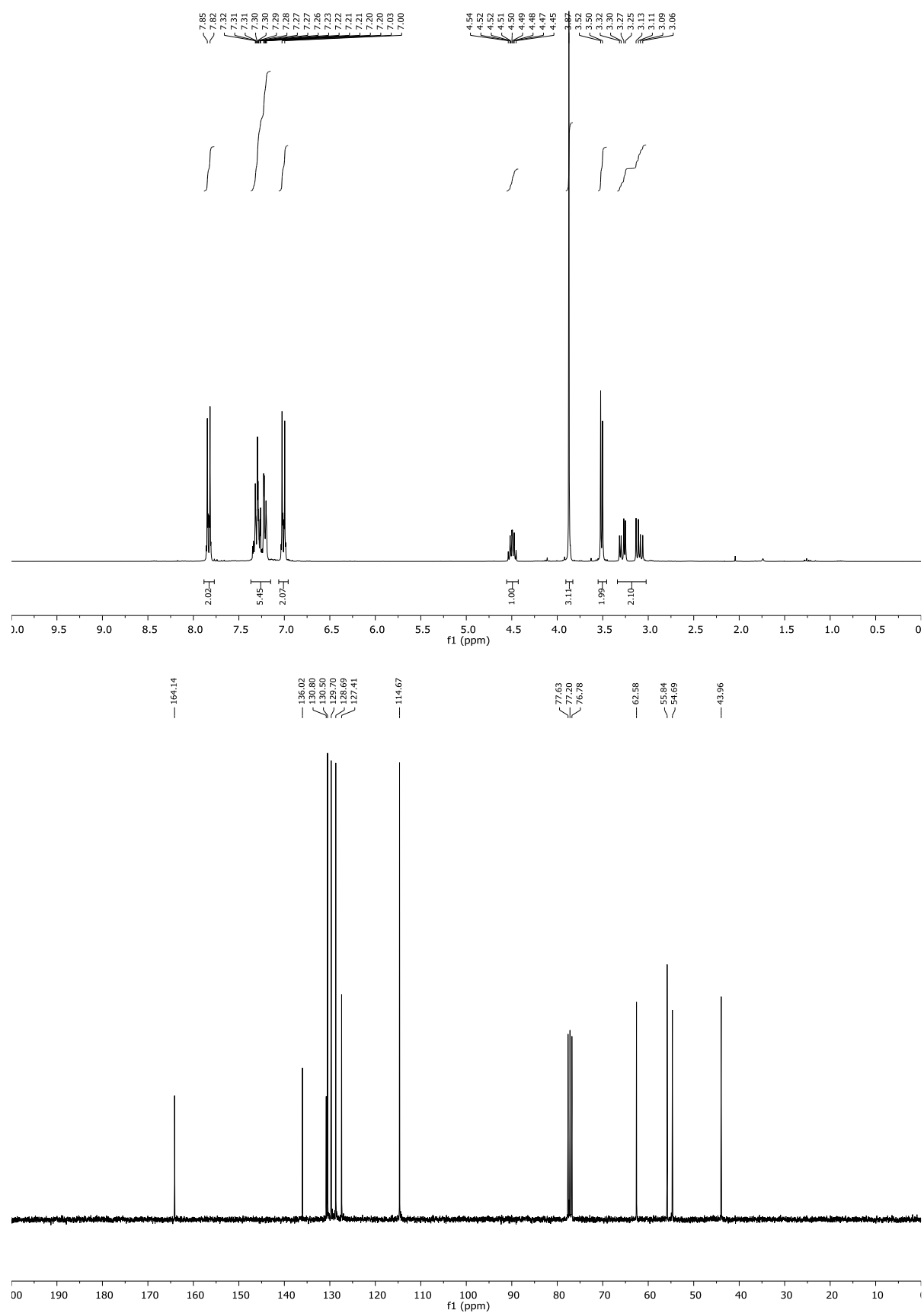
## Chapter 6: Introducing Copper(II)-Catalyst to Photochemical ATRA Reactions

$^1\text{H}$  and  $^{13}\text{C}$  NMR of **7f**:



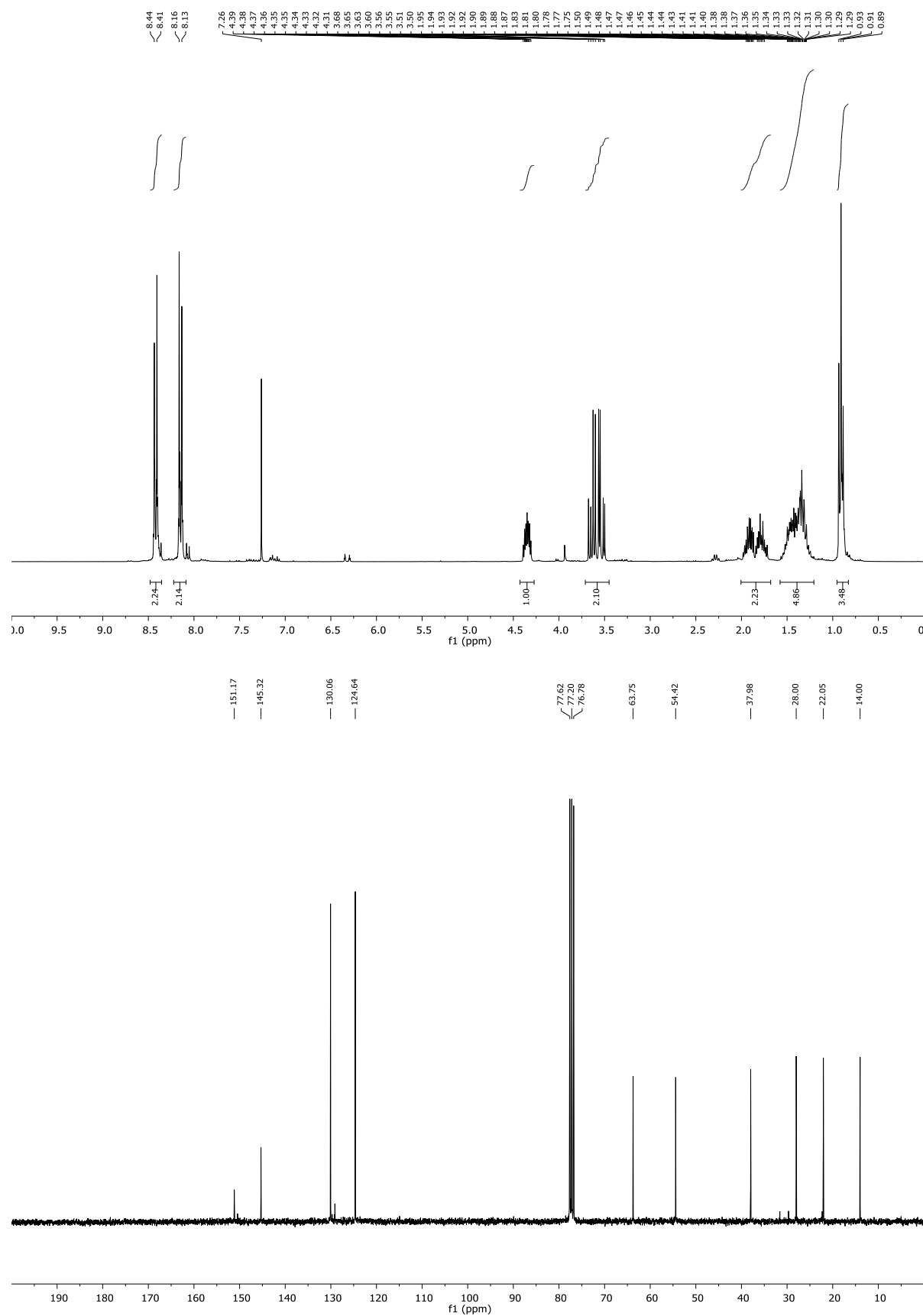
## Chapter 6: Introducing Copper(II)-Catalyst to Photochemical ATRA Reactions

$^1\text{H}$  and  $^{13}\text{C}$  NMR of **7g**:



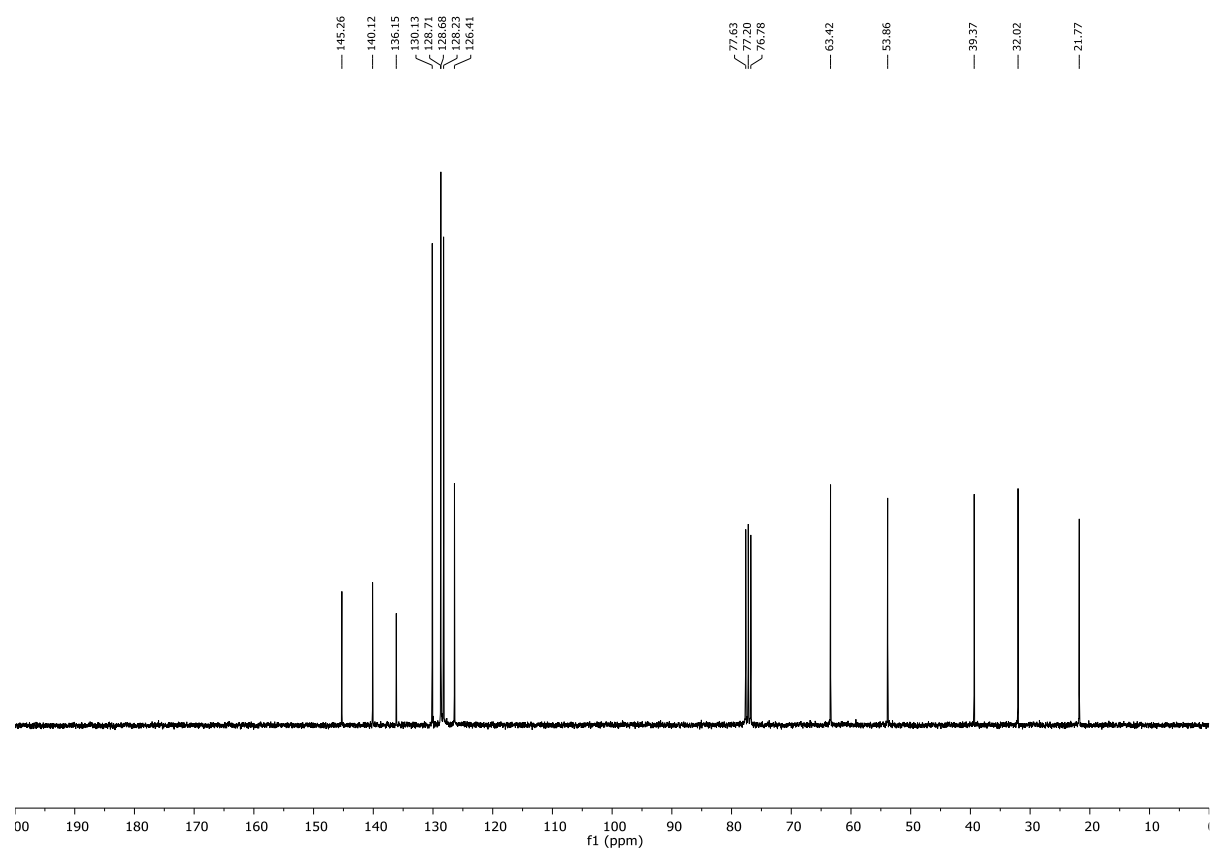
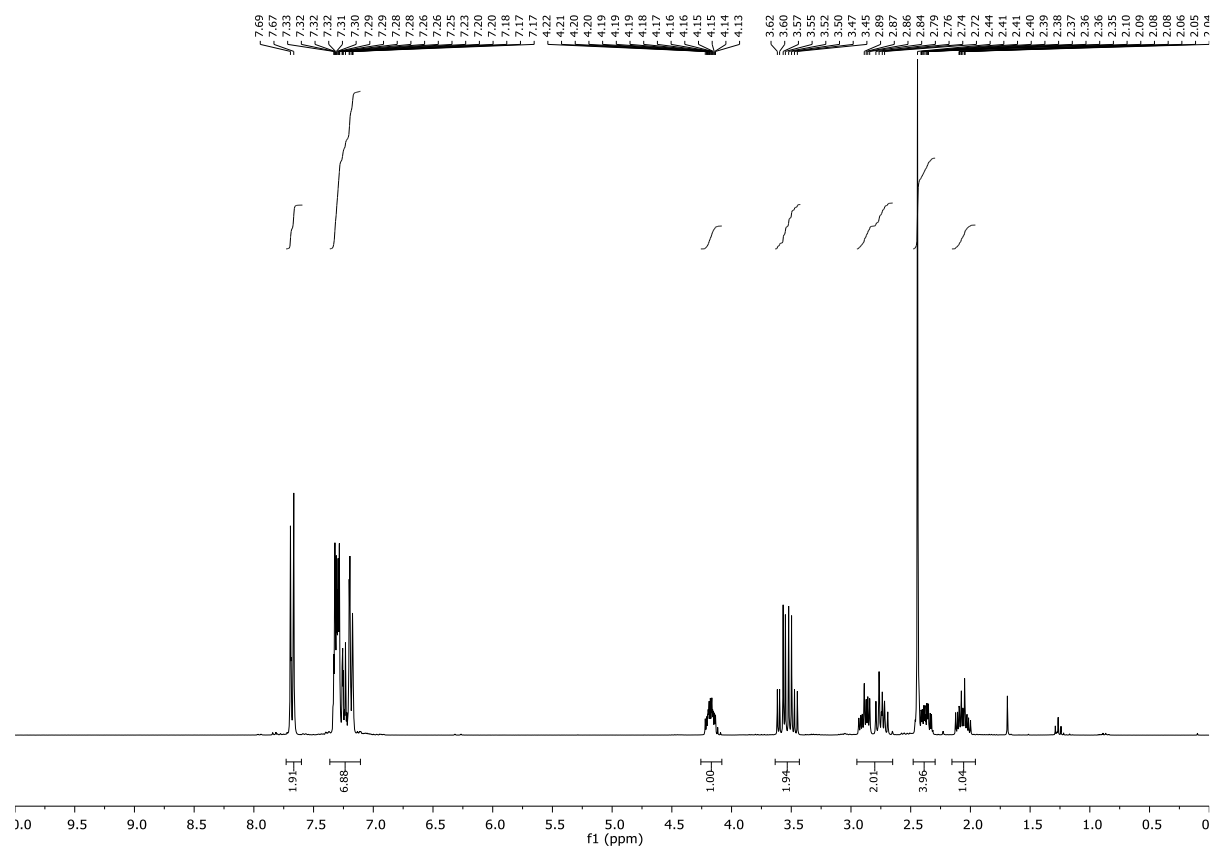
# Chapter 6: Introducing Copper(II)-Catalyst to Photochemical ATRA Reactions

$^1\text{H}$  and  $^{13}\text{C}$  NMR of **7i**:



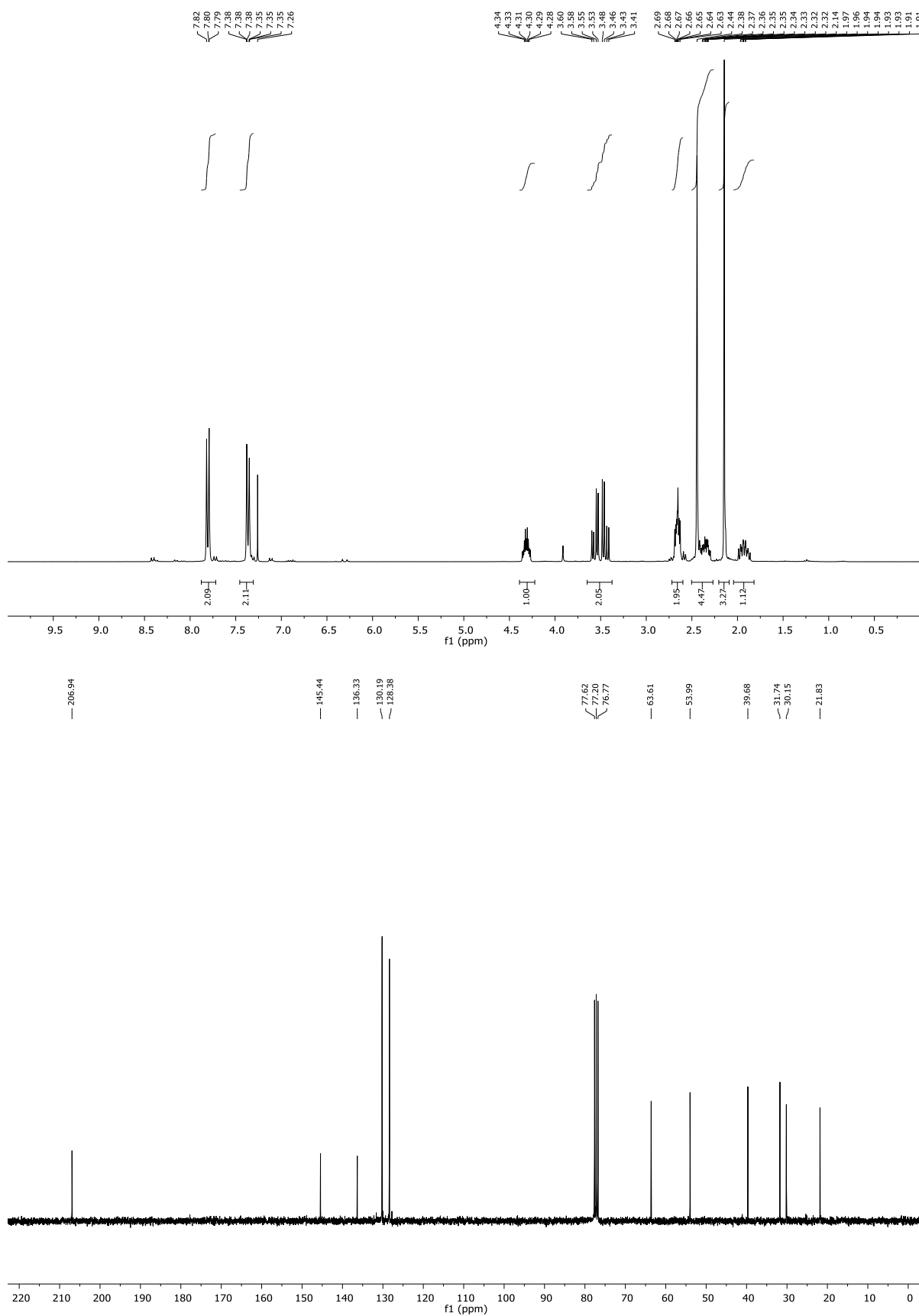
## Chapter 6: Introducing Copper(II)-Catalyst to Photochemical ATRA Reactions

$^1\text{H}$  and  $^{13}\text{C}$  NMR of **7j**:



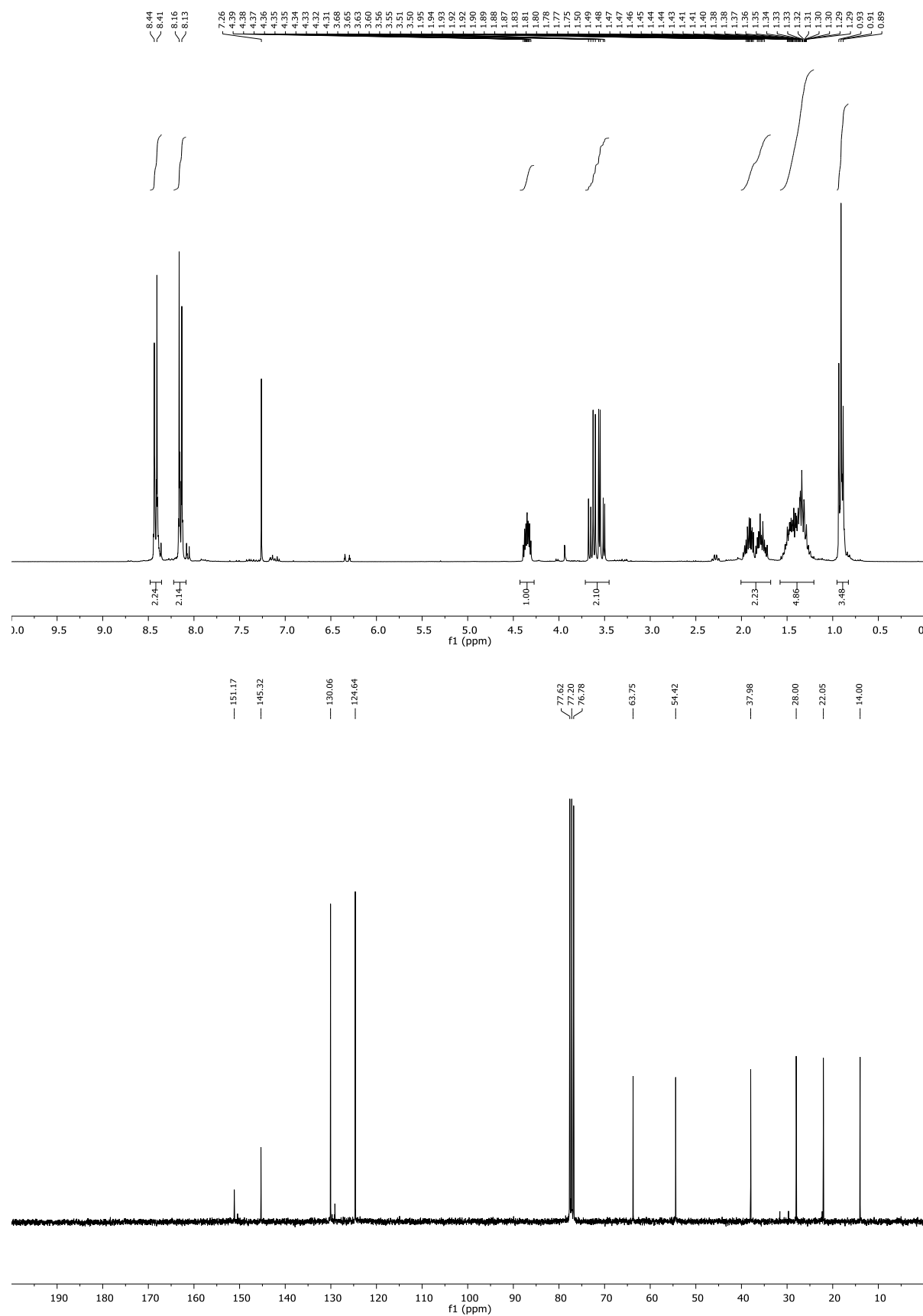
# Chapter 6: Introducing Copper(II)-Catalyst to Photochemical ATRA Reactions

$^1\text{H}$  and  $^{13}\text{C}$  NMR of **7k**:



# Chapter 6: Introducing Copper(II)-Catalyst to Photochemical ATRA Reactions

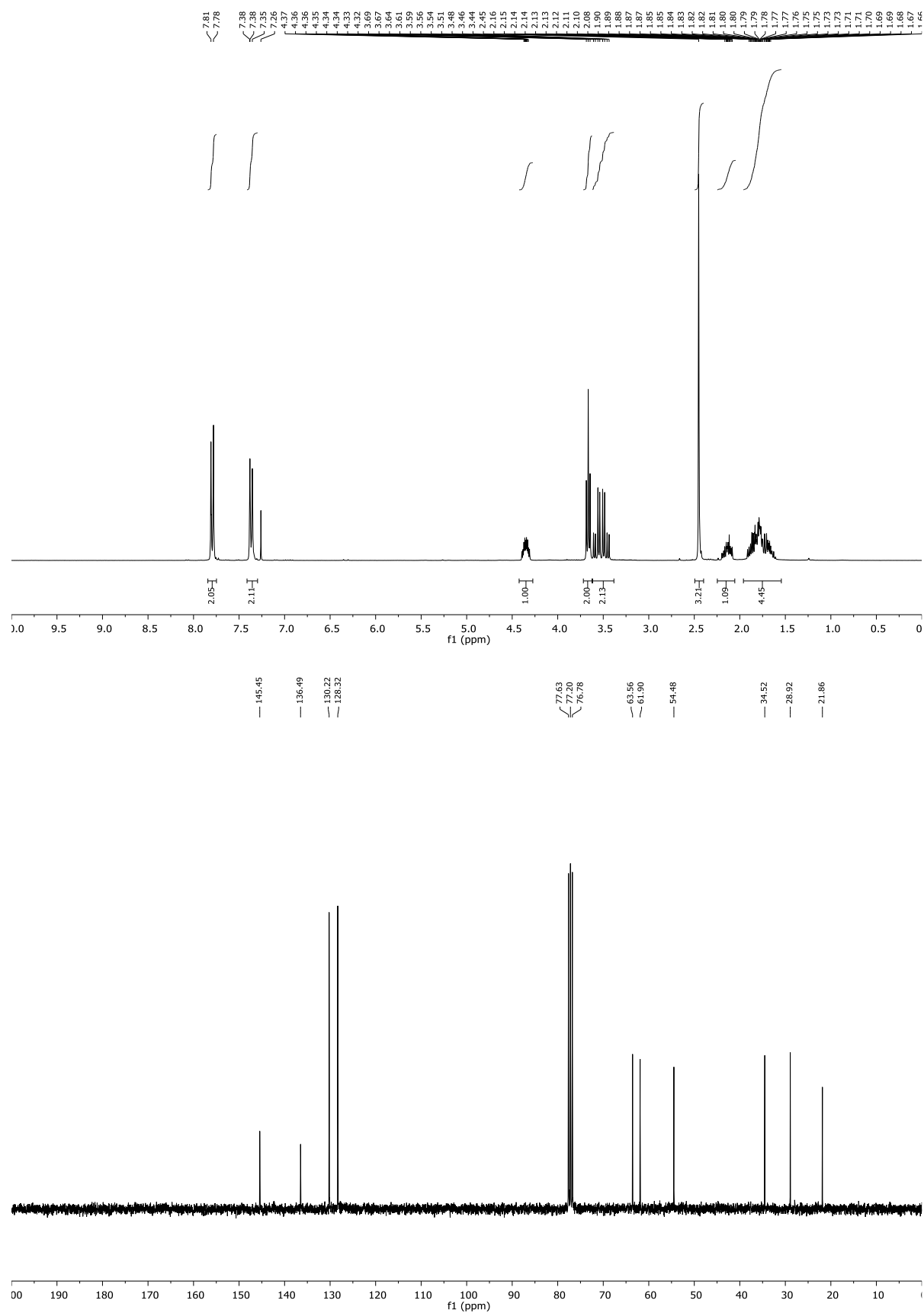
$^1\text{H}$  and  $^{13}\text{C}$  NMR of **7l**:





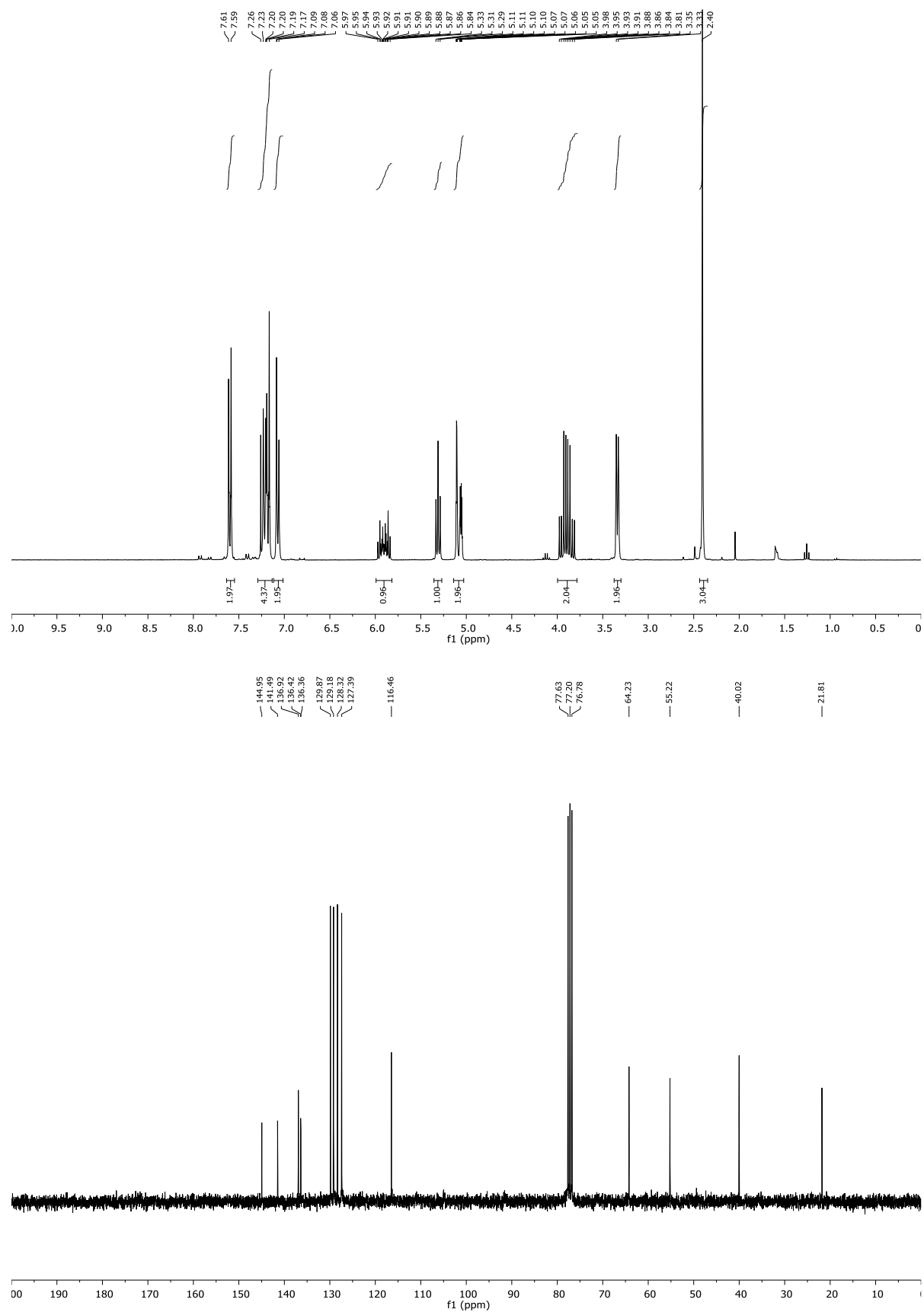
## Chapter 6: Introducing Copper(II)-Catalyst to Photochemical ATRA Reactions

$^1\text{H}$  and  $^{13}\text{C}$  NMR of **7m**:



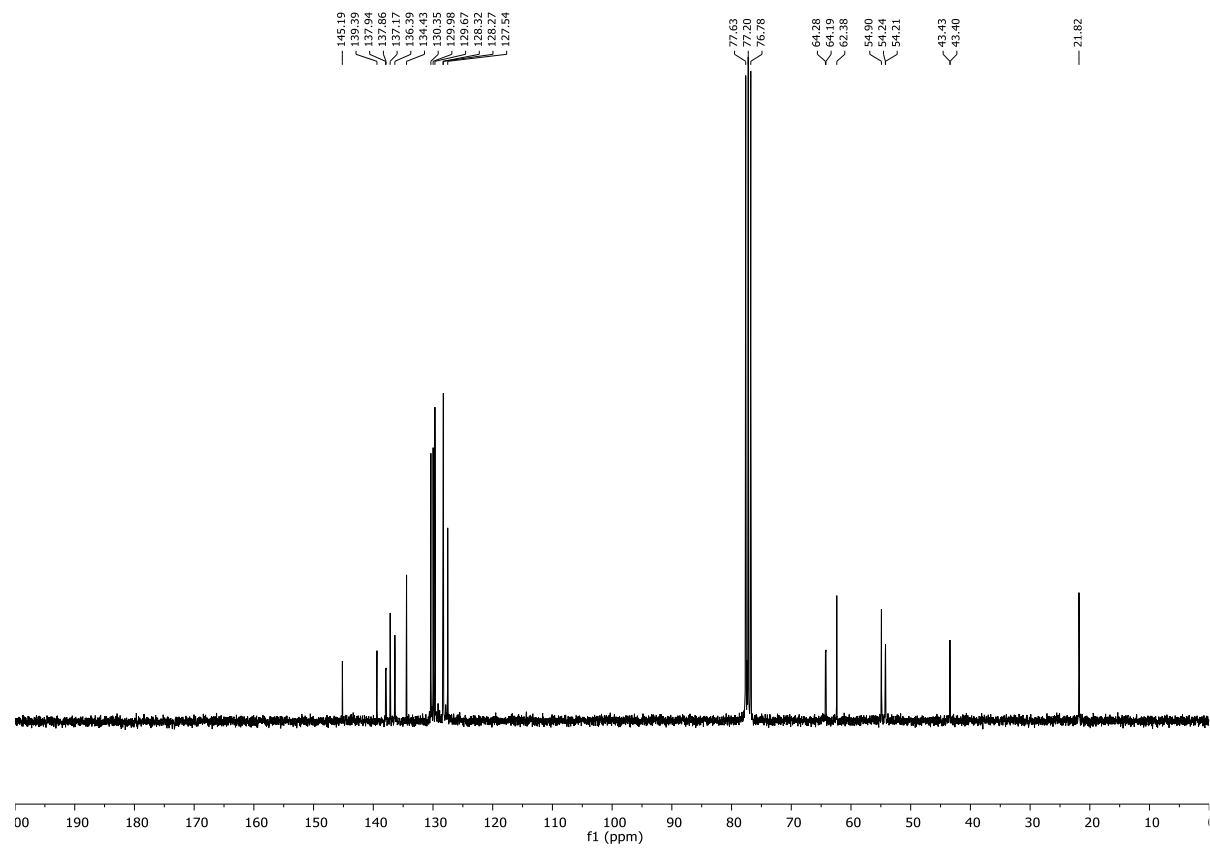
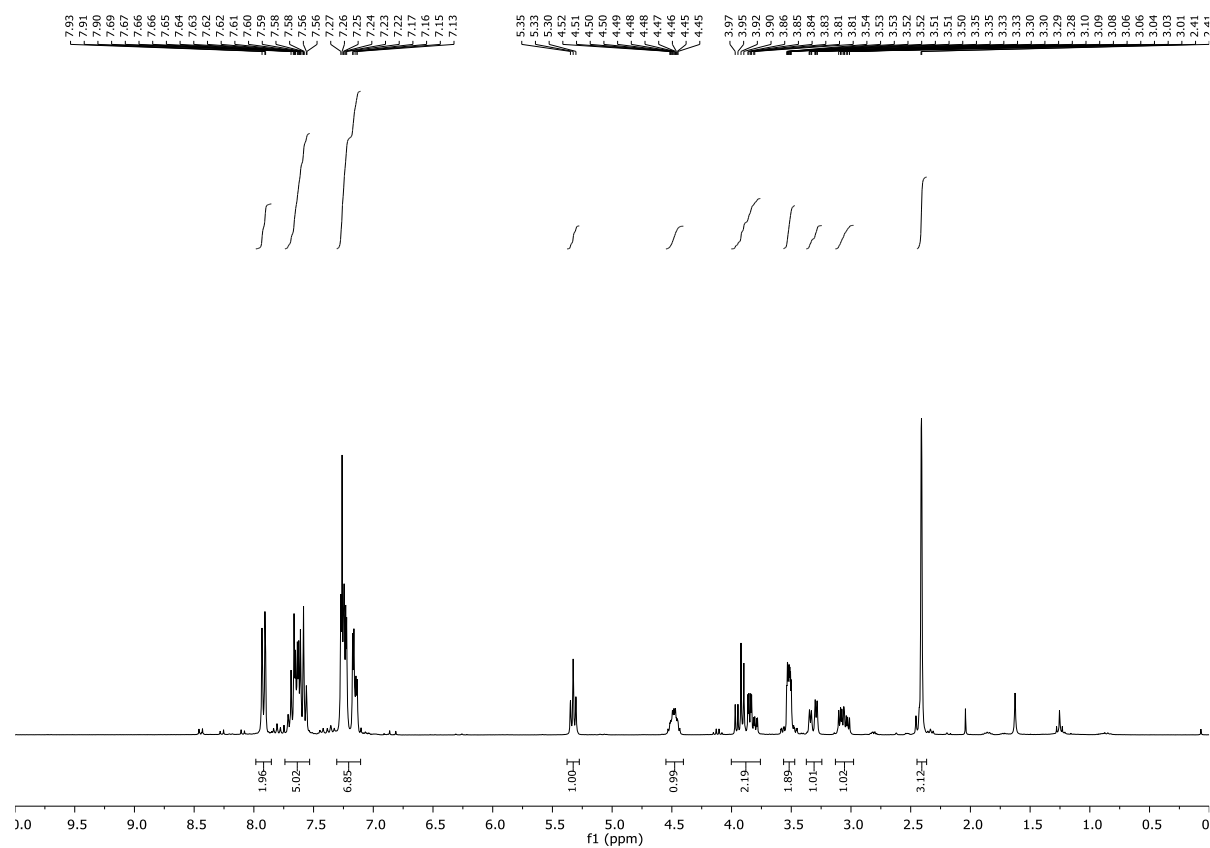
## Chapter 6: Introducing Copper(II)-Catalyst to Photochemical ATRA Reactions

$^1\text{H}$  and  $^{13}\text{C}$  NMR of **8a**:



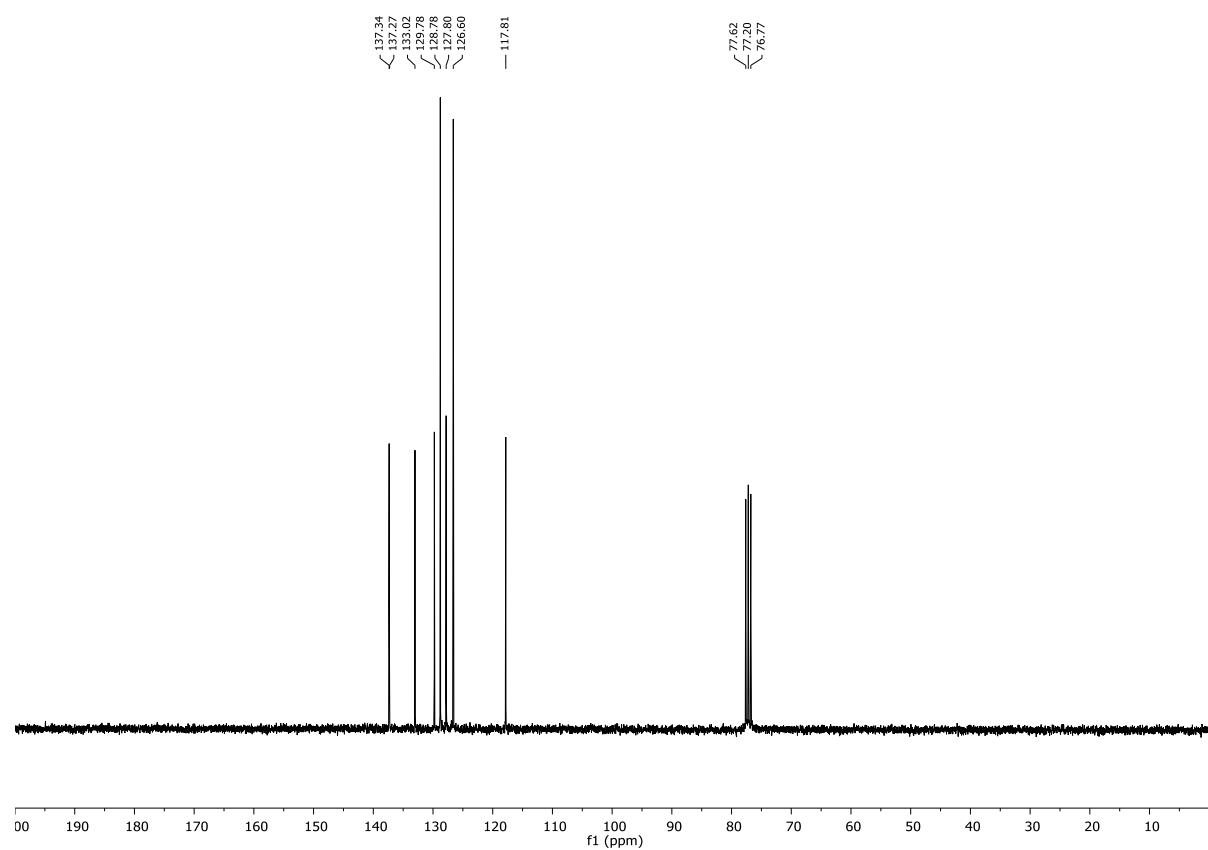
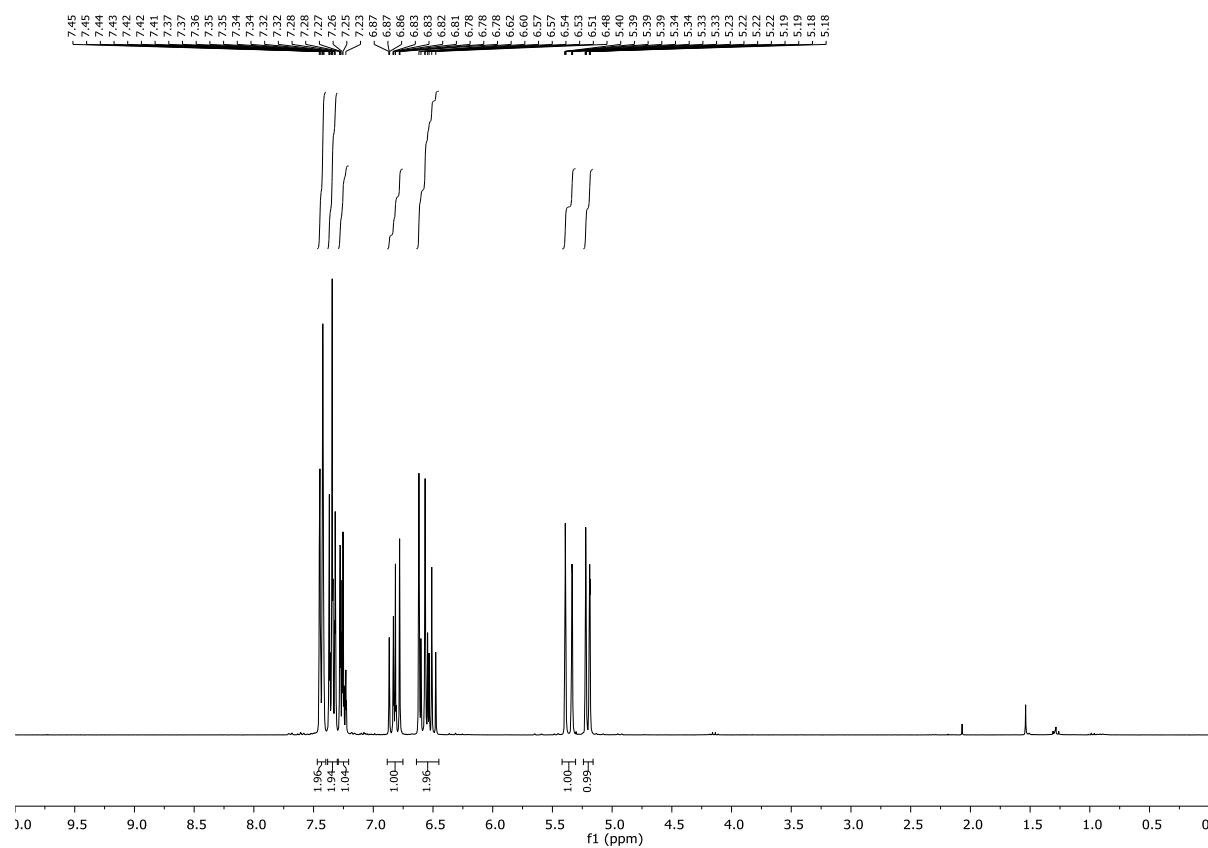
# Chapter 6: Introducing Copper(II)-Catalyst to Photochemical ATRA Reactions

$^1\text{H}$  and  $^{13}\text{C}$  NMR of **8b**:



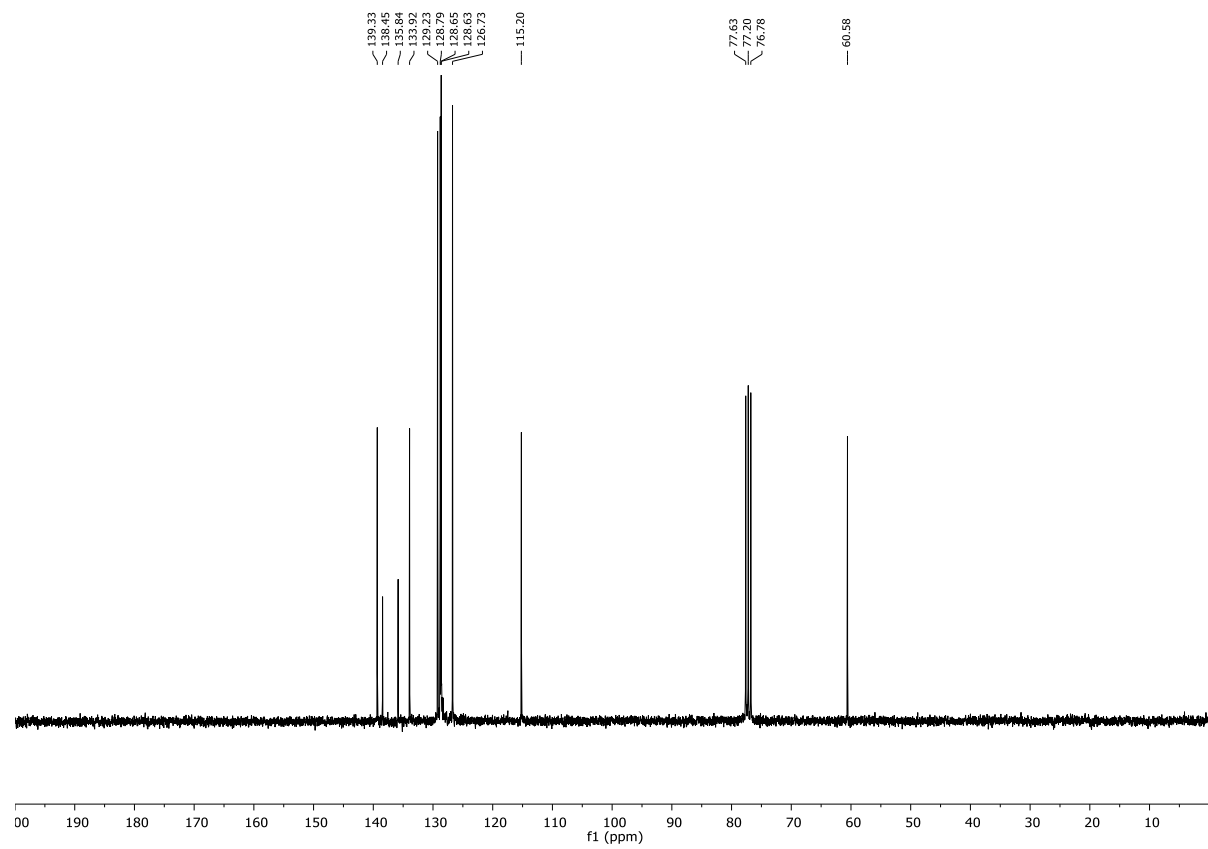
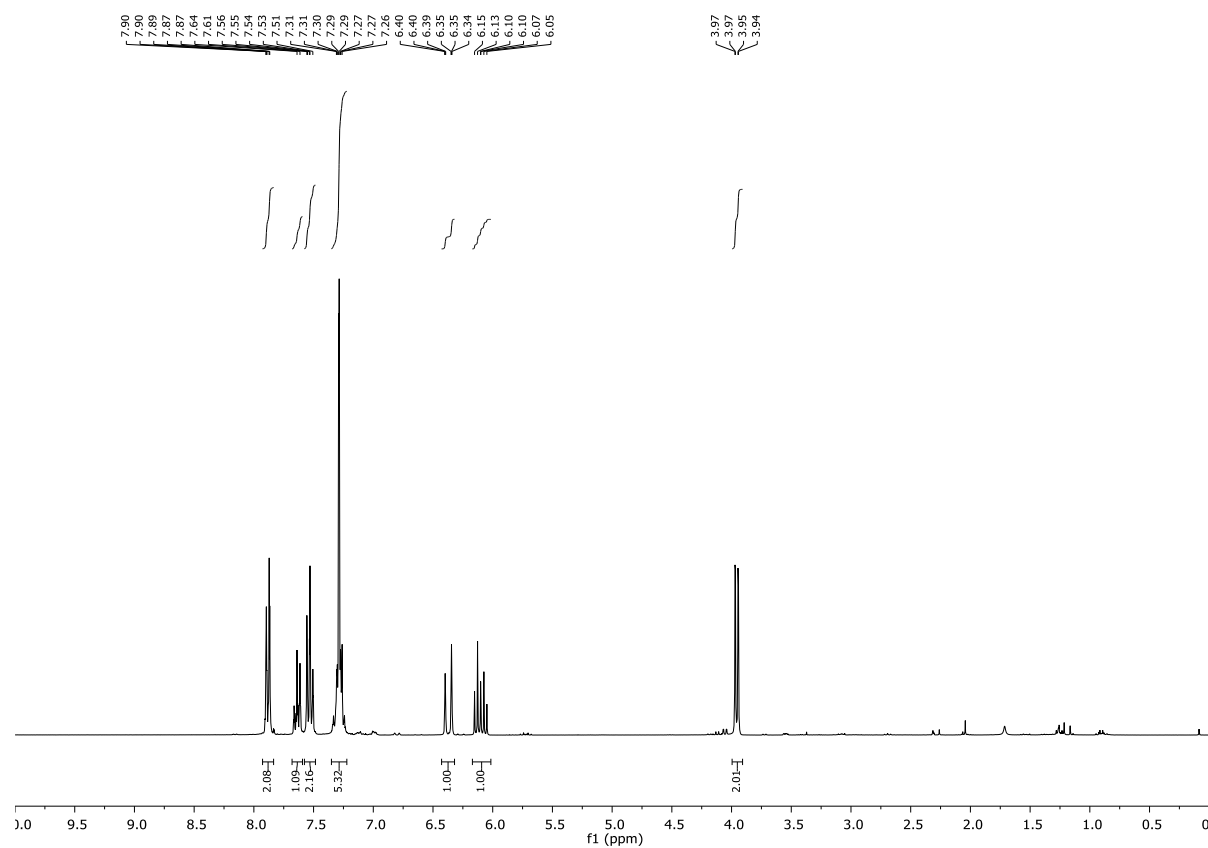
## Chapter 6: Introducing Copper(II)-Catalyst to Photochemical ATRA Reactions

$^1\text{H}$  and  $^{13}\text{C}$  NMR of **11**:



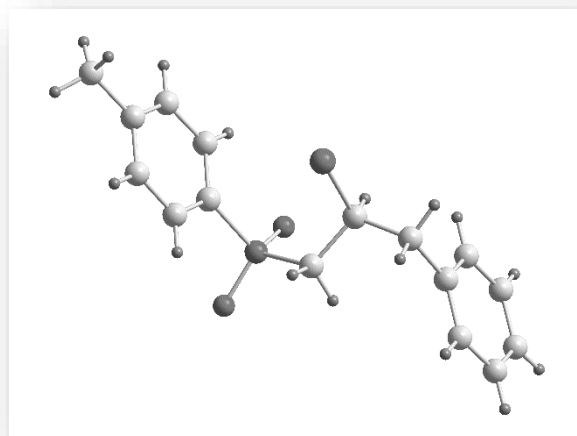
## Chapter 6: Introducing Copper(II)-Catalyst to Photochemical ATRA Reactions

$^1\text{H}$  and  $^{13}\text{C}$  NMR of **12**:



## Chapter 6: Introducing Copper(II)-Catalyst to Photochemical ATRA Reactions

### Crystal Data of 7a:



**Experimental.** Single clear white block-shaped crystals of **7a** were obtained by recrystallisation from dichloromethane. A suitable crystal (0.30×0.22×0.19) mm<sup>3</sup> was selected and mounted on a Lindemann tube oil on a SuperNova, Single source at offset/far, Atlas diffractometer. The crystal was kept at  $T = 123.01(10)$  K during data collection. Using **Olex2** (Dolomanov et al., 2009), the structure was solved with the **ShelXT** (Sheldrick, 2015) structure solution program, using the Intrinsic Phasing solution method. The model was refined with version 2016/6 of **ShelXL** (Sheldrick, 2015) using Least Squares minimisation.

**Crystal Data.** C<sub>16</sub>H<sub>17</sub>ClO<sub>2</sub>S,  $M_r = 308.80$ , orthorhombic,  $Pca2_1$  (No. 29),  $a = 20.3055(4)$  Å,  $b = 7.7348(2)$  Å,  $c = 9.6943(2)$  Å,  $\alpha = \beta = \gamma = 90^\circ$ ,  $V = 1522.58(6)$  Å<sup>3</sup>,  $T = 123.01(10)$  K,  $Z = 4$ ,  $Z' = 1$ ,  $\mu(\text{CuK}\alpha) = 3.486$ , 10815 reflections measured, 3038 unique ( $R_{int} = 0.0437$ ) which were used in all calculations. The final  $wR_2$  was 0.1050 (all data) and  $R_1$  was 0.0400 ( $I > 2(I)$ ).

Compound	7a
Formula	C <sub>16</sub> H <sub>17</sub> ClO <sub>2</sub> S
$D_{calc.}/\text{g cm}^{-3}$	1.347
$\mu/\text{mm}^{-1}$	3.486
Formula Weight	308.80
Colour	clear white
Shape	block
Size/mm <sup>3</sup>	0.30×0.22×0.19

**Chapter 6: Introducing Copper(II)-Catalyst to Photochemical ATRA  
Reactions**

---

<i>T</i> /K	123.01(10)
Crystal System	orthorhombic
Flack Parameter	-0.02(2)
Hoofit Parameter	-0.013(9)
Space Group	<i>Pca</i> 2 <sub>1</sub>
<i>a</i> /Å	20.3055(4)
<i>b</i> /Å	7.7348(2)
<i>c</i> /Å	9.6943(2)
$\alpha$ /°	90
$\beta$ /°	90
$\gamma$ /°	90
<i>V</i> /Å <sup>3</sup>	1522.58(6)
<i>Z</i>	4
<i>Z'</i>	1
Wavelength/Å	1.54184
Radiation type	CuK $\alpha$
$\theta_{min}$ /°	4.355
$\theta_{max}$ /°	76.456
Measured Refl.	10815
Independent Refl.	3038
Reflections Used	2958
<i>R</i> <sub>int</sub>	0.0437
Parameters	225
Restraints	181
Largest Peak	0.490
Deepest Hole	-0.274
Goof	1.054
<i>wR</i> <sub>2</sub> (all data)	0.1050
<i>wR</i> <sub>2</sub>	0.1034
<i>R</i> <sub>1</sub> (all data)	0.0412
<i>R</i> <sub>1</sub>	0.0400

## Chapter 6: Introducing Copper(II)-Catalyst to Photochemical ATRA Reactions

### Structure Quality Indicators

**Reflections:** d min (Cu) 0.79  $I/\sigma$  20.0  $R_{int}$  4.37% complete at  $2\theta=144^\circ$  95%

**Refinement:** Shift 0.001 Max Peak 0.5 Min Peak -0.3 GooF 1.054 Flack -0.02(2)

A clear white block-shaped crystal with dimensions  $0.30 \times 0.22 \times 0.19 \text{ mm}^3$  was mounted on a Lindemann tube oil. X-ray diffraction data were collected using a SuperNova, Single source at offset/far, Atlas diffractometer equipped with an Oxford Cryosystems low-temperature device, operating at  $T = 123.01(10) \text{ K}$ .

Data were measured using  $\omega$  scans of  $1.0^\circ$  per frame for 1.0/4.0 s using  $\text{CuK}\alpha$  radiation (micro-focus sealed X-ray tube, n/a kV, n/a mA). The total number of runs and images was based on the strategy calculation from the program **CrysAlisPro** (Rigaku, V1.171.39.37b, 2017). The maximum resolution achieved was  $\theta = 76.456^\circ$ .

Cell parameters were retrieved using the **CrysAlisPro** (Rigaku, V1.171.39.37b, 2017) software and refined using **CrysAlisPro** (Rigaku, V1.171.39.37b, 2017) on 6937 reflections, 64 % of the observed reflections. Data reduction was performed using the **CrysAlisPro** (Rigaku, V1.171.39.37b, 2017) software which corrects for Lorentz polarisation. The final completeness is 99.90 % out to  $76.456^\circ$  in  $\theta$ .

A gaussian absorption correction was performed using CrysAlisPro 1.171.39.37b (Rigaku Oxford Diffraction, 2017). Numerical absorption correction based on gaussian integration over a multifaceted crystal model. Empirical absorption correction using spherical harmonics, implemented in SCALE3 ABSPACK scaling algorithm. The absorption coefficient  $\mu$  of this material is  $3.486 \text{ mm}^{-1}$  at this wavelength ( $\lambda = 1.54184 \text{ \AA}$ ) and the minimum and maximum transmissions are 0.601 and 0.772.

The structure was solved in the space group  $Pca2_1$  (# 29) by Intrinsic Phasing using the **ShelXT** (Sheldrick, 2015) structure solution program and refined by Least Squares using version 2016/6 of **ShelXL** (Sheldrick, 2015). All non-hydrogen atoms were refined anisotropically. Hydrogen atom positions were calculated geometrically and refined using the riding model.

There is a single molecule in the asymmetric unit, which is represented by the reported sum formula. In other words: Z is 4 and Z' is 1.

The Flack parameter was refined to -0.02(2). Determination of absolute structure using Bayesian statistics on Bijvoet differences using the Olex2 results in -0.015(9). Note: The Flack

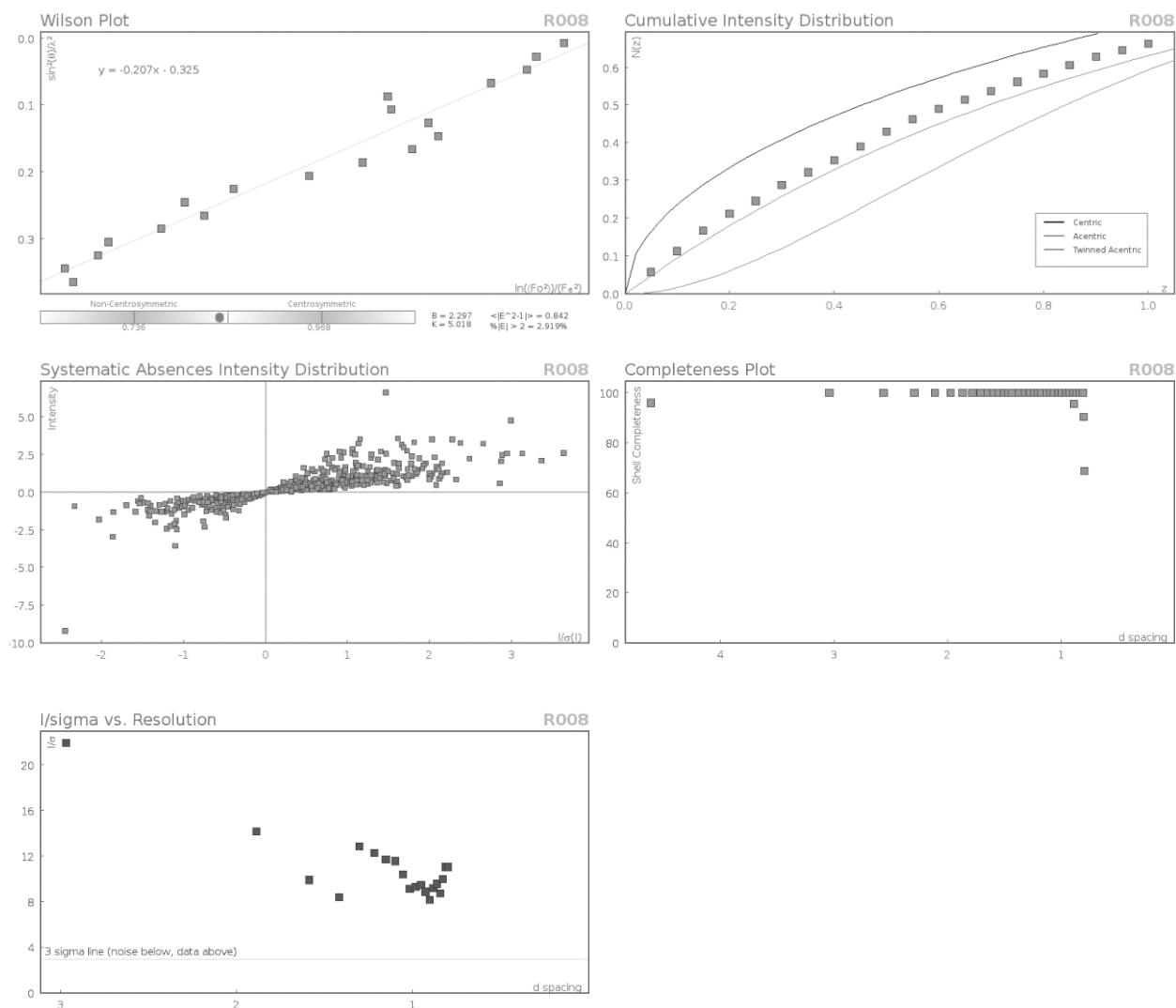


## Chapter 6: Introducing Copper(II)-Catalyst to Photochemical ATRA Reactions

parameter is used to determine chirality of the crystal studied, the value should be near 0, a value of 1 means that the stereochemistry is wrong and the model should be inverted. A value of 0.5 means that the crystal consists of a racemic mixture of the two enantiomers.

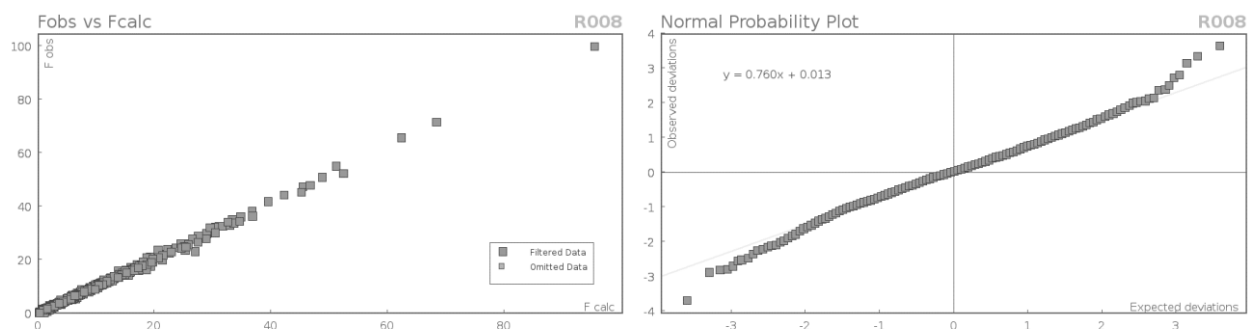
*\_exptl\_absorpt\_process\_details*: CrysAlisPro 1.171.39.37b (Rigaku Oxford Diffraction, 2017) Numerical absorption correction based on gaussian integration over a multifaceted crystal model. Empirical absorption correction using spherical harmonics, implemented in SCALE3 ABSPACK scaling algorithm.

### Data Plots: Diffraction Data



## Chapter 6: Introducing Copper(II)-Catalyst to Photochemical ATRA Reactions

### Data Plots: Refinement and Data

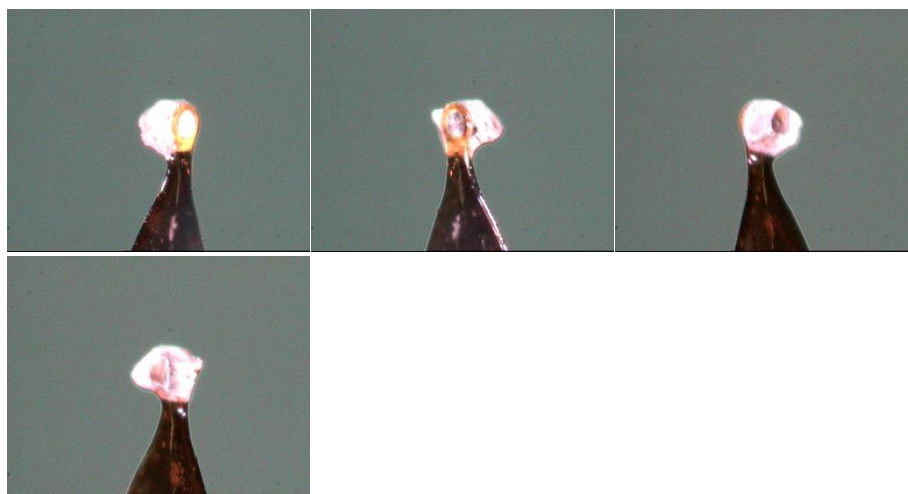


### Reflection Statistics

Total reflections (after filtering)	11592	Unique reflections	3038
Completeness	0.949	Mean $I/\sigma$	20.0
$hkl_{\max}$ collected	(25, 9, 12)	$hkl_{\min}$ collected	(-25, -8, -12)
$hkl_{\max}$ used	(25, 9, 12)	$hkl_{\min}$ used	(0, 0, -12)
Lim $d_{\max}$ collected	100.0	Lim $d_{\min}$ collected	0.77
$d_{\max}$ used	10.15	$d_{\min}$ used	0.79
Friedel pairs	3018	Friedel pairs merged	0
Inconsistent equivalents	2	$R_{\text{int}}$	0.0437
$R_{\text{sigma}}$	0.0355	Intensity transformed	0
Omitted reflections	0	Omitted by user (OMIT)	hkl)
Multiplicity	(5945, 2078, 419, 51, 6)	Maximum multiplicity	15
Removed systematic absences	777	Filtered	off0 (Shel/OMIT)

## Chapter 6: Introducing Copper(II)-Catalyst to Photochemical ATRA Reactions

### Images of the Crystal on the Diffractometer



Fractional Atomic Coordinates ( $\times 10^4$ ) and Equivalent Isotropic Displacement Parameters ( $\text{\AA}^2 \times 10^3$ ) for **7a**.  $U_{eq}$  is defined as 1/3 of the trace of the orthogonalised  $U_{ij}$ .

Atom	x	y	z	$U_{eq}$
S1	5155.6(3)	5468.9(9)	6009.1(9)	24.9(2)
O1	4975.9(13)	6480(3)	7196(3)	33.5(6)
O2	4854.8(13)	3800(3)	5832(3)	36.1(6)
C4	6298.2(17)	4157(5)	5005(4)	29.2(7)
C6	6395.4(18)	5946(4)	7045(4)	29.4(7)
C3	6976.4(18)	3920(5)	5010(4)	33.0(7)
C5	6014.5(14)	5171(4)	6025(4)	24.7(6)
C7	7074.4(19)	5676(4)	7030(4)	33.1(7)
C8	4964.1(16)	6686(4)	4508(4)	25.8(6)
C10	4808.3(18)	9634(5)	3460(4)	35.9(8)
C9	5177.8(15)	8562(4)	4527(4)	29.3(7)
C2	7368.6(15)	4677(4)	6020(5)	33.1(7)
C1	8107.3(17)	4391(5)	6010(6)	45.0(9)
C13	3260(3)	10867(8)	5389(9)	31.4(6)
C12A	3917(3)	10611(10)	5031(9)	30.9(6)
C11	4077(3)	9807(11)	3797(10)	30.2(5)
C16	3569(3)	9237(9)	2932(8)	30.9(6)
C15	2914(3)	9524(9)	3286(10)	31.5(6)
C14	2763(3)	10332(8)	4503(10)	31.7(6)

**Chapter 6: Introducing Copper(II)-Catalyst to Photochemical ATRA Reactions**

Atom	x	y	z	$U_{eq}$
Cl1	6047.3(4)	8723.6(14)	4134.0(14)	51.5(3)
C11A	4105(3)	9859(17)	3796(15)	30.5(6)
C16A	3707(6)	9157(14)	2774(12)	30.9(6)
C15A	3026(5)	9285(13)	2878(14)	31.4(6)
C14A	2743(3)	10116(13)	4003(18)	31.6(6)
C13A	3142(5)	10818(12)	5025(14)	31.4(6)
C12B	3823(5)	10690(15)	4922(12)	30.9(6)

Anisotropic Displacement Parameters ( $\times 10^4$ ) **7a**. The anisotropic displacement factor exponent takes the form:  $-2\pi^2 [h^2 a^{*2} \times U_{11} + \dots + 2hka^* \times b^* \times U_{12}]$

Atom	$U_{11}$	$U_{22}$	$U_{33}$	$U_{23}$	$U_{13}$	$U_{12}$
S1	31.3(3)	20.7(3)	22.6(3)	2.1(3)	2.7(3)	-1.1(2)
O1	43.2(13)	31.8(13)	25.6(12)	1.9(11)	7.4(10)	5.0(11)
O2	40.5(13)	24.9(11)	42.9(16)	4.6(12)	2.3(11)	-7.6(9)
C4	36.5(16)	27.4(15)	23.8(15)	-2.5(14)	-1.9(13)	0.2(13)
C6	39.7(17)	23.8(15)	24.6(15)	0.2(13)	-4.3(13)	3.8(13)
C3	39.0(17)	29.5(16)	30.5(17)	1.6(15)	3.1(14)	7.5(14)
C5	33.1(13)	19.7(12)	21.3(13)	3.0(15)	0.3(14)	1.7(10)
C7	39.2(17)	27.1(16)	32.9(17)	1.9(15)	-9.0(14)	1.3(13)
C8	26.7(13)	26.2(16)	24.4(14)	2.1(13)	-4.4(11)	-2.2(12)
C10	40.2(18)	36(2)	31.9(18)	12.5(15)	1.7(14)	-0.4(14)
C9	28.3(15)	26.5(16)	33.2(17)	8.2(15)	-0.2(12)	-4.7(11)
C2	32.2(15)	29.3(15)	37.6(16)	10.3(16)	-1.8(15)	2.6(12)
C1	34.0(16)	46(2)	55(2)	14(2)	-2(2)	3.6(15)
C13	34.1(11)	26.1(10)	34.0(14)	-0.2(10)	-8(1)	1.2(9)
C12A	33.8(11)	25.2(10)	33.8(13)	0.1(10)	-7.6(10)	0.7(9)
C11	33.7(11)	23.9(9)	33.2(13)	0.9(9)	-7.4(9)	0.5(9)
C16	34.1(11)	25.0(9)	33.5(13)	0.6(10)	-7.6(10)	0.8(9)
C15	34.3(11)	26.4(10)	33.8(14)	0(1)	-7.9(10)	0.4(9)
C14	34.2(11)	26.8(10)	34.0(14)	0(1)	-7.8(10)	1.3(9)
Cl1	28.4(4)	51.8(6)	74.3(7)	29.2(5)	-1.1(4)	-8.5(4)

**Chapter 6: Introducing Copper(II)-Catalyst to Photochemical ATRA  
Reactions**

Atom	$U_{11}$	$U_{22}$	$U_{33}$	$U_{23}$	$U_{13}$	$U_{12}$
C11A	33.8(11)	24.3(10)	33.3(13)	0.7(10)	-7.5(10)	0.6(9)
C16A	34.0(11)	25(1)	33.6(14)	0.4(10)	-7.6(10)	0.9(9)
C15A	34.3(11)	25.9(10)	33.9(14)	-0.2(10)	-7.7(10)	1.1(9)
C14A	34.2(11)	26.3(10)	34.2(15)	-0.4(11)	-7.8(11)	1.0(9)
C13A	34.2(11)	26(1)	34.0(14)	-0.3(11)	-7.6(10)	1.1(9)
C12B	33.9(11)	25.1(10)	33.7(14)	0.1(10)	-7.6(10)	0.8(9)

Bond Lengths in Å for **7a**.

Atom	Atom	Length/Å
S1	O1	1.439(3)
S1	O2	1.438(2)
S1	C5	1.759(3)
S1	C8	1.777(3)
C4	C3	1.389(5)
C4	C5	1.387(5)
C6	C5	1.391(5)
C6	C7	1.395(5)
C3	C2	1.391(6)
C7	C2	1.383(6)
C8	C9	1.515(5)
C10	C9	1.523(5)
C10	C11	1.525(7)
C10	C11A	1.474(7)
C9	C11	1.810(3)
C2	C1	1.516(4)
C13	C12A	1.393(8)
C13	C14	1.389(7)
C12A	C11	1.387(8)
C11	C16	1.402(7)
C16	C15	1.391(8)
C15	C14	1.369(9)

**Chapter 6: Introducing Copper(II)-Catalyst to Photochemical ATRA  
Reactions**

Atom	Atom	Length/Å
C11A	C16A	1.3900
C11A	C12B	1.3900
C16A	C15A	1.3900
C15A	C14A	1.3900
C14A	C13A	1.3900
C13A	C12B	1.3900

Bond Angles in ° for **7a**.

Atom	Atom	Atom	Angle/°
O1	S1	C5	108.41(17)
O1	S1	C8	108.16(15)
O2	S1	O1	118.42(16)
O2	S1	C5	107.72(15)
O2	S1	C8	106.55(16)
C5	S1	C8	107.06(16)
C5	C4	C3	118.9(3)
C5	C6	C7	118.5(3)
C4	C3	C2	121.0(3)
C4	C5	S1	118.7(3)
C4	C5	C6	121.3(3)
C6	C5	S1	120.0(3)
C2	C7	C6	121.2(3)
C9	C8	S1	115.8(2)
C9	C10	C11	112.4(4)
C11A	C10	C9	113.0(7)
C8	C9	C10	111.8(3)
C8	C9	Cl1	110.0(2)
C10	C9	Cl1	107.4(2)
C3	C2	C1	120.0(4)
C7	C2	C3	119.1(3)
C7	C2	C1	120.9(4)

**Chapter 6: Introducing Copper(II)-Catalyst to Photochemical ATRA  
Reactions**

Atom	Atom	Atom	Angle/°
C14	C13	C12A	120.0(6)
C11	C12A	C13	120.2(5)
C12A	C11	C10	116.9(6)
C12A	C11	C16	119.0(5)
C16	C11	C10	124.1(6)
C15	C16	C11	120.4(5)
C14	C15	C16	119.9(5)
C15	C14	C13	120.4(5)
C16A	C11A	C10	111.1(9)
C16A	C11A	C12B	120.0
C12B	C11A	C10	128.9(9)
C11A	C16A	C15A	120.0
C16A	C15A	C14A	120.0
C13A	C14A	C15A	120.0
C12B	C13A	C14A	120.0
C13A	C12B	C11A	120.0

Hydrogen Fractional Atomic Coordinates ( $\times 10^4$ ) and Equivalent Isotropic Displacement Parameters ( $\text{\AA}^2 \times 10^3$ ) for **7a**.  $U_{eq}$  is defined as 1/3 of the trace of the orthogonalised  $U_{ij}$ .

Atom	x	y	z	$U_{eq}$
H4	6038.69	3644.54	4328.05	35
H6	6201.43	6628.83	7721.82	35
H3	7171.12	3245.28	4328.71	40
H7	7334.11	6176.84	7711.71	40
H8A	5168.22	6127.14	3720.67	31
H8B	4491.33	6647.87	4368.15	31
H10A	4856.1	9096.32	2561.69	43
H10B	5003.39	10776.8	3412.07	43
H10C	5013.73	10762.48	3390.5	43
H10D	4845.45	9075.22	2567.69	43
H9	5097.19	9044.37	5446.89	35

**Chapter 6: Introducing Copper(II)-Catalyst to Photochemical ATRA  
Reactions**

<b>Atom</b>	<b>x</b>	<b>y</b>	<b>z</b>	<b><math>U_{eq}</math></b>
H1A	8199.36	3204.76	5792.38	68
H1B	8284.69	4662.5	6901.58	68
H1C	8305.6	5126.01	5327.94	68
H13	3154.36	11395.58	6221.72	38
H12A	4249.9	10979.7	5621.61	37
H16	3669.46	8663.73	2116.05	37
H15	2578.63	9167.41	2697.7	38
H14	2325.03	10523.34	4736.58	38
H16A	3895.72	8600.62	2021.39	37
H15A	2759.07	8814.42	2194.14	38
H14A	2287.76	10201.27	4072.48	38
H13A	2953.08	11374.32	5778.09	38
H12B	4089.74	11160.55	5605.36	37

Atomic Occupancies for all atoms that are not fully occupied in **7a**.

<b>Atom</b>	<b>Occupancy</b>
H10A	0.648(16)
H10B	0.648(16)
H10C	0.352(16)
H10D	0.352(16)
C13	0.648(16)
H13	0.648(16)
C12A	0.648(16)
H12A	0.648(16)
C11	0.648(16)
C16	0.648(16)
H16	0.648(16)
C15	0.648(16)
H15	0.648(16)
C14	0.648(16)
H14	0.648(16)



**Chapter 6: Introducing Copper(II)-Catalyst to Photochemical ATRA  
Reactions**

---

Atom	Occupancy
C11A	0.352(16)
C16A	0.352(16)
H16A	0.352(16)
C15A	0.352(16)
H15A	0.352(16)
C14A	0.352(16)
H14A	0.352(16)
C13A	0.352(16)
H13A	0.352(16)
C12B	0.352(16)
H12B	0.352(16)

**References:**

- [1] S. Mao, Y.-R. Gao, X.-Q. Zhu, D.-D. Guo, Y.-Q. Wang, *Org. Lett.* **2015**, *17*, 1692.  
[2] Q. Liu *et al.*, *Org. Lett.* **2013**, *15*, 6054.



### Summary

This thesis describes two different Cu(II)-catalyzed photochemical transformations, namely, oxo-azidation of vinylarenes and chloro-sulfonation of unactivated olefins. In addition, a photochemical route for the synthesis of pyrazines from corresponding vinyl azides has been delineated.

In **Chapter 1**, the historical background, revolution as well as recent developments in the field of visible-light photoredox catalysis have been outlined. In addition, the discovery of different modes of photochemical activation of small organic molecules and their application in organic synthesis have been shown by the selection of a few pioneering examples.

In **Chapter 2**, the synthesis of pyrazine cores from vinyl azides has been described via a photocascade process which involves the utilization of two photons by a single photocatalyst ( $[\text{Ru}(\text{bpy})_3]\text{Cl}_2$ ) for producing one molecule of the pyrazine product. In the first catalytic cycle, photoexcited  $^*[\text{Ru}(\text{bpy})_3]\text{Cl}_2$  transfers energy to the vinyl azide to form an azirine intermediate which further reacts with water to form an 1,4-dihydropyrazine intermediate. In the subsequent catalytic cycle, this intermediate underwent oxidation to the corresponding 1,4-pyrazine in the presence of oxygen (air, as terminal oxidant).

The **Chapter 3** describes the use of copper in various visible-light-mediated transformations. Copper is not only an earth-abundant or cost-alternative metal for photocatalysis, but it has several special features beyond single-electron transfer. In the first part of this chapter, a few unique transformations have been discussed which could be achieved only in the presence of a copper(I)-photocatalyst (organic dyes, iridium or ruthenium-based photocatalyst failed in all these transformations). In the second part, the ability of copper to form a photoactive-species and their interaction with various organic compounds under photochemical conditions has been discussed. Recently, copper has also been employed as a co-catalyst in combination with the commonly used photocatalysts in order to achieve various cross-coupling reactions. This discussion, including the mechanistic paradigms are shown in the third part of this chapter. While in the last part, a conceptual description of copper(II)-photocatalyzed processes have been demonstrated with a few examples. The concept of visible-light-induced homolysis (VLIH) of photoactive Cu(II)-complexes has been introduced in this chapter.

The **Chapter 4** illustrates an unprecedented visible-light mediated copper(II)-photocatalyzed process. A visible-light-accelerated, copper(II)-catalyzed method for oxoazidation of vinylarenes has been developed which proceeds at room temperature and utilizes molecular oxygen as the stoichiometric oxidant. In contrast to commonly used iridium, ruthenium or organic dye based photocatalysts, copper-based photocatalysts have been found to be unique for this transformation. With spectroscopic evidences, Cu(II) has been proposed as the catalytically active species. In the key-step, a copper(II)-azide intermediate species undergoes light-accelerated homolysis to form a Cu(I)-species and an azido radical. This study also represents the first catalytic synthesis of azidoketones directly from olefins.

In **Chapter 5**, the use of different sulfonyl chlorides in visible-light-mediated transformations have been discussed. Direct trifluoromethylation, sulfonation and arylation of organic compounds could be achieved in single photocatalytic steps as demonstrated by a few properly selected examples.

In **Chapter 6**, visible-light induced, copper catalyzed chloro-sulfonation of unactivated olefin has been delineated. This protocol utilizes commercially available precursors (sulfonyl chlorides and olefins) and proceeds at room temperature. Besides the Cu(I) complex  $[\text{Cu}(\text{dap})_2]\text{Cl}$ , the corresponding Cu(II) complex  $[\text{Cu}(\text{dap})\text{Cl}_2]$  has been proven to be an efficient catalyst in this reaction, being advantageous from an economic point of view but also opening up new avenues for photoredox catalysis. Moreover, these copper complexes have also outperformed commonly used ruthenium, iridium, or organic dye based photocatalysts. The use of stoichiometric  $\text{Na}_2\text{CO}_3$  in combination with the copper photocatalysts was found to be essential for this reaction. As suggested by appropriate control experiments, the role of  $\text{Na}_2\text{CO}_3$  is attributed to prevention of poisoning of the catalyst.

### Zusammenfassung

Diese Arbeit zeigt zwei verschiedene mit Cu(II)-katalysierte photochemische Transformationen. Zum einen die Oxo-Azidierung von Vinylarenen, zum Anderen die Chloro-Sulfonierungen von nicht aktivierten Olefinen. Außerdem wurde eine photochemische Route zur Synthese von Pyrazinen aus den entsprechenden Vinylaziden beschrieben.

In **Kapitel 1** wird ein Überblick über den historischen Hintergrund, die Revolution sowie jüngste Entwicklungen im Feld der Photoredoxkatalyse mit sichtbarem Licht gegeben. Darüber hinaus wird anhand einer Auswahl wegweisender Beispiele die Entdeckung von verschiedenen photochemischen Aktivierungsmoden von kleinen organischen Molekülen und ihre Anwendung in der organischen Synthese aufgezeigt.

In **Kapitel 2** konnte die Synthese einer Pyrazingrundstruktur aus Vinylaziden über einen photokaskaden Prozess gezeigt werden. In anderen Worten wurden zur Herstellung eines Moleküls des Pyrazinproduktes zwei Photonen eines einzelnen Photokatalysators ( $[\text{Ru}(\text{bpy})_3]\text{Cl}_2$ ) genutzt. Im ersten katalytischen Zyklus findet ein Energietransfer des durch Licht angeregten  $^*[\text{Ru}(\text{bpy})_3]\text{Cl}_2$  zum Vinylazid statt um ein Azirinintermediat zu bilden. Dieses reagiert mit Wasser weiter zum 1,4-Dihydropyrazinintermediat, welches in einem weiteren katalytischen Zyklus in Anwesenheit von Sauerstoff (Luftsauerstoff, als abschließendes Oxidationsmittel) zum entsprechenden 1,4-Pyrazin oxidiert.

**Kapitel 3** beschreibt den Einsatz von Kupfer in verschiedenen durch sichtbares Licht vermittelten Transformationen. Kupfer ist nicht nur ein reichlich vorkommendes und kostengünstiges Metall zur Photokatalyse, sondern weist neben der Möglichkeit eines Einzel-Elektronentransfers zahlreiche weitere Besonderheiten auf. Im ersten Teil dieses Kapitels wurden einige einzigartige Transformationen behandelt, die nur in Anwesenheit eines Kupfer(I)-Photokatalysators möglich sind (organische Farbstoffe und Iridium- oder Ruthenium-basierte Photokatalysatoren waren in allen Fällen erfolglos). Der zweite Teil befasst sich mit der Fähigkeit von Kupfer, unter photochemischen Bedingungen, photoaktive Spezies zu bilden und sie mit verschiedenen organischen Verbindungen zu koppeln. Erst kürzlich wurde Kupfer in Kombination mit herkömmlichen Photokatalysatoren sogar als Co-Katalysator verwendet, um verschiedene Kreuzkopplungsreaktionen zu verwirklichen. Die Diskussion darüber, einschließlich mechanistischer Paradigmen werden im dritten Teil dieses Kapitels aufgezeigt. Im letzten Teil wurde anhand einiger Beispiele eine konzeptuelle Beschreibung von Kupfer(II)-photokatalysierten Prozessen aufgezeigt.

**Kapitel 4** veranschaulicht einen noch nie gezeigten, durch sichtbares Licht vermittelten, Kupfer(II)-photokatalysierten Prozess. Eine durch sichtbares Licht beschleunigte, Kupfer(II) katalysierte Methode zur oxo-Azidierung von Vinylarenen wurde erschlossen. Diese läuft bei Raumtemperatur ab und nutzt molekularen Sauerstoff als stöchiometrisches Oxidationsmittel. Dabei erwiesen sich, im Gegensatz zu herkömmlich benutzten Iridium, Ruthenium oder auf organischen Farbstoffen basierende Photokatalysatoren, Kupfer-basierte Photokatalysatoren als einzigartig für diese Transformation. Spektroskopisch nachgewiesen, wurde Cu(II) als die katalytisch aktive Spezies vorgeschlagen. Im Schlüsselschritt durchläuft eine Kupfer-Azid Spezies eine durch Licht beschleunigte Homolyse, wobei sich Cu(I) und Azidoradikale bilden. Darüber hinaus repräsentiert diese Studie die erste direkt von Olefinen ausgehende katalytische Synthese von Azidoketonen.

In **Kapitel 5** wurde die Verwendung von verschiedenen Sulfonylchloriden in durch sichtbares Licht vermittelte Transformationen erörtert. In nur einem photokatalytischen Schritt kann die direkte Trifluoromethylierung, Sulfonylierung und Arylierung von organischen Verbindungen verwirklicht werden. Dies wurde anhand ausgewählter Beispiele dargestellt.

In **Kapitel 6** wurde die durch sichtbares Licht induzierte, kupferkatalysierte Chlorosulfonylierung von nicht aktivierten Olefinen dargestellt. Dieses Protokoll nutzt käuflich erwerbliche Startmaterialien (Sulfonylchloride und Olefine) und läuft bei Raumtemperatur ab. Es wurde gezeigt, dass neben dem Cu(I) Komplex  $[\text{Cu}(\text{dap})_2]\text{Cl}$ , auch der korrespondierende Cu(II) Komplex  $[\text{Cu}(\text{dap})\text{Cl}_2]$  diese Reaktion effektiv katalysieren konnte. Dies ist nicht nur aus ökonomischer Sicht vorteilhaft, sondern eröffnet auch neue Wege in der Photoredoxkatalyse. Ferner übertrafen diese Kupferkomplexe auch die herkömmlich genutzten Ruthenium-, Iridium- oder auf organischen Farbstoffen basierenden Photokatalysatoren. Es erwies sich, dass stöchiometrische Mengen von  $\text{Na}_2\text{CO}_3$  in Kombination mit den Kupferphotokatalysatoren für diese Reaktion essenziell sind. Wie durch geeignete Kontrollexperimente suggeriert wurde, wurde die Rolle von  $\text{Na}_2\text{CO}_3$  der Prävention der Katalysatorvergiftung zugeschrieben.

**Asik Hossain (M. Sc.)**

**Present Address:**

**Asik Hossain**

C/o. Prof. Dr. Oliver Reiser

Institut für Organische Chemie

Universität Regensburg

Universitätsstraße 31, 93053

Regensburg, Germany

Email: [asik.hossain@chemie.uni-regensburg.de](mailto:asik.hossain@chemie.uni-regensburg.de) (Institute)

[asikhossain93@gmail.com](mailto:asikhossain93@gmail.com) (Personal)

**Education:**

- 01/04/2016 to **Doctor of Philosophy (Ph.D.): Organic Chemistry**  
**present** University of Regensburg, Germany  
*Research Advisor:* Prof. Dr. Oliver Reiser  
*Research Topic:* Visible-Light Photocatalysis  
*Funding:* GRK 1626 (Chemical Photocatalysis, DFG)
- 01/10/2015- **Research Trainee: Organic Chemistry**  
31/03/2016 University of Regensburg, Germany  
In the research group of Prof. Dr. Oliver Reiser  
*Research Topic:* Photocatalysis with Copper Complexes  
*Funding:* University of Regensburg
- 24/07/2015 **Master of Science (M.Sc.): Chemistry (Organic Chemistry Specialized)**  
CGPA **8.45** (out of 10)  
Indian Institute of Technology (IIT) Madras, Chennai, India  
*M.Sc. Thesis Advisor:* Prof. Indrapal Singh Aidhen  
*Research Topic:* Development of Sulphone-based Building Blocks for the  
Synthesis of Natural Product.
- 17/06/2013 **Bachelor of Science (B.Sc.): Honours in Chemistry**  
Obtained marks **71.62%** (1<sup>st</sup> class)  
St. Paul's Cathedral Mission College  
University of Calcutta, Kolkata, India

**List of Publications:**

**During PhD:**

- 1) **A. Hossain**, O. Reiser\*. Recent developments in visible-light photocatalysis. (Tutorial review). **2019**, *manuscript in preparation*.
- 2) **A. Hossain**,<sup>#</sup> A. Bhattacharyya,<sup>#</sup> O. Reiser\*. Copper's rapid ascent in visible-light photoredox catalysis. *Science* **2019**, *364*, eaav9713. **DOI:** 10.1126/science.aav9713. (#contributed equally).  
Altmetric score 39 (*top 5% of all research outputs ever tracked by Altmetric*).
- 3) **A. Hossain**,<sup>#</sup> S. Engl,<sup>#</sup> E. Lutsker,<sup>#</sup> O. Reiser\*. Visible-Light-Mediated Regioselective Chlorosulfonylation of Alkenes and Alkynes: Introducing the Cu(II) Complex [Cu(dap)Cl<sub>2</sub>] to Photochemical ATRA Reactions. *ACS Catal.* **2019**, *9*, 1103-1109; **DOI:** 10.1021/acscatal.8b04188. (#contributed equally).  
Among the *most read articles* (2<sup>nd</sup>) of the months January and February 2019.
- 4) **A. Hossain**, A. Vidyasagar, C. Eichinger, C. Lankes, J. Phan, J. Rehbein,\* O. Reiser\*. Visible-Light-Accelerated Copper(II)-Catalyzed Regio- and Chemoselective Oxo-Azidation of Vinyl Arenes. *Angew. Chem. Int. Ed.* **2018**, *57*, 8288-8292; **DOI:** 10.1002/anie.201801678. *Angew. Chem.* **2018**, *130*, 8420-8424; **DOI:** 10.1002/ange.201801678.  
This article appears in *HOT Topic: Photocatalysis*.
- 5) S. K. Pagire, **A. Hossain**, O. Reiser\*. Temperature Controlled Selective C-S or C-C Bond Formation: Photocatalytic Sulfonylation versus Arylation of Unactivated Heterocycles Utilizing Aryl Sulfonyl Chlorides. *Org. Lett.* **2018**, *20*, 648-651; **DOI:** 10.1021/acs.orglett.7b03790.  
This article was highlighted in *Nature Index*.
- 6) **A. Hossain**, S. K. Pagire, O. Reiser\*. Visible-Light-Mediated Synthesis of Pyrazines from Vinyl Azides Utilizing a Photocascade Process. *Synlett* **2017**, *28*, 1707-1714; **DOI:** 10.1055/s-0036-1590888.  
This article is a part of *Heterocycles: Special Issue*, ISHC Conference held in Regensburg, Germany (September 2017).
- 7) S. K. Pagire, **A. Hossain**, L. Traub, S. Kerres, O. Reiser\*. Photosensitised regioselective [2+2]-cycloaddition of cinnamates and related alkenes. *Chem. Commun.* **2017**, *53*, 12072-12075; **DOI:** 10.1039/C7CC06710K.  
Selected for inside front *cover picture* of the article.



- 8) T. Rawner, M. Knorn, E. Lutsker, **A. Hossain**, O. Reiser\*. Synthesis of Trifluoromethylated Sultones from Alkenols Using a Copper Photoredox Catalyst. *J. Org. Chem.* **2016**, *81*, 7139-7147; **DOI**: 10.1021/acs.joc.6b01001.

This article is a part of *Photocatalysis* special issue.

**During M.Sc.:**

- 9) R. Mukkamala, **A. Hossain**, I. S. Aidhen\*. Valuable building blocks for the synthesis of lunularic acid, hydrangeic acid and their analogues. *Nat. Prod. Res.* **2017**, *31*, 1085-1090; **DOI**: 10.1080/14786419.2016.1274891.

This article is part of my *Master Thesis*.

**Awards and Achievements in Academics and Research:**

- **Fellowship for pursuing Ph.D.** from GRK 1626 (Chemical Photocatalysis, DFG) at University of Regensburg.
- Received a **Scholarship** from GRK 1626 (Chemical Photocatalysis, DFG) for attending Conferences in Italy and Germany.
- Institute **Merit Scholarship** for outstanding academic performance throughout all four semesters during MSc.
- Earned 'A' **Grade (9/10)** for Master Thesis work at IIT Madras.
- Awarded a **Junior Research Fellowship (J.R.F)** for qualifying National Eligibility Test (NET) conducted by Council of Scientific and Industrial Research (CSIR), New Delhi, India. All India Rank 35.
- Awarded a **Research Fellowship** for qualifying Graduate Aptitude Test in Engineering (GATE) with 98.5 percentile marks conducted by IIT Kanpur, India.

**Selected Oral and Poster Presentations:**

- 1) *Oral Presentation*: **A. Hossain**, O. Reiser. Unique Features of Copper in Visible-light Photocatalysis. At 35<sup>th</sup> *GRK Seminar Day* in Kostenz, Germany (2019).
- 2) *Poster Presentation*: **A. Hossain**, A. Vidyasagar, C. Eichinger, C. Lankes, J. Phan, J. Rehbein, O. Reiser. Visible-Light-Accelerated Cu(II)-Catalyzed Oxo-Azidation of Vinyl Arenes. In the **22<sup>nd</sup> IUPAC International Conference on Organic Synthesis (ICOS)** in Florence, Italy (2018).
- 3) *Poster Presentation*: E. Lutsker, T. Rawner, M. Knorn, **A. Hossain**, O. Reiser (Group Presentation). Copper Based Photocatalysts for Visible Light Mediated Organic Transformations. At the **Lecture Conference on Photochemistry** in Munich, Germany (2018).

- 4) *Oral Presentation*: **A. Hossain**, O. Reiser. Visible-Light-Accelerated Oxo-Azidation of Alkenes. At 32<sup>nd</sup> GRK Seminar Day in Regensburg, Germany (2018).
- 5) *Poster Presentation*: **A. Hossain**, S. K. Pagire, O. Reiser. Visible-Light-Mediated Synthesis of Pyrazines from Vinyl Azides Utilizing a Photocascade Process. In the *International Society of Heterocyclic Chemistry (ISHC) Conference* at University of Regensburg, Germany (2017).
- 6) *Oral Presentation*: **A. Hossain**, R. Mukkamala, I. S. Aidhen: New Strategy and Building Blocks towards Synthesis of Lunularic Acid, Hydrangeic Acid and Their Analogues. At 23<sup>rd</sup> GRK Seminar day in Kostenz, Germany (2015).
- 7) *Oral Presentation*: **A. Hossain**, R. Mukkamala, I. S. Aidhen: Valuable Building Blocks towards Synthesis of Lunularic Acid, Hydrangeic Acid and Their Analogues. At Indian Institute of Technology Madras, India (2015).

### **Teaching Experience:**

Supervised one Master student of Synthesis and Catalysis (*SynCat*) programme at the **University of Regensburg**, Germany.

### **Selected Participation:**

- 1) Attended *Münster Symposium on Cooperative Effects in Chemistry 2019* held at Westfälische Wilhelms-Universität (WWU) Münster, Germany (2019).
- 2) Participated in visiting a pharmaceutical company (*Aurigene Discovery*) as part of Medicinal Chemistry course work during M.Sc. in Bangalore, India (2015).
- 3) Attended *MedChem Conference* at IIT Madras (2014).
- 4) Attended *Chemistry In-House Symposium* held at IIT Madras (2014).
- 5) Attended University Grants Commission (UGC) sponsored national conference on *Modern Trends of Chemistry in the 21<sup>st</sup> Century* held in Kolkata (2012).
- 6) Attended UGC sponsored national conference on *Non-conventional Energy Resources and Sustainable Development: Current Perspective* held at St. Paul's Cathedral Mission College, Kolkata (2010).

**Personal Information:**

Full Name: **Asik Hossain**  
Date of Birth: March 22, 1993  
Gender: Male  
Nationality: Indian  
Languages known: English, Bengali (native), Hindi  
Marital Status: Single  
Hobbies: Travelling  
Permanent Address: Vill-Bajitpur, P.O.-Bhalukabazar, P.S.-Ratua, Dist-Malda, PIN-732125  
West Bengal, India

**References:**

**Prof. Dr. Oliver Reiser** (Ph.D. Supervisor)

Institute of Organic Chemistry  
University of Regensburg, Germany  
*E-mail:* [oliver.reiser@chemie.uni-regensburg.de](mailto:oliver.reiser@chemie.uni-regensburg.de)  
*Homepage:* [http://www-oc.chemie.uni-regensburg.de/reiser/index\\_e.html](http://www-oc.chemie.uni-regensburg.de/reiser/index_e.html)

**Prof. Dr. Burkhard König**

Institute of Organic Chemistry  
University of Regensburg, Germany  
*E-mail:* [burkhard.koenig@chemie.uni-regensburg.de](mailto:burkhard.koenig@chemie.uni-regensburg.de)  
*Homepage:* <http://www-oc.chemie.uni-regensburg.de/koenig/index.php>

**Prof. Dr. Julia Rehbein**

Institute of Organic Chemistry  
University of Regensburg, Germany  
*E-mail:* [julia.rehbein@chemie.uni-regensburg.de](mailto:julia.rehbein@chemie.uni-regensburg.de)  
*Homepage:* <http://www.reaction-dynamics.de/>

## *Declaration*

---

### **Declaration:**

Herewith I declare that this Ph.D. thesis has been prepared single-handedly which is an outline of my original work. Contributions from the co-authors has been marked clearly.

Regensburg, September 2019

**Asik Hossain**